Human cytomegalovirus-induced oncogenesis in breast cancer, glioblastoma, and epithelial ovarian cancer

Ranim El Baba

▶ **To cite this version:**

Ranim El Baba. Human cytomegalovirus-induced oncogenesis in breast cancer, glioblastoma, and epithelial ovarian cancer. Human health and pathology. Université Bourgogne Franche-Comté, 2023. English. NNT : 2023UBFCE028 . tel-04457277

HAL Id: tel-04457277

https://theses.hal.science/tel-04457277

Submitted on 14 Feb 2024

HAL is a multi-disciplinary open access archive for the deposit and dissemination of scientific research documents, whether they are published or not. The documents may come from teaching and research institutions in France or abroad, or from public or private research centers.

L'archive ouverte pluridisciplinaire **HAL**, est destinée au dépôt et à la diffusion de documents scientifiques de niveau recherche, publiés ou non, émanant des établissements d'enseignement et de recherche français ou étrangers, des laboratoires publics ou privés.

THESE DE DOCTORAT DE L'ETABLISSEMENT UNIVERSITE BOURGOGNE FRANCHE-COMTE

Préparée à l'UFR Santé-EPILAB 4266

Ecole doctorale n°554

Environnement-Santé

Doctorat de Médecine, cancérologie, génétique, hématologie, immunologie

Par

EL BABA Ranim

Oncogénicité du cytomégalovirus humain dans le cancer du sein, le glioblastome et le cancer épithélial de l'ovaire

Thèse présentée et soutenue à Besançon, le Mardi 28 Novembre 2023

Composition du Jury :

M. ADOTEVI Olivier	Professeur, Université de Bourgogne-Franche-Comté	Président
Mme. VAN LINT Carine	Professeure, Université Libre de Bruxelles	Rapporteuse
M. SCHWARTZ Christian	Professeur, Université de Strasbourg	Rapporteur
M. HERBEIN Georges	Professeur, Université de Bourgogne-Franche-Comté	Directeur de thèse

Invités

Mme. DIAB-ASSAF Mona	Professeure, Université Libanaise

Acknowledgement

As I reach the culmination of my academic journey with this thesis, I would like to express my profound gratitude to the following individuals and entities who have played a pivotal role in my PhD journey.

First and foremost, I would like to praise and thank GOD, the almighty, who has granted me countless blessings, strength, perseverance, knowledge, and opportunities so that I have been finally able to accomplish my thesis.

I sincerely thank Pr. Georges Herbein, my supervisor, for providing me with the opportunity to pursue the PhD under his supervision. I'm beyond grateful for the exceptional support, guidance, presence, and knowledge you've shared with me during my thesis research. Your mentorship has been an invaluable and transformative part of my academic experience. Your supportive input and constructive feedbacks propelled me forward, broaden my knowledge, and challenged me to strive highest standards. Not to forget your presence, both in terms of physical presence during meetings and your willingness to be available when needed, has made a world of difference.

My gratitude knows no bounds for Pr. Mona Diab-Assaf. I appreciate her recommendation to Pr. Georges Herbein, which led to my acceptance as a PhD candidate in his laboratory. Throughout this journey, she offered continuous positive reinforcement and support.

I am extremely thankful to the members of my PhD jury including Pr. Olivier Adotevi, Pr. Carine Van Lint, and Pr. Christian Schwartz. I am well aware of the time you invested in reading my manuscript, providing feedback, and offering your expertise which significantly enhanced the quality of this research.

I am indebted to Apex Biosolutions company and the Hariri Foundation for Sustainable Human Development for their financial assistance that contributed to the successful completion of my PhD.

I extend my heartfelt thanks to my lab colleagues (Sébastien, Zeina, Sandy, Jihan, and Fidaa) for being an essential part of my academic journey. A special thanks to Sébastien who facilitated my integration into the lab environment and acquainted me with various laboratory methods. Thank you for your willingness to share your scientific knowledge and experience with me. I also deeply acknowledge the support of Jihan and Fidaa. I'm thankful for their friendship and encouragement. To all my lab colleagues, may your paths ahead be filled with success, growth, and endless opportunities. Here's to each of you and the bright futures you're destined to create. Here's to your ambitions!

To my guardians, "Baba Yehya" and "Mama Ghada", thank you for being the pillar of my PhD journey. You have provided me with strength during life's triumphs and tribulations; you amplified the joy during my successes. Knowing that I can count on you, no matter what, has been a priceless gift. I am forever grateful for your irreplaceable presence in my life. To my gems, my brother "Zakaria" and my sister "Wafaa", your love, support, empathy, listening ear, and words of encouragement have been a source of solace and strength. My love for all of you goes beyond what words can convey. I truly cherish our bond and I love you all!

My deepest gratitude goes for my big family (aunts, uncles, and cousins) for their unwavering love and support. Their presence and encouragement have been the cornerstone of my success.

Finally, I would like to extend my sincere gratitude to my close friends who reside in distant corners of the world 'Lebanon, France, Dubai, Canada, Germany, and America'. Although miles apart, your care packages, video calls, love, moral support, and encouragement have been an invaluable source of strength throughout my academic journey. Your friendship has transcended borders and time zones. Your friendship is a treasure that I will forever hold close to my heart.

Table of Contents

Chapter 1 ..... **18**

1 Human Cytomegalovirus (HCMV) in Focus: An Overview of the Virology, Immunology, and Clinical Aspects **18**

1.1 *Herpesviridae* Family and HCMV Discovery 18

1.2 HCMV Genome 19

1.3 Virion Structure 21

1.3.1 The Envelope 22

1.3.2 The Capsid 22

1.3.3 The Tegument 23

1.4 HCMV Life Cycle 23

1.4.1 Attachment and Viral Entry 23

1.4.2 Lytic Cycle 24

1.4.3 Latent Cycle 26

1.5 HCMV Prevalence and Spread 27

1.6 Clinical Aspects of HCMV and HCMV-Related Diseases 27

1.7 HCMV Detection and Diagnosis 28

1.7.1 Serology 28

1.7.2 Virus Culture 28

1.7.3 Identification of Viral Antigens 29

1.7.4 PCR Amplification 29

1.8 Therapeutic Approaches for HCMV Infection 29

1.8.1 HCMV Antivirals 30

1.8.2 Immunotherapy 31

Chapter 2 ..... **34**

2. HCMV-Induced Polyploid Giant Cancer Cells and Their Significance in Tumorigenesis **34**

2.1 Morphological Characteristics of PGCCs 34

2.2 PGCCs Stimuli and Mechanisms of Generation 34

2.3 Characteristics of PGCCs and Potential Biomarkers 35

2.4 Potential Involvement of PGCCs in Cancer Progression 38

2.5 PGCCs and Oncoviruses 39

2.5.1 HPV 40

2.5.2 EBV 41
2.5.3 KSHV 42
2.5.4 HTLV-1 43
2.5.5 HBV 44
2.5.6 HCV 45
2.5.7 MCPyV 46
2.6 HCMV and PGCCs 47
Chapter 3 49
3. HCMV-Mediated Oncogenesis 49
3.1 HCMV Prevalence in Diverse Forms of Cancer 49
3.2 HCMV, A Candidate Oncogenic Virus, Fulfilling Cancer Hallmarks 51
3.2.1 Sustaining Proliferative Signaling 52
3.2.2 Evading Tumor Suppressors 53
3.2.3 Activating Invasion and Metastasis 54
3.2.4 Enabling Replicative Immortality 54
3.2.5 Inducing Angiogenesis 55
3.2.6 Resisting Cell Death 55
3.2.7 Evading Immune Suppression 57
3.2.8 Reprogramming of Energy Metabolism 58
3.2.9 Enabling Characteristics: Genomic Instability, Mutation, and Tumor-promoting Inflammation 59
3.2.10 Tumor Promoting Microenvironment 60
3.3 HCMV and Its Association with Breast Cancer 63
3.4 The Potential Link Between HCMV and Glioblastoma 64
3.5 The Interplay Between HCMV and Ovarian cancer 65
Chapter 4 67
4. Emerging Threats: Decoding The Molecular Pathways in Cancer Development and Understanding Viral Variants 67
4.1 Decoding The Molecular Pathways in Cancer Development 67
4.2 Viral Variants and Their Oncogenic Potential 68
Chapter 5 72
5. Study Objectives 72

Chapter 6 ..... **74**
6. Materials And Methods **74**
6.1 Reagents 74
6.2 Cell Cultures 76
6.3 HCMV Isolates Growth and Detection 77
6.4 Microscopy 78
6.5 Soft Agar Colony Formation Assay 78
6.6 Tumorsphere and Spheroid formation Assays 79
6.7 Flow Cytometry Analysis 79
6.8 Western Blotting 80
6.9 RT^2 Profiler PCR Array 80
6.10 RNA Cross-linking Immunoprecipitation (RNA CLIP) assay 80
6.11 Assessment of telomerase activity 81
6.12 Quantitative Reverse Transcription PCR (RT-qPCR) 81
6.13 Invasion Assay 81
6.14 Treatments 82
6.15 Tumor Biopsies and HCMV isolation 82
6.15.1 Tumor Biopsies 82
6.15.2 Genes and Transcripts Expression As Well As Polyploidy Detection Within Tumor Biopsies 85
6.15.3 HCMV Isolation From Tumor Biopsies 85
6.16 Statistical Analyses 86
Chapter 7 ..... **87**
7. Results **87**
7.1 Oncogenic and Stemness Signatures of the High-Risk HCMV Strains in Breast Cancer Progression 87
7.1.1 Growth of Two HCMV Clinical Strains Isolated from TNBC in HMECs and the Emergence of Morphologically Distinct Cells 87
7.1.2 Transformation Capacity of CTH Cells and the Induction of an Oncogenic Environment 87
7.1.3 CTH Cells Promote Embryonic Stemness and Develop an Epithelial/Mesenchymal Hybrid State 91
7.1.4 Persistent HCMV Replication in CTH-B544 and CTH-B693 Long-Term Cultures 95

7.1.5 A Specific Molecular Landscape Unveiled in the Tumor Microenvironment of TNBC Harboring High-Risk HCMV 97
7.1.6 Restricting Soft Agar Colony Formation, Controlling PGCCs Count and Proliferation by Paclitaxel and Ganciclovir Therapy 97
7.2 EZH2-Myc Driven Glioblastoma Elicited by Cytomegalovirus Infection of Human Astrocytes ... 99
7.2.1 HCMV Clinical Isolates Permissively Infect HAs Inducing Increased Myc and EZH2 Expression 99
7.2.2 Emergence of a Glioblastoma-Like Phenotype With CEGBCs in HAs Chronically Infected With High-Risk HCMV Strains 102
7.2.3 CEGBCs Productively Infected With High-Risk HCMV Display Invasiveness 107
7.2.4 Detection of lncRNA4.9/EZH2 and HOTAIR/EZH2 Complexes in CEGBCs Cultures 110
7.2.5 Upregulation of EZH2 and Myc in HCMV-positive GBM Tissues 112
7.2.6 Isolation of Oncogenic HCMV Strains From GBM Tumors 114
7.2.7 EZH2 inhibitor, TMZ, and GCV tritherapy Curtails CEGBCs Growth 120
7.3 Polyploidy, EZH2 Upregulation, and Transformation in CMV-infected Human Ovarian Epithelial Cells 122
7.3.1 OECs Chronically Infected With HCMV-DB and BL Strains Generated CTO Cells With PGCCs 122
7.3.2 CTO cells Display Dedifferentiation, Stemness, and EMT Characteristics 127
7.3.3 Lytic and Latent HCMV Replication in Transformed OECs 136
7.3.4 EZH2 Upregulation in HCMV-positive HGSOC Biopsies and The Isolation of Three Oncogenic HCMV Strains From EZH2^{High} HGSOC Biopsies 139
Chapter 8 144
8. Discussion 144
Chapter 9 155
9. Conclusion 155
10. Bibliographic References 160
11. Annex 192
11.1 Publication N°1 192
11.2 Publication N°2 205
11.3 Publication N°3 218
11.4 Publication N°4 236
11.5 Publication N°5 254

11.6 Publication N°6 275
11.7 Publication N°7 294
11.8 Publication N°8 306
11.9 Publication N°9 322
11.10 Publication N°10 337
11.11 Publication N°11 353

Abstract

On a worldwide scale, breast cancer, glioblastoma, and ovarian cancer present a significant health obstacle, being responsible for cancer-related fatalities. Cancer etiological factors are assorted into genetic or environmental risk factors of which viruses are estimated to contribute to 20% of all cancer cases. Human cytomegalovirus (HCMV) is a herpesvirus that infects a substantial portion of the global population, ranging from 40% to 95%. The variability in the HCMV genome may contribute to its oncomodulatory potential, as it can promote the initiation and dissemination of cancerous cells. Recently, increasing attention has been directed towards the oncogenic role of HCMV, particularly high-risk HCMV strains that can directly induce transformation in primary cells. Polyploid giant cancer cells (PGCCs), have been definitively shown to exhibit cancer stem cells (CSCs) characteristics. These PGCCs give rise to descendant cells through asymmetric division, the latter express markers associated with epithelial-mesenchymal transition (EMT), which in turn promotes invasion and migration. Research indicated that PGCCs generation can be triggered by anti-cancer therapies. PGCCs presence has been particularly linked to cases with poor prognosis, contributing to tumor relapse and resistance to therapy. Previous investigations by our group have highlighted the presence of PGCCs containing HCMV in cancer biopsies, establishing a noteworthy correlation between the presence of PGCCs and HCMV.

HCMV has been implicated in oncogenesis, particularly in breast cancers, glioblastoma (GBM), and epithelial ovarian cancer. Herein, we investigated the oncogenic potential of HCMV in various cancer contexts and explored the molecular mechanisms and transforming capabilities of different HCMV strains isolated from these distinct cancer types and their impact on patient outcomes. To start with breast cancer, we assessed HCMV-B544 and B693 strains, isolated from EZH2HighMycHigh triple-negative breast cancer (TNBC) biopsies. These strains transformed human mammary epithelial cells (HMECs) resulting in CMV-Transformed-HMECs (CTH cells) and PGCCs displaying stemness phenotype. Notably, HCMV persists in long-term cultures, indicating sustained viral replication with alternance of lytic and latent states. In glioblastoma, HCMV was explored as a reprogramming vector, dedifferentiating mature human astrocytes into CMV-Elicited Glioblastoma Cells (CEGBCs) with glioblastoma-like traits. HCMV influences the transformation, invasion, and spheroid formation processes, correlating with increased EZH2 and

Myc expression in GBM biopsies. Eleven clinical HCMV strains isolated from GBM tissues further validated their role in glioblastoma oncogenesis. These CEGBCs exhibit sensitivity to therapeutic interventions, including an EZH2 inhibitor, ganciclovir, and temozolomide triple therapy, offering potential avenues for glioblastoma treatment. In the context of high-grade serous ovarian carcinoma (HGSOC), HCMV-DB and BL high-risk strains transformed ovarian epithelial cells (OECs) into "CMV-transformed Ovarian cells" (CTO). HCMV infection was associated with EZH2 upregulation and the presence of PGCCs with cancer stem cell-like properties expressing EMT markers. From HGSOC biopsies, we isolated three clinical HCMV strains. The high-risk strains transformed OECs resulting in CTO cells that displayed proliferative capacities and revealed an increase in EZH2 levels, along with the generation of PGCCs. Notably, the observed features were curtailed upon the inhibition of EZH2.

All in all, this study emphasizes the diverse oncogenic potential of HCMV in breast cancer, glioblastoma, and ovarian cancer, shedding light on molecular mechanisms, transformation processes, and targeted therapies that may improve the overall survival of cancer patients.

Keywords : Human Cytomegalovirus, High-risk strains, oncogenesis, PGCCs, Myc, EZH2, CTH cells, CEGBCs, CTO cells, breast cancer, glioblastoma, high-grade serous ovarian carcinoma.

Résumé

Le cancer du sein, le glioblastome et le cancer de l'ovaire représentent un problème majeur de santé publique. Les facteurs étiologiques du cancer se répartissent en facteurs de risque génétiques ou environnementaux, parmi ces derniers les virus contribueraient à environ 20% de tous les cas de cancer. Le cytomégalovirus humain (HCMV) est un virus herpès qui infecte une part importante de la population mondiale, avec une prévalence de 40% à 95%. La variabilité génomique du HCMV pourrait contribuer à son potentiel oncomodulateur, car il semble accélérer les mécanismes d'oncogenèse. Les cellules cancéreuses géantes polyploïdes (PGCC) ont des caractéristiques semblables à celles des cellules souches cancéreuses (CSC) et donnent naissance à des cellules « filles» lesquelles expriment des marqueurs associés à la transition épithélio-mésenchymateuse (TEM). La présence de PGCC est particulièrement observée dans les cancers de mauvais pronostic. De précédentes études de notre groupe ont mis en évidence la présence de PGCC infectées par le HCMV dans les biopsies de cancer du sein, évoquant ainsi un rôle oncogène direct du HCMV, notamment de certaines souches virales « à haut risque ». Le HCMV a été suggéré comme participant à l'oncogenèse, en particulier dans les cancers du sein, le glioblastome et le cancer épithélial de l'ovaire. Notre travail de thèse a consisté à examiner le potentiel oncogène du HCMV dans ces cancers. Nous avons évalué les souches virales HCMV-B544 et B693, isolées de biopsies de cancer du sein triple négatif $EZH2^{High}Myc^{High}$. Ces souches virales transforment les cellules épithéliales mammaires humaines (HMEC), donnant naissance à « des cellules HMEC transformées par le CMV » (cellules CTH) d'une grande hétérogénéité cellulaire comprenant notamment des PGCC présentant des traits de cellules souches. Une persistance du HCMV est notée dans les cultures à long terme, indiquant une réplication virale continue avec alternance de phase lytique et de latence. Dans le glioblastome, le HCMV a été étudié en tant que vecteur de reprogrammation, dédifférenciant les astrocytes humains matures en « cellules glioblastomateuses induites par le CMV » (cellules CEGBC) présentant des caractéristiques similaires aux cellules de malades. Le HCMV favorise la transformation cellulaire, l'invasion et la de formation de sphéroïdes, corrélé avec une augmentation de l'expression d'EZH2 et de Myc observée également dans les biopsies de glioblastome provenant de malades. Onze souches cliniques de HCMV ont été isolées à partir de biopsies de glioblastome de malades qui reproduisent la transformation

d’astrocytes normaux en cellules glioblastomateuses suite à l’infection virale. Ces cellules CEGBC sont sensibles aux interventions thérapeutiques, notamment à un inhibiteur d'EZH2, au ganciclovir et à une triple thérapie incluant temozolomide-inhibiteur d’EZH2-ganciclovir, offrant ainsi des perspectives nouvelles pour le traitement de ce cancer de très mauvais pronostic. Concernant le cancer séreux épithélial de l'ovaire de haut grade (HGSOC), les souches « à haut risque » HCMV-DB et de BL transforment les cellules épithéliales ovariennes (OEC) en "cellules ovariennes transformées par le CMV" (cellules CTO). Dans ces cellules CTO une augmentation de l'expression d'EZH2 ainsi que la présence de PGCC avec des traits de cellules souches cancéreuses avec TEM ont été observées. À partir de biopsies de HGSOC, nous avons réussi à isoler trois souches cliniques de HCMV qui en infectant les cellules OEC donnent naissance à des cellules CTO hautement prolifératives surexprimant EZH2 et générant des PGCCs ; leur transformation étant réduite par les inhibiteurs d’EZH2 in vitro. En résumé, notre travail met en évidence le potentiel oncogène du HCMV dans trois cancers graves, en dévoilant certains des mécanismes moléculaires mis en œuvre lors de la transformation cellulaire et ouvre la voie à des thérapies ciblées qui pourraient améliorer la survie des patients.

Mots clés: Cytomégalovirus humain, souches virales à haut risque, oncogenèse, PGCCs, Myc, EZH2, cellules CTH, CEGBCs, cellules CTO, cancer du sein, glioblastome, cancer séreux épithélial de l'ovaire de haut grade

List of Figures

Figure 1: Schematic representations comparing genome organizations. 20
Figure 2: HCMV Virion. 22
Figure 3: HCMV Life cycle. 25
Figure 4: Scheme illustrating PGCCs formation mechanisms. 35
Figure 5: A scheme illustrating the giant cell cycle. 37
Figure 6: Generation of PGCCS in various cancer types. 39
Figure 7: The Hallmarks of Cancer. 52
Figure 8: Modulation of the host immune system. 58
Figure 9: HCMV Oncomodulation and Its Significance in Tumor Microenvironment. 61
Figure 10: Replication of B544 and B693 strains in MRC5 cultures, and the appearance of morphologically distinct cells following the infection of HMECs with these high-risk strains. 89
Figure 11: Colony formation in soft agar and Myc expression in CTH-B544 and B693 cells. 89
Figure 12: CTH proliferation capacities and AKT activation. 90
Figure 13: Tumorspheres formation and the expression of stemness markers in CTH cells. 92
Figure 14: Expression of embryonic stem cell markers in CTH-B544 and B693 cells. 93
Figure 15: Penotypic analysis of CTH cells. 94
Figure 16: Sustained viral replication in CTH cells. 96
Figure 17: Distinct responses of CTH cells to paclitaxel/ganciclovir (PTX/GCV) treatment in vitro recapitulates distinct TNBC molecular signatures in vivo. 98
Figure 18: Replication of two high-risk oncogenic HCMV strains in HAs cultures, the activation of oncogenic pathways, and reduced apoptosis rates. 100
Figure 19: Long-term cultures of HAs infected with the two low-risk HCMV strains. 101
Figure 20: Long-term replication of two high-risk HCMV strains in HAs cultures. 103
Figure 21: Chronic infection of HAs with HCMV clinical isolates, the appearance of CEGBCs as well as colony formation in soft agar, and the phenotypic characterization of CEGBCs. 104
Figure 22: Spheroid-forming potentials of CEGBCs as well as invasiveness and migration. 106
Figure 23: Stemness potential of CEGBCs-DB and BL. 106
Figure 24: The invasion capacities of CEGBCs-DB and BL. 108
Figure 25: Cellular migration of CEBGCs. 108
Figure 26: The three major invasion mechanisms of CEGBCs-DB and BL. 109
Figure 27: Detection of replicative HCMV and identification of the lncRNA4.9 and HOTAIR/EZH2 complex in CEGBCs cultures. 111
Figure 28: HCMV detection as well as EZH2, and Myc expression in glioblastoma biopsies. 113
Figure 29: Akt expression in glioblastoma biopsies. 114
Figure 30: Isolation of oncogenic HCMV strains from GBM biopsies. 116
Figure 31: Spheroid forming and invasion potentials of the HCMV-GBM strains and the detection of lncRNA 4.9 and HOTAIR transcripts. 120
Figure 32: The effect of diverse single and combination therapies on CEGBCs' growth. 121
Figure 33: Replication of high-risk HCMV strains in OECs cultures. 122
Figure 34: Replication of low risk HCMV strains in OECs cultures. 123
Figure 35: Flow cytometric analysis based on FSC and SSC of uninfected OECs as well as chronically infected OECs. 124

Figure 36: Chronic infection of OECs with the high-risk HCMV clinical isolates and polyploidy detection in OECs cultures. 126
Figure 37: Colony formation in soft agar and the phenotypic characterization of HCMV-transformed OECs. 129
Figure 38: The assessment of the correlation between EZH2 and Myc expression in CTO cells. 129
Figure 39: Expression of SUZ12 in CTO-DB and BL cells. 130
Figure 40: HCMV-transformed OECs display an embryonic stemness phenotype and possess spheroid-forming potential. 131
Figure 41: Expression of Oct4 in CTO-DB and BL cells. 132
Figure 42: Expression of CD44 in CTO-DB and BL cells. 133
Figure 43: HCMV infection of OECs enhances EMT/MET hybrid traits. 134
Figure 44: Detection of high expression of E-cadherin in several small cells present in CTO-DB and BL cultures. 135
Figure 45: FACS staining of EZH2, Myc, Ki67Ag, Vimentin, E-cadherin, and CD44 in the subpopulations of uninfected OECs. 135
Figure 46: Sustained HCMV replication in chronically HCMV-infected OECs. 137
Figure 47: Expression of IE1 in CTO-DB and CTO-BL subpopulations by FACS. 138
Figure 48: CTO cultures post-TPA treatment. 138
Figure 49: EZH2 expression in untreated CTO-DB/BL and CTO-DB/BL treated with 0.1 µM of GSK343 and EPZ6438 by FACS. 139
Figure 50: HCMV detection, PGCCs presence as well as EZH2 expression in ovarian cancer biopsies. 142
Figure 51: Myc Expression in ovarian cancer biopsies. 142
Figure 52: Akt Expression in ovarian cancer biopsies. 143
Figure 53: Potential model depicting the course of events leading to the initiation of the giant cell cycle. 156
Figure 54: Glioblastoma generation scheme. 157
Figure 55: A schematic representing the giant cell cycling following HCMV infection of OECs. 158

List of Tables

Table 1: Oncoviruses. 46
Table 2: HCMV Gene Products. 49
Table 3: HCMV enabling the characteristics of cancer. 62
Table 4: Primers Used. 74
Table 5: Antibodies Used. 75
Table 6: Treatments Used. 76
Table 7: Clinical and biological data of the GBM patients. 83
Table 8: Clinical data and treatments of the OC patients. 84
Table 9: Characteristics of HCMV-GBM strains. 117

List of Abbreviations

ACT:	Adoptive Cell Therapy
ALDH1A:	Aldehyde dehydrogenase-1A
ATL:	Adult T-cell leukemia
BAX:	Bcl2 associated X
BKPyV:	BK Polyomavirus
BRD4:	Bromodomain-4 protein
CCND1:	Cyclin D1
CDK1:	Cyclin-dependent kinase 1
CDV:	Cidofovir
CEGBCs:	CMV-Elicited Glioblastoma Cells
CID:	Cytomegalic inclusion disease
CNDK2A:	Cyclin dependent kinase inhibitor 2A
CNS:	Central nervous system
$CoCl_2$:	Cobalt chloride
COX-2:	Cyclooxygenase-2
CPE:	Cytopathic effects
CSC:	Cancer stem cell
CTH:	CMV-Transformed HMECs
CTL:	Cytotoxic T lymphocyte
CTO cells:	CMV-transformed Ovarian cells
DBs:	Dense bodies
DC:	Dendritic cell
dsDNA:	Double-stranded DNA
E:	Early
EBNA:	Epstein–Barr virus nuclear antigen
EBV:	Epstein-Barr virus
EGFRs:	Epidermal growth factor receptors
EGR1:	Early growth response 1
ELISA:	Enzyme-linked immunosorbent assay
EMT:	Epithelial-mesenchymal transition
ER:	Endoplasmic reticulum
FAO:	Fatty acid oxidation
FOS:	Foscarnet
FTPs:	Fusion toxin proteins
gB:	Glycoprotein B
GBM:	Glioblastoma multiforme
GCV:	Ganciclovir
GFI1:	Growth factor independence1
gH:	Glycoprotein H
GLUT:	Glucose transporter

gL:	Glycoprotein L
gO:	Glycoprotein O
GRIM-19:	Gene associated with retinoid/interferon-induced mortality-19
GSCs:	Glioblastoma stem cells
HAs:	Human astrocytes
HBV:	Hepatitis B virus
HBx:	Hepatitis B virus X protein
HCC:	Hepatocellular carcinoma
HCMV:	Human Cytomegalovirus
HCV:	Hepatitis C virus
HDACs:	Histone deacetylases
HGSIL:	High-grade squamous intraepithelial lesions
HGSOC:	High-grade serous ovarian cancer
HHV-5:	Human Herpesvirus 5
HIF:	Hypoxia-inducible factor
HLTF:	Helicase like transcription factor
HMECs:	Human Mammary Epithelial Cells
HMTs:	Histone methyltransferases
HPV:	Human papillomavirus
HR:	High-risk
HSCT:	Hematopoietic stem cell transplantation
HSV:	Herpes simplex virus
hTERT:	Human telomerase reverse transcriptase
HTLV-1:	Human T-cell lymphotropic virus-1
ICAM-1:	Intercellular adhesion molecule 1
ICIs:	Immune checkpoint inhibitors
ICs:	Intermediate cells
IE:	Immediate-early
IRS/TRS:	Internal repeat short/terminal repeat short
ITAM:	Immunoreceptor tyrosine-based activation motif
JCPyV:	John Cunningham Polyomavirus
KICS:	KSHV-associated inflammatory syndrome
KS:	Kaposi sarcoma
KSHV:	Kaposi's sarcoma-associated herpesvirus
L:	Late
LAcmvIL-10:	Latency-associated viral homolog of IL-10
LAMP1:	Lysosome-associated membrane protein 1
LANA:	Latency-associated nuclear antigen
LCs:	Large tetraploid cells
LDs:	Lipid droplets
LHBs:	HBV large surface protein
LMP1:	Latent membrane protein 1
lncRNA HOTAIR:	LncRNA HOX antisense intergenic RNA
lncRNAs:	Long non-coding RNAs

LR:	Low-risk
LTAg:	Large T antigen
LUNA:	Latent unique nuclear antigen
MAPK:	Mitogen-activated protein kinase
MCC:	Merkel cell carcinoma
MCD:	Multicentric Castleman's disease
MCP-1:	Monocyte chemoattractant protein-1
MCPyV:	Merkle Polyomavirus
MES:	Mesenchymal
MGMT:	O (6)-methylguanine DNA methyltransferase
MHC:	Major histocompatibility complex
MIEP:	Major immediate early promoter
miR34:	MicroRNA
MOI:	Multiplicity of infection
NCAM:	Neural cell adhesion molecule
ND10:	Nuclear domain 10
NFκB:	Nuclear factor kappa B
NIEPs:	Non-infectious enveloped particles
NOS:	Nitric oxide synthase
NPC:	Nasopharyngeal carcinoma
NPC:	Neural progenitor cell
OC:	Epithelial ovarian cancer
OECs:	Ouman ovarian epithelial cells
PBMCs:	Peripheral blood mononuclear cells
PCR:	Polymerase chain reaction
PD-1:	Programmed cell death protein 1
PD-L1:	Programmed death ligand 1
PEL:	Primary effusion lymphoma
PGCCs:	Polyploid giant cancer cells
PI:	Post-infection
PI3k:	Phosphatidylinositol 3-kinase
Plin4:	Perilipin 4
Plk1:	Polo-like kinase 1
PML:	Promyelocytic leukemia protein
PN:	Proneural
PRC2:	Polycomb repressive complex 2
PTX:	Paclitaxel
qPCR:	Real-time quantitative PCR
RANTES:	Regulated on activation normal T expressed and secreted
Rb:	Retinoblastoma protein
RNA CLIP:	RNA Cross-linking Immunoprecipitation
RT-PCR:	Reverse transcriptase PCR
RT-qPCR:	Quantitative Reverse Transcription PCR
SCs:	Small cells

SOT:	Solid organ transplantation
sTAg:	Small T antigen
STAT-3:	Signal transducer and activator of transcription 3
SV40:	Simian virus 40
TAMs:	Tumor-associated macrophages
TGF-β:	Transforming growth factor-β
TME:	Tumor microenvironment
TMZ:	Temozolomide
TNBC:	Triple-negative breast cancer
TNFR1:	Tumor necrosis factor receptor 1
TRAIL:	TNF-related apoptosis-inducing ligand
TRL/IRL:	Terminal repeat long/internal repeat long
TUSC3:	Tumor suppressor candidate 3
UL:	Unique long
UNITE:	Universal intracellular targeted expression
US:	Unique short
VEGF:	Vascular endothelial growth factor
vFLIP :	Viral FLICE-inhibitory protein
VGCV:	Valganciclovir
vIRF-3:	Viral interferon regulatory factor 3
vMIA:	Viral mitochondria-localized inhibitor of apoptosis
VZV:	Varicella-zoster virus
WHO:	World Health Organization
γH2AX:	Gamma histone variant H2AX

Chapter 1

1 Human Cytomegalovirus (HCMV) in Focus:An Overview of the Virology, Immunology, and Clinical Aspects

1.1 *Herpesviridae* Family and HCMV Discovery

Herpesviridae is a family of viruses that includes a large and diverse group of viruses known as herpesviruses. These viruses are characterized by their ability to establish latent infections by remaining dormant within the host's body and reactivate later under certain conditions. Herpesviruses can infect a wide range of species [1,2]. The family Herpesviridae is divided into three subfamilies: *Alphaherpesvirinae, Betaherpesvirinae, and Gammaherpesvirinae*. Each subfamily has distinct characteristics in terms of virus-host interactions, replication strategies, and clinical manifestations. To start with *Alphaherpesvirinae,* these viruses are known for their rapid replication cycle and ability to establish lytic and latent infections, they are often associated with lesions and sores on the skin and mucous membranes. Examples of alphaherpesviruses include Herpes simplex virus 1 (HSV-1), Herpes simplex virus 2 (HSV-2), and Varicella-zoster virus (VZV), which causes chickenpox and shingles. Second, the *Betaherpesvirinae* comprising betaherpesviruses that have a slower replication cycle compared to alphaherpesviruses; they are often associated with persistent infections and can cause long-term health issues. Human Cytomegalovirus (HCMV), also known as Human Herpesvirus 5 (HHV-5), belongs to this subfamily, within the genera *Cytomegalovirus*. On the other hand, we have HHV6A, HHV6B, and HHV7, which belongs to the genera *Roseolovirus*. Third, the *Gammaherpesvirinae* including Gammaherpesviruses that are associated with certain types of cancers, particularly in immunocompromised individuals. Epstein-Barr virus (EBV) or (HHV4), belonging to genera *Lymphocryptovirus*, is associated with infectious mononucleosis and various cancers, and Kaposi's sarcoma-associated herpesvirus (KSHV) or (HHV8), belongs to genera *Rhadinovirus* [1,3]. Both viruses are classified as oncogenic pathogens that infect lymphoblastoid cells such as T or B lymphocytes and establish latency. However, it's worth noting that a lytic infection has also been observed in epithelioid and fibroblastic cells [3].

One of the numerous breakthroughs and advancements documented during the 20th century involved the identification and characterization of HCMV, which stands as one of the most

prevalent viruses and opportunistic pathogens encountered worldwide. Within this discovery, several specific dates stand out [4,5]. In 1881, the German pathologist Ribbert documented the presence of cells containing inclusions in the kidney of a stillborn infant affected by syphilis and in the parotid gland of an infant. These same "protozoan-like" cells were also observed by Jesionek and Kiolemenoglou in 1904 in the lungs, kidneys, and liver of an 8-month-old fetus with syphilis and by Löwenstein in 1907. These cells, characterized by their large eccentrically placed nuclei, appear to represent the earliest descriptions of typical cytomegalic cells, which were later termed 'cytomegalia' in 1907 [6]. In 1921, Goodpasture and Talbert first suggested a definitive connection between viral diseases and cells exhibiting characteristic intranuclear inclusion bodies. This concept was further elucidated by Wyatt et al., who later in 1932 referred to it as "generalized cytomegalic inclusion disease (CID)." This notion was in alignment with the observations and hypotheses put by other researchers, such as Von Glahn, Pappenheimer, Minder, and others. Significantly, the mid-1950s saw a breakthrough with the advent of human cell culture techniques, enabling the isolation of a virus that was later identified as cytomegalovirus [6]. This achievement was the result of independent efforts by three different laboratories: Smith in 1956, Rowe and colleagues in 1956, and Weller and colleagues in 1957. It was subsequently named 'cytomegalovirus' (CMV) [7,8]. This marked a significant milestone in advancing our comprehension of various aspects of the virus, including but not limited to epidemiology, structure, life cycle, replication, latency, pathogenesis, and treatment modalities. These advancements were greatly facilitated by the development of animal models for studying CMV's pathogenesis [9].

1.2 HCMV Genome

HCMV stands out as having the largest genome among human herpesviruses, spanning a length of 235 kilobases (kb) [10]. This genome comprises a linear double-stranded DNA (dsDNA) helix, with more than 751 translated open reading frames (ORFs) [11,12]. Furthermore, HCMV produces polyadenylated non-coding RNAs, including four notable long non-coding RNAs (lncRNAs), notably RNA2.7, RNA1.2, RNA4.9, and RNA5.0 [13]. Additionally, it generates non-polyadenylated RNAs, such as microRNAs, which play pivotal roles in various processes like regulating host cell metabolism, immune evasion, and the maintenance of latency [14]. The genome of HCMV is highly complex and encodes a wide range of proteins involved in various

aspects of the virus's life cycle, including replication, immune evasion, and pathogenesis. The organization of the HCMV genome adheres to the characteristic architecture of herpesviruses classified under class E [15]. HCMV genome features two inverted domains: the unique long (UL) and unique short (US) domains, each flanked by a pair of inverted repeats, one at the terminal end (terminal repeat long/internal repeat long (TRL/IRL)) and the other at the junction with the other unique domain (internal repeat short/terminal repeat short (IRS/TRS)). This results in a genome organization denoted as TR_L–U_L–IR_L–IR_S–U_S–TR_S. Consequently, HCMV gene annotations are based on their respective positions within these genome segments, specifically UL, US, IRL, IRS, TRL, and TRS **(Figure 1)** [16].

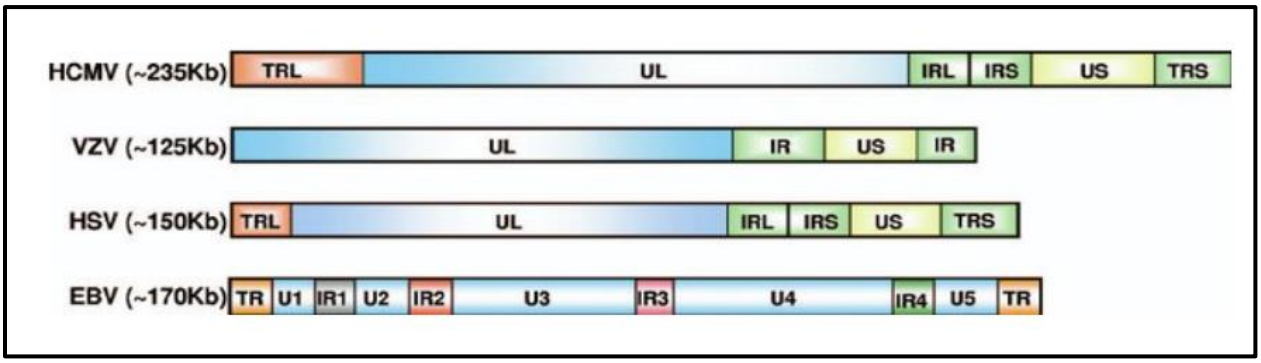

Figure 1: Schematic representations comparing genome organizations.

Genome organizations of various human herpesviruses including varicella zoster virus (VZV), human simplex virus (HSV), and Epstein-Barr virus (EBV). The labels within each segment of the genome illustrate the following characteristics: terminal repeat long (TRL), unique long (UL), unique short (US), internal repeat long (IRL), internal repeat short (IRS), terminal repeat short (TRS), and internal repeat (IR). Adapted from Crough et al [17].

HCMV displays a remarkably broad tropism, encompassing a diverse range of cell types including epithelial cells, fibroblasts, endothelial cells, monocytes and macrophages, dendritic cells, smooth muscle cells, neural cells, and placental cells [18]. This trait can significantly impact the pathogenesis of acute HCMV infections in vivo. For instance, infecting epithelial cells facilitates transmission between hosts, while infecting endothelial and hematopoietic cells can support systemic spread within the host. Additionally, infecting ubiquitous cell types, such as fibroblastic and smooth muscle cells, provides a conducive environment for efficient viral proliferation [18,19]. It's worth emphasizing that HCMV tropism varies considerably among different HCMV

strains and is primarily influenced by variations within the UL128-131 gene locus. This region has been associated with viral persistence, reactivation, and the ability to infect different cell types. The resulting genetic differences account for inter-strain variations in viral entry. Notably, the UL128, UL130, and UL131 proteins form complexes with the virion envelope glycoprotein gH/gL, specifically the pentamer gH/gL/UL128-131. This complex is responsible for mediating entry into epithelial and endothelial cells [20,21]. Furthermore, laboratory-adapted strains, such as the widely used reference strain AD169 and other well-known strains like Towne or Davis, have lost substantial DNA fragments within their ULb' region due to extensive passaging in human fibroblast cell cultures. Consequently, these laboratory strains replicate efficiently in fibroblasts but exhibit limited replication in other cell types like endothelial or epithelial cells. This is in contrast to clinical isolates, which replicate less efficiently in cultured cells but demonstrate nearly equivalent replication efficiency in endothelial cells [22–24]. Understanding the role of the UL128-131 gene locus and its impact on viral entry and tropism is essential for unraveling the complex interactions between HCMV and its host. This knowledge has implications for vaccine development and antiviral strategies aimed at targeting specific strains or cell types.

1.3 Virion Structure

The HCMV virion structure consists of several components **(Figure *2*)** that are orchestrated to ensure successful attachment, entry, and establishment of infection in target cells [25].

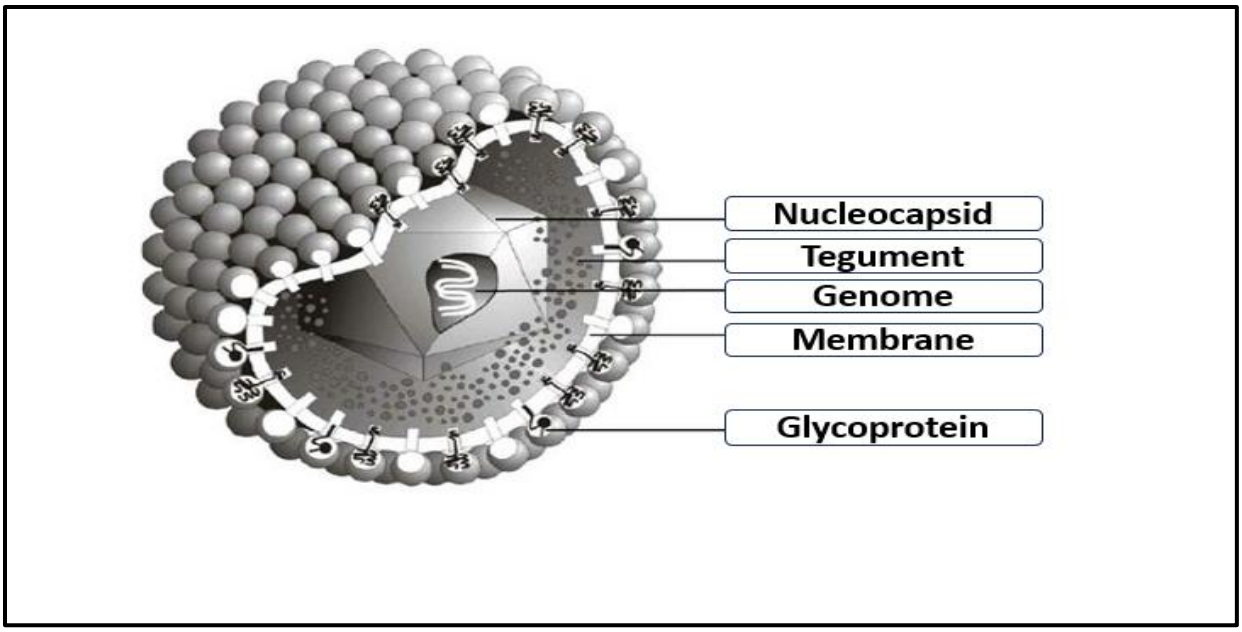

Figure 2: HCMV Virion.

Double-stranded DNA genome is enclosed within an icosahedral symmetry capsid which is further enveloped by a layer called tegument. Mature virions are enveloped; viral glycoproteins protrusions are found on the envelope surface. This description has been adapted and altered based on Tomtishen's work [24].

1.3.1 The Envelope

The HCMV virion is enveloped by a lipid bilayer derived from the host cell membrane during the process of virus assembly and budding. The lipid bilayer is approximately 10 nm thick and contains a minimum of 19 integral membrane proteins that play a crucial role in binding to host cells, facilitating viral entry, and, in some instances, evading the host immune response by sequestering human chemokines [21,26]. Among these proteins, key players in virus entry, cell-to-cell transmission, and virion maturation include viral glycoproteins like gpUL55 (gB), gpUL73 (gN), gpUL74 (gO), gpUL75 (gH), gpUL100 (gM), gpUL115 (gL), and the pentameric complex composed of gL, gH, and UL128-131 [21].

1.3.2 The Capsid

Measuring about 100 nm in diameter, the icosahedral HCMV capsid, also known as the nucleo-capsid, serves as the innermost core layer of the virion particle. It’s a proteinaceous shell that encloses the viral genome. Its primary roles are to safeguard and deliver the genetic material to the

host cell's nucleus. This capsid is constructed from a minimum of five distinct proteins, which are meticulously organized into 162 capsomeres. These five proteins encompass the major capsid protein (UL86), the minor capsid protein (UL85), the smallest capsid protein (UL48-49), the assembly protein comprising fragments of UL80, and the minor capsid binding protein (UL46) [27,28].

1.3.3 The Tegument

The tegument layer in the HCMV virion is around 50 nm thick and occupies the space between the lipid envelope and the protein capsid [29]. This layer is characterized by its high protein content, accounting for approximately half of all viral proteins present in an infectious virion. Many of these proteins are phosphorylated. These proteins play crucial roles in various aspects of the viral life cycle, including replication, gene expression regulation, viral particle assembly, immune system evasion, and other essential functions. Beyond viral proteins, the tegument layer also contains approximately 70 cellular proteins, as well as viral and cellular RNAs [30,31].

1.4 HCMV Life Cycle

The HCMV life cycle is a complex process involving various stages from viral attachment and entry into host cells to replication, assembly, and release of new virions [32].

1.4.1 Attachment and Viral Entry

During the viral entry process, HCMV achieves its tropism by employing cell receptor-mediated endocytosis, which is facilitated by virally encoded glycoproteins binding to specific cellular receptors. This entry mechanism can be delineated into three key stages. Initially, the virus adheres to the host cell's surface by binding to heparan sulfate glycosaminoglycans via the virion glycoprotein B (gB) in conjunction with the glycoprotein M/glycoprotein N complex [33]. Subsequently, there is an interaction with entry receptors located on the host cell membrane, including integrins and epidermal growth factor receptors (EGFRs), both of which bind to gB [34,35]. The third step involves either the internalization of the viral particle or the fusion of the viral envelope with the cell membrane, a process also mediated by gB. In addition to gB, this step may involve the trimeric complex comprised of glycoprotein H, glycoprotein L, and glycoprotein O (gH/gL/gO) in fibroblasts, likely due to interactions with platelet-derived growth factor-α

(PDGF-alpha). In epithelial and endothelial cells, it may alternatively entail the pentameric complex of glycoproteins gH/gL, in conjunction with UL128-131 [36,37].

1.4.2 Lytic Cycle

Viral tegument proteins that are bound to the capsid engage with the host microtubule machinery, leading to the transportation of viral capsids to the nuclear envelope and subsequently into the nucleus, where the viral DNA is released [38]. Within this context, two crucial players in nucleocapsid translocation, uncoating, and the release of the viral genome are the large tegument protein (product of UL48) and the large tegument protein binding protein (product of UL47) [39,40]. In the nucleus, the processes of viral transcription, genome replication, and encapsidation occur. Lytic replication is a regulated sequence of events, with immediate early genes (IE) being expressed first, followed by early (E) and late genes (L). The IE gene products function as transcription factors and expression regulators for the E and L genes. The E proteins primarily interact with host proteins while also impacting the transcriptional and replication machinery for viral proteins. The L proteins serve primarily as structural components of the virions, and they also encompass proteins crucial for the assembly and release of infectious particles [41–43]. In this intricate process, UL54 (the viral DNA polymerase) and UL70 (DNA primase) play pivotal roles in regulating the replication machinery and ensuring an efficient production of new virus progeny. Additionally, various viral-encoded proteins contribute to the regulation of cell signaling pathways and cellular metabolism, as well as the inhibition of initial steps in the immune response to support viral replication and immune evasion [44–48]. For instance, the viral US3 protein sequesters the major histocompatibility complex (MHC) class I within the endoplasmic reticulum (ER), while the US2 and US11 proteins induce the destruction of class I heavy chains, thereby impeding viral clearance by cytotoxic T lymphocytes (CTL) [49].

The nucleocapsid, containing DNA, assembles within the nucleus and exits into the cytoplasm by inducing changes in nuclear lamina components. This process is facilitated by two highly conserved viral proteins, specifically pUL50 and pUL53 [50]. The assembly and transportation of virions involve the integration of various cellular trafficking pathways such as the hijacking of the endoplasmic reticulum (ER), Golgi apparatus, and endosomal machinery, forming the cytoplasmic

viral assembly complex. It is within this complex that capsids acquire their tegument layer and viral envelope from intracellular vesicles [51]. Subsequently, infectious particles are released either by fusing with the plasma membrane or by causing cell lysis, releasing them into the extracellular space **(Figure *3*)** [52]. Beside mature virions, two types of defective particles are also released: dense bodies (DBs) and non-infectious enveloped particles (NIEPs) [53]. DBs are larger and denser than mature virions, ranging in size from approximately 250 to 600 nm in diameter; they contain most of the structural proteins but lack a viral genome, which is normally packed into the protective capsid. NIEPs are similar in size to virions but lack a viral genome [54]. The entire lytic replication cycle for HCMV takes approximately 72 hours before new mature virions are prepared to infect further cells, either through release from the infected cells or via cell-to-cell transmission mechanisms [55].

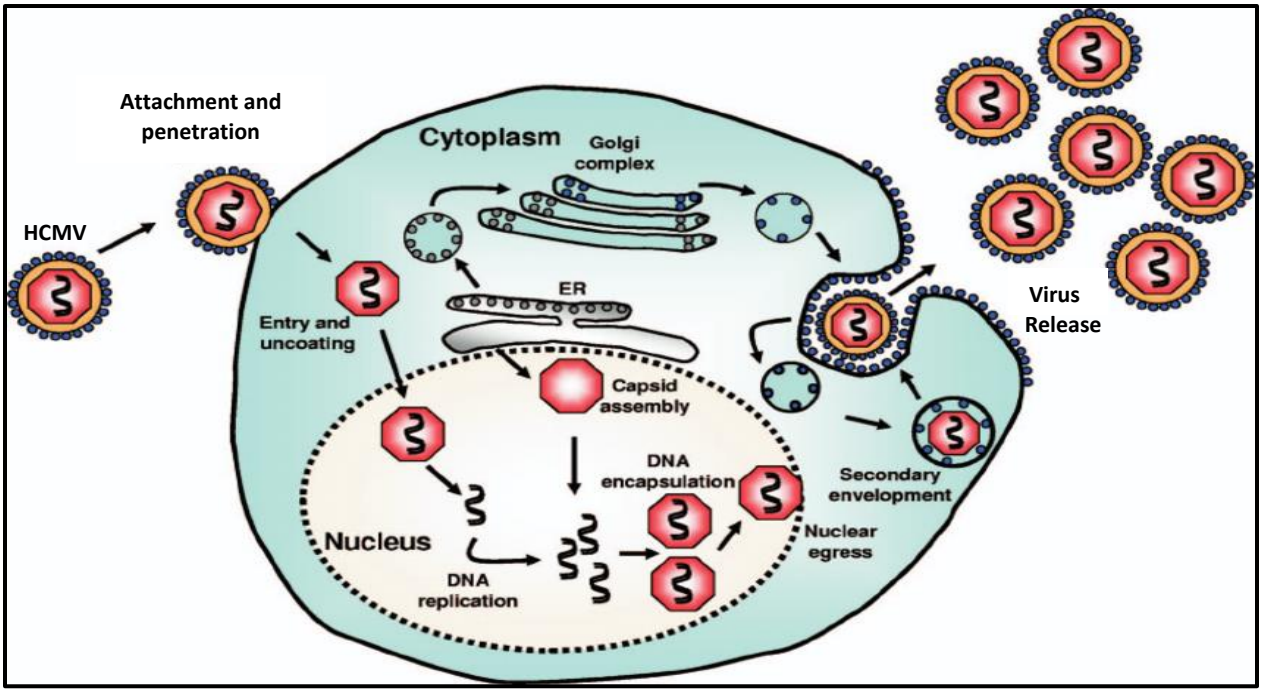

Figure 3: HCMV Life cycle.

The life cycle of HCMV involves a series of steps. Initially, HCMV gains entry into the host cell through the interaction of host receptors with specific viral glycoproteins. Following this, capsid and tegument proteins are liberated into the host cytosol. The capsid then releases the viral genome into the nucleus, initiating the expression of immediate early (IE) genes. These IE proteins, in turn, activate the expression of early (E) genes. Early proteins boost

viral genome replication and the expression of late (L) genes. The L gene expression leads to capsid assembly and the expression of tegument and glycoproteins. The genome loaded capsid exits the nucleus through nuclear egress and associates with the tegument proteins. Subsequently, the capsid acquires a viral envelope by budding into intracellular vesicles. Finally, these enveloped viral particles are released into the extracellular space, completing the HCMV life cycle. Figure has been adapted from Crough et al [17].

1.4.3 Latent Cycle

Latency in the context of HCMV infection refers to a dormant phase where the viral genome is retained without active virus replication or the release of infectious viral particles, occasionally interrupted by reactivation events [56]. Multiple latency reservoirs have been identified in the blood and bone marrow including mainly CD34+ hematopoietic progenitor cells and CD14+ monocytes. HCMV reactivation could be triggered by monocytes harboring latent viral genomes differentiating into macrophages or dendritic cells (DCs) [57,58]. During latency, only a limited set of genes are expressed, including genes from the UL133-UL138 locus, UL144, the latent unique nuclear antigen (LUNA), the US28 viral G-coupled receptor and chemokine receptor homologue, the latency-associated viral homolog of IL-10 (LAcmvIL-10) encoded by UL111A, a shorter variant of the UL123-encoded IE1 protein (IE1×4), a transcript associated with latency originating from a distant promoter within the MIE region, and long non-coding RNAs of 2.7 kb and 4.9 kb [59]. The establishment of HCMV latency is a complex process that involves epigenetic silencing of the viral genome through chromatin remodeling around the viral major immediate early promoter (MIEP) and the presence of latency-associated repressors. Histone methyltransferases (HMTs) and histone deacetylases (HDACs) play roles in maintaining latency [60–62]. Cellular defenses and controls, such as nuclear domain 10 (ND10) structures or promyelocytic leukemia protein (PML) nuclear bodies, also contribute to suppressing viral replication by modifying chromatin around the viral MIEP [63–65]. On the other hand, reactivation involves the transition to lytic replication [66]. Various factors can trigger this switch, including cellular differentiation, stress conditions, and certain drugs like histone deacetylase inhibitors; the latter have been shown to alleviate the repressive marks on chromatin, resulting in IE gene expression [67]. Reactivation of latent HCMV can have significant clinical consequences, ranging from severe inflammatory conditions in immunocompromised patients to complications like allograft rejection and graft-versus-host disease in transplant recipients [68,69].

1.5 HCMV Prevalence and Spread

HCMV is widely recognized as a ubiquitous virus, with seroprevalence rates ranging from 40% to 90% in the adult population [70]. HCMV infection is considered endemic and doesn't exhibit seasonal variations [71]. The prevalence of HCMV infection varies depending on geographic and socioeconomic factors. In developing regions, more than 90% of preschool children are found to have acquired HCMV during early childhood. In contrast, in industrialized countries, less than 20% of children are seropositive [72,73]. As individuals age, the percentage of seropositive individuals continues to rise, reaching levels between 40% and 70% [74].

The transmission of HCMV is influenced by a multitude of potential sources of exposure [75]. The primary route for acquiring HCMV is the direct contact with body fluids from an infected individual. These fluids encompass saliva, oropharyngeal secretions, urine, cervical and vaginal secretions, semen, breast milk, allografts, and blood products from donors who are seropositive [74]. Another means of contracting the virus is through perinatal or vertical transmission, where HCMV is transmitted through the placenta, a condition known as congenital infection. It's important to mention that infected infants typically excrete substantial amounts of the virus for months to years following infection, as do older children and adults following a primary HCMV infection [76].

1.6 Clinical Aspects of HCMV and HCMV-Related Diseases

HCMV infection is mostly asymptomatic yet it can result in a mild illness in immunocompetent individuals. Primary HCMV infection can occasionally lead to a mild syndrome resembling mononucleosis [77]. On the contrary, severe CMV disease occurs in individuals with immature, suppressed, or compromised immune systems, such as neonates, transplant recipients receiving immunosuppressive drugs, and patients with AIDS. This severe form of the disease can have life-threatening consequences or cause significant long-term complications [78]. These complications encompass a wide range of potential clinical manifestations due to the virus's ability to spread through the bloodstream and infect various tissues. This includes gastrointestinal issues, respiratory problems, hematological abnormalities, cardiovascular complications, neurological symptoms, and urological manifestations. Additionally, severe HCMV infection can indirectly

lead to atherosclerosis acceleration, graft rejection, and increased susceptibility to opportunistic infections [17]. In cases of congenital HCMV infection, approximately 90% of infected infants show no symptoms at birth, although about 5% of them may develop complications later in life [79]. Common initial symptoms include jaundice, petechiae, and hepatosplenomegaly [80]. Major long-term complications of congenital HCMV infection encompass prematurity, restricted intrauterine growth, hypotonia, poor feeding, cerebral ventriculomegaly, microcephaly, intracranial periventricular calcifications, sensorineural hearing loss, and, in 10 to 20% of affected infants, chorioretinitis and mental retardation [81,82].

1.7 HCMV Detection and Diagnosis

Numerous diagnostic approaches are accessible for detecting HCMV infection, primarily encompassing serological testing, virus culture, identification of viral antigens, and CMV DNA detection through polymerase chain reaction (PCR) [83].

1.7.1 Serology

This method relies on assessing the levels of IgM and IgG antibodies in the serum or plasma of patients. The enzyme-linked immunosorbent assay (ELISA) is the most commonly employed technique. The presence or absence of CMV IgG serves as a marker to identify whether the individual has previously experienced a CMV infection. Meanwhile, the detection of IgM antibodies has been employed as an indicator of a recent, acute infection, or viral reactivation [81,84]. Furthermore, by determining the avidity of IgG antibodies, it will be possible to differentiate between an early primary infection (low avidity) and a latter infection (high avidity) during pregnancy [85].

1.7.2 Virus Culture

The conventional method for detecting HCMV is through traditional cell culture. In this approach, clinical samples are introduced to human fibroblast cells (MRC5 cells), and their development is observed over a period ranging from 2 to 21 days. The presence of cytopathic effects (CPE), characterized by clusters of flattened and swollen cells, is then directly correlated with the virus's titer. However, the limitation of this method is the extended time required, with results often taking 2 to 3 weeks. To expedite this process, an alternative approach involves the detection of viral

antigens using monoclonal antibodies directed against CMV immediate-early viral antigens via indirect immunofluorescence after a 16-hour incubation period [86,87].

1.7.3 Identification of Viral Antigens

This assay relies on the detection of the viral pp65 antigen within blood specimens, specifically within leukocytes, as this antigen is expressed in these cells during the early stages of the HCMV replication cycle [88]. An immunofluorescence assay that identifies pp65 in a sample of peripheral blood leukocytes not only allows for the quantification of positive leukocyte nuclei but also closely correlates with viremia and the severity of clinical disease in immunosuppressed populations [89]. However, a significant limitation of this technique is its lack of automation, requiring skilled individuals for accurate test execution and result interpretation. Furthermore, results should be assessed within a 6-hour window, as delays in processing can significantly reduce the assay's sensitivity, potentially leading to false-negative results, especially in patients with neutropenia [90,91].

1.7.4 PCR Amplification

PCR is a widely accessible, rapid, sensitive and specific method for detecting HCMV in various types of samples, including blood, leukocytes, plasma, tissue biopsy specimens, and fluids for instance urine, bronchoalveolar lavage, or cerebrospinal fluid [92]. PCR for HCMV DNA can be conducted in either a qualitative or quantitative manner (Real-Time PCR), enabling continuous monitoring of immunocompromised individuals to identify those at risk for HCMV-related diseases, implement preemptive therapy, and assess treatment response [93]. Additionally, the detection of viral mRNA transcripts in peripheral blood leukocytes can be accomplished through reverse transcriptase PCR (RT-PCR) during active HCMV infection. However, it's worth noting that this method is less sensitive than the pp65 antigen test and PCR in diagnosing HCMV-related diseases [94].

1.8 Therapeutic Approaches for HCMV Infection

Effective management of HCMV infection is particularly important for immunocompromised individuals, such as transplant recipients and people with HIV/AIDS, as well as newborns infected with HCMV [95]. Below are the approved therapies for HCMV, their mechanism of action, and

their associated benefits and potential adverse effects in addition to the ongoing research and emerging therapies that hold promise for improving the therapeutic strategies against HCMV infection, offering better patient outcomes [96].

1.8.1 HCMV Antivirals

Most of the current FDA-approved drugs for treatment of HCMV, including ganciclovir, valganciclovir, foscarnet, cidofovir, letermovir, and Maribavir target late stages of the virus life cycle including viral replication and DNA packaging with varying efficacy and dose-related cytotoxicity [97].

1.8.1.1 Ganciclovir (GCV) is a nucleoside analogue commonly used to treat HCMV infections, especially in immunocompromised individuals [98]. GCV and its valine ester derivative, valganciclovir (VGCV), are primary treatments for CMV disease. GCV is phosphorylated by the HCMV kinase pUL97 to create ganciclovir monophosphate, which accumulates in infected cells, inhibiting viral DNA replication. While GCV can add one more base to the DNA chain, it triggers nucleotide removal downstream, preventing further elongation. GCV selectively targets infected cells due to its activation by a viral kinase and superior inhibition of viral DNA polymerase over cellular DNA polymerase. Resistance usually arises from UL97 and UL54 mutations. VGCV improves GCV absorption but can lead to adverse effects like neutropenia and nephrotoxicity. VGCV has received approval for use in both the initiation and maintenance treatment of AIDS-related HCMV retinitis. It is also administered for the prevention of HCMV infection and related complications in individuals who have undergone kidney, pancreas, or heart transplantation [99,100].

1.8.1.2 In case of GCV resistance, Foscarnet (FOS), a pyrophosphate analogue, can be used for the treatment of HCMV infections. FOS represents the second medication authorized for addressing HCMV retinitis in AIDS patients. It acts by inhibiting viral DNA polymerase. Unlike some other drugs, FOS doesn't rely on viral kinase-mediated intracellular phosphorylation to exert its antiviral effects, nor does it become incorporated into the developing viral DNA chain. This unique feature positions it as the preferred rescue therapy for patients encountering treatment challenges due to GCV-resistant HCMV strains or those experiencing GCV-induced neutropenia

or leucopenia. However, FOS does come with potential adverse effects including nephrotoxicity as well as hypocalcemia, hypomagnesemia, and hypokalemia, which could be associated with seizures [101,102].

1.8.1.3 Cidofovir (CDV) is a second-line treatments for GCV and FOS-resistant cases. CDV is classified as an acyclic nucleoside phosphonate analogue. Its primary indication is for treating HCMV retinitis in AIDS patients. It is formulated for intravenous use because of its limited oral bioavailability. Additionally, CDV is recognized for its extended intracellular half-life, enabling less frequent drug administration. This characteristic can be advantageous for patients who may have difficulty adhering to daily intravenous dosing schedules. However, CDV is nephrotoxic and causes neutropenia, metabolic acidosis and ocular hypotony [96,103].

1.8.1.4 Letermovir is effective in preventing or treating HCMV infections in recipients of hematopoietic stem cells, thoracic organs, and lung transplants. It offers several advantages over traditional antiviral drugs. Notably, it has a low level of toxicity and excellent oral bioavailability, preventing the urge for hospitalization or intravenous administration. Moreover, letermovir operates by targeting the viral terminase complex and interfering with the viral UL56 gene product, instead of DNA polymerase. This unique mechanism of action reduces the risk of cross-resistance with anti-CMV medications [104,105].

1.8.1.5 Maribavir was being studied for the treatment of resistant or refractory HCMV infections in transplant recipients. It has shown encouraging outcomes in clinical trials. This medication functions by competing with ATP to attach itself to the viral kinase pUL97. Interestingly, Maribavir retains its effectiveness against certain HCMV strains that have developed resistance to GCV, despite the fact that most GCV-resistant strains possess mutations in the UL97 gene. It's important to emphasize that Maribavir cannot be employed concurrently with GCV treatment, as it would impede the initial phosphorylation and activation process of GCV. MBV showed reduced haematotoxicity and nephrotoxicity compared to GCV and VGCV [106,107].

1.8.2 Immunotherapy

With the advancement of immunotherapy, a growing cohort of scientists has been exploring its application in the context of HCMV infection.

1.8.2.1 Vaccines

Vaccination against HCMV infection remains high priority. In recent years, there has been significant interest among pharmaceutical researchers in developing an effective and safe HCMV vaccine, as immunity can lessen the severity of the disease. Researchers have explored various types of HCMV vaccines, including live vaccines (such as live-attenuated and chimeric viral vaccines) and non-living vaccines (including subunit, RNA-based, virus-like particle, and plasmid-based DNA vaccines) [108,109]. While clinical trials have yielded promising data, it's important to note that an approved HCMV vaccine has not yet been authorized for use. Designing a vaccine for HCMV presents unique challenges. First, the virus can establish lifelong latency in the host after a subclinical primary infection and can spread from cell to cell, evading antibodies in extracellular fluids. Additionally, HCMV can reactivate when the host's immune defenses are weakened. Another obstacle is the diversity of HCMV strains, as the virus frequently undergoes recombination with disruptive mutations identified in clinical isolates, even exhibiting rapid evolution within the host [110]. In summary, the development of an effective HCMV vaccine has been hindered by these complex challenges, despite the pressing need for such a vaccine.

1.8.2.2 Antibody Therapy

The FDA has granted approval for passive immunization using HCMV immunoglobulin as a prophylactic measure. This is typically administered alongside GCV, especially in high-risk recipients of lung and cardiothoracic transplants. It is also considered in cases of GCV resistance or poor tolerance. However, when it comes to congenital HCMV, passive immunization with HCMV immunoglobulin has not shown significant reductions in congenital HCMV disease [111]. Therefore, it is not recommended for use in pregnant women with primary HCMV infection.

1.8.2.3 Adoptive Cell Therapy (ACT)

T cells isolated from healthy donors who have previously been exposed to HCMV can be expanded in vitro and transferred to immunocompromised patients. These "donor-derived" T cells can help control HCMV reactivation. ACT is now being used as a treatment approach for HCMV reactivation in patients who have undergone allogeneic hematopoietic stem cell transplantation (HSCT) and solid organ transplantation (SOT). Research has demonstrated that autologous

HCMV-specific T cells can directly eliminate primary glioblastoma (GBM) cells. Some researchers have even devised an innovative adoptive immunotherapy approach targeting CMV antigens for patients with recurrent GBM. Experimental results from this approach have shown it to be both safe and linked to extended progression-free survival in 4 out of 10 patients [112].

1.8.2.4 Checkpoint Blockade Therapy

Research has shown that the use of immune checkpoint inhibitors (ICIs) can potentially revive immune function and elicit an immune response to CMV antigens even when in a latent state. One promising approach involves a vector called pS-CIFT-aPD-1, which is designed to express the gene for an antibody targeting the programmed cell death protein 1 (anti-PD-1) [112].

1.8.2.5 Novel US28-targeting Strategies

In search of innovative treatments against HCMV infection, a recent approach has emerged focusing on the role of the surface protein US28, which plays a crucial part during both lytic and latent infections. The methods for therapeutically targeting US28 can be broadly categorized into three distinct categories: small molecules, single-domain antibodies (referred to as nanobodies), and fusion toxin proteins (FTPs) [112,113].

Chapter 2

2. HCMV-Induced Polyploid Giant Cancer Cells and Their Significance in Tumorigenesis

2.1 Morphological Characteristics of PGCCs

Polyploid giant cancer cells (PGCCs) are characterized as either gigantic mononuclear cells with multiple genome copies or multinuclear cells [114]. According to the definition by Zhang et al., a PGCC is delineated as a cell three times larger than a typical diploid cancer cell. However, the size of a PGCC can vary significantly depending on the DNA content and the number of nuclei within the cells, sometimes reaching dimensions that are 10 to 20 times larger than a regular diploid cell [115]. PGCCs have a slow cell cycle and divide through asymmetric cell division patterns, which include budding and bursting. Budding is characterized by the release of numerous small daughter cells resembling the growth and division mechanisms seen in simpler organisms like yeasts. Additionally, dormant PGCCs are associated with the induction of quiescence and increased storage capacity through the presence of vacuoles and accumulation of lipid droplets, increased metabolic capacity, and elevated energy production [116–118].

2.2 PGCCs Stimuli and Mechanisms of Generation

PGCCs frequently emerge as a result of various stressors, such as exposure to chemotherapy, ionizing radiation, conditions of hypoxia, viruses, and other stimuli that lead to DNA double-strand breaks **(Figure 4)**. CoCl2 serves as a mimic for hypoxia-induced cellular responses in vitro and activates signaling pathways associated with hypoxia. CoCl2 plays a role in stabilizing hypoxia-inducible factor (HIF)-1α by inhibiting proline hydroxylase. Additionally, chemotherapy drugs like capecitabine, oxaliplatin, and irinotecan, as well as radiation therapy, can induce PGCCs formation. Tumor tissues rich in PGCCs are associated with higher risks of recurrence, metastasis, chemoresistance, and poor prognosis [119,120].

The generation of PGCCs involves a complex interplay of cellular processes and signaling pathways. The giant cell cycle, which leads to the formation of PGCCs, differs from the regular cell cycle in certain aspects. While the exact mechanisms can vary between different types of cancer, here are some general insights into how PGCCs are generated and the characteristics of

the giant cell cycle **(Figure 5)**. PGCCs formation can occur through various mechanisms, including endoreplication, mitotic slippage, cytokinesis failure, cell fusion, or cell cannibalism with the former being the predominant mechanism. While studies have documented the occurrence of PGCCs resulting from cell fusion in Hodgkin's lymphoma and glioblastoma cell lines, it's worth noting that, in MDA-MB-231 and ovarian cancer cells, cell fusion contributes to only a modest fraction, ranging from 10% to 20%, of all PGCCs [119,121].

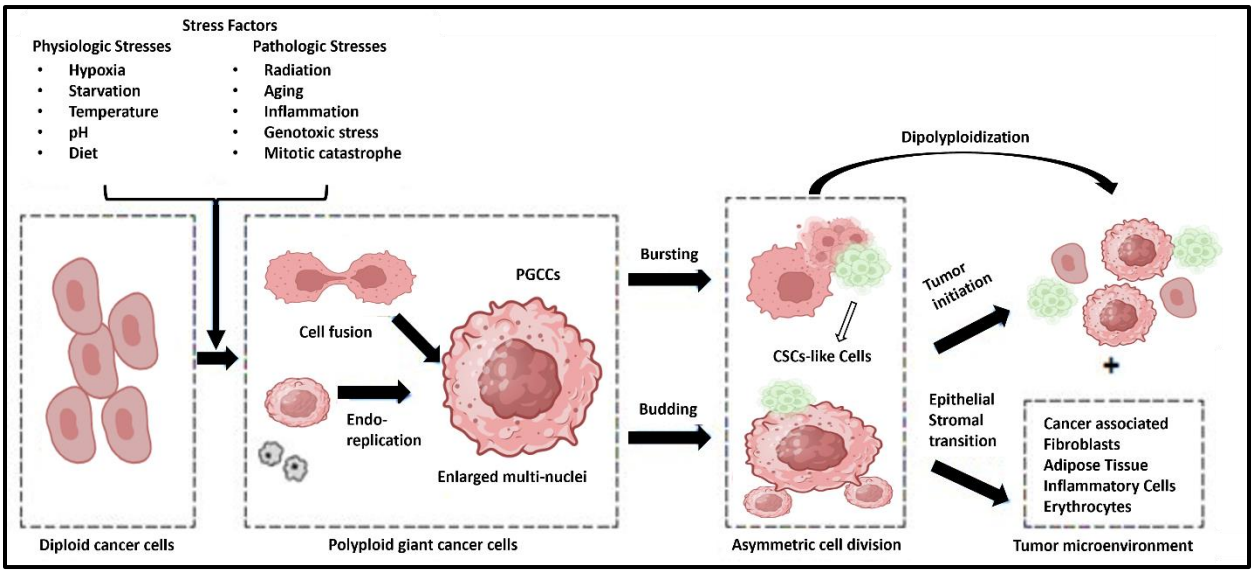

Figure 4: Scheme illustrating PGCCs formation mechanisms.

PGCCs formed through endoreplication and cell fusion have developed the capacity to undergo division using mechanisms similar to those seen in single-celled organisms, such as budding and viral-like amitotic division, which leads to the production of tumor-initiating cells. Adapted from Chen et al. [120].

2.3 Characteristics of PGCCs and Potential Biomarkers

PGCCs exhibit a unique combination of markers, encompassing both normal and cancer stem cell (CSC) indicators [115,119]. These markers include OCT4, NANOG, SOX2, CD44, and CD133. Notably, the daughter cells originating from PGCCs also display characteristics similar to stem cells and continue to express CSC markers, specifically the surface glycoproteins CD44 and

CD133. PGCCs maintain a highly dedifferentiated state, reminiscent of embryonic cells, and possess more pluripotency compared to typical CSCs. Furthermore, these PGCC progeny share similarities with blastomeres observed during embryonic development, possessing the capability to differentiate into various cell types representing the three germ layers: ectoderm, mesoderm, and endoderm, as demonstrated in vitro. Their expression profile includes spatiotemporal markers associated with embryonic development and self-renewal, such as NANOG, OCT3, OCT4, aldehyde dehydrogenase-1A (ALDH1A), and SOX-2. These daughter cells exhibit the potential to differentiate into diverse benign cell types, such as adipocytes, chondrocytes, erythrocytes, and osteocytes, or give rise to carcinomas with differing grades [119]. In a study by Zhang and colleagues, PGCCs progeny derived from the MCF-7 cell line were observed to differentiate into benign stromal cells, including myoepithelial, endothelial, and erythroid cells. Considering the role of the tumor stroma in modulating drug bioavailability and enzymatic degradation, PGCCs can exert a significant influence on promoting resistance to various anticancer therapies [115]. Further, PGCCs and their progeny often undergo epithelial-mesenchymal transition (EMT). EMT involves significant cytoskeletal transformations that lead to alterations in cell adhesion and morphology, playing a critical role in the metastatic dissemination of cancer cells. PGCCs, along with their progeny, have been observed to exhibit distinct expression patterns, characterized by elevated levels of mesenchymal markers like vimentin, fibronectin, and N-cadherin, accompanied by reduced levels of epithelial markers such as cytokeratin and E-cadherin. This pattern mirrors the connection often seen in cancer cells, where EMT and the acquisition of stem cell-like features are closely intertwined. Likewise, in PGCC progeny cells, there is a notable association between the expression of EMT markers and stemness markers. This association is exemplified by the induction of EMT in human mammary epithelial cells triggered by transforming growth factor-β (TGF-β), which also facilitates the generation of cells exhibiting stem cell-like properties, such as CD44 expression and self-renewal capacity [119,122].

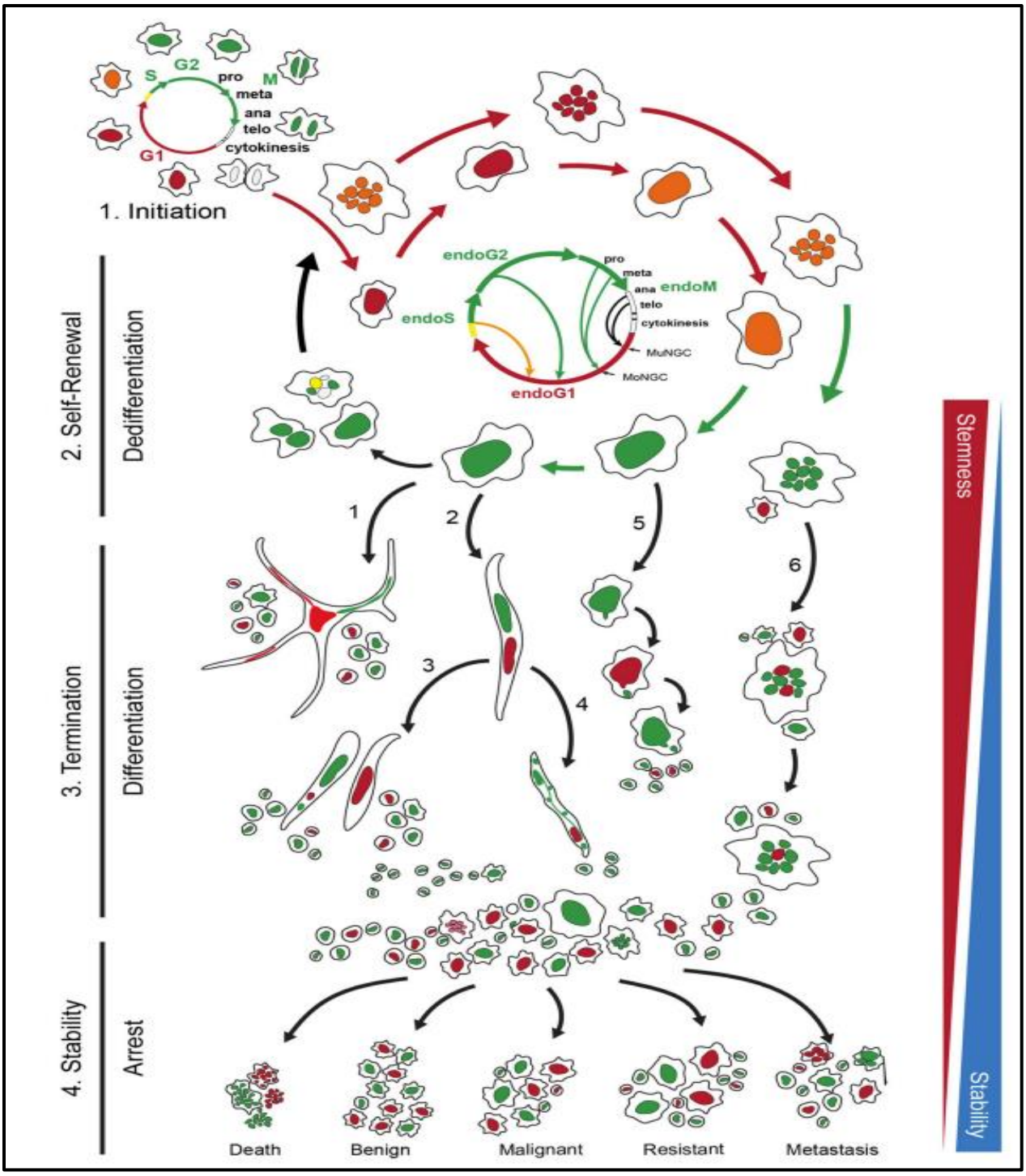

Figure 5: A scheme illustrating the giant cell cycle.

The giant cell cycle closely mimics the division of blastomeres. Upon initiation by either intrinsic genetic factors or external stresses, a somatic cell enters a phase of self-renewal endoreplication and initiates dedifferentiation or

reprogramming. Subsequently, the reprogrammed cell enters a termination phase to start differentiation. During this phase, giant cells employ multiple primitive cell division mechanisms to generate diploid daughter cells. These include (1) horizontal genetic transfer, where DNA migrates horizontally into adjacent cells through cytoplasmic extensions followed by budding, (2) the formation of elongated cells with two giant nuclei, as well as (3) splitting in the middle of the giant cell or (4) direct budding from both (5) mononucleated and (6) multinucleated giant cells. In the stability phase, differentiated cells gradually organize themselves out of chaos, reaching a specific developmental level. Dominant clones emerge from this chaos, resulting in the formation of a visible tumor which can behave as benign, malignant, resistant, metastasis or death. Cells that immediately bud off from the giant cells exhibit a high level of stemness, symbolized by a red triangle, and progressively attain stability during the process of differentiation, represented by a blue triangle. Adapted from Liu et al [122].

2.4 Potential Involvement of PGCCs in Cancer Progression

Accumulating evidence underscores the significance of genome duplication, or polyploidization, as a fundamental genetic trait in cancer [114,118,121]. Recently, polyploidy was found to be present in approximately 37% of human tumors [123,124]. Polyploidization is recognized for its role in promoting chromosomal instability, primarily through the frequent missegregation of chromosomes during cell proliferation, and by creating conditions conducive to aneuploidy [123]. This, in turn, fosters cancer evolution by introducing genetic diversity. PGCCs have been described in a broad spectrum of high-grade and chemoresistant tumors, as well as in various cancer cell lines [114,119]. These encompass breast and colorectal cancer, glioma, lung, prostate, ovarian, cervical, lymphoma, nasopharyngeal, pancreatic carcinoma, neuroblastoma, renal, thyroid, bowel sarcoma, and melanoma [114,125,126]. It's worth noting that the presence of PGCCs has been preferentially reported in poor prognosis cancers participating in tumor relapse and therapy resistance. PGCCs play a role in contributing to the heterogeneity of tumors **(Figure 6)** and have been identified in well-established cancer cell lines, including MDA-MB231, MCF-7, U87MG, SKOV-3, HeLa, A549, PC-3, SW620, and HCT-116 cell lines [119]. Thus, discovering distinctive traits that symbolize polyploid tumors has the potential to enhance the clinical management and classification of tumors based on their ploidy status.

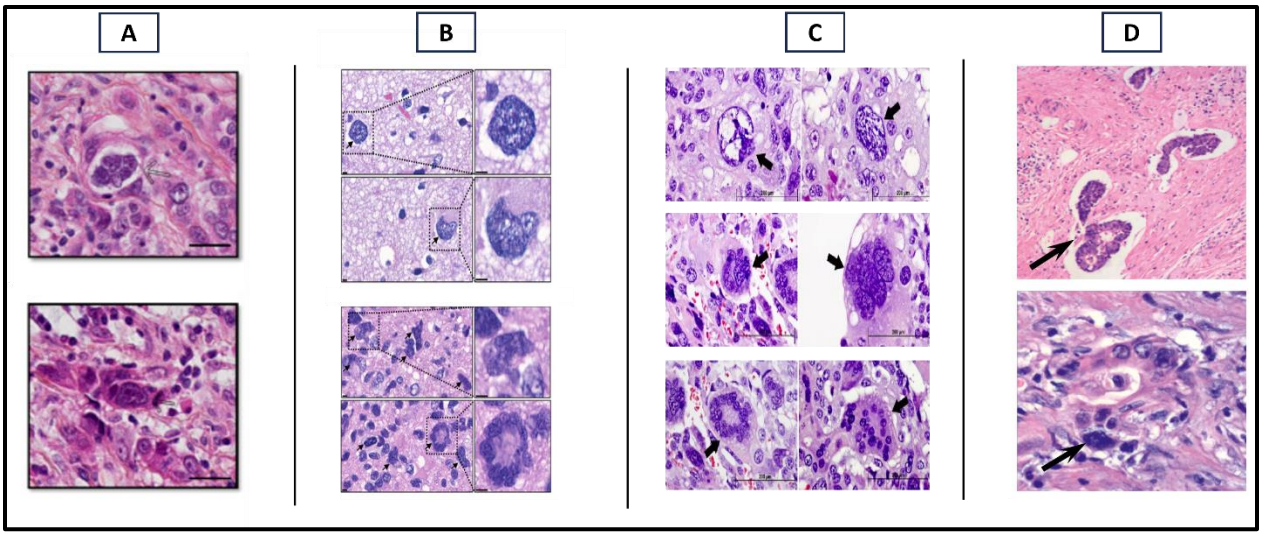

Figure 6: Generation of PGCCS in various cancer types.

Representative images of PGCCs in (A) breast cancer tissues, (B) WHO grade II gliomas where the black arrow points a single PGCC, and the black frame shows a PGCC with single giant-nucleus as well as in WHO grade IV gliomas where the black arrow points a single PGCC, and the lower black frame shows a PGCC with multi-nucleus, (C) high grade ovarian serous carcinoma, and (D) colorectal cancers. Adapted and modified from several studies considering the link between PGCCs and cancer [120,126–128].

2.5 PGCCs and Oncoviruses

Since its inception, the field of viral oncogenesis has yielded groundbreaking insights into the origins of human cancer, illuminating the intricate molecular mechanisms and multifaceted interactions between the host and oncogenic viruses. Approximately 15 to 20% of human cancers worldwide can be attributed to infections caused by oncoviruses. These oncoviruses include human papillomaviruses (HPV), Epstein-Barr virus (EBV), hepatitis B and C viruses (HBV, HCV, respectively), human T-cell lymphotropic virus-1 (HTLV-1), Kaposi's sarcoma herpesvirus (KSHV), and Merkle Polyomavirus (MCPyV) **(Table *1*)** [127]. Although significant advancements have expanded our understanding of how these pathogens designate cellular machinery to establish infection and initiate common pathways leading to tumorigenesis, as well as to replicate and maintain persistence, the development of targeted therapies and definitive curative clinical treatments remains a formidable challenge. This challenge primarily stems from the limitations of equivalent animal models and the mysterious nature of certain mechanistic

aspects involved in cancer induction by these agents, given their diverse characteristics. Nonetheless, polyploidy emerges as a pivotal common trait shared among oncoviruses, where distinct viral proteins can act as catalysts for the induction of polyploidy. Polyploidy is increasingly recognized as an initial trigger for cellular transformation within this context [128–130].

2.5.1 HPV

HPV, a small double-stranded circular DNA virus belonging to the Papillomaviridae family, encompasses more than 200 identified types categorized by tissue tropism (skin or mucosa) and malignant transformation potential (high risk and low risk). Low-risk (LR) HPVs cause benign warts, while high-risk (HR) HPVs are associated with high-grade cervical lesions and cancers, particularly HPV-16 and -18 [131,132]. The oncogenic potential of HR-HPVs is primarily attributed to the HPV-E6 and -E7 proteins [133]. Polyploidy is commonly observed in the context of HPV infection, particularly in cervical carcinogenesis. Tetraploidy is an early event, and tetrasomy is detected in cervical squamous intraepithelial lesions caused by HR-HPVs [134,135]. Additionally, polyploidy is linked to high-grade squamous intraepithelial lesions (HGSIL) [136,137]. The expression of E6 and E7 oncoproteins is associated with a higher proportion of cells with >4N DNA content [138]. The mechanisms behind HPV-induced polyploidy are diverse. E6 and E7 can induce abnormal centrosome duplication and erroneous mitotic spindle pole formation, decoupling centrosome duplication from cell cycle division and causing genomic instability [139]. Furthermore, E6 disrupts the mitotic checkpoint by interfering with p53-mediated functions, while E7 overcomes the mitotic checkpoint through a p53-independent mechanism, possibly by modulating Rb function [140]. Further, E6 and E7 downregulate nuclear p21 localization and upregulate cyclin-dependent kinase 1 (CDK1) upon microtubule disruption, contributing to postmitotic checkpoint abrogation-induced polyploidy [141]. This effect is also observed with E7 through its role in Rb downregulation [142]. Simultaneous expression of E6 and E7 induces polyploidy by disrupting the spindle checkpoint and upregulating G2-M proteins. Endoreplication, characterized by multiple S phases without mitosis, is associated with HPV-16 E5 and E6 oncoproteins, leading to enlarged nuclei and increased cellular DNA content [143,144]. Multinucleated cells with enlarged nuclei result from two consecutive S phases without cytokinesis upon HPV-18 E7 transduction [145]. Re-replication is induced by HPV-16 E7 in response to DNA

damage, mediated by the DNA replication initiation factor [146,147]. E6 and E7 enhance HIF protein accumulation and activity in human cervical cancers [148]. In summary, HPV oncoproteins, particularly E6 and E7, employ various mechanisms to induce polyploidy, contributing to cervical carcinogenesis. These mechanisms encompass centrosome abnormalities, mitotic checkpoint abrogation, endoreplication, multinucleation, and re-replication, with downstream effects on genomic stability and cellular transformation. Additionally, HPV infection is associated with increased HIF activity in cervical cancers.

2.5.2 EBV

EBV, a member of the Herpesviridae family within the Gammaherpesvirinae subfamily, is a linear, double-stranded DNA virus [149]. It is the first isolated tumor virus and primarily infects B lymphocytes [150]. EBV is associated with a variety of malignancies, including lymphomas such as Hodgkin's lymphoma, diffuse large B-cell lymphoma, and Burkitt's lymphoma, as well as carcinomas like gastric and nasopharyngeal carcinoma (NPC) [150]. Several viral latent antigens, including Epstein–Barr virus nuclear antigen 1 (EBNA1), EBNA2, EBNA3, and the latent membrane protein 1 (LMP1), play essential roles in B-cell transformation [151]. In tissue biopsies of NPC, polynuclear giant cancer cells are observed, often surrounded by small nucleus-containing bodies indicative of budding cells [152]. Multinucleated giant cells are also formed following EBV replication in epithelial NPC hybrid cells [153]. EBV-infected nasal mucosal neoplasms display cells with increased volume and pronounced multinucleation, some containing over 12 nuclei [154]. Chromosomal integration of the viral genome into primary human B cells has been linked to polyploidy [155]. Infection of B cells with an EBV strain isolated from nasopharyngeal carcinoma predisposes them to polyploidy, with cells exhibiting multiple micronuclei or a single large polyploid nucleus [156]. Multinucleation and micronucleus formation have been detected in human laryngeal carcinoma Hep-2 and osteosarcoma U-2 OS cells following EBNA2 expression [157]. Stable expression of LMP1 in Burkitt's lymphoma cell lines is associated with multinuclearity, indicating a close correlation between polyploidy and EBV infection or the expression of EBV-latent oncoproteins [158]. Additionally, EBV latent genes compromise the mitotic spindle assembly checkpoint, preventing metaphase arrest [159]. Cell cycle progression without cytokinesis, G1 checkpoint disruption, and spindle assembly checkpoint disruption can

lead to polyploidy upon EBNA3C or EBNA2 expression [157]. Expression of EBNA2 or LMP1 triggers cell re-entry into S phase. EBNA-1, EBNA-3, and EBNA-5 expression enhances the synthesis, transcription, and stability of HIF-1α, respectively [160,161]. In terms of telomere dysfunction, LMP1 expression is associated with an increase in telomeric aggregates, a decrease in total telomere number, an increase in multinucleated cells, and an increase in nuclear volume. In brief, EBV infection and the expression of EBV-latent oncoproteins are closely linked to polyploidy, which can occur through various mechanisms, including disruption of cell cycle checkpoints, centrosome abnormalities, and telomere dysfunction [162,163]. These interactions contribute to the oncogenic potential of EBV in various malignancies.

2.5.3 KSHV

Kaposi's sarcoma-associated herpesvirus (KSHV), also known as human herpesvirus 8 (HHV-8), is a double-stranded DNA gamma-herpesvirus capable of infecting various cell types, including monocytes, dendritic cells, keratinocytes, B lymphocytes, oral epithelial cells, and endothelial cells [164]. It exists in both lytic and latent forms and is responsible for several malignancies, including Kaposi sarcoma (KS), primary effusion lymphoma, multicentric Castleman disease, and plasmablastic lymphoma [165]. KSHV encodes several viral oncogenes, such as latency-associated nuclear antigen (LANA), K cyclin, and viral FLICE-inhibitory protein (vFLIP), which play roles in inactivating tumor suppressor pathways, promoting cell cycle progression and DNA replication, as well as activating nuclear factor kappa B (NFκB) to support cell survival [166,167]. In terms of polyploidy, KSHV infection induces a multinucleation state characterized by enlarged and irregularly shaped nuclei in various cell types [168]. Constitutive expression of LANA in different cell lines results in a dramatic increase in the multinucleated phenotype, characterized by cells with two or more polarized nuclei. K cyclin expression leads to cells with enlarged nuclei and multiple large multi-lobular nuclei, highlighting a strong association between KSHV and polyploidy. Several mechanisms contribute to KSHV-induced polyploidy. KSHV can induce abnormal centrosome duplication and multipolar or monopolar spindle formation, mediated by LANA and K cyclin proteins. Aurora kinase B cleavage by serine protease-N terminus in KSHV-latently infected tumor cells promotes the transition from metaphase to telophase, enhancing mitotic progress and tumorigenesis. LANA induces S-phase entry and multinucleation by

protecting cells from cell cycle arrest; it also interacts with the spindle checkpoint protein Bub1, leading to Bub1 ubiquitination and degradation, favoring multinucleation. K cyclin expression results in DNA replication and cell nuclei division without simultaneous cell division [169,170]. Hypoxia, a condition of reduced oxygen availability, is linked to KSHV-induced polyploidy. KSHV viral interferon regulatory factor 3 (vIRF-3) interacts with and enhances the activity of HIF-1α, leading to increased angiogenesis through vascular endothelial growth factor (VEGF) activation [171]. Regarding senescence, viral v-cyclin protein induces senescence during latent infection by disrupting the cell cycle and activating the DNA damage response. However, viral FLICE inhibitory protein (v-FLIP) can bypass senescence, allowing the growth and division of latently infected cell populations, which may include a subpopulation of polyploid cells [172]. In summary, KSHV is associated with polyploidy through various mechanisms, including centrosome abnormalities, spindle checkpoint disruption, cell cycle deregulation, and interactions with cellular proteins involved in mitosis and senescence. These mechanisms contribute to the complex interplay between KSHV infection and the development of malignancies.

2.5.4 HTLV-1

Human T-cell lymphotropic virus type 1 (HTLV-1), the first human retrovirus discovered, belongs to the Retroviridae family. While it can infect various human cell types in vitro, HTLV-1 primarily undergoes productive replication within CD4+ T helper cells. HTLV-1 is the causative agent of adult T-cell leukemia/lymphoma (ATL), a highly aggressive non-Hodgkin's peripheral T-cell malignancy. The viral oncoprotein Tax plays a central role in the development of ATL. Tax activates genes that prevent cell death and disrupts the normal cell cycle, leading to DNA damage. This results in the clonal expansion of T cells harboring the HTLV-1 provirus, eventually leading to cellular immortalization and malignant transformation. HTLV-1 infection can lead to the formation of large lymphoma cells, especially in the presence of Tax [173,174]. Specifically, HTLV-1-induced multinucleated giant cells, characterized by giant lobulated nuclei or enlarged nuclei, have been observed in mammalian cells with elevated Tax expression [175–178]. HeLa cells expressing Tax also displayed larger cell sizes and DNA content greater than that of cells lacking Tax expression [179]. HTLV-1-infected CD4+ cell clones exhibited enlarged, well-separated nuclei in binucleated and multinucleated cells, and this morphological feature correlated

with Tax expression levels [180]. Thus, HTLV-1 plays a significant role in inducing polyploidy, leading to the formation of multinucleated cells and contributing to the pathogenesis of ATL. This occurs through various mechanisms involving disruption of the mitotic checkpoint, alteration of cell cycle regulation, and enhanced HIF-1α expression.

2.5.5 HBV

Hepatitis B virus (HBV), as the prototype member of the Hepadnaviridae family, is an enveloped virus with partly double-stranded DNA. It shares some characteristics with retroviruses, involving the use of reverse transcriptase during its replication cycle [181]. HBV is primarily a hepatotropic virus, with hepatocytes being its major target and the confirmed site for HBV replication. Infection and replication of HBV in the liver can lead to various complications, ranging from acute hepatitis to severe conditions like liver failure and hepatocellular carcinoma (HCC) [182]. In terms of oncogenic proteins, the hepatitis B virus X protein (HBx or pX) plays a significant role in promoting the progression of the cell cycle, inhibits the expression of tumor suppressor genes, including p53, and affects the transcription of methyltransferases [183]. It has been shown that HBx hinders the suppression of E2F1 activity, which is a key promoter of cell cycle progression, through the deactivation of the Rb gene promoter and consequently the tumor suppressor Rb. Furthermore, HBx augments CDK2 activity, resulting in a disruption of the balance between E2F1 and Rb [184]. These functions suggest its potential involvement in the pathogenesis of HCC and cellular transformation [183]. Another oncogenic factor is the HBV large surface protein (LHBs), which exhibits properties that may contribute to hepatocarcinogenesis [185]. Polyploidy, mainly endoreduplication and hyperploidy, have been exclusively identified in peripheral blood cells of individuals with chronic HBV infection when compared to HBV-negative individuals. Nuclear ploidy is positively correlated with poor prognosis and HBV infection [186,187]. Notably, DNA polyploidy is significantly increased in the liver tissues of HCC patients with a history of HBV infection [188]. This observation is consistent with cellular models where HBV-positive hepatoma cell lines exhibit higher levels of hyperploidy than HBV-negative cells [189]. Mechanistically, the expression of HBV pX can lead to the depletion of p53, suggesting an antagonistic relationship between p53 and pX-induced polyploidy [190]. Moreover, both LHBs and pX protein contribute to the override of the G2/M checkpoint. This results in the attenuation of the DNA damage

checkpoint and inhibition of p53-mediated apoptosis. Furthermore, cells expressing HBV LHBs experience cytokinesis failure compared to controls [189]. In HBV pX-induced polyploid cells, DNA re-replication occurs alongside aberrant mitotic spindle formation [191]. This DNA re-replication is associated with the upregulation of Cdt1 and Cdc6, which are essential for pre-replicative complex assembly [190]. Lastly, HBx interferes with the degradation of HIF-1α protein and enhances its synthesis [192,193]. Hence, HBV, especially through the actions of HBx and LHBs, is strongly linked to the induction of polyploidy, which can contribute to hepatocellular carcinoma development. This occurs through mechanisms involving the disruption of cell cycle checkpoints, cytokinesis failure, DNA re-replication, and interference with HIF-1α regulation.

2.5.6 HCV

Hepatitis C virus (HCV), a member of the Flaviviridae family, is a small, hepatotropic virus with a single-stranded RNA genome that is enveloped and replicates in the cytoplasm. Various cell types, including dendritic cells, epithelial cells, lymph nodes, and others, can support HCV replication [195]. Similar to HBV, HCV infection can lead to cirrhosis, severe liver disease, and ultimately HCC [194]. There is also a strong potential association between HCV infection and non-Hodgkin's B-cell lymphoma [195]. The development of HCV-mediated HCC is driven by long-standing hepatic inflammation, oxidative stress, and the potential for DNA damage. Additionally, it involves the alteration of normal cellular signaling pathways and the stimulation of host cell growth, potentially mediated by specific HCV proteins, including the core proteins NS3, NS5A, and NS5B [196]. Polyploidy has been observed in the context of HCV infection. In comparison to peripheral blood mononuclear cells (PBMCs) isolated from healthy individuals, PBMCs from HCV-infected patients have been found to exhibit chromosomal polyploidy [197]. Furthermore, primary human and mouse hepatocytes infected with the HCV strain showed a higher frequency of polyploidy compared to non-infected cells. The expression of the viral core protein was found to induce extensive polyploidy in various cell lines, including the human liver cell line HepG2 and the embryonic kidney cell line HEK293. Moreover, it led to a two-fold increase in polyploidy in primary splenocytes, hepatocytes, and embryo fibroblasts isolated from transgenic mice [197]. The HCV core protein appears to trigger polyploidy by upregulating the transcription of HIF-1α mRNA [198].

2.5.7 MCPyV

Merkel cell polyomavirus (MCPyV) belongs to a family of small, non-enveloped, icosahedral viruses with double-stranded DNA. MCPyV stands out as an oncogenic virus known to cause a rare and aggressive skin cancer called Merkel cell carcinoma (MCC) [199,200]. The key players in MCPyV-induced transformation and tumorigenesis are the transforming large T antigen (LTAg) and small T antigen (sTAg), which interact with important cellular factors disrupting the role of tumor suppressors like Rb and p53, contributing to the development of cancer [201,202]. The expression of MCPyV sTAg has been shown to lead to the formation of multinucleated cells and an increase in the population of cells with more than four sets of chromosomes (>4N) in human diploid fibroblastic cells known as WI38 [203]. Moreover, when sTAg was induced in C57BL/6 mice, it resulted in the development of poorly differentiated neoplasia. These tumors exhibited pleomorphic nuclei with variations in size and shape, along with multiple nucleoli [204]. This phenomenon is similar to the induction of polyploidy observed in the context of John Cunningham Polyomavirus (JCPyV) and BK Polyomavirus (BKPyV) infections, as well as infection with simian virus 40 (SV40), which is a closely related oncogenic primate virus [124].

Table 1: Oncoviruses.

Oncogenic Viruses	Genome	Human Cancers	Mode of infection	Oncoproteins
EBV	dsDNA	Burkitt's lymphoma, Hodgkin's lymphoma, posttransplantation lymphoma, nasopharyngeal carcinoma	Saliva, milk, blood, organ transplantation	EBNA1, EBNA2, EBNA3A, EBNA3B, EBNA3C, LMP1
HBV	dsDNA	Hepatocarcinoma	Transplacentally, milk, sexually, parenteraly, percutaneously	HBx
HCV	ssRNA	Hepatocarcinoma	Injection equipment, blood transfusion, sexually	Core protein
HPV	dsDNA	Cervical cancer, penis cancer, anal cancer, head and neck carcinoma	Sexually	E6, E7
HTLV-1	ssRNA	Adult T-cell leukemia (ATL)	Transplacentally, milk, sexually, blood	Tax, HBZ
KSHV	dsDNA	Kaposi's sarcoma, primary effusion lymphoma (PEL), multicentric Castleman's disease (MCD), KSHV-associated inflammatory syndrome (KICS)	Sexually, via drug injection, blood transfusion, solid organ transplantation	LANA, RTA, vFLIP, vIL-6, vGPCR

Merkel cell polyomavirus (MCV)	dsDNA	Merkel cell carcinoma	Saliva and/or skin between siblings and between mothers and their children	Unknown

2.6 HCMV and PGCCs

In general, oncoviruses employ various mechanisms that can be considered as early events leading to polyploidy, tumor advancement, and diversity within tumors. Interestingly, HCMV shares many of these mechanisms involved in inducing polyploidy [124–126,205]. For example, HCMV infection leads to the generation of excess centrosomes and the formation of abnormal mitotic spindles [205]. Moreover, HCMV proteins interact with the p53 protein, both in vitro and in vivo, resulting in the functional inactivation of p53. Additionally, HCMV affects the Rb protein through the HCMV UL97 protein, leading to Rb inactivation by phosphorylation, and it binds to pp71, which is part of the Rb protein family, ultimately causing their degradation [206,207]. Furthermore, HCMV has been shown to activate Myc at both the transcriptional and translational levels and induce the expression of HIF-1α [208–210]. HCMV infection also gives rise to multinucleated giant cells through cell fusion and upregulates the expression of G2/M transition regulators, including polo-like kinase 1 (Plk1) [205]. These findings suggest a potential connection between HCMV infection, the induction of polyploidy, and the development of tumors. It's worth noting that there may be a possible link between oncogenic viruses, the presence of a polyploid phenotype, and resistance to therapy, metastasis, and disease recurrence, as discussed in previous reviews [124]. This connection is strengthened by observations that chromosomal alterations coincide with morphological transformation [211], and the multinucleated cell phenotype is triggered by the expression of viral oncoproteins rather than simple cell fusion, a phenomenon also observed with other non-oncogenic pathogens [177,212]. Additionally, the emergence of a blastomere-like cycle with “CMV-transformed HMECs” or CTH cells in HMECs long-term cultures infected with HCMV as well as the detection of polyploidy and oncogenic potential in CTH cells have been previously shown, by our laboratory [125,126]. Several HCMV clinical strains were used to infect Human Mammary Epithelial Cells (HMECs) cultures which were grown for an extended period of time. Cultures of uninfected HMECs were terminated after fifty days

due to cellular senescence, similarly the cultures that became senescent when infected with HCMV-SD, HCMV-FS, HCMV-KM, HCMV-RM, or HCMV-PJ strains. While all clinical isolates could be cultured for about two months in HMECs, only HCMV-BL strain, along with the previously described HCMV-DB, exhibited sustained growth. These cells were termed 'CMV-transformed HMECs' or CTH cells. In CTH cultures, several atypical cells with distinct morphologies were observed including giant cells with a blastomere-like appearance, numerous small round daughter cells, a combination of epithelial and mesenchymal cells, filopodia, and patterns indicating asymmetric cell division [125,126]. All of these patterns may represent slow self-renewing cells undergoing various stages of the previously described giant cell cycle. This cycle consists of a series of synchronized events characterized by the emergence and dominance of enlarged giant cells, which then produce multiple small daughter cells. Furthermore, using confocal microscopy, common morphological features of PGCCs, characterized by their large size and giant nuclei, were detected, along with a broad range of cell sizes. Nehme et al. detected polyploidy in cultures infected with HCMV-BL as shown by flow cytometric analysis with propidium iodide staining. A significant percentage of cells with polyploidy, including polyploid giant cells (>4N), as well as other subpopulations like large tetraploid cells (LCs), intermediate cells (ICs), and diploid small cells (SCs) were observed. To assess the transforming potential of immortalized CTH cells, they performed a soft agar colony formation assay, which showed an increase in colony formation in CTH-BL and CTH-DB cells. This was associated with a significant increase in cell proliferation, as evidenced by a seven-fold rise in Ki67 antigen expression, increasing from 6.9% in control cells to 51.5% and 53.9% in CTH-BL and CTH-DB cells, respectively. Among these, PGCCs exhibited the highest level of Ki67 antigen expression [125,126]. Consequently, there is a growing need for novel treatment approaches that not only disrupt the replicative machinery of viral infections and inhibit the immortalizing and transforming capabilities of oncoviruses but also target PGCCs as a therapeutic strategy.

Chapter 3

3. HCMV-Mediated Oncogenesis

3.1 HCMV Prevalence in Diverse Forms of Cancer

While the frequency of HCMV detection remains a subject of debate, several research groups have detected HCMV and linked it to various human malignancies. HCMV-associated nucleic acids and proteins have been found in tumors and peripheral blood of patients with breast cancer, glioblastoma multiforme (GBM), high-grade serous ovarian carcinoma, neuroblastoma, medulloblastomas, colorectal cancer, and prostate cancer. These findings suggest a potential correlation between HCMV and cancer progression, with some studies reporting poorer prognosis in cases with extensive HCMV expression [70,209,213,214]. It has been proposed that HCMV gene products may modulate oncogenesis development and activate transformation-related pathways (**Table 2**). This concept aligns with the idea of oncomodulation, where disturbances in intracellular signaling pathways, transcription factors, and tumor suppressor proteins in the tumor environment create opportunities for HCMV to exert its oncomodulatory effects, potentially enhancing malignancy [215,216]. The variability in detecting HCMV, ranging from no detection to a high percentage of positivity, can be attributed to the specific methods employed for its detection, including IHC, PCR, histopathology, serology, antigenemia, etc.. [217].

Table 2: HCMV Gene Products.

HCMV Gene Products	Mechanism of Action	Oncogenic Characteristic
US2, US3, US6, US10, US11	▪ MHC class I expression impairment, reducing HCMV antigen presentation to CD8+ cells and evasion of CD8+ T cell immunity, superinfection ▪ US2 down regulates MHC class II and reduces HCMV antigen presentation to CD4+ cells	➢ Preventing host cell MHC class I antigen expression that is required for CD8+ cytotoxic tumor killing
US18 and US20	▪ Interfere with B7-H6 surface expression involving endosomal degradation, evades NK cells' immune recognition	➢ HCMV-immune evasion might indirectly affect tumor environment
US28 (viral GPCR)	▪ Promotes chemotaxis	➢ Cellular proliferation, tumor growth, enhanced angiogenesis and cell survival

UL16	▪ Regulation of NK cell ligand NKG2D and impairing NK cells function	➢ Immune evasion, protects the cells from cytotoxic peptides-mediated lysis, and protects cancer cells from both NK and T cells
UL40	▪ NK cell evasion ▪ HLA-E over expression, potentiating its interaction with the inhibitory receptor CD94/NKG2A	➢ HLA-E Over expression
UL83 (pp65)	▪ IE-1 sequestration, inhibit proteasome processing, reduce NKp30 effect and delays antiviral gene expression	➢ Genomic mutation, immune evasion
UL122 (IE2)	▪ Overexpression of anti-apoptotic FLIP protein	➢ Elevated immune suppression, cellular proliferation, escaping growth suppressors and enhanced cell survival
UL123 (IE1)	▪ Induction of TGF-b	➢ Cellular proliferation, genome instability and mutation, escaping growth suppressors, and ameliorated cell survival
UL82 (pp71)	▪ Inhibit antiviral response by binding to interferon stimulator gene	➢ Cellular proliferation, sscaping growth suppressors, and genomic mutation
UL111A (cmvIL-10)	▪ Inhibits MHC class II expression and suppresses CD4(+) T-cell recognition	➢ Immunosuppression, cellular proliferation, stimulates migration and metastasis, telomerase activation
UL142	▪ Inhibiting major stress protein (MICA)	➢ HCMV-immune evasion might indirectly affect tumor environment
UL36	▪ Complexing with pro-caspase-8 thus suppressing its proteolytic activation and prompting its designation as viral inhibitor of caspase-8-induced apoptosis (vICA)	➢ Enhanced cell survival
UL37	▪ Inhibition of pro-apoptotic Bcl-2 family Bak and Bax protein, thus inhibiting apoptosis	➢ Enhanced cell survival
UL76	▪ Activation of the DNA damage response thus inducing IL-8 expression	➢ Genome instability and mutation
UL97	▪ Forms a complex with pp65 and mediates immune evasion	➢ Escaping growth suppressors
UL141- UL144	▪ Encodes for homolog of TNFR, inhibits cell surface expression of CD155 and CD112 (NK	➢ HCMV-immune evasion might indirectly affect tumor environment

	cell activating ligands) and the death receptor for the TNF family ligand TRAIL	
UL145	▪ Degradation of helicase like transcription factor (HLTF) through the recruitment of Cullin4/DDB ligase complex	➢ Impeding innate immunity might indirectly affect tumor environment
UL146	▪ Promotes neutrophil chemotaxis, immune escape	➢ HCMV-immune evasion might indirectly affect tumor environment
UL148	▪ Suppression of CD58; potent modulator of CTL function, increases degranulation in both cytotoxic T lymphocytes and NK cells against HCMV-infected cells	➢ HCMV-immune evasion might indirectly affect tumor environment
miR-UL112	▪ Down regulation of MICB thus escaping NK cells, and decreased T-cell recognition	➢ Exerts its oncogene function by directly targeting tumor suppressor candidate 3 (TUSC3) in GBM
LncRNA	▪ Function in both innate and adaptive immunity including the development, activation, and homeostasis of the immune system	➢ Cellular proliferation and transformation, facilitating signal transductions in cancer signaling pathways, it's also involved in angiogenesis

3.2 HCMV, A Candidate Oncogenic Virus, Fulfilling Cancer Hallmarks

Hanahan and Weinberg updated their framework to include new additional hallmarks, and the list has continued to evolve to reflect our growing knowledge of cancer **(Figure 7)**. Originally and in 2000, Douglas Hanahan and Robert Weinberg outlined six key hallmarks of cancer including sustaining proliferative signaling, evading growth suppressors, resisting cell death, enabling replicative immortality, inducing angiogenesis, as well as activating invasion and metastasis [218]. Afterwards, in 2011, they expanded on the initial hallmarks and introduced two additional ones that involves reprogramming of energy metabolism and evading immune destruction [219]. In 2022, Douglas Hanahan further incorporated two hallmarks, tumor-promoting inflammation and genome instability and mutation [220] as depicted in the figure below. HCMV fulfills all the criteria associated with cancer hallmarks, as elaborated in the subsequent discussion below and in **Table 3**.

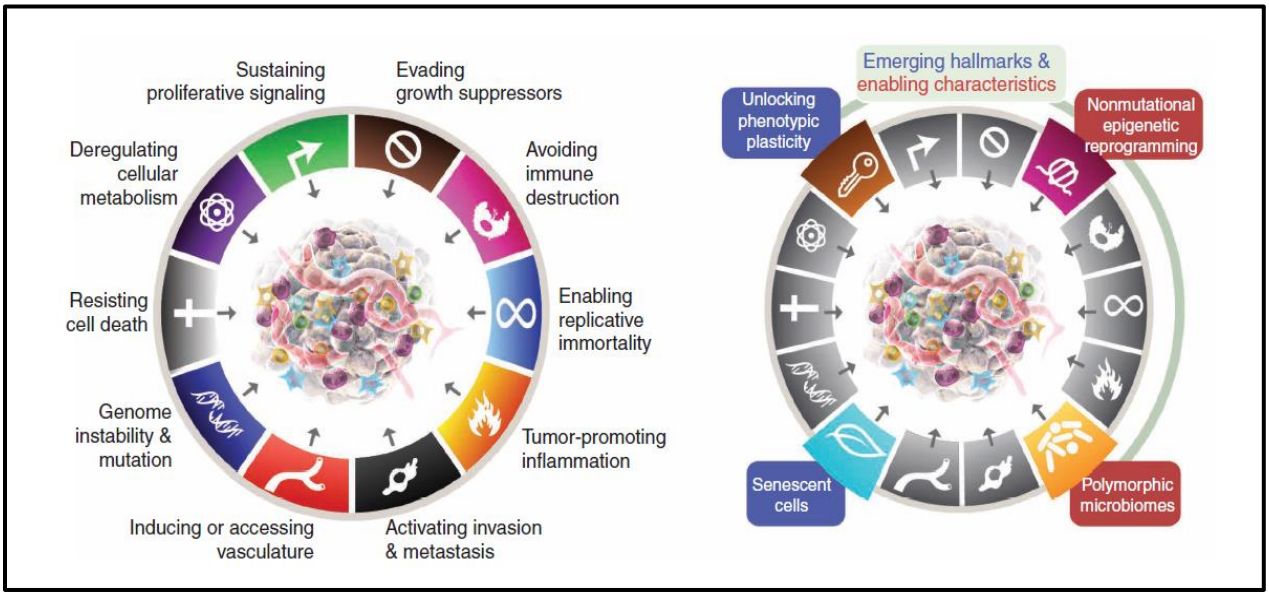

Figure 7: The Hallmarks of Cancer.

The conceptualization of the hallmarks of cancer serves as a exploratory instrument, aiming to simplify the immense complexities of cancer's various phenotypes and genotypes into a working framework of fundamental principles. The hallmarks of cancer graphic has been adapted from Hanahan and Weinberg [218–220].

3.2.1 Sustaining Proliferative Signaling

One of the primary characteristics of cancer cells is their capacity for continuous and uncontrolled proliferation, leading to unlimited growth [221]. This phenomenon is primarily achieved through several mechanisms including independent production of growth factors, stimulation of neighboring tumor-associated cells to produce various growth factors that support cancer cells via paracrine signals, and the constant activation of downstream signaling pathways [222]. Notably, certain HCMV proteins, including IE1, IE2, pUL44, and pUL84, have been shown to play a role in regulating the tumor suppressor protein p53 by interacting with it and influencing p53-mediated transcription, thereby exerting control over the cell cycle at various checkpoints [223–225]. HCMV IE1-72 hindered the ability of p53 to bind to its specific DNA sequences, whereas IE2-86 and/or UL84 augmented p53 binding, resulting in an altered DNA-protein complex [226].

Additionally, the induction of the transcription factor NF-kB by HCMV IE proteins has been found to activate cell survival pathways in both normal and tumor cells. Further, HCMV significantly elevates the activity of mitogen-activated protein kinase (MAPK) p38 and ERK1/2 through various mechanisms [227,228]. The expression of HCMV-US28 has been shown to enhance the secretion of biologically active VEGF and activate multiple cellular kinases, thereby promoting glioma growth and invasion [229]. Moreover, it induces the production of IL-6 through NF-kB activation, resulting in the potent activation of the signal transducer and activator of transcription 3 (STAT-3) [230].

3.2.2 Evading Tumor Suppressors

By inactivating p53 function and Rb, DNA oncoviruses overpass the G1/S check point and force the cell to enter into the S phase, resulting in unregulated cell division and tumor formation. Numerous studies have documented HCMV interference with the cell cycle, showing p53 and Rb being targeted. HCMV-IE1, and IE2 allow the evasion of tumor suppressors p53 and Rb [215]. HCMV-IE1 and IE2 proteins interact with p53 *in vitro* and *in vivo*, transcriptionally inactivating the latter [226,231]. The aforementioned HCMV-IE proteins have the potential to deactivate the Rb protein family, which consequently stimulates the entry of cells into the S phase of the cell cycle [232]. Additionally, the IE1 protein drives cell cycle progression toward the G1/S transition point by increasing the expression of E2F-responsive genes. Among these genes are cellular regulators of the cell cycle, as well as essential enzymes required for DNA precursor synthesis and the initiation of cellular DNA replication, such as cyclin E and cdk-2 [233]. HCMV pUL97 phosphorylates and renders inactive proteins belonging to the Rb family, facilitating the promotion of the cell cycle. Additionally, the pUL82 protein works to reduce the levels of Rb family proteins. One such protein is encoded by the viral UL82 gene and is termed pp71; HCMV pp71 protein targets the hypo-phosphorylated forms of the Rb proteins for proteasome-dependent degradation through a ubiquitin-independent pathway [234]. In HCMV-infected HMECs, there is a decrease in the detection of the Rb protein and an enhanced expression of the UL82 transcript [235]. Further, a study showed that the proliferation of IE1-expressing glioblastoma cells depends on p53 and Rb inhibition and PI3K/AKT activation [236].

3.2.3 Activating Invasion and Metastasis

The capacity for invasion and formation of distant metastases are recognized as critical characteristics of tumor cells, regulated by a complex network of interactions and regulatory mechanisms. This enables them to intravasate into blood and lymphatic vessels while evading immune surveillance, displaying anchorage-independent growth. Subsequently, cancer cells extravasate from these vessels into their target tissues, where they establish micrometastases [219]. The epithelial-mesenchymal transition (EMT) process plays a significant role in this cascade of invasion and metastasis [222]. Studies have shown that persistent HCMV infection of neuroblastoma cells leads to increased motility and adhesion of human endothelial cells [237]. It's worth noting that the transmigration of tumor cells is facilitated by the focal disruption of endothelial cell integrity, mediated by the activation of β1α5 integrin on the surface of infected tumor cells. This phenomenon is accompanied by HCMV-induced downregulation of neural cell adhesion molecule (NCAM; CD56) receptors, which promotes transendothelial penetration [238]. HCMV infection augments glioma invasiveness by enhancing extracellular matrix-dependent migration and invasion, specifically through the phosphorylation of FAK at Tyrosine397, which is observed exclusively in human malignant glioma cells [239]. In neuroblastoma cell lines persistently infected with HCMV, gene microarray analysis has revealed an upregulation of genes associated with cancer cell invasion [240]. Furthermore, vIL-10 and US28 will enhance cancer cell invasion and metastasis [241].

3.2.4 Enabling Replicative Immortality

It is widely acknowledged that cancer cells possess the capability for endless replication. This immortality is achieved by their capacity to overcome two significant barriers to proliferation: senescence and crisis, with the latter eventually resulting in cell death [219]. Additionally, tumor cells find ways to evade the loss of telomeres, which protect the ends of chromosomes, thereby preventing telomere erosion and the entry into crisis, enabling them to sustain unlimited proliferation [222]. HCMV has been demonstrated to trigger the continuous expression of human telomerase reverse transcriptase (hTERT) and the activation of telomerase. In this context, CMV-IE and hTERT proteins were observed to co-localize in human primary glioblastoma multiforme cells, and their levels correlated with each other. This effect is facilitated by IE1's ability to

stimulate telomerase activity and promote telomere lengthening through a specific interaction with the hTERT promoter [242]. Previously, in our laboratory, the infection of HMECs with HCMV-DB resulted in the overexpression of hTERT mRNA and increased telomerase activity [209].

3.2.5 Inducing Angiogenesis

During the progression of tumors, an "angiogenic switch" is triggered to ensure the continuous development of new blood vessels that serve not only to sustain tumor growth by providing essential nutrients and oxygen but also facilitate the removal of metabolic waste products and enable the tumor to enter the process of hematogenous metastasis [222]. This process primarily involves the induction of pro-angiogenic factors or the suppression of antiangiogenic signals [219]. HCMV typically promotes angiogenesis through both direct and indirect mechanisms. Infections occurring near blood vessels may stimulate angiogenesis by releasing angiogenic factors or by increasing local inflammation [243]. When fibroblasts and endothelial cells are infected, they promote the synthesis and release of various angiogenic factors that facilitate multiple stages of angiogenesis [244]. US28-induced angiogenic activity, characterized by the production of VEGF, is initiated through an increase in cyclooxygenase-2 (COX-2) expression mediated by US28, which activates the NF-κB pathway [245]. Furthermore, HCMV infection of endothelial cells induces an angiogenic response through viral binding to the epidermal growth factor receptor, as well as β1 and β3 integrins, leading to the activation of the phosphatidylinositol 3-kinase (PI3k) and mitogen-activated protein kinase signaling pathways [246]. HCMV also infects lymphatic endothelial cells and induces the release of a set of molecules that promote angiogenesis and lymphangiogenesis. These molecules include IL-6, granulocyte-macrophage colony-stimulating factor, and IL-8 [247,248]. In addition, HCMV induces the production of proinflammatory and angiogenic cytokines in retinal pericytes, contributing to angiogenesis in conditions such as retinopathy and congenital ocular disease [249].

3.2.6 Resisting Cell Death

In addition to sustaining continuous proliferation and manipulating cellular growth processes, cancer cells possess the ability to avoid pathways leading to cell death. While three primary pathways apoptosis, necrosis, and autophagy can potentially induce cell death, their activation needs to be regulated by tumor cells. Apoptosis, in particular, has been extensively studied in the

context of malignant transformation, where the initiation of apoptosis is finely tuned by balancing pro-apoptotic and anti-apoptotic factors [220,222]. Numerous HCMV proteins can modulate apoptosis through diverse mechanisms, ultimately resulting in the inhibition of both intrinsic and extrinsic apoptotic signaling pathways [250]. For instance, pUL38, UL37, and US21 have been demonstrated to exert anti-apoptotic effects [70,251,252]. Notably, HCMV encodes a cell death-suppressing protein known as viral mitochondria-localized inhibitor of apoptosis (vMIA), which binds to Bcl2 associated X (BAX) and impedes BAX-mediated mitochondrial membrane permeabilization by sequestering BAX within the mitochondria [253]. Another HCMV protein, pUL36, interacts with pro-caspase-8 thereby inhibiting apoptosis initiated through death receptors [254]. Moreover, HCMV adopts strategies to evade extrinsic pro-apoptotic pathways by downregulating the cell surface expression of death receptors, including tumor necrosis factor receptor 1 (TNFR1), TNF-related apoptosis-inducing ligand (TRAIL) receptor 1, TRAIL receptor 2, and Fas [255]. Additionally, the long non-coding RNA lncRNA2.7 directly interacts with the gene associated with retinoid/interferon-induced mortality-19 (GRIM-19), leading to the stabilization of mitochondrial respiratory chain complex I and the continuous production of ATP [256]. Furthermore, HCMV employs alternative mechanisms to block apoptosis, such as the expression of the anti-apoptotic Bcl-2 protein or the inhibition of p53-mediated apoptosis by HCMV-IE2 [257,258].

While the role of autophagy in cancer regulation is a subject of contention, an increasing body of research predominantly underscores its pro-survival function in promoting cancer progression and metastasis [259]. Autophagy has the capacity to limit viral infections, but persistent viruses have developed diverse strategies to evade or hinder multiple stages of the autophagic process [260]. For instance, HCMV employs mechanisms to counteract autophagy, one of which involves TRS1 in addition to IRS1 that hinder autophagy by binding to Beclin 1 [260,261]. Autophagy also regulates the properties of CSCs by contributing to the maintenance of stemness, induction of recurrence, as well as tumor resistance [262]. On the other hand, in early tumorgenesis, it acts as a tumor suppressor and survival pathway by preventing the accumulation of damaged proteins and organelles [263]. Hence, autophagy plays dual roles in tumor promotion and suppression [262,263].

3.2.7 Evading Immune Suppression

HCMV has developed various immune evasion tactics to manipulate the host immune system, enhancing its infection and spread within the host **(Figure 8)** [70]. A significant strategy involves hindering MHC class I-restricted antigen presentation. During the immediate early phase of HCMV infection, cytotoxic T-lymphocytes (CTLs) counteract antigenic peptides produced by the IE1 transcription factor. However, the matrix protein pp65, which possesses kinase activity, phosphorylates IE1, specifically blocking the presentation of IE-derived antigenic peptides. This allows HCMV to evade immune recognition of early viral proteins. Additionally, pp65 is introduced directly into cells during viral fusion, enabling HCMV to escape immunological surveillance until other immune evasion-related proteins are released. HCMV-specific viral proteins and genes associated with host interferon responses further inhibit NK cell detection and activation, as well as hinder the recognition of CD4+ and CD8+ T-cells by preventing MHC Class I and II antigen processing and presentation. Furthermore, HCMV-infected cells produce a viral IL-10 homolog, which suppresses CD4+ and CD8+ T-cell responses [70].

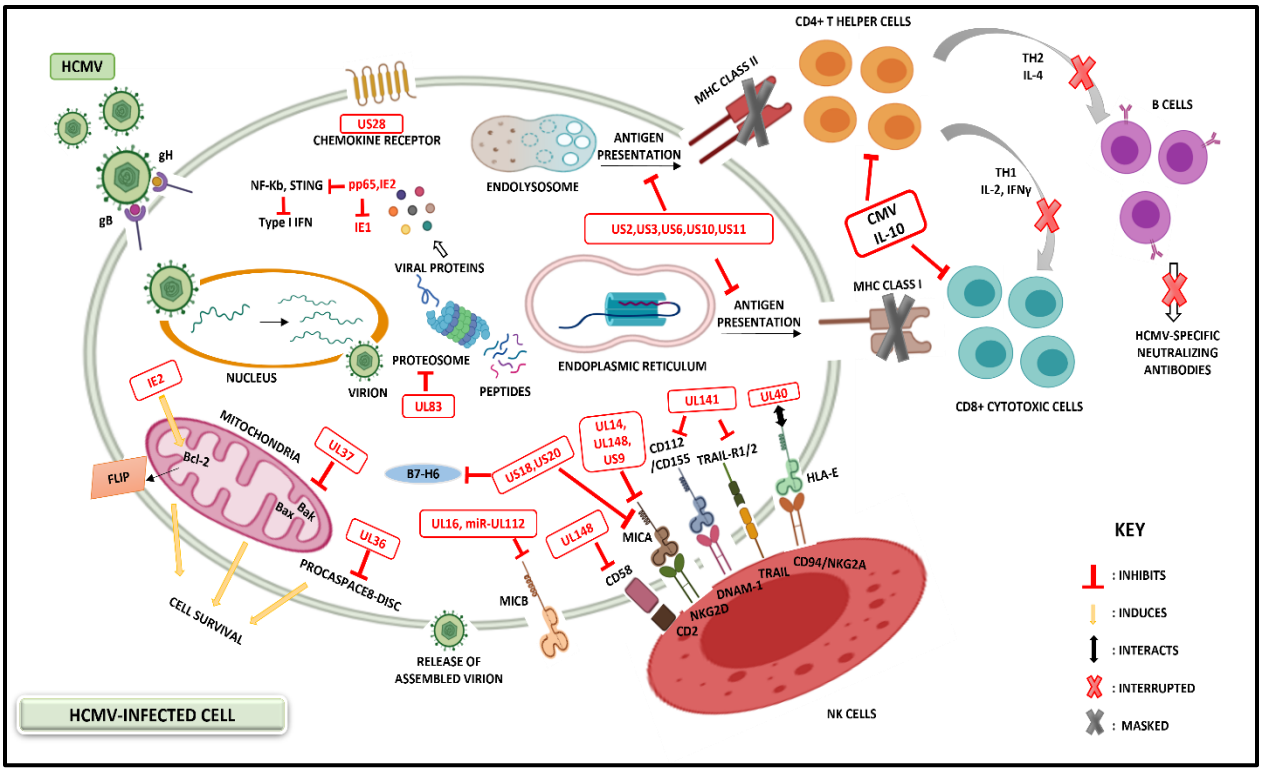

Figure 8: Modulation of the host immune system.

HCMV-induced modulation of the host immune system. The battle between the host immunity and HCMV is permanent, with HCMV developing various mechanisms to evade the host immune system. Immunosuppression may be ascribed to the variety of immune modulators encoded by HCMV-specific gene products. HCMV viral genes prevent MHC Class I and II antigen presentation and thus interfere with interferon responses, NK cell recognition as well as $CD4^+$ and $CD8^+$ T-cell recognition. Additional HCMV genes for instance IL-10 homologue (UL111a), and viral proteins acting as receptors for host inflammatory cytokines (US28), further suppress the host immune responses [70].

3.2.8 Reprogramming of Energy Metabolism

Dysregulation of energy metabolism has been well established as a hallmark of cancer. Lipid droplets (LDs) accumulation has gradually been recognized as a prominent characteristic in a variety of cancers and attracts increasing attention. In case of nutrient deprivation, fatty acids released from LDs are used for energy production via mitochondria β-oxidation and Kreb's cycle. Compared to healthy tissues, higher LD content have been reported in cancer cells and cancerous tissues such as colorectal cancer, breast and prostate cancers, hepatocellular carcinoma, renal cell carcinoma and glioblastoma. Thereby, during the aggressive process of cancer cells, LDs can

function as energy source to support distant dissemination of cells. Notably, not only LD density but also their motility was correlated with cancer aggressiveness [264]. Further, HCMV infection disrupts cellular energy metabolism and induces significant alterations in metabolic processes including increased glucose uptake, elevated glycolysis, diversion of glucose carbon, and the induction of the Warburg effect [46]. HCMV-IE1 protein appears to modulate the mRNA levels, eliminating glucose transporter 1 (GLUT1) mRNA and increasing GLUT4 mRNA. The elevated GLUT4 in infected cells is driven onto the cell surface, verifying that glucose uptake increases regardless of Akt function [265]. Further, HCMV-pUL38 is capable of initiating glycolytic activation and prompting the breakdown of specific amino acids [266]; HCMV-pUL13 targets mitochondrial cristae architecture to increase cellular respiration during infection [267].

3.2.9 Enabling Characteristics: Genomic Instability, Mutation, and Tumor-promoting Inflammation

Throughout the multistep progression of tumors, cancer cells often exhibit an increased rate of mutations, wherein a favorable mutant genotype provides a selective advantage to certain subclones of cells. This advantage supports their proliferation and eventual dominance within a local tissue environment [219,220]. Several mechanisms contribute to this phenomenon, including increased sensitivity to mutagenic agents, compromised surveillance systems responsible for monitoring genomic integrity (such as p53), as well as increased defects in detecting DNA damage and activating the repair mechanisms responsible for DNA damage repair and deactivating mutagenic substances. On the other hand, the inflammatory response associated with tumor growth has been linked to enhanced tumorigenesis and progression. This is attributed to the release of various chemicals, notably mutagenic reactive oxygen species, as well as factors promoting growth, survival, and angiogenesis. These factors collectively facilitate proliferative signaling, inhibit cell death, and enable processes like angiogenesis, invasion, and metastasis [219].

In the context of HCMV infection, it has been shown that HCMV-UL76 induces DNA damage as well as the accumulation of chromosome abnormalities, including micronuclei, misaligned chromosomes, and issues like lagging and bridging [268]. Further, viral replication activates the checkpoint response to DNA double-strand breaks, and this replication alters the localization of

checkpoint proteins to the cytoplasm, thus inhibiting the signaling pathway [269]. Furthermore, lytic HCMV infection disrupts ataxia telangiectasia mutated protein (ATM)-related kinases and triggers DNA damage responses [270]. Specifically, IE1 has been shown to activate ATM kinase [223], while E2F1 contributes to the accumulation of the gamma histone variant H2AX (γH2AX) during HCMV infection or IE protein expression [271]. On the other hand, pUS28 exacerbates tumor-related inflammation by inducing the production of various proinflammatory mediators, including IL-6, regulated on activation normal T expressed and secreted (RANTES), monocyte chemoattractant protein-1 (MCP-1), and fractalkine [272,273]. HCMV augments the recruitment of leukocytes and prompts the production of proinflammatory substances like IL-8 and IL-6, along with the expression of the leukocyte intercellular adhesion molecule 1 (ICAM-1) receptor [274–276]. Furthermore, CMV infection generates intracellular reactive oxygen intermediates in smooth muscle cells and human diploid fibroblasts [277,278].

3.2.10 Tumor Promoting Microenvironment

As cancer evolves, it can resist immune clearance by prompting tolerance in the presence of tumor-associated inflammatory cells. Consequently, a tumor microenvironment (TME) is generated and controlled by tumor-induced molecular and cellular interactions in which immune cells not only fail to exert anti-tumor effector functions, but also promote tumor development [279]. HCMV expresses several gene products that modulate the host immune response and promote modifications in non-coding RNA and regulatory proteins. These changes are linked to several complications, such as immunosenescence and malignant phenotypes leading to immunosuppressive TME and oncomodulation **(Figure 9)** [70]. NF-κB and PI3K activity play a role in facilitating the HCMV-induced transformation of monocytes into macrophages with a dual phenotype, exhibiting characteristics of both inflammatory macrophages (M1) and immunosuppressive macrophages (M2). In this context, M1 macrophages are responsible for releasing inflammatory factors such as TNF-alpha, IL-6, and nitric oxide synthase 2, while M2 macrophages exhibit an immunosuppressive profile similar to tumor-associated macrophages (TAMs), characterized by the secretion of immunosuppressive cytokines like TGF-β and IL-10 [280]. It's worth noting that a significant portion of TAMs in breast cancer cells display activated M2 features, accompanied by the secretion of elevated levels of immunosuppressive cytokines,

including IL-10, TGF-β, and, to a lesser extent, pro-inflammatory cytokines [281]. Notably, research from our laboratory has demonstrated that the highly macrophage-tropic HCMV-DB strain can induce the activation of an M2-like state [282]. This underscores the potential contribution of HCMV infection to the development of neoplastic transformation in breast epithelial cells, partially through the recruitment and polarization of macrophages [283]. The oncomodulatory potential of HCMV catalyzes an oncogenic process by producing viral proteins, helping tumor cells to evade the immune system, and preventing and/or delaying cell death. The lack of HCMV specific cellular immune responses in these immune-privileged tumor sites would definitely enhance HCMV replication. On the other hand, cancer cells on their own can escape immune responses by diverse mechanisms. Thus, the combination of intrinsic cellular with viral immune escape machineries in cancer cells may offer an environment which enhances HCMV replication and boost cancer cells to evade from immune surveillance showing the bidirectional relationship between tumor cells and HCMV [70].

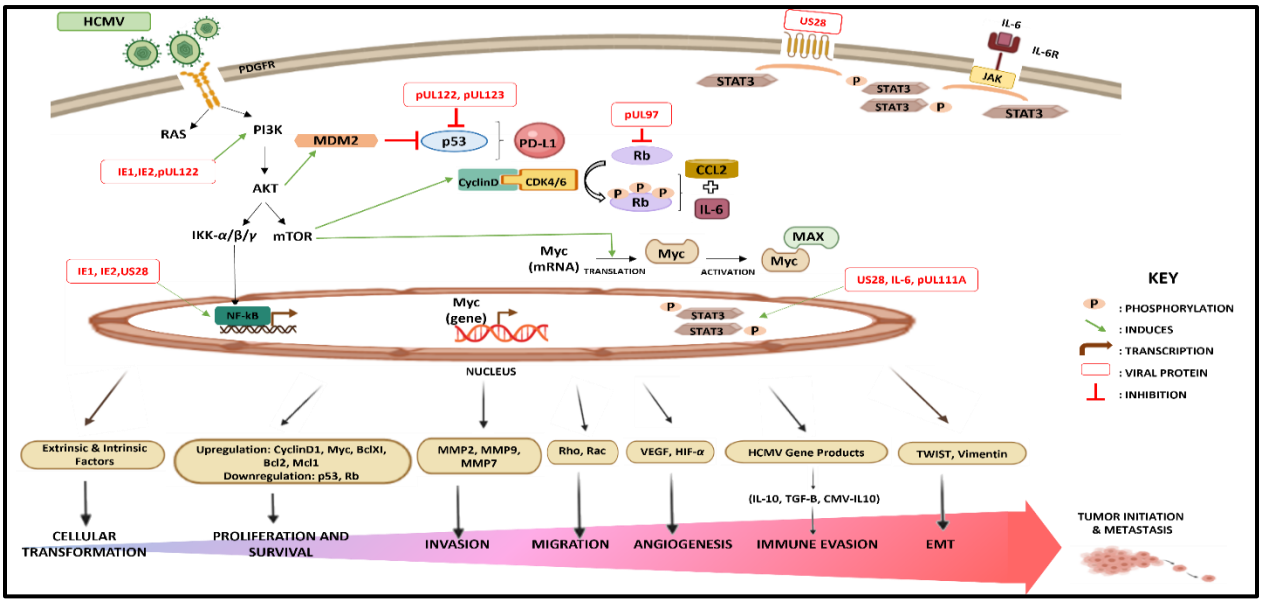

Figure 9: HCMV Oncomodulation and Its Significance in Tumor Microenvironment.

Major signaling pathways stimulated by HCMV that modulate the immune landscape. HCMV-infected cells produce elevated levels of interleukin-6 (IL-6) that activates signal transduction *via* IL-6 receptor (IL6R)-STAT3 axis. US28, an active chemokine receptor, also plays a major role in activating STAT3 in cancer cells. The combination of STAT3

activation and the impact of HCMV on cancer cell apoptosis, invasion, migration, adhesion, angiogenesis, and immunogenicity significantly exacerbates malignancy. In contrast to p53 and Rb, the upregulation of Akt, Myc, PD-L1, and CCL2 strongly exerts immunosuppressive and oncomodulatory effects. HCMV-induced alterations in the TME may contribute to oncomodulation [70].

Table 3: HCMV enabling the characteristics of cancer.

Cancer Hallmarks	HCMV Mechanism of Action	HCMV Proteins
Sustaining Proliferative Signaling	Induces cell cycle progression to S phase	**IE2**
	Induces expression of E2F genes	**pp71**
	Phosphorylates Rb	**UL97**
Evading Growth Suppressors	Activates EGFR	**HCMV infection**
	Dysregulates Cyclin E expression	**IE1**
	Inhibits p53 degradation Decreases levels of p21 Induces expression of p53 Binds to p53	**mtrII**
Activating Invasion and Metastasis	Activation of RhoA dependent motility of U373 cells as well as smooth muscle cells	**US28**
Enabling Replicative Immortality	Activation of telomerase	**IE1**
Inducing Angiogenesis	Induction of VEGF expression	**US28**
	Induction of IL-8	**IE1**
Resisting Cell Death	Inhibits apoptosis	**IE1**
	Activates PI3-K/Akt pathway	**IE2, vMIA, vICA**
Deregulating Cellular Energetics	Increases flux through glycolytic pathway, acetyl CoA, flux of carbon, nucleotide biosynthesis	**HCMV infection**
Avoiding Immune Destruction	Production of homologs to immunosuppressive cyto-kines	**HCMV IL-10**

	Inhibits expression of MCH I	**US2**
	Intracellular retention of NKG2D	**UL16**
	Induces expression of TGF-β1	**IE2**
Genome Instability and Mutation	Inhibits DNA damage repair	**HCMV infection**
	Increases mutation frequency	**pp65 and pp71**
	Induces chromosome aberrations in cell lines	**IE1 and UL76**
Tumor Promoting Inflammation	Induces production of RANTES, fraktalkine, MCP-1	**HCMV infection**
	NF-κB activation & IL-6 production	**US28**

3.3 HCMV and Its Association with Breast Cancer

Globally, breast cancer poses a formidable health challenge as it is the most prevalent malignancy accounting for a high number of cancer deaths in women [284]. Breast cancer consists of a group of heterogeneous diseases driven by a multifactorial etiology involving genetic predisposition, hormones, and environmental factors; viruses are considered indisputable causal factors for nearly 20% of all human malignancies [285]. Triple-negative breast cancer (TNBC) comprises 15% of breast cancers globally [286]. Despite its susceptibility to standard chemotherapy, TNBC is highly invasive, has a high relapse tendency, and is associated with a poor overall prognosis [287]. Recently, more significant advances include characterizing the molecular features of TNBC which will maximize the efficacy of certain chemotherapeutic agents and aid in actively exploring novel therapeutic targets [288]. The majority of breast cancers originate from cells lining the milk-forming ducts within the mammary gland, known as carcinomas [289]. Following childbirth, HCMV can be detected in breast milk, potentially spreading to nearby mammary epithelial cells [290]. Moreover, HCMV has the ability to infect macrophages and induce an atypical M1/M2

phenotype that closely resembles the phenotype of tumor-associated macrophages. This alteration is linked to the release of cytokines that play a role in the initiation or promotion of cancer, particularly in cases of breast cancer with a poor prognosis [290]. Furthermore, HCMV antigens and DNA have been identified in tissue biopsies of individuals with breast cancer [291], and there have been reports of elevated serum HCMV IgG antibody levels occurring before the onset of breast cancer in certain women [292]. Further, previous studies demonstrated the ability of HCMV-DB and HCMV-BL strains in transforming primary HMECs into CMV-Transformed HMECs (CTH) cells in vitro [125,209]. CTH cells, which are slow self-renewing cells, undergo diverse stages of the giant cell cycle. They were shown to be heterogeneous, generate PGCCs, exhibit dedifferentiation, and display stemness and EMT/MET features [125,126]. HCMV oncomodulation, molecular mechanisms, and ability to support PGCCs generation might underscore its contribution to oncogenesis, especially breast cancers. The heterogeneity of strains can be linked to distinct properties influencing the virus-transforming potential, cancer types induced, and patient's clinical outcomes.

3.4 The Potential Link Between HCMV and Glioblastoma

GBM, a subtype of adult diffuse glioma, is a primary central nervous system (CNS) tumor presumed to arise from neuroglial stem cells or their progenitors in the subventricular zone [293,294]. There has been a recent paradigm shift, with increasing reliance on molecular information for diagnostic classification and prognostication within gliomas, as seen in the most recent World Health Organization (WHO) classification of CNS tumors [294]. Despite the molecular evolution of GBM, it continues to be an incurable disease with poor survival. HCMV infects neural stem/progenitor cells, and human astrocyte [295–298]. Although HCMV DNA and antigens, especially IE1, have been detected in GBM tissue [236,299], there is no conclusive evidence about HCMV oncogenicity in GBM, and the mechanisms by which the virus might contribute/induce oncogenesis remain elusive. The expression of HCMV proteins and oligonucleotides in high percentage of low- and high-grade malignant gliomas was first reported by Cobbs et al. in 2002 [213]. Although these data do not establish a causal role for HCMV in glioma pathogenesis, existing data indicates that HCMV could facilitate glioma progression. A study showed that HCMV-IE1 protein was detected in 100% of glioblastomas and 82% of low-

grade gliomas upon using immunohistochemistry. They further reported the detection of HCMV-specific oligonucleotides in the same areas of IE1 expression within the tumor. Their finding, as initially described by Cobbs et al. in 2002, is that HCMV IE1 and virus-specific oligonucleotides weren't detected in necrotic areas or outside the tumor margin [236]. Numerous reports have provided evidence of HCMV's presence in GBM, although typically confined to a small subset of cells [300]. Studies have also indicated that viral proteins can dysregulate cellular processes and intensify the malignancy of tumors [70,215,236,300]. Additionally, it has been observed that HCMV IgG seropositivity is linked to reduced overall survival rates among GBM patients [301]. These discoveries hold substantial implications for GBM screening and treatment, as anti-HCMV IgG testing may offer valuable prognostic insights. A study revealed a significant association between HCMV seropositivity and diminished overall survival in GBM patients, especially among those with unmethylated MGMT. This observation suggests that prior HCMV infection may have a noteworthy impact on the outcomes of GBM patients [301]. Consequently, anti-HCMV antibodies may prove to be a valuable prognostic tool in the management of GBM patients. Moreover, GBM cells exhibit HCMV proteins, presenting a unique opportunity for targeted therapy. A study utilized the universal intracellular targeted expression (UNITE) platform to develop a multi-antigen DNA vaccine encoding HCMV proteins pp65, gB, and IE1. The UNITE platform incorporates lysosomal targeting technology, involving the fusion of lysosome-associated membrane protein 1 (LAMP1) with target antigens. This study demonstrates compelling evidence of enhanced antigen presentation through both MHC-I and -II, resulting in a robust antigen-specific CD4 and CD8 T-cell response, along with a potent humoral response [302]. Thus, this research underscores that vaccination with HCMV antigens elicits robust cellular and humoral immune responses, triggering significant anti-tumor activity and leading to improved survival in a mouse model of GBM. Lastly and most recently, it's worth mentioning that Moderna's RNA vaccine for HCMV infection (CMVictory mRNA-1647) is currently undergoing Phase 3 clinical trials (NCT05085366) [303].

3.5 The Interplay Between HCMV and Ovarian cancer

Epithelial ovarian cancer (OC), the most common and life-threatening cancer amongst gynecologic malignancies, has a 5-year age-standardized survival rate of 30–40%. Nearly 75% of

all OC cases are diagnosed at late stages [304]. Despite the advances in treatment modalities, the overall survival remains low for stage III and stage IV accounting for 40% and 20%, respectively [305,306]. Currently, infection-triggered chronic inflammation is recognized as a crucial mechanism in the progression and spread of OC. In alignment with this observation, recent studies have identified elevated expressions of HCMV proteins in OC tissue samples that have been associated with poor survival outcomes [307]. One study revealed that HCMV-IE protein expression was present in 82% of OC cases and 36% of benign tumors, while pp65 was detected in 97% of EOC cases and 63% of benign tumors. Notably, pronounced HCMV-IE expression was correlated with a shorter median overall survival [308]. Additionally, the presence of HCMV DNA was found in 70% of cancerous ovarian tissues, significantly exceeding the detection rate in benign tumor cases [307]. These findings suggest that HCMV infection might potentially facilitate the progression of cancer. Within the ovarian cancer TME, active HCMV infection may directly contribute to OC progression. Once HCMV infects host cells, it initiates mechanisms to counteract key antiviral immune responses necessary for infection control. These mechanisms involve the secretion of immunosuppressive cytokines and the impairment of cell-mediated immune responses, which are also crucial for restraining tumor growth [304]. Previously existing data showed the detection of HCMV-gB by PCR in approximately 50% of OC tissues, with 80% of these cases being late-stage invasive tumors, suggesting that HCMV infection within the TME could potentially promote cancer progression or metastasis [304]. Another recent study by Radestad et al. explored the prevalence of HCMV in ovarian cancer and its association with clinical outcomes. Their research indicated higher levels of HCMV-IgG, HCMV-IE proteins, and pp65 proteins in OC patients with malignant or benign ovarian epithelial tumors compared to control subjects [309]. This observation underscores the need to investigate whether administering anti-HCMV treatment to OC patients experiencing active HCMV reactivation in their TME should be considered in future therapeutic approaches. In conclusion, HCMV proteins and nucleic acids are frequently detected at varying levels in high-grade serous ovarian carcinoma. The shorter median overall survival of patients with HCMV-IE and pp65 in their tumors underscores the imperative to further explore the role of HCMV in ovarian cancer patients.

Chapter 4

4. Emerging Threats: Decoding The Molecular Pathways in Cancer Development and Understanding Viral Variants

4.1 Decoding The Molecular Pathways in Cancer Development

The cumulative body of evidence underscores the pivotal roles played by EZH2 and Myc in the initiation of cancer and maintenance of stem cell properties [310]. Being the enzymatic subunit of polycomb repressive complex 2 (PRC2), EZH2 is a histone-lysine N-methyltransferase responsible of transcriptional silencing [311]. EZH2 dysregulation was associated with the development, progression, and therapeutic resistance of many tumors [312,313]. Additionally, it was shown to expand the stem cell pool and the tumor-initiating cells in glioma, breast, ovarian, and prostate cancer, hence enhancing accelerated initiation, metastasis, invasion and growth [314–316]. In breast cancer pathogenesis, EZH2 overexpression assumes a critical role as it suppresses the expression of early growth response 1 (EGR1), thus inhibiting EGR1-mediated tumor-suppressive signals [317]. Moreover, EZH2 mediates the stability of ribosomal DNA by silencing PHACTR2-AS1, thereby fostering genomic instability and promoting growth and metastasis in breast cancer [318]. Further, EZH2 was demonstrated to be overexpressed in GBM tissues harboring HCMV [319]. EZH2 was also shown to be recruited to the major immediate early promoter (MIEP) in CD14+ monocytes where HCMV establishes latent infection in vivo [320]. Furthermore, several studies showed that EZH2 overexpression is associated with HGSOC [321,322]. A study reported that EZH2 degradation profoundly blocked ovarian tumor cell proliferation and tumorigenesis in vitro and in vivo [323]. Another study revealed that invading PGCCs possess strong EZH2 expression [324]. Since EZH2 enhances cell proliferation, inhibits apoptosis, promotes angiogenesis, metastasis and therapy resistance in several tumors, inhibiting EZH2 suggests an effectual therapeutic strategy [325,326].

EZH2 was identified as a downstream target of Myc oncogene, the latter coordinately regulating EZH2 through transcriptional and post-transcriptional mechanisms during tumor initiation and disease progression [327]. Myc has been shown to stimulate EZH2 expression through direct binding and activation of its promoter, as well as by suppressing its negative regulator, miR-26a, or by directly repressing miR-137 [327,328]. The Myc-miR-137-EZH2 pathway has been linked

to cisplatin resistance in ovarian cancer [329]. Additionally, bromodomain-4 protein (BRD4) was shown to positively regulate EZH2 transcription through Myc upregulation [330]. Interestingly, Myc activation has been widely reported in the progression of breast cancer, especially in triple-negative breast cancer and in tumors that exhibit drug resistance, much like aggressive medulloblastoma tumors where elevated Myc levels are associated with increased EZH2 expression [126,331]. By uncoupling DNA replication from mitosis, Myc overexpression can induce DNA replication, thus opening the door toward polyploidy [332]. This intricate relationship between Myc, polyploidy, and cancer has been previously demonstrated [333], with Myc correlating with nuclear pleomorphism in both primary and metastatic renal cell carcinomas. Moreover, Myc has been found overexpressed in GBM; its expression correlates with glioma grade where 60-80% of GBM reveal elevated Myc levels [334]. In glioma cells, EZH2 knockdown depleted Myc expression [335]. Further, Myc direct transcriptional regulation by EZH2 may establish a new mechanism underlying glioma cancer stem cell maintenance [336]. Similarly, enhanced Myc expression have been observed in 20-50% of ovarian carcinoma [337,338].

4.2 Viral Variants and Their Oncogenic Potential

Viral variants acquire diverse capacities to manipulate host cell machinery, making them more or less efficient at promoting cellular transformation and cancer development. Some variants may be more efficient at evading the immune response, more prone to causing persistent infections, or more effective at disrupting cellular processes that regulate cell growth and division [339–341]. Oncoviruses could serve to emphasize the significance of HCMV in processes related to cellular transformation and oncogenesis. To start with, HPV strains were classified into high- and low-risk strains after being isolated from different lesions. These discoveries were shown to radically alter the tumor diagnosis, prognosis, and prevention approaches [342,343]. Low-risk HPV strains were generally not strongly linked to cancer development, for instance HPV-6 and HPV-11. On the other hand, certain high-risk HPV strains were strongly associated with the development of various cancers through persistent infections that may cause various cellular changes. The most notable high-risk HPV strains include HPV-16 and HPV-18, HPV-31, HPV-33, and HPV-45 [344,345]. Researchers have identified specific genetic sequences within high-risk HPV types that are associated with increased cellular transformation. The HPV E7 carboxyl terminus contains two

copies of a CXXC motif that are separated by a 29-amino-acid spacer. This domain may function as a dimerization domain [346]. Like adenovirus E1A and SV40 T antigen, the HPV E7 proteins interact with pRB and the related "pocket proteins" p107 and p130 through a conserved LXCXE sequence within the conserved region 2 sequences thereby impairing their ability to control cell-cycle dependent transcription [346,347]. These sequences often involve the viral E6 and E7 genes, which produce proteins that interfere with cellular regulatory mechanisms and contribute to the transformation of normal cells into cancerous cells. Variations in these genes can affect the severity of their oncogenic effects. Additionally, KSHV isolates were identified in patients of different geographical regions, indicating the importance of these newly isolated strains in developing better diagnostic procedures and novel treatment approaches in the context of KSHV-associated malignancies as well as enriching potential vaccine studies [348–350]. The cytoplasmic tail of KSHV-K1 protein contains two SH2 binding motifs that together constitute an immunoreceptor tyrosine-based activation motif (ITAM) [351]. ITAM motif consisting of six conserved amino acid residues spaced precisely over 26-amino acid sequence,$(D/E)X_7(D/E)X_2YX_2LX_7YX_2L/I$ [352], is able to constitutively induce angiogenic and inflammatory responses via AKT and NFkB [353]. Further, EBV was initially categorized into two primary sub-types, namely type 1 and type 2, based on the genetic sequences of two EBV-encoded genes, EBNA2 and EBNA3. Type 1 is widespread globally, whereas type 2 is primarily found in sub-Saharan Africa. Currently, more than 71 distinct EBV strains have been documented. These EBV variants exhibit varying replication characteristics, and individuals can potentially be infected with multiple strains. It has been observed that certain EBV strains possess a higher oncogenic potential compared to others. For instance, the EBV strain M81, derived from nasopharyngeal carcinoma (NPC), exhibits an elevated rate of replication in B cells and a remarkably strong tendency to infect epithelial cells [354,355]. Ongoing research efforts are increasingly delving into the diversity of EBV latent and lytic genes among the various EBV strains, aiming to discover high-risk EBV strains. This attempt holds the potential to identify individuals at a higher risk of infection and pave the way for the development of effective EBV vaccines and anti-EBV T-cell therapies [354].

Nonetheless, it is noteworthy that the oncogenic potency of HCMV clinical strains varies between low and high-risk strains. HCMV-DB and HCMV-BL have been classified as high-risk strains in

which they possessed their oncogenic potentials in acutely infected HMECs in vitro showing sustained transformation [125,126,209,356]. Upon infection with HCMV high-risk strains, there was an increase in the activation of Myc and EZH2 as well as the induction of polyploidy. This activation of the mentioned axis was significantly more pronounced in CTH cells. Moreover, it has been previously shown that the high-risk HCMV-BL strain robustly induces Myc expression while suppressing p53 levels [126]. This can enhance the replicative potential of stem cells and the reprogramming of progenitor cells in breast cancer, as Myc is identified as a transcriptional target of p53 in mammary stem cells and is activated upon p53 loss. Furthermore, HCMV-DB increases pRb repression [125], with the pRB-E2F pathway known to regulate the expression of EZH2 [357]. Previously, in experiments involving the infection of HMECs with KM, FS, and TB40/E strains, no significant activation of molecular oncogenic pathways was observed upon acute infection, nor were CTH cells detected in cultures [126,356]. This was especially notable when compared to the high-risk HCMV-DB and BL strains. Consequently, it is reasonable to classify HCMV-KM, FS, and TB40/E strains as low-risk strains. This conclusion is consistent with the absence of colony formation in soft agar assays following seeding HMECs infected with HCMV-KM, FS, and TB40/E strains. This underscores the hypothesis that the HCMV high-risk strains, namely DB and BL differentially induce Myc upregulation and consequently stimulating EZH2 overexpression and polyploidy induction, thus pointing to the presence of the Myc/EZH2/PGCCs axis as a key factor underlying these observed results [126]. With regard to immune responses, Myc suppresses immune surveillance by modulating the expression of the innate immune regulator (CD47, also known as integrin-associated protein) and the adaptive immune checkpoint namely, programmed death ligand 1 (PD-L1, also known as CD274 and B7-H1) [358]. Further, Myc suppresses thrombospondin-1 gene [359], type 1 IFN [360], interleukin-2, and perforin [358]. Hence, Myc initiates and maintains tumorigenesis through the modulation of immune regulatory molecules [361]. These high-risk strains were also characterized by PI3K/Akt pathway activation. PI3K/Akt activation induced inflammation and immunosuppression through nitric oxide synthase (NOS) overexpression; thus, resulting in tumor initiation *via* the activated Notch pathway leading to tumor progression. On the other hand, suppression or mutation of p53 has been shown to decrease MHC-I presentation, increase STAT3 phosphorylation,

upregulate PD-L1 *via* microRNA (miR34), elevate pro-inflammatory chemokine and cytokine production, and indirectly upregulate the expression of chemokine receptors (CXCR4 and CXCR5). Loss of Rb leads to the increase in CCL2 and IL6 secretion and this is because of the elevated fatty acid oxidation (FAO) activity and enhanced mitochondrial superoxide (MS) production. Indeed, those molecular alterations have been linked to immune suppression in the TME [70].

Chapter 5

5. Study Objectives

Objective 1:

In the context of breast cancer, previous studies that were conducted by our research team demonstrated the ability of HCMV-DB and HCMV-BL strains in transforming primary HMECs into CMV-Transformed HMECs (CTH) cells in vitro. CTH cells, which are slow self-renewing cells, undergo diverse stages of the giant cell cycle. They were shown to be heterogeneous, generate PGCCs, exhibit dedifferentiation, and display stemness and EMT/MET features. Herein, we aimed to:

- Characterize two HCMV strains, B544 and B693, isolated from TNBC biopsies and assess their transformation potential in vitro.
- Evaluate the resulting cellular phenotype and examine the genetic and molecular features induced by these strains.
- Examine the sensitivity of CTH cells to combination therapy using paclitaxel (PTX) and ganciclovir (GCV).

Objective 2:

With regards to GBM, since HCMV-DB and BL clinical strains previously transformed HMECs into CTH cells and as HCMV has been detected in malignant gliomas, we aimed to discover its transforming potential in human astrocytes (HAs) by setting the following objectives:

- Screening HCMV-DB and BL clinical strains for their transforming capacity in HAs and investigating the molecular and cellular characteristics of CMV-induced glioblastoma cells (CEGBCs) that emerge during long-term cultures.
- Examining the impact of temozolomide (TMZ), Ganciclovir (GCV), and the EZH2 inhibitor (GSK 343) on this glioblastoma model.

- Exploring the potential link between the triad of HCMV, CEGBCs and EZH2, as well as the potential interrelation with Myc in the context of glioblastoma carcinogenesis.
- Investigating the morphological and phenotypic characteristics of CEGBCs and assess the potential implication of Myc and EZH2 in both CEGBCs and GBM biopsies.
- Isolating eleven clinical HCMV strains from GBM biopsies, analyzing their oncogenic, stemness, and invasiveness properties when cultured on HAs, as well as evaluating the potential effectiveness of combination therapy in curtailing these effects.

Objective 3:

In the context of ovarian cancer and since HCMV-DB and BL clinical strains previously transformed HMECs and HAs into CTH and CEGBCs cells, respectively, we decided to investigate the potential association between HCMV infection and epithelial ovarian cancer, particularly in the case of high-grade serous ovarian cancer (HGSOC) through setting the objectives below:

- Assessing the transforming capacities of the two high-risk clinical strains namely, HCMV-DB and HCMV-BL, as well as exploring the molecular and cellular characteristics that emerged during long-term cultures of "CMV-transformed Ovarian cells" (CTO cells).
- Isolating clinical HCMV strains from HGSOC biopsies displaying high EZH2 expression and investigating their oncogenic and stemness properties when cultured on OECs.
- Evaluating the efficacy of EZH2 inhibitors in curtailing CTO's oncogenic and stemness features.

Chapter 6

6. Materials And Methods

6.1 Reagents

All the reagents that were used including primers, antibodies, and therapies were provided in the tables below **(Table 4, Table 5, and Table 6)**.

Table 4: Primers Used.

Primer	Primer Sequence
IE1-forward	5'-CGACGTTCCTGCAGACTATG-3'
IE1-reverse	5'-TCCTCGGTCACTTGTTCAAA-3'
UL69-forward	5'-GGGATGTCGATGACTCCCTTC-3'
UL69-reverse	5'-GTCGCTATTGGATCTCACCGT-3'
EZH2-forward	5'-TCGTGCCCTTGTGTGATAGC-3'
EZH2-reverse	5'-TCTCGGACAGCCAGGTAGC-3'
MYC-forward	5'-ACACCCTTCTCCCTTCG-3'
MYC-reverse	5'CCGCTCCACATACAGTCC3'
Akt-forward	5'-ATCCCCTCAACAACTTCTCAGT-3'
Akt-reverse	5'-CTTCCGTCCACTCTTCTCTTTC-3'
LncRNA4.9-forward	5'-GTGAACCGATACGGGTGGAG-3'
LncRNA4.9-reverse	5'-CATTTGAACAGAGAAAGGTGG-3'
LncRNA HOTAIR-forward	5'-GGTAGAAAAAGCAACCACGAAGC-3'
LncRNA HOTAIR-reverse	5'-ACATAAACCTCTGTCTGTGAGTGCC-3'
SOX2-forward	5′-GGGAAATGGAGG GGTGCAAAAGAGG-3′
SOX2-reverse	5′-TTGCGTGAGTGT GGATGG GATTGGTG-3′
Nanog-forward	5′-TCCTCCTCTTCCTCTATACTAAC-3′
Nanog-reverse	5′-CCCACAATCACAGGCATAG-3′
Oct4-forward	5′-TGGAGAAGGAGAAGCTGGAGCAAAA-3′
Oct4-reverse	5′-GGCAGAGGTCGTTTGGCTGAATAGACC-3′
OLIG2-forward	5'-CTCCTCAAATCGCATCCAG-3'
OLIG2-reverse	5'-AAAAGGTCATCGGGCTCTG-3'
CD133-forward	5'- GGGAGAACAA TAATAGGATATTTTGAA-3'
CD133-reverse	5'-CGATGCCACTTTCTCACTGAT3'
CD44-forward	5'-GACAAGTTTTGGTGGC ACG-3′
CD44-reverse	5'-CACGTGGAATACACCTGCAA-3′
c-MET-forward	5'-CATCTCAGAACGGTTCATGCC-3'
c-MET-reverse	5'- TGCACAATCAGGCTACTGGG-3'

EGFR-forward	5’-TGCGTCTCTTGCCGGAAT-3’
EGFR-reverse	5’- GGCTCACCCTCCAGAAGGTT-3’
CNDK2A-forward	5’-GGGAGCAGCATGGAGCCG-3’
CNDK2A-reverse	5’-AGTCGCCCGCCATCCCCT-3’
CCND1-forward	5’-GCGAGGAACAGAAGTGC-3’
CCND1-reverse	5’-GAGTTGTCGGTGTAGATGC-3’
GAPDH-forward	5’-CCCCTCTTCAAGGCCTCTAC-3’
GAPDH-reverse	5’-CGACCACTTTGTCAAGCTCA-3’
β-2-Microglobulin-forward	5’-GATGAGTATGCCTGCCGTGTG-3’
β-2-Microglobulin-reverse	5’-CAATCCAAATGCGGCATCT-3’

Table 5: Antibodies Used.

Antibody	Catalog Number/Source
Myc	06-549/Upstate, Lake Placid, NY, USA
Anti-Myc Tag	06-549-25UG/Merck KGaA, (Darmstadt, Germany)
EZH2	39875/Active Motif (Carlsbad, CA, USA)
Ki67 Ag	BD-556026/BD Biosciences (Franklin Lakes, USA)
CMV pp72 (IE1)	SC-69834/Santa Cruz Biotechnology (CA, USA)
HCMV Late antigen	11-005 Argene (Varilhes, France)
IE1/2	ab53495/Abcam (Cambridge, UK)
p53	SC-47698/Santa Cruz Biotechnology (CA, USA)
Rb	SC-102/Santa Cruz Biotechnology (CA, USA)
pRb	SC-377528/Santa Cruz Biotechnology (CA, USA)
Nestin	SC-23927/Santa Cruz Biotechnology (CA, USA)
GFAP	SC-166481/Santa Cruz Biotechnology (CA, USA)
Oct4	ab19857/Abcam (Cambridge, UK)
SOX2	ab97959/Abcam (Cambridge, UK)
Nanog	SC-293121/Santa Cruz Biotechnology (CA, USA)
SUZ12	AB_2614929/Active Motif (Carlsbad, CA, USA)
OLIG2	ab109186/Abcam (Cambridge, UK)
EpCAM	BD-347197/BD Biosciences (Franklin Lakes, USA)
pp65	SC-52401/Santa Cruz Biotechnology (CA, USA)
SSEA-4	SC-21704/Santa Cruz Biotechnology (CA, USA)
AKT	SC-5298/Santa Cruz Biotechnology (CA, USA)
pAKT (Ser473)	SC-293125/Santa Cruz Biotechnology (CA, USA)
CD44	BD-555478/BD Biosciences (Franklin Lakes, USA)

CD24	BD-555428/BD Biosciences (Franklin Lakes, USA)
CD49f	BD-555735/BD Biosciences (Franklin Lakes, USA)
Vimentin	SC-6260/Santa Cruz Biotechnology (CA, USA)
E-cadherin	SC-8426/Santa Cruz Biotechnology (CA, USA)
Phalloidine	ab235137/ Abcam (Cambridge, UK)
Propidium Iodide	P3566/Life Technologies (*Eugene*, USA)
Annexin V	BD-65874 BD Biosciences (Franklin Lakes, USA)
FITC-conjugated anti-mouse antibody	BD- 553399/BD Biosciences (Franklin Lakes, USA)
PE-conjugated anti-mouse antibody	BD-551436/BD Biosciences (Franklin Lakes, USA)
FITC-conjugated anti-rabbit antibody	ab6717/Abcam (Cambridge, UK)
FITC-conjugated Goat Anti-Mouse	BD-555988/BD Biosciences (Franklin Lakes, USA)
FITC-conjugated Rat Anti-Mouse	BD-553443/BD Biosciences (Franklin Lakes, USA)

Table 6: Treatments Used.

Drugs	**Dosage**
GCV	20 μM
PTX	20nM
TPA	100 nM
TMZ	50 μM
GSK343	0.1 μM
EPZ6438	0.1 μM

6.2 Cell Cultures

Human primary mammary epithelial cells (HMECs, A10565) were purchased from Life Technologies (Carlsbad, CA, USA), and were cultured in HMEC medium (Life Technologies) supplemented with HMEC supplement and bovine pituitary extract (Life Technologies). Human breast cancer cell lines MDA-MB231 and MCF7 were obtained from Institut Hiscia (Arlesheim, Switzerland). Human embryonic lung fibroblasts (MRC5, 84002) were purchased from RD-Biotech (Besançon, France). MRC5, MDA-MB231 and MCF7 cells were grown in Dulbecco's modified Eagle medium (DMEM) (PAN-Biotech, Aidenbach, Germany) supplemented with 10% fetal bovine serum (Dutscher, Bernolsheim, France) and penicillin (100U/mL)-streptomycin (100μg/mL) (Life Technologies, Eugene, OR). Primary human astrocytes (HAs) were purchased from Innoprot (Derio, Spain) and cultivated in astrocytes medium (Innoprot). Human ovarian

surface epithelial cells (HOSE cells or OECs, as mentioned in our study) were purchased from Innoprot (Derio, Spain), and cultivated in ovarian epithelial cell medium (serum-free) supplemented with ovarian epithelial cell growth supplement (OEpiCGS) and penicillin/streptomycin solution (P60132, Innoprot). To note that, HOSE cells or OECs were isolated from healthy human ovaries, as mentioned in the technical data sheet (P10982, Innoprot).

CTH and CTO cells emerging following chronic HCMV infection were cultured in the same condition as HMECs and OECs, respectively. With regards to CEGBCs isolation and growth, upon the appearance of large cellular clusters/structures in HAs cultures that were infected with HCMV-DB and BL isolates, clusters were gently detached. CEGBCs were initially cultivated in HAs medium complemented with low levels of fetal bovine serum (2%) as per the manufacturer's recommendations. At day 150 post-infection, since CEGBCs resemble stem cells compared to uninfected HAs, serum was excluded and this is to fit with the optimal conditions of serum-free stemness growth as requested for glioblastoma cell cultures [362]. Serum was omitted at day 5 post-infection of HAs with the HCMV strains that were isolated from GBM biopsies. CTH, CEGBCs, and CTO cultures used in this study were maintained for at least 9 months in culture.

All cells were cultured under standard conditions (37°C, 5% CO2, 95% humidity). Cultures were verified as mycoplasma-free as determined by monthly screenings (VenorGem classic mycoplasma detection, Minerva Biolabs).

6.3 HCMV Isolates Growth and Detection

Clinical HCMV strains, namely HCMV-DB (GenBank KT959235), BL (GenBank MW980585), KM, and FS were isolated from patients that were hospitalized at Besançon University Hospital (France) as described previously [125,209]. Data corresponding to TNBC biopsies and other HCMV strains were reported previously [125,126]. Cell-free virus stocks and infections were performed as previously detailed [125]; to prepare these stocks, HCMV strains were propagated in MRC5 cells for only few passages to avoid losing the ULb' region. It is worth mentioning that careful screening of our viral stocks was conducted to rule out the presence of other oncoviruses. Infections of cells (HMECs, HAs, MRC5, and OECs), quantification of viral replication, and HCMV detection were performed as previously described [125,126]. Briefly, the aforementioned

cells ($1x10^6$) infection with the clinical isolates was performed at a multiplicity of infection (MOI) of 1. Cells were incubated at 37 ℃ for two hours, after which the inoculum was dis-carded, and the cell monolayer was washed three times using 1X PBS and afterwards covered with fresh medium. HAs ($3x10^6$) cells infection with HSV was performed at a MOI of 1.

For HCMV quantification, cell-free infectious supernatant was collected, DNA was isolated (EZNA Blood DNA Kit, D3392-02, Omega BIO-TEK, Norcross, GA) and real-time quantitative PCR (qPCR) was performed using a Stratagene Mx3005P thermocycler (Agilent Technologies, Santa Clara, CA) and IE1 primers. Where specified, UL69 as well as HCMV lncRNA4.9 were detected by the qPCR assay. qPCR was performed using a KAPA SYBR FAST Master Mix (KAPA BIOSYSTEMS, KK4601, Potters Bar, UK); reactions were activated at 95 °C for 10 min, followed by 50 cycles (15 seconds at 95 °C and 1 min at 60 °C). Results were collected and analyzed using MxPro qPCR software.

6.4 Microscopy

Olympus optical microscope (Olympus Corporation, Tokyo, Japan) and OPTIKA digital camera (Optica Microscopy, Ponteranica, Italy) were used to monitor the short and long-term cultures of infected HMECs, MRC5, HAs, and OECs including CTH, CEGBCs, and CTO cells.

Confocal microscopy imaging for all the aforementioned cells was performed as described previously [125]. Briefly, cells were washed with 1X PBS, fixed and permeabilized (BD Cytofix/Cytoperm, 554722) and stained with primary antibodies and their corresponding secondary antibodies listed in **Table 5**. For visualization of the nucleus and the cytoplasm, DAPI (4′, 6′-diamidino-2- phenylindole) and phalloidin staining respectively were performed according to the manufacturer's protocol. Post-staining, the slides were assessed using a 63× oil immersion objective lens with a Carl-Zeiss confocal microscope (Jena, Germany); images were analyzed using ZenBlue Software (Carl-Zeiss Microscopy GmbH).

6.5 Soft Agar Colony Formation Assay

Colony formation in soft agar seeded with uninfected HMECs, B544, B693, DB, and BL-infected HMECs, untreated and PTX/GCV-treated CTH cells, uninfected HAs, CEGBCs, uninfected

OECs, and CTO cells was carried out as mentioned previously [125]. MCF7 and MDA-MB231 were used as positive controls. Briefly, cells were assayed using Cell Biolabs Cytosolic Cell Transformation Assay kit (Colorimetric assay, CB135; Cell Biolabs Inc., San Diego, CA) as per the manufacturer's protocol. The provided MTT solution and a microplate reader (*A*570 nm) were used for detection and quantification of the formation of colonies in soft agar (Cayman Chemical, Ann Arbor, MI). Olympus optical microscope (Olympus Corporation, Tokyo, Japan) and OPTIKA digital camera (Optica Microscopy, Ponteranica, Italy) were used to observe the formed colonies.

6.6 Tumorsphere and Spheroid formation Assays

Tumorsphere formation by uninfected HMECs and HMECs infected with HCMV-B544 and HCMV-B693 was assayed using StemXVivo serum-free tumorsphere media (R&D Systems) supplemented with heparin (2 U/ml) (Sigma) and hydrocortisone (0.5 microg/ml) (Sigma) following the manufacturer's protocol and as described previously [125].

Spheroids of CEGBCs were prepared as described previously [363,364]. Single cells ($1x10^4$) isolated by accutase were seeded in a serum-free astrocytes medium containing methylcellulose. Where indicated, drugs were mixed in serum-free astrocytes medium with 0.4% methylcellulose. Treatment was renewed daily. Spheroid size and surface area were determined using the ImageJ software, taking the mean length of the major and minor axis of the spheroid at a given time point compared to the initial measurements at time zero. Spheroids of OECs were prepared as described previously [365]. Single cells ($1x10^4$) isolated by accutase were seeded in a serum-free OECs medium containing methylcellulose.

6.7 Flow Cytometry Analysis

Cells (1×10^5) were collected from uninfected HMECs, HAs, OECs, as well as CTH cells, HCMV-infected HAs, CEGBCs, HCMV-infected OECs, and CTO cells including treated cells (where indicated). Cells were fixed, permeabilized, and stained as previously reported [125,126]. Briefly, cells were fixed and permeabilized using 100 µl of BD Biosciences Cytofix/Cytoperm solution for 20 minutes at 4°C and washed with BD Biosciences 1X BD perm/wash solution. One half of the cells were stained using the respective primary antibody and the remaining cells were mock stained

to identify secondary antibody background staining. Cells were incubated at 4°C for 1 hour in the dark, washed twice with BD Biosciences 1X BD perm/wash solution and incubated at 4°C for 1 hour in the dark with the corresponding secondary antibody. Cells were then washed twice and subjected to cytofluorometric analysis. For cell cycle analysis, uninfected OECs or CTO cells were washed in 1X PBS, fixed in 70% ethanol, and resuspended in 50 µg/ml propidium iodide (P3566, life technologies, Eugene, USA) with 0.1 mg/ml RNase (R4642, Sigma-Aldrich, Saint-Louis, MO, USA), then incubated at 37°C for 30 min as described previously. Cytofluorometric analysis was achieved using a BD LSRFortessa X-20 (BD Biosciences) flow cytometer. FACSDiva software (BD Biosciences) was used for data collection and analysis.

6.8 Western Blotting

Expression of IE1, pp65, Myc, EZH2, Akt, and pAkt in uninfected HAs and HCMV-infected HAs as well as IE1, pp65, Myc, EZH2, Sox2, Nanog, E-cadherin, and vimentin expression in uninfected OECs, HCMV-infected OECs and CTO cells were assessed as described previously [125]. Densitometry using ImageJ 1.40 software (National Institutes of Health, Bethesda, MA, USA) was applied to quantify protein levels. β-actin was used as a loading control.

6.9 RT^2 Profiler PCR Array

The RT^2 profiler PCR array was performed as detailed previously [356]. Total RNA was extracted from uninfected HAs, and CEGBCs-DB and BL using an RNA extraction kit (EZNATotal kit I,Omega BIO-TEK). Afterwards, cDNA was synthesized using the SuperScript IV First-Strand Synthesis kit (Invitrogen, Carlsbad, CA, USA) following the manufacturer's protocol. RT^2 Profiler PCR Arrays for human oncogenes & tumor suppressor genes (PAHS502ZR) (from Qiagen,Germantown,MD,USA) were performed using Mx3005P real-time PCR system as per manufacturer's instructions. Fold regulation was analyzed using the delta-delta Ct method [356,366].

6.10 RNA Cross-linking Immunoprecipitation (RNA CLIP) assay

RNA CLIP assay was performed on CEGBCs and uninfected HAs as previously reported [126,320]. qPCR analysis of EZH2 immunoprecipitated samples (IP EZH2) and negative control

(IP IgG) were normalized with respect to each input and expressed as (2(−ΔCt)) x100 (% Input) as previously reported [126].

6.11 Assessment of telomerase activity

Uninfected OECs and CTO cells were collected, washed with PBS, and resuspended in RIPA lysis buffer and 4% protease inhibitor on ice for 30 minutes. Samples were then centrifuged at 16,000 g for 30 minutes at 4°C and the protein concentration was determined using Bradford assay (DC Protein Assay kit, Bio-Rad Laboratories, Hercules, CA). Telomerase activity was assessed as described previously and according to the manufacturer's instructions.

6.12 Quantitative Reverse Transcription PCR (RT-qPCR)

In CTH cells, the detection of absolute mRNA levels of epidermal growth factor receptor (EGFR), cyclin dependent kinase inhibitor 2A (CNDK2A), cyclin D1 (CCND1), SOX2, Oct4, and Nanog was assessed by RT-qPCR. Furthermore, RT-qPCR was also used to detect the transcripts of IE1, UL69, Myc, EZH2, OLIG2, CD133, SOX2, CD44, EGFR, MET, HCMV lncRNA4.9, and cellular lncRNA HOTAIR in CEGBCs as well as the IE1, UL69, EZH2, Myc, Sox2, Nanog, and Oct4 transcripts in CTO cells. RT-qPCR was performed as detailed previously [126,356]. In brief, RNA was extracted from the biopsies or the aforementioned cells using the EZNA® Total RNA Kit I (Omega BIO-TEK, Norcross, GA, USA). Reverse transcription was carried out using the SuperScript IV First-Strand Synthesis kit (Invitrogen, Carlsbad, CA, USA). The expression of markers was assessed by performing real-time qPCR using a KAPA SYBR FAST Master mix (KAPA BIOSYSTEMS, KK4601) and specific primers according to the manufacturer's protocol. The fold change expression was calculated by adopting the delta-delta Ct method [356].

6.13 Invasion Assay

Collagen invasion assay: Collagen I (Corning, New York, NY) of 1 mg/ml concentration was prepared in 1X PBS with 7.2mM NaOH and 0.1% HCl was added. Where indicated, treatments, were mixed directly into the collagen gels. Prepared spheroids were incubated on ice for 30 min and then separately selected, washed in PBS, and subsequently included in the collagen solution.

After 1 hour at 37°C in a cell incubator, serum-free astrocytes medium including the diverse treatments was added. Secondly, 3D astrocyte scaffold invasion assay: scaffolds were formed by HAs in hyperconfluent culture. Afterwards, CEGBCs-DB and BL spheroids were cultured on top of HAs scaffolds. Spheroids' core area and invasion area were measured using ImageJ software; protrusions were measured using OPTIKA Vision Pro software and manually quantified.

6.14 Treatments

Where indicated, CTH cells were treated with ganciclovir (GCV) and paclitaxel (PTX). CEGBCs-DB and BL were under GCV, temozolomide (TMZ), and EZH2 inhibitor (GSK343). Treatments was renewed every day. Further, CTO-DB and BL were treated with the two EZH2 inhibitors (GSK343 and EPZ6438). Treatment was renewed every 2 days. CTH, CEGBCs, and CTO cells were also treated with 12-O-45 tetradecanoylphorbol-13-acetate (TPA); treatment was renewed daily. The dosages corresponding to each drug were provided in **Table 6**.

6.15 Tumor Biopsies and HCMV isolation

6.15.1 Tumor Biopsies

All tumor biopsies were provided by the Regional tumor bank (BB0033-00024 Tumorothèque Régionale de Franche-Comté). It's worth noting that a written informed consent for participation was obtained from all patients. The studies were authorized by the local ethics committees of Besançon University Hospital (Besançon, France) and the French Research Ministry (AC-2015-2496, CNIL n°1173545, NF-S-138 96900 n°F2015).

-Tumor breast biopsies (luminal tumor biopsies n=10 and basal tumor biopsies n=9) and adjacent healthy breast biopsies (n=8). The treatment, clinical outcome and pathological data for these two TNBC patients were described previously [126].

-GBM biopsies [n=37; O (6)-methylguanine DNA methyltransferase (MGMT) promoter methylated GBM biopsies n=17, and MGMT promoter unmethylated GBM biopsies n=20] as well as healthy brain biopsies (n=4). Clinical and biological data of the GBM patients were provided in **Table 7**.

Table 7: Clinical and biological data of the GBM patients.

GBM Patients N°	Age (years)	Sex (F/M)	CMV detection (IE1/UL69 Expression)	EZH2 Fold gene Expression (Low/Intermediate/ High)	Myc Fold gene Expression (Low/Intermediate/ High)	Akt Fold gene Expression (Low/Intermediate/ High)
MGMT PROMOTER METHYLATED GBM BIOPSIES (n=17)						
1	53	M	+/+	*	*	**
2	81	M	+/+	**	**	***
3	77	F	+/+	**	**	*
4	79	F	+/+	***	**	**
5	70	M	+ /+	*	*	*
6	68	F	+/+	**	**	*
7	85	M	+/+	**	**	*
8	72	F	+/+	*	*	*
9	75	F	+/+	**	*	*
10	76	M	+/+	***	**	*
11	69	F	+/+	*	*	*
12	22	M	+/+	*	*	*
13	76	M	+/+	***	**	**
14	68	M	+/+	*	*	*
15	84	F	+/+	*	*	**
16	64	F	+/+	*	*	**
17	59	M	+/+	*	*	*
Mean	**69.29**	**[8F/9M] 47-53%**	**[+/+]**	**[9*/5**/3***] 53-29-18%**	**[10*/7**/0***] 59-41-0%**	**[11*/5**/1***] 65-29-6%**
MGMT PROMOTER UNMETHYLATED GBM BIOPSIES (n=20)						
18	50	M	+/+	***	**	*
19	42	M	+/+	*	*	*
20	77	M	+/+	***	*	*
21	76	M	+/+	***	***	**
22	68	F	+/+	*	*	*
23	69	M	+/+	**	**	*
24	59	M	+/+	**	**	*
25	59	M	+/+	**	**	***
26	73	M	+/+	*	*	*
27	72	F	+/+	*	*	*
28	55	M	+/+	*	*	*
29	77	F	+/+	**	*	**
30	78	F	+/+	**	*	**
31	65	M	+/+	***	**	***
32	41	M	+/+	**	*	*
33	46	F	+/+	**	**	*
34	73	F	+/+	*	*	*
35	65	M	+/+	**	*	**
36	67	F	+/+	*	*	*

37	47	F	+/+	*	*	*
Mean	**62.95**	**[8F/12M] 40-60%**	**[+/+]**	**[8*/8**/4***] 40-40-20%**	**[13*/6**/1***] 65-30-5%**	**[14*/4**/2***] 70-20-10%**
TOTAL GBM BIOPSIES (n=37)						
Mean	**65.86**	**[16F/21M] 43-57%**	**[+/+]**	**[17*/13**/7***] 46-35-19%**	**[23*/13**/1***] 62-35-3%**	**[25*/9**/3***] 68-24-8%**

Key: Myc Fold gene expression: *Low: <10; **Intermediate:10-100; ***High: >100; EZH2 Fold gene expression: *Low: <10; **Intermediate:10-100; ***High: >100; Akt Fold gene expression: *Low: <1; **Intermediate:1-10; ***High: >10 .

-Ovarian biopsies (n=25; HGSOC biopsies n=18, and adjacent non-tumoral biopsies n=7) were provided by the Regional tumor bank (BB0033-00024 Tumorothèque Régionale de Franche-Comté). Clinical data and treatments of the OC patients were provided in **Table 8**.

Table 8: Clinical data and treatments of the OC patients.

Biopsy #	Age	Tumor	Metastasis	Chemotherapy
1	67	HGSOC	+	carboplatin – gemcitabine - bevacizumab
2	64	HGSOC	+	carboplatin -paclitaxel
3	50	HGSOC	+	bevacizumab-carboplatin -paclitaxel -pegylated liposomal doxorubicin-HIPEC
4	82	HGSOC	+	carboplatin – gemcitabine – bevacizumab - paclitaxel
5	63	HGSOC	+	carboplatin -paclitaxel - pegylated liposomal doxorubicin
6	48	HGSOC	+	bevacizumab – carboplatin – paclitaxel - pegylated liposomal doxorubicin
7	57	HGSOC	+	topotecan
8	79	HGSOC	-	carboplatin -paclitaxel
9	70	HGSOC	+	carboplatin – gemcitabine - bevacizumab
10	57	HGSOC	-	carboplatin - cyclophosphamide
11	70	HGSOC	+	carboplatin -paclitaxel - pegylated liposomal doxorubicin – gemcitabine -topotecan
12	54	HGSOC	+	carboplatin -paclitaxel - bevacizumab
13	56	HGSOC	+	carboplatin -paclitaxel
14	88	HGSOC	+	carboplatin -paclitaxel
15	60	HGSOC	+	carboplatin -paclitaxel
16	64	HGSOC	+	carboplatin -paclitaxel
17	57	HGSOC	+	docetaxel - carboplatin -paclitaxel
18	44	HGSOC	+	carboplatin - paclitaxel

6.15.2 Genes and Transcripts Expression As Well As Polyploidy Detection Within Tumor Biopsies

RNA was extracted from TNBC biopsies (B544 and B693) followed by reverse transcription to measure EGFR, CNDK2A, CCND1, SOX2, Oct4, and Nanog mRNA expression by RT-qPCR. Genomic DNA was isolated from GBM as well as OC biopsies, and HCMV presence was identified by qPCR using specific primers against IE1 and UL69 genes. Further, RNA was extracted from GBM and OC biopsies and reverse transcription was performed as reported previously. For GBM biopsies, expression of EZH2, Myc, Akt, and GAPDH was assessed by real-time qPCR using specific primers according to the manufacturer's protocol. For OC biopsies, the expression of EZH2, Myc, Akt, and β-2-Microglobulin was assessed by real-time qPCR using specific primers according to the manufacturer's protocol. Fold change expression in TNBC, GBM and OC biopsies versus healthy breast and brain biopsies as well as adjacent non-tumoral OC biopsies, respectively was calculated using the delta-delta Ct method.

In TNBC biopsies, hematoxylin and eosin slides were used to detect PGCCs presence based on Zhang et al. description, with PGCCs being defined as a cancer cell with a nucleus at least three times larger than that of a diploid cancer cell [115]. PGCCs presence in HGSOC biopsies was confirmed by hematoxylin and eosin staining; briefly, PGCCs were counted in five hot spots of each tumor sample (magnification x400, field diameter of 250 µm and 100 µm, Zeiss Axiostar).

6.15.3 HCMV Isolation From Tumor Biopsies

HCMV strains, B544 and B693, were isolated from TNBC patient biopsies by mechanical tissue disruption and filtration of the frozen biopsy through a 0.45 µm filter and initially grown on MRC5 cells. The supernatant from MRC5 culture was filtrated through a 0.45 µm filter and used to infect HMECs. The purity of our HCMV cultures was confirmed by ruling out the presence of other viruses (Epstein-Barr virus, human papillomavirus, Kaposi sarcoma herpesvirus and adenovirus). Eleven HCMV-GBM strains were isolated from MGMT promoter methylated (n=4) and promoter unmethylated (n=7) GBM biopsies by mechanical tissue disruption and filtration of the frozen biopsy through a 0.45 µm filter and initially grown on MRC5 cells. The supernatant from MRC5 culture was used to infect fresh human astrocytes. The purity of our HCMV cultures was confirmed by ruling out the presence of other viruses (Epstein-Barr virus and human papillomavirus). Three

HCMV-OC strains were isolated from HGSOC biopsies. Neither human papillomavirus (HPV) nor Epstein-Barr virus (EBV) was detected in the OC biopsies.

6.16 Statistical Analyses

All quantitative results are reported as mean ± SD of the independent experiments. Statistical analyses were done using Wilcoxon and Mann-Whitney tests; a p-value≤0.05 was considered to be statistically significant [*: ≤0.05; **: ≤0.01; ***: ≤0.001]. Correlation analyses were done using Spearman, Pearson, and Kendall's Tau correlation tests. Microsoft Excel was used to construct the plots and histogram data.

Chapter 7

7. Results

7.1 Oncogenic and Stemness Signatures of the High-Risk HCMV Strains in Breast Cancer Progression

7.1.1 Growth of Two HCMV Clinical Strains Isolated from TNBC in HMECs and the Emergence of Morphologically Distinct Cells

To assess the cellular environment achieved by HCMV, B544 and B693 were isolated from TNBC biopsies and grown in MRC5 cells, revealing a viral growth at days 3 and 5 post-infection (PI) **(Figure 10A)**. At day 1 post-HMECs infection, HCMV-IE1 and pp65 were detected with confocal microscopy **(Figure 10B)**. HCMV-B544 and B693 promoted the transformation of the infected HMECs toward CTH cells as previously reported [126]. Uninfected HMECs were used as controls which underwent cellular senescence in long-term cultures. At day 110 PI, we detected a wide variety of spheroids and giant cells distributed between round dense cells, flat, and elongated spindle-like cells. Afterwards, lipid droplet-packed cells, multinucleated giant cells, cell budding, and filopodium protrusions were observed in CTH cultures **(Figure 10C,D)**. Hence, this population displayed mesenchymal and fibroblastic-like structures in addition to epithelial and small cells. The above-mentioned detailed cell morphology is close to that of CTH cells which were previously detected in HMEC cultures acutely infected with high-risk BL and DB strains [126]. Thus, the CTH-B544 and CTH-B693 heterogeneous cell population represent transformed and self-renewing cells that are engaged in distinct phases of the giant cell cycle [117,118].

7.1.2 Transformation Capacity of CTH Cells and the Induction of an Oncogenic Environment

To evaluate the transformation of HCMV-B544 and B693 immortalized infected HMECs, cells were seeded in soft agar. Colony formation was detected at day 14 post-seeding in CTH-B544 and CTH-B693 cells (p-value ≤ 0.05) in contrast to uninfected HMECs which showed no changes **(Figure 11A)**. The resulting anchorage-independent growth in CTH cells is a crucial phase in the acquisition of malignancies. With regard to oncogenes, the expression of c-Myc was assessed by performing confocal microscopy imaging where large and elongated CTH cells showed remarkable c-Myc staining compared to uninfected HMECs **(Figure 11B)**. Using flow cytometry, a slightly higher expression of the proliferation marker (Ki67Ag) was detected in CTH-B693

compared to CTH-B544 cells with a limited expression in the uninfected HMECs. Only CTH-B544 and B693 cells were positively stained with Ki67 Ag as detected by confocal microscopy imaging **(Figure 12A)**. On the other hand, a slight increase in the expression of phosphorylated Akt (pAkt-ser473) along with a limited to nonexistent increase in Akt expression levels was shown in all CTH cells compared to uninfected HMECs **(Figure 12B)**. Overall, the acquisition of an immortal phenotype in CTH-B544 and B693 cells reflects their transformation potential.

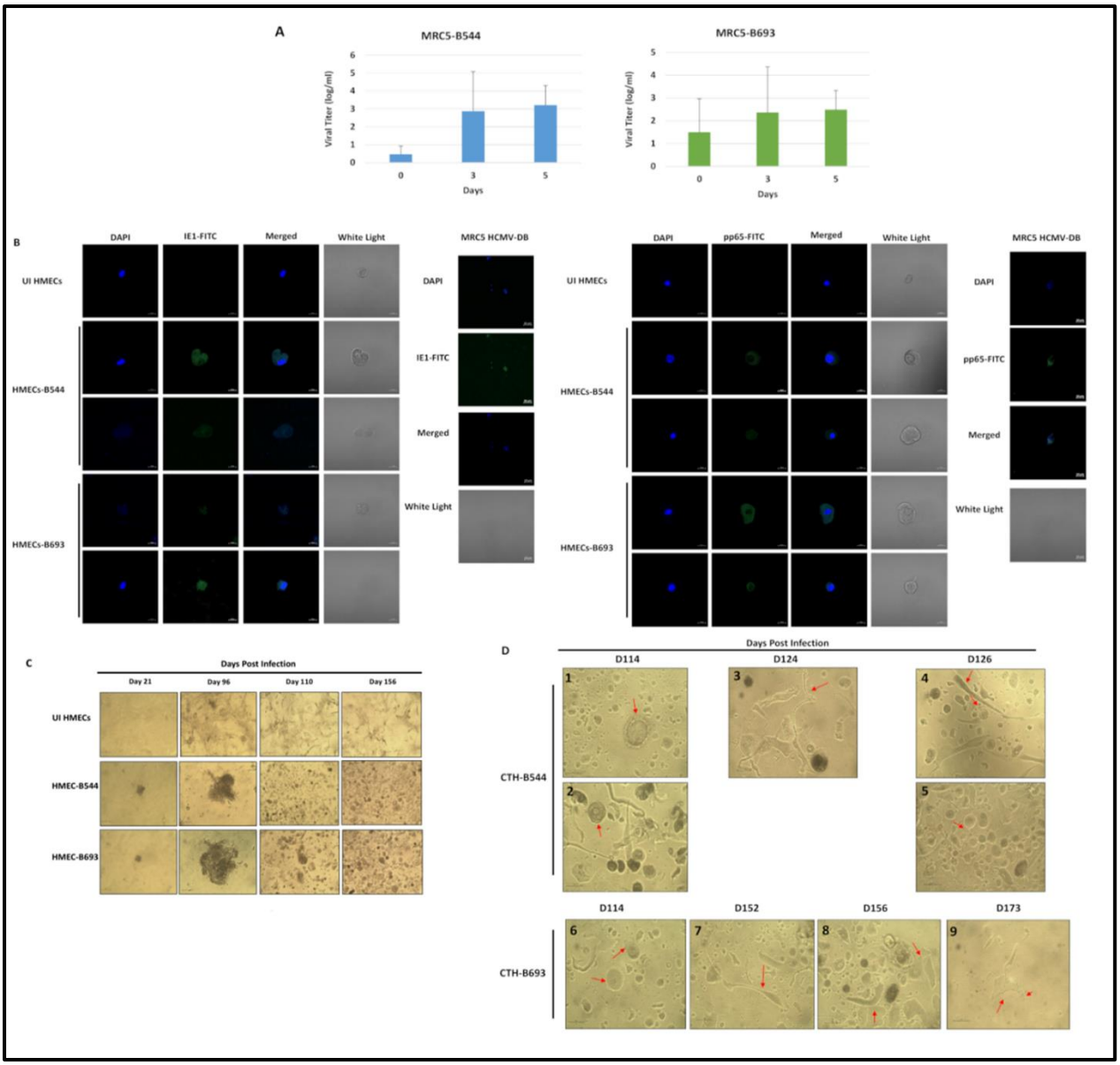

Figure 10: Replication of B544 and B693 strains in MRC5 cultures, and the appearance of morphologically distinct cells following the infection of HMECs with these high-risk strains.

(A) Time-course of the viral titer in the supernatant of MRC5 infected with the strains HCMV-B544 and HCMV-B693, as measured by IE1-qPCR. (B) Confocal microscopic images of HCMV-IE1 and pp65 staining in HMECs infected with HCMV-B544 and HCMV-B693 (day 1 post-infection). Uninfected HMECs were used as controls. Nuclei were counterstained with DAPI; magnification ×63, scale bar 10 µm. (C) HMECs time-course infection with HCMV-B544 and HCMV-B693 strains (MOI = 1). Magnification ×100, scale bar 100 µm. Uninfected HMECs were used as a control. (D) Presence of giant cells with blastomere-like morphology (1 and 6), mesenchymal cells (4 and 7), lipid droplet-packed cells (3, 8, and 9), cells displaying multiple nuclei (2) as well as cell budding (4, 5, and 6), and cells with filopodia protrusions (9) in CTH-B544 and CTH-B693 cells. The inverted light microscope scale bar represents 100 µm; magnification ×200.

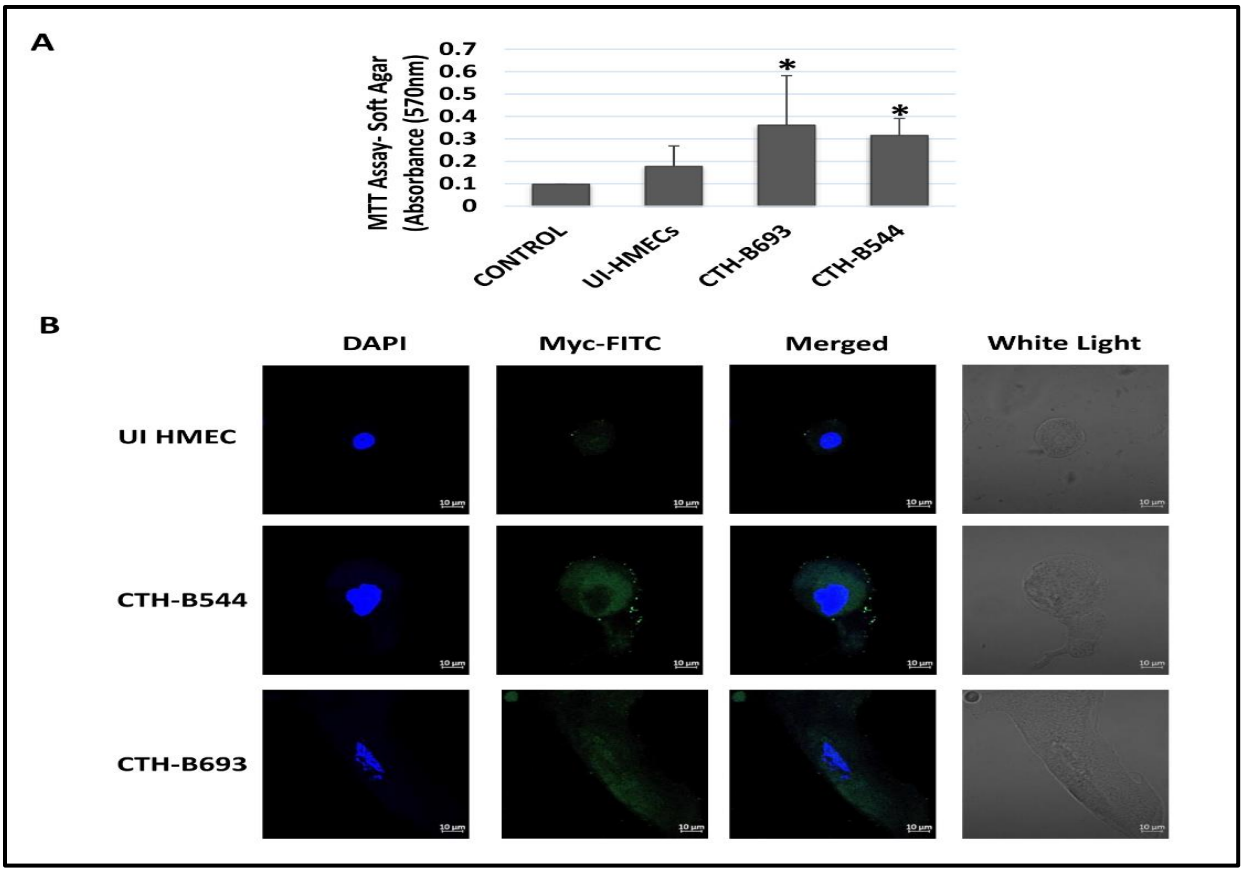

Figure 11: Colony formation in soft agar and Myc expression in CTH-B544 and B693 cells.

(A) Colony formation in soft agar seeded with uninfected HMECs, CTH-B544 and CTH-B693 cells. At day 15 post-seeding, quantification of colonies was performed; Histogram represents the mean data ± SD of three independent experiments. * p-value ≤ 0.05, (B) Confocal microscopic images of Myc and DAPI staining in CTH cells. Magnification ×63, scale bar 10 µm.

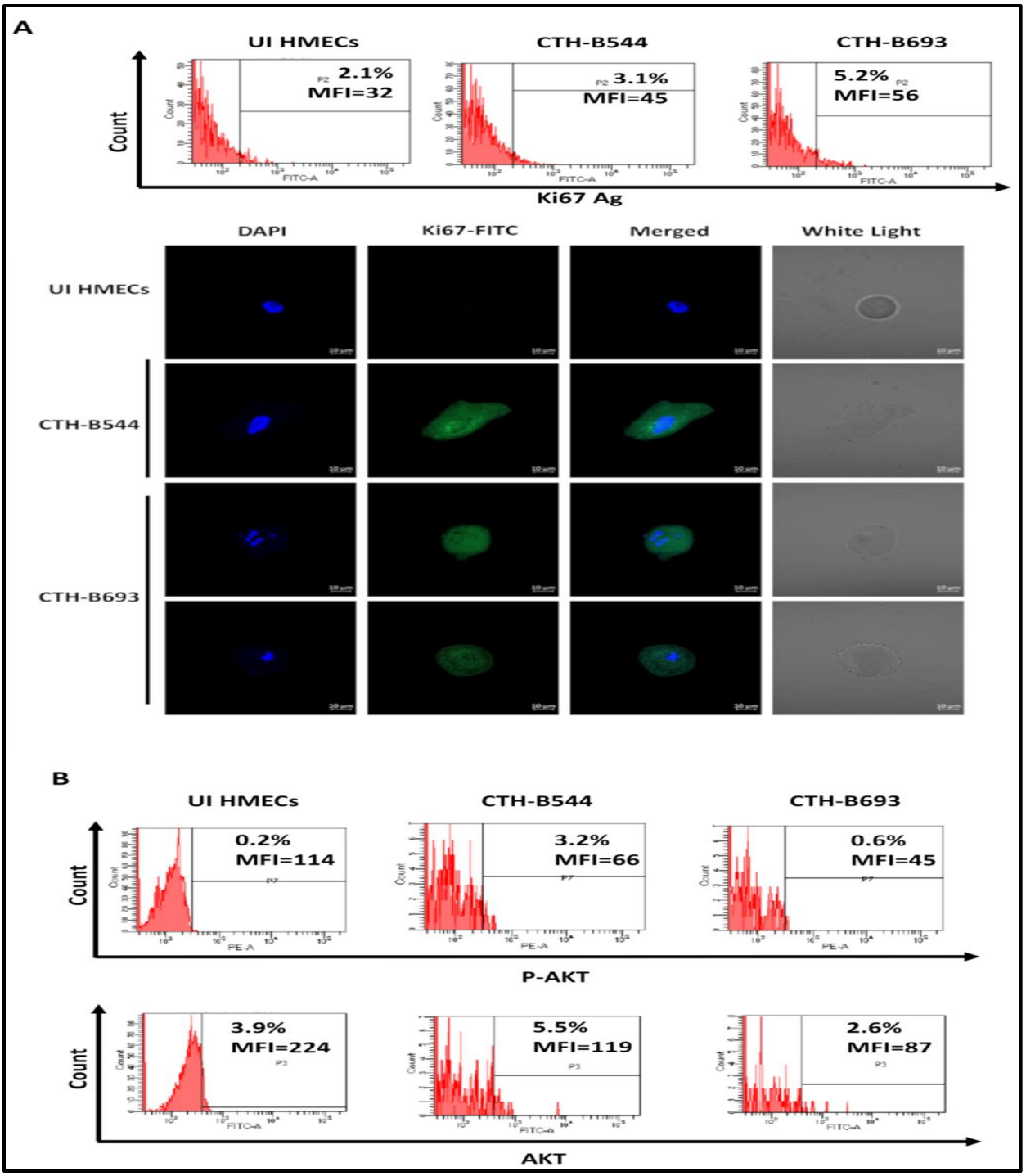

Figure 12: CTH proliferation capacities and AKT activation.

(A) Proliferation assessment by FACS and confocal microscopy; UI HMECs, CTH-B544 and CTH-B693 cells were stained for Ki67 Ag and DAPI. Magnification ×63, scale bar 10 µm. (B) P-AKT, and AKT expression in UI HMECs and CTH cells, as measured by FACS. Results are representative of three independent experiments.

7.1.3 CTH Cells Promote Embryonic Stemness and Develop an Epithelial/Mesenchymal Hybrid State

When cultured in serum-free tumorsphere medium, CTH-B544 and B693 cells gave rise to mammospheres at day 14 and expressed stemness markers versus uninfected HMECs **(Figure 13A)**. CTH cells revealed a rise in CD44 and CD24 expression when compared to uninfected HMECs **(Figure 13B)**, in line with CTH-DB and BL data. Activated expression of the embryonic stem cell markers, SSEA-4 and Nanog, was recognized in CTH-B544, CTH-B693, CTH-DB, and CTH-BL cells by performing flow cytometry **(Figure 14A)** and confocal microscopy imaging **(Figure 14B,C)**. Moreover, CTH-B544 and B693 cells gained embryonic stem-like properties by highly expressing Oct4 and SOX2 as demonstrated by confocal microscopy imaging **(Figure 14D,E)**. Similar to CTH-DB and BL, the newly discovered CTH cells showed an elevated expression of the stemness marker CD49f or Integrin alpha-6, and a limited EpCAM expression **(Figure 15)**. CTH-B544 and B693 as well as CTH-DB and BL cells were positive for both vimentin and E-cadherin staining **(Figure 15)** thereby signifying their ability to dynamically oscillate between the epithelial-hybrid-mesenchymal spectrum as reported previously in tumors with poor prognosis [367,368]. As a result, CTH-B544 and B693 cells exhibited the following two phenotypes: stemness and hybrid epithelial/mesenchymal phenotypes.

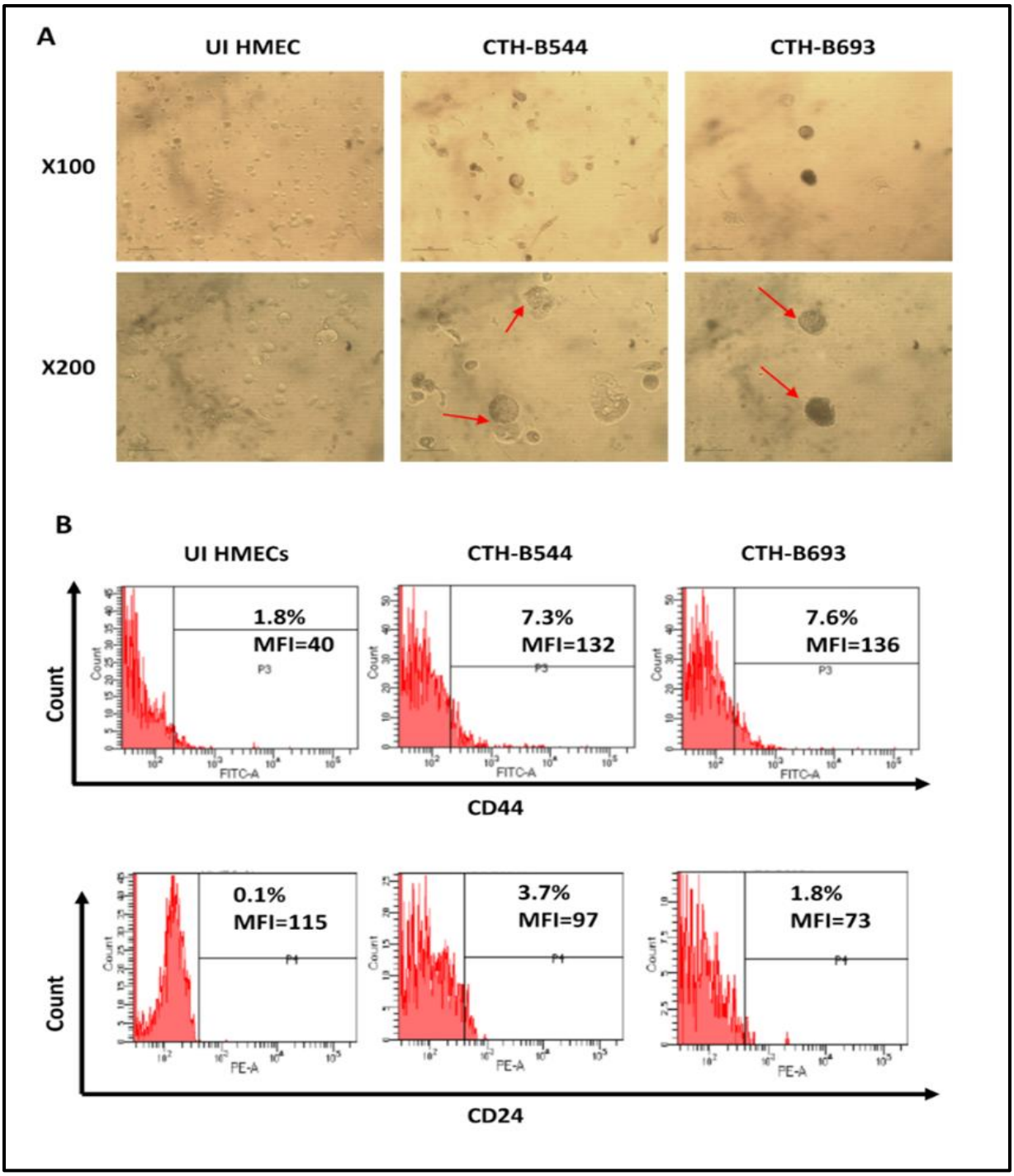

Figure 13: Tumorspheres formation and the expression of stemness markers in CTH cells.

(A) Tumorspheres were observed under an inverted light microscope in CTH-B544 and CTH-B693 cells. Magnification ×100 and ×200, scale bare 100 µm. Uninfected HMECs were used as a negative control. (B) FACS staining of CD44 and CD24 was performed in CTH cells. Results are representative of three independent experiments.

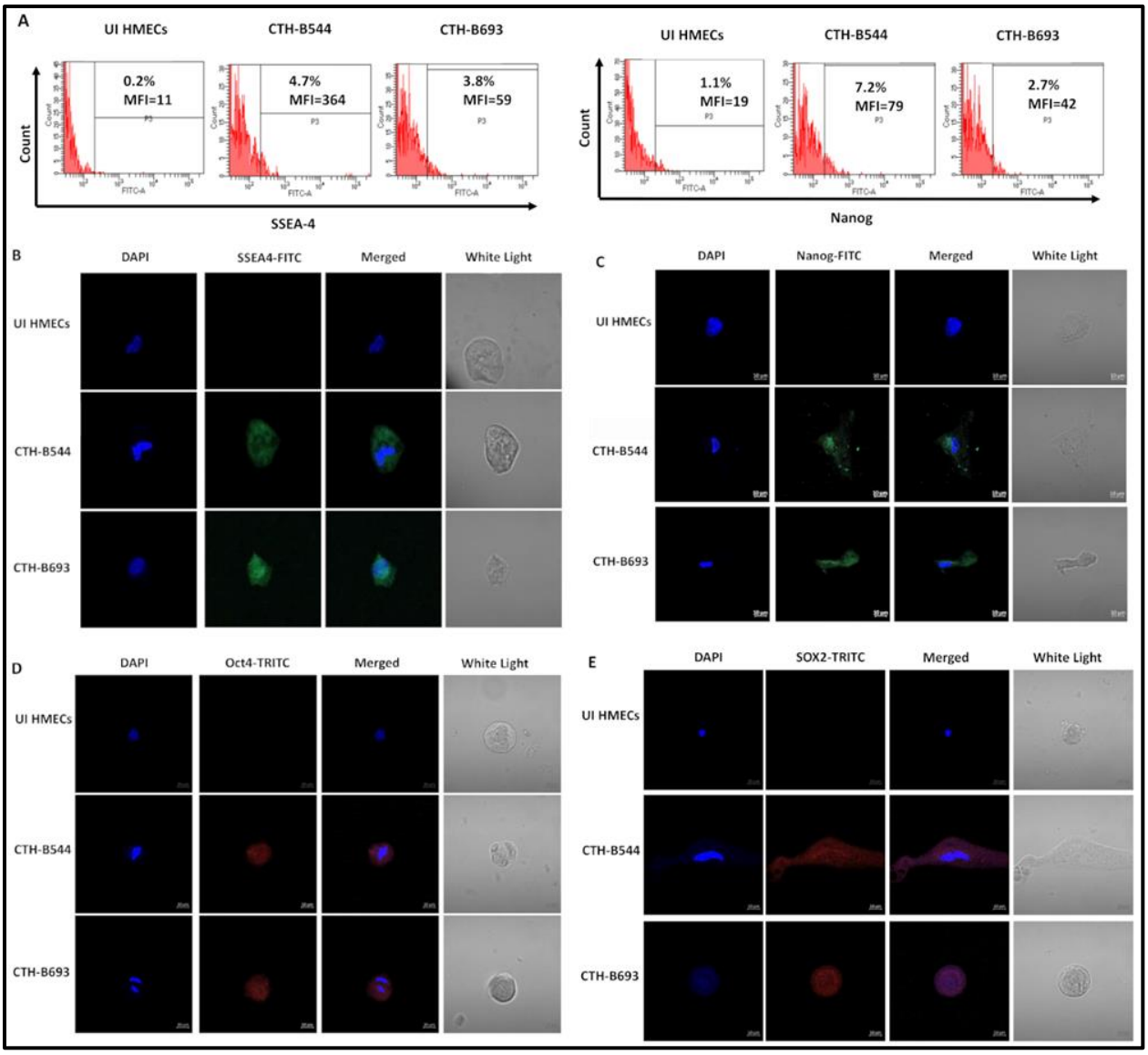

Figure 14: Expression of embryonic stem cell markers in CTH-B544 and B693 cells.

(A) Detection of SSEA4 and Nanog in CTH cells by FACS. Results are representative of three independent experiments. Confocal microscopy imaging demonstrating the expression of (B) SSEA-4, (C) Nanog, (D) Oct4, and (E) SOX2. Nuclei were counterstained with DAPI; magnification ×63, scale bar 10 μm.

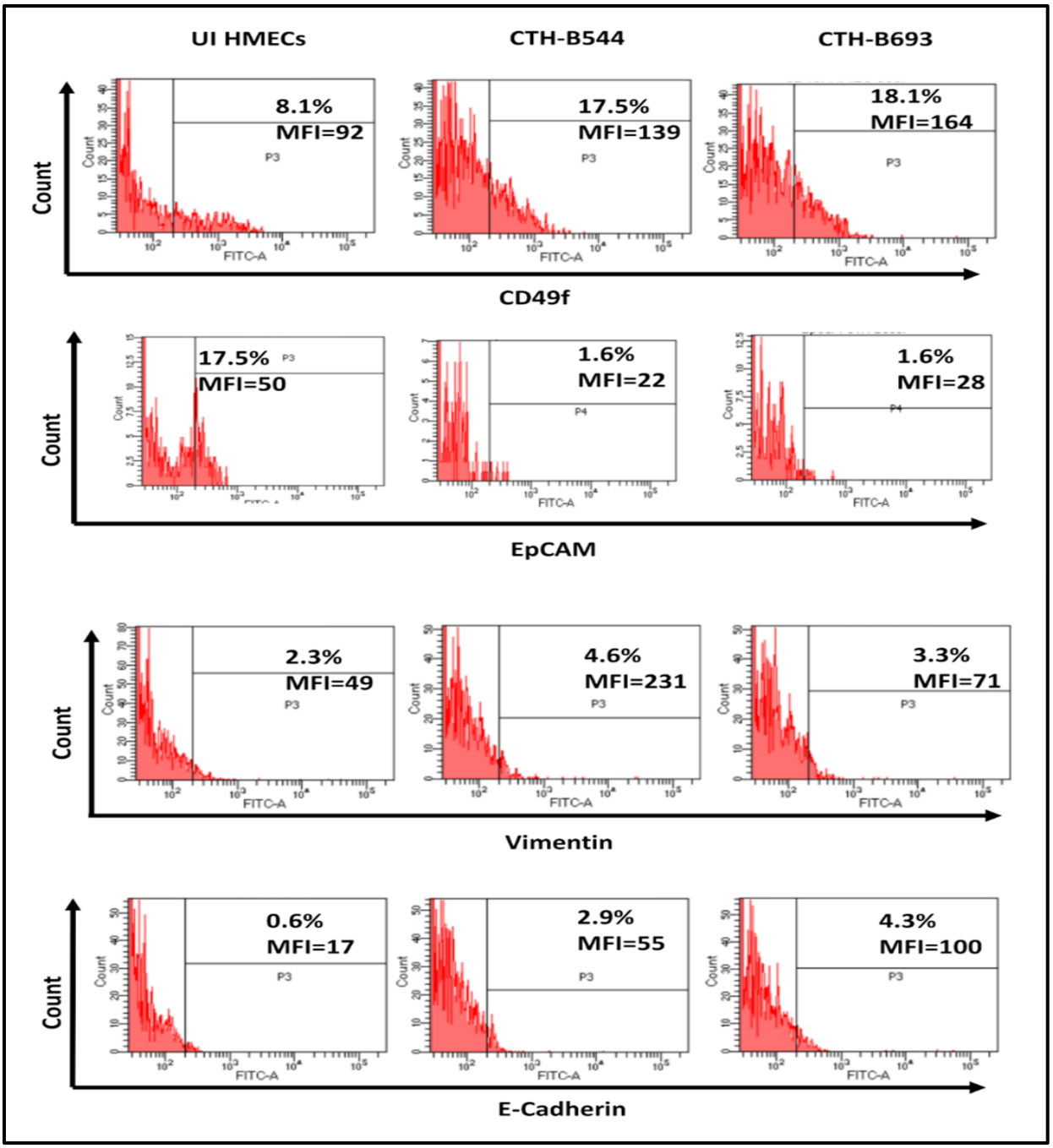

Figure 15: Penotypic analysis of CTH cells.

Detection of a panel of cell markers through FACS staining of CD49f, EpCAM, Vimentin, and E-cadherin in CTH-B544 and CTH-B693 versus UI HMECs. Results are representative of three independent experiments.

7.1.4 Persistent HCMV Replication in CTH-B544 and CTH-B693 Long-Term Cultures

To determine the sustained HCMV presence, HCMV-IE1 antigen was detected using flow cytometric analysis. IE1 was strongly expressed in CTH-B544 and CTH-B693; uninfected HMECs showed no staining for IE1 **(Figure 16A)**. Using qPCR, we detected HCMV (IE1 DNA) in the supernatant of CTH-B544 and CTH-B693 cultures **(Figure 16B)**. Further, CTH cells were positively stained for HCMV-pp65 antigen versus uninfected HMECs **(Figure 16C)**. CTH cells were treated with TPA to assess latency relevance **(Figure 16D,E)**. Post TPA treatment, the proliferation of CTH-B544 and CTH-B693 cells was promoted **(Figure 16D)**. IE1 detection was elevated at day 1 and day 2 post-treatment in CTH-B544 and CTH-B693, respectively (*p*-value= 0.33), and subsequently decreased **(Figure 16E)**.

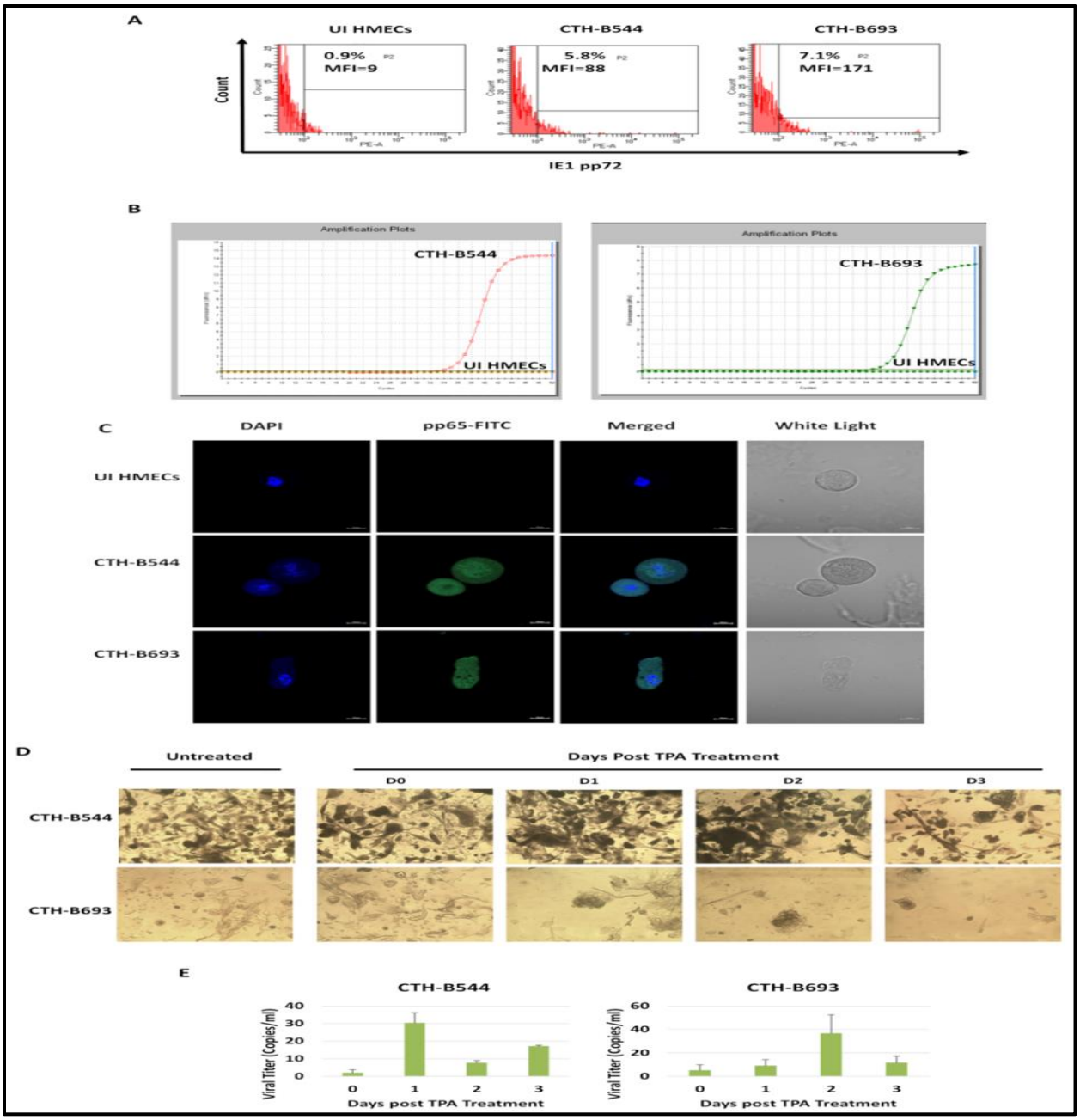

Figure 16: Sustained viral replication in CTH cells.

IE1 expression in CTH cells was assessed by (A) FACS and (B) qPCR. (C) pp65 detection in CTH-B544 and B693 cells as demonstrated by confocal microscopy imaging. As a negative control, uninfected HMECs were used; nuclei were counterstained with DAPI; magnification ×63, scale bar 10 µm. (D, E) Determination of viral reactivation from latency in CTH cells through the treatment of TPA. (D) Representative images of CTH cultures treated with TPA (100 nM). Untreated cells were used as a control. Magnification ×100, scale bar 100 µm. (E) HCMV lytic replication was induced by TPA in CTH cultures. Histograms represent the mean data ± SD of three independent experiments.

7.1.5 A Specific Molecular Landscape Unveiled in the Tumor Microenvironment of TNBC Harboring High-Risk HCMV

To evaluate the variation in strains' aggressiveness, we compared the transcriptomic profile corresponding to the two high-risk biopsies. The absolute mRNA level of epidermal growth factor receptor (EGFR), cyclin dependent kinase inhibitor 2A (CNDK2A), cyclin D1 (CCND1), SOX2, Oct4, and Nanog was assessed by RT-qPCR. EGFR, a proto-oncogene that enhances cell proliferation and survival, the cell cycle regulator CNDK2A, the proliferation marker CCND1, and the three embryonic markers were overexpressed in biopsy 693 compared to biopsy 544 (p-value ≤ 0.05 for all markers) **(Figure 17A)**. Our results indicated that biopsy 693, from which we isolated the HCMV-B693 strain, is associated with higher tumor aggressiveness and poor prognosis.

7.1.6 Restricting Soft Agar Colony Formation, Controlling PGCCs Count and Proliferation by Paclitaxel and Ganciclovir Therapy

To assess the colony formation in soft agar, CTH cells were treated by PTX/GCV combination therapy to target the oncogenic cellular environment as well as HCMV. Breast cancer cell lines, MDAMB231 and MCF7 were used as positive controls. PTX/GCV treatment of CTH-B544 cells resulted in the disappearance of colonies; however, colony formation was restricted in treated CTH-B693 cells versus untreated cells **(Figure 17B)**. Post therapy, the PGCCs count was reduced by 25% in CTH-B544 while it remained constant in CTH-B693 as measured by FACS **(Figure 17C)**. Further, the proliferation of PGCCs was assessed by Ki67 Ag measurement using flow cytometric analysis; Ki67 Ag expression was reduced in PTX/GCV-treated CTH-B544, but not in CTH-B693 **(Figure 17D)**. Our outcomes revealed that CTH-B544 cells are more responsive to PTX/GCV therapy compared to CTH-B693 cells implying that the latter exhibits aggressive behavior.

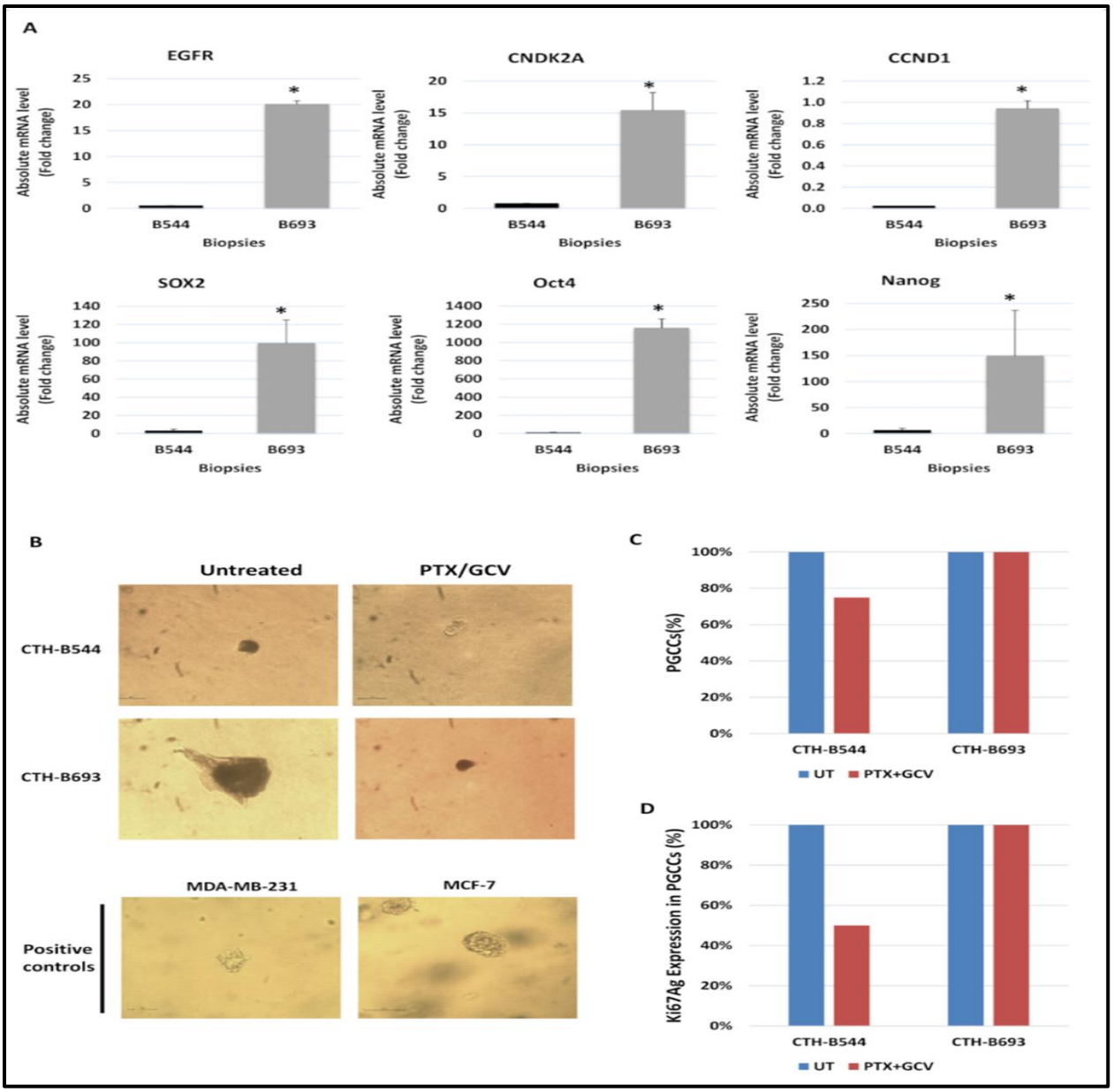

Figure 17: Distinct responses of CTH cells to paclitaxel/ganciclovir (PTX/GCV) treatment in vitro recapitulates distinct TNBC molecular signatures in vivo.

(A) EGFR, CNDK2A, CCND1, SOX2, Oct4, and Nanog mRNA expression was measured by RT-qPCR in TNBC biopsies B544 and B693. Histograms represent the mean ± SD of three independent experiments. * $p \leq 0.05$, determined by Mann–Whitney U test. (B) Soft agar seeded with CTH-B544 and CTH-B693 cells treated with PTX (20 nM)/GCV (20 µM) combination therapy. Untreated cells were used as negative controls; MCF7 and MDA-MB231 cells were used as positive controls. Magnification ×200, scale bar 100 µm. (C) Propidium iodide (PI) staining for detection of PGCCs in untreated and treated CTH cells by FACS analysis. (D) Ki67 Ag expression in PGGCs of untreated and treated CTH cells. Histograms represent the mean data ± SD of three independent experiments.

7.2 EZH2-Myc Driven Glioblastoma Elicited by Cytomegalovirus Infection of Human Astrocytes

7.2.1 HCMV Clinical Isolates Permissively Infect HAs Inducing Increased Myc and EZH2 Expression

The cellular environment induced by HCMV infection was assessed by studying the tropism of DB and BL high-risk HCMV strains **(Figure 18)** as well as KM and FS low-risk HCMV strains **(Figure 19)** to HAs. HCMV-DB and BL strains replicated in HAs with a burst of viral growth (6 logs for DB and 3 logs for BL) followed by occasional blips **(Figure 18A and Figure 20)**. Acute infection was then confirmed through immediate early gene (IE1), pp65, and the late HCMV antigens detection **(Figure 18B,C and Figure 19)**. In addition, IE1 and early/late gene (UL69) transcripts were detected in HAs infected with HCMV-DB and BL compared to controls **(Figure 18D)**. At day 3 post-infection, Myc was overexpressed in HAs-DB and BL compared to controls (p-value = 0.09), mostly in HAs-DB. Elevated EZH2 expression was detected in HAs-DB and BL compared to uninfected HAs (p-value = 0.02) **(Figure 18E)**. Myc and EZH2 transcripts were detected in HAs-DB and BL compared to controls **(Figure 18F)**. Lower apoptosis levels were recognized with the two strains **(Figure 18G)** in line with Akt and pAkt-Ser473 upregulation as confirmed by western blot and FACS, particularly with HCMV-DB **(Figure 18H)**. In contrast to the high-risk DB and BL strains, the low-risk FS and KM strains did not elicit any of the above-mentioned behavior **(Figure 19)**. Taken together, a Myc^{High} $EZH2^{High}$ molecular profile was observed with both high-risk strains, preferentially with HCMV-DB.

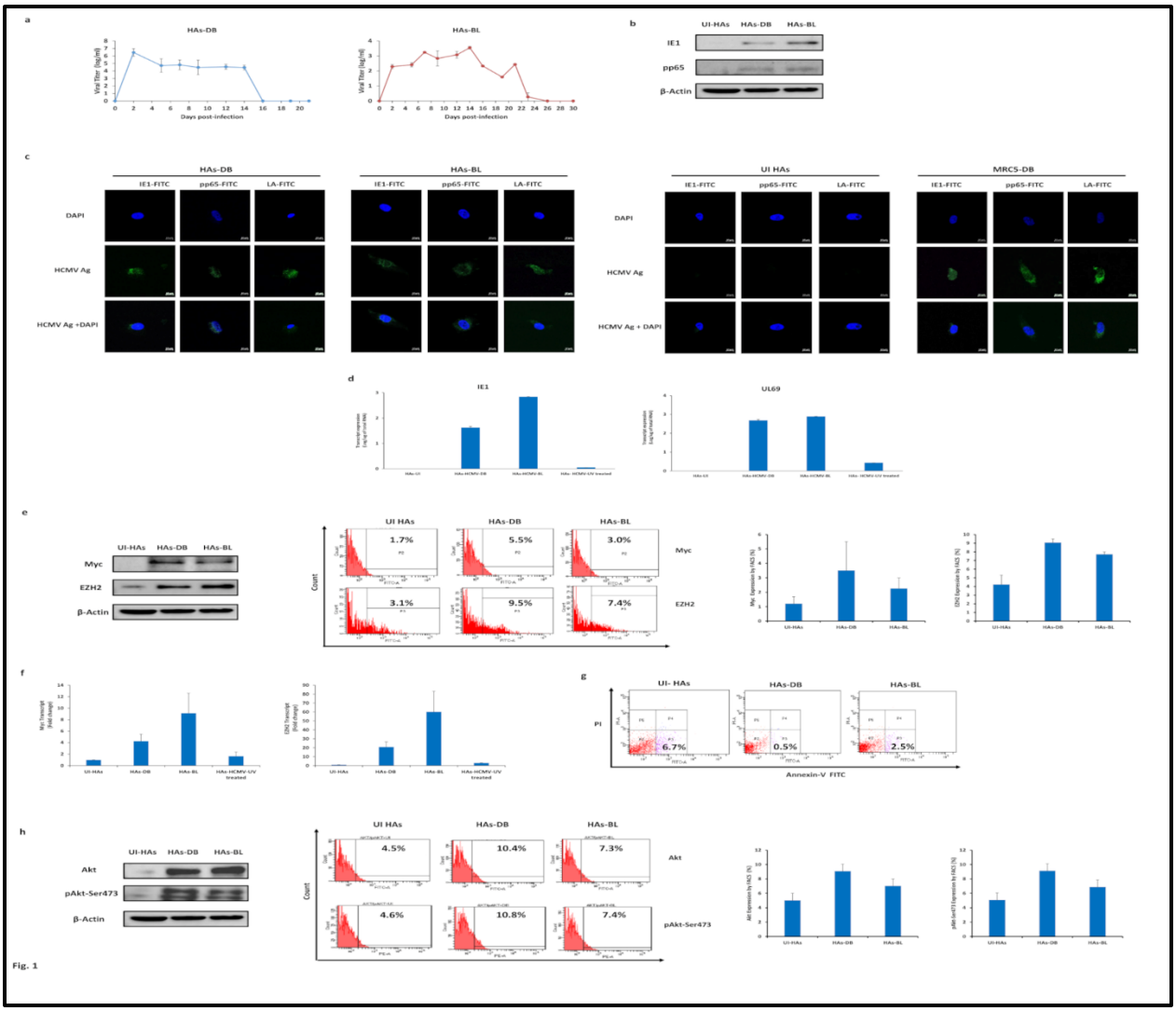

Figure 18: Replication of two high-risk oncogenic HCMV strains in HAs cultures, the activation of oncogenic pathways, and reduced apoptosis rates.

(A) Time-course of the viral titer in the supernatant of HAs infected with HCMV-DB and BL as measured by IE1-qPCR. (B) Immunoblotting data of IE1 and pp65 in uninfected HAs lysates and HAs infected with HCMV-DB and BL (day 5 post-infection). β-actin was used as loading control. (C) Confocal microscopic images of HCMV-IE1, pp65, and late antigen staining in HAs infected with HCMV-DB and BL (day 1 post-infection). Uninfected HAs and MRC5-DB cells were used as negative and positive controls, respectively. Nuclei were counterstained with DAPI; magnification ×63, scale bar 10 µm. (D) IE1 and UL69 transcripts detection by RT-qPCR in uninfected HAs, HAs-DB and BL as well as HAs infected with UV-treated HCMV. (E) Myc and EZH2 protein expression as measured by western blot (day 5 post-infection) and FACS (day 3 post-infection) in uninfected HAs and HAs infected with HCMV-DB and BL. β-actin was used as loading control. (F) Myc and EZH2 transcripts detection by RT-qPCR. (G) Early apoptosis assessment in HAs-DB and BL (MOI = 1). UI HAs were used as a control. (H) Akt, and pAkt-Ser473 protein expression as measured by western blot and FACS in uninfected HAs and HAs infected with HCMV-DB and BL. β-actin was used as loading control. Data are represented as mean ± SD of two independent experiments.

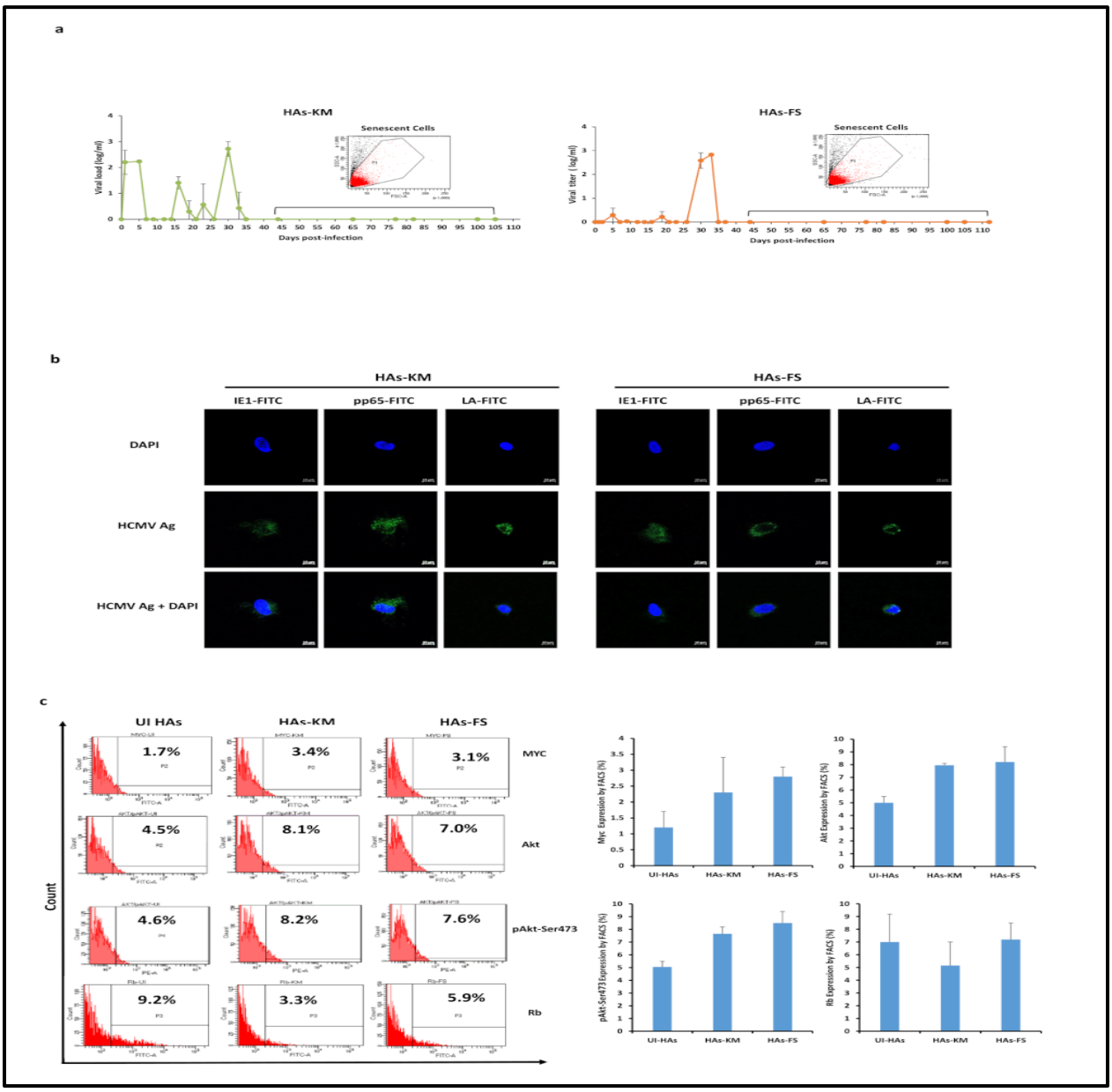

Figure 19: Long-term cultures of HAs infected with the two low-risk HCMV strains.

(A) Time-course of the viral titer in the supernatant of infected HAs as measured by IE1-qPCR along with the cellular analysis of HAs-KM and FS based on their size (FSC) and granularity (SSC). (B) Confocal microscopic images of HCMV-IE1, pp65, and late antigen staining in HAs infected with HCMV-KM and FS (day 1 post-infection). Nuclei were counterstained with DAPI; magnification ×63, scale bar 10 µm. (C) Myc, Akt, pAkt-Ser473, and Rb protein expression as measured by FACS in uninfected HAs and HAs infected with HCMV-KM and FS. Data are represented as mean ± SD of two independent experiments.

7.2.2 Emergence of a Glioblastoma-Like Phenotype With CEGBCs in HAs Chronically Infected With High-Risk HCMV Strains.

In contrast to the low-risk HCMV strains that didn't allow long-term replication in HA cultures and were senescent **(Figure 19)**, HAs infected with HCMV-DB and BL were maintained in culture for an extended period of time **(Figure 20)**. Around day 80–90 post-infection, dense cellular aggregates appeared in HCMV-BL and DB cultures with invasive-like cells irradiating from the main cellular structures resembling the formerly described "go or growth" phenotype of glioblastoma cells [369] **(Figure 21A,B)**. Cells with a glioblastoma-like phenotype were termed *"CMV-Elicited GlioBlastoma Cells*" or CEGBCs similar to the previously reported "CMV-Transformed Human mammary epithelial cells" or CTH cells [125,209].

We next assessed the protein expression of EZH2 and Myc in CEGBCs in which increased expression levels were observed compared to controls **(Figure 21C)**. CEGBCs characterization was achieved by assessing oncogenes, tumor suppressor genes and cell cycle genes. Oncogenes and cell cycle genes were mainly upregulated in CEGBCs-DB; however, tumor suppressor genes were down-regulated mostly in CEGBCs-BL **(Figure 21D,E)**. CEGBCs-DB and BL were seeded on a soft agar to evaluate their tumorigenic potential and colony formation was detected; uninfected HAs and HAs infected with herpes simplex virus (HSV) showed no colony formation **(Figure 21F)**. Primary GBM experiences the subtype switch during relapse, shifting from the proneural (PN) subtype to the mesenchymal (MES) one namely the proneural-mesenchymal transition (PMT), thus acquiring a therapy-resistant phenotype [370]. With regards to PMT markers, vimentin was elevated mostly in CEGBCs-DB, and to a lesser extent in CEGBCs-BL **(Figure 21G)**. CD44, a widely accepted marker for cancer stem cells and a mesenchymal marker regulating both stemness and epithelial-mesenchymal plasticity, was shown to be predominantly upregulated in CEGBCs-DB **(Figure 21H)**. EMT genes were mostly upregulated in CEGBCs-DB compared to CEGBCs-BL **(Figure 21I)**. CEGBCs-DB were shown to be close to the transcriptome profile of mesenchymal glioblastoma (mGB) whereas CEGBCs-BL expressed more PN traits **(**mesenchymal markers: p-value $_{(\text{CEGBCs-DB:CEGBCs-BL})} = 0.002$; proneural markers: p-value $_{(\text{CEGBCs-DB:CEGBCs-BL})} = 0.06$) **(Figure 21J)**. Taking into account the proteomic and transcriptome data, CEGBCs-DB mostly displayed a mesenchymal phenotype compared to

CEGBCs-BL. High levels of SOX2, Oct4, and SSEA4 were detected in CEGBCs **(Figure 22A and Figure 23A,B)**. Hence, the identified stemness features in CEGBCs indicated their relevance to glioblastoma stem cells (GSCs). Assessing the spheroid formation potential of CEGBCs, spheroids were generated 24–48 hours post-seeding; no spheroid formation was detected in HAs infected with HSV **(Figure 22B)**. Nestin and IE1 were concomitantly expressed in CEGBCs-DB and BL spheroids **(Figure 22C)**.

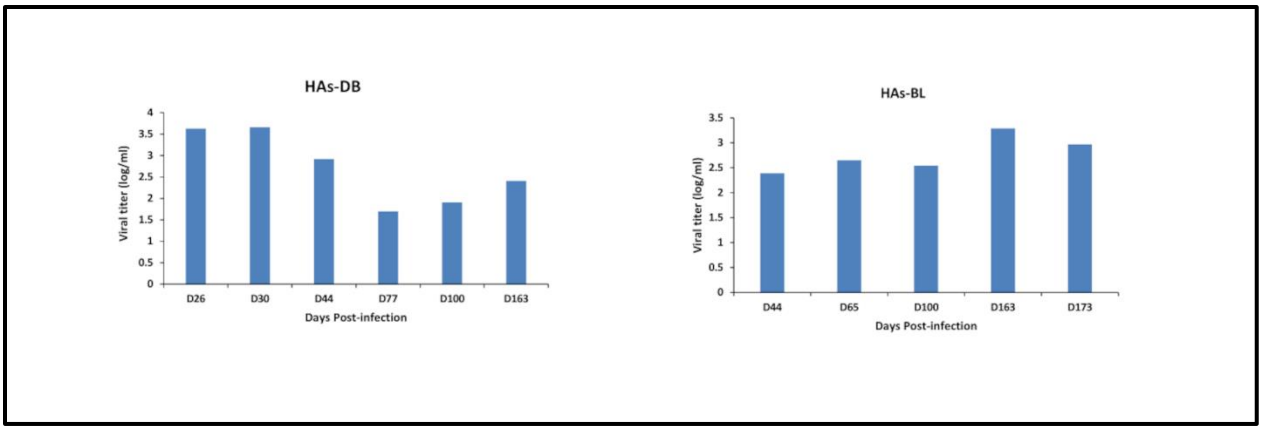

Figure 20: Long-term replication of two high-risk HCMV strains in HAs cultures.

Time-course of the viral titer in the supernatant of HAs infected with HCMV-DB and BL as measured by IE1-qPCR.

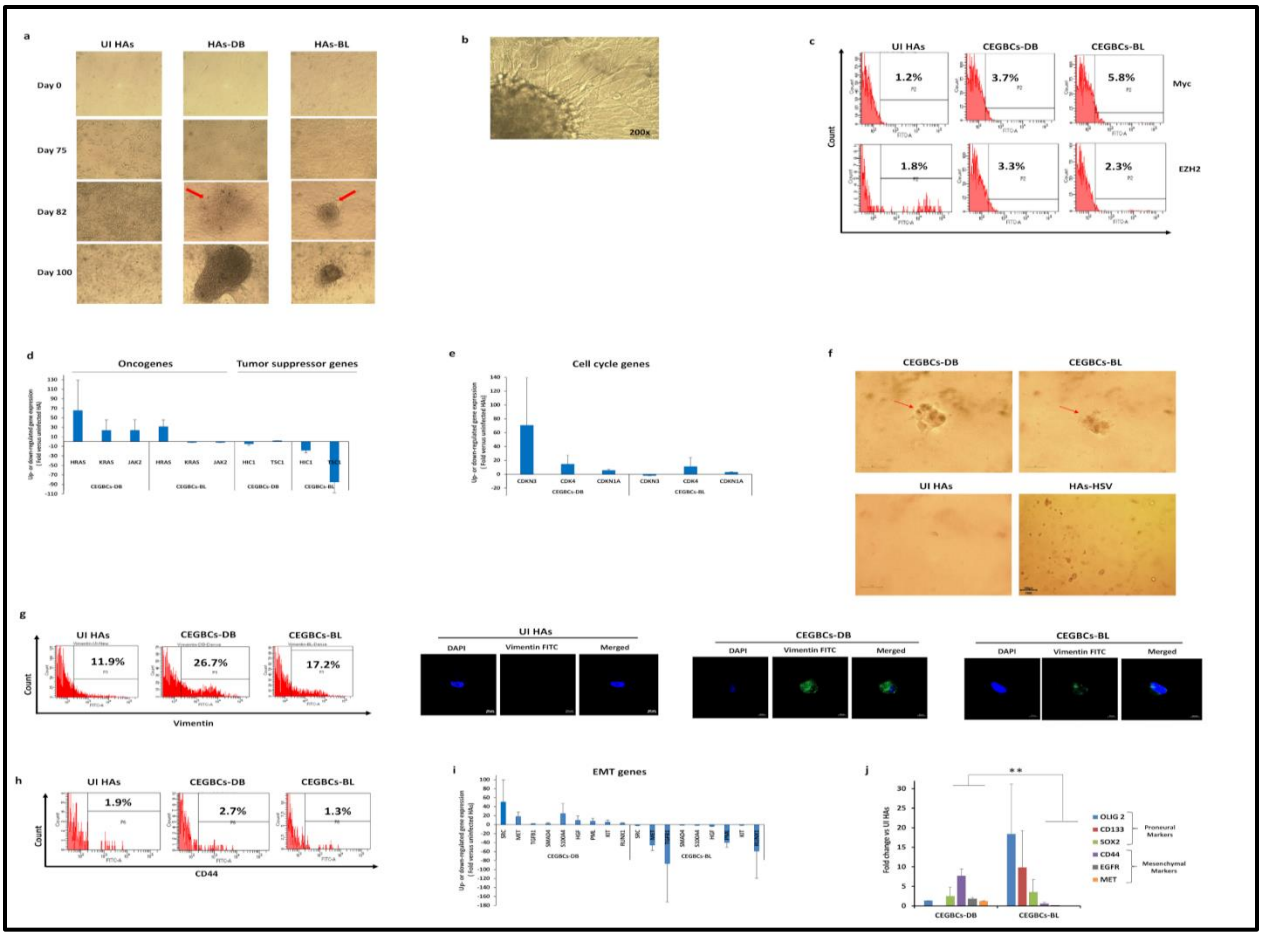

Figure 21: Chronic infection of HAs with HCMV clinical isolates, the appearance of CEGBCs as well as colony formation in soft agar, and the phenotypic characterization of CEGBCs.

(A) HAs time-course infection with HCMV-DB and BL strains (MOI = 1). Red arrows showing the generated CEGBCs. Magnification ×100, scale bar 100 µm. Uninfected HAs were used as a control. (B) An inverted light microscope was used to closely follow up the chronic CEGBCs-DB and BL cultures and the appearance of several structures; magnification 200x, scale bar 100 µm. (C) FACS staining of Myc and EZH2 in HAs infected with HCMV-DB and BL; uninfected HAs were used as a negative control. The fold regulation of oncogenes and tumor suppressor genes (D) as well as cell cycle genes (E) was assessed in uninfected HAs and HAs infected with HCMV-DB and BL using RT2 Profiler PCR Arrays. (F) Colony formation in soft agar seeded with CEGBCs-DB and BL (MOI = 1); UI HAs and HAs-HSV were used as controls. Formed colonies were observed under an inverted light microscope (Magnification 200x, scale bar 100 µm). (G) Vimentin expression by FACS and confocal microscopy in CEGBCs-DB and BL; uninfected HAs were used as a control. Nuclei were counterstained with DAPI; magnification ×63, scale bar 10 µm. (H) FACS staining of CD44 in CEGBCs-DB and BL. Uninfected HAs were used as controls. (I) The fold regulation of EMT genes was assessed in UI HAs and HAs infected with HCMV-DB and BL using RT2 Profiler PCR Arrays. (J) Histogram depicting the expression of PN markers (OLIG2, CD133, and SOX2), MES markers (CD44, EGFR, and MET), as quantified by RT-qPCR in CEGBCs-DB and BL. **p- value ≤ 0.01. Data are represented as mean ± SD of two independent experiments.

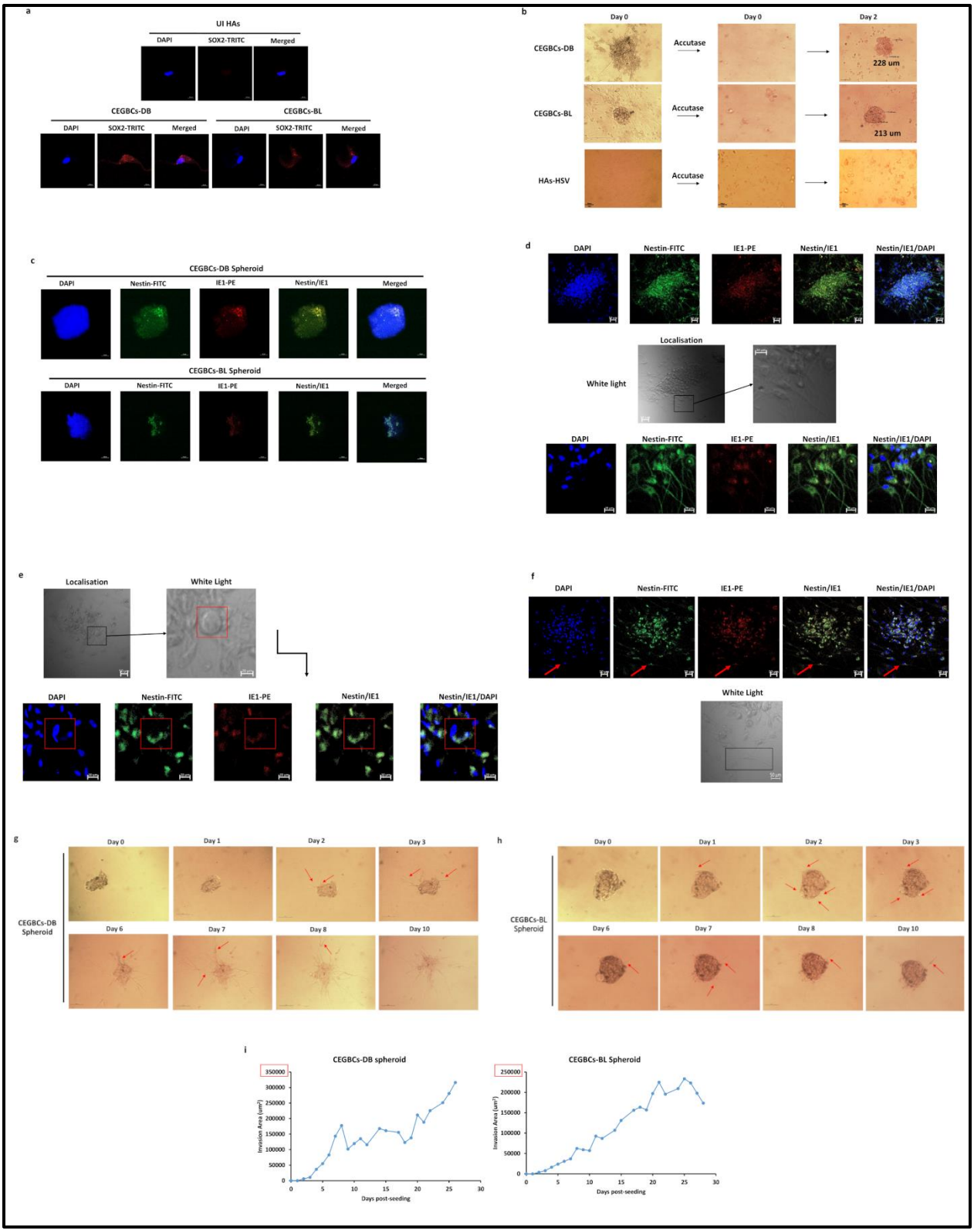
a
UI HAs
DAPI
SOX2-TRITC
Merged
CEGBCs-DB
CEGBCs-BL
b
Day 0
Day 0
Day 2
CEGBCs-DB
CEGBCs-BL
HAs-HSV
Accutase
228 um
213 um
c
CEGBCs-DB Spheroid
CEGBCs-BL Spheroid
Nestin-FITC
IE1-PE
Nestin/IE1
d
Nestin/IE1/DAPI
Localisation
White light
e
White Light
f
g
Day 0
Day 1
Day 2
Day 3
Day 6
Day 7
Day 8
Day 10
CEGBCs-DB Spheroid
h
CEGBCs-BL Spheroid
i
CEGBCs-DB spheroid
CEGBCs-BL Spheroid
Invasion Area (um²)
Days post-seeding

Figure 22: Spheroid-forming potentials of CEGBCs as well as invasiveness and migration.

(A) Confocal microscopic images of SOX2 and DAPI staining in CEGBCs-DB and BL. UI HAs were used as controls; magnification ×63, scale bar 10 µm. (B) Schematic for spheroid generation from the chronically infected DB and BL astrocytes (day 222 post-infection); magnification 100x, scale bar 100 µm. HAs-HSV were used as a negative control. (C) Concomitant staining of IE1 and Nestin in CEGBCs-DB and BL spheroids. Nuclei were counterstained with DAPI; magnification ×63, scale bar 10 µm. (D) HCMV-IE1 and Nestin staining in 3D-scaffolds formed by CEGBCs in confluent culture and seeded with CEGBCs-DB and BL spheroids using confocal microscopy; magnification x20, scale bar 20 µm. Confocal microscopic images of Nestin and IE1 staining in PGCCs (E) and isolated cells (F) present in CEGBCs-BL culture (red arrows). Nuclei were counterstained with DAPI; magnification ×20, scale bar 20 and 50 µm. Time-course of the 3D-invasion assay where CEGBCs-DB (G) and BL (H) spheroids were embedded into type-1 collagen in the presence of HCl; red arrows showing cell invasion. Magnification x100, scale bar 100 µm. (I) Graphs showing the variation in the invasion area of CEGBCs- DB and BL spheroids. Measurements were taken using ImageJ; data are represented as mean ± SD of two independent experiments.

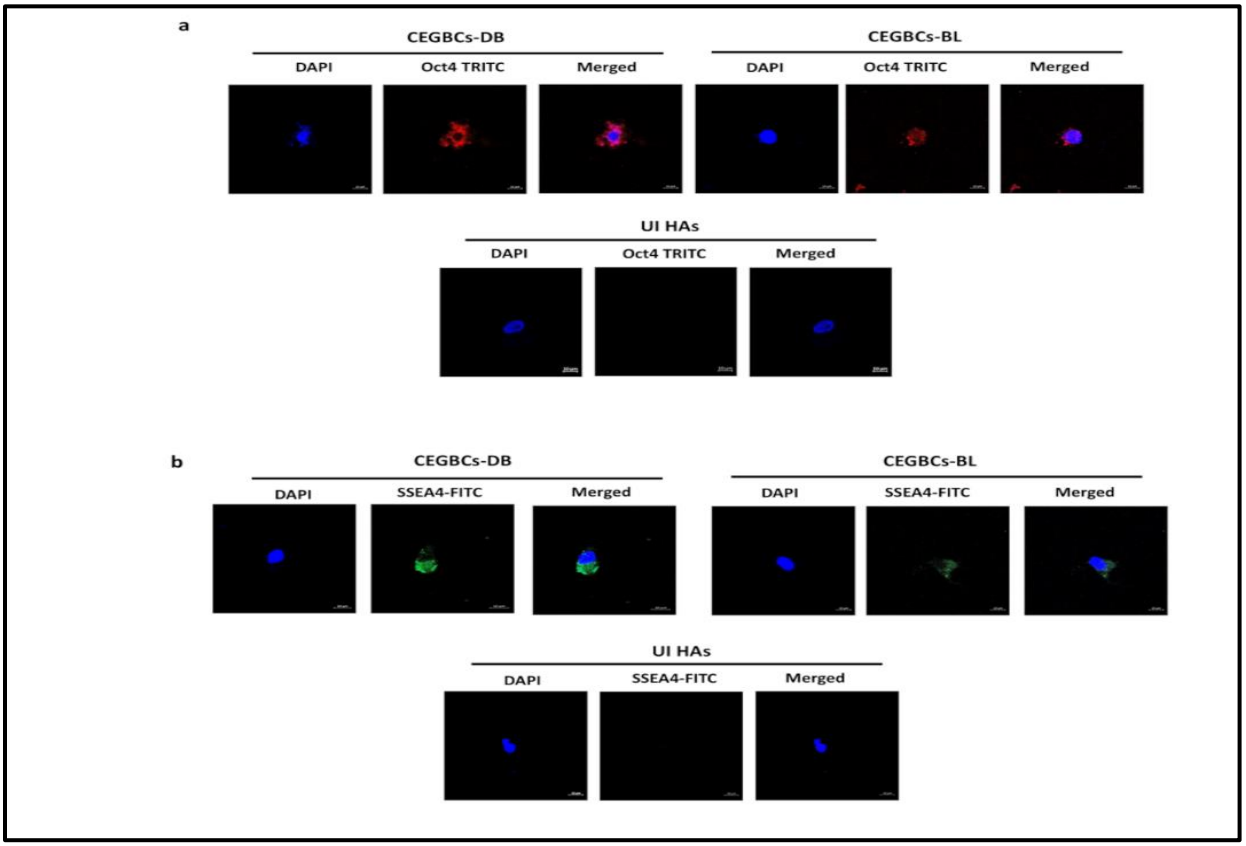

Figure 23: Stemness potential of CEGBCs-DB and BL.

Confocal microscopic images of Oct4 (A) and SSEA4 (B) staining in CEGBCs-DB and BL; UI HAs were used as a control. Nuclei were counterstained with DAPI; magnification ×63, scale bar 10 µm.

7.2.3 CEGBCs Productively Infected With High-Risk HCMV Display Invasiveness

CEGBCs from spheroids readily invaded astrocyte scaffolds, by aligning along and intercalating between astrocytes and penetrating all scaffold layers as measured by nestin detection. After 7 days, nestin was present in the spheroids' core and invasive part; cells were IE1 and nestin-positive. HCMV-IE1 was predominantly located in the spheroid core and present in the individual cells detaching from the core **(Figure 22D)**. Uninfected HAs expressed GFAP in the absence of nestin. PGCCs and neural progenitor cell (NPC)-like cells, positive for nestin and IE1, were also present **(Figure 22E,F)**; supernatants were positive for HCMV-IE1 indicating ongoing viral replication. Further, using a 3D collagen-invasion assay, invasiveness was noticed for CEGBCs-DB and to a lesser extent for CEGBCs-BL as measured by the invasion area **(Figure 22G,H)**; the protrusions' number and length were also recorded **(Figure 24)**. Within the CEGBCs-DB cultures, the majority of invading cells adopted a neural progenitor-like phenotype with a round small cell body and a long leading process characterized by high cell motility **(Figure 25, left panel)**. Cellular heterogeneity occurred among the invasive cells with random morphology in which low motility cells co-existed with highly motile cells **(Figure 25)**. Three mechanisms of invasiveness were detected in CEGBCs-DB and BL cultures as recently reported [371] **(Figure 26A,B, and C)**. Filopodia and lamellipodia were also observed **(Figure 26D)**.

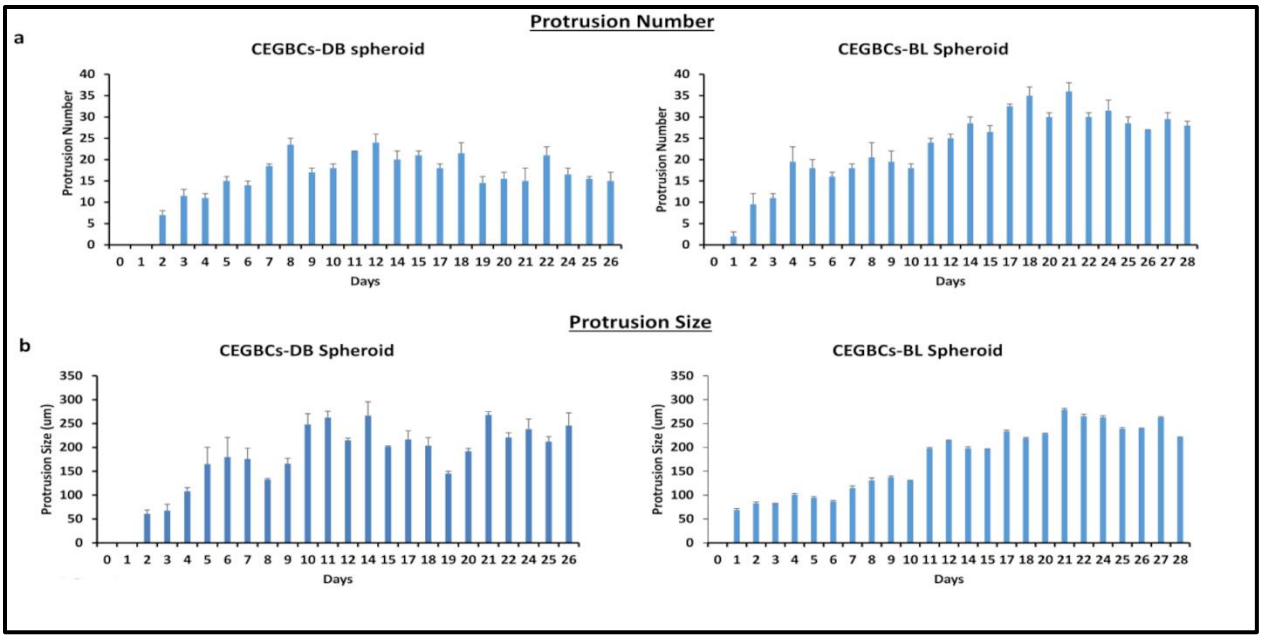

Figure 24: The invasion capacities of CEGBCs-DB and BL.

(A,B) Histograms representing the number (A) and size (B) of protrusions generated from CEGBCs-DB and BL spheroids. Data are represented as mean ± SD of two independent experiments.

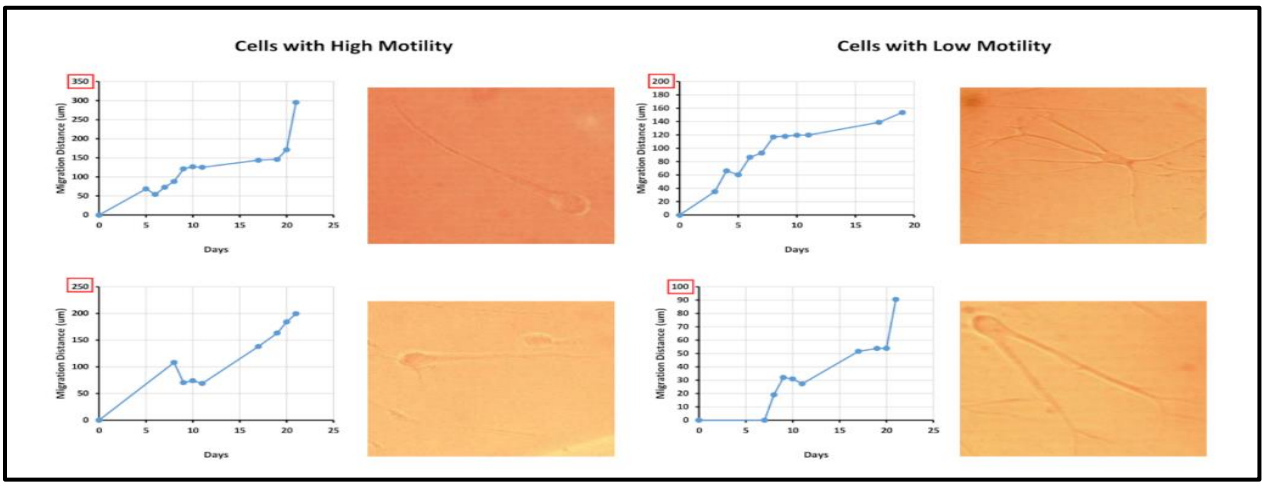

Figure 25: Cellular migration of CEBGCs.

Microscopic images showing the high and low motility cells that are invading from the CEGBCs-DB spheroid; magnification x100, scale bar 100µm. Graphs showing the variation in the migration distance of the selected cells using ImageJ.

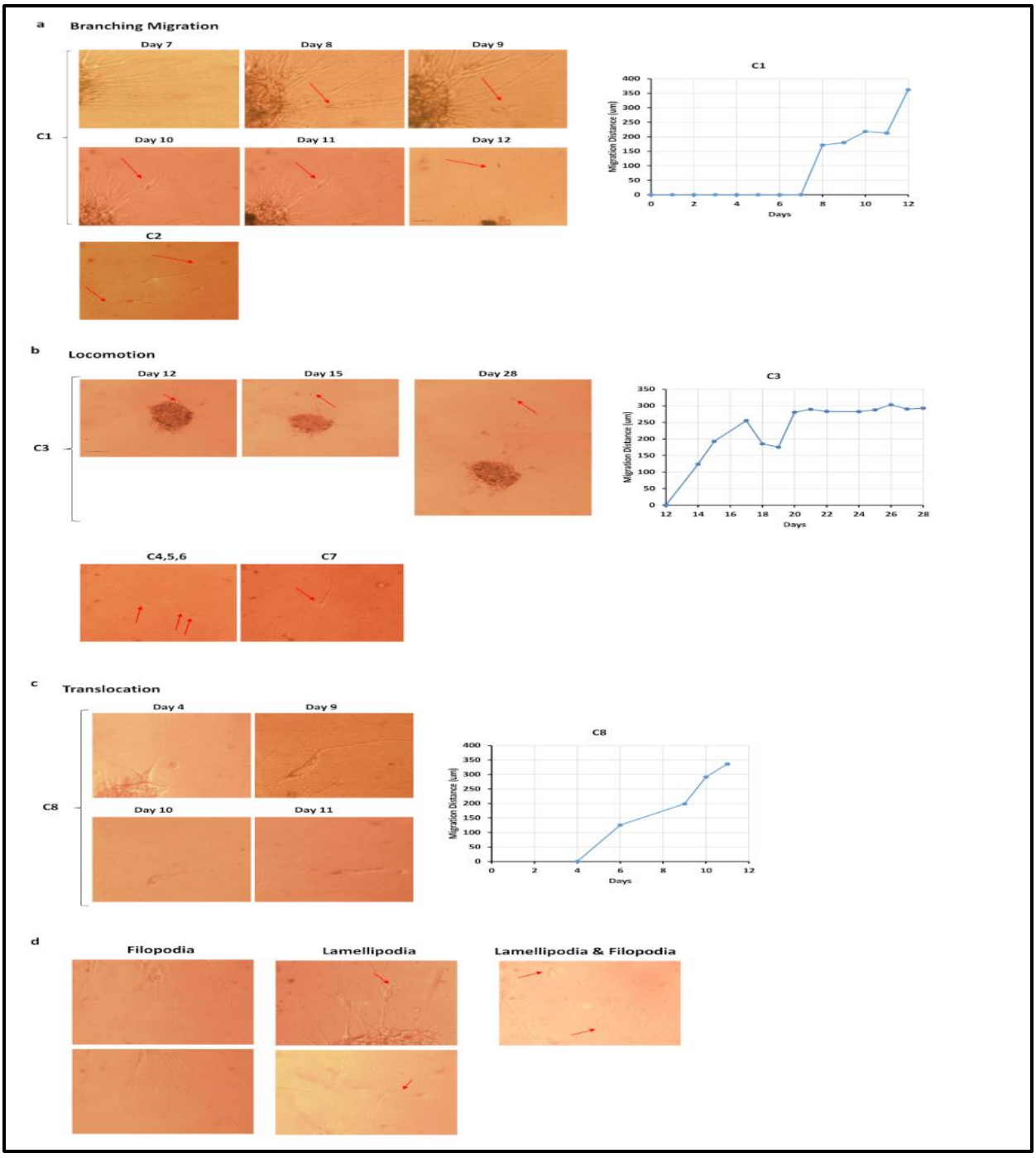

Figure 26: The three major invasion mechanisms of CEGBCs-DB and BL.

(A,B,C) Microscopic images illustrating the branching migration (A), locomotion (B), and translocation (C) invasion mechanisms in addition to the graphs showing the variation in the migration distance of the selected cells (C1, C3, and C8) using ImageJ. (D) Classification of specific structural features (filopodia and lamellipodia) of CEGBCs-DB and BL; magnification x100 and x200, scale bar 100µm.

7.2.4 Detection of lncRNA4.9/EZH2 and HOTAIR/EZH2 Complexes in CEGBCs Cultures

HCMV latency in CEGBCs cultures was established by IE1 expression that was observed at day 1 post-TPA treatment **(Figure 27A)** parallel to the detection of HCMV gene (lncRNA4.9) **(Figure 27B)**. In agreement with the presence of the lncRNA4.9 gene in EZH2-expressing CEGBCs, we observed the interaction of HCMV lncRNA4.9 and cellular lncRNA HOX antisense intergenic RNA (HOTAIR) transcripts with EZH2 using RNA CLIP assay **(Figure 27C,D)**. Cellular lncRNA HOTAIR transcript, reported as a poor prognostic factor in cancers [372] was detected particularly in the EZH2 immunoprecipitated samples corresponding to CEGBCs-DB compared to CEGBCs-BL **(Figure 27D)**.

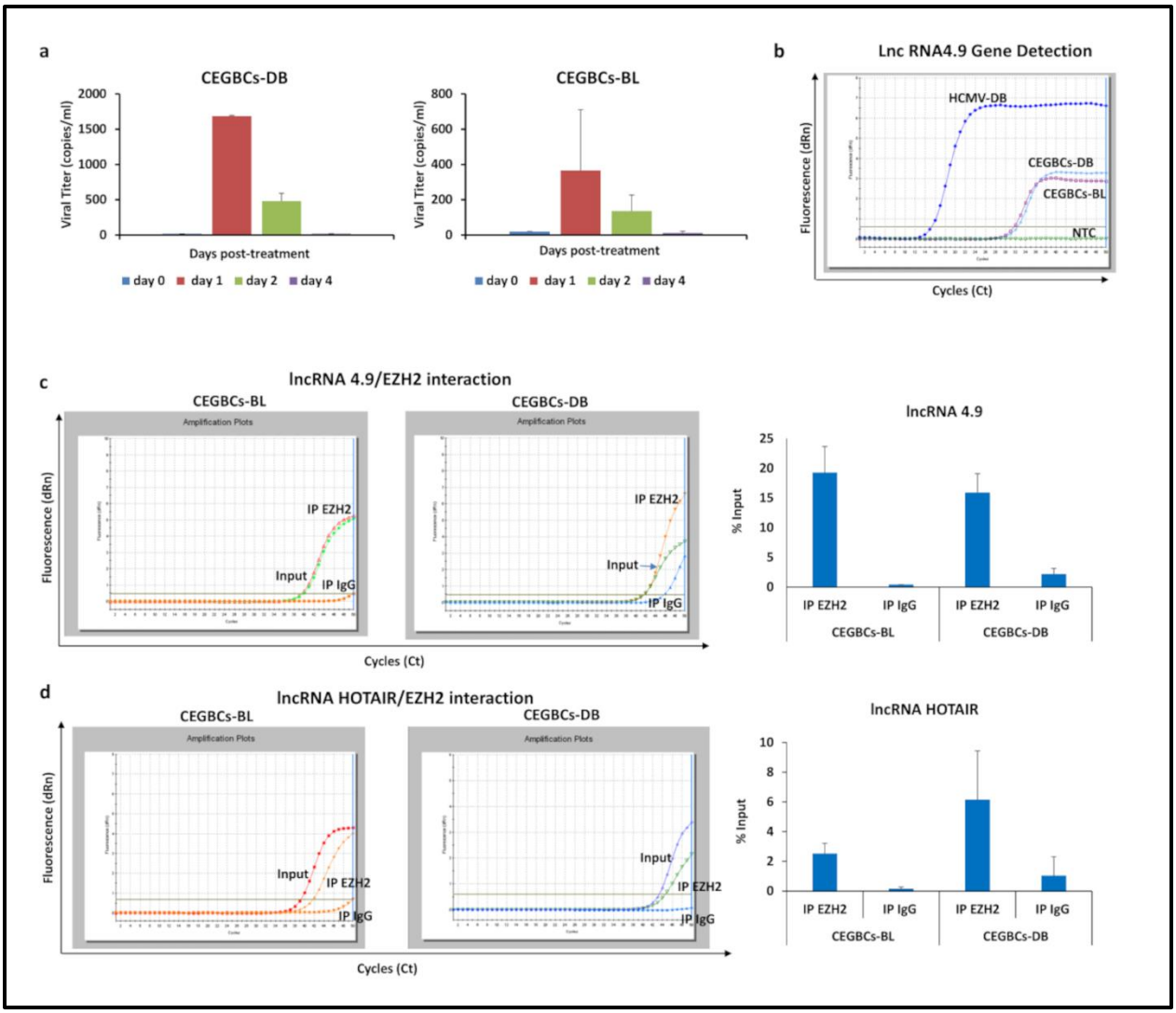

Figure 27: Detection of replicative HCMV and identification of the lncRNA4.9 and HOTAIR/EZH2 complex in CEGBCs cultures.

(A) Histograms representing the viral load post-TPA treatment (100 nM) in CEGBCs-DB and BL cultures as measured by IE1-qPCR. (B) lncRNA 4.9 gene detection in CEGBCs-DB and BL using RT-qPCR. HCMV-DB sample was used as a positive control. NTC: no template control. lncRNA 4.9 (C) and lncRNA HOTAIR (D) transcript detection in the EZH2 IP samples of CEGBCs-DB and BL, as measured by RT-qPCR. Mouse anti-IgG was used as an isotype control. Data are represented as mean ± SD of two independent experiments.

7.2.5 Upregulation of EZH2 and Myc in HCMV-positive GBM Tissues

To further decipher the role of HCMV and EZH2-Myc pathway in vivo, we analyzed 37 GBM biopsies (MGMT promoter methylated $n = 17$ and MGMT promoter unmethylated $n = 20$) for the presence of HCMV as well as EZH2 and Myc expression. Tumor biopsies displayed an enhanced EZH2 and Myc expression in both MGMT promoter methylated and unmethylated tissues, particularly in MGMT promoter unmethylated ones **(Figure 28B)**. HCMV was detected in all GBM samples (100%) **(Table 7)**. In all GBM biopsies, there was a statistically significant strong correlation between Myc and EZH2 expression **(Figure 28C)**. A significant strong correlation was found between HCMV presence (IE1 gene) and Myc/EZH2 expression in unmethylated GBM biopsies ($r = 0.690$, p-value $= 0.001$; $r = 0.589$, p-value $= 0.006$; respectively) **(Figure 28D)**. In unmethylated GBM biopsies, HCMV presence (UL69 gene) strongly correlated with Myc/EZH2 expression ($r = 0.507$, p-value $= 0.02$ and $r = 0.544$, p-value $= 0.01$, respectively) **(Figure 28E)**. On the other hand, a weak to moderate correlation was detected between HCMV presence and Myc/EZH2 expression in methylated GBM biopsies **(Figure 28D,E)**. Hence, we reported the detection of HCMV in GBM tumor biopsies displaying enhanced EZH2, Myc, and Akt expression **(Figure 28 and Figure 29)**.

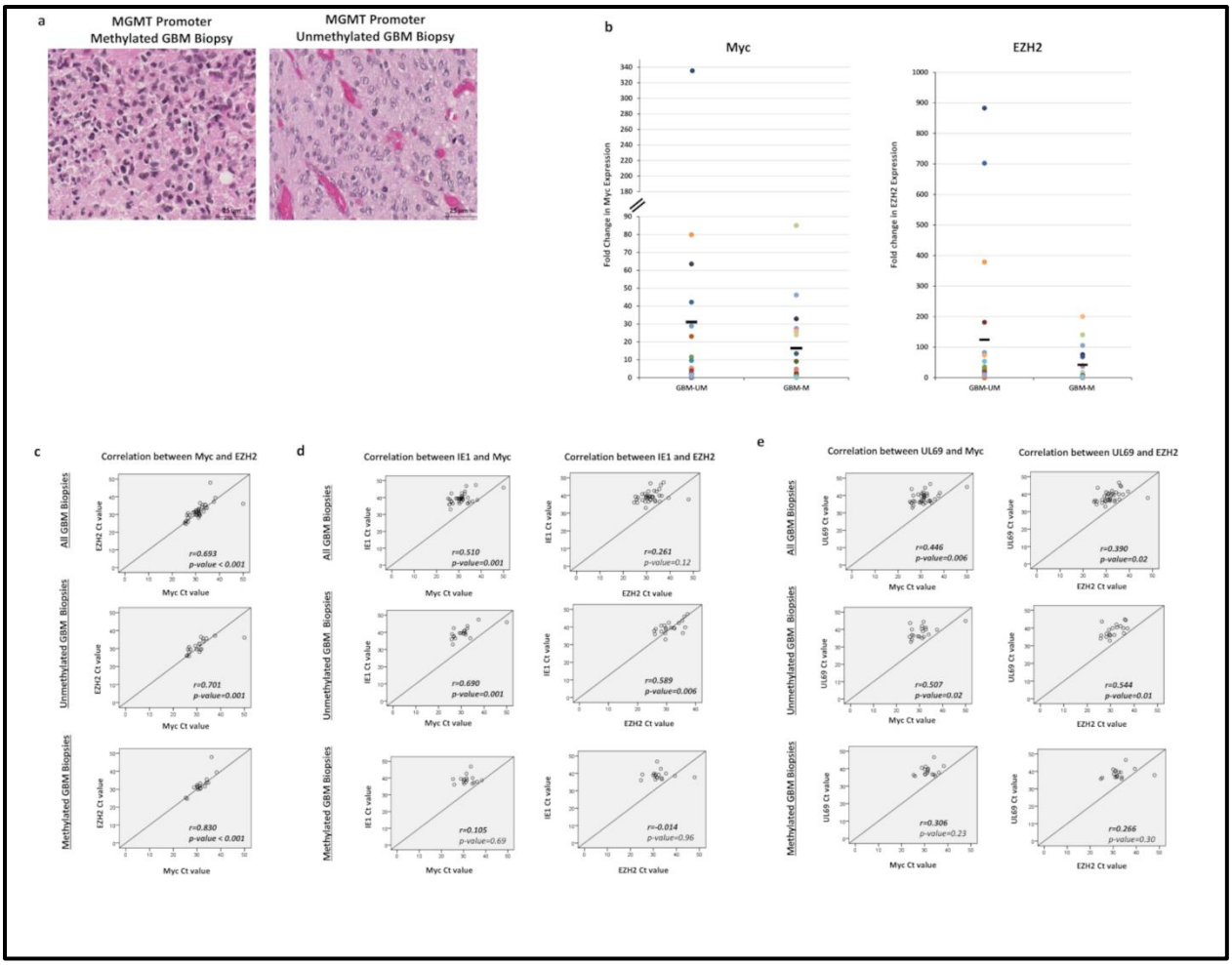

Figure 28: HCMV detection as well as EZH2, and Myc expression in glioblastoma biopsies.

(A) Glioblastoma multiforme tissue was stained using HES; magnification x40, scale bar 25 µm. (B) Scattered plots showing Myc, and EZH2 expression in individual methylated, and unmethylated HCMV-positive GBM biopsies. Mean values are indicated. (C) Correlation test between Myc and EZH2 expression in all GBM biopsies, methylated, and unmethylated HCMV-positive GBM biopsies. Correlation test between IE1 (D) and UL69 (E) presence and the expression of Myc and EZH2. *p*-values were determined by Pearson's correlation test.

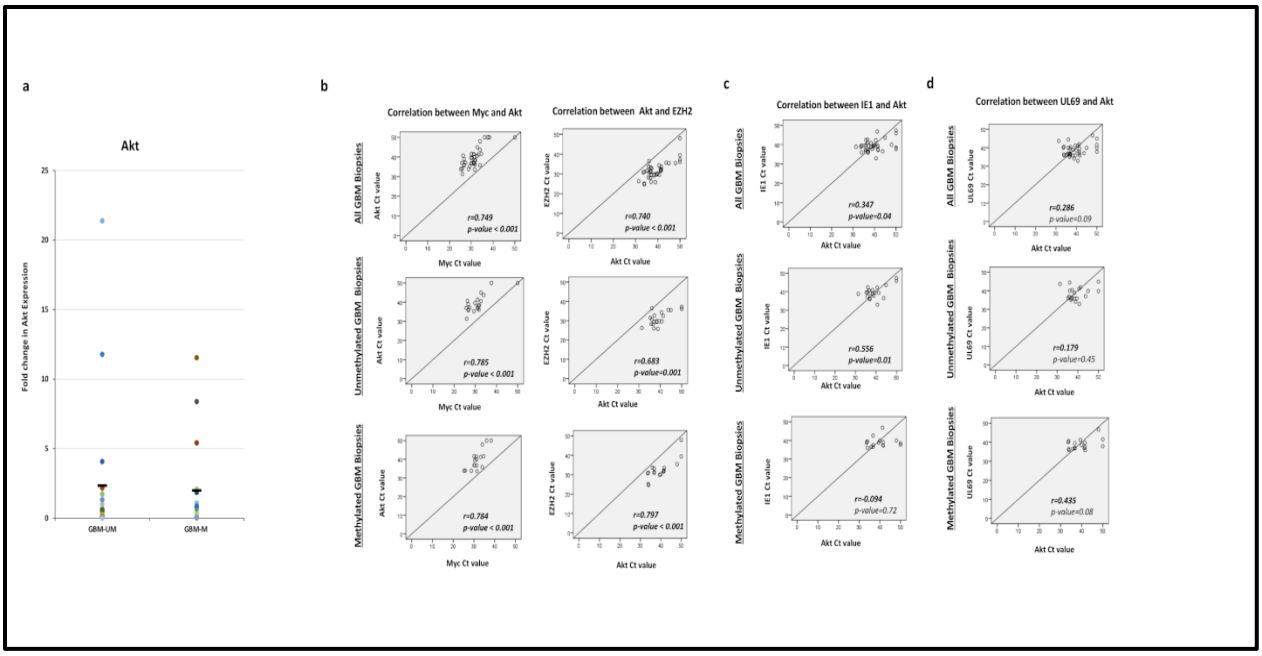

Figure 29: Akt expression in glioblastoma biopsies.

(A) Scattered plots showing Akt expression in individual methylated, and unmethylated HCMV-positive GBM biopsies. Mean values are indicated. (B) Correlation test between Myc and Akt expression, as well as EZH2 and Akt expression in all GBM biopsies, methylated, and unmethylated HCMV-positive GBM biopsies. Correlation test between IE1 (C) and UL69 (D) presence and Akt expression. p-values were determined by Pearson's correlation test.

7.2.6 Isolation of Oncogenic HCMV Strains From GBM Tumors

Among the thirty-seven GBM biopsies, eleven GBM biopsies were considered for HCMV isolation. Eleven HCMV-GBM strains were isolated from MGMT promoter methylated ($n = 4$) and MGMT promoter unmethylated ($n = 7$) GBM tumors by tissue disruption and filtration, and were subsequently grown in MRC5 cells showing a peak of viral load (1–3 log) around day 20 post-infection **(Figure 30A and Table 9)**. Following HAs infection with the eleven HCMV-GBM strains, we detected cell clusters with irradiating low and high motility cells displaying a neural progenitor-like phenotype **(Figure 30B)** parallel to the sustained viral replication confirmed by FACS **(Figure 30C)** and IE1 gene detection by qPCR **(Figure 30D)**. Viral transcripts (IE1 and UL69) were detected in HAs infected with methylated and unmethylated HCMV-GBM strains compared to uninfected HAs **(Figure 30E)**. Upregulated Myc and EZH2 proteins and transcripts were detected in HAs infected with methylated and unmethylated HCMV-GBM strains, unlike

uninfected HAs **(Figure 30F,G,H and Table 9)**. All HCMV-GBM isolates transformed HAs as measured by soft agar colony formation assay (*p*-value $_{(UI\ HAs:\ HCMV\text{-}GBM)} = 0.02$; *p*-value $_{(UI\ HAs:\ HCMV\text{-}GBM\text{-}M)} = 0.04$, *p*-value $_{(UI\ HAs:\ HCMV\text{-}GBM\text{-}UM)} = 0{\cdot}03$) **(Figure 30I)**.

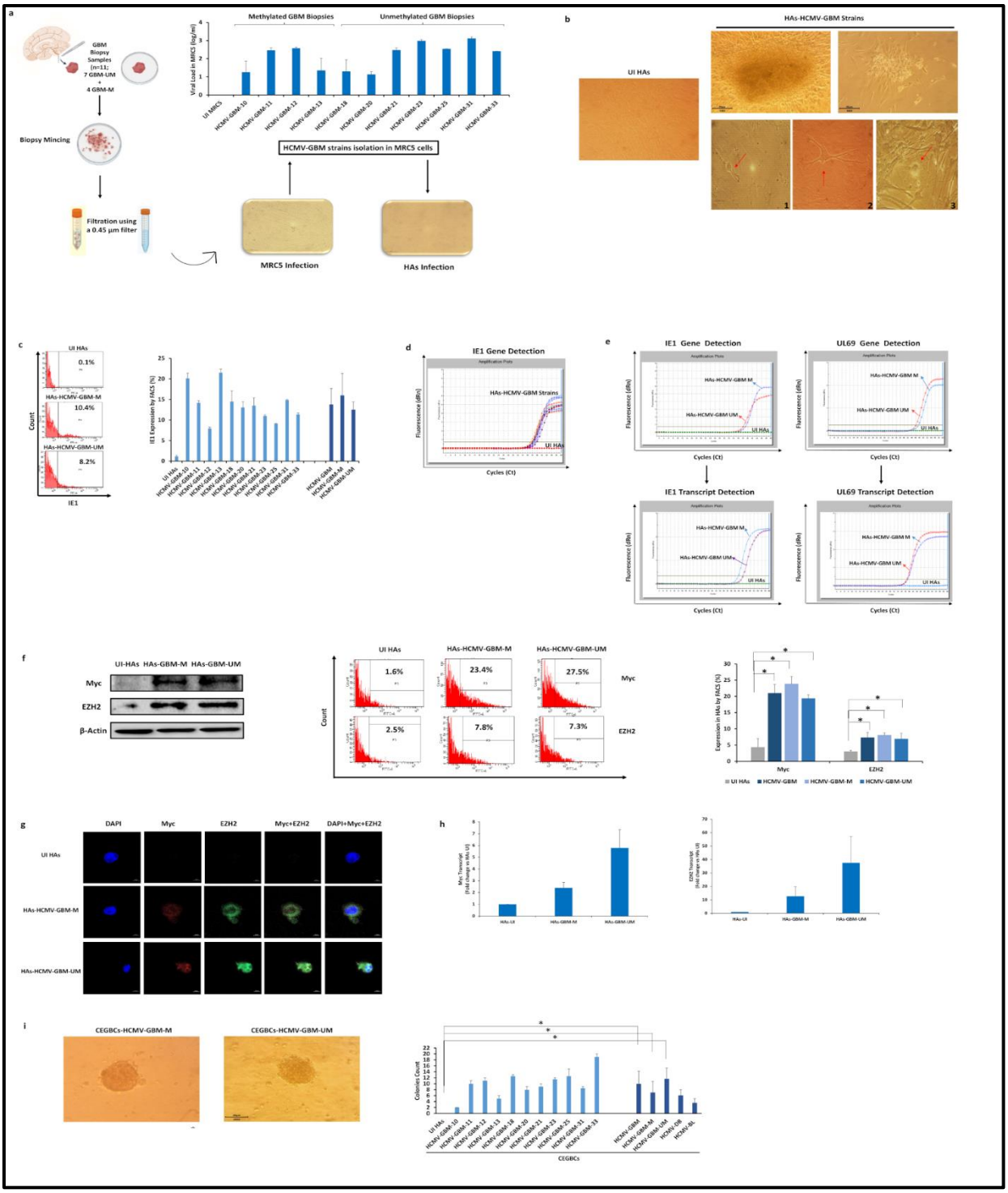

Figure 30: Isolation of oncogenic HCMV strains from GBM biopsies.

(A) Isolation protocol of eleven HCMV-GBM strains from GBM tissues; seven unmethylated and four methylated GBM biopsies. Histogram representing the viral replication of the isolated HCMV strains in MRC5 cultures. UI MRC5 cells were used as control. (B) The subsequent infection of HAs generating CEGBCs. Microscopic images showing the different cellular morphology (red arrows) generated in human astrocytes infected with the eleven isolated GBM HCMV strains; (1) neural progenitor cell (NPC)-like cells; (2) dendritic-like cells with cytoplasmic prolongation, and (3) PGCCs; magnification x100, scale bar 100 µm. IE1 protein and gene expression in the isolated methylated and unmethylated promoter HCMV-GBM strains as measured by FACS (C) and qPCR (D), respectively; UI HAs were used as a control. (E) IE1 and UL69 gene and transcript detection in HAs infected with the isolated methylated and unmethylated promoter HCMV-GBM strains as measured by qPCR and RT-qPCR, respectively. (F) Myc and EZH2 expression in the isolated methylated and unmethylated GBM strains, as measured by western blot and FACS; uninfected HAs were used as a control. β-actin was used as loading control. Histogram representing Myc and EZH2 expression in uninfected HAs, the total isolated HCMV-GBM strains, methylated and unmethylated HCMV-GBM strains as measured by FACS. (G) Confocal microscopic images of Myc and EZH2 staining in HAs infected with the isolated methylated and unmethylated promoter HCMV-GBM strains. Nuclei were counterstained with DAPI; magnification ×63, scale bar 10 µm. (H) Myc and EZH2 transcripts detection by RT-qPCR. (I) Colony formation in soft agar seeded with CEGBCs generated from HAs infection with the isolated methylated and unmethylated promoter HCMV-GBM strains; UI HAs were used as a control. Formed colonies were observed under an inverted light microscope (Magnification 200x, scale bar 100 µm). Histograms representing the number of colonies generated in all GBM strains as well as methylated and unmethylated HCMV-GBM strains. Data are represented as mean ± SD of two independent experiments. **p*-value ≤ 0.05.

Table 9: Characteristics of HCMV-GBM strains.

HCMV isolated from GBM Biopsy (HCMVGBM) N°	Human Astrocytes Infected with HCMV-GBM					
	Myc Expression by FACS	EZH2 Expression by FACS	SOX2 Expression by Confocal Staining	Soft Agar Colonies	Spheroids Formation	Invasion
MGMT PROMOTER METHYLATED GBM BIOPSIES (n=4)						
10	+	+	+	+	+	+/-
11	+	+	+	+	+	+
12	+	+	+	+	+	+
13	+	+	+	+	+	+
Positive	**[4/4]**	**[4/4]**	**[4/4]**	**[4/4]**	**[4/4]**	**[3/4]**
MGMT PROMOTER UNMETHYLATED GBM BIOPSIES (n=7)						
18	+	+	+	+	+	+
20	+	+	+	+	+	+
21	+	+	+	+	+	+
23	+	+	+	+	+	+
25	+	+	+	+	+	+
31	+	+	+	+	+	+
33	+	+	+	+	+	+
Positive	**[7/7]**	**[7/7]**	**[7/7]**	**[7/7]**	**[7/7]**	**[7/7]**
TOTAL ISOLATED GBM BIOPSIES (n=11)						
Positive	**[11/11]**	**[11/11]**	**[11/11]**	**[11/11]**	**[11/11]**	**[10/11]**

Spheroids were generated 24–48 hours post-seeding the HAs infected with the clinical HCMV-GBM strains (p-value $_{(UI\ HAs:\ HCMV\text{-}GBM)} = 0.02$; p-value $_{(UI\ HAs:\ HCMV\text{-}GBM\text{-}M)} = 0.04$, p-value $_{(UI\ HAs:\ HCMV\text{-}GBM\text{-}UM)} = 0.03$) **(Figure 31A)**. High SOX2 levels were detected in spheroids generated from the eleven HCMV-GBM strains **(Figure 31B and Table 9)**. Nestin and IE1 were concomitantly expressed in spheroids generated from all HCMV-GBM strains **(Figure 31C)**. Spheroids generated from the HCMV-GBM strains did not express GFAP unlike uninfected HAs. Further, a 3D collagen-invasion assay was performed to evaluate the invasiveness potential of the spheroids generated from HCMV-GBM strains **(Figure 31D)**. The lncRNA4.9 gene was detected in CEGBCs derived from HCMV-GBM strains **(Figure 31E).** Viral lncRNA4.9 and cellular lncRNA HOTAIR transcripts were detected in the EZH2 immunoprecipitated samples corresponding to CEGBCs derived from all HCMV-GBM strains, mostly from MGMT promoter unmethylated HCMV-GBM strains, using RNA CLIP assay (p-value $_{(UI\ HAs:GBM)} = 0.03$; p-value $_{(UI\ HAs:\ GBM\text{-}M)} = 0.07$; p-value $_{(UI\ HAs:\ GBM\text{-}UM)} = 0.04$) **(Figure 31F)**.

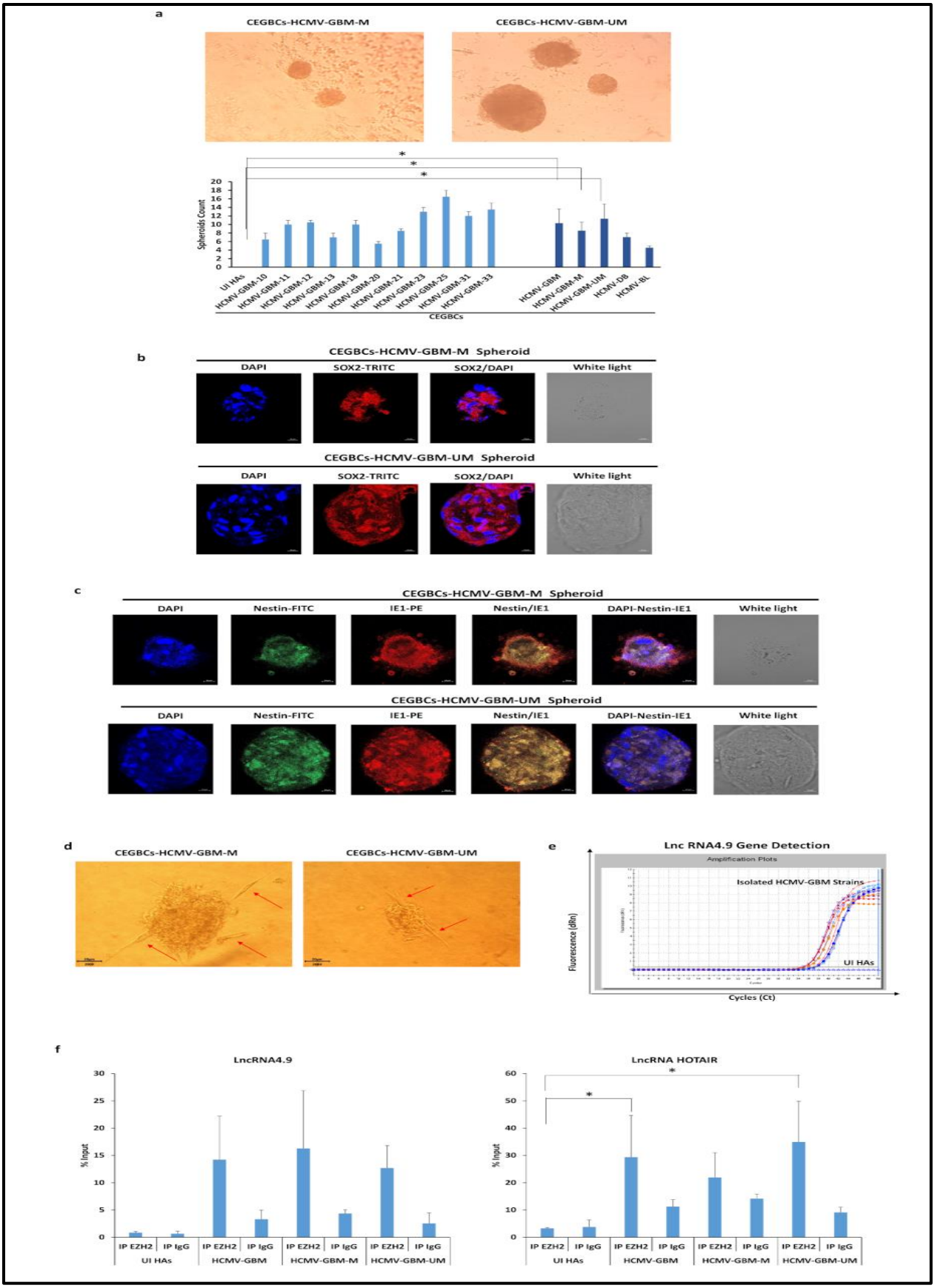
a
CEGBCs-HCMV-GBM-M
CEGBCs-HCMV-GBM-UM
Spheroids Count
UI HAs
HCMV-GBM-10
HCMV-GBM-11
HCMV-GBM-12
HCMV-GBM-13
HCMV-GBM-18
HCMV-GBM-20
HCMV-GBM-21
HCMV-GBM-23
HCMV-GBM-25
HCMV-GBM-31
HCMV-GBM-33
HCMV-GBM
HCMV-GBM-M
HCMV-GBM-UM
HCMV-DB
HCMV-BL
CEGBCs
b
CEGBCs-HCMV-GBM-M Spheroid
DAPI
SOX2-TRITC
SOX2/DAPI
White light
CEGBCs-HCMV-GBM-UM Spheroid
c
CEGBCs-HCMV-GBM-M Spheroid
DAPI
Nestin-FITC
IE1-PE
Nestin/IE1
DAPI-Nestin-IE1
White light
CEGBCs-HCMV-GBM-UM Spheroid
d
CEGBCs-HCMV-GBM-M
CEGBCs-HCMV-GBM-UM
e
Lnc RNA4.9 Gene Detection
Amplification Plots
Isolated HCMV-GBM Strains
UI HAs
Fluorescence (dRn)
Cycles (Ct)
f
LncRNA4.9
% Input
IP EZH2
IP IgG
UI HAs
HCMV-GBM
HCMV-GBM-M
HCMV-GBM-UM
LncRNA HOTAIR

Figure 31: Spheroid forming and invasion potentials of the HCMV-GBM strains and the detection of lncRNA 4.9 and HOTAIR transcripts.

(A) Microscopic images of the spheroids generated from the isolated GBM HCMV strains; magnification ×100, scale bar 20 μm. Histograms representing the number of spheroids generated in all HCMV GBM strains as well as methylated and unmethylated HCMV-GBM strains; UI HAs were used as a control. Confocal microscopic images of SOX2 (B) and concomitant Nestin/IE1 (C) staining in spheroids generated from the isolated HCMV-GBM strains. Nuclei were counterstained with DAPI; magnification ×63, scale bar 10 μm. (D) Microscopic images showing the invasion potential of CEBGCs through protrusions and cell migration (red arrows); magnification ×200, scale bar 20 μm. (E) lncRNA 4.9 gene detection in the supernatants of HAs infected with the isolated HCMV-GBM strains using qPCR; UI HAs were used as a control. (F) Interaction of lncRNA4.9 and HOTAIR transcripts with EZH2 in CEGBCs-GBM using RNA cross-linking immunoprecipitation (CLIP) assay.

7.2.7 EZH2 inhibitor, TMZ, and GCV tritherapy Curtails CEGBCs Growth

Although TMZ is known as the first-choice chemotherapeutic agent in glioblastoma, TMZ resistance often becomes a limiting factor in effective glioblastoma treatment [373,374]. Herein, we evaluated EZH2 inhibitor GSK343, GCV and TMZ efficacy as single therapies, as well as bi- or tri-combination therapy on CEGBCs-DB, BL, and GBM spheroids **(Figure 32)**. TMZ reduced spheroids' size by 23% only in CEGBCs-BL cultures, unlike CEGBCs-DB which displayed more mesenchymal traits (p-value $_{(CEGBCs\text{-}DB:CEGBCs\text{-}BL)} = 0.03$). GCV reduced the spheroids' size by 21% and 24% in CEGBCs-DB and BL, respectively (p-value $_{(CEGBCs\text{-}DB:CEGBCs\text{-}BL)} = 0.35$). On the other hand, GCV/TMZ combination therapy lead to a 27% size reduction of CEGBCs-BL spheroids, meanwhile having a very limited effect in CEGBCs-DB in which the spheroids' size was reduced by 9% (p-value $_{(CEGBCs\text{-}DB:CEGBCs\text{-}BL)} < 0.01$) **(Figure 32A)**. Spheroids of CEGBCs-DB and BL were treated by GSK343, GSK343/GCV, GSK343/TMZ, and GSK343/GCV/TMZ. CEGBCs-DB were resistant to mostly all therapies except the triple therapy (p-value $_{(CEGBCs\text{-}DB:CEGBCs\text{-}BL)} = 0.06$) unlike CEGBCs-BL that were mainly responsive to GSK343/TMZ (p-value $_{(CEGBCs\text{-}DB:CEGBCs\text{-}BL)} < 0.001$) and triple treatment ($p$-value $_{(CEGBCs\text{-}DB:CEGBCs\text{-}BL)} = 0.06$) **(Figure 32A)**. Under triple therapy (GSK343/GCV/TMZ), spheroids' size was reduced by around 90% in CEGBCs-DB and BL at day 10 post-treatment (p-value $_{(triple\ therapy:\ TMZ)} = 0.02$) **(Figure 32B)**. Spheroids' size was reduced by around 60% with all the eleven HCMV-GBM strains at day 10 post-triple treatment (GSK343/GCV/TMZ) (p-value $_{(triple\ therapy:\ TMZ)} < 0.001$) **(Figure 32C)**, similar to that reported for DB and BL strains.

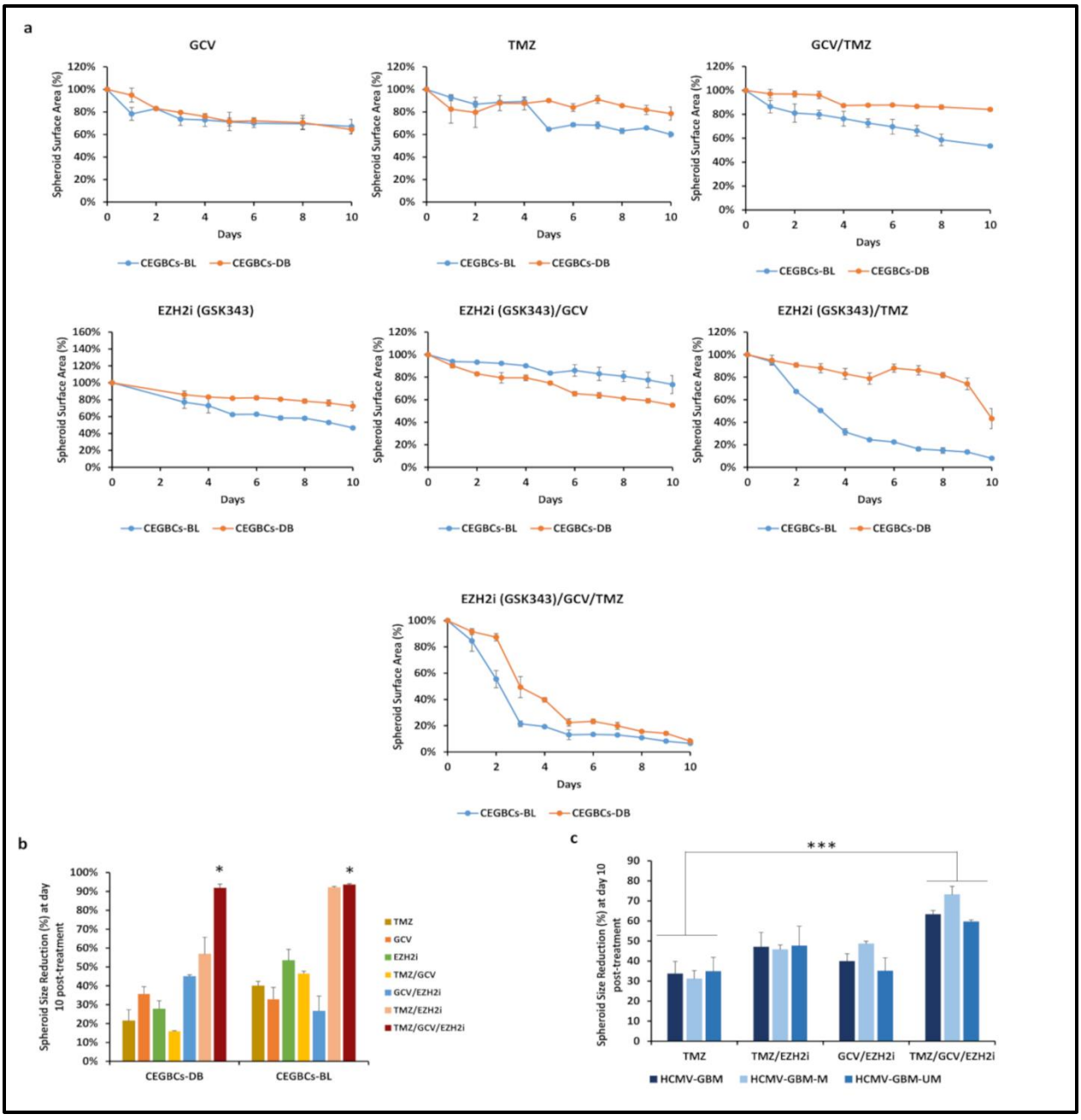

Figure 32: The effect of diverse single and combination therapies on CEGBCs' growth.

(A) Curves representing the spheroid surface area corresponding to CEGBCs-DB and BL under GCV(20 µM), TMZ(50 µM), GCV(20 µM)/TMZ(50 µM), GSK343 (0.1 µM), GSK343 (0.1 µM)/ GCV(20 µM), GSK343 (0.1 µM)/TMZ(50 µM), and GSK343 (0.1 µM)/GCV(20 µM)/TMZ(50 µM) therapies. (B) Histogram representing the CEGBCs-DB and BL spheroids size reduction 10 days post-treatment. Data are represented as mean ± SD of two independent experiments. **p*-value ≤ 0.05. (C) Histogram representing the CEGBCs-GBM spheroids size reduction at day 10 post-treatment. Data are represented as mean ± SD of two independent experiments. **p*-value ≤ 0.05; ****p*-value ≤ 0.001.

7.3 Polyploidy, EZH2 Upregulation, and Transformation in CMV-infected Human Ovarian Epithelial Cells

7.3.1 OECs Chronically Infected With HCMV-DB and BL Strains Generated CTO Cells With PGCCs

Upon studying the tropism exhibited by HCMV in OECs, all HCMV clinical strains replicated showing a peak viral replication at day 21, 16, 16, and 19 post-infection in OECs infected with HCVM-DB, HCMV-BL, HCMV-KM, and HCMV-FS, respectively **(Figure 33A and Figure 34A)**. The peak level of HCMV productive infection was 6 and 4 logs in OECs-DB and BL, respectively **(Figure 33A)**. HCMV-IE1 and pp65 proteins were detected in OECs-DB and BL **(Figure 33B)**.

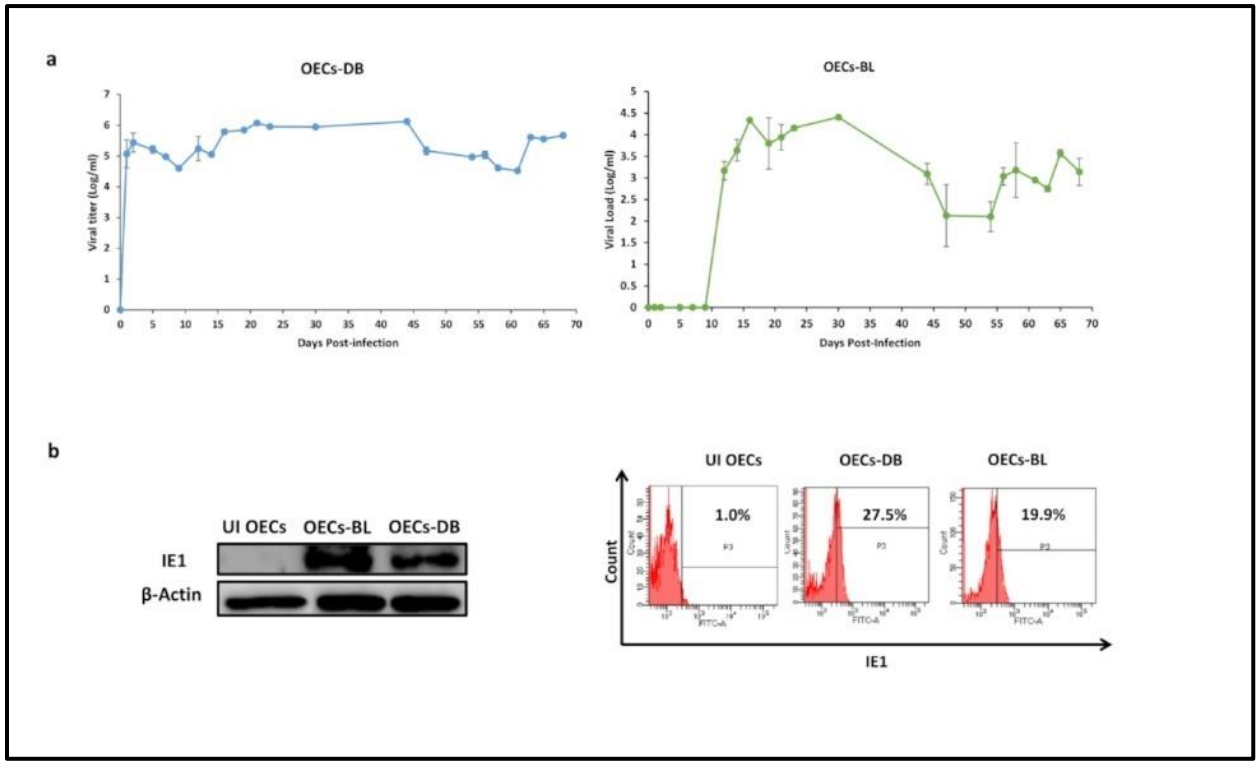

Figure 33: Replication of high-risk HCMV strains in OECs cultures.

(A)Time-course of the viral titer in the supernatant of OECs infected with HCMV-DB and BL as measured by IE1-qPCR. (B) Immunoblotting data of IE1 in uninfected OECs lysates and OECs infected with HCMV-DB and BL (day 5 post-infection). β-actin was used as loading control. IE1 expression by FACS in acutely infected OECs-DB and BL; UI OECs were used as a control.

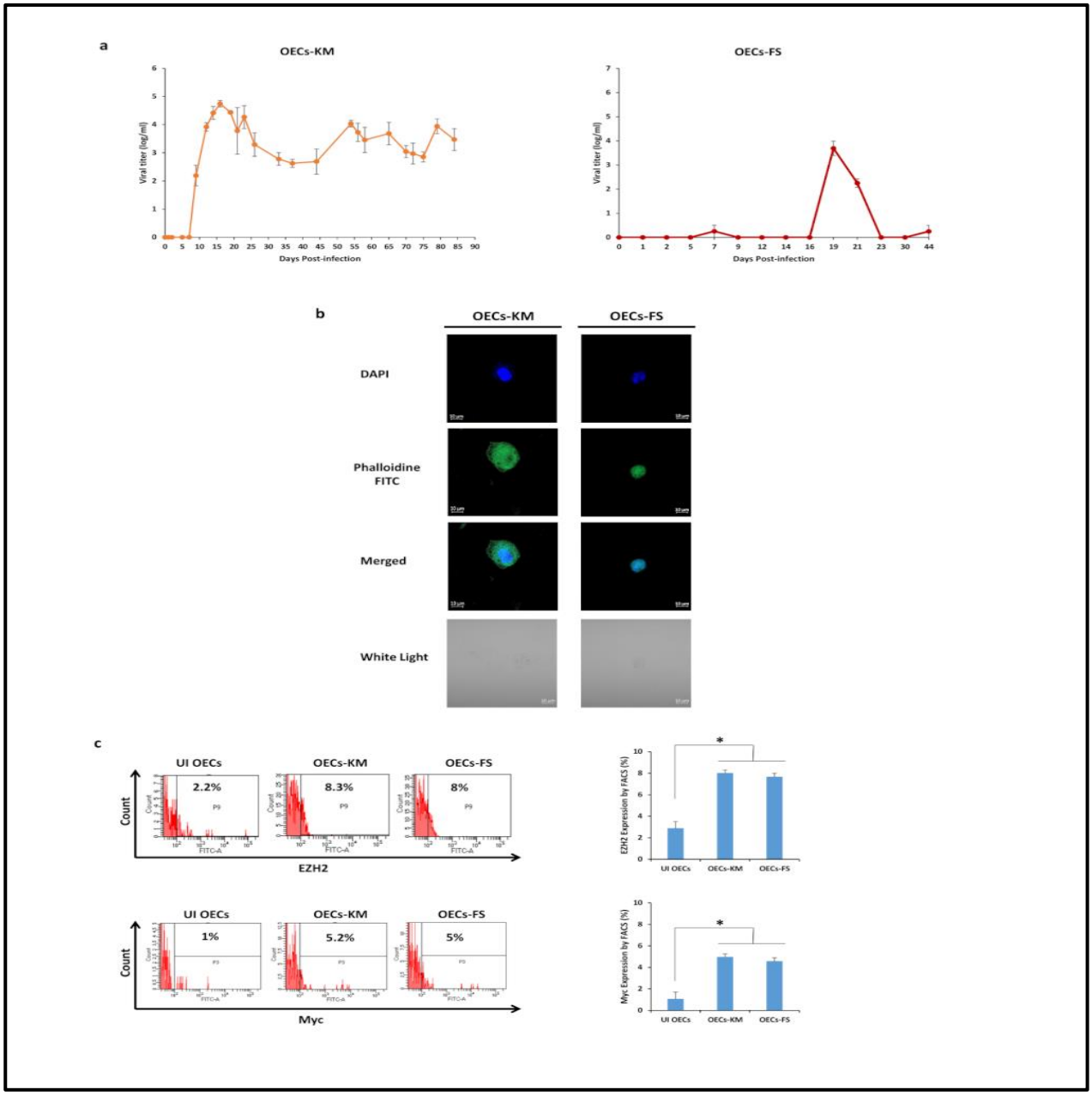

Figure 34: Replication of low risk HCMV strains in OECs cultures.

(A) Time-course of the viral titer in the supernatant of OECs infected with HCMV-KM and FS as measured by IE1-qPCR. (B) Confocal microscopic images of DAPI and phalloidine staining in OECs infected with HCMV-KM and FS. (C) FACS staining of EZH2 and Myc in uninfected OECs as well as OECs-KM and FS. Data are represented as mean ± SD of two independent experiments. * p-value≤0·05.

We noticed the existence of large-sized cells having large nuclei that were detected only in OECs chronically infected with the high-risk HCMV-DB and BL strains compared to uninfected OECs **(Figure 36A)** and OECs chronically infected with HCMV-KM and FS strains **(Figure 34B)**. Further, around three months post-infection, cellular survival was noted only in the chronically infected OECs-DB and BL compared to OECs-KM and FS **(Figure 35)**. The emerging cells were termed *"CMV-Transformed Ovarian epithelial cells*" or CTO similar to the transformed cells that were previously reported by our group, namely, "CMV-Transformed Human mammary epithelial cells" or CTH cells and "CMV-Elicited GlioBlastoma Cells" or CEGBCs [125,209,375].

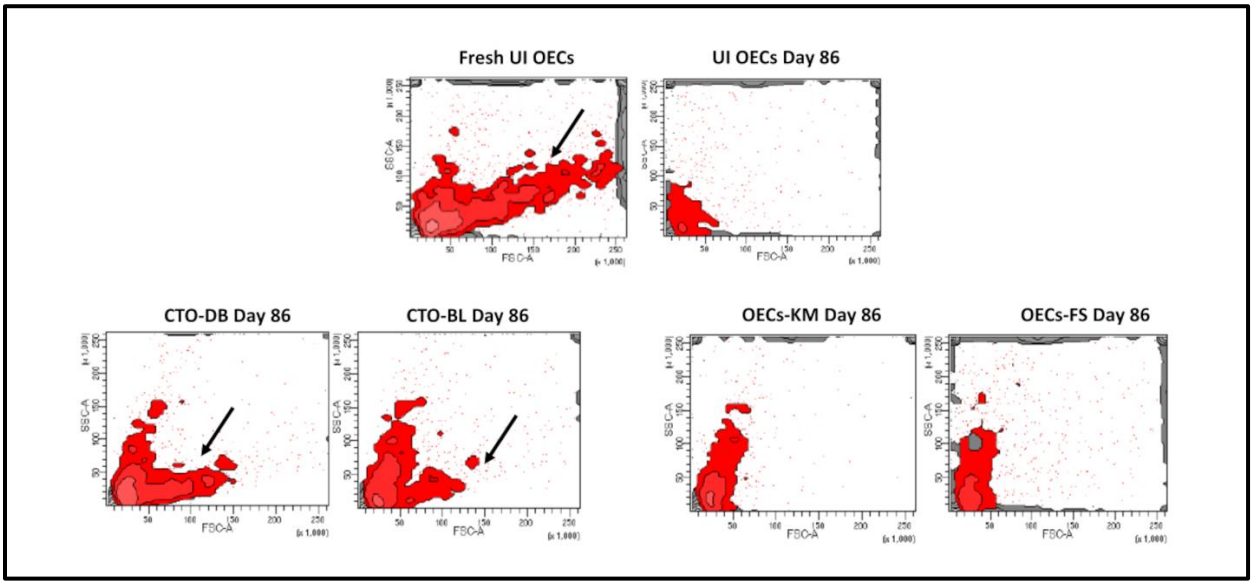

Figure 35: Flow cytometric analysis based on FSC and SSC of uninfected OECs as well as chronically infected OECs.

Only chronically-infected OECs-DB and BL, namely CTO-DB and CTO-BL cells, and not the chronically-infected OECs-KM and FS were alive at day 86 post-infection (black arrows).

After applying a morphology-based classification, cellular heterogeneity was detected in CTO-DB and BL cultures including giant cells, blastomeres, blastocytes, multinucleated, mesenchymal, budding, and lipid droplets-rich cells as well as cells exhibiting filopodia and cytoplasmic vacuolization **(Figure 36B)**. Some of the aforementioned morphologies were further confirmed by confocal microscopy showing mainly multinucleated and mesenchymal cells, asymmetric division, budding, and cells with giant nuclei **(Figure 36C)**. A high percentage of tetraploidization and polyploidy cells was detected in CTO-DB and BL compared to UI OECs **(Figure 36D)**. CTO-

DB and BL populations were classified into PGCCs (≥4 N), intermediate cells (ICs of 2–4 N), and small cells (SCs of 2 N) **(Figure 36D)**. As a positive control, cobalt chloride ($CoCl_2$) was used to induce PGCCs formation in OECs cultures **(Figure 36D)**.

Since the blockade of tumor suppressors and decreased telomerase activity have been correlated with tetraploidization in several human cancers [376], p53 and Rb expression as well as telomerase activity were assessed in uninfected OECs, CTO-DB, and CTO-BL **(Figure 36E,F)**. Downregulation of p53 and Rb proteins was noticed in CTO-DB and BL compared to controls (*p*-value $_{(UI\ OECs:CTO\text{-}HCMV)} = 0{\cdot}03$), unlike pRb which was upregulated in CTO-DB and BL (*p*-value $_{(UI\ OECs:CTO\text{-}HCMV)} = 0{\cdot}03$) **(Figure 36E)**. Notably, telomerase activity was relatively low or undetectable in CTO-DB and BL compared to uninfected OECs (*p*-value = 0·03) **(Figure 36F)**. Hence, p53 and Rb downregulation along with decreased telomerase activity are sufficient to drive polyploidization in CTO-DB and BL, as previously reported [376].

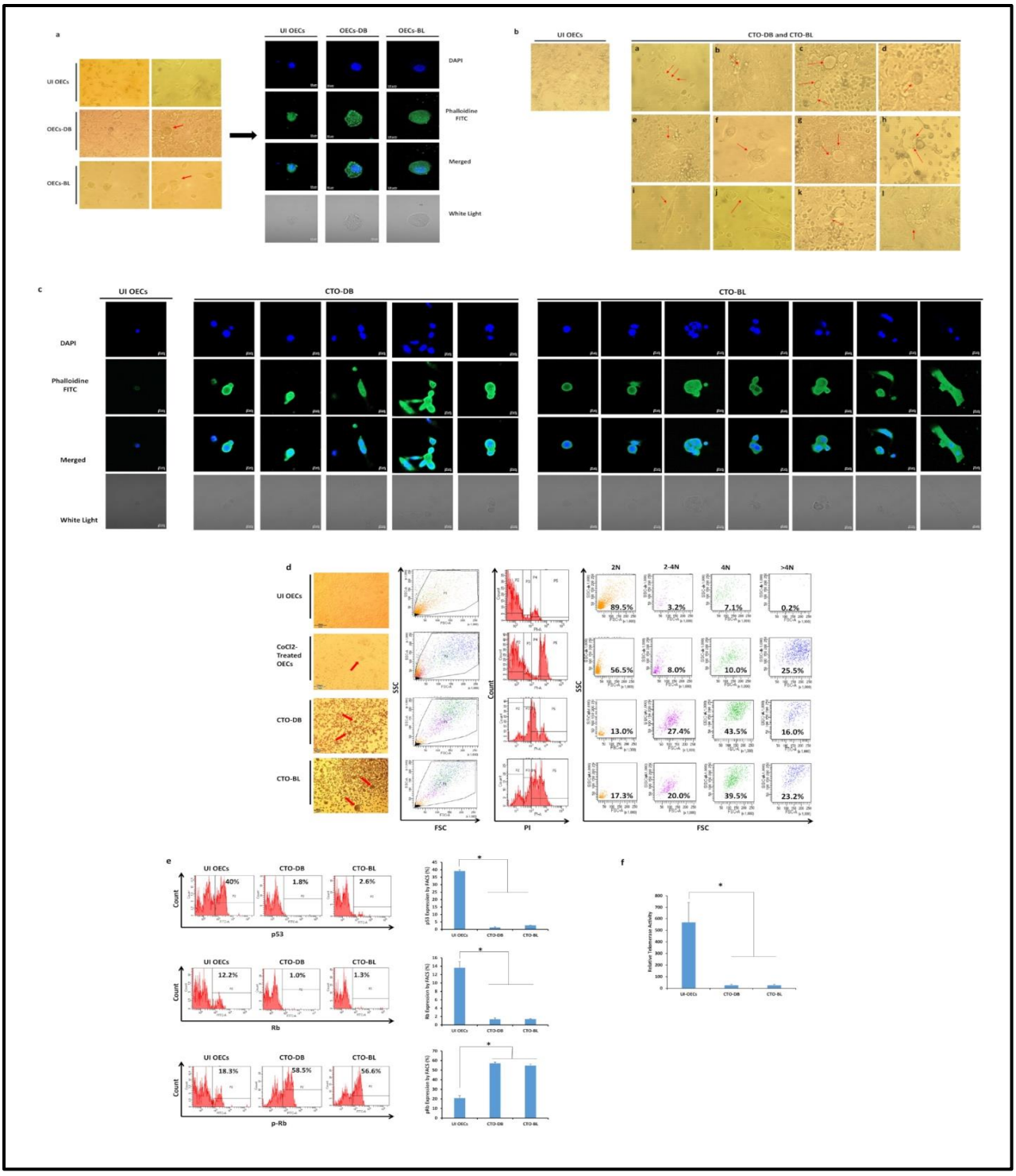

Figure 36: Chronic infection of OECs with the high-risk HCMV clinical isolates and polyploidy detection in OECs cultures.

(A) Microscopic images including confocal images of DAPI and phalloidine staining in OECs infected with HCMV-DB and BL; uninfected OECs were used as a negative control. Left panel: magnification ×100 and ×200, scale bar 100 and 50 µm; Right panel: magnification ×63, scale bar 10 µm. Red arrows showing the PGCCs detected in OECs cultures. (B) The appearance of distinct cellular morphologies of the giant cell cycle including (a) filopodia, (b, c, d) blastomeres and blastocytes, (e) lipid droplets-filled cells, (f) multinucleated, (g, h) budding, (i) mesenchymal cells as well as (j, k, l) few atypical morphologies; magnification ×100, scale bar 100 µm. Uninfected OECs were used as a control. (C) Confocal microscopic images of DAPI and phalloidine staining in CTO-DB and BL. Uninfected OECs were used as a negative control; magnification ×63, scale bar 10 µm. (D) Propidium iodide (PI) staining for polyploidy detection in HCMV-transformed OECs. Cobalt chloride (CoCl2)-treated OECs (450 µM) were used as a positive control. Microscopic images of uninfected OECs as well as the PGCCs generated in CTO-DB and BL cultures and post- CoCl2 treatment; magnification ×100, scale bar 100 µm. (E) p53, Rb, and p-Rb expression in uninfected OECs and CTO-DB and BL by FACS. (F) Histograms representing the relative telomerase activity in uninfected OECs as well as CTO-DB and BL. Data are represented as mean ± SD of two independent experiments. *p-value ≤ 0·05.

7.3.2 CTO cells Display Dedifferentiation, Stemness, and EMT Characteristics

CTO-DB and BL were seeded in soft agar to assess their oncogenic transforming potential. Colony formation was detected in the cultures seeded with CTO-DB and BL, compared to uninfected OECs **(Figure 37A)**. On the proteomic level, EZH2 and Myc upregulation was detected in CTO-DB and BL compared to uninfected OECs (p-value $_{(UI\ OECs:CTO\text{-}HCMV)} = 0{\cdot}03$) **(Figure 37B,C, and D)**; on the contrary, a limited EZH2 and Myc upregulation was observed in OECs-KM and FS (p-value $_{(UI\ OECs:OECs\text{-}HCMV)} = 0{\cdot}02$) **(Figure 34C)**. A significant positive correlation between EZH2 and Myc protein expression was detected in CTO cells ($r = 0.983$, p-value $< 0{\cdot}001$) **(Figure 38)**. Further, EZH2 and Myc transcripts were upregulated in CTO-DB and BL compared to uninfected controls (p-value $_{(UI\ OECs:CTO\text{-}HCMV)} = 0{\cdot}03$) **(Figure 37E)**. Altogether, a remarkable EZH2 upregulation parallel to the limited increase in Myc expression was noticed in CTO infected with the high-risk HCMV-DB and BL strains. EZH2 and Myc were expressed mainly in the PGCCs subpopulation of CTO-DB and BL **(Figure 37G)**. A limited increase in SUZ12 expression was observed in CTO-DB and BL compared to uninfected OECs (p-value $_{(UI\ OECs:CTO\text{-}HCMV)} = 0{\cdot}03$) **(Figure 39A,B)**. Upon assessing the proliferative potential of OECs chronically infected with HCMV high-risk strains, Ki67Ag was highly prominent in CTO-DB and BL compared to uninfected OECs (p-value $_{(UI\ OECs:CTO\text{-}HCMV)} = 0{\cdot}03$) **(Figure 37F)**. High Ki67Ag expression was detected in the large cells **(Figure 37G)**.

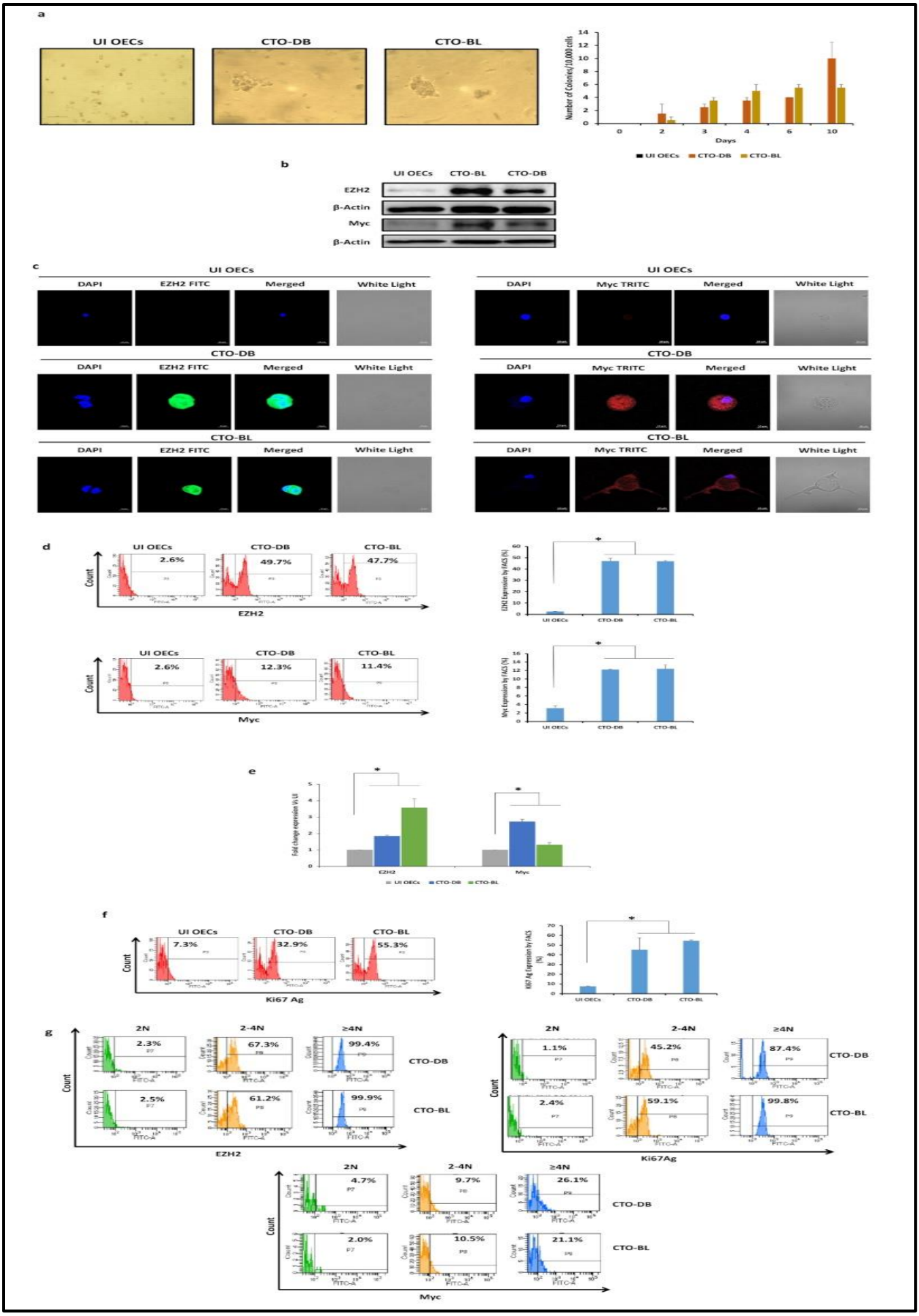
a
UI OECs
CTO-DB
CTO-BL
Number of Colonies/10,000 cells
Days
UI OECs CTO-DB CTO-BL
b
UI OECs CTO-BL CTO-DB
EZH2
β-Actin
Myc
β-Actin
c
UI OECs
DAPI
EZH2 FITC
Merged
White Light
Myc TRITC
CTO-DB
CTO-BL
d
Count
EZH2
Myc
2.6%
49.7%
47.7%
12.3%
11.4%
e
Fold change expression Vs UI
f
Ki67 Ag
7.3%
32.9%
55.3%
g
2N
2-4N
≥4N
2.3%
67.3%
99.4%
2.5%
61.2%
99.9%
1.1%
45.2%
87.4%
2.4%
59.1%
99.8%
4.7%
9.7%
26.1%
2.0%
10.5%
21.1%

Figure 37: Colony formation in soft agar and the phenotypic characterization of HCMV-transformed OECs.

(A) Colony formation in soft agar seeded with CTO-DB and BL (MOI = 1); UI OECs were used as a negative control. Formed colonies were observed under an inverted light microscope (Magnification ×200, scale bar 50 μm). Histogram representing the colony quantification/10,000 cells over days. (B) Immunoblotting data of EZH2 and Myc in uninfected OECs lysates and CTO-DB and BL. β-actin was used as loading control. (C) Confocal microscopic images of EZH2, Myc, and DAPI staining in CTO-DB and BL. UI OECs were used as controls; magnification ×63, scale bar 10 μm. (D) FACS staining of EZH2 and Myc in uninfected OECs as well as CTO-DB and BL. (E) EZH2 and Myc transcriptsVdetection by RT-qPCR. (F) FACS staining of Ki67Ag in uninfected OECs as well as CTO-DB and BL. (G) EZH2, Myc, and Ki67Ag expression in CTO-DB and BL subpopulations (2 N, 2–4 N, and ≥4 N). Data are represented as mean ± SD of two independent experiments. **p*-value ≤ 0·05.

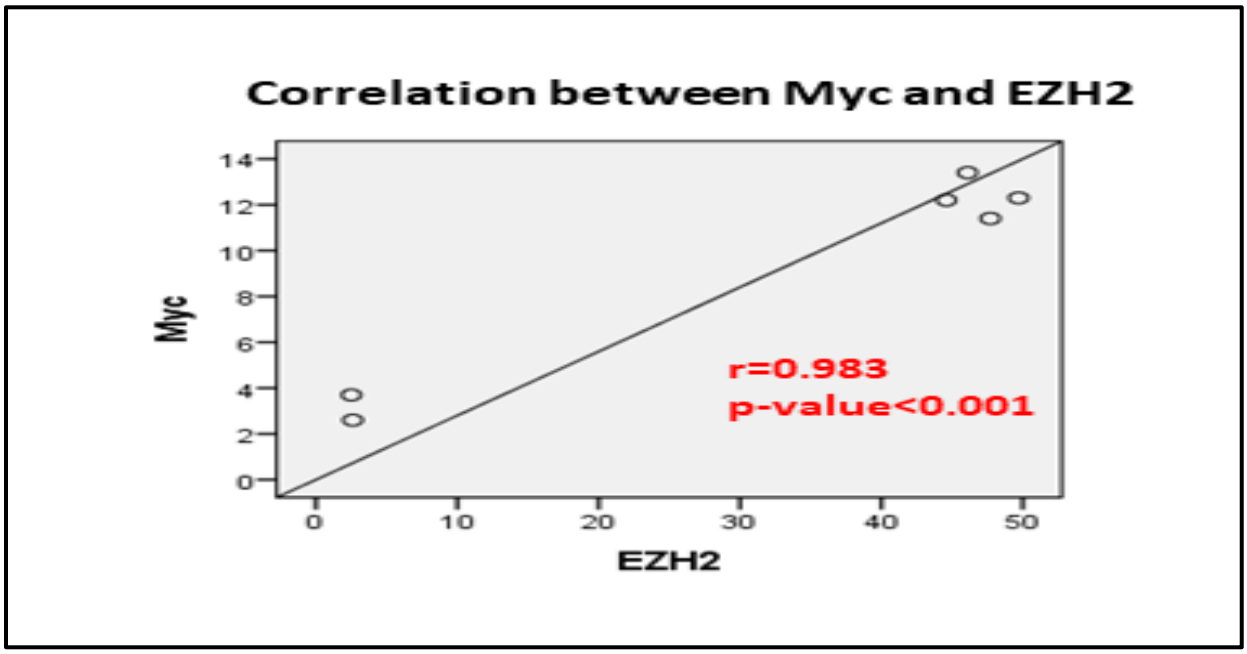

Figure 38: The assessment of the correlation between EZH2 and Myc expression in CTO cells.

A significant-positive correlation detected between EZH2 and Myc protein expression in CTO-DB and BL cells. p-values were determined by Pearson's test.

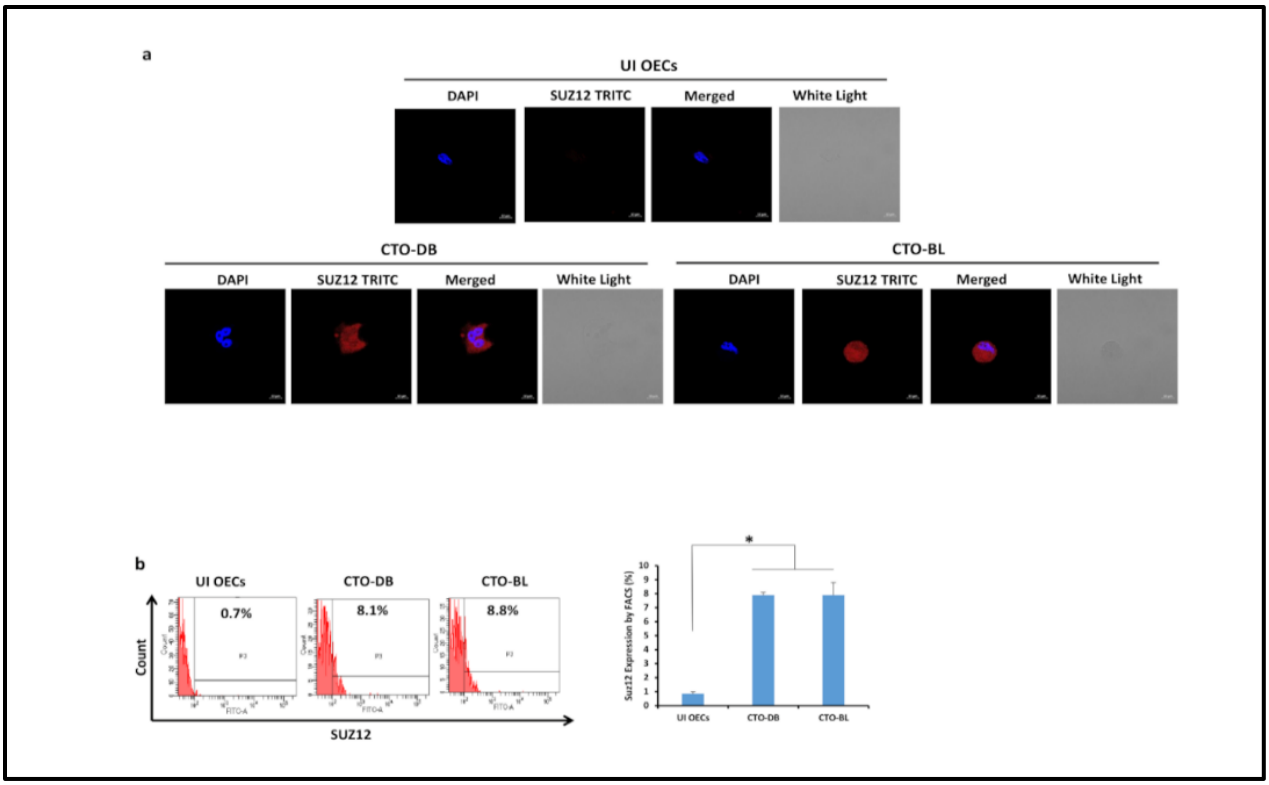

Figure 39: Expression of SUZ12 in CTO-DB and BL cells.

SUZ12 expression by (A) confocal microscopy and (B) FACS in CTO-DB and BL; uninfected OECs were used as a control. Nuclei were counterstained with DAPI; magnification ×63, scale bar 10 µm. Data are represented as mean ± SD of two independent experiments. * p-value≤0.05.

CTO-DB and BL displayed an embryonic stemness phenotype. The key regulatory genes maintaining the pluripotency and self-renewal properties of embryonic stem cells, Nanog, Sox2, and Oct4 were shown to be highly expressed in CTO-DB and BL compared to uninfected OECs **(Figure 40A,B, and Figure 41A)**. Additionally, transcripts of Nanog, Sox2, and Oct4 were elevated in CTO-DB and BL (Nanog, *p*-value $_{(\text{UI OECs:CTO-HCMV})} = 0{\cdot}06$; Sox2 and Oct4, *p*-value $_{(\text{UI OECs:CTO-HCMV})} = 0{\cdot}03$) **(Figure 40C, and Figure 41B)**. Besides PGCCs appearance in CTO-DB and BL cultures, it's worth mentioning the appearance of spontaneous spheroids in CTO-BL cultures **(Figure 40D)**. Further, in the presence of methylcellulose, spheroids were generated in CTO-DB and BL cultures **(Figure 40E)**. Finally, CD44, a marker of stemness and invasiveness, was upregulated in CTO-DB and BL cultures compared to uninfected OECs **(Figure 42)**.

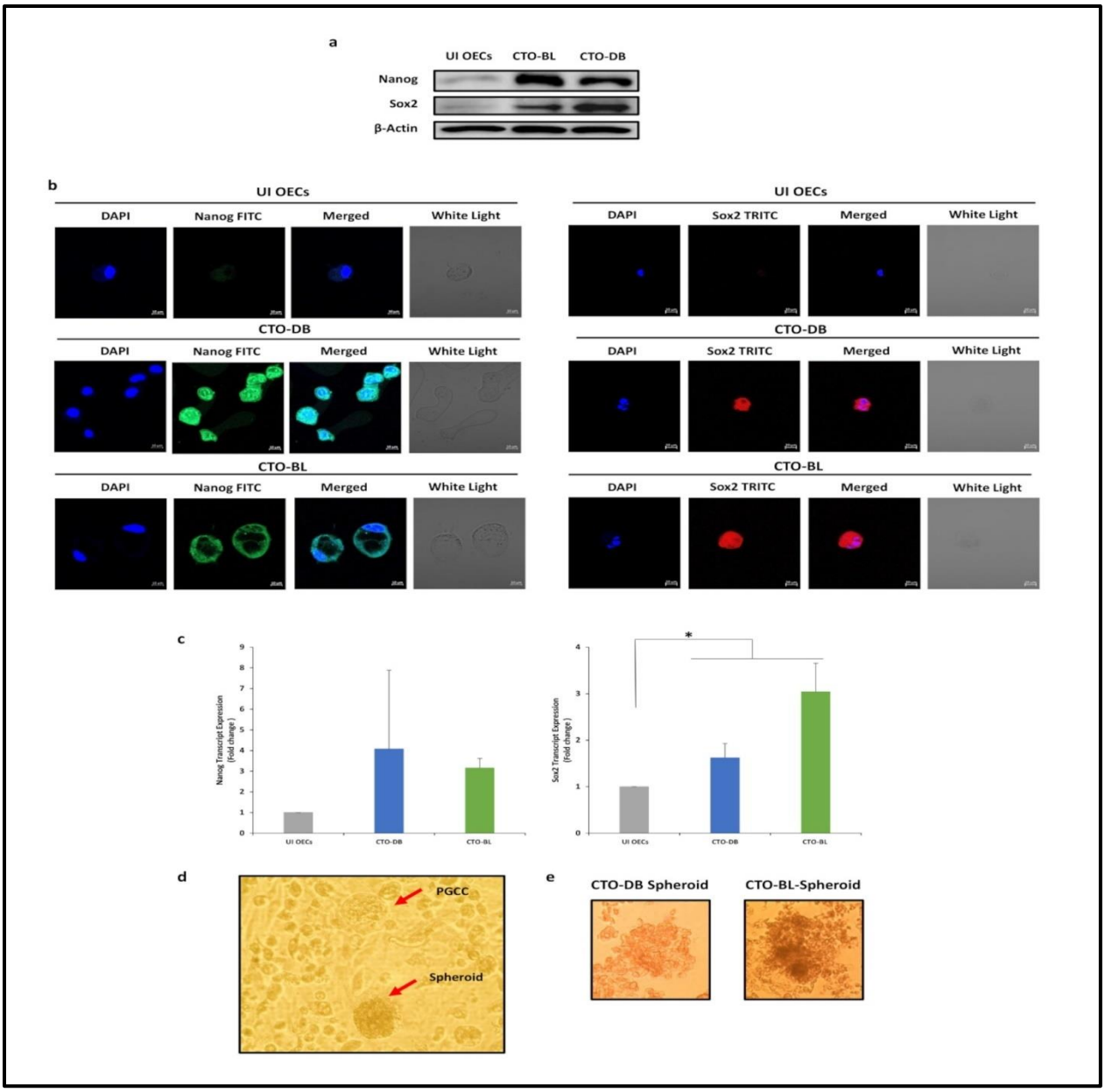

Figure 40: HCMV-transformed OECs display an embryonic stemness phenotype and possess spheroid-forming potential.

(A) Immunoblotting data of Nanog and Sox2 in uninfected OECs lysates and CTO-DB and BL. β-actin was used as loading control. (B) Confocal microscopic images of Nanog, Sox2, and DAPI staining in CTO-DB and BL. UI OECs were used as controls; magnification ×63, scale bar 10 μm. (C) Nanog and Sox2 transcripts detection by RT-qPCR. Data are represented as mean ± SD of two independent experiments. (D) Spontaneous spheroid formation and PGCCs were detected under an inverted light microscope in HCMV-transformed OECs cultures. Magnification ×100, scale bar 100 μm. (E) Spheroid generation from the chronically infected DB and BL OECs in methyl-cellulose assay; magnification ×100, scale bar 100 μm. *p- value ≤ 0·05.

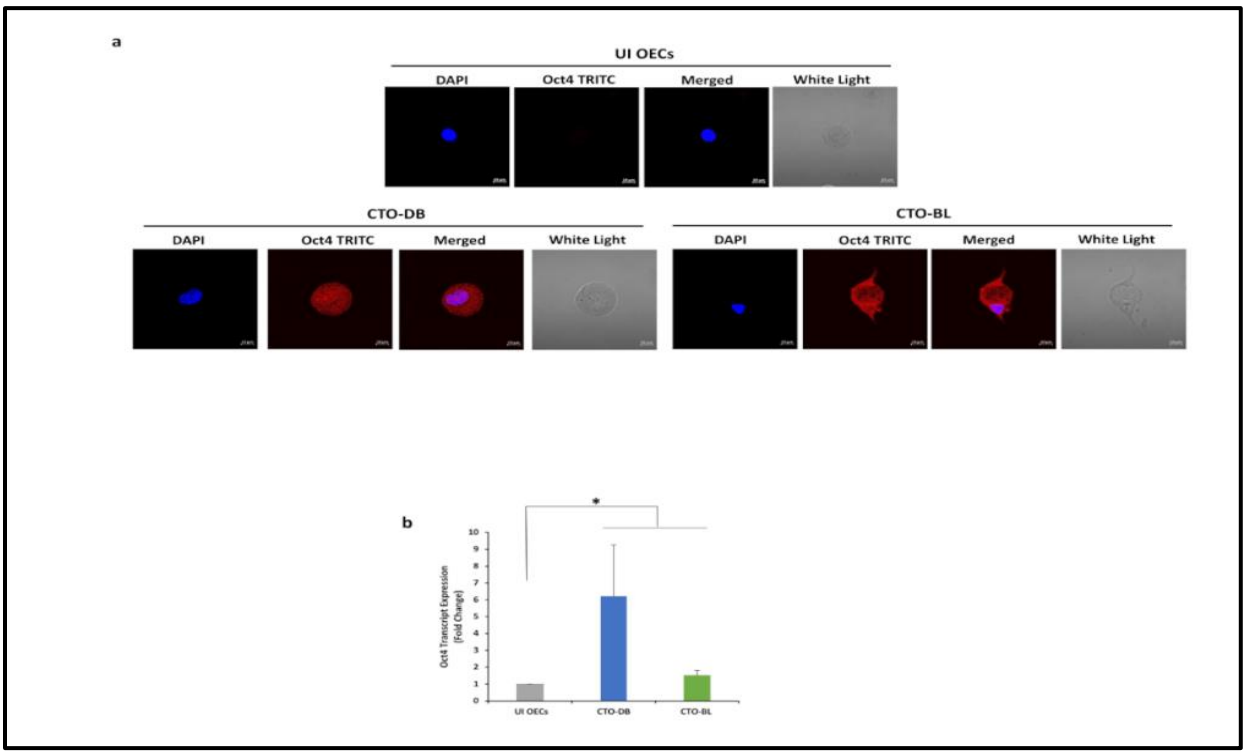

Figure 41: Expression of Oct4 in CTO-DB and BL cells.

(A) Confocal microscopic images of Oct4 and DAPI staining in CTO-DB and BL cells. UI OECs were used as controls; magnification ×63, scale bar 10 µm. (B) Oct4 transcript detection by RT-qPCR. Data are represented as mean ± SD of two independent experiments. * p-value≤0.05.

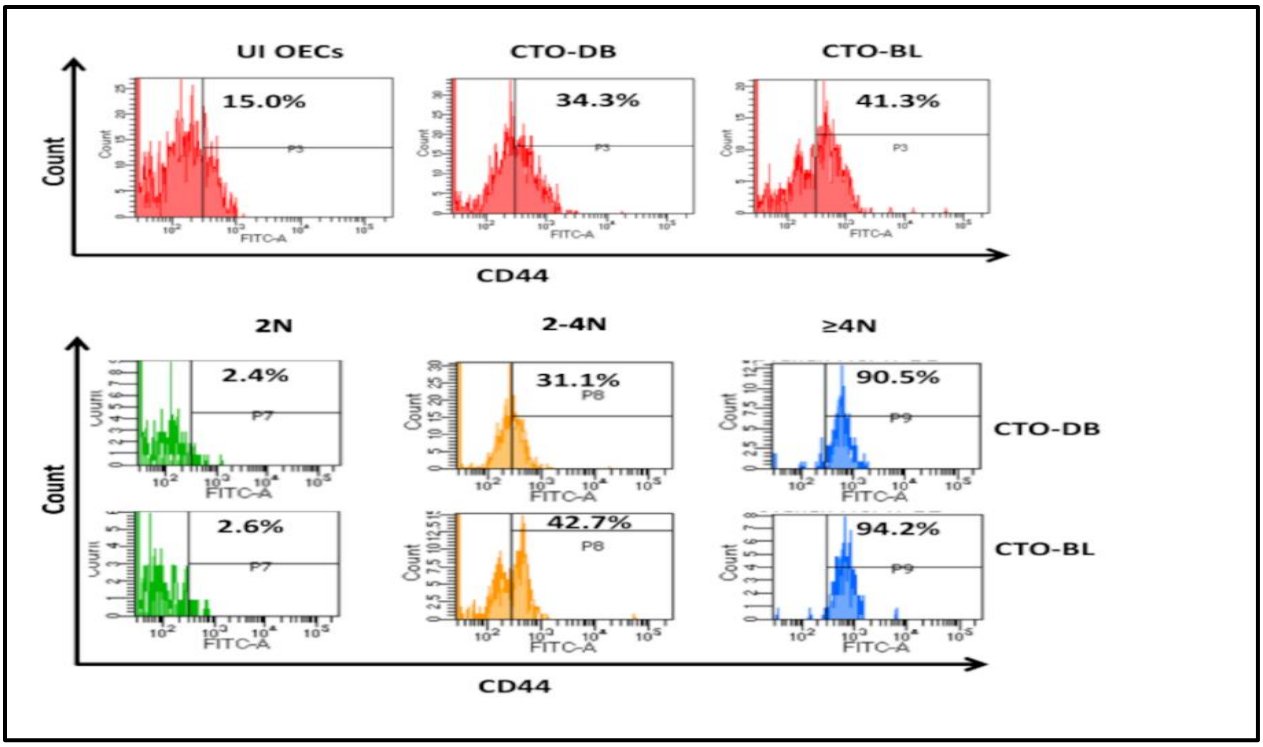

Figure 42: Expression of CD44 in CTO-DB and BL cells.

FACS staining of CD44 in CTO-DB and BL whole and subpopulations; uninfected OECs were used as a control.

EMT fuels cancer progression, tumor cell invasion, and therapy resistance [377]. PGCCs gain strong invasiveness and migration ability after they undergo EMT [378]. Vimentin was strongly upregulated in DB and BL-infected OECs (p-value $_{(UI\ OECs:CTO\text{-}HCMV)} = 0{\cdot}03$), whereas a slight decrease in E-cadherin was noticed compared to uninfected OECs (p-value $_{(UI\ OECs:CTO\text{-}HCMV)} = 0{\cdot}06$) **(Figure 43A,B, and C)**. Vimentin and E-cadherin were expressed mainly in the PGCCs and ICs subpopulations of CTO-DB and BL **(Figure 43D)**. Altogether, the co-existence of vimentin and E-cadherin was detected in CTO-DB and BL, indicating a mesenchymal/epithelial hybrid state that was also accompanied with occasionally existing small cells possessing an elevated E-cadherin expression **(Figure 43 and Figure 44)**. The co-existence of mesenchymal and epithelial phenotypes confirms the cellular plasticity of CTO-DB and BL. As a control, EZH2, Myc, Ki67Ag, Vimentin, E-cadherin, and CD44 protein expression in the subpopulations of uninfected OECs was provided in **Figure 45**.

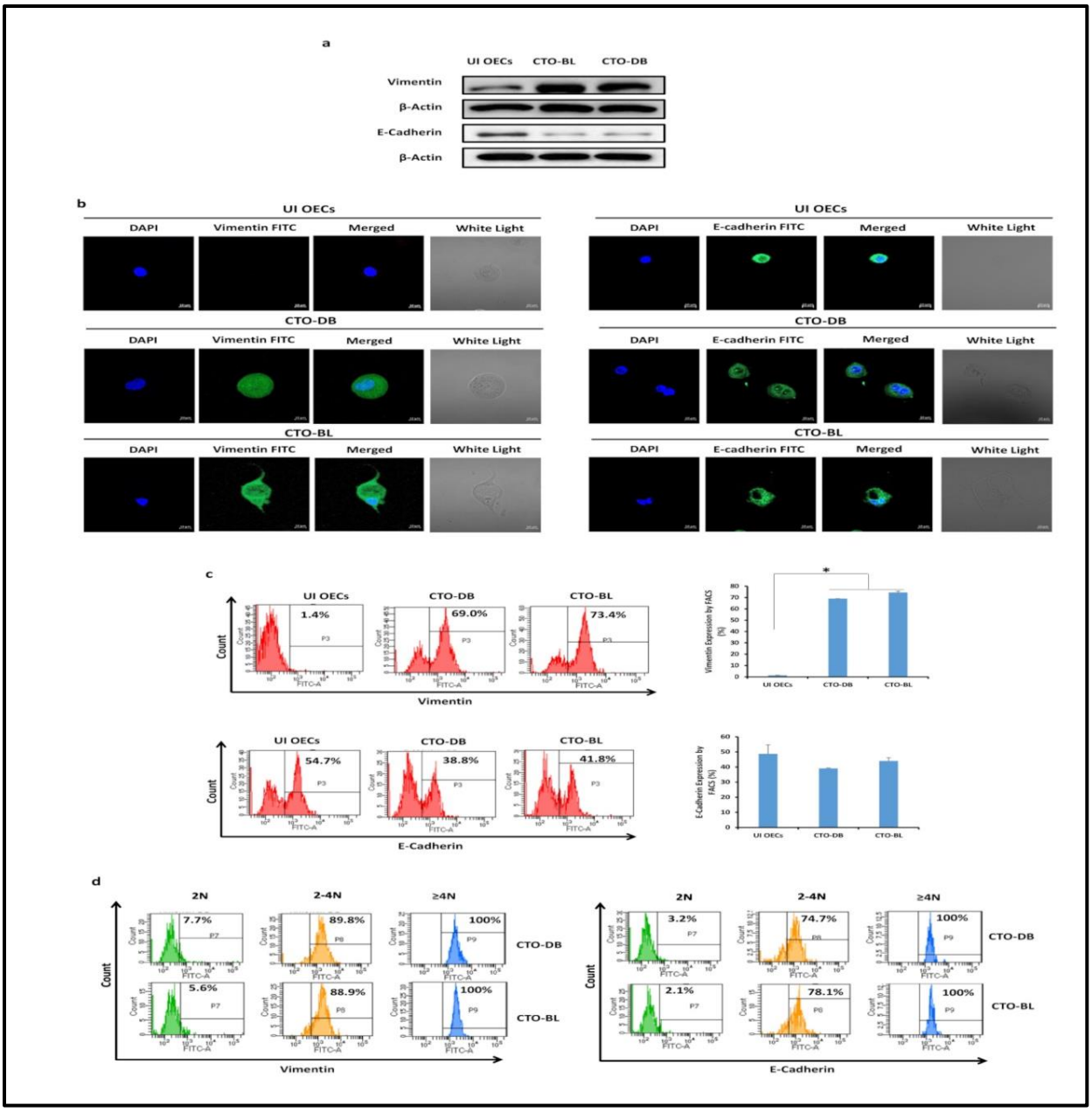

Figure 43: HCMV infection of OECs enhances EMT/MET hybrid traits.

Vimentin and E-cadherin expression by western blot (A), confocal microscopy (B), and FACS (C) in CTO-DB and BL. Uninfected OECs were used as controls. (D) Vimentin and E-cadherin expression in CTO-DB and BL subpopulations (2 N, 2–4 N, and ≥4 N). Data are represented as mean ± SD of two independent experiments. **p*-value ≤ 0·05.

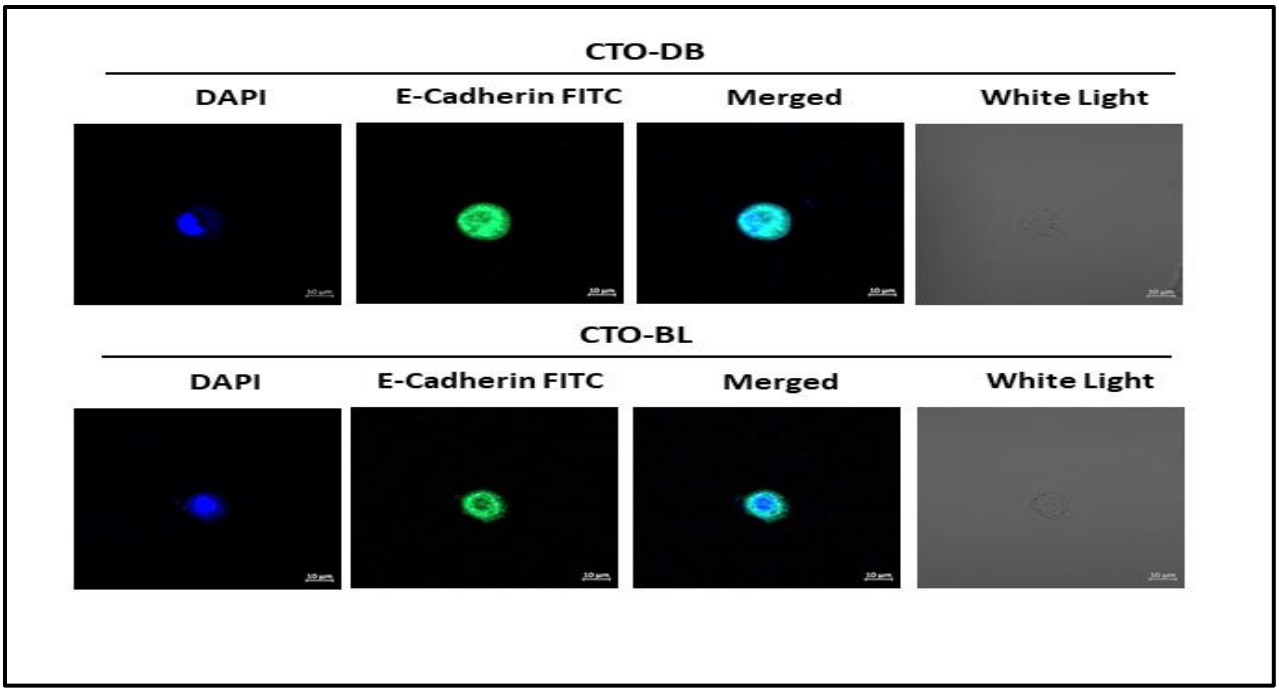

Figure 44: Detection of high expression of E-cadherin in several small cells present in CTO-DB and BL cultures.

Confocal microscopic images of E-cadherin and DAPI staining in CTO-DB and BL cultures; magnification ×63, scale bar 10 µm.

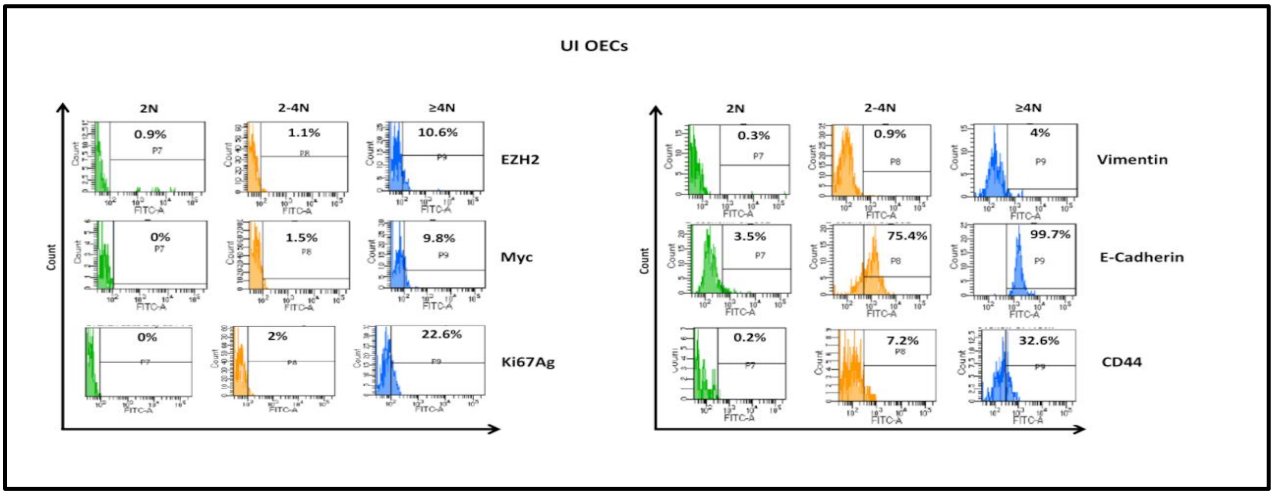

Figure 45: FACS staining of EZH2, Myc, Ki67Ag, Vimentin, E-cadherin, and CD44 in the subpopulations of uninfected OECs.

7.3.3 Lytic and Latent HCMV Replication in Transformed OECs

Sustained HCMV replication was confirmed in OECs chronically infected with HCMV-DB and BL, namely CTO-DB and BL **(Figure 46)**. IE1 protein was remarkably detected in CTO-DB and BL versus uninfected OECs **(Figure 46A,B)**; elevated IE1 expression was detected mainly in the PGCCs subpopulation compared to ICs and SCs **(Figure 47)**. IE1 and UL69 genes and transcripts were detected in CTO-DB and BL compared to uninfected OECs **(Figure 46C,D)**, indicating lytic HCMV replication. In addition, HCMV latency in CTO-DB and BL cultures was established by IE1 reactivation that was observed post-TPA treatment (p-value $_{(\text{CTO:TPA treated CTO})} = 0{\cdot}02$) **(Figure 46E and Figure 48).**

Given that EZH2 is considered a major tumor marker and an effective therapeutic target for OC, herein, we evaluated the impact of two EZH2 inhibitors (GSK343 and EPZ6438) on CTO proliferation and polyploidization. Upon EZH2 blockade **(Figure 49)**, detection of HCMV-IE1 gene was suppressed **(Figure 46F)**. Ki67Ag protein expression was decreased post-EZH2 inhibitor treatment of CTO-DB and BL compared to untreated CTO cells (p-value $_{(\text{CTO:EZH2 inhibitors treated CTO})} = 0{\cdot}004$) **(Figure 46G)**. Upon assessing the PI expression in the subpopulations of CTO cells, GSK343 and EPZ6438 reduced tetraploidization and polyploidization in treated CTO cells compared to controls (p-value $_{(\text{CTO:EZH2 inhibitors treated CTO})} = 0{\cdot}007$ and $0{\cdot}004$, respectively) **(Figure 46H)**.

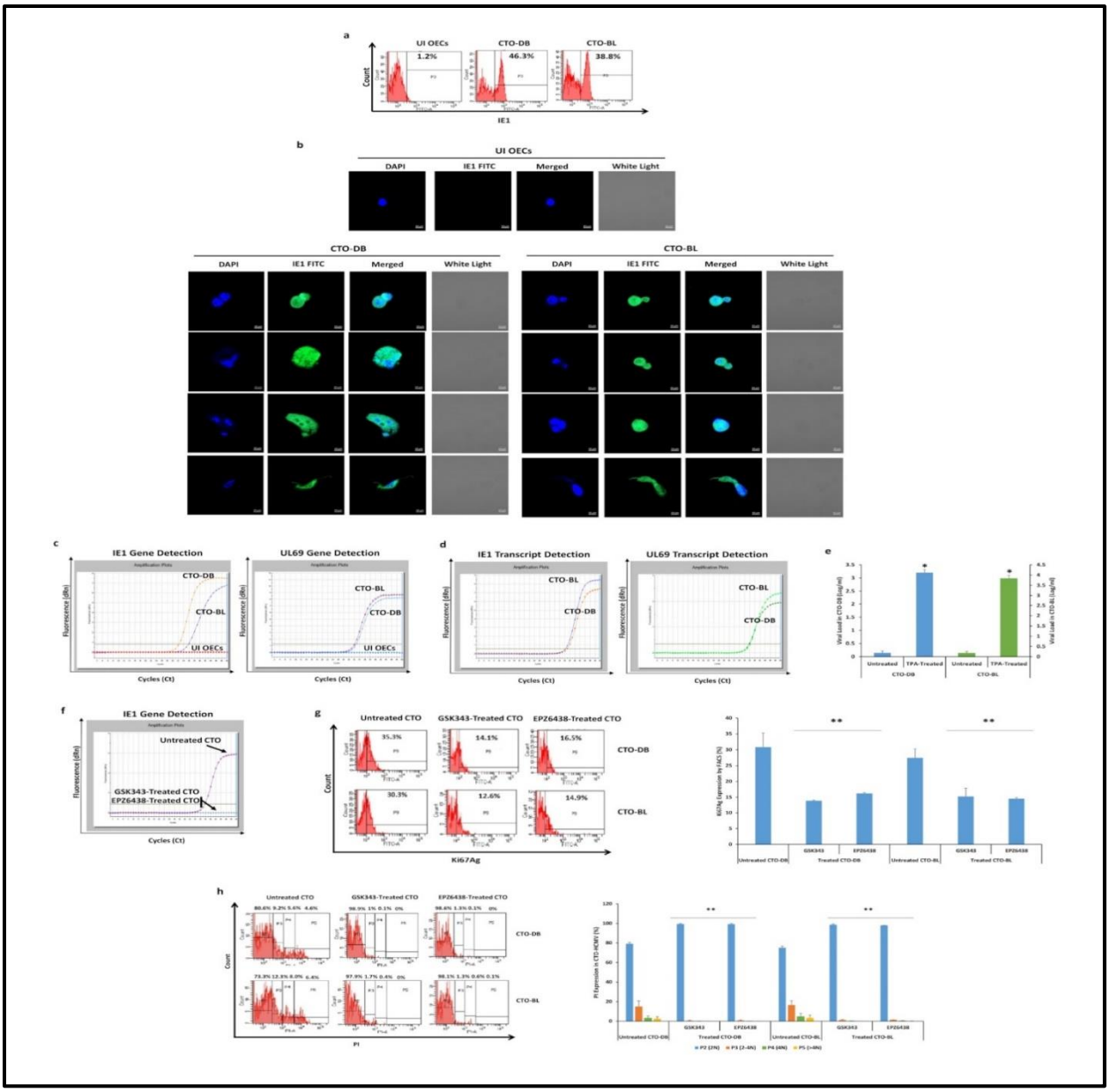

Figure 46: Sustained HCMV replication in chronically HCMV-infected OECs.

(A) IE1 expression by FACS in chronically infected OECs-DB and BL cultures. (B) IE1 expression by confocal microscopy in CTO-DB and BL; uninfected OECs were used as a control. Nuclei were counterstained with DAPI; magnification ×63, scale bar 10 µm. (C) IE1 and UL69 gene detection in chronically infected OECs-DB and BL as measured by qPCR. Uninfected OECs were used as a negative control. (D) IE1 and UL69 transcripts detection as measured by RT-qPCR. (E) Histogram representing the viral load post-TPA treatment in CTO-DB and BL cultures as measured by IE1-qPCR. (F) IE1 gene detection by qPCR in untreated CTO-DB, and CTO-DB treated with two EZH2 inhibitors (0.1 µM of GSK34 and EPZ6438). Ki67Ag expression (G) and PI staining (H) in untreated CTO-DB/BL and CTO-DB/BL treated with 0.1 µM of GSK34 and EPZ6438 by FACS. Data are represented as mean ± SD of two independent experiments. **p*-value ≤ 0·05; ***p*-value ≤ 0·01.

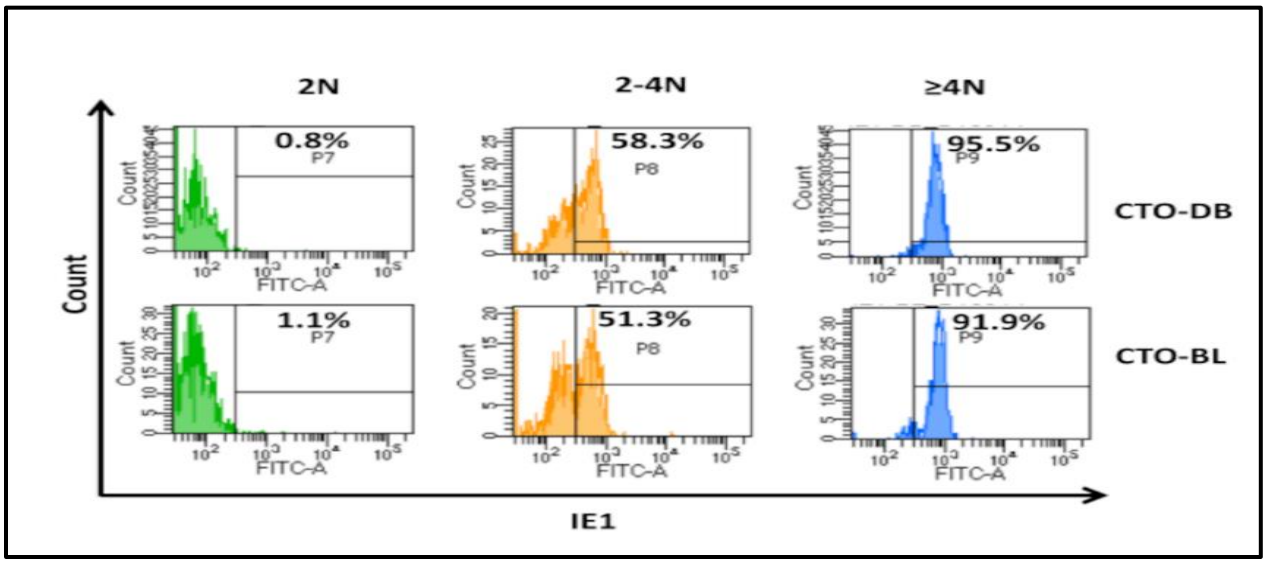

Figure 47: Expression of IE1 in CTO-DB and CTO-BL subpopulations by FACS.

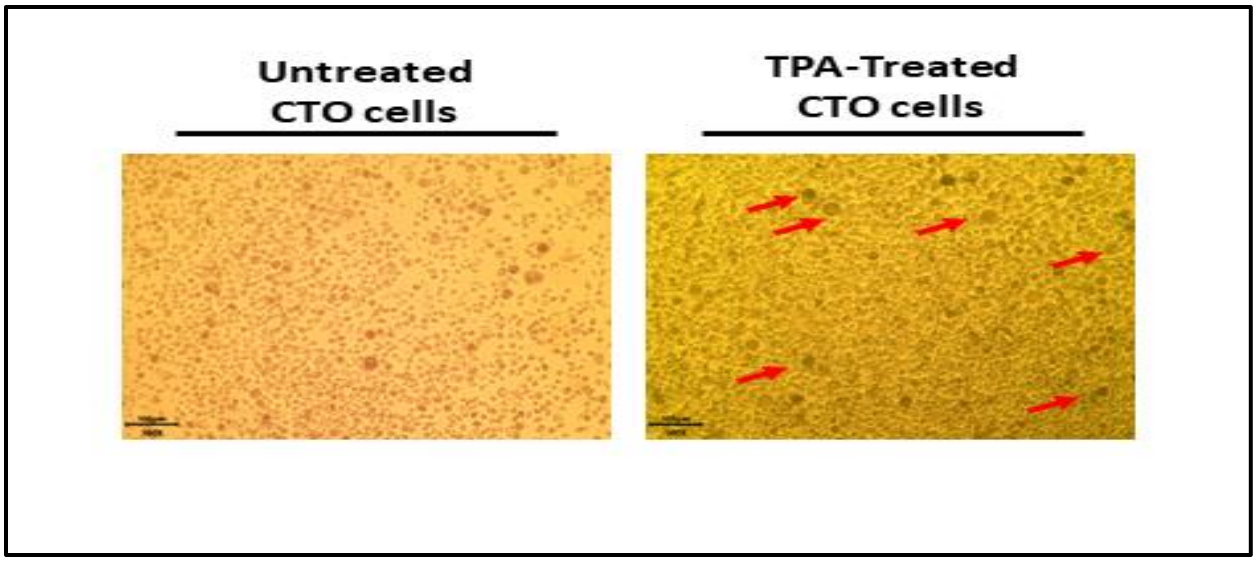

Figure 48: CTO cultures post-TPA treatment.

Microscopic images of TPA-treated CTO cells; untreated CTO cells were used as a control. Magnification ×100, scale bar 100 μm. Red arrows represent PGCCs found in TPA-treated CTO cultures.

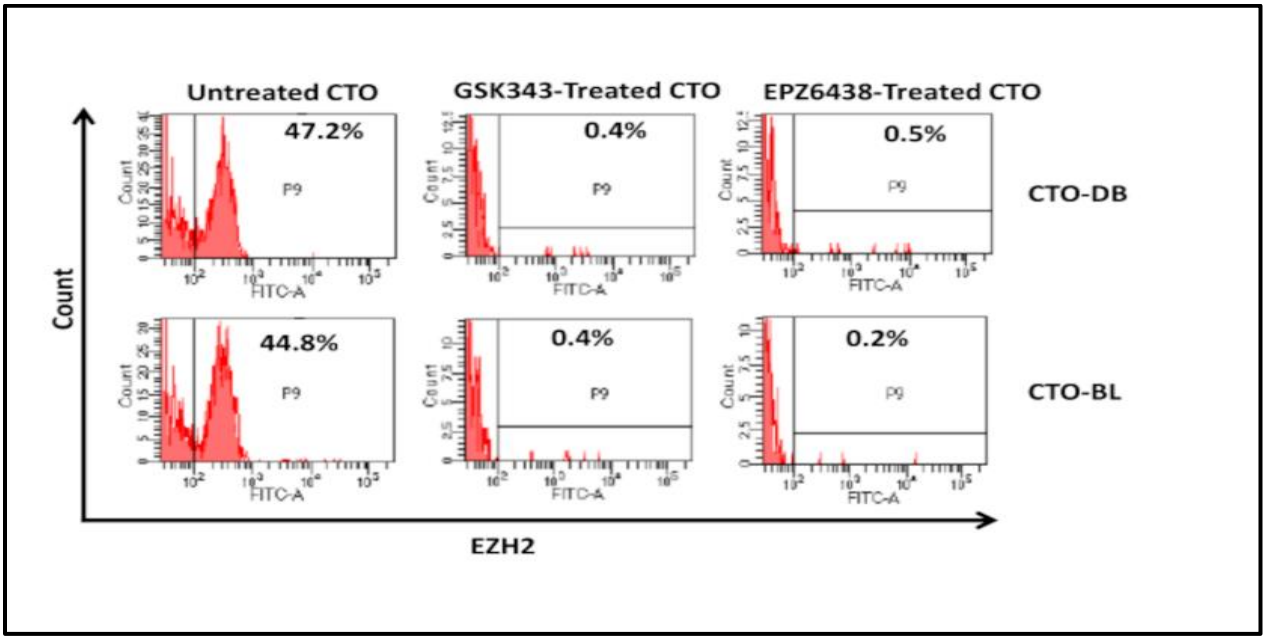

Figure 49: EZH2 expression in untreated CTO-DB/BL and CTO-DB/BL treated with 0.1 µM of GSK343 and EPZ6438 by FACS.

7.3.4 EZH2 Upregulation in HCMV-positive HGSOC Biopsies and The Isolation of Three Oncogenic HCMV Strains From EZH2^{High} HGSOC Biopsies

To further assess the role of HCMV, EZH2, and PGCCs induction in vivo, we analyzed 25 OC biopsies (HGSOC biopsies $n = 18$ and adjacent non-tumoral biopsies $n = 7$) **(Table 8)** for the presence of HCMV, PGCCs count, as well as EZH2, Myc, and Akt expression **(Figure 50, Figure 51, and Figure 52)**. PGCCs with giant or multiple nuclei were detected in the HGSOC biopsies **(Figure 50A)**. HCMV was detected in 72% of HGSOC biopsies **(Figure 50B)**. Elevated PGCCs count was mainly detected in HCMV-positive HGSOC biopsies **(Figure 50C)**. HCMV-positive tumor biopsies displayed mostly an enhanced EZH2 and Akt with a limited Myc expression **(Figure 50D, Figure 51, and Figure 52A)**. A significant positive correlation was found between HCMV presence and EZH2 as well as Akt expression ($r = -0.598$, p-value $= 0{\cdot}009$ and $r = -0.466$, p-value $= 0{\cdot}05$, respectively, based on Ct values) **(Figure 50E, and Figure 52B)**. A significant positive correlation was detected between Akt expression and EZH2 as well as Myc expression ($r = 0.420$, p-value $= 0{\cdot}015$ and $r = 0.620$, p-value $= 0{\cdot}006$, respectively) **(Figure 52B)**.

Among the eighteen HCMV-positive HGSOC biopsies, three biopsies with the highest EZH2 expression were considered for HCMV isolation. The three HCMV-OC strains were isolated by tissue disruption and filtration, and were subsequently grown in MRC5 cells showing a peak of viral load of 3 logs around day 7 post-infection **(Figure 50F)**. Following OECs infection with the three HCMV-OC strains, HCMV presence was confirmed by the detection of IE1 gene in addition to the morphological changes that appeared in the OECs infected cultures, for instance, giant and multinucleated cells showing cell budding as well as mesenchymal cells **(Figure 50F,G)**. Post-EZH2 inhibition, using GSK343, no HCMV replication was detected in addition to the absence of morphological heterogeneity in the infected cultures **(Figure 50G,H)**. Upregulation of Ki67Ag, EZH2, and Myc expression was observed in CTO-HCMV-OC compared to uninfected OECs and GSK-treated CTO-HCMV-OC cells (Ki67Ag p-value $_{(CTO:GSK343\text{-}CTO)} = 0{\cdot}01$; EZH2 p-value $_{(CTO:GSK343\text{-}CTO)} = 0{\cdot}002$; Myc p-value $_{(CTO:GSK343\text{-}CTO)} = 0{\cdot}002$). GSK343 reduced Ki67Ag, EZH2, and Myc expression by 56%, 79%, and 63%, respectively **(Figure 50I)**. EZH2 inhibition reduced PGCCs percentage in infected cultures compared to untreated CTO cells (p-value $= 0{\cdot}002$) **(Figure 50J)**.

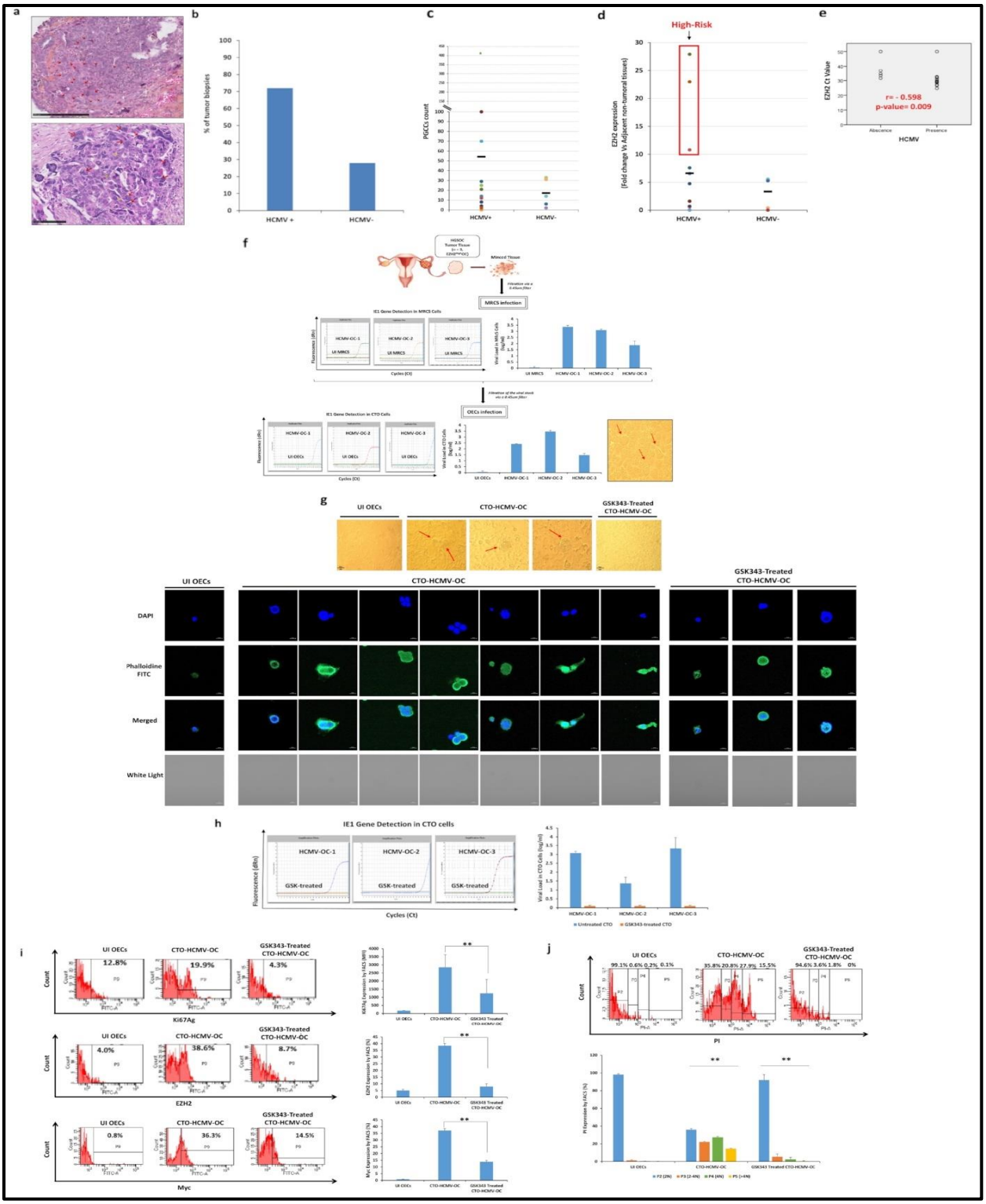
a
b
% of tumor biopsies
HCMV +
HCMV-
c
PGCCs count
HCMV+
HCMV-
d
High-Risk
EZH2 expression
(Fold change Vs Adjacent non-tumoral tissues)
HCMV+
HCMV-
e
EZH2 Ct Value
r= - 0.598
p-value= 0.009
Absecence
Presence
HCMV
f
Minced Tissue
MRCS infection
UI MRCS
HCMV-OC-1
HCMV-OC-2
HCMV-OC-3
OECs infection
UI OECs
g
UI OECs
CTO-HCMV-OC
GSK343-Treated CTO-HCMV-OC
DAPI
Phalloidine FITC
Merged
White Light
h
IE1 Gene Detection in CTO cells
GSK-treated
Fluorescence (dRn)
Cycles (Ct)
Viral Load in CTO Cells (log/ml)
Untreated CTO
GSK343-treated CTO
i
Ki67Ag
EZH2
Myc
12.8%
19.9%
4.3%
4.0%
38.6%
8.7%
0.8%
36.3%
14.5%
j
99.1% 0.6% 0.2% 0.1%
35.8% 20.8% 27.9% 15.5%
94.6% 3.6% 1.8% 0%
PI

Figure 50: HCMV detection, PGCCs presence as well as EZH2 expression in ovarian cancer biopsies.

(A) Ovarian cancer tissue HES staining; magnification ×400, scale bar 250 µm (upper panel) and 100 µm (lower panel). Red arrow representing the PGCCs while the yellow arrow represents the diploid carcinoma cells. (B) Histogram representing HCMV presence in the ovarian tumor biopsies. (C) Scattered plots showing the PGCCs count in HCMV-positive and negative ovarian tumor biopsies. (D) Scattered plots representing EZH2 expression in HCMV-positive and negative ovarian tumor biopsies by RT-qPCR. Red box indicates the high-risk HCMV strains with high EZH2 expression. (E) Correlation test between Ct value of EZH2 and HCMV presence *p*-values were determined by Spearman's correlation test. (F) Isolation protocol of the three high- risk HCMV-ovarian cancer strains from HGSOC tissues; histogram representing the viral replication of the isolated HCMV strains in MRC5 cells and CTO cultures by IE-qPCR. CTO cells were observed under an inverted light microscope (magnification ×200, scale bar 50 µm). (G) Light microscopic images (magnification ×200, scale bar 50 µm) as well as confocal images of DAPI and phalloidine staining in CTO-HCMV-OC and GSK343-treated CTO cells (magnification ×63, scale bar 10 µm); uninfected OECs were used as a negative control. (H) IE1 gene detection in CTO- HCMV-OC and GSK343-treated CTO cells by IE-qPCR. Ki67Ag, EZH2, Myc expression (I) and PI staining (J) in CTO-HCMV-OC, GSK343-treated CTO cells, and uninfected OECs by FACS. Data are represented as mean ± SD of two independent experiments. ***p*-value ≤ 0·01.

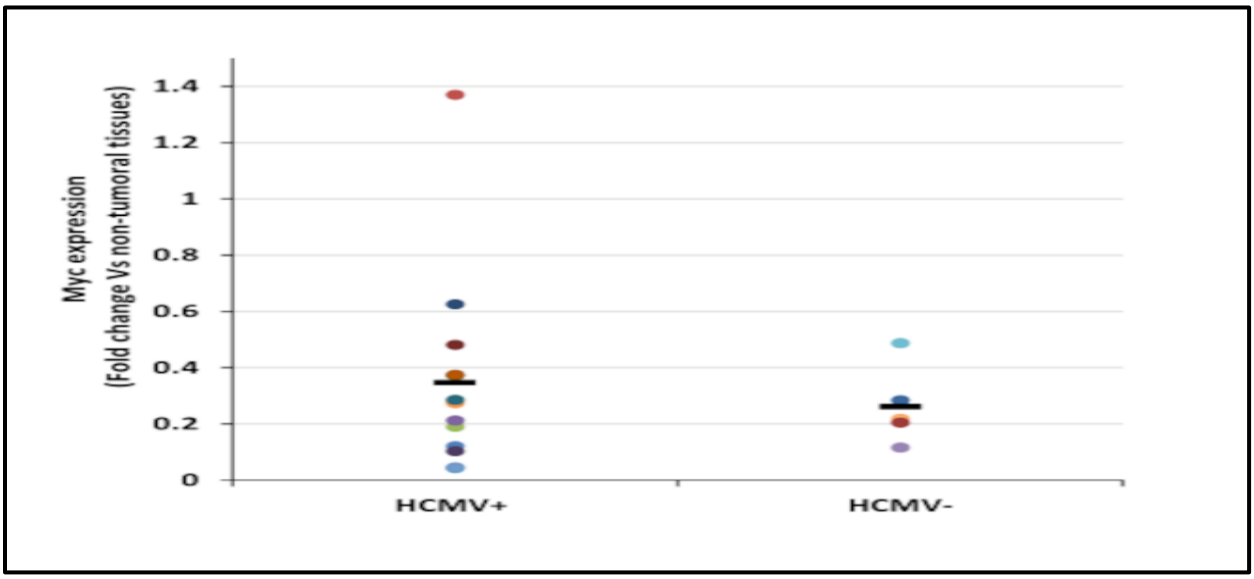

Figure 51: Myc Expression in ovarian cancer biopsies.

Scattered plot representing Myc expression in HCMV-positive and negative ovarian tumor biopsies by RT-qPCR.

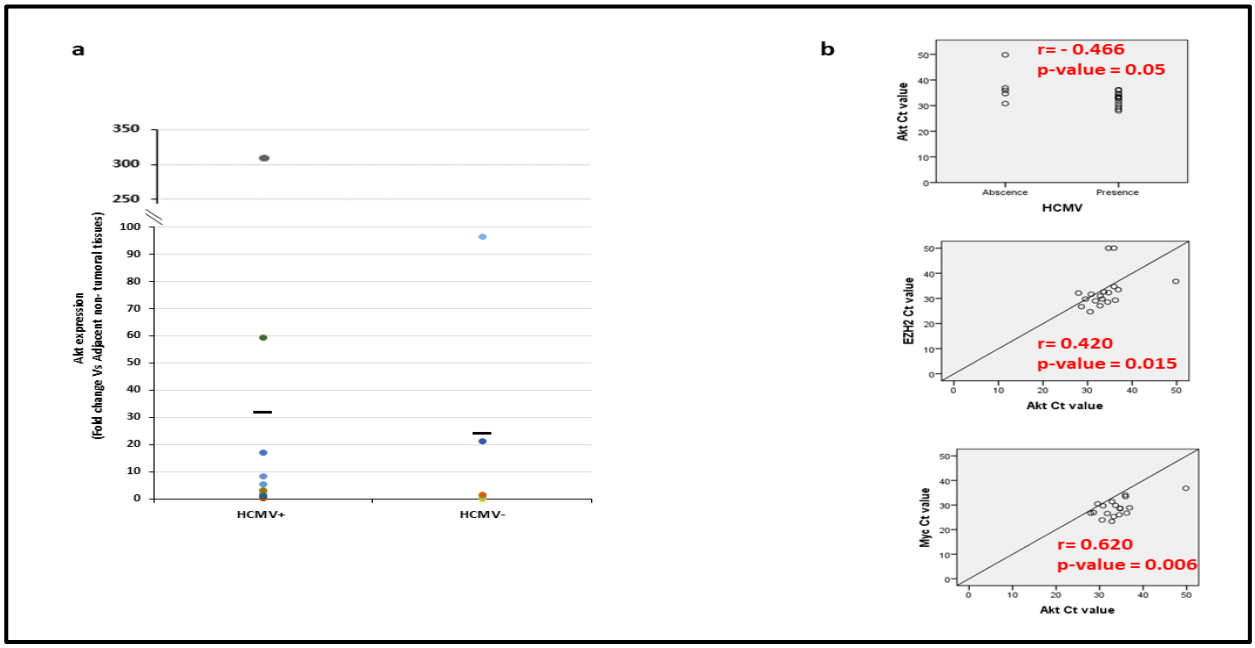

Figure 52: Akt Expression in ovarian cancer biopsies.

(A) Scattered plot representing Akt expression in HCMV-positive and negative ovarian tumor biopsies by RT-qPCR. (B) A correlation detected between Akt expression (Ct value) and HCMV presence, in addition to Akt expression and EZH2 as well as Myc expression. p-values were determined by Spearman, Kendall's Tau, and Pearson correlation tests, respectively.

Chapter 8

8. Discussion

Understanding the potential connections between viral infections and oncogenesis has been an ongoing area of research. In the context of breast cancer and to the best of our knowledge, our study demonstrated the oncogenic transformation and stemness potential of HCMV-B544 and B693 strains that were isolated from TNBC biopsies and indicated a differential treatment response depending on the HCMV strain present in the tumor. CTH-B544 and CTH-B693 cells are heterogeneous cellular populations that give rise to PGCCs, and display dedifferentiating phenotypes with stemness features as well as hybrid epithelial/mesenchymal phenotypes, resembling the morphological features found in aggressive cancers.

Myc activation has been widely described in breast cancer progression and can be used as a predictive marker for cancer staging, therapy resistance, and prognosis [331]. It is noteworthy that both B544 and B693 HCMV strains were isolated from $EZH2^{High}Myc^{High}$ -expressing TNBC [126], further indicating a potential link between the presence of these HCMV strains and cancer progression. The coupling of c-Myc overexpression with Akt pathway activation observed in CTH cells is in line with previous findings [125]. Moreover, colony formation was detected in CTH-B544 and CTH-B693 cells associated with a high expression level of Ki67 Ag and c-Myc overexpression, thus revealing cellular transformation and their oncogenic potential which is consistent with the previously reported CTH data [125]. Ki67, a prognostic biomarker in invasive breast cancer, is not only required for cell proliferation in tumors but is also strongly linked to tumor initiation, growth, and metastasis [379]. PGCCs formation was promoted in hypoxic environments. It is worth noting that hypoxia inducible factor 1 alpha (HIF-1α) expression is induced by HCMV infection [210]. In PGCCs, the evaluation of metabolic reprogramming revealed the presence of PLIN4, a perilipin covering the lipid droplets especially in chemo-resistant tumors [118]; the Warburg effect [380] and the involvement of the glycolytic pathway were also found to be induced in cancer environments and upon HCMV infection [117]. PGCC-bearing CTH cells acquired embryonic-like stemness and an epithelial-mesenchymal hybrid phenotype. Studies have shown that the acquisition of the EMT and stemness properties lead to an

increase in the invasiveness and the metastatic potential of cancer cells within tumors [367]. The embryonic stem cells transcriptional network is based on the presence of master pluripotency regulators, Oct4, SSEA-4, SOX2, and Nanog [381]. Besides mammosphere generation, CTH-B544 and CTH-B693 gained a stemness phenotype with increased expression of Oct4, SOX2, and Nanog promoting tumor progression; CTH cells were positively stained for SSEA4 which is associated with EMT and drug resistance [381]. SOX2, Nanog, and Oct4 expression was associated with poor differentiation, advanced cancer stages, and the worst outcomes in breast cancer patients [382]. Studies have implicated CD44 in breast cancer cell adhesion, proliferation, motility and migration, angiogenesis, and metastasis. Limited CD24 expression in breast cancer cells was shown to augment their growth and metastatic potential through a chemokine receptor response [381]. The $CD44^{high}/CD24^{low}$ phenotype was recognized in CTH-B544 and B693 cells indicating a tumor-initiating phenotype similar to that of the highly tumorigenic breast cancer cells [383]. The existence of an intermediate state between epithelial and mesenchymal phenotypes is considered a hybrid E/M state which is associated with elevated cellular plasticity, migration, stem-cell-like properties, metastatic potential, and therapy resistance [367]. In CTH cells, the co-existence of vimentin and E-cadherin resembled a partial EMT hence ensuring their plasticity while preserving the same tumor-propagating potential [125]. Since in breast tumors CD49f was considered a marker for distant metastasis and recurrence, $CD49f+/CD44^{high}/CD24^{low}$ CTH cells represented an aggressive phenotype which is associated with an increased risk for disease recurrence with poor clinical outcomes [384].

On the transcriptomic level, biopsy 693 overexpressed EGFR, CNDK2A, CCND1, SOX2, Oct4, and Nanog. It is known that EGFR promotes TNBC progression through JAK/STAT3 signaling [385], CNDK2A drives TNBC tumorigenesis [386], CCND1 has a prognostic significance in TNBC [387], and the three embryonic markers correlate with stemness, metastasis, tumor relapse, and poor clinical outcomes of TNBC [388]; therefore, we proposed that biopsy 693 maintains a tumor signature that is associated with an aggressive behavior predicting poor clinical outcome.

Studies reveal that the initiation of KSHV and EBV lytic cycles supported malignancies driven by the aforementioned oncogenic viruses [389,390]. HCMV persistence was established in CTH cells by detecting IE1 and pp65 throughout long-term cultures [125,126,209]. High-risk strains express

immediate-early (IE), early (E), and late (L) viral antigens including IE1 in agreement with a viral lytic cycle following the acute infection of permissive cells such as MCR5 cells. High-risk strains are detected in chronically infected cells, for instance CTH cells in our study, which is in line with the HCMV latency observed in Hodgkin's disease and Non-Hodgkin's lymphoma revealing the latent viral UL138 protein expression [391]. Nonetheless, a dynamic state of latency is recommended by novel transcriptomic studies. Since HCMV develops a complex relationship with the host, to define lytic and latency phases, several studies used the ratio of replicative and latency genes as a phase indicator [56,392]. To further highlight the role of the HCMV-IE1 gene, a study showed the potential of HCMV in regulating stemness in glioblastoma cells by specifically increasing SOX2 and Nestin, thus upregulating stemness and proliferation markers [393].

A study revealed the potential of combining GCV with certain chemotherapeutic agents to suppress EBV-positive NPC tumor growth [394]. In HPV-infected cervical cancer cells, cidofovir and cisplatin inhibited cellular proliferation, reduced E6 protein expression, and restored the activity of p53 [395]. A third study showed the effectiveness of anti-herpetic drugs, GCV and cidofovir, as single therapies or in combination with chemotherapy in treating KSHV-associated primary effusion lymphoma (PEL) [396]. Based on our results, the heterogeneity of HCMV strains including their distinct behavioral aspects had a major impact on CTH cells' response post-therapy. CTH-B544 cells were therapy sensitive whereas CTH-B693 cells displayed an aggressive behavior with lower sensitivity to PTX/GCV combination therapy. Generally, isolating distinct HCMV strains from tumors that possess potential prognostic biomarkers and behave differently depending on their own heterogeneity and various cell types may improve the diagnostic process and treatment options, provide effective follow-up strategies, and may be essentially pertinent in breast cancer pathophysiology and other adenocarcinomas, particularly of poor prognosis.

While our primary aim in this study was to investigate the potential link between breast cancer and the high-risk HCMV strains, we must not overlook the importance of the secondary goal of our research which was to examine the impact of these high-risk HCMV strains on the progression and clinical outcomes of GBM patients. Within the context of GBM, we presented the first experimental evidence for HCMV as a reprogramming vector, straight through the dedifferentiation of mature human astrocytes, and generation of CMV-Elicited Glioblastoma Cells

(CEGBCs) possessing glioblastoma-like traits. HCMV counterparts the progression of the perceived cellular and molecular mechanisms succeeding the transformation and invasion processes with CEGBCs involved in spheroid formation and invasiveness. Our study was conducted to assess the potential transforming capacities of HCMV-DB and BL following the HAs infection which were previously classified as high-risk transforming strains [125,126,241,397]. HAs infection with the high-risk HCMV-DB and BL strains resulted in a pro-oncogenic cellular environment and sustained growth of CEGBCs with soft agar colonies formation, unlike HAs infected with the low-risk HCMV-KM and FS strains that showed no transforming potentials and resulted in cell death in the long term cultures. CEGBCs displayed a "go and growth" phenotype in 2D monolayer cultures, dedifferentiated and displayed stemness as well as PMT features, and finally resulted in spheroid formation and invasion in 3D cultures. PGCCs appearance as well as cellular heterogeneity were previously allied to cultures of mammary epithelial cells infected with the high-risk HCMV strains [125,398]. Similar to HMECs transformed with the high-risk HCMV strains, around day 80 post-infection, we observed the appearance of dense cell aggregates, followed by the emergence of a wide array of morphologically distinct cells in HCMV-DB and BL cultures. We named these cells CMV-elicited glioblastoma cells (CEGBCs) with reference to the CMV-transformed HMECs (CTH) cells. PGCCs, NPC-like, neuron-like and mesenchymal-like cells were detected as well as filopodia, lamellipodia, and asymmetric cell division patterns. The described patterns could be representative of self-renewing cells undergoing diverse stages of the previously described giant cell cycle [125,398], although blastomere-like structures weren't so far detected as reported previously in CTH cells [125]. A replication-competent virus susceptible to reactivation from latency upon TPA treatment has been detected in CEGBC cultures. Activation of the Myc/EZH2 axis was observed in acute and sustained chronic infection with both high-risk HCMV strains. In agreement with EZH2 activation by HCMV, we observed a direct interaction between EZH2 and HCMV lncRNA4.9 transcript, likewise between EZH2 and cellular lncRNA HOTAIR transcript, a poor prognosis oncogenic factor for glioma patients. In line with EZH2 and HCMV involvement in our glioblastoma model, combination triple therapy (GSK343/GCV/TMZ) curtailed the growth of CEGBCs-derived spheroids. In vivo, all GBM tumor biopsies were found to harbor HCMV with enhanced EZH2 and Myc expression, possessing a strong positive

correlation between EZH2 and Myc expression as well as a strong correlation between EZH2/Myc and HCMV presence. Eleven HCMV-GBM strains were isolated from GBM tumors which acutely transformed HAs toward CEGBCs with increased EZH2/Myc expression that undergo dedifferentiation towards glioblastoma stem cells with spheroid formation and invasiveness capacities that could be curtailed by GSK343/GCV/TMZ triple therapy.

Among the mechanisms studied to transform HAs and promote disease progression in addition to poor prognosis in GBM, is the coupling of Myc and EZH2 overexpression as well as the depletion of retinoblastoma protein (Rb) which was observed in our study [336,399]. Although limited Myc upregulation and Rb downregulation were observed, none of the two low-risk HCMV-KM and FS strains transformed HAs as measured by soft agar colony formation in addition to the cell death observed in prolonged cultures. On the other hand, the high-risk clinical isolates HCMV-DB and BL can drive HAs towards oncogenic transformation in vitro. Our findings conform to the "astrocyte dedifferentiation theory" corresponding to glioblastoma origin [400–402]. In contrast to uninfected HAs, the distinct transcriptome profile including oncogenes, tumor suppressor genes and cell cycle genes facilitated the characterization of CEGBCs that possess a glioblastoma-like phenotype [403,404]. Stemness acquisition, commonly described in metastasis and poorly differentiated tumors [405–407], is in accordance with previous findings where GB-generated spheroids are composed of glioma stem cells (GSCs). The concomitant presence of the stemness marker nestin and HCMV-IE1 was detected in the spheroid structures generated from CEGBCs, as reported for nestin in the cell lines derived from GBM [408]. Highly motile Nestin/IE1-positive cells were spotted leaving the core which are similar to the neural-progenitor-like tumor cells detected in glioblastoma, especially the ones adopting the Lévy-like movement patterns [293,408]. The concomitant presence of viral proteins and nestin within transformed cells has been reported for the two herpes oncoviruses EBV and KSHV [409,410]. In agreement with enhanced CD44 and CD133 expression in CEGBCs, their expression in glioblastoma stem cells correlates with cell proliferation, intra-tumor heterogeneity, invasion and poor prognosis in CD44-expressing glioma [405,411]. The presence of vimentin^{+}/CD44^{+} cells in CEGBC cultures as well as the detection of stem cells expressing SOX2 and nestin confirms the PMT plasticity. In agreement with the proneural-mesenchymal plasticity described upon oncogenic stress activation highlighting

astrocyte plasticity/reactivity during tumorigenesis [370,412,413], a high invasive potential was observed in CEGBCs-DB compared to BL with increased mesenchymal traits indicating a more aggressive behavior that might drive therapeutic resistance.

Accumulated evidence highlighted Myc and EZH2 as key players in both oncogenesis and stemness. Myc stimulates EZH2 expression by activating the EZH2 promoter [328], repressing miR-26a [327], or directly suppressing miR-137. Bromodomain-4 protein (BRD4) positively regulates EZH2 transcription through Myc upregulation [330]. Myc activation was reported in glioblastoma progression, particularly in poor prognosis and therapy resistant-tumors [328,414]. EZH2 mediates proliferation, migration, and invasion in GBM. High-risk HCMV clinical strains DB and BL differentially induce Myc upregulation, and consequently stimulate EZH2 overexpression as well as CEGBCs induction, pointing toward the presence of Myc/EZH2/CEGBCs axis underlying the described results. Though, the interrelationship between HCMV and EZH2 is further complexed by the detection of HCMV lncRNA4.9 gene in CEGBCs which is in line with Rossetto et al. report [320]. Consistent with our data, the cellular lncRNA HOTAIR was described to interact with EZH2 in glioblastoma, thus linked to tumor dissemination, PMT, and drug resistance [414,415]. The noticeable detection of high lncRNA HOTAIR in the EZH2 IP samples corresponding to CEGBCs-DB explicates the aggressiveness of this particular high-risk HCMV strain, predicting poor prognosis. Indeed, EZH2-mediated stemness could underlie the appearance and maintenance of CEGBCs expressing a high degree of embryonic stemness, as EZH2 expression in astrocytes induced their dedifferentiation toward stem-like cells expressing nestin, SOX2, and CD133 [402]. Further, we reported the detection of HCMV in GBM tumor biopsies displaying enhanced EZH2, Myc, and Akt expression. HCMV-induced Myc and EZH2 expression along with the embryonic stem-like phenotype in the IE1-expressing CEGBCs could establish a significant model in the context of GBM. Since EZH2 and Myc have been implicated in tumor initiation and proven to impact glioblastoma appearance and development with the two high-risk HCMV DB and BL strains isolated from biological fluids (cervical swab and urine respectively), we evaluated EZH2/Myc expression and recovered HCMV strains directly from GBM biopsies thereby assessing their oncogenic potential. Eleven HCMV strains were isolated from GBM tumors (with unmethylated and methylated MGMT promoters). After HAs

infection, CEGBCs were generated with morphological features matching the previously described CEGBCs-DB and BL and led to the appearance of spheroids with invasiveness potential. HCMV-IE1 protein detection parallel to stemness markers and the upregulated Myc and EZH2 expression parallel to the detection of lncRNA4.9 gene, lncRNA4.9 and HOTAIR transcripts in cultures infected with the eleven HCMV-GBM strains recapitulates the previously observed molecular phenotype induced by HCMV-DB and BL strains. The expression of Myc was predominantly elevated in IE1-positive HAs. Altogether, HCMV strains are present in GBM tumors retaining tumor-promoting abilities, therefore considered as oncogenic strains.

Highlighting the critical role of EZH2 and HCMV in our glioblastoma model, the impact of EZH2 inhibitor (GSK343) and anti-HCMV drug ganciclovir (GCV) alone and in combination with TMZ was assessed. TMZ possessed a very limited effect on the growth of CEGBCs spheroids derived from HCMV-DB, HCMV-BL and the eleven HCMV-GBM strains. In agreement with our results, valganciclovir possessed a positive effect on glioblastoma tumors with an unmethylated or methylated MGMT promoter gene [416], potentially through its antiproliferative effect [417,418]. Although GSK343 single therapy had a limited effect on the growth of CEGBCs spheroids, its combination with TMZ enhanced the restriction of the CEGBCs spheroids growth derived from DB and BL, and to a lesser extent HCMV-GBM strains. EZH2 may modulate TMZ resistance where blocking EZH2 reverses TMZ chemosensitivity in GBM patients; an increased number of apoptotic cells were detected by knocking down EZH2 [419]. Although encouraging responses were detected post-dual therapy (GSK343/TMZ) in CEGBCs-DB and BL, and to a lesser extent from the eleven GBM HCMV strains, the triple therapy (TMZ/GSK343/GCV) was the most effective in CEGBCs derived from DB, BL, and the eleven GBM HCMV strains. Hence, triple therapy provides the foundation for a combinational therapeutic strategy to improve overall patient survival, reduce viral resistance, and lower drug toxicity.

While exploring the potential association between HCMV, BC, and GBM, we also recognized the significance of understanding how diverse HCMV viral strains may influence OC progression. Finally, we presented the experimental evidence for HCMV as a reprogramming vector that elicited human ovarian epithelial cells (OECs) transformation leading to the generation of "CMV-

transformed Ovarian cells" (CTO). Herein, we assessed the potential transforming capacities of the high-risk HCMV-DB and BL strains, following the OECs infection. The OECs infection with the high-risk HCMV-DB and BL strains resulted in a pro-oncogenic cellular environment and sustained growth of CMV-transformed OECs with soft agar colonies formation. The CTO cells dedifferentiated, displayed stemness as well as EMT-MET hybrid phenotype, and finally resulted in PGGCs generation and spheroid formation. HCMV presence accompanied by polyploidy, EZH2 upregulation, and malignant phenotype potentially confirm the transformation process. In vivo, 72% of HGSOC biopsies were found to harbor HCMV with elevated PGCCs count as well as enhanced EZH2 expression, revealing a strong correlation between HCMV, PGCCs, and EZH2 expression. Three HCMV-OC strains were isolated from $EZH2^{high}$ OC tumors that transformed OECs toward CTO possessing increased EZH2, Ki67Ag, and Myc expression parallel to polyploidy induction. The expression of the aforementioned markers and polyploidy were curtailed by EZH2 inhibitors therapy.

PGCCs play a fundamental role in tumor progression and in regulating tumor heterogeneity [115,420]. Accumulating evidence reveals the presence of PGCCs in OC, particularly the HGSOC, where PGCCs act as stem-like, self-renewing cells that are considered prognostic factors for OC [115,421]. In our study, CTO cells generated PGCCs, and were heterogeneous showing distinct morphological features including budding, filopodia, lipid droplets-filled cells, blastomere-like cells, and multinucleated cells that were previously detected in OC especially HGSOC [420,422–427] and reported upon HCMV infection of human mammary epithelial cells [125,126,397]. Our findings indicated that polyploidy harboring HCMV might induce the acquisition of a malignant phenotype via the giant cell cycling [118]. p53 and Rb inactivation have been correlated with tetraploidization in human tumors [428]. Indeed, p53 was shown to be mutated in more than 50% of human tumors, especially HGSOC; most of the p53 mutations acquired an oncogenic function. It's worth mentioning that tumor-promoting viruses reduce p53 activity [429]. Studies have shown that the incidence of tetraploidy occurs in p53-deficient cells possessing prolonged DNA damage due to persistent telomere dysfunction [430]. p53 and Rb expression was decreased in CTO-DB and BL that showed high percentages of tetraploidization and decreased telomerase activity, in line with the telomere-driven tetraploidization induced by critically short telomeres with the

potential to promote tumorigenesis in early cancerous lesions [376]. Several HCMV products have been involved in the cellular transformation including IE1, IE2, pp65, US28, cmvIL-10, UL76, UL44, and UL84, etc. Such expression of HCMV gene products could impair the pathways of p53 and Rb [70,215]. HCMV-IE1, IE2, and UL97 allow the evasion of p53 and Rb [215]. Hence, the impaired p53 and Rb pathways in CTO cells was due to the transforming potential of HCMV contrasting the Ras, human telomerase reverse transcriptase (hTERT), and SV40-mediated transformation of human ovarian cells [431].

Cells possessing sphere-forming potentials were shown to reside in the malignant ascites of OC patients [432–434]. In OC, the aforementioned cells are strong contributors to tumor progression, metastasis, chemotherapy resistance, and disease relapse [433]. The spontaneous spheroid generation along with the high expression of Nanog and Oct4 in CTO-DB and BL is in line with the previously described OC cell phenotype [435]. Given their role in maintaining pluripotency and long-term self-renewal, the embryonic transcription factors Oct4 and Nanog are recognized as part of the stem cell signature that strongly correlates with spheroid formation, tumor initiation, and chemoresistance in ovarian cancer cells [435,436]. CD44 was highly expressed in CTO-DB and BL cells; it has been previously shown to drive the progression of several tumors [437,438], maintain stem cell quiescence, and promote EMT in OC [439]. Further, CD44 has been linked to the sphere-forming, self-renewing and tumor-initiating potential of OC cells [440]. The co-existence of vimentin and E-cadherin in CTO-DB and BL highlights the high cellular plasticity. EMT plasticity with EMT and MET alternately taking place was revealed during HGSOC progression where cells co-express epithelial and mesenchymal determinants [427,441,442]. Besides cellular plasticity, the hybrid E/M state promotes stem-like properties as well as metastatic and tumorigenic potential [367,443].

Upon infecting OECs with HCMV-DB and BL strains, IE1 and pp65 proteins were detected which is in line with the recent studies that have identified high expressions of HCMV-IE or pp65 in ovarian tumor samples that were associated with poor survival outcomes [304,444], suggesting that HCMV infection could potentially promote cancer progression. All in all, HCMV-induced EZH2 expression along with the embryonic stem-like phenotype and cellular plasticity in the IE1-expressing OECs/CTO cells could establish a significant model in the context of OC. Several

studies shed light on the existence of herpesviruses DNA and proteins in ovarian tissues that may hold potential in the process of OC tumorigenesis [304,444,445]. Herein, we reported the detection of HCMV in HGSOC biopsies displaying elevated PGCCs count as well as enhanced EZH2 expression. It is worth mentioning that, neither HPV nor EBV was detected in the eighteen tested HGOSC biopsies.

Three HCMV strains with a strong transforming potential, so called high-risk strains, were isolated from $EZH2^{High}$ HGOSC biopsies. After OECs infection, CTO cells were generated with morphological features matching the previously described CTO-DB and BL. Additionally, we evaluated EZH2 expression in the high-risk HCMV strains that were recovered directly from HGSOC biopsies thereby assessing their oncogenic and stemness potential. Unlike GSK-treated CTO, the expression of EZH2, Myc, and Ki67Ag was predominantly elevated in untreated CTO-HCMV-OC cells parallel to the PGCCs appearance. In summary, HCMV clinical strains reside in HGOSC biopsies retaining cancer-promoting potentials.

Targeting HCMV might have a vital role in treating OC [444]. Post-anti-CMV therapy, a remarkably high extended survival was observed in both newly diagnosed and recurrent glioblastoma patients [446]. Current vaccine candidates have focused on several HCMV antigens/epitopes such as gB, gH, pentamer complex, pp65 and IE1 [447,448]. Recently, CMV-specific immunotherapy including cytotoxic T lymphocyte (CTL) or dendritic cell (DC)-based vaccines has contributed to minimal successful outcomes in glioblastoma treatment [8,448]. In addition, using EZH2 inhibitors to specifically target ovarian tumors could ultimately improve patients outcomes [322]. Two inhibitors triggering EZH2 degradation (DZNep and YM281) exhibited potent efficacy in OC cell lines and xenografts [323]. GSK343 significantly induced apoptosis and inhibited the invasion of ovarian epithelial cells in 3D cultures which more closely mimics the tumor microenvironment in vivo [449]. In patient-derived glioma stem cells, GSK343 was shown to suppress the stemness traits [335]. Interestingly, in the present study, EZH2 inhibitors totally blocked HCMV replication. It's worth noting that the HCMV major immediate early promoter (MIEP) transcriptional repressor, growth factor independence1 (GFI1), is controlled by the EZH2-NDY1/KDM2B-JARID2 axis. Therefore, EZH2 inhibitors might result in an enhanced GFI1 expression which could block viral replication [450]. Hence, combinational

therapies including EZH2 inhibitors may prove to be a promising milestone in developing therapeutic strategies for ovarian cancer treatment.

Overall, the existence of diverse strains expressing potential biomarkers and possessing various replication potentials in different tissues and/or cell types explain the distinct oncogenicity. So far, sixteen high-risk oncogenic clinical HCMV strains were isolated directly from tumor biopsies (breast cancer, N=2; glioblastoma, N=11; HGSOCs, N=3). These strains shared the same transforming potential. PGCCs were detected in the aforementioned cell cultures that were shown to highly express Myc and EZH2 pointing toward a potential link between HCMV, PGCCs, EZH2, and Myc. CTO and CTH cells dedifferentiated and revealed stemness as well as EMT traits. On the other hand, CEGBCs dedifferentiated and displayed stemness, PMT as well as invasiveness features. The phenotypic changes were similar in HCMV-infected ovarian and mammary epithelial cells. However, the difference was mainly the detection of high percentages of tetraploid cells in the CTO cultures compared to the >4N population detected in CTH cells. In both models, a high degree of cellular plasticity was detected knowing that ovarian and mammary epithelial cells are isolated from human glandular organs. Thus, discovering distinct viral strains will adjust the different adopted approaches to tumor diagnosis, prognosis, prevention, advanced treatment, as well as therapy monitoring and will enrich potential vaccine studies. In the forthcoming studies, it would be essential to sequence the isolated high-risk HCMV strains aiming to define the specific viral gene(s) that are responsible for driving the transformation process. Further, it is of high importance to conduct in vivo experimental studies since they can serve as a crucial bridge for extrapolating our findings to the patient context as well as translating the exact relevance of such models in the pathogenesis of breast cancer, GBM, and ovarian cancer. This could play a pivotal role in indicating and confirming HCMV as an oncogenic virus.

Chapter 9

9. Conclusion

As a conclusion, our findings elucidate the concept of how HCMV is linked to breast cancer, glioblastoma, and ovarian cancer as depicted in the figures below **(Figure 53, Figure 54, and Figure 55)**. The data that were provided proved that HCMV is not solely associated with oncomodulation; it is also recognized for its involvement in oncogenesis. The oncogenic and stemness signatures of the high-risk HCMV strains accentuate the oncogenic potential of HCMV in breast cancer, glioblastoma, and ovarian cancer progression and support the tumorigenic properties of EZH2 and Myc which might be highly pertinent in the pathophysiology of the aforementioned tumors. With respect to breast and ovarian cancer, HCMV triggered EZH2 and Myc expression, generated PGCCs, displayed dedifferentiating phenotypes with stemness features as well as hybrid EMT/MET phenotypes parallel to the existence of giant cell cycling. Further, HCMV induced a CEGBCs phenotype with tumor heterogeneity, proneural to mesenchymal plasticity, and embryonic-like stemness leading to spheroid formation and invasiveness in vitro and in GBM biopsies.

In accordance with the previous findings discussed, and considering that HCMV has been detected primarily within tumors correlating positively to poor prognosis, along with the potential influence of HCMV gene products on the regulation of tumorigenic pathways and processes associated with key cancer characteristics, and taking into account HCMV's wide tissue tropism, we deduce that HCMV harbors distinctive mechanisms that contribute to cancer progression.

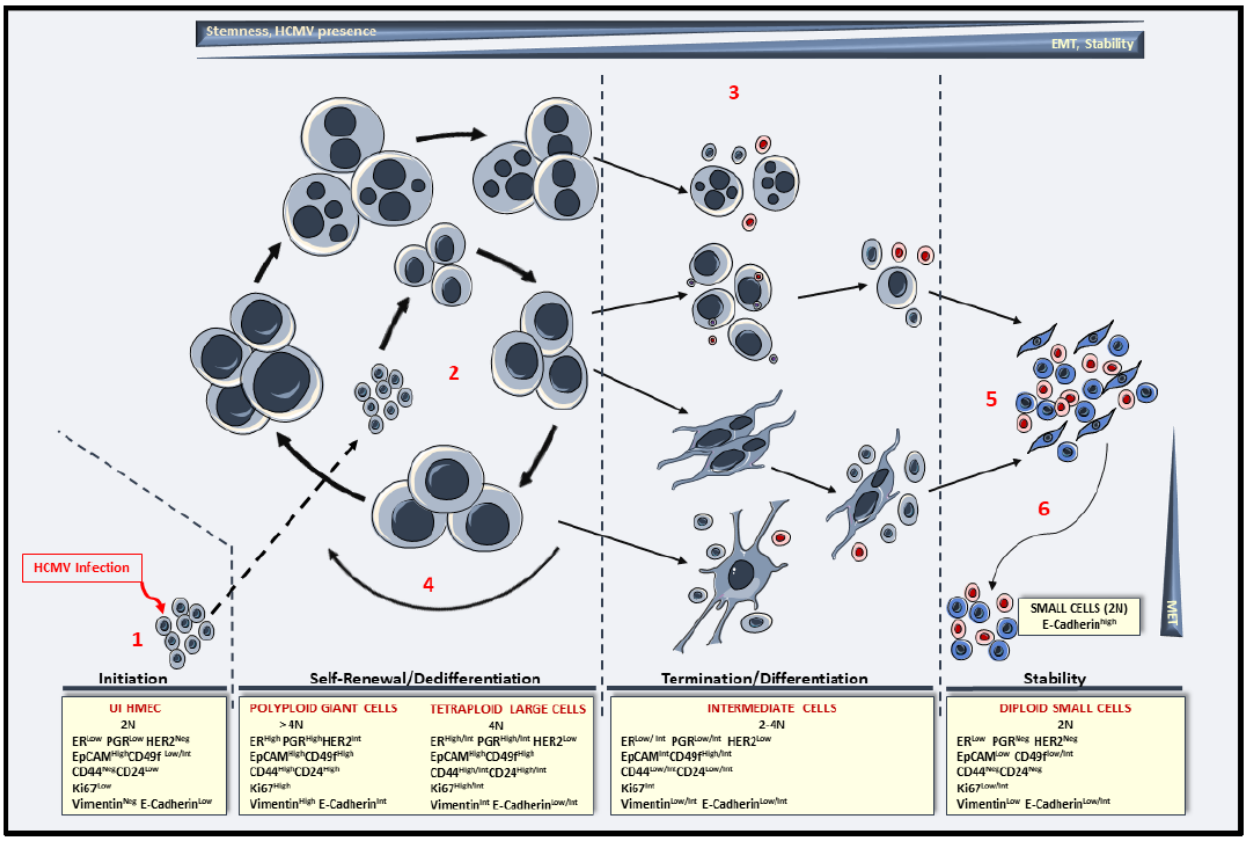

Figure 53: Potential model depicting the course of events leading to the initiation of the giant cell cycle.

In response to HCMV infection (1), the 2N human mammary epithelial cells (HMECs) enter the initiation phase of the giant cell cycle through endoreplication (2). Polyploid (>4N) cells in the dedifferentiation stage display a luminal-like phenotype with high to intermediate expression of epithelial and stemness markers. Cells directly bud from multinucleated or mononucleated giant cells (3) or alternatively continue endoreplication (4). The termination/differentiation step characterized by intermediate 2-4N cells profile gradually achieve stability into diploid 2N small cells (SCs) (5), where the latter are triple-negative with lower expression of epithelial and stemness markers. A small population of SCs could revert and show a mesenchymal-to-epithelial transition (6). A gradual decrease in HCMV presence is seen from left to right. Adapted from Nehme et al [125].

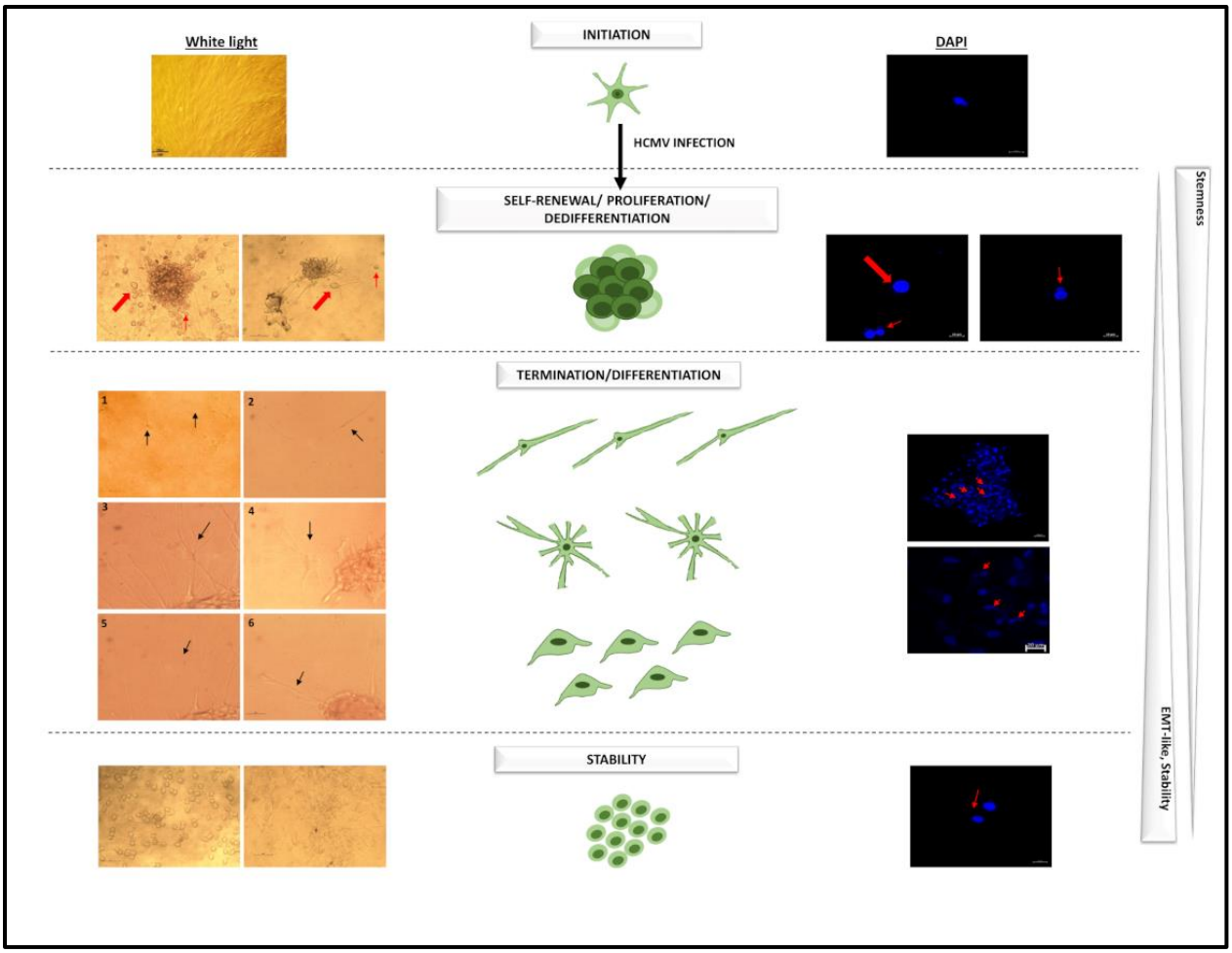

Figure 54: Glioblastoma generation scheme.

The scheme illustrates the four phases of the CEGBCs cycling including initiation, self-renewal, proliferation, and dedifferentiation, termination/differentiation, and stability. Large red arrows showed the large cells and PGCCs; Small red and black arrows showed the intermediate/small heterogeneous cells. In the termination/differentiation phase, NPC-like (1, 2), neuron-like (3, 4), and mesenchymal-like (5, 6) cells were detected.

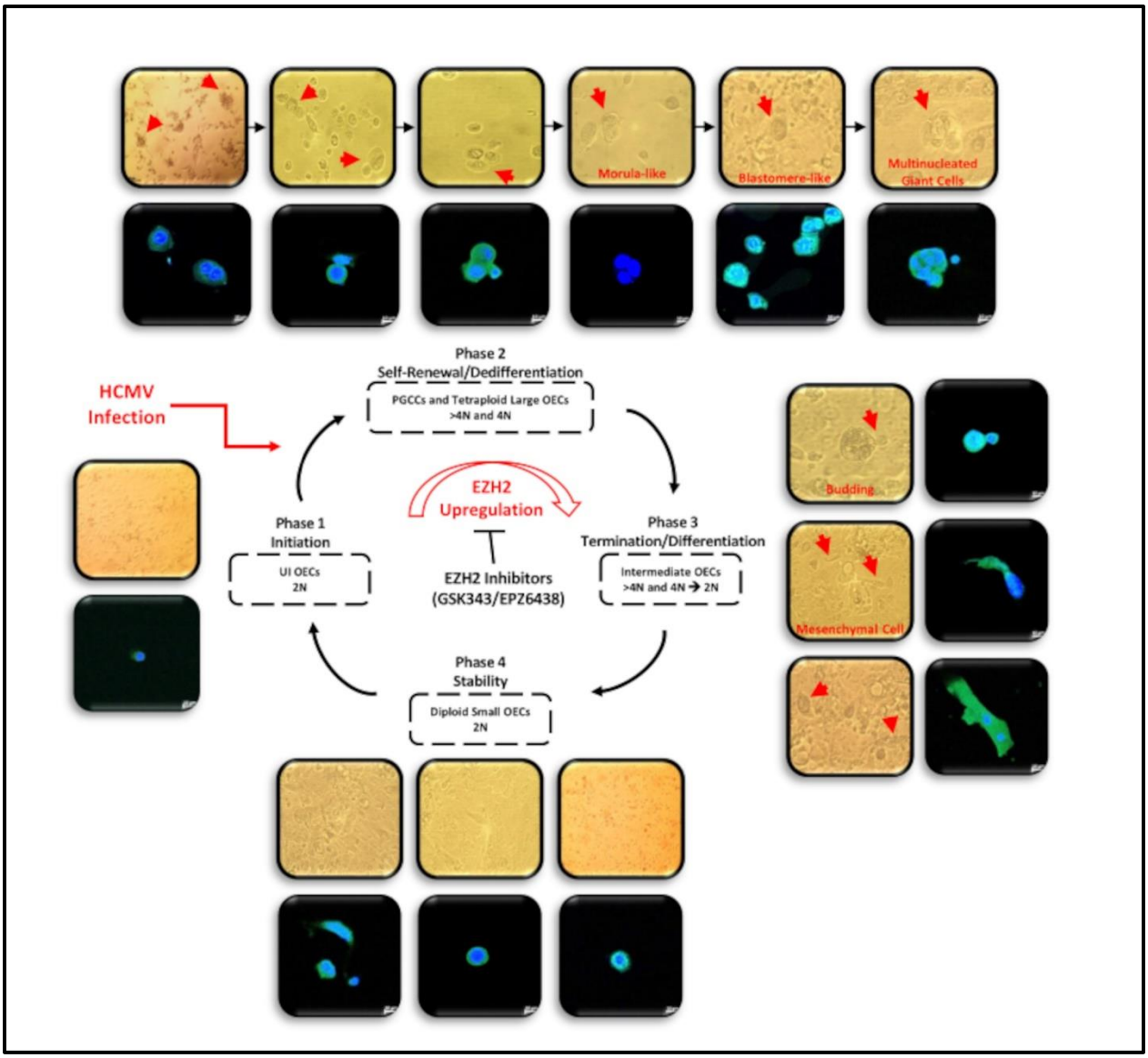

Figure 55: A schematic representing the giant cell cycling following HCMV infection of OECs.

Giant cell cycle representing four distinct phases including initiation, self-renewal, termination and stability. Upon HCMV infection, the 2 N OECs go into the initiation phase through endoreplication. Polyploid cells (> 4 N) and tetraploid cells (4 N) generate in the self-renewal/dedifferentiation stage due to HCMV infection and the subsequent EZH2 upregulation. Cell budding takes place from multinucleated or mononucleated giant cells generating intermediate 2–4 N OECs during the termination/differentiation phase. Intermediate OECs gradually reach stability and are converted into diploid small OECs (2 N).

Future studies, with more detailed analyses of target genes within the CMV-transformed cells namely, CTH, CEGBCs, and CTO cells and their corresponding response to inhibitors may establish new avenues to understand the complex pathogenesis of breast cancer, glioblastoma, and ovarian cancer. Additionally, large-scale experiments are highly encouraged to further validate our findings. Meanwhile, the presented data provides new insights into the oncogenic role of HCMV in cancer progression, thereby uncovering novel targeted therapeutic approaches and innovative clinical interventions that will improve cancer patient outcomes and their overall survival rates.

10. Bibliographic References

[1] Grinde B. Herpesviruses: latency and reactivation – viral strategies and host response. Journal of Oral Microbiology 2013;5:22766. https://doi.org/10.3402/jom.v5i0.22766.

[2] Sehrawat S, Kumar D, Rouse BT. Herpesviruses: Harmonious Pathogens but Relevant Cofactors in Other Diseases? Front Cell Infect Microbiol 2018;8:177. https://doi.org/10.3389/fcimb.2018.00177.

[3] Roizmann B, Desrosiers RC, Fleckenstein B, Lopez C, Minson AC, Studdert MJ. The familyHerpesviridae: an update. Archives of Virology 1992;123:425–49. https://doi.org/10.1007/BF01317276.

[4] Ho M. The history of cytomegalovirus and its diseases. Med Microbiol Immunol 2008;197:65–73. https://doi.org/10.1007/s00430-007-0066-x.

[5] Boeckh M, Geballe AP. Cytomegalovirus: pathogen, paradigm, and puzzle. J Clin Invest 2011;121:1673–80. https://doi.org/10.1172/JCI45449.

[6] Riley HD. History of the Cytomegalovirus: Southern Medical Journal 1997;90:184–90. https://doi.org/10.1097/00007611-199702000-00004.

[7] Smith MG. Propagation in Tissue Cultures of a Cytopathogenic Virus from Human Salivary Gland Virus (SGV) Disease. Experimental Biology and Medicine 1956;92:424–30. https://doi.org/10.3181/00379727-92-22498.

[8] Weller M, Roth P, Preusser M, Wick W, Reardon DA, Platten M, et al. Vaccine-based immunotherapeutic approaches to gliomas and beyond. Nat Rev Neurol 2017;13:363–74. https://doi.org/10.1038/nrneurol.2017.64.

[9] Crawford LB, Streblow DN, Hakki M, Nelson JA, Caposio P. Humanized mouse models of human cytomegalovirus infection. Current Opinion in Virology 2015;13:86–92. https://doi.org/10.1016/j.coviro.2015.06.006.

[10] Dolan A, Cunningham C, Hector RD, Hassan-Walker AF, Lee L, Addison C, et al. Genetic content of wild-type human cytomegalovirus. Journal of General Virology 2004;85:1301–12. https://doi.org/10.1099/vir.0.79888-0.

[11] Stern-Ginossar N, Weisburd B, Michalski A, Le VTK, Hein MY, Huang S-X, et al. Decoding Human Cytomegalovirus. Science 2012;338:1088–93. https://doi.org/10.1126/science.1227919.

[12] Ye L, Qian Y, Yu W, Guo G, Wang H, Xue X. Functional Profile of Human Cytomegalovirus Genes and Their Associated Diseases: A Review. Front Microbiol 2020;11:2104. https://doi.org/10.3389/fmicb.2020.02104.

[13] Gatherer D, Seirafian S, Cunningham C, Holton M, Dargan DJ, Baluchova K, et al. High-resolution human cytomegalovirus transcriptome. Proc Natl Acad Sci USA 2011;108:19755–60. https://doi.org/10.1073/pnas.1115861108.

[14] Van Damme E, Van Loock M. Functional annotation of human cytomegalovirus gene products: an update. Front Microbiol 2014;5. https://doi.org/10.3389/fmicb.2014.00218.

[15] Roizman B, Carmichael LE, Deinhardt F, de-The G, Nahmias AJ, Plowright W, et al. Herpesviridae. Intervirology 1981;16:201–17. https://doi.org/10.1159/000149269.

[16] Martí-Carreras J, Maes P. Human cytomegalovirus genomics and transcriptomics through the lens of next-generation sequencing: revision and future challenges. Virus Genes 2019;55:138–64. https://doi.org/10.1007/s11262-018-1627-3.
[17] Crough T, Khanna R. Immunobiology of Human Cytomegalovirus: from Bench to Bedside. Clin Microbiol Rev 2009;22:76–98. https://doi.org/10.1128/CMR.00034-08.
[18] Sinzger C, Digel M, Jahn G. Cytomegalovirus Cell Tropism. In: Shenk TE, Stinski MF, editors. Human Cytomegalovirus, vol. 325, Berlin, Heidelberg: Springer Berlin Heidelberg; 2008, p. 63–83. https://doi.org/10.1007/978-3-540-77349-8_4.
[19] Sinzger C, Jahn G. Human Cytomegalovirus Cell Tropism and Pathogenesis. Intervirology 1996;39:302–19. https://doi.org/10.1159/000150502.
[20] Loughney JW, Rustandi RR, Wang D, Troutman MC, Dick LW, Li G, et al. Soluble Human Cytomegalovirus gH/gL/pUL128–131 Pentameric Complex, but Not gH/gL, Inhibits Viral Entry to Epithelial Cells and Presents Dominant Native Neutralizing Epitopes. Journal of Biological Chemistry 2015;290:15985–95. https://doi.org/10.1074/jbc.M115.652230.
[21] Ryckman BJ, Rainish BL, Chase MC, Borton JA, Nelson JA, Jarvis MA, et al. Characterization of the Human Cytomegalovirus gH/gL/UL128-131 Complex That Mediates Entry into Epithelial and Endothelial Cells. J Virol 2008;82:60–70. https://doi.org/10.1128/JVI.01910-07.
[22] Wang D, Shenk T. Human Cytomegalovirus UL131 Open Reading Frame Is Required for Epithelial Cell Tropism. J Virol 2005;79:10330–8. https://doi.org/10.1128/JVI.79.16.10330-10338.2005.
[23] Murphy E, Yu D, Grimwood J, Schmutz J, Dickson M, Jarvis MA, et al. Coding potential of laboratory and clinical strains of human cytomegalovirus. Proc Natl Acad Sci USA 2003;100:14976–81. https://doi.org/10.1073/pnas.2136652100.
[24] Scrivano L, Sinzger C, Nitschko H, Koszinowski UH, Adler B. HCMV Spread and Cell Tropism are Determined by Distinct Virus Populations. PLoS Pathog 2011;7:e1001256. https://doi.org/10.1371/journal.ppat.1001256.
[25] Liu Y-T, Strugatsky D, Liu W, Zhou ZH. Structure of human cytomegalovirus virion reveals host tRNA binding to capsid-associated tegument protein pp150. Nat Commun 2021;12:5513. https://doi.org/10.1038/s41467-021-25791-1.
[26] Weekes MP, Tomasec P, Huttlin EL, Fielding CA, Nusinow D, Stanton RJ, et al. Quantitative Temporal Viromics: An Approach to Investigate Host-Pathogen Interaction. Cell 2014;157:1460–72. https://doi.org/10.1016/j.cell.2014.04.028.
[27] Yu X, Jih J, Jiang J, Zhou ZH. Atomic structure of the human cytomegalovirus capsid with its securing tegument layer of pp150. Science 2017;356:eaam6892. https://doi.org/10.1126/science.aam6892.
[28] Wood LJ, Baxter MK, Plafker SM, Gibson W. Human cytomegalovirus capsid assembly protein precursor (pUL80.5) interacts with itself and with the major capsid protein (pUL86) through two different domains. J Virol 1997;71:179–90. https://doi.org/10.1128/jvi.71.1.179-190.1997.
[29] Chen DH, Jiang H, Lee M, Liu F, Zhou ZH. Three-Dimensional Visualization of Tegument/Capsid Interactions in the Intact Human Cytomegalovirus. Virology 1999;260:10–6. https://doi.org/10.1006/viro.1999.9791.

[30] Terhune SS, Schröer J, Shenk T. RNAs Are Packaged into Human Cytomegalovirus Virions in Proportion to Their Intracellular Concentration. J Virol 2004;78:10390–8. https://doi.org/10.1128/JVI.78.19.10390-10398.2004.
[31] Varnum SM, Streblow DN, Monroe ME, Smith P, Auberry KJ, Paša-Tolić L, et al. Identification of Proteins in Human Cytomegalovirus (HCMV) Particles: the HCMV Proteome. J Virol 2004;78:13395–13395. https://doi.org/10.1128/JVI.78.23.13395.2004.
[32] Jean Beltran PM, Cristea IM. The life cycle and pathogenesis of human cytomegalovirus infection: lessons from proteomics. Expert Review of Proteomics 2014;11:697–711. https://doi.org/10.1586/14789450.2014.971116.
[33] Compton T, Nowlin DM, Cooper NR. Initiation of Human Cytomegalovirus Infection Requires Initial Interaction with Cell Surface Heparan Sulfate. Virology 1993;193:834–41. https://doi.org/10.1006/viro.1993.1192.
[34] Wang X, Huang DY, Huong S-M, Huang E-S. Integrin αvβ3 is a coreceptor for human cytomegalovirus. Nat Med 2005;11:515–21. https://doi.org/10.1038/nm1236.
[35] Chan G, Nogalski MT, Yurochko AD. Activation of EGFR on monocytes is required for human cytomegalovirus entry and mediates cellular motility. Proc Natl Acad Sci USA 2009;106:22369–74. https://doi.org/10.1073/pnas.0908787106.
[36] Mosher BS, Kowalik TF, Yurochko AD. Overview of how HCMV manipulation of host cell intracellular trafficking networks can promote productive infection. Front Virol 2022;2:1026452. https://doi.org/10.3389/fviro.2022.1026452.
[37] Ibig-Rehm Y, Götte M, Gabriel D, Woodhall D, Shea A, Brown NE, et al. High-content screening to distinguish between attachment and post-attachment steps of human cytomegalovirus entry into fibroblasts and epithelial cells. Antiviral Research 2011;89:246–56. https://doi.org/10.1016/j.antiviral.2011.01.007.
[38] Ogawa-Goto K, Tanaka K, Gibson W, Moriishi E, Miura Y, Kurata T, et al. Microtubule Network Facilitates Nuclear Targeting of Human Cytomegalovirus Capsid. J Virol 2003;77:8541–7. https://doi.org/10.1128/JVI.77.15.8541-8547.2003.
[39] Bechtel JT, Shenk T. Human Cytomegalovirus UL47 Tegument Protein Functions after Entry and before Immediate-Early Gene Expression. J Virol 2002;76:1043–50. https://doi.org/10.1128/JVI.76.3.1043-1050.2002.
[40] Ogawa-Goto K, Irie S, Omori A, Miura Y, Katano H, Hasegawa H, et al. An Endoplasmic Reticulum Protein, p180, Is Highly Expressed in Human Cytomegalovirus-Permissive Cells and Interacts with the Tegument Protein Encoded by UL48. J Virol 2002;76:2350–62. https://doi.org/10.1128/jvi.76.5.2350-2362.2002.
[41] Chambers J, Angulo A, Amaratunga D, Guo H, Jiang Y, Wan JS, et al. DNA Microarrays of the Complex Human Cytomegalovirus Genome: Profiling Kinetic Class with Drug Sensitivity of Viral Gene Expression. J Virol 1999;73:5757–66. https://doi.org/10.1128/JVI.73.7.5757-5766.1999.
[42] Sanchez V, Clark CL, Yen JY, Dwarakanath R, Spector DH. Viable Human Cytomegalovirus Recombinant Virus with an Internal Deletion of the IE2 86 Gene Affects Late Stages of Viral Replication. J Virol 2002;76:2973–89. https://doi.org/10.1128/JVI.76.6.2973-2989.2002.
[43] Perng Y-C, Qian Z, Fehr AR, Xuan B, Yu D. The Human Cytomegalovirus Gene UL79 Is Required for the Accumulation of Late Viral Transcripts. J Virol 2011;85:4841–52. https://doi.org/10.1128/JVI.02344-10.

[44] Loregian A, Appleton BA, Hogle JM, Coen DM. Residues of Human Cytomegalovirus DNA Polymerase Catalytic Subunit UL54 That Are Necessary and Sufficient for Interaction with the Accessory Protein UL44. J Virol 2004;78:158–67. https://doi.org/10.1128/JVI.78.1.158-167.2004.
[45] Shen A, Lei J, Yang E, Pei Y, Chen Y-C, Gong H, et al. Human Cytomegalovirus Primase UL70 Specifically Interacts with Cellular Factor Snapin. J Virol 2011;85:11732–41. https://doi.org/10.1128/JVI.05357-11.
[46] Yu Y, Clippinger AJ, Alwine JC. Viral effects on metabolism: changes in glucose and glutamine utilization during human cytomegalovirus infection. Trends in Microbiology 2011;19:360–7. https://doi.org/10.1016/j.tim.2011.04.002.
[47] Yurochko AD. Human Cytomegalovirus Modulation of Signal Transduction. In: Shenk TE, Stinski MF, editors. Human Cytomegalovirus, vol. 325, Berlin, Heidelberg: Springer Berlin Heidelberg; 2008, p. 205–20. https://doi.org/10.1007/978-3-540-77349-8_12.
[48] Li T, Chen J, Cristea IM. Human Cytomegalovirus Tegument Protein pUL83 Inhibits IFI16-Mediated DNA Sensing for Immune Evasion. Cell Host & Microbe 2013;14:591–9. https://doi.org/10.1016/j.chom.2013.10.007.
[49] Noriega VM, Hesse J, Gardner TJ, Besold K, Plachter B, Tortorella D. Human cytomegalovirus US3 modulates destruction of MHC class I molecules. Molecular Immunology 2012;51:245–53. https://doi.org/10.1016/j.molimm.2012.03.024.
[50] Camozzi D, Pignatelli S, Valvo C, Lattanzi G, Capanni C, Dal Monte P, et al. Remodelling of the nuclear lamina during human cytomegalovirus infection: role of the viral proteins pUL50 and pUL53. Journal of General Virology 2008;89:731–40. https://doi.org/10.1099/vir.0.83377-0.
[51] Moorman NJ, Sharon-Friling R, Shenk T, Cristea IM. A Targeted Spatial-Temporal Proteomics Approach Implicates Multiple Cellular Trafficking Pathways in Human Cytomegalovirus Virion Maturation. Molecular & Cellular Proteomics 2010;9:851–60. https://doi.org/10.1074/mcp.M900485-MCP200.
[52] Homman-Loudiyi M, Hultenby K, Britt W, Söderberg-Nauclér C. Envelopment of Human Cytomegalovirus Occurs by Budding into Golgi-Derived Vacuole Compartments Positive for gB, Rab 3, Trans-Golgi Network 46, and Mannosidase II. J Virol 2003;77:3191–203. https://doi.org/10.1128/JVI.77.5.3191-3203.2003.
[53] Roby C, Gibson W. Characterization of phosphoproteins and protein kinase activity of virions, noninfectious enveloped particles, and dense bodies of human cytomegalovirus. J Virol 1986;59:714–27. https://doi.org/10.1128/jvi.59.3.714-727.1986.
[54] Pepperl S, Münster J, Mach M, Harris JR, Plachter B. Dense Bodies of Human Cytomegalovirus Induce both Humoral and Cellular Immune Responses in the Absence of Viral Gene Expression. J Virol 2000;74:6132–46. https://doi.org/10.1128/JVI.74.13.6132-6146.2000.
[55] Landolfo S, Gariglio M, Gribaudo G, Lembo D. The human cytomegalovirus. Pharmacology & Therapeutics 2003;98:269–97. https://doi.org/10.1016/S0163-7258(03)00034-2.
[56] Forte E, Zhang Z, Thorp EB, Hummel M. Cytomegalovirus Latency and Reactivation: An Intricate Interplay With the Host Immune Response. Front Cell Infect Microbiol 2020;10:130. https://doi.org/10.3389/fcimb.2020.00130.

[57] Reeves MB, MacAry PA, Lehner PJ, Sissons JGP, Sinclair JH. Latency, chromatin remodeling, and reactivation of human cytomegalovirus in the dendritic cells of healthy carriers. Proc Natl Acad Sci USA 2005;102:4140–5. https://doi.org/10.1073/pnas.0408994102.
[58] Söderberg-Nauclér C, Fish KN, Nelson JA. Reactivation of Latent Human Cytomegalovirus by Allogeneic Stimulation of Blood Cells from Healthy Donors. Cell 1997;91:119–26. https://doi.org/10.1016/S0092-8674(01)80014-3.
[59] Goodrum F. Human Cytomegalovirus Latency: Approaching the Gordian Knot. Annu Rev Virol 2016;3:333–57. https://doi.org/10.1146/annurev-virology-110615-042422.
[60] Reeves MB. Chromatin-mediated regulation of cytomegalovirus gene expression. Virus Research 2011;157:134–43. https://doi.org/10.1016/j.virusres.2010.09.019.
[61] Murphy JC. Control of cytomegalovirus lytic gene expression by histone acetylation. The EMBO Journal 2002;21:1112–20. https://doi.org/10.1093/emboj/21.5.1112.
[62] Elder E, Sinclair J. HCMV latency: what regulates the regulators? Med Microbiol Immunol 2019;208:431–8. https://doi.org/10.1007/s00430-019-00581-1.
[63] Tavalai N, Papior P, Rechter S, Leis M, Stamminger T. Evidence for a Role of the Cellular ND10 Protein PML in Mediating Intrinsic Immunity against Human Cytomegalovirus Infections. J Virol 2006;80:8006–18. https://doi.org/10.1128/JVI.00743-06.
[64] Tavalai N, Papior P, Rechter S, Stamminger T. Nuclear Domain 10 Components Promyelocytic Leukemia Protein and hDaxx Independently Contribute to an Intrinsic Antiviral Defense against Human Cytomegalovirus Infection. J Virol 2008;82:126–37. https://doi.org/10.1128/JVI.01685-07.
[65] Woodhall DL, Groves IJ, Reeves MB, Wilkinson G, Sinclair JH. Human Daxx-mediated Repression of Human Cytomegalovirus Gene Expression Correlates with a Repressive Chromatin Structure around the Major Immediate Early Promoter. Journal of Biological Chemistry 2006;281:37652–60. https://doi.org/10.1074/jbc.M604273200.
[66] Sinclair J, Sissons P. Latency and reactivation of human cytomegalovirus. Journal of General Virology 2006;87:1763–79. https://doi.org/10.1099/vir.0.81891-0.
[67] Huang MM, Kew VG, Jestice K, Wills MR, Reeves MB. Efficient Human Cytomegalovirus Reactivation Is Maturation Dependent in the Langerhans Dendritic Cell Lineage and Can Be Studied using a CD14 $^{+}$ Experimental Latency Model. J Virol 2012;86:8507–15. https://doi.org/10.1128/JVI.00598-12.
[68] Walton AH, Muenzer JT, Rasche D, Boomer JS, Sato B, Brownstein BH, et al. Reactivation of Multiple Viruses in Patients with Sepsis. PLoS ONE 2014;9:e98819. https://doi.org/10.1371/journal.pone.0098819.
[69] Nett PC, Heisey DM, Fernandez LA, Sollinger HW, Pirsch JD. Association of Cytomegalovirus Disease and Acute Rejection with Graft Loss in Kidney Transplantation. Transplantation 2004;78:1036–41. https://doi.org/10.1097/01.TP.0000137105.92464.F3.
[70] El Baba R, Herbein G. Immune Landscape of CMV Infection in Cancer Patients: From "Canonical" Diseases Toward Virus-Elicited Oncomodulation. Front Immunol 2021;12:730765. https://doi.org/10.3389/fimmu.2021.730765.
[71] Staras SAS, Dollard SC, Radford KW, Flanders WD, Pass RF, Cannon MJ. Seroprevalence of Cytomegalovirus Infection in the United States, 1988-1994. Clinical Infectious Diseases 2006;43:1143–51. https://doi.org/10.1086/508173.

[72] Stagno S, Reynolds DW, Tsiantos A, Fuccillo DA, Long W, Alford CA. Comparative Serial Virologic and Serologic Studies of Symptomatic and Subclinical Congenitally and Natally Acquired Cytomegalovirus Infections. Journal of Infectious Diseases 1975;132:568–77. https://doi.org/10.1093/infdis/132.5.568.
[73] Revello MG, Campanini G, Piralla A, Furione M, Percivalle E, Zavattoni M, et al. Molecular epidemiology of primary human cytomegalovirus infection in pregnant women and their families. Journal of Medical Virology 2008;80:1415–25. https://doi.org/10.1002/jmv.21243.
[74] Schottstedt V. Human Cytomegalovirus (HCMV) – Revised. Transfus Med Hemother 2010;37:365–75. https://doi.org/10.1159/000322141.
[75] Forbes BA. Acquisition of cytomegalovirus infection: an update. Clin Microbiol Rev 1989;2:204–16. https://doi.org/10.1128/CMR.2.2.204.
[76] Pass RF, Anderson B. Mother-to-Child Transmission of Cytomegalovirus and Prevention of Congenital Infection. Journal of the Pediatric Infectious Diseases Society 2014;3:S2–6. https://doi.org/10.1093/jpids/piu069.
[77] Lancini D, Faddy HM, Flower R, Hogan C. Cytomegalovirus disease in immunocompetent adults. Medical Journal of Australia 2014;201:578–80. https://doi.org/10.5694/mja14.00183.
[78] Britt W. Manifestations of Human Cytomegalovirus Infection: Proposed Mechanisms of Acute and Chronic Disease. In: Shenk TE, Stinski MF, editors. Human Cytomegalovirus, vol. 325, Berlin, Heidelberg: Springer Berlin Heidelberg; 2008, p. 417–70. https://doi.org/10.1007/978-3-540-77349-8_23.
[79] Chiopris G, Veronese P, Cusenza F, Procaccianti M, Perrone S, Daccò V, et al. Congenital Cytomegalovirus Infection: Update on Diagnosis and Treatment. Microorganisms 2020;8:1516. https://doi.org/10.3390/microorganisms8101516.
[80] Dietrich ML, Schieffelin JS. Congenital Cytomegalovirus Infection. TOJ 2019;19:123–30. https://doi.org/10.31486/toj.18.0095.
[81] Xia W, Yan H, Zhang Y, Wang C, Gao W, Lv C, et al. Congenital Human Cytomegalovirus Infection Inducing Sensorineural Hearing Loss. Front Microbiol 2021;12:649690. https://doi.org/10.3389/fmicb.2021.649690.
[82] Syggelou A, Iacovidou N, Kloudas S, Christoni Z, Papaevangelou V. Congenital cytomegalovirus infection. Annals of the New York Academy of Sciences 2010;1205:144–7. https://doi.org/10.1111/j.1749-6632.2010.05649.x.
[83] Grangeot-Keros L. Diagnosis and prognostic markers of HCMV infection. Journal of Clinical Virology 2001;21:213–21. https://doi.org/10.1016/S1386-6532(00)00164-5.
[84] De Paschale M, Agrappi C, Manco MT, Clerici P. Positive predictive value of anti-HCMV IgM as an index of primary infection. Journal of Virological Methods 2010;168:121–5. https://doi.org/10.1016/j.jviromet.2010.05.001.
[85] Macé M, Sissoeff L, Rudent A, Grangeot-Keros L. A serological testing algorithm for the diagnosis of primary CMV infection in pregnant women: DIAGNOSIS OF CMV PRIMARY INFECTION IN PREGNANT WOMEN. Prenat Diagn 2004;24:861–3. https://doi.org/10.1002/pd.1001.
[86] A. Ross S, Novak Z, Pati S, B. Boppana S. Overview of the Diagnosis of Cytomegalovirus Infection. IDDT 2011;11:466–74. https://doi.org/10.2174/187152611797636703.
[87] Drew WL. Diagnosis of Cytomegalovirus Infection. Clinical Infectious Diseases 1988;10:S468–76. https://doi.org/10.1093/clinids/10.Supplement_3.S468.

[88] Grazia Revello M, Percivalle E, Zavattoni M, Parea M, Grossi P, Gerna G. Detection of human cytomegalovirus immediate early antigen in leukocytes as a marker of viremia in immunocompromised patients. J Med Virol 1989;29:88–93. https://doi.org/10.1002/jmv.1890290204.
[89] Niubò J, Pérez J, Martínez-Lacasa JT, García A, Roca J, Fabregat J, et al. Association of quantitative cytomegalovirus antigenemia with symptomatic infection in solid organ transplant patients. Diagnostic Microbiology and Infectious Disease 1996;24:19–24. https://doi.org/10.1016/0732-8893(95)00248-0.
[90] Schäfer P, Tenschert W, Gutensohn K, Laufs R. Minimal effect of delayed sample processing on results of quantitative PCR for cytomegalovirus DNA in leukocytes compared to results of an antigenemia assay. J Clin Microbiol 1997;35:741–4. https://doi.org/10.1128/jcm.35.3.741-744.1997.
[91] Boeckh M, Gallez-Hawkins GM, Myerson D, Zaia JA, Bowden RA. PLASMA POLYMERASE CHAIN REACTION FOR CYTOMEGALOVIRUS DNA AFTER ALLOGENEIC MARROW TRANSPLANTATION: Comparison with Polymerase Chain Reaction Using Peripheral Blood Leukocytes, pp65 Antigenemia, and Viral Culture1. Transplantation 1997;64:108–13. https://doi.org/10.1097/00007890-199707150-00020.
[92] Evans PC, Soin A, Wreghitt TG, Alexander GJ. Qualitative and semiquantitative polymerase chain reaction testing for cytomegalovirus DNA in serum allows prediction of CMV related disease in liver transplant recipients. Journal of Clinical Pathology 1998;51:914–21. https://doi.org/10.1136/jcp.51.12.914.
[93] Seehofer D, Meisel H, Rayes N, Stein A, Langrehr JM, Settmacher U, et al. Prospective Evaluation of the Clinical Utility of Different Methods for the Detection of Human Cytomegalovirus Disease after Liver Transplantation. American Journal of Transplantation 2004;4:1331–7. https://doi.org/10.1111/j.1600-6143.2004.00510.x.
[94] Meyer-Konig U, Serr A, Von Laer D, Kirste G, Wolff C, Haller O, et al. Human Cytomegalovirus Immediate Early And Late Transcripts In Peripheral Blood Leukocytes: Diagnostic Value In Renal Transplant Recipients. Journal of Infectious Diseases 1995;171:705–9. https://doi.org/10.1093/infdis/171.3.705.
[95] Ahmed A. Antiviral Treatment of Cytomegalovirus Infection. IDDT 2011;11:475–503. https://doi.org/10.2174/187152611797636640.
[96] Acosta E, Bowlin T, Brooks J, Chiang L, Hussein I, Kimberlin D, et al. Advances in the Development of Therapeutics for Cytomegalovirus Infections. The Journal of Infectious Diseases 2020;221:S32–44. https://doi.org/10.1093/infdis/jiz493.
[97] Britt WJ, Prichard MN. New therapies for human cytomegalovirus infections. Antiviral Research 2018;159:153–74. https://doi.org/10.1016/j.antiviral.2018.09.003.
[98] Biron KK. Antiviral drugs for cytomegalovirus diseases. Antiviral Research 2006;71:154–63. https://doi.org/10.1016/j.antiviral.2006.05.002.
[99] Tseng A, Foisy M. The Role of Ganciclovir for the Management of Cytomegalovirus Retinitis in HIV Patients: Pharmacological Review and Update on New Developments. Canadian Journal of Infectious Diseases 1996;7:183–94. https://doi.org/10.1155/1996/780831.
[100] Gilbert C, Boivin G. Human Cytomegalovirus Resistance to Antiviral Drugs. Antimicrob Agents Chemother 2005;49:873–83. https://doi.org/10.1128/AAC.49.3.873-883.2005.

[101] Bacigalupo A, Boyd A, Slipper J, Curtis J, Clissold S. Foscarnet in the management of cytomegalovirus infections in hematopoietic stem cell transplant patients. Expert Review of Anti-Infective Therapy 2012;10:1249–64. https://doi.org/10.1586/eri.12.115.
[102] Gérard L, Salmon-Céron D. Pharmacology and clinical use of foscarnet. International Journal of Antimicrobial Agents 1995;5:209–17. https://doi.org/10.1016/0924-8579(95)00008-V.
[103] Kendle JB, Fan-Havard P. Cidofovir in the Treatment of Cytomegaloviral Disease. Ann Pharmacother 1998;32:1181–92. https://doi.org/10.1345/aph.17312.
[104] Lin A, Maloy M, Su Y, Bhatt V, DeRespiris L, Griffin M, et al. Letermovir for primary and secondary cytomegalovirus prevention in allogeneic hematopoietic cell transplant recipients: Real-world experience. Transplant Infectious Dis 2019;21:e13187. https://doi.org/10.1111/tid.13187.
[105] Verghese PS, Schleiss MR. Letermovir. Drugs Fut 2013;38:291. https://doi.org/10.1358/dof.2013.38.5.1946425.
[106] Marty FM, Boeckh M. Maribavir and human cytomegalovirus—what happened in the clinical trials and why might the drug have failed? Current Opinion in Virology 2011;1:555–62. https://doi.org/10.1016/j.coviro.2011.10.011.
[107] Avery RK, Alain S, Alexander BD, Blumberg EA, Chemaly RF, Cordonnier C, et al. Maribavir for Refractory Cytomegalovirus Infections With or Without Resistance Post-Transplant: Results From a Phase 3 Randomized Clinical Trial. Clinical Infectious Diseases 2022;75:690–701. https://doi.org/10.1093/cid/ciab988.
[108] Cui X, Snapper CM. Development of novel vaccines against human cytomegalovirus. Human Vaccines & Immunotherapeutics 2019;15:2673–83. https://doi.org/10.1080/21645515.2019.1593729.
[109] Scarpini S, Morigi F, Betti L, Dondi A, Biagi C, Lanari M. Development of a Vaccine against Human Cytomegalovirus: Advances, Barriers, and Implications for the Clinical Practice. Vaccines 2021;9:551. https://doi.org/10.3390/vaccines9060551.
[110] Griffiths P, Reeves M. Pathogenesis of human cytomegalovirus in the immunocompromised host. Nat Rev Microbiol 2021;19:759–73. https://doi.org/10.1038/s41579-021-00582-z.
[111] Jückstock J, Rothenburger M, Friese K, Traunmüller F. Passive Immunization against Congenital Cytomegalovirus Infection: Current State of Knowledge. Pharmacology 2015;95:209–17. https://doi.org/10.1159/000381626.
[112] Long X, Qiu Y, Zhang Z, Wu M. Insight for Immunotherapy of HCMV Infection. Int J Biol Sci 2021;17:2899–911. https://doi.org/10.7150/ijbs.58127.
[113] Berg C, Rosenkilde MM. Therapeutic targeting of HCMV-encoded chemokine receptor US28: Progress and challenges. Front Immunol 2023;14:1135280. https://doi.org/10.3389/fimmu.2023.1135280.
[114] Zhou X, Zhou M, Zheng M, Tian S, Yang X, Ning Y, et al. Polyploid giant cancer cells and cancer progression. Front Cell Dev Biol 2022;10:1017588. https://doi.org/10.3389/fcell.2022.1017588.
[115] Zhang S, Mercado-Uribe I, Xing Z, Sun B, Kuang J, Liu J. Generation of cancer stem-like cells through the formation of polyploid giant cancer cells. Oncogene 2014;33:116–28. https://doi.org/10.1038/onc.2013.96.

[116] Pienta KJ, Hammarlund EU, Brown JS, Amend SR, Axelrod RM. Cancer recurrence and lethality are enabled by enhanced survival and reversible cell cycle arrest of polyaneuploid cells. Proc Natl Acad Sci USA 2021;118:e2020838118. https://doi.org/10.1073/pnas.2020838118.
[117] Liu J, Niu N, Li X, Zhang X, Sood AK. The life cycle of polyploid giant cancer cells and dormancy in cancer: Opportunities for novel therapeutic interventions. Seminars in Cancer Biology 2022;81:132–44. https://doi.org/10.1016/j.semcancer.2021.10.005.
[118] Liu J, Erenpreisa J, Sikora E. Polyploid giant cancer cells: An emerging new field of cancer biology. Seminars in Cancer Biology 2022;81:1–4. https://doi.org/10.1016/j.semcancer.2021.10.006.
[119] Saini G, Joshi S, Garlapati C, Li H, Kong J, Krishnamurthy J, et al. Polyploid giant cancer cell characterization: New frontiers in predicting response to chemotherapy in breast cancer. Seminars in Cancer Biology 2022;81:220–31. https://doi.org/10.1016/j.semcancer.2021.03.017.
[120] Was H, Borkowska A, Olszewska A, Klemba A, Marciniak M, Synowiec A, et al. Polyploidy formation in cancer cells: How a Trojan horse is born. Seminars in Cancer Biology 2022;81:24–36. https://doi.org/10.1016/j.semcancer.2021.03.003.
[121] Chen J, Niu N, Zhang J, Qi L, Shen W, Donkena KV, et al. Polyploid Giant Cancer Cells (PGCCs): The Evil Roots of Cancer. CCDT 2019;19:360–7. https://doi.org/10.2174/1568009618666180703154233.
[122] Wang H, Unternaehrer JJ. Epithelial-mesenchymal Transition and Cancer Stem Cells: At the Crossroads of Differentiation and Dedifferentiation: EMT in Differentiation and Dedifferentiation. Dev Dyn 2019;248:10–20. https://doi.org/10.1002/dvdy.24678.
[123] Matsumoto T, Wakefield L, Peters A, Peto M, Spellman P, Grompe M. Proliferative polyploid cells give rise to tumors via ploidy reduction. Nat Commun 2021;12:646. https://doi.org/10.1038/s41467-021-20916-y.
[124] Herbein G, Nehme Z. Polyploid Giant Cancer Cells, a Hallmark of Oncoviruses and a New Therapeutic Challenge. Front Oncol 2020;10:567116. https://doi.org/10.3389/fonc.2020.567116.
[125] Nehme Z, Pasquereau S, Haidar Ahmad S, Coaquette A, Molimard C, Monnien F, et al. Polyploid giant cancer cells, stemness and epithelial-mesenchymal plasticity elicited by human cytomegalovirus. Oncogene 2021;40:3030–46. https://doi.org/10.1038/s41388-021-01715-7.
[126] Nehme Z, Pasquereau S, Haidar Ahmad S, El Baba R, Herbein G. Polyploid giant cancer cells, EZH2 and Myc upregulation in mammary epithelial cells infected with high-risk human cytomegalovirus. eBioMedicine 2022;80:104056. https://doi.org/10.1016/j.ebiom.2022.104056.
[127] Mui U, Haley C, Tyring S. Viral Oncology: Molecular Biology and Pathogenesis. JCM 2017;6:111. https://doi.org/10.3390/jcm6120111.
[128] Mesri EA, Feitelson MA, Munger K. Human Viral Oncogenesis: A Cancer Hallmarks Analysis. Cell Host & Microbe 2014;15:266–82. https://doi.org/10.1016/j.chom.2014.02.011.
[129] Zur Hausen H. The search for infectious causes of human cancers: Where and why. Virology 2009;392:1–10. https://doi.org/10.1016/j.virol.2009.06.001.

[130] Yasunaga J, Jeang K. Viral transformation and aneuploidy. Environ and Mol Mutagen 2009;50:733–40. https://doi.org/10.1002/em.20480.
[131] Wang C, Hai Y, Liu X, Liu N, Yao Y, He P, et al. Prediction of High-Risk Types of Human Papillomaviruses Using Statistical Model of Protein "Sequence Space." Computational and Mathematical Methods in Medicine 2015;2015:1–9. https://doi.org/10.1155/2015/756345.
[132] Burd EM. Human Papillomavirus and Cervical Cancer. Clin Microbiol Rev 2003;16:1–17. https://doi.org/10.1128/CMR.16.1.1-17.2003.
[133] Yeo-Teh N, Ito Y, Jha S. High-Risk Human Papillomaviral Oncogenes E6 and E7 Target Key Cellular Pathways to Achieve Oncogenesis. IJMS 2018;19:1706. https://doi.org/10.3390/ijms19061706.
[134] Giannoudis A, Evans MF, Southern SA, Herrington CS. Basal keratinocyte tetrasomy in low-grade squamous intra-epithelial lesions of the cervix is restricted to high and intermediate risk HPV infection but is not type-specific. Br J Cancer 2000;82:424–8. https://doi.org/10.1054/bjoc.1999.0937.
[135] Olaharski AJ, Sotelo R, Solorza-Luna G, Gonsebatt ME, Guzman P, Mohar A, et al. Tetraploidy and chromosomal instability are early events during cervical carcinogenesis. Carcinogenesis 2006;27:337–43. https://doi.org/10.1093/carcin/bgi218.
[136] Lorenzato M, Clavel C, Masure M, Nou J-M, Bouttens D, Evrard G, et al. DNA image cytometry and human papillomavirus (HPV) detection help to select smears at high risk of high-grade cervical lesions. J Pathol 2001;194:171–6. https://doi.org/10.1002/path.874.
[137] Méhes G, Speich N, Bollmann M, Bollmann R. Chromosomal aberrations accumulate in polyploid cells of high-grade squamous intraepithelial lesions (HSIL). Pathol Oncol Res 2004;10:142–8. https://doi.org/10.1007/BF03033742.
[138] Patel D, Incassati A, Wang N, McCance DJ. Human Papillomavirus Type 16 E6 and E7 Cause Polyploidy in Human Keratinocytes and Up-Regulation of G2-M-Phase Proteins. Cancer Research 2004;64:1299–306. https://doi.org/10.1158/0008-5472.CAN-03-2917.
[139] Duensing S, Lee LY, Duensing A, Basile J, Piboonniyom S, Gonzalez S, et al. The human papillomavirus type 16 E6 and E7 oncoproteins cooperate to induce mitotic defects and genomic instability by uncoupling centrosome duplication from the cell division cycle. Proc Natl Acad Sci USA 2000;97:10002–7. https://doi.org/10.1073/pnas.170093297.
[140] Tomaić V. Functional Roles of E6 and E7 Oncoproteins in HPV-Induced Malignancies at Diverse Anatomical Sites. Cancers 2016;8:95. https://doi.org/10.3390/cancers8100095.
[141] Zhang W, Liu Y, Zhao N, Chen H, Qiao L, Zhao W, et al. Role of Cdk1 in the p53-Independent Abrogation of the Postmitotic Checkpoint by Human Papillomavirus E6. J Virol 2015;89:2553–62. https://doi.org/10.1128/JVI.02269-14.
[142] Heilman SA, Nordberg JJ, Liu Y, Sluder G, Chen JJ. Abrogation of the Postmitotic Checkpoint Contributes to Polyploidization in Human Papillomavirus E7-Expressing Cells. J Virol 2009;83:2756–64. https://doi.org/10.1128/JVI.02149-08.
[143] Araldi RP, Mazzuchelli-de-Souza J, Modolo DG, Souza EBD, Melo TCD, Spadacci-Morena DD, et al. Mutagenic Potential of *Bos taurus* Papillomavirus Type 1 E6 Recombinant Protein: First Description. BioMed Research International 2015;2015:1–15. https://doi.org/10.1155/2015/806361.

[144] Hu L, Potapova TA, Li S, Rankin S, Gorbsky GJ, Angeletti PC, et al. Expression of HPV16 E5 produces enlarged nuclei and polyploidy through endoreplication. Virology 2010;405:342–51. https://doi.org/10.1016/j.virol.2010.06.025.
[145] Chien W-M, Noya F, Benedict-Hamilton HM, Broker TR, Chow LT. Alternative Fates of Keratinocytes Transduced by Human Papillomavirus Type 18 E7 during Squamous Differentiation. J Virol 2002;76:2964–72. https://doi.org/10.1128/JVI.76.6.2964-2972.2002.
[146] Fan X, Liu Y, Heilman SA, Chen JJ. Human Papillomavirus E7 Induces Rereplication in Response to DNA Damage. J Virol 2013;87:1200–10. https://doi.org/10.1128/JVI.02038-12.
[147] Dorn ES, Chastain PD, Hall JR, Cook JG. Analysis of re-replication from deregulated origin licensing by DNA fiber spreading. Nucleic Acids Research 2009;37:60–9. https://doi.org/10.1093/nar/gkn912.
[148] Tang X, Zhang Q, Nishitani J, Brown J, Shi S, Le AD. Overexpression of Human Papillomavirus Type 16 Oncoproteins Enhances Hypoxia-Inducible Factor 1α Protein Accumulation and Vascular Endothelial Growth Factor Expression in Human Cervical Carcinoma Cells. Clinical Cancer Research 2007;13:2568–76. https://doi.org/10.1158/1078-0432.CCR-06-2704.
[149] Zanella L, Riquelme I, Buchegger K, Abanto M, Ili C, Brebi P. A reliable Epstein-Barr Virus classification based on phylogenomic and population analyses. Sci Rep 2019;9:9829. https://doi.org/10.1038/s41598-019-45986-3.
[150] Farrell PJ. Epstein–Barr Virus and Cancer. Annu Rev Pathol Mech Dis 2019;14:29–53. https://doi.org/10.1146/annurev-pathmechdis-012418-013023.
[151] Saha A, Robertson ES. Epstein-Barr Virus–Associated B-cell Lymphomas: Pathogenesis and Clinical Outcomes. Clinical Cancer Research 2011;17:3056–63. https://doi.org/10.1158/1078-0432.CCR-10-2578.
[152] Jiang Q, Zhang Q, Wang S, Xie S, Fang W, Liu Z, et al. A Fraction of CD133+ CNE2 Cells Is Made of Giant Cancer Cells with Morphological Evidence of Asymmetric Mitosis. J Cancer 2015;6:1236–44. https://doi.org/10.7150/jca.12626.
[153] Sato H, Takimoto T, Tanaka S, Ogura H, Shiraishi K, Tanaka J. Cytopathic effects induced by Epstein-Barr virus replication in epithelial nasopharyngeal carcinoma hybrid cells. J Virol 1989;63:3555–9. https://doi.org/10.1128/jvi.63.8.3555-3559.1989.
[154] Gelardi M, Tomaiuolo M, Cassano M, Besozzi G, Fiorella ML, Calvario A, et al. Epstein-barr virus induced cellular changes in nasal mucosa. Virol J 2006;3:6. https://doi.org/10.1186/1743-422X-3-6.
[155] Humme S, Reisbach G, Feederle R, Delecluse H-J, Bousset K, Hammerschmidt W, et al. The EBV nuclear antigen 1 (EBNA1) enhances B cell immortalization several thousandfold. Proc Natl Acad Sci USA 2003;100:10989–94. https://doi.org/10.1073/pnas.1832776100.
[156] Shumilov A, Tsai M-H, Schlosser YT, Kratz A-S, Bernhardt K, Fink S, et al. Epstein–Barr virus particles induce centrosome amplification and chromosomal instability. Nat Commun 2017;8:14257. https://doi.org/10.1038/ncomms14257.
[157] Pan S-H, Tai C-C, Lin C-S, Hsu W-B, Chou S-F, Lai C-C, et al. Epstein-Barr virus nuclear antigen 2 disrupts mitotic checkpoint and causes chromosomal instability. Carcinogenesis 2009;30:366–75. https://doi.org/10.1093/carcin/bgn291.

[158] Parker GA, Touitou R, Allday MJ. Epstein-Barr virus EBNA3C can disrupt multiple cell cycle checkpoints and induce nuclear division divorced from cytokinesis. Oncogene 2000;19:700–9. https://doi.org/10.1038/sj.onc.1203327.
[159] Leao M, Anderton E, Wade M, Meekings K, Allday MJ. Epstein-Barr Virus-Induced Resistance to Drugs That Activate the Mitotic Spindle Assembly Checkpoint in Burkitt's Lymphoma Cells. J Virol 2007;81:248–60. https://doi.org/10.1128/JVI.01096-06.
[160] Wakisaka N, Kondo S, Yoshizaki T, Murono S, Furukawa M, Pagano JS. Epstein-Barr Virus Latent Membrane Protein 1 Induces Synthesis of Hypoxia-Inducible Factor 1α. Molecular and Cellular Biology 2004;24:5223–34. https://doi.org/10.1128/MCB.24.12.5223-5234.2004.
[161] Darekar S, Georgiou K, Yurchenko M, Yenamandra SP, Chachami G, Simos G, et al. Epstein-Barr Virus Immortalization of Human B-Cells Leads to Stabilization of Hypoxia-Induced Factor 1 Alpha, Congruent with the Warburg Effect. PLoS ONE 2012;7:e42072. https://doi.org/10.1371/journal.pone.0042072.
[162] Lajoie V, Lemieux B, Sawan B, Lichtensztejn D, Lichtensztejn Z, Wellinger R, et al. LMP1 mediates multinuclearity through downregulation of shelterin proteins and formation of telomeric aggregates. Blood 2015;125:2101–10. https://doi.org/10.1182/blood-2014-08-594176.
[163] Knecht H, Mai S. LMP1 and Dynamic Progressive Telomere Dysfunction: A Major Culprit in EBV-Associated Hodgkin's Lymphoma. Viruses 2017;9:164. https://doi.org/10.3390/v9070164.
[164] Wen KW, Damania B. Kaposi sarcoma-associated herpesvirus (KSHV): Molecular biology and oncogenesis. Cancer Letters 2010;289:140–50. https://doi.org/10.1016/j.canlet.2009.07.004.
[165] Goncalves PH, Ziegelbauer J, Uldrick TS, Yarchoan R. Kaposi sarcoma herpesvirus-associated cancers and related diseases. Current Opinion in HIV and AIDS 2017;12:47–56. https://doi.org/10.1097/COH.0000000000000330.
[166] Radkov SA, Kellam P, Boshoff C. The latent nuclear antigen of Kaposi sarcoma-associated herpesvirus targets the retinoblastoma–E2F pathway and with the oncogene Hras transforms primary rat cells. Nat Med 2000;6:1121–7. https://doi.org/10.1038/80459.
[167] Zhu Y, Haecker I, Yang Y, Gao S-J, Renne R. γ-Herpesvirus-encoded miRNAs and their roles in viral biology and pathogenesis. Current Opinion in Virology 2013;3:266–75. https://doi.org/10.1016/j.coviro.2013.05.013.
[168] Pan H, Zhou F, Gao S-J. Kaposi's Sarcoma-Associated Herpesvirus Induction of Chromosome Instability in Primary Human Endothelial Cells. Cancer Research 2004;64:4064–8. https://doi.org/10.1158/0008-5472.CAN-04-0657.
[169] Verschuren EW, Klefstrom J, Evan GI, Jones N. The oncogenic potential of Kaposi's sarcoma-associated herpesvirus cyclin is exposed by p53 loss in vitro and in vivo. Cancer Cell 2002;2:229–41. https://doi.org/10.1016/S1535-6108(02)00123-X.
[170] Si H, Robertson ES. Kaposi's Sarcoma-Associated Herpesvirus-Encoded Latency-Associated Nuclear Antigen Induces Chromosomal Instability through Inhibition of p53 Function. J Virol 2006;80:697–709. https://doi.org/10.1128/JVI.80.2.697-709.2006.
[171] Shin YC, Joo C-H, Gack MU, Lee H-R, Jung JU. Kaposi's Sarcoma–Associated Herpesvirus Viral IFN Regulatory Factor 3 Stabilizes Hypoxia-Inducible Factor-1α to Induce

Vascular Endothelial Growth Factor Expression. Cancer Research 2008;68:1751–9. https://doi.org/10.1158/0008-5472.CAN-07-2766.
[172] Leidal AM, Cyr DP, Hill RJ, Lee PWK, McCormick C. Subversion of Autophagy by Kaposi's Sarcoma-Associated Herpesvirus Impairs Oncogene-Induced Senescence. Cell Host & Microbe 2016;19:901. https://doi.org/10.1016/j.chom.2016.05.006.
[173] Panfil AR, Martinez MP, Ratner L, Green PL. Human T-cell leukemia virus-associated malignancy. Current Opinion in Virology 2016;20:40–6. https://doi.org/10.1016/j.coviro.2016.08.009.
[174] Mohanty S, Harhaj EW. Mechanisms of Oncogenesis by HTLV-1 Tax. Pathogens 2020;9:543. https://doi.org/10.3390/pathogens9070543.
[175] Grassmann R, Aboud M, Jeang K-T. Molecular mechanisms of cellular transformation by HTLV-1 Tax. Oncogene 2005;24:5976–85. https://doi.org/10.1038/sj.onc.1208978.
[176] Ducu RI, Dayaram T, Marriott SJ. The HTLV-1 Tax oncoprotein represses Ku80 gene expression. Virology 2011;416:1–8. https://doi.org/10.1016/j.virol.2011.04.012.
[177] Liang M-H, Geisbert T, Yao Y, Hinrichs SH, Giam C-Z. Human T-Lymphotropic Virus Type 1 Oncoprotein Tax Promotes S-Phase Entry but Blocks Mitosis. J Virol 2002;76:4022–33. https://doi.org/10.1128/JVI.76.8.4022-4033.2002.
[178] Jin D-Y, Spencer F, Jeang K-T. Human T Cell Leukemia Virus Type 1 Oncoprotein Tax Targets the Human Mitotic Checkpoint Protein MAD1. Cell 1998;93:81–91. https://doi.org/10.1016/S0092-8674(00)81148-4.
[179] Yang L, Kotomura N, Ho Y-K, Zhi H, Bixler S, Schell MJ, et al. Complex Cell Cycle Abnormalities Caused by Human T-Lymphotropic Virus Type 1 Tax. J Virol 2011;85:3001–9. https://doi.org/10.1128/JVI.00086-10.
[180] Sibon D. HTLV-1 propels untransformed CD4+ lymphocytes into the cell cycle while protecting CD8+ cells from death. Journal of Clinical Investigation 2006;116:974–83. https://doi.org/10.1172/JCI27198.
[181] Caballero A, Tabernero D, Buti M, Rodriguez-Frias F. Hepatitis B virus: The challenge of an ancient virus with multiple faces and a remarkable replication strategy. Antiviral Research 2018;158:34–44. https://doi.org/10.1016/j.antiviral.2018.07.019.
[182] Liang TJ. Hepatitis B: The virus and disease. Hepatology 2009;49:S13–21. https://doi.org/10.1002/hep.22881.
[183] Kew MC. Hepatitis B virus x protein in the pathogenesis of hepatitis B virus-induced hepatocellular carcinoma. J of Gastro and Hepatol 2011;26:144–52. https://doi.org/10.1111/j.1440-1746.2010.06546.x.
[184] Sivasudhan E, Blake N, Lu Z, Meng J, Rong R. Hepatitis B Viral Protein HBx and the Molecular Mechanisms Modulating the Hallmarks of Hepatocellular Carcinoma: A Comprehensive Review. Cells 2022;11:741. https://doi.org/10.3390/cells11040741.
[185] Musa J, Li J, Grünewald TG. Hepatitis B virus large surface protein is priming for hepatocellular carcinoma development via induction of cytokinesis failure. The Journal of Pathology 2019;247:6–8. https://doi.org/10.1002/path.5169.
[186] Donne R, Saroul-Aïnama M, Cordier P, Celton-Morizur S, Desdouets C. Polyploidy in liver development, homeostasis and disease. Nat Rev Gastroenterol Hepatol 2020;17:391–405. https://doi.org/10.1038/s41575-020-0284-x.

[187] Bou-Nader M, Caruso S, Donne R, Celton-Morizur S, Calderaro J, Gentric G, et al. Polyploidy spectrum: a new marker in HCC classification. Gut 2020;69:355–64. https://doi.org/10.1136/gutjnl-2018-318021.
[188] Gramantieri L, Melchiorri C, Chieco P, Gaiani S, Stecca B, Casali A, et al. Alteration of DNA ploidy and cell nuclearity in human hepatocellular carcinoma associated with HBV infection. Journal of Hepatology 1996;25:848–53. https://doi.org/10.1016/S0168-8278(96)80288-1.
[189] Li T, Wu Y, Tsai H, Sun C, Wu Y, Wu H, et al. Intrahepatic hepatitis B virus large surface antigen induces hepatocyte hyperploidy via failure of cytokinesis. The Journal of Pathology 2018;245:502–13. https://doi.org/10.1002/path.5102.
[190] Rakotomalala L, Studach L, Wang W-H, Gregori G, Hullinger RL, Andrisani O. Hepatitis B Virus X Protein Increases the Cdt1-to-Geminin Ratio Inducing DNA Re-replication and Polyploidy. Journal of Biological Chemistry 2008;283:28729–40. https://doi.org/10.1074/jbc.M802751200.
[191] Studach L, Wang W-H, Weber G, Tang J, Hullinger RL, Malbrue R, et al. Polo-like Kinase 1 Activated by the Hepatitis B Virus X Protein Attenuates Both the DNA Damage Checkpoint and DNA Repair Resulting in Partial Polyploidy. Journal of Biological Chemistry 2010;285:30282–93. https://doi.org/10.1074/jbc.M109.093963.
[192] Yoo Y-G, Cho S, Park S, Lee M-O. The carboxy-terminus of the hepatitis B virus X protein is necessary and sufficient for the activation of hypoxia-inducible factor-1α. FEBS Letters 2004;577:121–6. https://doi.org/10.1016/j.febslet.2004.10.004.
[193] Yoo Y-G, Oh SH, Park ES, Cho H, Lee N, Park H, et al. Hepatitis B Virus X Protein Enhances Transcriptional Activity of Hypoxia-inducible Factor-1α through Activation of Mitogen-activated Protein Kinase Pathway. Journal of Biological Chemistry 2003;278:39076–84. https://doi.org/10.1074/jbc.M305101200.
[194] Moosavy SH, Dvoodian P, Nazarnezhad MA, Nejatizaheh A, Ephtekhar E, Mahboobi H. Epidemiology, transmission, diagnosis, and outcome of Hepatitis C virus infection. Electron Physician 2017;9:5646–56. https://doi.org/10.19082/5646.
[195] Zhu X, Jing L, Li X. Hepatitis C virus infection is a risk factor for non-Hodgkin lymphoma: A MOOSE-compliant meta-analysis. Medicine 2019;98:e14755. https://doi.org/10.1097/MD.0000000000014755.
[196] Banerjee A, Ray RB, Ray R. Oncogenic Potential of Hepatitis C Virus Proteins. Viruses 2010;2:2108–33. https://doi.org/10.3390/v2092108.
[197] Machida K, Liu J-C, McNamara G, Levine A, Duan L, Lai MMC. Hepatitis C Virus Causes Uncoupling of Mitotic Checkpoint and Chromosomal Polyploidy through the Rb Pathway. J Virol 2009;83:12590–600. https://doi.org/10.1128/JVI.02643-08.
[198] Abe M, Koga H, Yoshida T, Masuda H, Iwamoto H, Sakata M, et al. Hepatitis C virus core protein upregulates the expression of vascular endothelial growth factor via the nuclear factor-κB/hypoxia-inducible factor-1α axis under hypoxic conditions. Hepatology Research 2012;42:591–600. https://doi.org/10.1111/j.1872-034X.2011.00953.x.
[199] White MK, Gordon J, Khalili K. The Rapidly Expanding Family of Human Polyomaviruses: Recent Developments in Understanding Their Life Cycle and Role in Human Pathology. PLoS Pathog 2013;9:e1003206. https://doi.org/10.1371/journal.ppat.1003206.

[200] Prado JCM, Monezi TA, Amorim AT, Lino V, Paladino A, Boccardo E. Human polyomaviruses and cancer: an overview. Clinics 2018;73:e558s. https://doi.org/10.6061/clinics/2018/e558s.
[201] Verhaegen ME, Mangelberger D, Harms PW, Vozheiko TD, Weick JW, Wilbert DM, et al. Merkel Cell Polyomavirus Small T Antigen Is Oncogenic in Transgenic Mice. Journal of Investigative Dermatology 2015;135:1415–24. https://doi.org/10.1038/jid.2014.446.
[202] Dalianis T, Hirsch HH. Human polyomaviruses in disease and cancer. Virology 2013;437:63–72. https://doi.org/10.1016/j.virol.2012.12.015.
[203] Kwun HJ, Wendzicki JA, Shuda Y, Moore PS, Chang Y. Merkel cell polyomavirus small T antigen induces genome instability by E3 ubiquitin ligase targeting. Oncogene 2017;36:6784–92. https://doi.org/10.1038/onc.2017.277.
[204] Shuda M, Guastafierro A, Geng X, Shuda Y, Ostrowski SM, Lukianov S, et al. Merkel Cell Polyomavirus Small T Antigen Induces Cancer and Embryonic Merkel Cell Proliferation in a Transgenic Mouse Model. PLoS ONE 2015;10:e0142329. https://doi.org/10.1371/journal.pone.0142329.
[205] Hertel L, Mocarski ES. Global Analysis of Host Cell Gene Expression Late during Cytomegalovirus Infection Reveals Extensive Dysregulation of Cell Cycle Gene Expression and Induction of Pseudomitosis Independent of US28 Function. J Virol 2004;78:11988–2011. https://doi.org/10.1128/JVI.78.21.11988-12011.2004.
[206] Kwon Y, Kim M-N, Young Choi E, Heon Kim J, Hwang E-S, Cha C-Y. Inhibition of p53 transcriptional activity by human cytomegalovirus UL44: Inhibition of p53 by HCMV UL44. Microbiology and Immunology 2012;56:324–31. https://doi.org/10.1111/j.1348-0421.2012.00446.x.
[207] Iwahori S, Umaña AC, VanDeusen HR, Kalejta RF. Human cytomegalovirus-encoded viral cyclin-dependent kinase (v-CDK) UL97 phosphorylates and inactivates the retinoblastoma protein-related p107 and p130 proteins. Journal of Biological Chemistry 2017;292:6583–99. https://doi.org/10.1074/jbc.M116.773150.
[208] Boldogh I, AbuBakar S, Deng CZ, Albrecht T. Transcriptional activation of cellular oncogenes fos, jun, and myc by human cytomegalovirus. J Virol 1991;65:1568–71. https://doi.org/10.1128/jvi.65.3.1568-1571.1991.
[209] Kumar A, Tripathy MK, Pasquereau S, Al Moussawi F, Abbas W, Coquard L, et al. The Human Cytomegalovirus Strain DB Activates Oncogenic Pathways in Mammary Epithelial Cells. EBioMedicine 2018;30:167–83. https://doi.org/10.1016/j.ebiom.2018.03.015.
[210] McFarlane S, Nicholl MJ, Sutherland JS, Preston CM. Interaction of the human cytomegalovirus particle with the host cell induces hypoxia-inducible factor 1 alpha. Virology 2011;414:83–90. https://doi.org/10.1016/j.virol.2011.03.005.
[211] Lehman JM. Early chromosome changes in diploid Chinese hamster cells after infection with simian virus 40. Int J Cancer 1974;13:164–72. https://doi.org/10.1002/ijc.2910130203.
[212] Lehman JM, Mauel J, Defendi V. Regulation of DNA synthesis in macrophages infected with simian virus 40. Experimental Cell Research 1971;67:230–3. https://doi.org/10.1016/0014-4827(71)90644-6.
[213] Cobbs C, Harkins L, Samanta M, Gillespie G, Bharara S, King P, et al. Human cytomegalovirus infection and expression in human malignant glioma. Cancer Res 2002;62:3347–50.

[214] Xu S, Schafer X, Munger J. Expression of Oncogenic Alleles Induces Multiple Blocks to Human Cytomegalovirus Infection. J Virol 2016;90:4346–56. https://doi.org/10.1128/JVI.00179-16.
[215] Herbein G. The Human Cytomegalovirus, from Oncomodulation to Oncogenesis. Viruses 2018;10:408. https://doi.org/10.3390/v10080408.
[216] Herbein G. High-Risk Oncogenic Human Cytomegalovirus. Viruses 2022;14:2462. https://doi.org/10.3390/v14112462.
[217] Razonable RR, Inoue N, Pinninti SG, Boppana SB, Lazzarotto T, Gabrielli L, et al. Clinical Diagnostic Testing for Human Cytomegalovirus Infections. The Journal of Infectious Diseases 2020;221:S74–85. https://doi.org/10.1093/infdis/jiz601.
[218] Hanahan D, Weinberg RA. The Hallmarks of Cancer. Cell 2000;100:57–70. https://doi.org/10.1016/S0092-8674(00)81683-9.
[219] Hanahan D, Weinberg RA. Hallmarks of Cancer: The Next Generation. Cell 2011;144:646–74. https://doi.org/10.1016/j.cell.2011.02.013.
[220] Hanahan D. Hallmarks of Cancer: New Dimensions. Cancer Discovery 2022;12:31–46. https://doi.org/10.1158/2159-8290.CD-21-1059.
[221] Feitelson MA, Arzumanyan A, Kulathinal RJ, Blain SW, Holcombe RF, Mahajna J, et al. Sustained proliferation in cancer: Mechanisms and novel therapeutic targets. Seminars in Cancer Biology 2015;35:S25–54. https://doi.org/10.1016/j.semcancer.2015.02.006.
[222] Gutschner T, Diederichs S. The hallmarks of cancer: A long non-coding RNA point of view. RNA Biology 2012;9:703–19. https://doi.org/10.4161/rna.20481.
[223] Castillo JP, Frame FM, Rogoff HA, Pickering MT, Yurochko AD, Kowalik TF. Human Cytomegalovirus IE1-72 Activates Ataxia Telangiectasia Mutated Kinase and a p53/p21-Mediated Growth Arrest Response. J Virol 2005;79:11467–75. https://doi.org/10.1128/JVI.79.17.11467-11475.2005.
[224] Castillo JP, Yurochko AD, Kowalik TF. Role of Human Cytomegalovirus Immediate-Early Proteins in Cell Growth Control. J Virol 2000;74:8028–37. https://doi.org/10.1128/JVI.74.17.8028-8037.2000.
[225] Speir E, Modali R, Huang E-S, Leon MB, Shawl F, Finkel T, et al. Potential Role of Human Cytomegalovirus and p53 Interaction in Coronary Restenosis. Science 1994;265:391–4. https://doi.org/10.1126/science.8023160.
[226] Hwang E-S, Zhang Z, Cai H, Huang DY, Huong S-M, Cha C-Y, et al. Human Cytomegalovirus IE1-72 Protein Interacts with p53 and Inhibits p53-Dependent Transactivation by a Mechanism Different from That of IE2-86 Protein. J Virol 2009;83:12388–98. https://doi.org/10.1128/JVI.00304-09.
[227] Johnson RA, Huong S-M, Huang E-S. Activation of the Mitogen-Activated Protein Kinase p38 by Human Cytomegalovirus Infection through Two Distinct Pathways: a Novel Mechanism for Activation of p38. J Virol 2000;74:1158–67. https://doi.org/10.1128/JVI.74.3.1158-1167.2000.
[228] Boyle KA, Pietropaolo RL, Compton T. Engagement of the Cellular Receptor for Glycoprotein B of Human Cytomegalovirus Activates the Interferon-Responsive Pathway. Molecular and Cellular Biology 1999;19:3607–13. https://doi.org/10.1128/MCB.19.5.3607.
[229] Soroceanu L, Matlaf L, Bezrookove V, Harkins L, Martinez R, Greene M, et al. Human Cytomegalovirus US28 Found in Glioblastoma Promotes an Invasive and Angiogenic

Phenotype. Cancer Research 2011;71:6643–53. https://doi.org/10.1158/0008-5472.CAN-11-0744.
[230] Slinger E, Maussang D, Schreiber A, Siderius M, Rahbar A, Fraile-Ramos A, et al. HCMV-Encoded Chemokine Receptor US28 Mediates Proliferative Signaling Through the IL-6–STAT3 Axis. Sci Signal 2010;3. https://doi.org/10.1126/scisignal.2001180.
[231] Tsai H-L, Kou G-H, Chen S-C, Wu C-W, Lin Y-S. Human Cytomegalovirus Immediate-Early Protein IE2 Tethers a Transcriptional Repression Domain to p53. Journal of Biological Chemistry 1996;271:3534–40. https://doi.org/10.1074/jbc.271.7.3534.
[232] Hume AJ, Kalejta RF. Regulation of the retinoblastoma proteins by the human herpesviruses. Cell Div 2009;4:1. https://doi.org/10.1186/1747-1028-4-1.
[233] Song Y-J, Stinski MF. Effect of the human cytomegalovirus IE86 protein on expression of E2F-responsive genes: A DNA microarray analysis. Proc Natl Acad Sci USA 2002;99:2836–41. https://doi.org/10.1073/pnas.052010099.
[234] Kalejta RF, Shenk T. Proteasome-dependent, ubiquitin-independent degradation of the Rb family of tumor suppressors by the human cytomegalovirus pp71 protein. Proc Natl Acad Sci USA 2003;100:3263–8. https://doi.org/10.1073/pnas.0538058100.
[235] Moussawi FA, Kumar A, Pasquereau S, Tripathy MK, Karam W, Diab-Assaf M, et al. The transcriptome of human mammary epithelial cells infected with the HCMV-DB strain displays oncogenic traits. Sci Rep 2018;8:12574. https://doi.org/10.1038/s41598-018-30109-1.
[236] Dziurzynski K, Chang SM, Heimberger AB, Kalejta RF, McGregor Dallas SR, Smit M, et al. Consensus on the role of human cytomegalovirus in glioblastoma. Neuro-Oncology 2012;14:246–55. https://doi.org/10.1093/neuonc/nor227.
[237] Cinatl J, Scholz M, Kotchetkov R, Vogel J-U, Wilhelm Doerr H. Molecular mechanisms of the modulatory effects of HCMV infection in tumor cell biology. Trends in Molecular Medicine 2004;10:19–23. https://doi.org/10.1016/j.molmed.2003.11.002.
[238] Blaheta RA, Beecken W-D, Engl T, Jonas D, Oppermann E, Hundemer M, et al. Human Cytomegalovirus Infection of Tumor Cells Downregulates NCAM (CD56): A Novel Mechanism for Virus-Induced Tumor Invasiveness'. Neoplasia 2004;6:323–31. https://doi.org/10.1593/neo.03418.
[239] Cobbs CS, Soroceanu L, Denham S, Zhang W, Britt WJ, Pieper R, et al. Human cytomegalovirus induces cellular tyrosine kinase signaling and promotes glioma cell invasiveness. J Neurooncol 2007;85:271–80. https://doi.org/10.1007/s11060-007-9423-2.
[240] Hoever G, Vogel J-U, Lukashenko P, Hofmann W-K, Komor M, Doerr HW, et al. Impact of persistent cytomegalovirus infection on human neuroblastoma cell gene expression. Biochemical and Biophysical Research Communications 2005;326:395–401. https://doi.org/10.1016/j.bbrc.2004.11.042.
[241] Herbein G. Tumors and Cytomegalovirus: An Intimate Interplay. Viruses 2022;14:812. https://doi.org/10.3390/v14040812.
[242] Straat K, Liu C, Rahbar A, Zhu Q, Liu L, Wolmer-Solberg N, et al. Activation of Telomerase by Human Cytomegalovirus. JNCI Journal of the National Cancer Institute 2009;101:488–97. https://doi.org/10.1093/jnci/djp031.
[243] Caposio P, Orloff SL, Streblow DN. The role of cytomegalovirus in angiogenesis. Virus Research 2011;157:204–11. https://doi.org/10.1016/j.virusres.2010.09.011.

[244] Dumortier J, Streblow DN, Moses AV, Jacobs JM, Kreklywich CN, Camp D, et al. Human Cytomegalovirus Secretome Contains Factors That Induce Angiogenesis and Wound Healing. J Virol 2008;82:6524–35. https://doi.org/10.1128/JVI.00502-08.
[245] Maussang D, Langemeijer E, Fitzsimons CP, Stigter-van Walsum M, Dijkman R, Borg MK, et al. The Human Cytomegalovirus–Encoded Chemokine Receptor US28 Promotes Angiogenesis and Tumor Formation via Cyclooxygenase-2. Cancer Research 2009;69:2861–9. https://doi.org/10.1158/0008-5472.CAN-08-2487.
[246] Bentz GL, Yurochko AD. Human CMV infection of endothelial cells induces an angiogenic response through viral binding to EGF receptor and β_1 and β_3 integrins. Proc Natl Acad Sci USA 2008;105:5531–6. https://doi.org/10.1073/pnas.0800037105.
[247] Fiorentini S, Luganini A, Dell'Oste V, Lorusso B, Cervi E, Caccuri F, et al. Human cytomegalovirus productively infects lymphatic endothelial cells and induces a secretome that promotes angiogenesis and lymphangiogenesis through interleukin-6 and granulocyte-macrophage colony-stimulating factor. Journal of General Virology 2011;92:650–60. https://doi.org/10.1099/vir.0.025395-0.
[248] Botto S, Streblow DN, DeFilippis V, White L, Kreklywich CN, Smith PP, et al. IL-6 in human cytomegalovirus secretome promotes angiogenesis and survival of endothelial cells through the stimulation of survivin. Blood 2011;117:352–61. https://doi.org/10.1182/blood-2010-06-291245.
[249] Wilkerson I, Laban J, Mitchell JM, Sheibani N, Alcendor DJ. Retinal pericytes and cytomegalovirus infectivity: implications for HCMV-induced retinopathy and congenital ocular disease. J Neuroinflammation 2015;12:2. https://doi.org/10.1186/s12974-014-0219-y.
[250] Brune W. Inhibition of programmed cell death by cytomegaloviruses. Virus Research 2011;157:144–50. https://doi.org/10.1016/j.virusres.2010.10.012.
[251] Terhune S, Torigoi E, Moorman N, Silva M, Qian Z, Shenk T, et al. Human Cytomegalovirus UL38 Protein Blocks Apoptosis. J Virol 2007;81:3109–23. https://doi.org/10.1128/JVI.02124-06.
[252] Luganini A, Di Nardo G, Munaron L, Gilardi G, Fiorio Pla A, Gribaudo G. Human cytomegalovirus US21 protein is a viroporin that modulates calcium homeostasis and protects cells against apoptosis. Proc Natl Acad Sci USA 2018;115. https://doi.org/10.1073/pnas.1813183115.
[253] Arnoult D, Bartle LM, Skaletskaya A, Poncet D, Zamzami N, Park PU, et al. Cytomegalovirus cell death suppressor vMIA blocks Bax- but not Bak-mediated apoptosis by binding and sequestering Bax at mitochondria. Proc Natl Acad Sci USA 2004;101:7988–93. https://doi.org/10.1073/pnas.0401897101.
[254] Chaudhry MZ, Kasmapour B, Plaza-Sirvent C, Bajagic M, Casalegno Garduño R, Borkner L, et al. UL36 Rescues Apoptosis Inhibition and In vivo Replication of a Chimeric MCMV Lacking the M36 Gene. Front Cell Infect Microbiol 2017;7:312. https://doi.org/10.3389/fcimb.2017.00312.
[255] Seirafian S, Prod'homme V, Sugrue D, Davies J, Fielding C, Tomasec P, et al. Human cytomegalovirus suppresses Fas expression and function. Journal of General Virology 2014;95:933–9. https://doi.org/10.1099/vir.0.058313-0.

[256] Reeves MB, Davies AA, McSharry BP, Wilkinson GW, Sinclair JH. Complex I Binding by a Virally Encoded RNA Regulates Mitochondria-Induced Cell Death. Science 2007;316:1345–8. https://doi.org/10.1126/science.1142984.
[257] Collins-McMillen D, Kim JH, Nogalski MT, Stevenson EV, Chan GC, Caskey JR, et al. Human Cytomegalovirus Promotes Survival of Infected Monocytes via a Distinct Temporal Regulation of Cellular Bcl-2 Family Proteins. J Virol 2016;90:2356–71. https://doi.org/10.1128/JVI.01994-15.
[258] Tanaka K, Zou J-P, Takeda K, Ferrans VJ, Sandford GR, Johnson TM, et al. Effects of Human Cytomegalovirus Immediate-Early Proteins on p53-mediated Apoptosis in Coronary Artery Smooth Muscle Cells. Circulation 1999;99:1656–9. https://doi.org/10.1161/01.CIR.99.13.1656.
[259] Das CK, Banerjee I, Mandal M. Pro-survival autophagy: An emerging candidate of tumor progression through maintaining hallmarks of cancer. Seminars in Cancer Biology 2020;66:59–74. https://doi.org/10.1016/j.semcancer.2019.08.020.
[260] Chen T, Tu S, Ding L, Jin M, Chen H, Zhou H. The role of autophagy in viral infections. J Biomed Sci 2023;30:5. https://doi.org/10.1186/s12929-023-00899-2.
[261] Mouna L, Hernandez E, Bonte D, Brost R, Amazit L, Delgui LR, et al. Analysis of the role of autophagy inhibition by two complementary human cytomegalovirus BECN1/Beclin 1-binding proteins. Autophagy 2016;12:327–42. https://doi.org/10.1080/15548627.2015.1125071.
[262] Yun C, Lee S. The Roles of Autophagy in Cancer. IJMS 2018;19:3466. https://doi.org/10.3390/ijms19113466.
[263] Li X, He S, Ma B. Autophagy and autophagy-related proteins in cancer. Mol Cancer 2020;19:12. https://doi.org/10.1186/s12943-020-1138-4.
[264] Li Z, Liu H, Luo X. Lipid droplet and its implication in cancer progression. Am J Cancer Res 2020;10:4112–22.
[265] Yu Y, Maguire TG, Alwine JC. Human Cytomegalovirus Activates Glucose Transporter 4 Expression To Increase Glucose Uptake during Infection. J Virol 2011;85:1573–80. https://doi.org/10.1128/JVI.01967-10.
[266] Rodríguez-Sánchez I, Schafer XL, Monaghan M, Munger J. The Human Cytomegalovirus UL38 protein drives mTOR-independent metabolic flux reprogramming by inhibiting TSC2. PLoS Pathog 2019;15:e1007569. https://doi.org/10.1371/journal.ppat.1007569.
[267] Betsinger CN, Jankowski CSR, Hofstadter WA, Federspiel JD, Otter CJ, Jean Beltran PM, et al. The human cytomegalovirus protein pUL13 targets mitochondrial cristae architecture to increase cellular respiration during infection. Proc Natl Acad Sci USA 2021;118:e2101675118. https://doi.org/10.1073/pnas.2101675118.
[268] Siew V-K, Duh C-Y, Wang S-K. Human cytomegalovirus UL76 induces chromosome aberrations. J Biomed Sci 2009;16:107. https://doi.org/10.1186/1423-0127-16-107.
[269] Gaspar M, Shenk T. Human cytomegalovirus inhibits a DNA damage response by mislocalizing checkpoint proteins. Proc Natl Acad Sci USA 2006;103:2821–6. https://doi.org/10.1073/pnas.0511148103.
[270] Luo MH, Rosenke K, Czornak K, Fortunato EA. Human Cytomegalovirus Disrupts both Ataxia Telangiectasia Mutated Protein (ATM)- and ATM-Rad3-Related Kinase-Mediated

DNA Damage Responses during Lytic Infection. J Virol 2007;81:1934–50. https://doi.org/10.1128/JVI.01670-06.
[271] E X, Pickering MT, Debatis M, Castillo J, Lagadinos A, Wang S, et al. An E2F1-Mediated DNA Damage Response Contributes to the Replication of Human Cytomegalovirus. PLoS Pathog 2011;7:e1001342. https://doi.org/10.1371/journal.ppat.1001342.
[272] Maussang D, Verzijl D, Van Walsum M, Leurs R, Holl J, Pleskoff O, et al. Human cytomegalovirus-encoded chemokine receptor US28 promotes tumorigenesis. Proc Natl Acad Sci USA 2006;103:13068–73. https://doi.org/10.1073/pnas.0604433103.
[273] Casarosa P, Bakker RA, Verzijl D, Navis M, Timmerman H, Leurs R, et al. Constitutive Signaling of the Human Cytomegalovirus-encoded Chemokine Receptor US28. Journal of Biological Chemistry 2001;276:1133–7. https://doi.org/10.1074/jbc.M008965200.
[274] Craigen JL, Yong KL, Jordan NJ, Maccormac LP, Westwick J, Akbar AN, et al. Human cytomegalovirus infection up-regulates interleukin-8 gene expression and stimulates neutrophil transendothelial migration. Immunology 1997;92:138–45. https://doi.org/10.1046/j.1365-2567.1997.00310.x.
[275] Visseren FLJ, Verkerk MSA, Bouter KP, Diepersloot RJA, Erkelens DW. Interleukin-6 production by endothelial cells after infection with influenza virus and cytomegalovirus. Journal of Laboratory and Clinical Medicine 1999;134:623–30. https://doi.org/10.1016/S0022-2143(99)90103-8.
[276] Moss P. Intercellular adhesion molecule-1 expression in endothelial cells is activated by cytomegalovirus immediate early proteins. Transplantation 1999;67:2–3. https://doi.org/10.1097/00007890-199901150-00002.
[277] Speir E, Shibutani T, Yu Z-X, Ferrans V, Epstein SE. Role of Reactive Oxygen Intermediates in Cytomegalovirus Gene Expression and in the Response of Human Smooth Muscle Cells to Viral Infection. Circulation Research 1996;79:1143–52. https://doi.org/10.1161/01.RES.79.6.1143.
[278] Mao G, Li H, Ding X, Meng X, Wang G, Leng SX. Suppressive effects of sirtinol on human cytomegalovirus (hCMV) infection and hCMV-induced activation of molecular mechanisms of senescence and production of reactive oxygen species. Mechanisms of Ageing and Development 2016;158:62–9. https://doi.org/10.1016/j.mad.2015.12.005.
[279] Tiwari A, Trivedi R, Lin S-Y. Tumor microenvironment: barrier or opportunity towards effective cancer therapy. J Biomed Sci 2022;29:83. https://doi.org/10.1186/s12929-022-00866-3.
[280] Chan G, Bivins-Smith ER, Smith MS, Yurochko AD. NF-κB and phosphatidylinositol 3-kinase activity mediates the HCMV-induced atypical M1/M2 polarization of monocytes. Virus Research 2009;144:329–33. https://doi.org/10.1016/j.virusres.2009.04.026.
[281] Tang X. Tumor-associated macrophages as potential diagnostic and prognostic biomarkers in breast cancer. Cancer Letters 2013;332:3–10. https://doi.org/10.1016/j.canlet.2013.01.024.
[282] Khan KA, Coaquette A, Davrinche C, Herbein G. Bcl-3-Regulated Transcription from Major Immediate-Early Promoter of Human Cytomegalovirus in Monocyte-Derived Macrophages. The Journal of Immunology 2009;182:7784–94. https://doi.org/10.4049/jimmunol.0803800.

[283] Pasquereau S, Al Moussawi F, Karam W, Diab Assaf M, Kumar A, Herbein G. Cytomegalovirus, Macrophages and Breast Cancer. TOVJ 2017;11:15–27. https://doi.org/10.2174/1874357901711010015.
[284] Sung H, Ferlay J, Siegel RL, Laversanne M, Soerjomataram I, Jemal A, et al. Global Cancer Statistics 2020: GLOBOCAN Estimates of Incidence and Mortality Worldwide for 36 Cancers in 185 Countries. CA A Cancer J Clinicians 2021;71:209–49. https://doi.org/10.3322/caac.21660.
[285] Zur Hausen H. Cancers in Humans: A Lifelong Search for Contributions of Infectious Agents, Autobiographic Notes. Annu Rev Virol 2019;6:1–28. https://doi.org/10.1146/annurev-virology-092818-015907.
[286] Guarneri V, Dieci MV, Conte P. Relapsed Triple-Negative Breast Cancer: Challenges and Treatment Strategies. Drugs 2013;73:1257–65. https://doi.org/10.1007/s40265-013-0091-6.
[287] Yin L, Duan J-J, Bian X-W, Yu S. Triple-negative breast cancer molecular subtyping and treatment progress. Breast Cancer Res 2020;22:61. https://doi.org/10.1186/s13058-020-01296-5.
[288] Yao H, He G, Yan S, Chen C, Song L, Rosol TJ, et al. Triple-negative breast cancer: is there a treatment on the horizon? Oncotarget 2017;8:1913–24. https://doi.org/10.18632/oncotarget.12284.
[289] Twite N, Andrei G, Kummert C, Donner C, Perez-Morga D, De Vos R, et al. Sequestration of human cytomegalovirus by human renal and mammary epithelial cells. Virology 2014;460–461:55–65. https://doi.org/10.1016/j.virol.2014.04.032.
[290] Herbein G, Kumar A. The Oncogenic Potential of Human Cytomegalovirus and Breast Cancer. Front Oncol 2014;4. https://doi.org/10.3389/fonc.2014.00230.
[291] Rahbar A, Touma J, Costa H, Davoudi B, Bukholm IR, Sauer T, et al. Low Expression of Estrogen Receptor-α and Progesterone Receptor in Human Breast Cancer Tissues Is Associated With High-Grade Human Cytomegalovirus Protein Expression. Clinical Breast Cancer 2017;17:526-535.e1. https://doi.org/10.1016/j.clbc.2017.04.013.
[292] Cox B, Richardson A, Graham P, Gislefoss RE, Jellum E, Rollag H. Breast cancer, cytomegalovirus and Epstein–Barr virus: a nested case–control study. Br J Cancer 2010;102:1665–9. https://doi.org/10.1038/sj.bjc.6605675.
[293] Lee JH, Lee JE, Kahng JY, Kim SH, Park JS, Yoon SJ, et al. Human glioblastoma arises from subventricular zone cells with low-level driver mutations. Nature 2018;560:243–7. https://doi.org/10.1038/s41586-018-0389-3.
[294] Louis DN, Perry A, Wesseling P, Brat DJ, Cree IA, Figarella-Branger D, et al. The 2021 WHO Classification of Tumors of the Central Nervous System: a summary. Neuro-Oncology 2021;23:1231–51. https://doi.org/10.1093/neuonc/noab106.
[295] Belzile J-P, Stark TJ, Yeo GW, Spector DH. Human Cytomegalovirus Infection of Human Embryonic Stem Cell-Derived Primitive Neural Stem Cells Is Restricted at Several Steps but Leads to the Persistence of Viral DNA. J Virol 2014;88:4021–39. https://doi.org/10.1128/JVI.03492-13.
[296] Odeberg J, Wolmer N, Falci S, Westgren M, Seiger Å, Söderberg-Nauclér C. Human Cytomegalovirus Inhibits Neuronal Differentiation and Induces Apoptosis in Human Neural Precursor Cells. J Virol 2006;80:8929–39. https://doi.org/10.1128/JVI.00676-06.

[297] Kossmann T, Morganti-Kossmann MC, Orenstein JM, Britt WJ, Wahl SM, Smith PD. Cytomegalovirus Production by Infected Astrocytes Correlates with Transforming Growth Factor-β Release. J INFECT DIS 2003;187:534–41. https://doi.org/10.1086/373995.
[298] Luo MH, Hannemann H, Kulkarni AS, Schwartz PH, O'Dowd JM, Fortunato EA. Human Cytomegalovirus Infection Causes Premature and Abnormal Differentiation of Human Neural Progenitor Cells. J Virol 2010;84:3528–41. https://doi.org/10.1128/JVI.02161-09.
[299] Mitchell DA, Xie W, Schmittling R, Learn C, Friedman A, McLendon RE, et al. Sensitive detection of human cytomegalovirus in tumors and peripheral blood of patients diagnosed with glioblastoma. Neuro-Oncology 2008;10:10–8. https://doi.org/10.1215/15228517-2007-035.
[300] Dos Santos CJ, Ferreira Castro FL, De Aguiar RB, Menezes IG, Santos AC, Paulus C, et al. Impact of human cytomegalovirus on glioblastoma cell viability and chemotherapy treatment. Journal of General Virology 2018;99:1274–85. https://doi.org/10.1099/jgv.0.001118.
[301] Foster H, Piper K, DePledge L, Li H-F, Scanlan J, Jae-Guen Y, et al. Human cytomegalovirus seropositivity is associated with decreased survival in glioblastoma patients. Neuro-Oncology Advances 2019;1:vdz020. https://doi.org/10.1093/noajnl/vdz020.
[302] Adhikari AS, Macauley J, Johnson Y, Connolly M, Coleman T, Heiland T. Development and Characterization of an HCMV Multi-Antigen Therapeutic Vaccine for Glioblastoma Using the UNITE Platform. Front Oncol 2022;12:850546. https://doi.org/10.3389/fonc.2022.850546.
[303] ModernaTX, Inc. A Study to Evaluate the Efficacy, Safety, and Immunogenicity of mRNA-1647 Cytomegalovirus (CMV) Vaccine in Healthy Participants 16 to 40 Years of Age. NCT05085366 2023. https://clinicaltrials.gov/study/NCT05085366.
[304] Cox M, Kartikasari AER, Gorry PR, Flanagan KL, Plebanski M. Potential Impact of Human Cytomegalovirus Infection on Immunity to Ovarian Tumours and Cancer Progression. Biomedicines 2021;9:351. https://doi.org/10.3390/biomedicines9040351.
[305] Delga B, Classe J-M, Houvenaeghel G, Blache G, Sabiani L, El Hajj H, et al. 30 Years of Experience in the Management of Stage III and IV Epithelial Ovarian Cancer: Impact of Surgical Strategies on Survival. Cancers 2020;12:768. https://doi.org/10.3390/cancers12030768.
[306] Steinberga I, Jansson K, Sorbe B. Quality Indicators and Survival Outcome in Stage IIIB-IVB Epithelial Ovarian Cancer Treated at a Single Institution. In Vivo 2019;33:1521–30. https://doi.org/10.21873/invivo.11632.
[307] Paradowska E, Jabłońska A, Studzińska M, Wilczyński M, Wilczyński JR. Detection and genotyping of CMV and HPV in tumors and fallopian tubes from epithelial ovarian cancer patients. Sci Rep 2019;9:19935. https://doi.org/10.1038/s41598-019-56448-1.
[308] Yin M, Chen A, Zhao F, Ji X, Li C, Wang G. Detection of human cytomegalovirus in patients with epithelial ovarian cancer and its impacts on survival. Infect Agents Cancer 2020;15:23. https://doi.org/10.1186/s13027-020-00289-5.
[309] Rådestad AF, Estekizadeh A, Cui HL, Kostopoulou ON, Davoudi B, Hirschberg AL, et al. Impact of Human Cytomegalovirus Infection and its Immune Response on Survival of Patients with Ovarian Cancer. Translational Oncology 2018;11:1292–300. https://doi.org/10.1016/j.tranon.2018.08.003.

[310] Wang L, Chen C, Song Z, Wang H, Ye M, Wang D, et al. EZH2 depletion potentiates MYC degradation inhibiting neuroblastoma and small cell carcinoma tumor formation. Nat Commun 2022;13:12. https://doi.org/10.1038/s41467-021-27609-6.
[311] Cao R, Wang L, Wang H, Xia L, Erdjument-Bromage H, Tempst P, et al. Role of Histone H3 Lysine 27 Methylation in Polycomb-Group Silencing. Science 2002;298:1039–43. https://doi.org/10.1126/science.1076997.
[312] Veneti Z, Gkouskou K, Eliopoulos A. Polycomb Repressor Complex 2 in Genomic Instability and Cancer. IJMS 2017;18:1657. https://doi.org/10.3390/ijms18081657.
[313] Kim KH, Roberts CWM. Targeting EZH2 in cancer. Nat Med 2016;22:128–34. https://doi.org/10.1038/nm.4036.
[314] Gonzalez ME, Moore HM, Li X, Toy KA, Huang W, Sabel MS, et al. EZH2 expands breast stem cells through activation of NOTCH1 signaling. Proc Natl Acad Sci USA 2014;111:3098–103. https://doi.org/10.1073/pnas.1308953111.
[315] Chang C-J, Yang J-Y, Xia W, Chen C-T, Xie X, Chao C-H, et al. EZH2 Promotes Expansion of Breast Tumor Initiating Cells through Activation of RAF1-β-Catenin Signaling. Cancer Cell 2011;19:86–100. https://doi.org/10.1016/j.ccr.2010.10.035.
[316] Wu J, Crowe DL. The histone methyltransferase EZH2 promotes mammary stem and luminal progenitor cell expansion, metastasis and inhibits estrogen receptor-positive cellular differentiation in a model of basal breast cancer. Oncology Reports 2015;34:455–60. https://doi.org/10.3892/or.2015.4003.
[317] Guan X, Deng H, Choi UL, Li Z, Yang Y, Zeng J, et al. EZH2 overexpression dampens tumor-suppressive signals via an EGR1 silencer to drive breast tumorigenesis. Oncogene 2020;39:7127–41. https://doi.org/10.1038/s41388-020-01484-9.
[318] Chu W, Zhang X, Qi L, Fu Y, Wang P, Zhao W, et al. The EZH2–PHACTR2–AS1–Ribosome Axis induces Genomic Instability and Promotes Growth and Metastasis in Breast Cancer. Cancer Research 2020;80:2737–50. https://doi.org/10.1158/0008-5472.CAN-19-3326.
[319] Ahani N, Shirkoohi R, Rokouei M, Alipour Eskandani M, Nikravesh A. Overexpression of enhancer of zeste human homolog 2 (EZH2) gene in human cytomegalovirus positive glioblastoma multiforme tissues. Med Oncol 2014;31:252. https://doi.org/10.1007/s12032-014-0252-9.
[320] Rossetto CC, Tarrant-Elorza M, Pari GS. Cis and Trans Acting Factors Involved in Human Cytomegalovirus Experimental and Natural Latent Infection of CD14 (+) Monocytes and CD34 (+) Cells. PLoS Pathog 2013;9:e1003366. https://doi.org/10.1371/journal.ppat.1003366.
[321] Leitner K, Tsibulak I, Wieser V, Knoll K, Reimer D, Marth C, et al. Clinical impact of EZH2 and its antagonist SMARCA4 in ovarian cancer. Sci Rep 2020;10:20412. https://doi.org/10.1038/s41598-020-77532-x.
[322] Jones BA, Varambally S, Arend RC. Histone Methyltransferase EZH2: A Therapeutic Target for Ovarian Cancer. Molecular Cancer Therapeutics 2018;17:591–602. https://doi.org/10.1158/1535-7163.MCT-17-0437.
[323] Chen J, Hong JH, Huang Y, Liu S, Yin J, Deng P, et al. EZH2 mediated metabolic rewiring promotes tumor growth independently of histone methyltransferase activity in ovarian cancer. Mol Cancer 2023;22:85. https://doi.org/10.1186/s12943-023-01786-y.

[324] Zhang L, Ding P, Lv H, Zhang D, Liu G, Yang Z, et al. Number of Polyploid Giant Cancer Cells and Expression of EZH2 Are Associated with VM Formation and Tumor Grade in Human Ovarian Tumor. BioMed Research International 2014;2014:1–9. https://doi.org/10.1155/2014/903542.
[325] Coughlan AY, Testa G. Exploiting epigenetic dependencies in ovarian cancer therapy. Intl Journal of Cancer 2021;149:1732–43. https://doi.org/10.1002/ijc.33727.
[326] Reid BM, Vyas S, Chen Z, Chen A, Kanetsky PA, Permuth JB, et al. Morphologic and molecular correlates of EZH2 as a predictor of platinum resistance in high-grade ovarian serous carcinoma. BMC Cancer 2021;21:714. https://doi.org/10.1186/s12885-021-08413-3.
[327] Sander S, Bullinger L, Klapproth K, Fiedler K, Kestler HA, Barth TFE, et al. MYC stimulates EZH2 expression by repression of its negative regulator miR-26a. Blood 2008;112:4202–12. https://doi.org/10.1182/blood-2008-03-147645.
[328] Nie Z, Guo C, Das SK, Chow CC, Batchelor E, Simons SS, et al. Dissecting transcriptional amplification by MYC. eLife 2020;9:e52483. https://doi.org/10.7554/eLife.52483.
[329] Sun J, Cai X, Yung MM, Zhou W, Li J, Zhang Y, et al. miR-137 mediates the functional link between c-Myc and EZH2 that regulates cisplatin resistance in ovarian cancer. Oncogene 2019;38:564–80. https://doi.org/10.1038/s41388-018-0459-x.
[330] Wu X, Liu D, Tao D, Xiang W, Xiao X, Wang M, et al. BRD4 Regulates EZH2 Transcription through Upregulation of C-MYC and Represents a Novel Therapeutic Target in Bladder Cancer. Molecular Cancer Therapeutics 2016;15:1029–42. https://doi.org/10.1158/1535-7163.MCT-15-0750.
[331] Fallah Y, Brundage J, Allegakoen P, Shajahan-Haq AN. MYC-Driven Pathways in Breast Cancer Subtypes. Biomolecules 2017;7:53. https://doi.org/10.3390/biom7030053.
[332] Li Q, Dang CV. c-Myc Overexpression Uncouples DNA Replication from Mitosis. Molecular and Cellular Biology 1999;19:5339–51. https://doi.org/10.1128/MCB.19.8.5339.
[333] Anatskaya OV, Vinogradov AE. Polyploidy and Myc Proto-Oncogenes Promote Stress Adaptation via Epigenetic Plasticity and Gene Regulatory Network Rewiring. IJMS 2022;23:9691. https://doi.org/10.3390/ijms23179691.
[334] Annibali D, Whitfield JR, Favuzzi E, Jauset T, Serrano E, Cuartas I, et al. Myc inhibition is effective against glioma and reveals a role for Myc in proficient mitosis. Nat Commun 2014;5:4632. https://doi.org/10.1038/ncomms5632.
[335] Yu T, Wang Y, Hu Q, Wu W, Wu Y, Wei W, et al. The EZH2 inhibitor GSK343 suppresses cancer stem-like phenotypes and reverses mesenchymal transition in glioma cells. Oncotarget 2017;8:98348–59. https://doi.org/10.18632/oncotarget.21311.
[336] Suvà M-L, Riggi N, Janiszewska M, Radovanovic I, Provero P, Stehle J-C, et al. EZH2 Is Essential for Glioblastoma Cancer Stem Cell Maintenance. Cancer Research 2009;69:9211–8. https://doi.org/10.1158/0008-5472.CAN-09-1622.
[337] Reyes-González JM, Vivas-Mejía PE. c-MYC and Epithelial Ovarian Cancer. Front Oncol 2021;11:601512. https://doi.org/10.3389/fonc.2021.601512.
[338] Bast RC, Hennessy B, Mills GB. The biology of ovarian cancer: new opportunities for translation. Nat Rev Cancer 2009;9:415–28. https://doi.org/10.1038/nrc2644.
[339] LaTourrette K, Garcia-Ruiz H. Determinants of Virus Variation, Evolution, and Host Adaptation. Pathogens 2022;11:1039. https://doi.org/10.3390/pathogens11091039.

[340] Dayaram T, Marriott SJ. Effect of Transforming Viruses on Molecular Mechanisms Associated With Cancer. Journal Cellular Physiology 2008;216:309–14. https://doi.org/10.1002/jcp.21439.
[341] Bayliss RJ, Piguet V. Masters of manipulation: Viral modulation of the immunological synapse. Cellular Microbiology 2018;20. https://doi.org/10.1111/cmi.12944.
[342] Reddout N, Christensen T, Bunnell A, Jensen D, Johnson D, O'Malley S, et al. High risk HPV types 18 and 16 are potent modulators of oral squamous cell carcinoma phenotypes in vitro. Infect Agents Cancer 2007;2:21. https://doi.org/10.1186/1750-9378-2-21.
[343] Pešut E, Đukić A, Lulić L, Skelin J, Šimić I, Milutin Gašperov N, et al. Human Papillomaviruses-Associated Cancers: An Update of Current Knowledge. Viruses 2021;13:2234. https://doi.org/10.3390/v13112234.
[344] Yousefi Z, Aria H, Ghaedrahmati F, Bakhtiari T, Azizi M, Bastan R, et al. An Update on Human Papilloma Virus Vaccines: History, Types, Protection, and Efficacy. Front Immunol 2022;12:805695. https://doi.org/10.3389/fimmu.2021.805695.
[345] Egawa N, Doorbar J. The low-risk papillomaviruses. Virus Research 2017;231:119–27. https://doi.org/10.1016/j.virusres.2016.12.017.
[346] Münger K, Baldwin A, Edwards KM, Hayakawa H, Nguyen CL, Owens M, et al. Mechanisms of Human Papillomavirus-Induced Oncogenesis. J Virol 2004;78:11451–60. https://doi.org/10.1128/JVI.78.21.11451-11460.2004.
[347] Münger K, Basile JR, Duensing S, Eichten A, Gonzalez SL, Grace M, et al. Biological activities and molecular targets of the human papillomavirus E7 oncoprotein. Oncogene 2001;20:7888–98. https://doi.org/10.1038/sj.onc.1204860.
[348] Bhutani M, Polizzotto MN, Uldrick TS, Yarchoan R. Kaposi Sarcoma–Associated Herpesvirus-Associated Malignancies: Epidemiology, Pathogenesis, and Advances in Treatment. Seminars in Oncology 2015;42:223–46. https://doi.org/10.1053/j.seminoncol.2014.12.027.
[349] Pérez CL, Tous MI. Diversity of human herpesvirus 8 genotypes in patients with AIDS and non-AIDS associated Kaposi's sarcoma, Castleman's disease and primary effusion lymphoma in Argentina. J Med Virol 2017;89:2020–8. https://doi.org/10.1002/jmv.24876.
[350] Moorad R, Juarez A, Landis JT, Pluta LJ, Perkins M, Cheves A, et al. Whole-genome sequencing of Kaposi sarcoma-associated herpesvirus (KSHV/HHV8) reveals evidence for two African lineages. Virology 2022;568:101–14. https://doi.org/10.1016/j.virol.2022.01.005.
[351] Wang L, Dittmer DP, Tomlinson CC, Fakhari FD, Damania B. Immortalization of Primary Endothelial Cells by the K1 Protein of Kaposi's Sarcoma–Associated Herpesvirus. Cancer Research 2006;66:3658–66. https://doi.org/10.1158/0008-5472.CAN-05-3680.
[352] Lee H, Guo J, Li M, Choi J-K, DeMaria M, Rosenzweig M, et al. Identification of an Immunoreceptor Tyrosine-Based Activation Motif of K1 Transforming Protein of Kaposi's Sarcoma-Associated Herpesvirus. Molecular and Cellular Biology 1998;18:5219–28. https://doi.org/10.1128/MCB.18.9.5219.
[353] Cavallin LE, Goldschmidt-Clermont P, Mesri EA. Molecular and Cellular Mechanisms of KSHV Oncogenesis of Kaposi's Sarcoma Associated with HIV/AIDS. PLoS Pathog 2014;10:e1004154. https://doi.org/10.1371/journal.ppat.1004154.

[354] Chakravorty S, Afzali B, Kazemian M. EBV-associated diseases: Current therapeutics and emerging technologies. Front Immunol 2022;13:1059133. https://doi.org/10.3389/fimmu.2022.1059133.
[355] Tsai M-H, Raykova A, Klinke O, Bernhardt K, Gärtner K, Leung CS, et al. Spontaneous Lytic Replication and Epitheliotropism Define an Epstein-Barr Virus Strain Found in Carcinomas. Cell Reports 2013;5:458–70. https://doi.org/10.1016/j.celrep.2013.09.012.
[356] Haidar Ahmad S, Pasquereau S, El Baba R, Nehme Z, Lewandowski C, Herbein G. Distinct Oncogenic Transcriptomes in Human Mammary Epithelial Cells Infected With Cytomegalovirus. Front Immunol 2021;12:772160. https://doi.org/10.3389/fimmu.2021.772160.
[357] Bracken AP. EZH2 is downstream of the pRB-E2F pathway, essential for proliferation and amplified in cancer. The EMBO Journal 2003;22:5323–35. https://doi.org/10.1093/emboj/cdg542.
[358] Li J, Dong T, Wu Z, Zhu D, Gu H. The effects of MYC on tumor immunity and immunotherapy. Cell Death Discov 2023;9:103. https://doi.org/10.1038/s41420-023-01403-3.
[359] Chan TSY, Picard D, Hawkins CE, Lu M, Pfister S, Korshunov A, et al. Thrombospondin-1 mimetics are promising novel therapeutics for MYC-associated medulloblastoma. Neuro-Oncology Advances 2021;3:vdab002. https://doi.org/10.1093/noajnl/vdab002.
[360] Zhou L, Picard D, Ra Y-S, Li M, Northcott PA, Hu Y, et al. Silencing of Thrombospondin-1 Is Critical for Myc-Induced Metastatic Phenotypes in Medulloblastoma. Cancer Research 2010;70:8199–210. https://doi.org/10.1158/0008-5472.CAN-09-4562.
[361] Casey SC, Tong L, Li Y, Do R, Walz S, Fitzgerald KN, et al. MYC regulates the antitumor immune response through CD47 and PD-L1. Science 2016;352:227–31. https://doi.org/10.1126/science.aac9935.
[362] Hong X, Chedid K, Kalkanis SN. Glioblastoma cell line-derived spheres in serum-containing medium versus serum-free medium: A comparison of cancer stem cell properties. International Journal of Oncology 2012;41:1693–700. https://doi.org/10.3892/ijo.2012.1592.
[363] Guyon J, Andrique L, Pujol N, Røsland GV, Recher G, Bikfalvi A, et al. A 3D Spheroid Model for Glioblastoma. JoVE 2020:60998. https://doi.org/10.3791/60998.
[364] Daubon T, Guyon J, Raymond A-A, Dartigues B, Rudewicz J, Ezzoukhry Z, et al. The invasive proteome of glioblastoma revealed by laser-capture microdissection. Neuro-Oncology Advances 2019;1:vdz029. https://doi.org/10.1093/noajnl/vdz029.
[365] Bilandzic M, Stenvers KL. Assessment of Ovarian Cancer Spheroid Attachment and Invasion of Mesothelial Cells in Real Time. JoVE 2014:51655. https://doi.org/10.3791/51655.
[366] Schmittgen TD, Livak KJ. Analyzing real-time PCR data by the comparative CT method. Nat Protoc 2008;3:1101–8. https://doi.org/10.1038/nprot.2008.73.
[367] Liao T-T, Yang M-H. Hybrid Epithelial/Mesenchymal State in Cancer Metastasis: Clinical Significance and Regulatory Mechanisms. Cells 2020;9:623. https://doi.org/10.3390/cells9030623.
[368] Grosse-Wilde A, Fouquier d'Hérouël A, McIntosh E, Ertaylan G, Skupin A, Kuestner RE, et al. Stemness of the hybrid Epithelial/Mesenchymal State in Breast Cancer and Its

Association with Poor Survival. PLoS ONE 2015;10:e0126522. https://doi.org/10.1371/journal.pone.0126522.
[369] Engwer C, Knappitsch M, Surulescu C, 1. WWU Münster, Institute for Computational und Applied Mathematics and Cluster of Excellence EXC 1003, Cells in Motion, Orleans-Ring 10, 48149 Münster, 2. Technische Universität Kaiserslautern, Felix-Klein-Zentrum für Mathematik, Paul-Ehrlich-Str. 31, 67663 Kaiserslautern. A multiscale model for glioma spread including cell-tissue interactions and proliferation. Mathematical Biosciences and Engineering 2016;13:443–60. https://doi.org/10.3934/mbe.2015011.
[370] Fedele M, Cerchia L, Pegoraro S, Sgarra R, Manfioletti G. Proneural-Mesenchymal Transition: Phenotypic Plasticity to Acquire Multitherapy Resistance in Glioblastoma. IJMS 2019;20:2746. https://doi.org/10.3390/ijms20112746.
[371] Venkataramani V, Yang Y, Schubert MC, Reyhan E, Tetzlaff SK, Wißmann N, et al. Glioblastoma hijacks neuronal mechanisms for brain invasion. Cell 2022;185:2899-2917.e31. https://doi.org/10.1016/j.cell.2022.06.054.
[372] Xin X, Li Q, Fang J, Zhao T. LncRNA HOTAIR: A Potential Prognostic Factor and Therapeutic Target in Human Cancers. Front Oncol 2021;11:679244. https://doi.org/10.3389/fonc.2021.679244.
[373] Singh N, Miner A, Hennis L, Mittal S. Mechanisms of temozolomide resistance in glioblastoma - a comprehensive review. CDR 2020. https://doi.org/10.20517/cdr.2020.79.
[374] Virrey JJ, Golden EB, Sivakumar W, Wang W, Pen L, Schönthal AH, et al. Glioma-associated endothelial cells are chemoresistant to temozolomide. J Neurooncol 2009;95:13–22. https://doi.org/10.1007/s11060-009-9891-7.
[375] El Baba R, Pasquereau S, Haidar Ahmad S, Monnien F, Abad M, Bibeau F, et al. EZH2-Myc driven glioblastoma elicited by cytomegalovirus infection of human astrocytes. Oncogene 2023;42:2031–45. https://doi.org/10.1038/s41388-023-02709-3.
[376] Davoli T, de Lange T. Telomere-Driven Tetraploidization Occurs in Human Cells Undergoing Crisis and Promotes Transformation of Mouse Cells. Cancer Cell 2012;21:765–76. https://doi.org/10.1016/j.ccr.2012.03.044.
[377] Dudás J, Ladányi A, Ingruber J, Steinbichler TB, Riechelmann H. Epithelial to Mesenchymal Transition: A Mechanism that Fuels Cancer Radio/Chemoresistance. Cells 2020;9:428. https://doi.org/10.3390/cells9020428.
[378] Zhao Q, Zhang K, Li Z, Zhang H, Fu F, Fu J, et al. High Migration and Invasion Ability of PGCCs and Their Daughter Cells Associated With the Nuclear Localization of S100A10 Modified by SUMOylation. Front Cell Dev Biol 2021;9:696871. https://doi.org/10.3389/fcell.2021.696871.
[379] Davey MG, Hynes SO, Kerin MJ, Miller N, Lowery AJ. Ki-67 as a Prognostic Biomarker in Invasive Breast Cancer. Cancers 2021;13:4455. https://doi.org/10.3390/cancers13174455.
[380] Warburg O. On the Origin of Cancer Cells. Science 1956;123:309–14. https://doi.org/10.1126/science.123.3191.309.
[381] Hadjimichael C. Common stemness regulators of embryonic and cancer stem cells. WJG 2015;7:1150. https://doi.org/10.4252/wjsc.v7.i9.1150.
[382] Sridharan S, Howard CM, Tilley AMC, Subramaniyan B, Tiwari AK, Ruch RJ, et al. Novel and Alternative Targets Against Breast Cancer Stemness to Combat Chemoresistance. Front Oncol 2019;9:1003. https://doi.org/10.3389/fonc.2019.01003.

[383] Velasco-Velázquez MA, Popov VM, Lisanti MP, Pestell RG. The Role of Breast Cancer Stem Cells in Metastasis and Therapeutic Implications. The American Journal of Pathology 2011;179:2–11. https://doi.org/10.1016/j.ajpath.2011.03.005.
[384] Ye F, Zhong X, Qiu Y, Yang L, Wei B, Zhang Z, et al. CD49f Can Act as a Biomarker for Local or Distant Recurrence in Breast Cancer. J Breast Cancer 2017;20:142. https://doi.org/10.4048/jbc.2017.20.2.142.
[385] Song X, Liu Z, Yu Z. EGFR Promotes the Development of Triple Negative Breast Cancer Through JAK/STAT3 Signaling. CMAR 2020;Volume 12:703–17. https://doi.org/10.2147/CMAR.S225376.
[386] Nie L, Wei Y, Zhang F, Hsu Y-H, Chan L-C, Xia W, et al. CDK2-mediated site-specific phosphorylation of EZH2 drives and maintains triple-negative breast cancer. Nat Commun 2019;10:5114. https://doi.org/10.1038/s41467-019-13105-5.
[387] Velasco-Velázquez MA, Li Z, Casimiro M, Loro E, Homsi N, Pestell RG. Examining the role of cyclin D1 in breast cancer. Future Oncology 2011;7:753–65. https://doi.org/10.2217/fon.11.56.
[388] Fultang N, Chakraborty M, Peethambaran B. Regulation of cancer stem cells in triple negative breast cancer. CDR 2021. https://doi.org/10.20517/cdr.2020.106.
[389] Jary A, Veyri M, Gothland A, Leducq V, Calvez V, Marcelin A-G. Kaposi's Sarcoma-Associated Herpesvirus, the Etiological Agent of All Epidemiological Forms of Kaposi's Sarcoma. Cancers 2021;13:6208. https://doi.org/10.3390/cancers13246208.
[390] Münz C. Latency and lytic replication in Epstein–Barr virus-associated oncogenesis. Nat Rev Microbiol 2019;17:691–700. https://doi.org/10.1038/s41579-019-0249-7.
[391] Mehravaran H, makvandi manoochehr, Samarbaf Zade A, Neisi N, Kiani H, Radmehr H, et al. Association of Human Cytomegalovirus with Hodgkin's Disease and Non-Hodgkin's lymphomas. APJCP 2017;18. https://doi.org/10.22034/APJCP.2017.18.3.593.
[392] Collins-McMillen D, Kamil J, Moorman N, Goodrum F. Control of Immediate Early Gene Expression for Human Cytomegalovirus Reactivation. Front Cell Infect Microbiol 2020;10:476. https://doi.org/10.3389/fcimb.2020.00476.
[393] Soroceanu L, Matlaf L, Khan S, Akhavan A, Singer E, Bezrookove V, et al. Cytomegalovirus Immediate-Early Proteins Promote Stemness Properties in Glioblastoma. Cancer Research 2015;75:3065–76. https://doi.org/10.1158/0008-5472.CAN-14-3307.
[394] Feng W hai, Bruce I, Nancy R-T, Pierre B, Shannon CK. Chemotherapy Induces Lytic EBV Replication and Confers Ganciclovir Susceptibility to EBV-positive Epithelial Cell Tumors. Cancer Res 2002;62:1920–6.
[395] Yang J, Dai L-X, Chen M, Li B, Ding N, Li G, et al. Inhibition of antiviral drug cidofovir on proliferation of human papillomavirus-infected cervical cancer cells. Experimental and Therapeutic Medicine 2016;12:2965–73. https://doi.org/10.3892/etm.2016.3718.
[396] Coen N, Duraffour S, Snoeck R, Andrei G. KSHV Targeted Therapy: An Update on Inhibitors of Viral Lytic Replication. Viruses 2014;6:4731–59. https://doi.org/10.3390/v6114731.
[397] El Baba R, Pasquereau S, Haidar Ahmad S, Diab-Assaf M, Herbein G. Oncogenic and Stemness Signatures of the High-Risk HCMV Strains in Breast Cancer Progression. Cancers 2022;14:4271. https://doi.org/10.3390/cancers14174271.

[398] Liu J. The dualistic origin of human tumors. Seminars in Cancer Biology 2018;53:1–16. https://doi.org/10.1016/j.semcancer.2018.07.004.
[399] Furnari FB, Fenton T, Bachoo RM, Mukasa A, Stommel JM, Stegh A, et al. Malignant astrocytic glioma: genetics, biology, and paths to treatment. Genes Dev 2007;21:2683–710. https://doi.org/10.1101/gad.1596707.
[400] Stiles CD, Rowitch DH. Glioma Stem Cells: A Midterm Exam. Neuron 2008;58:832–46. https://doi.org/10.1016/j.neuron.2008.05.031.
[401] Beiriger J, Habib A, Jovanovich N, Kodavali CV, Edwards L, Amankulor N, et al. The Subventricular Zone in Glioblastoma: Genesis, Maintenance, and Modeling. Front Oncol 2022;12:790976. https://doi.org/10.3389/fonc.2022.790976.
[402] Sher F, Boddeke E, Copray S. Ezh2 Expression in Astrocytes Induces Their Dedifferentiation Toward Neural Stem Cells. Cellular Reprogramming 2011;13:1–6. https://doi.org/10.1089/cell.2010.0052.
[403] Sasmita AO, Wong YP, Ling APK. Biomarkers and therapeutic advances in glioblastoma multiforme. Asia-Pac J Clncl Oncology 2018;14:40–51. https://doi.org/10.1111/ajco.12756.
[404] Senhaji N, Squalli Houssaini A, Lamrabet S, Louati S, Bennis S. Molecular and Circulating Biomarkers in Patients with Glioblastoma. IJMS 2022;23:7474. https://doi.org/10.3390/ijms23137474.
[405] Guerra-Rebollo M, Garrido C, Sánchez-Cid L, Soler-Botija C, Meca-Cortés O, Rubio N, et al. Targeting of replicating CD133 and OCT4/SOX2 expressing glioma stem cells selects a cell population that reinitiates tumors upon release of therapeutic pressure. Sci Rep 2019;9:9549. https://doi.org/10.1038/s41598-019-46014-0.
[406] Ben-Porath I, Thomson MW, Carey VJ, Ge R, Bell GW, Regev A, et al. An embryonic stem cell–like gene expression signature in poorly differentiated aggressive human tumors. Nat Genet 2008;40:499–507. https://doi.org/10.1038/ng.127.
[407] Lou Y-W, Wang P-Y, Yeh S-C, Chuang P-K, Li S-T, Wu C-Y, et al. Stage-specific embryonic antigen-4 as a potential therapeutic target in glioblastoma multiforme and other cancers. Proc Natl Acad Sci USA 2014;111:2482–7. https://doi.org/10.1073/pnas.1400283111.
[408] Veselska R, Kuglik P, Cejpek P, Svachova H, Neradil J, Loja T, et al. Nestin expression in the cell lines derived from glioblastoma multiforme. BMC Cancer 2006;6:32. https://doi.org/10.1186/1471-2407-6-32.
[409] Kondo S, Wakisaka N, Muramatsu M, Zen Y, Endo K, Murono S, et al. Epstein-Barr Virus Latent Membrane Protein 1 Induces Cancer Stem/Progenitor-Like Cells in Nasopharyngeal Epithelial Cell Lines. J Virol 2011;85:11255–64. https://doi.org/10.1128/JVI.00188-11.
[410] Li Y, Zhong C, Liu D, Yu W, Chen W, Wang Y, et al. Evidence for Kaposi Sarcoma Originating from Mesenchymal Stem Cell through KSHV-induced Mesenchymal-to-Endothelial Transition. Cancer Research 2018;78:230–45. https://doi.org/10.1158/0008-5472.CAN-17-1961.
[411] Xiao Y, Yang K, Wang Z, Zhao M, Deng Y, Ji W, et al. CD44-Mediated Poor Prognosis in Glioma Is Associated With M2-Polarization of Tumor-Associated Macrophages and Immunosuppression. Front Surg 2022;8:775194. https://doi.org/10.3389/fsurg.2021.775194.

[412] Yabo YA, Niclou SP, Golebiewska A. Cancer cell heterogeneity and plasticity: A paradigm shift in glioblastoma. Neuro-Oncology 2022;24:669–82. https://doi.org/10.1093/neuonc/noab269.
[413] Li F, Liu X, Sampson JH, Bigner DD, Li C-Y. Rapid Reprogramming of Primary Human Astrocytes into Potent Tumor-Initiating Cells with Defined Genetic Factors. Cancer Research 2016;76:5143–50. https://doi.org/10.1158/0008-5472.CAN-16-0171.
[414] Chen X, Guo Z-Q, Cao D, Chen Y, Chen J. MYC-mediated upregulation of PNO1 promotes glioma tumorigenesis by activating THBS1/FAK/Akt signaling. Cell Death Dis 2021;12:244. https://doi.org/10.1038/s41419-021-03532-y.
[415] Yadav B, Pal S, Rubstov Y, Goel A, Garg M, Pavlyukov M, et al. LncRNAs associated with glioblastoma: From transcriptional noise to novel regulators with a promising role in therapeutics. Molecular Therapy - Nucleic Acids 2021;24:728–42. https://doi.org/10.1016/j.omtn.2021.03.018.
[416] Pantalone MR, Rahbar A, Söderberg-Naucler C, Stragliotto G. Valganciclovir as Add-on to Second-Line Therapy in Patients with Recurrent Glioblastoma. Cancers 2022;14:1958. https://doi.org/10.3390/cancers14081958.
[417] Ding Z, Mathur V, Ho PP, James ML, Lucin KM, Hoehne A, et al. Antiviral drug ganciclovir is a potent inhibitor of microglial proliferation and neuroinflammation. Journal of Experimental Medicine 2014;211:189–98. https://doi.org/10.1084/jem.20120696.
[418] Zhang S, Mu Z, He C, Zhou M, Liu D, Zhao X-F, et al. Antiviral Drug Ganciclovir Is a Potent Inhibitor of the Proliferation of Müller Glia–Derived Progenitors During Zebrafish Retinal Regeneration. Invest Ophthalmol Vis Sci 2016;57:1991. https://doi.org/10.1167/iovs.15-18669.
[419] Fan, TY, Wang, H, Xiang, P, Liu, YW, Li, HZ, Lei, BX, et al. Inhibition of EZH2 reverses chemotherapeutic drug TMZ chemosensitivity in glioblastoma. Int J Clin Exp Pathol n.d.;7:6662–70.
[420] Richards JS, Candelaria NR, Lanz RB. Polyploid giant cancer cells and ovarian cancer: new insights into mitotic regulators and polyploidy. Biology of Reproduction 2021;105:305–16. https://doi.org/10.1093/biolre/ioab102.
[421] Bowers RR, Andrade MF, Jones CM, White-Gilbertson S, Voelkel-Johnson C, Delaney JR. Autophagy modulating therapeutics inhibit ovarian cancer colony generation by polyploid giant cancer cells (PGCCs). BMC Cancer 2022;22:410. https://doi.org/10.1186/s12885-022-09503-6.
[422] Niu N, Mercado-Uribe I, Liu J. Dedifferentiation into blastomere-like cancer stem cells via formation of polyploid giant cancer cells. Oncogene 2017;36:4887–900. https://doi.org/10.1038/onc.2017.72.
[423] Iwahashi N, Ikezaki M, Fujimoto M, Komohara Y, Fujiwara Y, Yamamoto M, et al. Lipid Droplet Accumulation Independently Predicts Poor Clinical Prognosis in High-Grade Serous Ovarian Carcinoma. Cancers 2021;13:5251. https://doi.org/10.3390/cancers13205251.
[424] Yoshihara M, Yamakita Y, Kajiyama H, Senga T, Koya Y, Yamashita M, et al. Filopodia play an important role in the trans-mesothelial migration of ovarian cancer cells. Experimental Cell Research 2020;392:112011. https://doi.org/10.1016/j.yexcr.2020.112011.
[425] Zhang S, Mercado-Uribe I, Hanash S, Liu J. iTRAQ-Based Proteomic Analysis of Polyploid Giant Cancer Cells and Budding Progeny Cells Reveals Several Distinct Pathways

for Ovarian Cancer Development. PLoS ONE 2013;8:e80120. https://doi.org/10.1371/journal.pone.0080120.
[426] Lv H, Shi Y, Zhang L, Zhang D, Liu G, Yang Z, et al. Polyploid giant cancer cells with budding and the expression of cyclin E, S-phase kinase-associated protein 2, stathmin associated with the grading and metastasis in serous ovarian tumor. BMC Cancer 2014;14:576. https://doi.org/10.1186/1471-2407-14-576.
[427] Davidson B, Tropé CG, Reich R. Epithelial–Mesenchymal Transition in Ovarian Carcinoma. Front Oncol 2012;2:33. https://doi.org/10.3389/fonc.2012.00033.
[428] Castedo M, Senovilla L, Vitale I, Kroemer G. Tetraploid cancer cell precursors in ovarian carcinoma. Cell Cycle 2012;11:3157–8. https://doi.org/10.4161/cc.21722.
[429] Aloni-Grinstein R, Charni-Natan M, Solomon H, Rotter V. p53 and the Viral Connection: Back into the Future ‡. Cancers 2018;10:178. https://doi.org/10.3390/cancers10060178.
[430] Davoli T, Denchi EL, De Lange T. Persistent Telomere Damage Induces Bypass of Mitosis and Tetraploidy. Cell 2010;141:81–93. https://doi.org/10.1016/j.cell.2010.01.031.
[431] Liu J, Yang G, Thompson-Lanza JA, Glassman A, Hayes K, Patterson A, et al. A Genetically Defined Model for Human Ovarian Cancer. Cancer Research 2004;64:1655–63. https://doi.org/10.1158/0008-5472.CAN-03-3380.
[432] Velletri T, Villa CE, Cilli D, Barzaghi B, Lo Riso P, Lupia M, et al. Single cell-derived spheroids capture the self-renewing subpopulations of metastatic ovarian cancer. Cell Death Differ 2022;29:614–26. https://doi.org/10.1038/s41418-021-00878-w.
[433] Liao J, Qian F, Tchabo N, Mhawech-Fauceglia P, Beck A, Qian Z, et al. Ovarian Cancer Spheroid Cells with Stem Cell-Like Properties Contribute to Tumor Generation, Metastasis and Chemotherapy Resistance through Hypoxia-Resistant Metabolism. PLoS ONE 2014;9:e84941. https://doi.org/10.1371/journal.pone.0084941.
[434] Shepherd TG, Dick FA. Principles of dormancy evident in high-grade serous ovarian cancer. Cell Div 2022;17:2. https://doi.org/10.1186/s13008-022-00079-y.
[435] Pease JC, Brewer M, Tirnauer JS. Spontaneous spheroid budding from monolayers: a potential contribution to ovarian cancer dissemination. Biology Open 2012;1:622–8. https://doi.org/10.1242/bio.2012653.
[436] Robinson M, Gilbert SF, Waters JA, Lujano-Olazaba O, Lara J, Alexander LJ, et al. Characterization of SOX2, OCT4 and NANOG in Ovarian Cancer Tumor-Initiating Cells. Cancers 2021;13:262. https://doi.org/10.3390/cancers13020262.
[437] Martincuks A, Li P-C, Zhao Q, Zhang C, Li Y-J, Yu H, et al. CD44 in Ovarian Cancer Progression and Therapy Resistance—A Critical Role for STAT3. Front Oncol 2020;10:589601. https://doi.org/10.3389/fonc.2020.589601.
[438] Gao Y, Foster R, Yang X, Feng Y, Shen JK, Mankin HJ, et al. Up-regulation of CD44 in the development of metastasis, recurrence and drug resistance of ovarian cancer. Oncotarget 2015;6:9313–26. https://doi.org/10.18632/oncotarget.3220.
[439] Zhou J, Du Y, Lu Y, Luan B, Xu C, Yu Y, et al. CD44 Expression Predicts Prognosis of Ovarian Cancer Patients Through Promoting Epithelial-Mesenchymal Transition (EMT) by Regulating Snail, ZEB1, and Caveolin-1. Front Oncol 2019;9:802. https://doi.org/10.3389/fonc.2019.00802.
[440] Lupia M, Cavallaro U. Ovarian cancer stem cells: still an elusive entity? Mol Cancer 2017;16:64. https://doi.org/10.1186/s12943-017-0638-3.

[441] Loret N, Denys H, Tummers P, Berx G. The Role of Epithelial-to-Mesenchymal Plasticity in Ovarian Cancer Progression and Therapy Resistance. Cancers 2019;11:838. https://doi.org/10.3390/cancers11060838.
[442] Ricci F, Bernasconi S, Perego P, Ganzinelli M, Russo G, Bono F, et al. Ovarian carcinoma tumor-initiating cells have a mesenchymal phenotype. Cell Cycle 2012;11:1966–76. https://doi.org/10.4161/cc.20308.
[443] Tedja R, Alvero AB, Fox A, Cardenas C, Pitruzzello M, Chehade H, et al. Generation of Stable Epithelial–Mesenchymal Hybrid Cancer Cells with Tumorigenic Potential. Cancers 2023;15:684. https://doi.org/10.3390/cancers15030684.
[444] Carlson JW, Rådestad AF, Söderberg-Naucler C, Rahbar A. Human cytomegalovirus in high grade serous ovarian cancer possible implications for patients survival. Medicine 2018;97:e9685. https://doi.org/10.1097/MD.0000000000009685.
[445] Pathak S, Wilczyński JR, Paradowska E. Factors in Oncogenesis: Viral Infections in Ovarian Cancer. Cancers 2020;12:561. https://doi.org/10.3390/cancers12030561.
[446] Stragliotto G, Pantalone MR, Rahbar A, Bartek J, Söderberg-Naucler C. Valganciclovir as Add-on to Standard Therapy in Glioblastoma Patients. Clinical Cancer Research 2020;26:4031–9. https://doi.org/10.1158/1078-0432.CCR-20-0369.
[447] Nelson CS, Herold BC, Permar SR. A new era in cytomegalovirus vaccinology: considerations for rational design of next-generation vaccines to prevent congenital cytomegalovirus infection. Npj Vaccines 2018;3:38. https://doi.org/10.1038/s41541-018-0074-4.
[448] Yu C, He S, Zhu W, Ru P, Ge X, Govindasamy K. Human cytomegalovirus in cancer: the mechanism of HCMV-induced carcinogenesis and its therapeutic potential. Front Cell Infect Microbiol 2023;13:1202138. https://doi.org/10.3389/fcimb.2023.1202138.
[449] Amatangelo M, Garipov A, Li H, Conejo-Garcia JR, Speicher D, Zhang R. Three-dimensional culture sensitizes epithelial ovarian cancer cells to EZH2 methyltransferase inhibition. Cell Cycle 2013;12:2113–9. https://doi.org/10.4161/cc.25163.
[450] Sourvinos G, Morou A, Sanidas I, Codruta I, Ezell SA, Doxaki C, et al. The Downregulation of GFI1 by the EZH2-NDY1/KDM2B-JARID2 Axis and by Human Cytomegalovirus (HCMV) Associated Factors Allows the Activation of the HCMV Major IE Promoter and the Transition to Productive Infection. PLoS Pathog 2014;10:e1004136. https://doi.org/10.1371/journal.ppat.1004136.

11. Annex

11.1 Publication N°1

El Baba R, Herbein G. Management of epigenomic networks entailed in coronavirus infections and COVID-19. Clin Epigenet 2020;12:118. https://doi.org/10.1186/s13148-020-00912-7.

Coronaviruses (CoVs) are highly variable single-stranded RNA viruses susceptible to genetic mutations and recombination. They include pathogens like SARS-CoV, MERS-CoV, and the highly infectious SARS-CoV-2, responsible for the COVID-19 pandemic. Severe outcomes of COVID-19 are linked to older age and compromised immune systems, often involving a cytokine storm marked by excessive inflammation. The molecular processes governing coronavirus infection encompass interactions between the virus and host, affecting viral entry, replication, escape, and immune control. Exploring coronavirus infections and COVID-19 from an epigenetic perspective may lead to altered gene expression, potentially limiting infection. Clinical trials of epigenetic therapies, approved epigenetic agents, and combining antivirals with epigenetic drugs are viewed as effective strategies for controlling viral replication and excessive inflammation.

El Baba and Herbein *Clinical Epigenetics* (2020) 12:118
https://doi.org/10.1186/s13148-020-00912-7

Clinical Epigenetics

REVIEW Open Access

Management of epigenomic networks entailed in coronavirus infections and COVID-19

Ranim El Baba[1,2] and Georges Herbein[1,3*]

Abstract

Coronaviruses (CoVs) are highly diverse single-stranded RNA viruses owing to their susceptibility to numerous genomic mutations and recombination. Such viruses involve human and animal pathogens including the etiologic agents of acute respiratory tract illnesses: severe acute respiratory syndrome coronavirus (SARS-CoV), Middle East respiratory syndrome coronavirus (MERS-CoV), and the highly morbific SARS-CoV-2. Coronavirus disease 2019 (COVID-19), an emerging disease with a quick rise in infected cases and deaths, was recently identified causing a worldwide pandemic. COVID-19 disease outcomes were found to increase in elderly and patients with a compromised immune system. Evidences indicated that the main culprit behind COVID-19 deaths is the cytokine storm, which is illustrated by an uncontrolled over-production of soluble markers of inflammation. The regulation process of coronavirus pathogenesis through molecular mechanism comprise virus-host interactions linked to viral entry, replication and transcription, escape, and immune system control. Recognizing coronavirus infections and COVID-19 through epigenetics lens will lead to potential alteration in gene expression thus limiting coronavirus infections. Focusing on epigenetic therapies reaching clinical trials, clinically approved epigenetic-targeted agents, and combination therapy of antivirals and epigenetic drugs is currently considered an effective and valuable approach for viral replication and inflammatory overdrive control.

Keywords: Coronavirus, SARS-CoV, MERS-CoV, SARS-CoV-2, COVID-19, Epigenetic, Inflammation

Background

Coronaviruses are non-segmented, enveloped viruses with a positive-sense single-stranded RNA genome belonging to Coronaviridae family [1–3]. CoVs share similar genome organization, but differ phenotypically and genotypically [4, 5]. High frequency of RNA recombination, RNA-dependent RNA polymerase (RdRp) fickleness, and the bulky genomes for RNA viruses are considered leading factors for CoVs' diversity [5]. Humans are infected by seven CoVs, including HCoV-229E and HCoV-NL63 belonging to Alphacoronavirus; HCoV-OC43 and HCoV HKU1 belonging to Betacoronavirus lineage A; these four viruses are known to be endemic [4–6]. Three human coronaviruses (HCoVs) caused epidemics expressing high morbidity and mortality rates: SARS-CoV belonging to Betacoronavirus lineage B, MERS-CoV or HCoV-EMC belonging to Betacoronavirus lineage C, and the 2019 novel coronavirus 2019-nCoV/SARS-CoV-2 [6–8].

SARS-CoV emerged in Guangdong Province, China, in February, 2003 [9, 10]. It resulted in 8098 human infections and 774 deaths, and it disseminated into 37 countries [3, 11]. In 2012, MERS-CoV was initially detected in the Kingdom of Saudi Arabia revealing 2494 confirmed infected cases and 858 mortalities. It was spread

* Correspondence: georges.herbein@univ-fcomte.fr
[1]Department Pathogens & Inflammation-EPILAB, UPRES EA4266, University of Franche-Comté and University of Bourgogne Franche-Comté, F-25030 Besançon, France
[3]Department of Virology, CHRU Besancon, F-25030 Besançon, France
Full list of author information is available at the end of the article

© The Author(s). 2020 **Open Access** This article is licensed under a Creative Commons Attribution 4.0 International License, which permits use, sharing, adaptation, distribution and reproduction in any medium or format, as long as you give appropriate credit to the original author(s) and the source, provide a link to the Creative Commons licence, and indicate if changes were made. The images or other third party material in this article are included in the article's Creative Commons licence, unless indicated otherwise in a credit line to the material. If material is not included in the article's Creative Commons licence and your intended use is not permitted by statutory regulation or exceeds the permitted use, you will need to obtain permission directly from the copyright holder. To view a copy of this licence, visit http://creativecommons.org/licenses/by/4.0/. The Creative Commons Public Domain Dedication waiver (http://creativecommons.org/publicdomain/zero/1.0/) applies to the data made available in this article, unless otherwise stated in a credit line to the data.

to 27 additional countries [3, 12]. While the MERS-CoV outbreak has been mostly limited to the Middle Eastern region, it is likely that more re-emerging HCoVs might endanger the global communal health condition. SARS-CoV-2 was identified in late December, 2019 in Wuhan, China [8]. The World Health Organization (WHO) declared that COVID-19 was listed as the sixth Public Health Emergency of International Concern (PHEIC), implicating that it may pose risks to various countries and entail an international response [8, 13, 14]. A situation report showed COVID-19 data as received by WHO in 9 June 2020: 7,039,918 confirmed cases and 404,396 deaths were globally reported in American, European, Eastern Mediterranean, Western Pacific, South-East Asia, and African regions [15]. However, underestimating COVID-19's burden was due to the fact that patients with mild COVID-19 symptoms or asymptomatic patients might not seek medical care for proper diagnosis.

As outbreaks can ensue rapidly worldwide, it is quite necessary to emphasize on novel therapeutic approaches. Although investment in biomedical and pharmaceutical research has increased significantly, the annual number of new treatments approved by the Food and Drug Administration (FDA) has remained relatively limited [11, 16]. Generally, the available treatment strategies for emerging coronavirus' strains, that led to significant pandemics, are inadequate to effectively advance patient's outcome [17]. These strategies have been less successful for RNA viruses compared to DNA viruses as the former mutates at a higher rate resulting in drug resistance [4]. Yet, HCoVs potentially influence the host's epigenome, and this will aid in discovering new targets for therapeutic interventions to gain more insights for the development of antiviral therapeutics and vaccines [9, 18]. The primary objective of this review is to evaluate the epigenetic mechanisms involved in HCoVs' infection and to highlight on epigenetic therapies in order to reduce peak incidence and global deaths resulting from HCoVs' outbreaks worldwide.

Epigenetic mechanisms at work in coronavirus replication

Epigenetic regulation of coronavirus replication

The genome of SARS-CoV-2 is composed of a single-stranded positive RNA of 29 kb; it is considered the largest of all RNA virus genomes (Fig. 1a) [3, 11]. So far, 14 open reading frames (ORF) have been described in the SARS-CoV-2 genome [11, 19]. SARS-CoV-2 genome encodes for viral proteins involved in viral replication named non-structural proteins (Nsp) including the replicase complex coded by ORF1ab, and structural viral proteins involved in viral assembly including the spike (S), envelope (E), membrane (M), and nucleocapsid (NP) protein [3, 11]. The S protein, a class I fusion glycoprotein, forms homotrimers bulging in the viral surface facilitating the viral envelope binding to host cells by attraction with angiotensin-converting enzyme 2 (ACE2). This transmembrane protein is cleaved by the host cell furin-like protease into 2 subunits labeled S1 which binds to the receptor on the host cell surface and S2 is responsible for fusion activity [1, 3]. Hence, disparities in the S protein would directly impact the viral

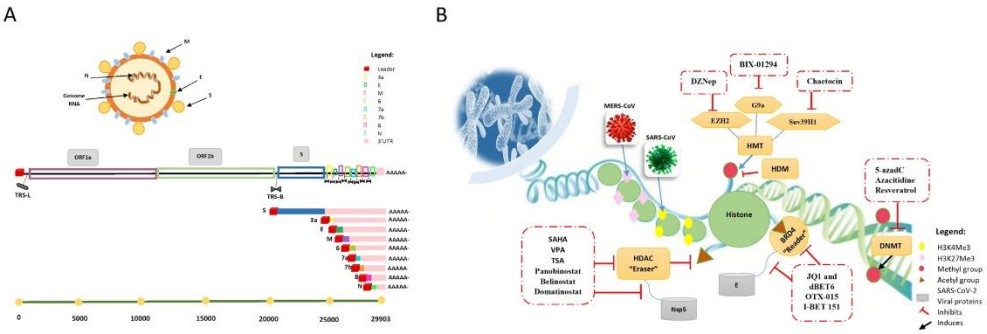

Fig. 1 Epigenetics in coronavirus replication and targeted therapies. **a** SARS-CoV-2 genomic map, canonical subgenomic RNAs, and virion structure. Both ORF1a and ORF1b are translated from the genomic RNA. Eight subgenomic RNAs are formed in addition to the genomic RNA. **b** Epigenetic marks and their therapeutic control in HCoV infection. This figure illustrates the epigenetics landscape during coronavirus replication through representing various epigenetic targets (DNMT, HDM, HDAC, and HMT) and their regulation by epigenetic therapy (HDACi, DNMTi, and HMTi). Inhibiting some epigenetic targets leads to a decrease in viral replication load; thus, acting as a vital therapeutic strategy in treating coronavirus infected patients. MERS-CoV in contrast to SARS-CoV increases the repressive epigenetic mark H3k27me3 and decreases the active mark H3k4me3 thus impeding transcription and expression of ISGs. BRD4, a bromodomain and extraterminal (BET) protein, is involved in histone acetylation; besides, it binds to protein E of SARS-CoV-2 accelerating the latter's entry. Nsp5 binds to HDAC2 and inhibits its entry into the nucleus affecting IFN response

biological characteristics including pathogenicity and antigenicity. Spike protein has been considered as the ultimate target for COVID-19 immunotherapies, and this is based on SARS-CoV and MERS-CoV preceding evidence. Recently, studies have found that SARS-CoV S protein induced polyclonal antibody responses and counteracted SARS-CoV-2 S-mediated entry into host cells, thus favoring the use of this ideal molecular target for vaccination and immunotherapies [20]. Even though SARS-CoV-2 crisis is noteworthy, referring to HCoVs' data is eminently required since HCoV and SARS-CoV-2 share genomic and biological properties.

Epigenetic regulation of HCoV entry

ACE2, a significant player in the renin-angiotensin system (RAS), was recognized as vital factor that attaches to spike protein and eases SARS-CoV-2 binding and host cell entry. Early studies have shown that this receptor acts as a protective mechanism to block the early stages of COVID-19 [11, 21]. ACE2 is significantly expressed in the lower respiratory tract such as type II alveolar cells (AT2) of the lungs, upper esophagus, and stratified epithelial cells, as well as in kidney proximal tubule cells, bladder urothelial cells, absorptive enterocytes, cardiomyocytes, and cholangiocytes. Such cellular outspreading elucidates the consequences of SARS-CoV-2 infection that is not only limited to respiratory disorders but also to kidney, liver, heart, and gastrointestinal tract illnesses [19]. Sirtuins, a family of nicotinamide adenine dinucleotide (NAD)+ dependent deacetylases, play an important role in cellular homeostasis [22]. Silent information regulator T1 (SIRT1), a histone deacetylase (HDAC) class III, is a key regulator of ACE2 levels via binding to its promoter [23]. In fact, resveratrol a well-known activator of SIRT1 increases the ACE2/angiotensin 1-7 (Ang1-7)/Mas receptor (MasR) axis parallel to the downregulation of the Angiotensin II receptor type 1 (AT1R) expression belonging to the prorenin receptor (PRR)/ACE/angiotensin II (Ang II)/AT1R axis [24–28]. Although it was not shown so far that SIRT1 increases SARS-CoV-2 entry into the cell due to increased ACE2 expression, COVID-19 patients with high levels of ACE2 have a better prognosis probably due to decreased hyperinflammation [28–30]. Similarly, SIRT1 could impact viral entry of SARS-CoV and HCoV-NL63 which also use ACE2 for viral entry [31]. Foremost host cellular receptors significantly utilized by other HCoVs for entry and viral replication are aminopeptidase N (APN) by HCoV-229E, dipeptidyl peptidase 4 (DPP4) by MERS-CoV and 9-O-acetylated sialic acid by HCoV-OC43 and HCoV-HKU1 [5, 6, 32, 33]. Any mutations in human APN cell surface receptor will directly inhibit virus-receptor interaction [33]. Promoter hypermethylation downregulates APN gene expression and azacitidine (5-azaC) induces APN protein expression [34]. In melanoma cells, the combination of HDAC inhibitor CHR-3996 and APN inhibitor tosedostat activated synergistically NF-kB [35]. Glucocorticoids directly upregulate the DPP4 gene expression in macrophages due to the presence of two GC-binding motifs in the DPP4 gene promoter [36]. Therefore, the cell surface expression of HCoV entry receptors can be modulated by epigenetic drugs which could be used to discover new therapeutic approaches to curtail HCoV infections.

Epigenetic regulation of HCoV replication and transcription

Coronaviruses employ a multisubunit machinery for replication and transcription. The RdRp, also known as Nsp12, catalyzes the synthesis of viral RNA and thus plays a central role in the replication and transcription cycle of SARS-CoV-2, possibly with the assistance of Nsp7 and Nsp8 as cofactors [37]. Nsp7 interacts with the 7SK small nuclear ribonucleoprotein (7SK snRNP) complex comprising La-related protein (LARP7), methyl-phosphate capping enzyme (MEPCE), and hexamethylene bisacetamide inducible protein (HEXIM1). This complex sequesters positive transcription elongation factor (P-TEFb) which is critical for the replication of several viruses including herpesviruses, human immunodeficiency viruses (HIV), human T-lymphotropic virus (HTLV), human adenovirus (HAdV), influenza A virus and Dengue virus (DENV) [38]. The interaction between Nsp7 and P-TEFb will result in the release of the active form of P-TEFb known to bind bromodomain-containing protein 4 (BRD4); similar interaction has been reported previously for HIV Tat and P-TEFb. Interestingly, bromodomain and extra-terminal motif (BET) inhibitors such as JQ1, I-BET, I-BET151, OTX015, UMB-136, MMQO, CPI-203, RVX-208, PFI-1, BI-2536, and BI-6727 induce P-TEFb release and have been reported to be latency reversal agents in HIV infection [39]. Nsp14, a 3′-5′ exonuclease, is critical for coronavirus RNA synthesis [40]; Nsp14 interacts with SIRT5 acting as a weak deacetylase but with desuccinylase and demalonylase activities regulating several metabolic pathways [41]. Recently, SIRT5 inhibitors have been developed [42]. Nsp13 helicase/triphosphatase participate in the release of newly synthesized RNA strand and thus the production of infectious viral particles [43]. Since p300 expression is under HDACs' control [44], helicases such as Nsp13 might be under the control of p300 and thereby HDAC inhibitors might interfere with coronavirus replication. The Nsp3-Nsp4-Nsp6 complex is also involved in viral replication. Remarkably, Nsp4 interacts with HDAC2, and this could emphasize the role of epigenetic therapies in blocking HDAC2 [45]. Nsp10 is

essential for the RNA cap methyl transferase of Nsp16. During RNA capping, Nsp16 methyl transferase activity coud be blocked by methyltransferase inhibitors such as sinefungin, dAPPMA 2′-O MTase inhibitors, aurintricaboxylic acid and inhibitor 7 [46]. Finally, Nsp15 is a uridine-specific RNA endonuclease which has been shown to cleave a highly conserved RNA structure in the 3′ non-translated region of the SARS virus [47]. Most recurrent transcription regulating sequence (TRS) related to MERS-CoV is TRS2. Generally, MERS-CoV transcribes 11 subgenomic mRNAs, including various ORFs translating polypeptide chains and fusion proteins. Unlike MERS-CoV, SARS-CoV includes TRS3 that exists also in SARS-CoV-2. SARS-CoV possesses several accessory proteins (AP), which are translated directly from mRNAs. SARS-CoV-2 grants comparative differences in transcription and subgenomic mRNAs translation compared to other beta-coronavirus. SARS-CoV-2 initiates transcription in 20 TRS sites, transcribing much more forms of subgenomic mRNAs than SARS-CoV and MERS-CoV; this could correlate to the severity and high infectivity of COVID-19 on host patients. SARS-CoV-2 produces around nine forms of fusion proteins, with higher concentrations of Nsp12, Nsp3, Nsp5, and AP12 [48].

Epigenetic regulation of HCoV protein maturation

Newly synthesized viral polyproteins are cleaved by viral proteases, namely, the 3C-like protease (3CLpro) and the papain-like protease (PLpro) [49]. ORF1a encodes the two cysteine proteases, 3CLpro and PLpro. While PLpro cuts the first three cleavage sites of its polyprotein, 3CLpro is responsible for cleavage of the residual 11 locations resulting in release of a total of 16 Nsp in both SARS-CoV and MERS-CoV [45]. Upon comparing SARS-CoV and SARS-CoV-2, correspondences have been detected in 5′UTR and 3′UTR regions, protease cleavage positions and amino acid conformation of both structural and non-structural proteins. Yet, the number of spike precursors and specificity of accessory proteins differ in SARS viruses. SARS-CoV processes two spike precursors (S1p and S2p), while SARS-CoV-2 and MERS-CoV produce only one. AP11 is characteristic for SARS-CoV, whereas SARS-CoV-2 translates a specific accessory protein AP12 [48]. Nsp5, the coronavirus 3CLpro, is critical for the maturation of non-structural SARS-CoV-2 proteins. Actively, 3CLpro binds to HDAC2 and tRNA methyl transferase 1 (TRMT1) resulting in their cleavage [45]. Thus, 3CLpro mimics HDAC2 inhibitor and might therefore facilitate viral and/or cellular gene expression in infected cells. TRMT1-catalyzed tRNA modifications are required for redox homeostasis to ensure proper cellular proliferation and oxidative stress survival [50]. Since TRMT1 is cleaved by 3CLpro, SARS-CoV-2 might interfere with tRNA methylation in infected cells. Numerous drugs have been reported to inhibit the activity of 3CLpro including the anti-HIV drug lopinavir [16]. The structural viral proteins (NP, M, E, and S) participate in the formation of new virions across the endoplasmic reticulum. SIRT1 activation following treatment of the infected cells with resveratrol results in decreased viral replication [51]. The viral envelope E binds to BRD2 and BRD4 and could be the target for BET inhibitors [39, 45]. Therefore, blocking SARS-CoV-2 structural proteins' maturation could result firstly from the usage of SARS-CoV-2 protease inhibitors to annihilate the viral polyprotein cleavage by 3CL pro and/or PLpro, and secondly from the epigenetic treatments to decrease the amount and/or activity of structural viral proteins.

Epigenetic-targeted therapies controlling coronavirus replication

Understanding fundamental elements of epigenetic regulation is progressively contributing to concepts of viral epigenetic therapeutics. Epigenetic therapies are among the most active areas of research and this is because of their potential specific targeting mechanisms compared to the conventional therapies. Manipulating gene regulatory networks using epidrugs could be associated with a risk generating from the systemic effect of such therapies. Yet, knowing that HCoVs including SARS-CoV-2 may infect more than one cell type it is advantageous to rely on systemically acting agents. Besides, some proposed epigenetic treatments can be site-directed and consequently minimize unwanted systemic risk. Furthermore, it is imperative to spotlight the SARS-CoV-2 direct RNA sequence data including RNA modifications, the viral transcriptome and epitranscriptome as it could anticipate novel-targeted strategies for the management of SARS-CoV-2 infection [52]. Antiviral therapies targeting the pathogen itself act by inhibiting enzymes responsible for viral genome replication, the viral assembly process, and preventing viral entry by blocking the virus-host receptor binding. Remdesivir, favipiravir, ribavirin, galidesivir, and its salt form (BCX-4430) targeting RdRp; ritonavir and darunavir targeting viral proteases (3CLpro or PLpro) in addition to camostat mesylate which is a serine protease inhibitor directly acting on SARS-CoV-2. Moreover, the FDA approved lopinavir/ritonavir as a target of the coronavirus protease enzyme and arbidol (umifenovir) targeting ACE2 and S protein showed efficacy against SARS-CoV-2 as well as chloroquine which possesses an antiviral and an anti-inflammatory effect [16]. In the primary stages of SARS-CoV epidemic, an empirical treatment of broad spectrum antiviral agents and immunosuppressive

doses of steroids were used along with the supportive treatment [53]. Despite the available treatment options, studies documenting the therapies' efficacy are lacking especially for the SARS-CoV-2 outbreak [11, 54–56]. Nevertheless, extending the choices of treatment by generating epigenetic therapies would provide a real improvement to healthcare community struggling to cope during an outbreak of emerging viral infections (Table 1). Histone deacetylases (HDACs) resemble a main epigenetic target for the treatment of viral infections [64, 65] (Fig. 1b). Hence, HDACs class III such as SIRT1 and resveratrol have been previously described as antiviral effectors [22]. Resveratrol was found to modulate SIRTs' activity (SIRT 1,2,3,5) especially as a SIRT1 activator, 5' AMP-activated protein kinase (AMPK), protein kinase C, NF-kB, p53, activator protein 1 (AP-1), early growth regulator 1 (EGR-1), sterol regulatory element-binding protein 1 (SREBP-1), and DNA methyltransferase (DNMT)1 thus targeting the regulation of viral infection [22, 57]. Significant downregulation of apoptosis induced by MERS-CoV, prolonged cellular survival post-MERS-CoV infection, potential decrease in viral NP protein expression, and decreased viral replication were detected after resveratrol administration [51]. Besides HDACs class III, the inhibition of the class II HDAC2 is achieved by the approved drug valproic acid (VPA) and the pre-clinical candidate apicidin [45, 59]. VPA displayed minimal control of SARS-CoV-2 growth regardless of drug concentration along with high cytotoxicity levels [45]. In addition to VPA and apicidin, HDAC inhibitors include the broad spectrum trichostatin A (TSA) which reduced the pro-inflammatory mediator's production, MS-275, and depsipeptide [63, 66, 67]. Other potent HDACi such as vorinostat or

Table 1 Epigenetics involved in coronavirus infection and their therapeutic control

Epigenetic drug target		Antagonism "inhibitors"		Potential outcome	Combination therapy(few require clinical validation)
HDAC	Pan-HDAC class I and II	VPA		Affecting inflammatory functions and interferon response [45].	VPA + antivirals (remdesivir, ribavirin, favipiravir, galidesivir) or (rapamycin, selumetinib, trametinib) or prostatin
		TSA		Reduced pro-inflammatory mediator's production and increased IL-10 production [55].	TSA + antivirals or (rapamycin, selumetinib, trametinib)
		Vorinostat (SAHA)		Diminished genomes initiating gene replication, and induced the expression of cellular proteins responsible for viral inhibition [57].	SAHA + antivirals or (rapamycin, selumetinib, trametinib) or prostatin or BIX-01294 or DZNep
	All HDAC classes including class I, II, and IV	Panobinostat		Affecting EGFR/HER2 signaling, MAPK signaling, PI3K-Akt, and NFκB pathway [58].	Panobinostat + antivirals or (rapamycin, selumetinib, trametinib)
		Belinostat and domatinostat		Enhanced TGF-β expression [58].	Belinostat or domatinostat + antivirals or (rapamycin, selumetinib, trametinib)
HKMT	Pan-HKMT EZH2	DZNep		Attained cellular antiviral state and reduced viral yields [57].	DZNep + vorinostat
	HKMT G9a	BIX-01294		Enhancing antiviral state [57].	BIX-01294 + vorinostat
	HMT Suv39H1	Chaetocin		Permanent cell cycle arrest and RNA transcript blockage [59].	
HAT		Anacardic acid, MG149, C646		Suppressed IL-6 levels [60, 61].	
DNMT		Resveratrol		Down-regulation of apoptosis, decrease in (N) protein expression, and RNA viral replication antagonism [51].	
		Decitabine (5-azadC)		Counteracting hyper-inflammation: lowering pro-inflammatory cytokines (TNF-α, IL-6, IL-1β) and chemokines, inducing IL-10 marker and TGF-β [58].	5-azadC + antivirals or (rapamycin, selumetinib, trametinib)
		Azacitidine		Viral mimicry [62].	Azacitidine + antivirals or (rapamycin, selumetinib, trametinib)
BET proteins (BRD4)		Clinical	ABBV-744, CPI-0610, RVX-208	BRD4 inhibition boosts a potential innate immune response, blocks viral attachment, inducts DNA damage response (DDR), decreases viral replication, and arrests cell-cycle with no apoptotic signs [63].	
		Preclinical	dBET6, JQ-1, MZ1		

suberanilohydroxamic acid (SAHA), belinostat, romidepsin, and panobinostat were already used for the treatment of several cancers such as T cell lymphoma and relapse of multiple myeloma [68–70]. Knowing that viruses depend on host's epigenetic machinery, some epigenetic drugs used in cancer therapies were shown to give a potential broad spectrum antiviral action against novel emerging viruses. The histone methyltransferases-enhancer of zeste homolog 2/1 (HMT EZH2/1) inhibitors have the ability to attain cellular antiviral state and reduce viral yields instead of inducing activation [68, 71]. A pan-HKMT antagonist, 3-deazaneplanocin-A (DZNep), prove to be therapeutically superior to BIX-01294 which antagonizes HKMT G9a [71]. Chaetocin is a fungal mycotoxin which inhibits HMT Suv39H1, promotes permanent cell cycle arrest, and RNA transcript blockage [72]. Chaetocin is contraindicated with SAHA and JQ-1 as it causes cytotoxicity [73]. On the contrary, a possible synergism was revealed combining BIX-01294 with vorinostat and DZNep with vorinostat [71]. BRD4, a chief gene expression regulator, is involved in recognizing and modifying histone acetylation. Inhibition of BRD4 exhibits an effective antiviral effect against a wide range of RNA and DNA viruses by boosting a potential innate immune response, blocking viral attachment, inducting DNA damage response (DDR), decreasing viral replication, and arresting cell-cycle with no apoptotic signs. Bromodomain and extraterminal protein inhibitors are subdivided into clinical (ABBV-744, CPI-0610, RVX-208) and preclinical (dBET6, JQ-1, MZ1) candidates [45, 74]. By hindering the communication of BRD4 and transmembrane E protein, JQ-1, and dBET6 effectively inhibit the replication of SARS-CoV-2 genome [45, 75]. JQ-1 exhibited a potential viral inhibition at low doses; dBET6 expressed lower cytotoxicity levels than JQ-1. Knowing that the bromodomain and extraterminal protein inhibitors possess varying cytotoxicity further drug assessments must be performed prior patient use [45].

Epigenetic regulation of cellular and immune landscape during coronavirus infection

Cellular and immune landscape during coronavirus infection

In the course of viral infections, innate immune cells initiate a transcriptional signal that is cell and stimulus specific. Several main performers of innate immunity, such as signal transducer and activator of transcription 1 (STAT1), myeloid differentiation primary response gene 88 (MyD88), *Toll-like receptor (*TLR)4, TLR7, and TLR3/TIR-domain-containing adapter-inducing interferon-beta (TRIF) diminish infection severity during HCoV infection in vivo. Moreover, interferons (IFN-alpha, IFN-beta, IFN-gamma) which are regulated by histone marks aid in controlling HCoV infections in vivo and in vitro. IFN and tumor necrosis factor (TNF) are the primary response genes of the innate immune system whose promoters show poised promoter features. H3K4me3, H3k27me3, and H3k9me2 are responsible for modulating the activation of the main player IFN. H3K9me2, a repressive histone mark, contributes to DNA methylation and heterochromatin formation and hence stopping histone tail acetylation by recruiting the transcriptional repressor of the heterochromatin protein 1 family. H3K4me3, a histone modification enriched in promoter regions, regulates Toll-like receptors (TLRs). As a result, IFN and innate immune responses are subject to epigenetic regulation mediated by specific epigenetic marks, the operation of histone modification enzymes, DNA methylases, and chromatin remodeling complexes. CoVs have progressed genetic functions that antagonize or delay pathogen recognition as well as IFN sensitive gene (ISG) effector functions. Upon the activation of danger sensors, dendritic cells (DCs), and macrophages a temporal and spatial response is epigenetically initiated. The ability of their epigenome to change within minutes after a stimulus is essential for initiating a speedy antiviral host response and to ensure a persistent/specific defense response. Hence, epigenetic mechanisms are responsible guaranteeing a functional and highly regulated host response beyond the initial activation wave [18, 76]. Several epigenetic factors were shown to be effective in the activation of immune responses: recruitment of transcription machinery, prevention of undesired expression of compelling mediators, and repression or stimulation of secondary gene programs [18]. Upon utilizing chromatin immuno-precipitation (ChIP) PCR approaches, it is possible to determine differential occupancy of histone marks at the promoters of ISG genes. During SARS-CoV infection, the promoter regions of ISG genes had more histones with active marks of H3K4me than the repressive H3K27me3 mark, therefore favoring open chromatin and promoting active transcription and ISG expression. MERS-CoV infection of Calu3, a continuous human airway epithelial cell line, resulted in increased levels of H3K27me3 and depletion of H3K4me3 occupancy at the promoter regions of subsets of specific ISGs. These viruses favored a closed chromatin conformation that inhibits ISG expression, which rather was regulated by epigenetic control mechanisms [9, 18, 76]. Thus, the setting of histone methylation marks could be different in two close CoV members, namely SARS-CoV and MERS-CoV.

Acute respiratory distress syndrome (ARDS) is a common immunopathological event for SARS-CoV, MERS-CoV, and SARS-CoV-2. A massive cytokine storm is considered as one of ARDS' principle mechanisms which is the chief death cause of COVID-19 in addition to MERS-CoV and SARS-CoV severe diseases [14]. During the cytokine storm, pro-inflammatory cytokines (IL-1β,

IL-6, IL-12, IL-18, IL-33, TNF-α) and chemokines (CCL2, CCL3, CCL5, CXCL8, CXCL9, CXCL10) are upregulated by effector cells in SARS-CoV infection linked with respiratory distress [14, 77–79]. Unlike the proinflammatory cytokine IL-6, the anti-inflammatory Th2 cytokine TGF-β is not overproduced in COVID-19 patients [77]. Augmented levels of IL-2, IL-6, IL-7, IL-10, granulocyte-colony stimulating factor (G-CSF), TNF-α, IFN-γ-inducible protein 10 (IP10), macrophage inflammatory protein 1-α (MIP1A), and monocyte chemoattractant protein (MCP1) were associated with COVID-19 severity; a cytokine outline favoring secondary hemophagocytic lymphohistiocytosis (sHLH) [80, 81]. Poor prognosis of SARS-CoV-2 infected patients can be forecasted by SARS-CoV-2 viral load which is concomitant with cytokine storm caused by the extremely high IL-6 levels [82]. Older, chronically ill and immunocompromised patients are expected to be more susceptible to hyperinflammation. Demethylation of IFN-regulated genes, NF-kB, and key cytokine genes favors the expression of proinflammatory cytokines and chemokines thus increasing cytokine storm incidence [83]. As a result, minimizing IL-6 plasma concentrations and controlling ACE2 gene epigenetically might be a target for prevention and therapy in COVID-19 [82, 83]. In contrast to SARS-CoV-2, delayed serum levels of IFN, IL-1β, IL-6, IL-8, CCL-2, CCL-3, CCL-5, and IL-2 were detected in MERS-CoV-infected patients. Recent data revealed that pro-inflammatory cytokines (IL-6) and chemokines (IL-8, CXCL-10, and CCL5) responses were elevated in severe MERS-CoV cases [14, 78]. Low levels of the anti-inflammatory cytokine IL-10 was seen in confirmed SARS cases with severe disease. It is noteworthy that SARS-CoV infects monocyte-macrophages, DCs, and T cells which produce IL-10 [78]. In addition to the role of immune cells, the immune landscape in the lung of COVID-19 patients can also be shaped by SARS-CoV-2 infection of the airway epithelial cells. Thus, prominent epigenetic regulators including HDAC2 and BRDs (BRD2, BRD4) interact with viral proteins Nsp5 and E, respectively. Nsp5 antagonizes HDAC2 transport into the nucleus; therefore, affecting HDAC2-induced inflammatory functions and IFN response [18, 45]. Altogether, the hyperinflammatory cytokine and chemokine storm observed in ARDS patients result from epigenetic modifications present in both HCoV infected epithelial cells and immune cells present in their vicinity.

Epigenetic treatments controlling immune hyperactivation

Epigenetic interventions must be urgently directed against cytokine storm to avoid or reduce ARDS and rising mortality (Fig. 2). Targeted anti-cytokine methodologies have proven efficacious in handling cytokine storm syndrome [77]. Dexamethasone, an effectual corticosteroid, was shown recently to decrease the cytokine storm syndrome with reduced mortality rates in COVID19 patients [84, 85]. IL-1 inhibitor anakinra and the IL-6 receptor inhibitor tocilizumab proved a remarkable survival benefit in patients experiencing hyperinflammation post-SARS-CoV-2 infection [80, 81]. IFN-αβ and IFN-γ inhibitors mitigate HCoV-induced inflammation; the timing of IFN antagonism therapy must be taken into consideration as it defines the disease outcome. An early IFN response was protective in SARS-CoV-infected mice unlike a delayed IFN signaling. During delayed severe stages of SARS-CoV, IFN-αβ receptor antagonists prevent inflammatory responses; IFNγ neutralization limited IFN-α production [78, 79]. Supplementary, anti-TNFα antibody administration significantly dampened IFNγ content [79]. DNA methylation is directed via DNA methylase DNMT3a/b by binding of H3K9 histone methyltransferase G9a to the TNFα promoter which will then render TNFα promoter in a transcriptionally repressive state, resulting in reduced TNFα protein levels. Histone acetylation (H3K9ac, H3K36ac, and H4K5ac) triggers the suppression of IL-8 and TNFα levels which were majorly produced in response to CoV. By means of broad spectrum HDACi, TSA, the production of these proinflammatory mediators was curbed [64, 76].

Resveratrol counteracts hyperinflammation by interfering with NF-kB pathway [51]. It potentiates SIRT1 which directly interacts with p65 via deacetylation on lysine 310 resulting in the inhibition of NF-κB activation. Additionally, inhibiting NF-κB activity via SIRT1-AMPK signaling pathway in the cytoplasm promotes an enhanced anti-inflammatory effect. In fact, NF-kB activation is required for the production of numerous proinflammatory cytokines including TNF-α, IL-1β, IL-6, and proinflammatory chemokines. Besides, resveratrol reduces TNF-α-induced phospho-p38 MAPK expression [86–88].

Baricitinib, a JAK inhibitor as well as an AP2-associated protein kinase 1 (AAK1) inhibitor, was approved for inhibiting IFN-α production in hyperinflammatory cases caused by SARS-CoV-2 [81, 89]. Epigenetic drugs targeting proinflammatory and anti-inflammatory cytokines/chemokines act as a beneficial forecaster of long-term outcome for CoVs infections. The aim is to dampen the major proinflammatory cytokines (IL-6, TNF-α, IL-1β) and chemokines (IL-8, MCP-1, CCL5) response while enhancing the role of anti-inflammatory cytokines (IL-10 and TGF-β). Altering DNA methylation and histone acetylation states in the IL-6 promoter will impact IL-6 expression [90–92]. Histone acetyltransferase inhibitors (HATi) such as anacardic acid, MG149, and C646 suppress IL-6 levels [60, 61]. Decitabine or 5-aza-2-deoxycytidine (5-azadC), a nucleoside-based DNMT inhibitor, is widely used to inhibit DNA methylation in macrophages; thus, suppressing inflammation [58, 70, 93]. A recent

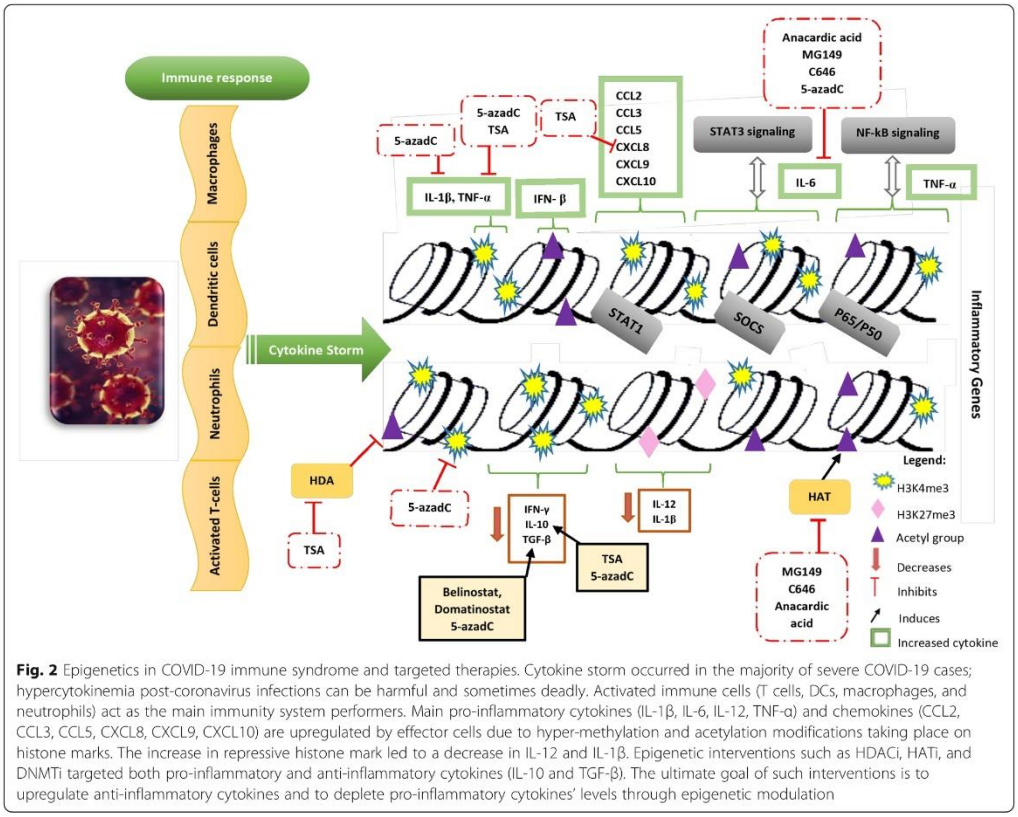

Fig. 2 Epigenetics in COVID-19 immune syndrome and targeted therapies. Cytokine storm occurred in the majority of severe COVID-19 cases; hypercytokinemia post-coronavirus infections can be harmful and sometimes deadly. Activated immune cells (T cells, DCs, macrophages, and neutrophils) act as the main immunity system performers. Main pro-inflammatory cytokines (IL-1β, IL-6, IL-12, TNF-α) and chemokines (CCL2, CCL3, CCL5, CXCL8, CXCL9, CXCL10) are upregulated by effector cells due to hyper-methylation and acetylation modifications taking place on histone marks. The increase in repressive histone mark led to a decrease in IL-12 and IL-1β. Epigenetic interventions such as HDACi, HATi, and DNMTi targeted both pro-inflammatory and anti-inflammatory cytokines (IL-10 and TGF-β). The ultimate goal of such interventions is to upregulate anti-inflammatory cytokines and to deplete pro-inflammatory cytokines' levels through epigenetic modulation

study suggested that the decrease of suppressor of cytokine signaling 1 (SOCS1) via promoter hypermethylation is strongly associated with overproduction of proinflammatory cytokines (TNF-α and IL-6) illuminating the use of DNMTi [90]. Besides, 5-azadC induced IL-10 marker and TGF-β [58, 70, 93]. Belinostat and domatinostat enhanced the expression of TGF-β [58]. Moreover, treatment with TSA resulted in increased production of IL-10 [63, 67, 69]. Hence, elevation of IL-10 and TGF-β levels might curtail the hyperinflammatory storm observed in COVID-19 patients associated with poor prognosis.

Combination therapy to fight coronavirus infections including antiviral and epigenetic drugs

Suitable combination therapies reduce the likelihood of drug resistance, suppress viral replication, lower toxicity levels, and provide synergistic effects (Table 1). Achieving high potency intensities, combinatorial treatments were employed especially in RNA viruses which mutate at higher rate than DNA viruses. However, care must be taken in order to avoid unwanted contraindications. Although there is no clinically approved antiviral drug or vaccine available to be used against COVID-19, few therapeutic combinations have been evaluated to cope with this viral outbreak. Some patients were clinically recovered after the administration of remdesivir combined with chloroquine (CQ) or IFN-β due to the significant blockade of the SARS-CoV-2 replication [89]. In Saudi Arabia, a clinical trial discovered that a combination of lopinavir/ritonavir and IFN-β1b was shown to be effective among MERS-CoV-infected patients [12]. It is also hypothesized that the combination of lopinavir/ritonavir and arbidol will deliver enhanced efficacy against SARS-CoV-2 for a synergistic effect is predictable [16]. A higher potency of antiviral therapy was achieved after the fusion of ribavirin and IFN with immunomodulating agents such as intravenous N-acetylcysteine [94]. Few synergistic combinations resulting from a network-based analysis include sirolimus and dactinomycin, an approved RNA synthesis inhibitor, target HCoV-associated

host protein subnetwork by "complementary exposure" pattern, resulting in potential combination regimens for treatment of HCoVs. To successfully inhibit MERS-CoV replication, kinase inhibitors were combined with other host-targeting molecules such as peroxisome proliferator-activated receptor alpha (PPAR-α) agonists [11]. In a retrospective analysis, ribavirin was tested in combination with corticosteroids, immunoglobulins, and/or antibiotics for SARS-CoV; no efficacy and high fatality rates were shown. Since ribavirin treatment did not improve patient outcome health, Canada stopped permitting the use of ribavirin. Additional studies tested the activity of ribavirin jointly with lopinavir against SARS-CoV. Compared to the control groups, confirmed SARS-CoV cases undergo a milder disease progression with no consequences. In another retrospective analysis, patients were treated with oral ribavirin and SC pegylated IFN-α2a for 2 weeks. At day 14 after confirmed diagnosis of MERS, survival was increased in the tested group (70%) compared to the control (29%). In an additional case study, an elderly patient who was infected with MERS in Jeddah was treated with oral lopinavir/ritonavir, pegylated IFN, and ribavirin. Viral RNA was detected in feces, serum, and respiratory secretions' samples after 2 days for initiating the therapy and up to 2 weeks. An ongoing randomized clinical trial in Saudi Arabia is evaluating treatment of MERS patients with IFN-β1b conjointly with lopinavir/ritonavir due to the latter's high efficacy [4]. Among clinical treatments studied for treating SARS-CoV, combinations of steroid with either alfacon-1, a recombinant consensus IFN-α, or protease inhibitors and ribavirin were found to improve patients' health [56]. Patients with COVID-19 are being recruited in randomized trials to evaluate the efficacy of favipiravir plus IFN-α and favipiravir plus baloxavir marboxil (an approved influenza inhibitor targeting the cap-dependent endonuclease). The synergism between a pegylated-IFN and a nucleoside compound against COVID-19 is still ambiguous [16]. In spite of drug repurposing and the use of targeted antiviral therapies (CQ, remdesivir, rapamycin, ribavirin), epigenetic drugs such as BRD4 inhibitors, DNMT1 inhibitors, and HDAC inhibitors have been demonstrated to potentially inhibit SARS-CoV-2 [4, 14, 45, 95]. Novel broad spectrum replication inhibitors such as remdesivir or GS-5734 (Gilead Sciences, in phase I clinical trial), and immunomodulators along with direct-acting antiviral agents that are in development could make an efficient amalgamation for treating HCoVs [4]. Knowing that the core treatment for eradicating HCoVs is controlling replication and immune response, offering drug therapies that target both pathways could be the best approach. Some epigenetic therapies have a dual action; resveratrol decreased the expression of NP protein in addition to SIRT-1 activation which counteracts viral replication and hyperinflammation [51]. The anti-viral and anti-inflammatory effects of CQ may play a crucial role in prevention and treatment of COVID-19 as it operated at entry and post-entry phases of SARS-CoV-2 infection [16, 96–98]. Generally, CQ blocks viral infection by elevating endosomal pH necessary for entry, replication, and maturation. For MERS-CoV and SARS-CoV, CQ interfered with cellular proteases and glycosylation of ACE2, respectively [16, 98]. Along with CQ's antiviral effect, CQ decreases the production of pro-inflammatory indicators and cytokines reducing cytokine storm destruction [96, 97]. Merging antiviral drugs with epigenetic therapies targeting hyperinflammation is considered as an alternative. Antivirals (remdesivir, ribavirin, favipiravir, and galidesivir) could be combined with DNMTi (decitabine, azacitidine) or HDACi (vorinostat, belinostat, panobinostat, TSA). However, further preclinical experiments and clinical trials are required to validate the clinical benefits of these combined candidates. Epidemiological studies showed that the majority of severe SARS-CoV-2 cases were elderly patients with comorbid conditions whereas children cases have been rarely reported [3, 54] suggesting the use of anti-aging drugs targeting epigenetics (resveratrol), other anti-aging drugs (CQ, rapamycin, and doxycycline) and senolytics (azithromycin and quercetin) which could decrease substantial morbidity and mortality [99, 100]. Several anti-aging therapeutics exists as FDA-approved drugs with acceptable safety profile proposing their use in COVID-19 prevention [99].

Conclusion and perspectives

Providing more research to generate infection control therapeutic interventions is a major challenge. The three coronavirus global outbreaks emphasized the exigent need for curtailing CoVs infections despite the presence of many therapeutic options including epigenetic therapy, antivirals, and repurposing drugs. Cationic amphiphilic drugs, analogs of previously developed drugs, antibody therapy, structure-based drug design, and combination therapies are considered as researchers' key for further novel antiviral drug development [4, 89]. Safe and effective coronavirus vaccine is the ultimate weapon for reducing morbidity and mortality rates. Coronavirus S protein is considered a strategic board for vaccines [89, 101]. Although several vaccination strategies are being tested against CoVs, these studies are still in progress [14, 89]. Live attenuated and deactivated virus, viral vectors, recombinant DNA, subunit, and protein vaccines are considered as the main approaches [14]. Additional clinical and laboratory evidences must be investigated to validate the use of vaccines proposed by several academic institutions [11, 14, 17, 89, 101]. A recent study specified the clinical benefits of the

microneedle array (MNA) delivered recombinant protein subunit vaccines as a favorable immunization strategy against SARS-CoV, MERS-CoV, and SARS-CoV-2 [101]. In closing, research efforts must be deepened through all outbreak stages to end coronavirus pandemic and epigenetic-targeted therapy could be a major asset in restricting severe HCoV infections.

Abbreviations

3CLpro: 3C-like protease; 5-azadC: 5-aza-2-deoxycytidine; 7SK snRNP: 7SK small nuclear ribonucleoprotein; AAK1: AP2-associated protein kinase 1; ACE: Angiotensin-converting enzyme; ACE2: Angiotensin-converting enzyme 2; ALI: Acute lung injury; AMPK: 5' AMP-activated protein kinase; Ang II: Angiotensin II; Ang1-7: Angiotensin 1-7; AP: Accessory proteins; AP-1: Activator protein 1; APN: Aminopeptidase N; ARDS: Acute respiratory distress syndrome; AT1R: Angiotensin II receptor type 1; AT2: Type II alveolar cells; BET: Bromodomain and extra-terminal motif; BRD: Bromodomain-containing protein; CCL/CXCL: Chemokine; ChIP: Chromatin immuno-precipitation; COVID-19: Coronavirus infectious disease 2019; CoVs: Coronaviruses; CQ: Chloroquine; DCs: Dendritic cells; DDR: DNA damage response; DENV: Dengue virus; DNMT: DNA methyltransferase; DPP4: Dipeptidyl peptidase 4; DZNep: 3Deazaneplanocin-A; E: Envelope; EGR-1: Early growth regulator 1; EZH2/1: Enhancer of zeste homolog 2/1; FDA: Food and Drug Administration; G-CSF: Granulocyte-colony stimulating factor; GS: Gilead Sciences; HAdV: Human adenovirus; HATi: Histone acetyltransferase inhibitors; HCoVs: Human coronaviruses; HDAC: Histone deacetylase; HIV: Human immunodeficiency viruses; HMT: Histone methyltransferases; HPV: Human papilloma virus; HTLV: Human T-lymphotropic virus; HXIM1: Hexamethylene bisacetamide inducible protein; IFN: Interferons; IL: Interleukine; IP10: IFN-γ-inducible protein 10; ISG: IFN sensitive gene; LARP7: La-related protein; M: Membrane; MasR: Mas receptor; MCP1: Monocyte chemoattractant protein; MEPCE: Methyl-phosphate capping enzyme; MERS-CoV: Middle East respiratory syndrome coronavirus; MIP1A: Macrophage inflammatory protein 1-α; MNA: Microneedle array; MyD88: Myeloid differentiation primary response gene 88; NAD: Nicotinamide adenine dinucleotide; NP: Nucleocapsid; Nsp: Non-structural proteins; ORF: Open reading frames; PHEIC: Public Health Emergency of International Concern; PLpro: Papain-like protease; PPAR-α: Peroxisome proliferator-activated receptor alpha; PRR: Prorenin receptor; P-TEFb: Positive transcription elongation factor beta; RAS: Renin-angiotensin system; RdRp: RNA dependent RNA polymerase; S: Spike; SAHA: Suberanilohydroxamic acid; SARS-CoV: Severe acute respiratory syndrome coronavirus; sHLH: Secondary haemophagocytic lymphohistiocytosis; SIRT1: Silent information regulator T1; SOCS1: Suppressor of cytokine signaling 1; SREBP-1: Sterol regulatory element-binding protein 1; STAT1: Signal transducer and activator of transcription 1; TLRs: Toll-like receptors; TNF: Tumor necrosis factor; TNFR: Tumor necrosis factor receptor; *TRIF*: TIR-domain-containing adapter-inducing interferon-β; TRMT1: tRNA methyl transferase 1; TRS: Transcription regulating sequence; TRS-B: Transcription-regulatory sequences in the body; TRS-L: Transcription-regulatory sequences in the leader; TSA: Trichostatin A; VPA: Valproic acid; WHO: World Health Organization

Acknowledgements

Not applicable.

Authors' contributions

ER and HG wrote the paper. All authors read and approved the final manuscript.

Funding

This work was supported by grants from the University of Franche-Comté (UFC). Ranim El Baba is a recipient of a doctoral scholarship from the Hariri Foundation for Sustainable Human Development.

Avaibility of data and materials

Not applicable.

Ethics approval and consent to participate

Not applicable.

Consent for publication

Not applicable.

Competing interests

The authors declare that they have no competing interests.

Author details

[1]Department Pathogens & Inflammation-EPILAB, UPRES EA4266, University of Franche-Comté and University of Bourgogne Franche-Comté, F-25030 Besançon, France. [2]Université Libanaise, Beirut, Lebanon. [3]Department of Virology, CHRU Besancon, F-25030 Besançon, France.

Received: 11 June 2020 Accepted: 22 July 2020
Published online: 05 August 2020

References

1. Shirato K, Kawase M, Watanabe O, Hirokawa C, Matsuyama S, Nishimura H, et al. Differences in neutralizing antigenicity between laboratory and clinical isolates of HCoV-229E isolated in Japan in 2004-2008 depend on the S1 region sequence of the spike protein. J Gen Virol. 2012;93:1908–17.
2. Kooraki S, Hosseiny M, Myers L, Gholamrezanezhad A. Coronavirus (COVID-19) Outbreak: What the Department of Radiology Should Know. J Am Coll Radiol. 2020;17:447–51.
3. Lu R, Zhao X, Li J, Niu P, Yang B, Wu H, et al. Genomic characterisation and epidemiology of 2019 novel coronavirus: implications for virus origins and receptor binding. The Lancet. 2020;395:565–74.
4. Dyall J, Gross R, Kindrachuk J, Johnson RF, Olinger GG, Hensley LE, et al. Middle East respiratory syndrome and severe acute respiratory syndrome: current therapeutic options and potential targets for novel therapies. Drugs. 2017;77:1935–66.
5. Zaki AM, Van Boheemen S, Bestebroer TM, Osterhaus ADME, Fouchier RAM. Isolation of a novel coronavirus from a man with pneumonia in Saudi Arabia. N Engl J Med. 2012;367:1814–20.
6. Lau SKP, Fan RYY, Luk HKH, Zhu L, Fung J, Li KSM, et al. Replication of MERS and SARS coronaviruses in bat cells offers insights to their ancestral origins. Emerg Microbes Infect. 2018;7:209.
7. Josset L, Menachery VD, Gralinski LE, Agnihothram S, Sova P, Carter VS, et al. Cell host response to infection with novel human coronavirus EMC predicts potential antivirals and important differences with SARS coronavirus. mBio. 2013;4:e00165–13.
8. Lai CC, Liu YH, Wang CY, Wang YH, Hsueh SC, Yen MY, et al. Asymptomatic carrier state, acute respiratory disease, and pneumonia due to severe acute respiratory syndrome coronavirus 2 (SARS-CoV-2): Facts and myths. J Microbiol Immunol Infect. 2020;53:404–12.
9. Lim Y, Ng Y, Tam J, Liu D. Human coronaviruses: a review of virus–host interactions. Diseases. 2016;4:26.
10. Mizutani T, Fukushi S, Saijo M, Kurane I, Morikawa S. JNK and PI3k/Akt signaling pathways are required for establishing persistent SARS-CoV infection in Vero E6 cells. Biochim Biophys Acta - Mol Basis Dis. 1741;2005:4–10.
11. Zhou Y, Hou Y, Shen J, Huang Y, Martin W, Cheng F. Network-based drug repurposing for novel coronavirus 2019-nCoV/SARS-CoV-2. Cell Discov. 2020;6:14.
12. Peeri NC, Shrestha N, Rahman MS, Zaki R, Tan Z, Bibi S, et al. The SARS, MERS and novel coronavirus (COVID-19) epidemics, the newest and biggest global health threats: what lessons have we learned? Int J Epidemiol. 2020:1–10.
13. Lai CC, Shih TP, Ko WC, Tang HJ, Hsueh PR. Severe acute respiratory syndrome coronavirus 2 (SARS-CoV-2) and coronavirus disease-2019 (COVID-19): The epidemic and the challenges. Int J Antimicrob Agents. 2020;55:105924.
14. Li X, Geng M, Peng Y, Meng L, Lu S. Molecular immune pathogenesis and diagnosis of COVID-19. J Pharm Anal. 2020;10:102–8.
15. WHO. Coronavirus disease. World Health Organization. 2020. Available at: https://www.who.int/docs/default-source/coronaviruse/situation-reports/20200519-covid-19-sitrep-120.pdf?sfvrsn=515cabfb_4.

16. Omolo CA, Soni N, Fasiku VO, Mackraj I, Govender T. Update on therapeutic approaches and emerging therapies for SARS-CoV-2 virus. Eur J Pharmacol. 2020;173348.
17. Menachery VD, Schäfer A, Burnum-Johnson KE, Mitchell HD, Eisfeld AJ, Walters KB, et al. MERS-CoV and H5N1 influenza virus antagonize antigen presentation by altering the epigenetic landscape. Proc Natl Acad Sci. 2018; 115:E1012–21.
18. Schäfer A, Baric RS. Epigenetic landscape during coronavirus infection. Pathogens. 2017;6:8.
19. Astuti I. Ysrafil. Severe Acute Respiratory Syndrome Coronavirus 2 (SARS-CoV-2): An overview of viral structure and host response. Diabetes Metab Syndr Clin Res Rev. 2020;14:407–12.
20. Salvatori G, Luberto L, Maffei M, Aurisicchio L, Roscilli G, Palombo F, et al. SARS-CoV-2 SPIKE PROTEIN: an optimal immunological target for vaccines. J Transl Med. 2020;18:222.
21. Pinto BG, Oliveira AE, Singh Y, Jimenez L, Goncalves AN, Ogava RL, et al. ACE2 expression is increased in the lungs of patients with comorbidities associated with severe COVID-19. Preprint at: http://medrxiv.org/lookup/doi/10.1101/2020.03.21.20040261 (2020).
22. Yang T, Li S, Zhang X, Pang X, Lin Q, Cao J. Resveratrol, sirtuins, and viruses. Rev Med Virol. 2015;25:431–45.
23. Clarke NE, Belyaev ND, Lambert DW, Turner AJ. Epigenetic regulation of angiotensin-converting enzyme 2 (ACE2) by SIRT1 under conditions of cell energy stress. Clin Sci. 2014;126:507–16.
24. Jang IA, Kim EN, Lim JH, Kim MY, Ban TH, Yoon HE, et al. Effects of resveratrol on the renin-angiotensin system in the aging kidney. Nutrients. 2018;10:1741.
25. Magrone T, Magrone M, Jirillo E. Focus on receptors for coronaviruses with special reference to angiotensin-converting enzyme 2 as a potential drug target - a perspective. endocr metab immune disord - Drug. Targets. 2020;20:807–11.
26. D'Onofrio N, Vitiello M, Casale R, Servillo L, Giovane A, Balestrieri ML. Sirtuins in vascular diseases: Emerging roles and therapeutic potential. Biochim Biophys Acta BBA - Mol Basis Dis. 1852;2015:1311–22.
27. Yacoub R, Lee K, He JC. The Role of SIRT1 in Diabetic Kidney Disease. Front Endocrinol. 2014;5:166.
28. Kim EN, Kim MY, Lim JH, Kim Y, Shin SJ, Park CW, et al. The protective effect of resveratrol on vascular aging by modulation of the renin–angiotensin system. Atherosclerosis. 2018;270:123–31.
29. Cheng H, Wang Y, Wang G. Organ-protective effect of angiotensin-converting enzyme 2 and its effect on the prognosis of COVID-19. J Med Virol. 2020;92:726–30.
30. Verdecchia P, Cavallini C, Spanevello A, Angeli F. The pivotal link between ACE2 deficiency and SARS-CoV-2 infection. Eur J Intern Med. 2020;76:14–20.
31. Devaux CA, Rolain J-M, Raoult D. ACE2 receptor polymorphism: Susceptibility to SARS- CoV-2, hypertension, multi-organ failure, and COVID-19 disease outcome. J Microbiol Immunol Infect. 2020;53:425–35.
32. Wentworth DE, Tresnan DB, Turner BC, Lerman IR, Bullis B, Hemmila EM, et al. Cells of human aminopeptidase N (CD13) transgenic mice are infected by human coronavirus-229E in vitro, but not in vivo. Virology. 2005;335:185–97.
33. Wentworth DE, Holmes KV. Molecular Determinants of Species Specificity in the Coronavirus Receptor Aminopeptidase N (CD13): Influence of N-Linked Glycosylation. J Virol. 2001;75:9741–52.
34. Wulfänger J, Schneider H, Wild P, Ikenberg K, Rodolfo M, Rivoltini L, et al. Promoter methylation of aminopeptidase N/CD13 in malignant melanoma. Carcinogenesis. 2012;33:781–90.
35. Smith EM, Zhang L, Walker BA, Davenport EL, Aronson LI, Krige D, et al. The combination of HDAC and aminopeptidase inhibitors is highly synergistic in myeloma and leads to disruption of the NFκB signalling pathway. Oncotarget. 2015;6:17314–27.
36. Diaz-Jimenez D, Petrillo MG, Busada JT, Hermoso MA, Cidlowski JA. Glucocorticoids mobilize macrophages by transcriptionally up-regulating the exopeptidase DPP4. J Biol Chem. 2020;295:3213–27.
37. Subissi L, Posthuma CC, Collet A, Zevenhoven-Dobbe JC, Gorbalenya AE, Decroly E, et al. One severe acute respiratory syndrome coronavirus protein complex integrates processive RNA polymerase and exonuclease activities. Proc Natl Acad Sci. 2014;111:E3900–9.
38. Zaborowska J, Isa NF, Murphy S. P-TEFb goes viral: The role of P-TEFb in viral infection. BioEssays. 2016;38:S75–85.
39. Ait-Ammar A, Kula A, Darcis G, Verdikt R, De Wit S, Gautier V, et al. Current status of latency reversing agents facing the heterogeneity of HIV-1 cellular and tissue reservoirs. Front Microbiol. 2020;10:3060.
40. Minskaia E, Hertzig T, Gorbalenya AE, Campanacci V, Cambillau C, Canard B, et al. Discovery of an RNA virus 3′→5′ exoribonuclease that is critically involved in coronavirus RNA synthesis. Proc Natl Acad Sci U S A. 2006;103: 5108–13.
41. Budayeva HG, Rowland EA, Cristea IM. Intricate Roles of Mammalian Sirtuins in Defense against Viral Pathogens. J Virol. 2016;90:5–8.
42. Kalbas D, Liebscher S, Nowak T, Meleshin M, Pannek M, Popp C, et al. Potent and Selective Inhibitors of Human Sirtuin 5. J Med Chem. 2018;61: 2460–71.
43. Gu B, Liu C, Lin-Goerke J, Maley DR, Gutshall LL, Feltenberger CA, et al. The RNA helicase and nucleotide triphosphatase activities of the bovine viral diarrhea virus NS3 protein are essential for viral replication. J Virol. 2000;74: 1794–800.
44. Li X, Yang H, Huang S, Qiu Y. Histone deacetylase 1 and p300 can directly associate with chromatin and compete for binding in a mutually exclusive manner. PLoS One. 2014;9:e94523.
45. Gordon DE, Jang GM, Bouhaddou M, Xu J, Obernier K, White KM, et al. A SARS-CoV-2 protein interaction map reveals targets for drug repurposing. Nature. Available at: http://www.nature.com/articles/s41586-020-2286-9 (2020).
46. Ferron F, Decroly E, Selisko B, Canard B. The viral RNA capping machinery as a target for antiviral drugs. Antiviral Res. 2012;96:21–31.
47. Bhardwaj K, Sun J, Holzenburg A, Guarino LA, Kao CC. RNA recognition and cleavage by the SARS coronavirus endoribonuclease. J Mol Biol. 2006;361: 243–56.
48. Pascual MR. Coronavirus SARS-CoV-2: Analysis of subgenomic mRNA transcription, 3CLpro and PL2pro protease cleavage sites and protein synthesis. https://arxiv.org/abs/2004.00746 (2020). Accessed 4 July 2020.
49. Báez-Santos YM, St. John SE, Mesecar AD. The SARS-coronavirus papain-like protease: Structure, function and inhibition by designed antiviral compounds. Antiviral Res. 2015;115:21–38.
50. Dewe JM, Fuller BL, Lentini JM, Kellner SM, Fu D. TRMT1-catalyzed tRNA modifications are required for redox homeostasis to ensure proper cellular proliferation and oxidative stress survival. Mol Cell Biol. 2017;37:e00214–7.
51. Lin SC, Ho CT, Chuo WH, Li S, Wang TT, Lin CC. Effective inhibition of MERS-CoV infection by resveratrol. BMC Infect Dis. 2017;17:144.
52. Taiaroa G, Rawlinson D, Featherstone L, Pitt M, Caly L, Druce J, et al. Direct RNA sequencing and early evolution of SARS-CoV-2. Preprint at: http://biorxiv.org/lookup/doi/10.1101/2020.03.05.976167 (2020).
53. Chu CM, Cheng VCC, Hung IFN, Wong MML, Chan KH, Chan KS, et al. Role of lopinavir/ritonavir in the treatment of SARS: Initial virological and clinical findings. Thorax. 2004;59:252–6.
54. Peiris JSM, Yuen KY, Osterhaus ADME, Stöhr K. The Severe Acute Respiratory Syndrome. N Engl J Med. 2003;349:2431–41.
55. Adhikari SP, Meng S, Wu YJ, Mao YP, Ye RX, Wang QZ, et al. Epidemiology, causes, clinical manifestation and diagnosis, prevention and control of coronavirus disease (COVID-19) during the early outbreak period: A scoping review. Infect Dis Poverty. 2020;9:29.
56. Cheng VCC, Lau SKP, Woo PCY, Kwok YY. Severe acute respiratory syndrome coronavirus as an agent of emerging and reemerging infection. Clin Microbiol Rev. 2007;20:660–94.
57. Koyuncu E, Budayeva HG, Miteva YV, Ricci DP, Silhavy TJ, Shenk T, et al. Sirtuins are evolutionarily conserved viral restriction factors. mBio. 2014;5: e02249–14.
58. Patnaik S. Anupriya. Drugs targeting epigenetic modifications and plausible therapeutic strategies against colorectal cancer. Front Pharmacol. 2019;10: 588.
59. Dejligbjerg M, Grauslund M, Litman T, Collins L, Qian X, Jeffers M, et al. Differential effects of class I isoform histone deacetylase depletion and enzymatic inhibition by belinostat or valproic acid in HeLa cells. Mol Cancer. 2008;7:70.
60. Hu L, Yu Y, Huang H, Fan H, Hu L, Yin C, et al. Epigenetic regulation of interleukin 6 by histone acetylation in macrophages and its role in paraquat-induced pulmonary fibrosis. Front Immunol. 2017;7:696.
61. Dekker FJ, Van Den Bosch T, Martin NI. Small molecule inhibitors of histone acetyltransferases and deacetylases are potential drugs for inflammatory diseases. Drug Discov Today. 2014;19:654–60.
62. Li G, De Clercq E. Therapeutic options for the 2019 novel. Nat Rev Drug Discov. 2020;19:149–50.
63. Zhang H, Kuchroo V. Epigenetic and transcriptional mechanisms for the regulation of IL-10. Semin Immunol. 2019;44:101324.

64. Herbein G, Wendling D. Histone deacetylases in viral infections. Clin Epigenetics. 2010;1:13–24.
65. Zwergel C, Stazi G, Valente S, Mai A. Histone deacetylase inhibitors : updated studies in various epigenetic-related diseases. J Clin Epigenetics. 2016;2:1.
66. Carson WF IV, Cavassani KA, Dou Y, Kunkel SL. Epigenetic regulation of immune cell functions during post-septic immunosuppression. Epigenetics. 2011;6:273–83.
67. Zhao M, Tang J, Gao F, Wu X, Liang Y, Yin H, et al. Hypomethylation of IL10 and IL13 promoters in CD4 + T cells of patients with systemic lupus erythematosus. J Biomed Biotechnol. 2010;2010:1–9.
68. Nehme Z, Pasquereau S, Herbein G. Control of viral infections by epigenetic-targeted therapy. Clin Epigenetics. 2019;11:55.
69. Larsson L, Thorbert-Mros S, Rymo L, Berglundh T. Influence of epigenetic modifications of the interleukin-10 promoter on IL10 gene expression. Eur J Oral Sci. 2012;120:14–20.
70. Iyer SS, Cheng G. Role of interleukin 10 transcriptional regulation in inflammation and autoimmune disease. Crit Rev Immunol. 2012;32:23–63.
71. Cole J, Morris P, Dickman MJ, Dockrell DH. The therapeutic potential of epigenetic manipulation during infectious diseases. Pharmacol Ther. 2016;167:85–99.
72. Keppler BR, Archer TK. Chromatin-modifying enzymes as therapeutic targets – Part 1. Expert Opin Ther Targets. 2008;12:1301–12.
73. Lai YS, Chen JY, Tsai HJ, Chen TY, Hung WC. The SUV39H1 inhibitor chaetocin induces differentiation and shows synergistic cytotoxicity with other epigenetic drugs in acute myeloid leukemia cells. Blood Cancer J. 2015;5:e313.
74. Wang J, Li GL, Ming SL, Wang CF, Shi LJ, Su BQ, et al. BRD4 inhibition exerts anti-viral activity through DNA damage-dependent innate immune responses. PLoS Pathog. 2020;16:e1008429.
75. Mehta S, Jeffrey KL. Beyond receptors and signaling: Epigenetic factors in the regulation of innate immunity. Immunol Cell Biol. 2015;93:233–44.
76. Poppe M, Wittig S, Jurida L, Bartkuhn M, Wilhelm J, Müller H, et al. The NF-κB-dependent and -independent transcriptome and chromatin landscapes of human coronavirus 229E-infected cells. PLoS Pathog. 2017;13:e1006286.
77. Chiusano ML. The modelling of COVID19 pathways sheds light on mechanisms, opportunities and on controversial interpretations of medical treatments. v2. ArXiv200311614 Q-Bio. Available at: http://arxiv.org/abs/2003.11614 (2020).
78. Channappanavar R, Perlman S. Pathogenic human coronavirus infections: causes and consequences of cytokine storm and immunopathology. Semin Immunopathol. 2017;39:529–39.
79. Walsh KB, Teijaro JR, Brock LG, Fremgen DM, Collins PL, Rosen H, et al. Animal model of respiratory syncytial virus: CD8+ T cells cause a cytokine storm that is chemically tractable by sphingosine-1-phosphate 1 receptor agonist therapy. J Virol. 2014;88:6281–93.
80. Mehta P, McAuley DF, Brown M, Sanchez E, Tattersall RS, Manson JJ. COVID-19: consider cytokine storm syndromes and immunosuppression. The Lancet. 2020;395:1033–4.
81. Zhang W, Zhao Y, Zhang F, Wang Q, Li T, Liu Z, et al. The use of anti-inflammatory drugs in the treatment of people with severe coronavirus disease 2019 (COVID-19): The Perspectives of clinical immunologists from China. Clin Immunol. 2020;214:108393.
82. Chen X, Zhao B, Qu Y, Chen Y, Xiong J, Feng Y, et al. Detectable serum SARS-CoV-2 viral load (RNAaemia) is closely associated with drastically elevated interleukin 6 (IL-6) level in critically ill COVID-19 patients. Preprint at: http://medrxiv.org/lookup/doi/10.1101/2020.02.29.20029520 (2020).
83. Sawalha AH, Zhao M, Coit P, Lu Q. Epigenetic dysregulation of ACE2 and interferon-regulated genes might suggest increased COVID-19 susceptibility and severity in lupus patients. Clin Immunol. 2020;215:108410.
84. Ledford H. Coronavirus breakthrough: dexamethasone is first drug shown to save lives. Nature. 2020;582:469.
85. Horby P, Lim WS, Emberson J, Mafham M, Bell J, Linsell L, et al. Effect of Dexamethasone in Hospitalized Patients with COVID-19: Preliminary Report. Preprint at: http://medrxiv.org/lookup/doi/10.1101/2020.06.22.20137273 (2020).
86. Ren Z, Wang L, Cui J, Huoc Z, Xue J, Cui H, et al. Resveratrol inhibits NF-kB signaling through suppression of p65 and Ikappaß kinase activities. Pharmazie. 2013;68:689–94.
87. Pan W, Yu H, Huang S, Zhu P. Resveratrol protects against TNF-α-induced injury in human umbilical endothelial cells through promoting sirtuin-1-induced repression of NF-KB and p38 MAPK. PLoS One. 2016;11:e0147034.
88. Xu L, Botchway BOA, Zhang S, Zhou J, Liu X. Inhibition of NF-κB signaling pathway by resveratrol improves spinal cord injury. Front Neurosci. 2018;12:690.
89. Shereen MA, Khan S, Kazmi A, Bashir N, Siddique R. COVID-19 infection: origin, transmission, and characteristics of human coronaviruses. J Adv Res. 2020;24:91–8.
90. Yasmin R, Siraj S, Hassan A, Khan AR, Abbasi R, Ahmad N. Epigenetic regulation of inflammatory cytokines and associated genes in human malignancies. Mediators Inflamm. 2015;2015:1–8.
91. Yang F, Zhou S, Wang C, Huang Y, Li H, Wang Y, et al. Epigenetic modifications of interleukin-6 in synovial fibroblasts from osteoarthritis patients. Sci Rep. 2017;7:43592.
92. Chen S, Yang J, Wei Y, Wei X. Epigenetic regulation of macrophages: from homeostasis maintenance to host defense. Cell Mol Immunol. 2020;17:36–49.
93. Wang X, Cao Q, Yu L, Shi H, Xue B, Shi H. Epigenetic regulation of macrophage polarization and inflammation by DNA methylation in obesity. JCI Insight. 2016;1:e87748.
94. Thomas G. Middle East respiratory syndrome coronavirus Joint Kingdom of Saudi Arabia/WHO mission. WHO. 2013; https://www.who.int/mediacentre/news/releases/2013/mers_cov_20130610/en/. .
95. Rothan HA, Byrareddy SN. The epidemiology and pathogenesis of coronavirus disease (COVID-19) outbreak. J Autoimmun. 2020;109:102433.
96. Principi N, Esposito S. Chloroquine or hydroxychloroquine for prophylaxis of COVID-19. Lancet Infect Dis. 2020;S1473309920302966.
97. Singh AK, Singh A, Shaikh A, Singh R, Misra A. Chloroquine and hydroxychloroquine in the treatment of COVID-19 with or without diabetes: A systematic search and a narrative review with a special reference to India and other developing countries. Diabetes Metab Syndr Clin Res Rev. 2020;14:241–6.
98. Wang M, Cao R, Zhang L, Yang X, Liu J, Xu M, et al. Remdesivir and chloroquine effectively inhibit the recently emerged novel coronavirus (2019-nCoV) in vitro. Cell Res. 2020;30:269–71.
99. Sargiacomo C, Sotgia F, Lisanti MP. COVID-19 and chronological aging: senolytics and other anti-aging drugs for the treatment or prevention of corona virus infection? Aging. 2020;12:6511–7.
100. Li J, Zhang CX, Liu YM, Chen KL, Chen G. A comparative study of anti-aging properties and mechanism: Resveratrol and caloric restriction. Oncotarget. 2017;8:65717–29.
101. Kim E, Erdos G, Huang S, Kenniston TW, Balmert SC, Carey CD, et al. Microneedle array delivered recombinant coronavirus vaccines: Immunogenicity and rapid translational development. EBioMedicine. 2020;55:102743.

Publisher's Note

Springer Nature remains neutral with regard to jurisdictional claims in published maps and institutional affiliations.

Ready to submit your research? Choose BMC and benefit from:

- fast, convenient online submission
- thorough peer review by experienced researchers in your field
- rapid publication on acceptance
- support for research data, including large and complex data types
- gold Open Access which fosters wider collaboration and increased citations
- maximum visibility for your research: over 100M website views per year

At BMC, research is always in progress.

Learn more biomedcentral.com/submissions

11.2 Publication N°2

Haidar Ahmad S, Al Moussawi F, **El Baba R**, Nehme Z, Pasquereau S, Kumar A, et al. Identification of UL69 Gene and Protein in Cytomegalovirus-Transformed Human Mammary Epithelial Cells. Front Oncol 2021;11:627866. https://doi.org/10.3389/fonc.2021.627866.

A growing body of evidence suggests that human cytomegalovirus (HCMV) is involved in cancer development, particularly in breast tumors. HCMV-infected human mammary epithelial cells (HMECs) give rise to rapidly proliferating, spheroid-shaped cells called CTH cells, indicating HCMV's contribution to oncogenesis. This study focused on the UL69 gene in HCMV, which was detected in CTH cells and breast cancer biopsies. In our experiments, ganciclovir treatment reduced UL69 gene presence and cell proliferation, while UL69 knockdown using siRNA affected HCMV replication and CTH cell growth. These findings highlight the direct role of HCMV in breast tumor development, particularly through the UL69 gene.

frontiers in Oncology

ORIGINAL RESEARCH
published: 16 April 2021
doi: 10.3389/fonc.2021.627866

Identification of UL69 Gene and Protein in Cytomegalovirus-Transformed Human Mammary Epithelial Cells

Sandy Haidar Ahmad[1,2†], *Fatima Al Moussawi*[1,2†], *Ranim El Baba*[1,2], *Zeina Nehme*[1,2], *Sébastien Pasquereau*[1], *Amit Kumar*[1], *Chloé Molimard*[3], *Franck Monnien*[3], *Marie-Paule Algros*[3], *Racha Karaky*[2], *Thomas Stamminger*[4], *Mona Diab Assaf*[2] *and Georges Herbein*[1,5*]

[1] Department Pathogens & Inflammation-EPILAB EA4266, University of Bourgogne France-Comté, Besançon, France, [2] Molecular Cancer and Pharmaceutical Biology Laboratory, Lebanese University, Beyrouth, Lebanon, [3] Department of Pathology, CHRU Besançon, Besançon, France, [4] Institute for Clinical Virology, Ulm University, Ulm, Germany, [5] Department of Virology, CHRU Besancon, Besancon, France

OPEN ACCESS

Edited by:
Victoria Virador,
Virador and Associates, United States

Reviewed by:
Benjamin Anthony Krishna,
Cleveland Clinic, United States
Cyprian Rossetto,
University of Nevada, United States

***Correspondence:**
Georges Herbein
georges.herbein@univ-fcomte.fr

[†]These authors have contributed equally to this work

Specialty section:
This article was submitted to Molecular and Cellular Oncology, a section of the journal Frontiers in Oncology

Received: 10 November 2020
Accepted: 26 March 2021
Published: 16 April 2021

Citation:
Haidar Ahmad S, Al Moussawi F, El Baba R, Nehme Z, Pasquereau S, Kumar A, Molimard C, Monnien F, Algros M-P, Karaky R, Stamminger T, Diab Assaf M and Herbein G (2021) Identification of UL69 Gene and Protein in Cytomegalovirus-Transformed Human Mammary Epithelial Cells. Front. Oncol. 11:627866. doi: 10.3389/fonc.2021.627866

A growing body of evidence addressing the involvement of human cytomegalovirus (HCMV) in malignancies had directed attention to the oncomodulation paradigm. HCMV-DB infected human mammary epithelial cells (HMECs) in culture showed the emergence of clusters of rapidly proliferating, spheroid-shaped transformed cells named CTH (CMV-Transformed HMECs) cells. CTH cells assessment suggests a direct contribution of HCMV to oncogenesis, from key latent and lytic genes activating oncogenic pathways to fueling tumor evolution. We hypothesized that the presence of HCMV genome in CTH cells is of pivotal importance for determining its oncogenic potential. We previously reported the detection of a long non-coding (lnc) *RNA4.9* gene in CTH cells. Therefore, we assessed here the presence of *UL69* gene, located nearby and downstream of the *lncRNA4.9* gene, in CTH cells. The HCMV *UL69* gene in CTH cells was detected using polymerase chain reaction (PCR) and sequencing of *UL69* gene was performed using Sanger method. The corresponding amino acid sequence was then blasted against the *UL69* sequence derived from HCMV-DB genome using NCBI Protein BLAST tool. A 99% identity was present between the nucleotide sequence present in CTH cells and HCMV-DB genome. *UL69* transcript was detected in RNA extracts of CTH cells, using a reverse transcription polymerase chain reaction (RT-PCR) assay, and pUL69 protein was identified in CTH lysates using western blotting. Ganciclovir-treated CTH cells showed a decrease in *UL69* gene detection and cellular proliferation. In CTH cells, the knockdown of *UL69* with siRNA was assessed by RT-qPCR and western blot to reveal the impact of pUL69 on HCMV replication and CTH cell proliferation. Finally, *UL69* gene was detected in breast cancer biopsies. Our results indicate a close link between the *UL69* gene detected in the HCMV-DB isolate used to infect HMECs, and the *UL69* gene present in transformed CTH cells and tumor biopsies, further highlighting a direct role for HCMV in breast tumor development.

Keywords: cytomegalovirus - HCMV, UL69, CTH cells, oncogenesis, latency

INTRODUCTION

Human cytomegalovirus (HCMV) is a large double-stranded DNA virus of the Betaherpesvirinae subfamily, with a genome length of approximately 230 kbp (1). HCMV genome encodes for more than 700 short open reading frames (sORFs) and is composed of two unique regions, each flanked by inverted repeats (2, 3). During the lytic cycle, active viral genome replication results in the release of new viral particles, in contrast to the latency phase, during which a limited number of viral gene products are expressed. Latency is established depending on cell type-specified mechanisms related to transcriptional silencing unlike the reactivation phase triggered by diverse stimuli, for instance infection, inflammation, and injury (4). Studies have shown that HCMV activates pro-oncogenic pathways in infected cells, resulting in a modified cellular phenotype that favors transformation (5, 6). Indeed, HCMV gained a considerable attention in cancer due to many factors that could underlie its potential oncogenic role. The latter includes supporting proliferative signals, evading growth suppression while stimulating metastasis and invasion, permitting replicative immortality and angiogenesis, resisting cell death, escaping immune destruction, as well as inducing genome variability including mutations, and tumor stimulating inflammation (7, 8).

We previously observed that the infection with the clinical strain HCMV-DB resulted in the transformation of HMECs in culture, with the appearance of clusters of spheroid cells that contributed to the formation of CMV-transformed HMECs or CTH cells (6). When xenografted in NOD SCID gamma (NSG) mice, CTH cells underwent unchecked proliferation and gave rise to tumors (6). To determine the potential causal role of HCMV in the transformation of CTH cells, it is critical to detect the presence of HCMV genome in those transformed cells. Since the two oncogenic herpesviruses discovered so far, Epstein-Barr virus (EBV) and Kaposi's sarcoma-associated herpesvirus (KSHV) exploit both latency and low lytic viral replication to fuel the oncogenic process (9–11), we decided to study HCMV genes and proteins expressed in CTH cells, even at low levels. In this context, studies have shown that few HCMV genes such as *UL123* and *UL122* immediate early genes, *UL7*, *UL111A*, *UL112*, *US28*, *US33*, *UL135*, *UL136*, and *lncRNA4.9* could be responsible for the tumorigenic phenotype observed in some human malignancies (12). Previously, we detected the presence of a 126 bp amplicon corresponding to the sequence of *lncRNA4.9* gene (nt95592- nt95717) of HCMV-DB strain in CTH cells (6). Since the previously detected *lncRNA4.9* is a non-coding sequence (6), we decided to further assess the presence of the nearby coding HCMV gene *UL69*, which might be a part of the transformation machinery.

Herein, we detected the presence of *UL69* gene in CTH cells using extensive PCR analysis and sequencing. Using phylogenic analysis, we confirmed that the detected *UL69* gene in CTH cells matches the *UL69* gene sequence of HCMV-DB strain originally used to infect and transform HMECs into CTH cells by 99%. At the proteomic level, the pUL69 sequence present in CTH cells differs from the HCMV-DB original pUL69 only in two amino acid point mutations. At the transcriptome level, we detected the transcript of *UL69* and pUL69 in CTH cells. Besides, in agreement with a coding role for *UL69* HCMV gene, we detected the expression of the pUL69 in CTH cells *in vitro*. Upon *UL69* knockdown using siRNA, we observed a decrease in viral replication and CTH proliferation. *In vivo*, we identified *UL69* gene with a high frequency in biopsies of breast cancer patients.

MATERIALS AND METHODS

Isolation and Culture of CTH Cells

Several clusters of spheroid-cells were observed in HCMV-DB infected HMECs around day 20 post-infection in some of the cultures. These clusters were gently detached and the floating detached cells named CTH cells were cultured in HMEC Ready medium (Cat#12752010, Gibco, Grand Island, NY) for numerous passages, currently >150 passages (6). CTH cells used in this study were cultivated for approximately 410 days. HMECs cultures were infected with HCMV-DB at MOI of 1 as previously reported (13). An inverted light microscope (Olympus, Japan) was used to count cells in CTH cultures.

Detection of the *UL69* Gene in CTH Cells Using PCR and qPCR Assay

Total DNA derived from uninfected HMECs, HCMV-DB infected HMECs, CTH, and MRC5 cells was extracted using a DNA extraction Kit (EZNA Blood DNA Kit, Omega BIO-TEK, Norcross, GA, USA). The presence of the HCMV sequence spanning the *UL69* gene was determined by qualitative PCR assay. The list of primer sets used to screen for the presence of *UL69* from HCMV-DB genome in CTH cells is described in **Supplementary Table 1**. Primer sets were provided by Eurogentec (Seraing, Belgium). Several Taq polymerases were used depending on the size and GC percent content of the amplified fragment. Dream Taq polymerase, KAPA hot start Taq polymerase, and KAPA fast Taq polymerase were ordered from Thermofisher (EP0701) and Sigma-Aldrich (KK1512 and KK4601) respectively. HCMV-DB DNA and lysates of HCMV-DB infected HMECs were used as positive controls. As negative controls, both uninfected HMECs and uninfected MRC5 cells were tested in parallel. Amplified products were electrophoresed in 2% agarose gel stained with Sybr green I nucleic acid stain. As an equal loading control, β-globin gene was amplified (sense: 5′-TCCCCTCCTACC CCTACTTTCTA-3′; antisense: 5′TGCCTGGACTAATC TGCAAGAG-3′). Using real-time qPCR assay, *UL69* load was

Abbreviations: A, adenine; C, cytosine; CDK19, cyclin dependent kinase 19; CTH cells, CMV Transformed HMECs; EBV, Epstein-Barr virus; G, guanine; HCMV, human cytomegalovirus; HMECs, human mammary epithelial cells; IFN, interferon; IHD, ICP27 homology domain; KSHV, Kaposi's sarcoma-associated herpesvirus; LncRNA4.9, long non-coding RNA4.9; MMP-10, matrix metalloproteinase-10; MSA, multi-sequences alignments; NTC, no template control; PCR, polymerase chain reaction; RT, reverse transcriptase; RT-PCR, reverse transcription polymerase chain reaction; SIMs, SUMO-interacting sequences; sORFs, short open reading frames; STING, stimulator of interferon genes; SUMOs, small ubiquitin-like modifiers; T, thymine; WES, whole exome sequencing.

measured in ganciclovir-treated (20 μM for 4 days) and untreated CTH cultures in parallel with the cell counting.

Sequencing of the *UL69* Gene Present in CTH Cells

Fragments amplified by PCR were sequenced using the Sanger method (Genoscreen, Lille, France; GATC, Köln, Germany). PCR products were sent either directly after amplification or after gel cutting to harvest the band of the expected size (in case of several bands). **Supplementary Table 1** includes the primers used for sequencing. PCR amplifications and Sanger's sequencing were repeated twice. The obtained sequences were prepared using the BIOEDIT software (14). Sequences were compared against the sequence of the HCMV-DB strain (accession number KT959235) (13) using NCBI nucleotide blast tool (https://blast.ncbi.nlm.nih.gov/BlastAlign.cgi).

Detection of the *UL69* Transcript by RT-PCR

RNA was extracted from CTH cells using RNA extraction kit (EZNA Total RNA Kit I, Omega BIO-TEK). Following DNAse I treatment for 30 minutes (ThermoFisher), cDNA was synthesized from extracted RNA using Superscript IV First-strand synthesis kit (ThermoFisher) as per manufacturer instructions. cDNA was then used as a template for qualitative PCR amplification using *UL69* primers and Dream Taq polymerase (ThermoFisher) as described above. Lysates of HCMV-DB infected HMECs were used as positive controls. The amplified product was electrophoresed in 2% agarose gel stained with Sybr green I nucleic acid stain.

UL69 knockdown with siRNA performed on CTH cells was assessed by the quantification of *UL69* RNA transcripts. Following RNA extraction and DNAse I treatment as described above, cDNA synthesis was performed. Real-time qPCR detection of UL69 was performed using KAPA SYBR FAST Master Mix (KAPA BIOSYSTEMS, KK4601) and *UL69* gene primers (sense: 5'-GGGATGTCGATGACTCCCTTC-3'; antisense: 5'- GTCG CTATTGGATCTCACCGT-3'), according to the manufacturers' instructions. Real-time qPCR reactions were activated at 95°C for 10 minutes and then 50 cycles (15 s at 95°C and 1 min at 60°C) were conducted using a Stratagene Mx3005P thermocycler (Agilent Technology, Santa Clara, CA, USA). The results were recorded and analyzed using MxPro qPCR software.

Western Blotting

Western blot was performed as described previously (13). Both controls and CTH cells were lysed and proteins were separated by electrophoresis on SDS-PAGE gel. Proteins were transferred to a nitrocellulose membrane. After blocking in 5% milk, the membrane was incubated overnight with 1 μg/ml anti-pUL69 polyclonal antibody (kindly provided by Dr. Stamminger, Erlangen University, Germany). Blots were developed with the ECL detection kit (Amersham Biosciences, Piscataway, NJ).

The siRNA-mediated knockdown of UL69 was assessed by western blot. Cellular extracts of transfected CTH cells with scramble siRNA and UL69 siRNA were prepared at day 1 post-transfection. In addition, cellular extracts of MRC5 infected with HCMV-DB and transfected with scramble siRNA and UL69 siRNA were prepared 24 hours post-transfection. β-actin was used as a control to normalize sample loading.

Flow Cytometry Analysis

The proliferation of CTH cells was assessed using the measurement of Ki67 antigen expression by intracellular flow cytometry as described previously (15).

Soft Agar Assay

Colony formation in soft agar seeded with ganciclovir-treated (20 μM for 4 days) and untreated CTH cells was assayed. Ganciclovir-treated and untreated CTH cells were incubated for 14 days in the semisolid agar medium. Colonies were observed under an Olympus microscope as previously reported (6).

Transfection Assay

A total of 0.25×10^6 cells (HMECs and CTH cells) were transfected with 1-2 μg total plasmid DNA, namely plasmids pUL69, empty pcDNA3.1 (16) and pGFP (17) using JetPEI transfection reagent (Polyplus Transfection, Illkirch, France) as per manufacturers' protocol. pGFP-positive cells were gated and Ki67Ag expression was measured 24 hours post-transfection in pGFP-positive cells using flow cytometry.

RNA Interference

HCMV-DB infected MRC5 and CTH cells were transfected with scramble siRNA or *UL69* siRNA (sense:ACUCAGCCGUU UGAUCGAATT; anti-sense:UUCGAUCAAAC GGCU GAGUTG) (Life Technologies, Carlsbad, CA, USA) using Lipofectamine RNAiMAX (Life Technologies) according to the manufacturer's protocol. Transfection efficiency was monitored 24 hours post-transfection for HCMV-DB infected MRC5 cells by western blot and for CTH cells by RT-qPCR and western blot as described above.

Determination of Amino Acid Sequences

Amino acid sequence derived from *UL69* gene present in CTH cells was obtained using the MBS translator software (http://insilico.ehu.es/translate/) (18). The *UL69* amino acid sequence existing in CTH cells was blasted against the pUL69 sequences derived from the HCMV-DB genome (KT959235) (13) using NCBI protein blast tool (https://blast.ncbi.nlm.nih.gov/Blast.cgi).

Phylogenic Analysis

Multi-sequences alignments (MSA) were performed using CLUSTAL W. Phylogenic tree was obtained using the neighbor-joining method and MEGA7 software (http://www.megasoftware.net/) as previously described (6).

Measurement of HCMV Growth

Viral replication was assessed by the quantification of HCMV load following DNA extraction (EZNA Blood DNA Kit, D3392-02, Omega BIO-TEK) by real-time qPCR detection using KAPA SYBR FAST Master Mix (KAPA BIOSYSTEMS, KK4601) and

primers specific for the IE1 gene (sense: 5'-CGACGTTC CTGCAGACTATG-3'; antisense: 5'-TCCTCGGTCACTTGT TCAAA-3') according to the manufacturer's protocol. Real-time qPCR reactions were activated at 95°C for 10 minutes, followed by 50 cycles (15 seconds at 95°C and 1 minute at 60°C) using a Stratagene Mx3005P thermocycler (Agilent). Results were collected and analyzed using MxPro qPCR software.

Detection of *UL69* DNA in Breast Tumor Tissue

All patients who were admitted to Besançon University Hospital (Besançon, France) gave their written informed consent to participate in the study according to the Helsinki declaration. The study was approved by the local ethics committees of Besançon University Hospital (Besançon, France) and the French Research Ministry (AC-2015-2496, CNIL n°1173545, NF-S-96900 n°F2015). Genomic DNA isolated from biopsies of breast cancer patients (n=30) was provided by the regional tumor bank (BB-0033-00024 Tumorothèque Régionale de Franche-Comté). Paired adjacent healthy tissue (n=29) was utilized in the study. 29 paired adjacent healthy samples match 29 tumor samples, but only one of the tumor samples lacks the corresponding healthy tissue. Breast tissues from non-tumor breast disease (n=4) were used as control. For histological grading of breast cancer biopsies, the Elston-Ellis grade was used with the three factors of grading: tubule formation, nuclear pleomorphism, and mitotic count. Each factor is given a score of 1 to 3 (1 being the best; 3 the worst) and the scores of all the three factors are then added up to give a total of 3 to 9 points indicating the tumor grade. Tumor grade is allocated on the following basis: 3 to 5 points: grade I (well-differentiated); 6 to 7 points: grade II (moderately differentiated); 8 to 9 points: grade III (poorly differentiated) (19). The presence of HCMV was determined by quantitative PCR using *UL69* primers (sense: 5'-GGGATGTCGATGACTCCCTTC-3'; antisense: 5'- GTCGCTA TTGGATCTCACCGT-3') as reported previously (6).

Statistical Analysis

The reported values represent the mean and SD of independent experiments. Statistical analysis was performed using Mann Whitney U test and differences were considered significant at a value of p-value < 0.05. Microsoft Excel was used for plot construction. Correlation analysis was done using Spearman test (Statistical software SPSS 23). Based on Spearman's rank correlation coefficient (rho), all bivariate correlation analyses express the strength of association between two variables where r = +1 (positive correlation) and the value r = -1 (negative correlation). Results were interpreted according to the degree of association as strong (0.7–1), moderate (0.5–0.7), or low (0.3–0.5), taking significant correlation (p-value < 0.05) values into consideration.

RESULTS

Presence of HCMV-DB *UL69* Gene Signature in CTH Cells

Since we previously identified *lncRNA4.9* sequences in CTH cells (7), we screened for the presence of the downstream and nearby *UL69* gene using primers spanning the complete gene region (**Figure 1A**, **Supplementary Table 1**). Using PCR assay, we first detected two HCMV-DB sequences in CTH cells corresponding to 160 bp and 245 bp *UL69* gene amplicons (**Figure 1B**), indicating that the complete *UL69* gene could be present in CTH cells. After

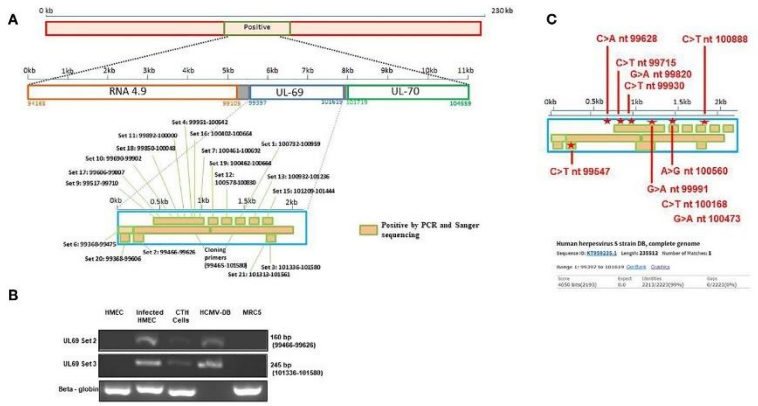

FIGURE 1 | Detection of *UL69* gene in CTH cells. **(A)** Screening strategy used to detect HCMV *UL69* sequences in CTH cells using PCR assay. **(B)** *UL69* amplicons detection in CTH cells using conventional PCR. Uninfected HMECs and MRC5 cells were used as negative controls; HCMV-DB viral stock and infected HMECs were considered as positive controls. β-globin was used as an internal control. Agarose gels show results representative of three independent experiments. The complete primer sets used are described in **Supplementary Table 1**. **(C)** Detection of nucleotide point mutations in HCMV-DB *UL69* sequence present in CTH cells compared to wild-type HCMV-DB virus.

demonstrating the presence of *UL69* genomic sequences in CTH cells, we used several primers sets to span the complete *UL69* gene (**Table 1**). Overall, we were able to detect the existence of a set of viral sequences in CTH cells that corresponds to the complete *UL69* gene (nt99397- nt101619) (**Figure 1B**, **Table 1**). *UL69* amplicons of the same size were also amplified in positive controls, including HMECs infected acutely with HCMV-DB and HCMV-DB viral stock (**Figure 1B**), whereas no HCMV sequences were detected in uninfected HMECs and uninfected MRC5 cells used as negative controls (**Figure 1B**).

Detection of Nucleotide Point Mutations in *UL69* Gene Present in CTH Cells Compared to the Original HCMV-DB Strain

To definitively confirm the presence of *UL69* gene in CTH cells, obtained *UL69* amplicons covering the complete gene were sequenced using the Sanger's method. *UL69* sequences present in CTH cells were then compared to the HCMV-DB genome sequence (KT959235) by using BLAST analysis. We detected ten nucleotide point mutations in the *UL69* sequence obtained from CTH cells compared to the parental HCMV-DB sequence (**Figure 1C**, **Table 2**, **Supplementary Figure 1**). Thoroughly, a 99% identity was established between the *UL69* nucleotide sequence present in CTH cells and HCMV-DB genome (**Figure 1C**, **Supplementary Figure 1**).

Detection of the *UL69* Transcript and Protein in CTH Cells

Following the detection of *UL69* sequence in CTH cells, we subsequently assessed the presence of *UL69* transcript and pUL69 protein in CTH cells. Using RT-PCR assay, we detected *UL69* transcript in RNA extracts of CTH cells (**Figure 2A**). We next analyzed the presence of pUL69 protein in CTH cells using western blotting. MRC5 cells infected with HCMV-DB were used as a positive control (**Figure 2B**). Despite its low levels, pUL69 protein was detected in CTH cells lysates at the expected size (82 kDa) (**Figure 2B**, red arrow). Intriguingly, one additional band of approximately 60 kDa was observed in CTH lysates compared to HCMV-infected MRC5 cells (**Figure 2B**, unidentified band). Amino acid sequence derived from *UL69* gene present in CTH cells was obtained using the MBS translator software (http://insilico.ehu.es/translate/) (18). UL69 amino acid sequence existing in CTH cells was blasted against pUL69 sequence derived from the HCMV-DB genome (KT959235) (13) using NCBI Protein BLAST tool (https://blast.ncbi.nlm.nih.gov/Blast.cgi). Two residue mutations were detected in pUL69 protein in CTH cells compared to the original HCMV-DB strain. The first mutation is at position 564, where the amino acid threonine (T) in HCMV-DB is changed to alanine (A) in CTH cells. The second one is at position 664, where the amino acid aspartic acid (D) is replaced by glutamic acid (E) (**Figure 2C**, **Table 2**).

TABLE 1 | Amplicon positions and sizes of the *UL69* HCMV-DB gene screened in CTH cells using qualitative and/or quantitative PCR.

Gene	Amplicon position	Amplicon size (bp)	PCR amplification result in CTH cells
UL69	99368-99475	108	Positive
	99368-99606	258	Positive
	99465-101580	2115	Positive
	99466-99625	160	Positive
	99517-99710	194	Positive
	99606-99807	202	Positive
	99690-99902	213	Positive
	99850-100048	199	Positive
	99892-100000	109	Positive
	99951-100542	592	Positive
	100402-100664	263	Positive
	100461-100692	232	Positive
	100462-1000664	203	Positive
	100578-100830	253	Positive
	100732-100959	228	Positive
	100932-101236	305	Positive
	101209-101444	236	Positive
	101313-101561	249	Positive
	101336-101580	245	Positive

Phylogenetic Analysis of *UL69* Gene and pUL69 Protein Present in CTH Cells

UL69 gene present in CTH cells was compared to its counterpart present in HCMV-DB genome, in parallel to comparison with ten other clinical and laboratory-adapted HCMV strains described previously (**Figure 3**) (5). We observed that *UL69* genomic sequence in CTH cells was mostly analogous to the *UL69* gene of TB40/E clinical strain than to that of the parental HCMV-DB strain (**Figure 3A**), indicating a shift of the *UL69* genomic sequence from HCMV-DB strain toward TB40/E strain. Similarly, at the protein level, we observed a shift from pUL69 protein of HCMV-DB strain toward TB40/E strain in CTH cells (**Figure 3B**). This analysis was performed over three independent experiments.

Ganciclovir Treatment of CTH Cells Decreases Both *UL69* Gene Detection and Cell Proliferation

Since *UL69* and the previously described *lncRNA4.9* genes are detected in CTH cells, we assessed the presence of *UL69* gene in culture supernatants of CTH cells. We detected a very low viral load (around 2 log copies/ml) in culture supernatants of CTH cells, indicating the incidence of a relatively slow viral lytic cycle rate. Upon ganciclovir treatment, a 95% decrease in the viral load was detected in CTH cultures as measured by *UL69* quantification, further indicating that HCMV is replicating in CTH cells. Interestingly, parallel to the *UL69* decrease, ganciclovir treatment diminished the CTH cell count in culture by 41%, the CTH cell proliferation by 54%, and the size of the colonies observed in soft agar (**Figures 4A–D**).

pUL69 Favors HCMV Replication and CTH Cell Proliferation

To further clarify the role of UL69 protein in CTH cells, we treated CTH cells with *UL69* siRNA and a scramble control. Knockdown of *UL69* transcript and protein in CTH cells was monitored by RT-qPCR assay and western blot, respectively (**Figures 5A, B**). In addition, knockdown of UL69 protein was assessed in MRC5 cells acutely infected with HCMV-DB (**Supplementary Figure 2A**) in parallel with decreased HCMV

TABLE 2 | Detection of nucleotide point mutations in the *UL69* gene present in CTH cells compared to the HCMV-DB.

Mutation position	Nucleotide change between HCMV-DB and CTH cells	Codon change between HCMV-DB and CTH cells	Transcribed Codon change between HCMV-DB and CTH cells	Amino acid in HCMV-DB and CTH cells
99547	T → C	TTG→ CTG	CAA → CAG	Glutamine
99628	A→ C	ATC→CTC	GAU → GAG	Aspartic acid → Glutamic acid
99715	T→ C	TCG→CCG	CGA → CGG	Arginine
99820	A→ G	AGC→GGC	GCU → GCC	Alanine
99930	T→ C	TGT→TGC	ACA → GCU	Threonine → Alanine
99991	A→ G	ATG→GTG	CAU → CAC	Histidine
100168	T→ C	TGA→ CGA	UCA → UCG	Serine
100473	A→ G	CAA→CAG	UUG → CUG	Leucine
100560	G→ A	CAG→CAA	CUG → UUG	Leucine
100888	T→ C	TGA→CGA	UCA → UCG	Serine

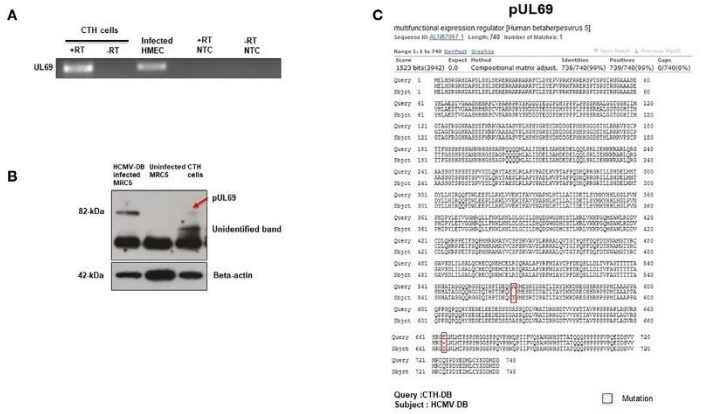

FIGURE 2 | Detection of *UL69* transcript and pUL69 protein in CTH cells. **(A)** RT-PCR assay to detect the presence of *UL69* transcript in RNA extracts of CTH cells in the presence (+) and absence (-) of reverse transcriptase (RT). Infected HMECs were used as a positive control and no template control (NTC) as a negative control. **(B)** Detection of pUL69 protein in CTH cells by western blot. **(C)** Two residue point mutations present in pUL69 in CTH cells when compared to the original pUL69 from HCMV-DB isolate.

replication in culture (**Supplementary Figure 2B**). Knockdown of *UL69* decreased both HCMV growth in CTH cell culture (**Figure 5C**) and CTH cell proliferation (**Figure 5D**). In addition, after overexpressing pUL69 in HMECs and CTH cells, we observed an increase in cell proliferation at 24 hours post-transfection using Ki67Ag detection by flow cytometry (**Figure 5E**). Altogether, our data indicate that *UL69* favors both HCMV replication and cell proliferation in CTH culture.

Detection of *UL69* DNA Within Breast Cancer Biopsies

To further demonstrate the pathophysiological relevance of the CTH cell model *in vivo*, we assessed the expression of the *UL69* gene in the genomic DNA obtained from human breast cancer biopsies and paired adjacent healthy tissue. Breast cancer biopsies were classified into luminal and basal-like biopsies based on the IHC analysis of a pathologist. Breast tissue from patients with non-tumor breast disease was used as control. Using quantitative PCR, *UL69* gene was detected in 43.33% (n=13/30) and 75.85% (n=22/29) of biopsies from breast tumor and paired adjacent healthy breast tissue (**Figure 6A**) (*p*-value=0.01). In addition, *UL69* gene was detected in 53.33% (n=8/15) and 33.33% (n=5/15) of biopsies from luminal and basal-like breast cancer, respectively (**Figure 6A**). In breast tissue taken from patients with non-tumor breast disease, we detected the *UL69* gene in 50% of the cases in agreement with approximately 40%-50% of the French healthy adults harboring the virus (20) with a Ct value of 44.35. Among HCMV-positive (*UL69* gene positive) biopsies, we did not find significant differences in the viral load between paired healthy breast tissue (Ct=44.24), tumor breast tissue (Ct=44.01), luminal breast biopsies (Ct=43.16), and basal-like breast biopsies (Ct=45.38) as measured by quantitative PCR (*UL69* Ct value) (**Figure 6B**). In tumor biopsies, a significant positive correlation was detected between *UL69* Ct value and tubule formation (rho=0.53, *p*-value=0.038). In luminal breast cancer biopsies, a

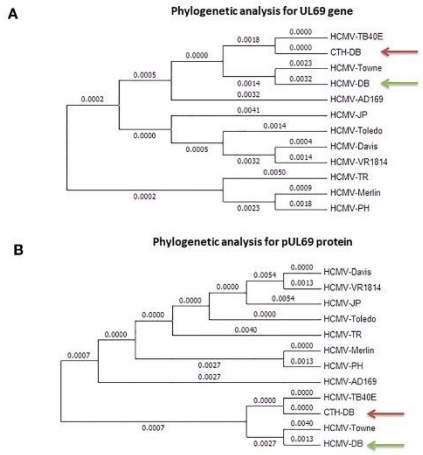

FIGURE 3 | Phylogenetic analysis of *UL69* gene and pUL69 protein present in CTH cells. Phylogenetic analysis of *UL69* gene **(A)** and pUL69 protein **(B)** present in CTH cells compared to the original HCMV-DB strain in addition to other clinical and laboratory-adapted HCMV strains. This analysis was performed over three independent experiments.

significant positive correlation was also found between *UL69* Ct value and tubule formation (rho=0.62, *p*-value=0.05). In addition, in basal-like breast cancer biopsies a significant negative correlation was observed between *UL69* Ct value and nuclear pleomorphism (rho=-0.89, *p*-value=0.05) (**Table 3**).

DISCUSSION

Previously, we reported the transformation of HMECs infected with the HCMV-DB strain, namely the CTH cells (6). To substantiate the causative role of HCMV-DB in HMECs transformation, it is imperative to demonstrate the presence of coding HCMV-DB genes in CTH cells. One short DNA sequence related to the viral *lncRNA4.9* was previously detected in CTH cells. In the present study, we assessed the presence of *UL69* gene located downstream and nearby the *lncRNA4.9*. Upon sequencing the *UL69* gene present in CTH cells, we detected ten nucleotide point mutations that resulted in two amino acid point mutations in pUL69 in comparison with HCMV-DB genome. Remarkably, pUL69 protein, along with its transcript, were detected in CTH cells. Moreover, *UL69* gene was detected in breast cancer biopsies. Overall, our data denote the occurrence of the coding *UL69* gene in CTH cells, with potential pathophysiological relevance in breast cancer.

Earlier, we aimed to determine HCMV-DB signature in CTH cells by whole exome sequencing (WES) adopting Sureselect target enrichment method (21). Using WES, we detected limited sequences of HCMV-DB genomic DNA in the CTH cells genome, where the observed signals were close to the "background noise". Among those weak WES signals in CTH cells, we noticed some hits corresponding to *lncRNA4.9* sequence of HCMV-DB. This was further confirmed by both qualitative and quantitative PCR that amplified a 126 bp fragment of *lncRNA4.9* originating from HCMV-DB, as confirmed by Sanger's sequencing (6).

In the present study, *UL69* gene, its corresponding transcript, and pUL69 protein were detected in CTH cells confirming the availability of the *UL69* gene. The *UL69* gene covers a genomic region of 2.2 kb and encodes for 744 amino acids protein (pUL69) (22). pUL69 is a multifunctional regulatory protein belonging to

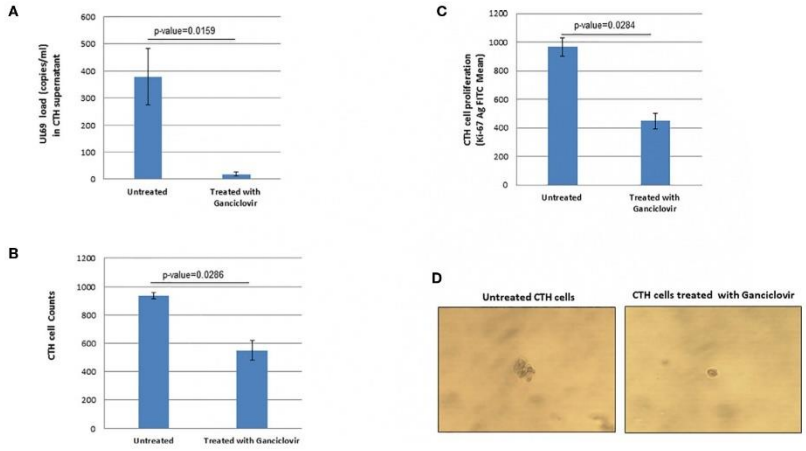

FIGURE 4 | Ganciclovir treatment of CTH cells decreases *UL69* viral load, cell count, and cellular proliferation in culture and reduces colony formation in soft agar. **(A)** Untreated and ganciclovir-treated (20 μM for 4 days) CTH cells were compared for detection of *UL69* gene by qPCR, **(B)** cell counting under the microscope (total magnification of 200x), **(C)** cellular proliferation as measured by Ki67 antigen quantification by flow cytometry, and **(D)** colony formation in soft agar.

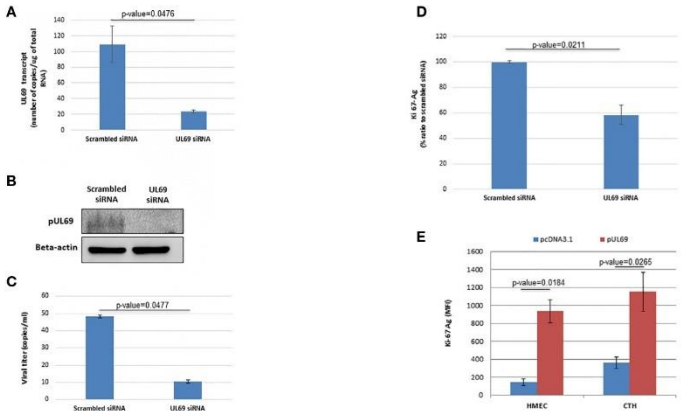

FIGURE 5 | pUL69 favors HCMV replication and cellular proliferation in CTH cells. **(A, B)** Knockdown of *UL69* transcript and protein in CTH cells was monitored by RT-qPCR assay **(A)** and western blot **(B)** respectively. CTH cells were treated with *UL69* siRNA and a scramble control. RT-qPCR assay and western blot were performed as specified in Methods. **(C)** Knockdown of UL69 resulted in decreased HCMV replication in CTH cell cultures as measured by detection of IE1 in culture supernatants by qPCR assay. **(D)** *UL69* knockdown decreased CTH cell proliferation as measured by Ki67Ag quantification (MFI, mean fluorescence intensity) by flow cytometry. **(E)** Overexpression of pUL69 favors the proliferation of HMECs and CTH cells. Increased cellular proliferation as measured by Ki67 antigen quantification (MFI) by flow cytometry in HMEC and CTH cells transfected with pUL69 plasmid. Empty pcDNA3.1 transfected cells were used as control. Results are means (± SD) of three independent experiments.

the ICP27 herpesvirus family (23) which contains the ICP27 homology domain (IHD) (24). pUL69 could participate in the transformation of CTH cells *via* two distinct mechanisms: low viral replication levels in parallel to viral latency as already reported for the two oncoviruses (EBV and KSHV), and/or through a direct oncogenic potential of the viral protein (9–11, 25). Those two mechanisms might not be exclusive to each other. In agreement with low levels of viral replication in sustained CTH transformation by HCMV, we observed decreased levels of *UL69* gene in CTH cells treated with ganciclovir. In parallel, this was accompanied by a decrease in CTH cell count in culture, indicating reduced CTH cell proliferation, in addition to a lower number of colony formation in soft agar. Although we cannot exclude the role of other viral proteins in the maintenance of the CTH cell transformation throughout a prolonged cell culture, *UL69* gene and pUL69 might contribute to the exquisite balance between low viral replication and the transformation process. Thus, comparable to EBV and KSHV, HCMV low replication level could fuel oncogenesis, where pUL69 could be part of this process since it targets several stages of the lytic viral cycle such as transcription, mRNA nuclear export, and translation. Indeed, pUL69 is involved in gene transcription and binds *via* its IHD domain to the cellular transcriptional elongation factor SPT6 which favors chromatin remodeling. Upon knocking-down SPT6, an approximately 90% inhibition of the wild-type replication was detected, thus highlighting the significance of SPT6-UL69 binding in HCMV replication (24, 26, 27). Besides, pUL69 possesses binding motifs for UAP56/URH49 known as cellular mRNA adaptor proteins (28). pUL69 binding to the cellular helicase UAP56 has a role in transcriptional elongation and also promotes the mRNA nuclear export (16, 29). Additionally, pUL69 contains nuclear export and localization sequences that play a vital role in facilitating the shuttle between the nucleus and the cytoplasm (24). Finally, to modulate translation in HCMV-infected cells, pUL69 interacts with part of the cap-binding complex, eIF4A1, and poly (A) binding protein (30). The detection of low levels of pUL69 protein and low viral replication rate in CTH cells are in line with the previously described constrained viral replication in sustained long term cultures of cancerous cell lines infected acutely with HCMV (31, 32). In fact, it has been shown that persistent HCMV infection of tumor cells may lead to the selection of novel virus variants characterized by changes in the coding sequences for virus regulatory proteins that have lost their ability to induce cell cycle arrest. Thus, persistent HCMV infection of tumor cells results in the development of mutant viral variants, that grow slowly and yield lower amounts of progeny virus compared to the wild-type viral strains originally used for infection (31, 33).

Based on *UL69* knockdown (**Figures 5A–D**) and overexpression (**Figure 5E**) experiments, we observed that *UL69* favors both HCMV replication and cell proliferation in CTH cultures. Enhanced cell proliferation could be involved in the sustained growth of CTH cells in culture. In contrast to our data in CTH cells, a pUL69-mediated cell cycle block in G1/S phase has been reported previously in acutely HCMV-infected MRC5 cells (34, 35). The difference in the cell type used (fibroblast versus epithelial cells) and in acute (MRC5 cells) versus chronic (CTH cells) infection could explain the observed discrepancies. In addition, cells with disrupted cell cycle tend to control mechanisms in a similar manner to tumor cells; the function of virus regulatory proteins may depend

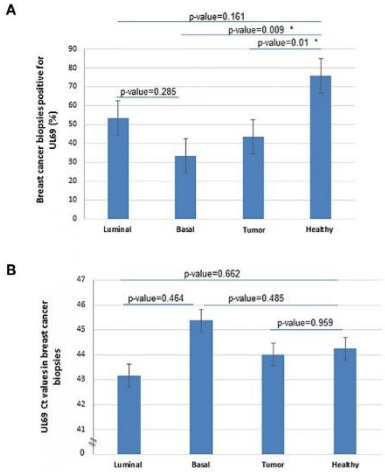

FIGURE 6 | Detection of *UL69* DNA in human breast cancer biopsies. **(A)** Percentage of *UL69*-positive samples (Ct<50) in breast tumor biopsies (n=30), including luminal (n=15) and basal-like (n=15) tumors, and in adjacent healthy paired breast tissue (n=29) using *UL69* quantitative PCR measurement. **(B)** Quantification of HCMV *UL69* DNA in breast tumor biopsies (n=30) compared to healthy adjacent paired breast tissue (n=29), and in patients with basal-like breast cancer (n=15) compared to patients with luminal breast cancer (n=15), as measured by quantitative PCR *UL69* Ct value. * A statistically significant difference at p-value < 0.05. Histogram data are represented as mean ± SD of two independent experiments.

on the internal landscape of tumor cells including p53 and Rb expression/mutation (36). For example, HCMV IE2 protein induces a G1/S block in human cells with wild-type pRb, but not in the human Rb-deficient osteosarcoma cell line Saos-2. Similarly, sustained HCMV infection did not induce cell cycle arrest in T89G glioblastoma cells with disrupted p53 signaling, but virus antigen-positive cells continued to divide (37). Interestingly, we previously reported both a functional defect of p53 and Rb downregulation in CTH cells infected with HCMV-DB (6). These findings indicate that the effects of HCMV on cell cycle and cell proliferation may depend on both the landscape of the internal cellular environment (e.g. p53, Rb) and the properties of virus regulatory proteins such as pUL69 (38). Although we did not yet decipher the molecular mechanism(s) involved in HCMV transformation and the role played by pUL69 (alone or in conjunction with other viral proteins) in this phenomenon, pUL69 favors sustained proliferation of CTH cells in parallel with low sustained viral growth in culture which have been reported as key elements for the transforming capabilities of the two oncogenic herpesviruses EBV and KSHV (25).

In addition to the role of pUL69 in low level viral replication detected in CTH cell cultures, it might also be directly involved in the oncogenic process fueled by HCMV. Notably, the functions of several cellular proteins involved in anti-viral responses and oncogenesis are under the control of certain modifications caused by the small ubiquitin-like modifiers (SUMOs), referred to as SUMOylation. These modifications can change the stability or localization of a specific protein and are capable of enhancing protein-protein interactions through the binding process of SUMOs to the SUMO-interacting sequences (SIMs) (39, 40). SUMOylation acts as a fundamental controller of cell cycle progression, genome stability, senescence, gene expression, stress, and innate immune responses (39, 41, 42). SUMO signal transduction has been identified as a key factor in the development of various cancer types, and SUMOylation was shown to be highly upregulated in several malignancies including breast cancer (39, 43–45). A recent report indicates that pUL69 has a SUMO E3 ligase activity and it can potentially bind to SUMO and Ubc9 (46). Besides, pUL69 takes over the induction of p53 SUMOylation when in complex with Ubc9 and SAE (46). Moreover, in Kaposi's sarcoma-associated herpesvirus (KSHV), K-bZIP represents a SUMO2/3-specific E3 ligase, leading to its own SUMOylation in addition to that of p53 and Rb (47). Since pUL69 protein present in CTH cells possesses an E3 ligase activity, it might induce the inactivation of p53 through SUMOylation, thereby potentially leading to the development of cancer. In addition, a virally-encoded deSUMOylase activity is required for HCMV reactivation from latency (48). In line with the fact that SUMOylation is involved in HCMV latency, it is often considered as a prerequisite for cellular transformation by herpes oncoviruses (7, 25). It should be pointed out that the binding of pUL69 to PRMT6 could be another mechanism elucidating its role in cancer development. We previously noted the upregulation of PRMT6 gene expression in HCMV-infected HMECs (5). The binding of pUL69 to PRMT6 could favor oncogenesis as already reported with the upregulated expression of PRMT6 in prostate cancer (17, 49). Therefore, the multifunctional pUL69 protein might play a complex role in controlling CTH cell transformation. Future studies adopting *UL69* deletion and/or point mutation constructs and UL69-defective HCMV might further assess its direct (or indirect) role in oncogenesis.

TABLE 3 | Correlation between *UL69* Ct value and tumor grade (Elston-Ellis), tubule formation, nuclear pleomorphism and mitotic count in breast cancer biopsies.

	Correlation between UL69 Ct value and			
	Tumor grade	**Tubule formation**	**Nuclear pleomorphism**	**Mitotic count**
			Rho	
All Tumor Biopsies	0.22 (p>0.05)	0.53 (p=0.038)	0.12 (p>0.05)	-0.12 (p>0.05)
Luminal Biopsies	0.109 (p>0.05)	0.62 (p=0.05)	0.50 (p>0.05)	-0.29 (p>0.05)
Basal Biopsies*	NA	NA	-0.89 (p=0.05)	NA

**Since the values for Tumor grade, Tubule formation and Mitotic count in Basal biopsies are constant, the covariance of both variables is zero. Since a non-null covariance is required for correlation tests, the correlation cannot be applied to these constant values, making the correlation coefficient undefined.*

It is worth noting that in macrophages, interferon (IFN) production is inhibited through ICP27-mediated interaction with the active stimulator of interferon genes (STING) signalosome. Knowing that UL69 protein represents the HCMV homolog of ICP27, it compromises the STING signaling pathway and type I IFN production, which might favor viral immune evasion and further cancer cell proliferation and migration (50, 51). Furthermore, a previous study indicated a potential role of the viral immunomodulator cytokine IL-10 during HCMV infection in enhancing breast tumor development and metastasis (52). Likewise, HCMV IL-10 exposed MCF-7 human breast cancer cells showed a significant up-regulation of matrix metalloproteinase-10 (MMP-10) gene expression, thus promoting excessive proliferation and tissue invasion (53).

Although *lncRNA4.9* has been shown to physically interact with the HCMV latent viral chromosome (54), we previously reported the presence of HCMV *lncRNA4.9* gene in breast cancer biopsies (6). In the present study, we detected the presence of the nearby *UL69* gene in breast cancer biopsies. A lower detection of the *UL69* gene (as measured by the percentage of *UL69* positive samples) was observed in breast tumor tissue compared to paired healthy breast tissue, in agreement with the previously reported block of HCMV replication in tumor tissue (55, 56). Since HCMV is detected in both tumor tissue and healthy tissue present in the vicinity of the breast tumor, the presence of HCMV in epithelial cells, tissue macrophages, or endothelial cells in normal breast tissue could fuel cellular transformation leading to breast cancer in some patients.

In conclusion, our findings highlight the potential of a clinical HCMV strain, namely the HCMV-DB isolate, to fulfill all the requirements contributing to the transformation of HMECs *in vitro*, causing the genesis of CTH cells. HCMV could possibly induce transformation through viral gene expression, including the *UL69* gene, which has been hijacked by latent and/or lytic viral cycle toward cellular transformation. The presence of *UL69* DNA in the majority of biopsies isolated from women with breast cancer indicates a potential relevance of *UL69* gene in breast cancer pathophysiology. The study of the *UL69* gene in CTH cells could be relevant to understand the molecular mechanisms involved in the development of breast cancer.

DATA AVAILABILITY STATEMENT

The datasets presented in this study can be found in online repositories. The names of the repository/repositories and accession number(s) can be found in the article/**Supplementary Material**.

ETHICS STATEMENT

The studies involving human participants were reviewed and approved by the study was approved by the local ethics committees of Besançon University Hospital (Besançon, France) and the French Research Ministry (AC-2015-2496, CNIL n°1173545, NF-S-96900 n°F2015). Genomic DNA isolated from biopsies of breast cancer patients (n=30) was provided by the regional tumor bank (BB-0033-00024 Tumorothèque Régionale de Franche-Comté). The patients/participants provided their written informed consent to participate in this study.

AUTHOR CONTRIBUTIONS

SH, FAM, RB, ZN, SP, AK, FM and CM performed experiments. SP, GH, RK, M-PA, MD and TS participated to the data analysis. GH conceived and designed the project. SH, RB, SP and GH wrote the manuscript. All authors contributed to the article and approved the submitted version.

FUNDING

This work was supported by grants from the University of Franche-Comté (CR3300), and the Région Franche-Comté (2020-11890). The funders had no role in the data collection, analysis, patient recruitment, or decision to publish.

SUPPLEMENTARY MATERIAL

The Supplementary Material for this article can be found online at: https://www.frontiersin.org/articles/10.3389/fonc.2021.627866/full#supplementary-material

Supplementary Figure 1 | Blast analysis of *UL69* nucleotide sequence. Comparison of *UL69* gene sequence present in CTH cells (Query) to the wild type HCMV-DB (Subject).

Supplementary Figure 2 | Assessment of pUL69 protein expression and HCMV growth in MRC5 cells treated with UL69 siRNA and siRNA scramble. **(A)** pUL69 expression and **(B)** HCMV growth were monitored 24 hours post transfection with siRNA in HCMV-DB infected MRC5 cells by western blot and detection of IE1 in culture supernatants by qPCR assay, respectively. Results are representative of two independent experiments.

REFERENCES

1. Dolan A, Cunningham C, Hector RD, Hassan-Walker AF, Lee L, Addison C, et al. Genetic content of wild-type human cytomegalovirus. *J Gen Virol* (2004) 85(5):1301–12. doi: 10.1099/vir.0.79888-0
2. Tirosh O, Cohen Y, Shitrit A, Shani O, Le-Trilling VTK, Trilling M, et al. The Transcription and Translation Landscapes during Human Cytomegalovirus Infection Reveal Novel Host-Pathogen Interactions. *PloS Pathog* (2015) 11 (11):e1005288. doi: 10.1371/journal.ppat.1005288
3. Van Damme E, Van Loock M. Functional annotation of human cytomegalovirus gene products: an update. *Front Microbiol* (2014) 5:218. doi: 10.3389/fmicb.2014.00218
4. Forte E, Zhang Z, Thorp EB, Hummel M. Cytomegalovirus Latency and Reactivation: An Intricate Interplay With the Host Immune Response. *Front Cell Infect Microbiol* (2020) 10:130. doi: 10.3389/fcimb.2020.00130
5. Moussawi FA, Kumar A, Pasquereau S, Tripathy MK, Karam W, Diab-Assaf M, et al. The transcriptome of human mammary epithelial cells infected with the HCMV-DB strain displays oncogenic traits. *Sci Rep* (2018) 8(1):12574. doi: 10.1038/s41598-018-30109-1
6. Kumar A, Tripathy MK, Pasquereau S, Al Moussawi F, Abbas W, Coquard L, et al. The Human Cytomegalovirus Strain DB Activates Oncogenic Pathways in Mammary Epithelial Cells. *EBioMedicine* (2018) 30:167–83. doi: 10.1016/j.ebiom.2018.03.015
7. Herbein G. The Human Cytomegalovirus, from Oncomodulation to Oncogenesis. *Viruses* (2018) 10(8):408. doi: 10.3390/v10080408

8. Pasquereau S, Al Moussawi F, Karam W, Diab Assaf M, Kumar A, Herbein G. Cytomegalovirus, Macrophages and Breast Cancer. *Open Virol J* (2017) 11 (1):15–27. doi: 10.2174/1874357901711010015
9. Bristol JA, Djavadian R, Albright ER, Coleman CB, Ohashi M, Hayes M, et al. A cancer-associated Epstein-Barr virus BZLF1 promoter variant enhances lytic infection. *PloS Pathog* (2018) 14(7):e1007179. doi: 10.1371/journal.ppat.1007179
10. Grundhoff A, Ganem D. Inefficient establishment of KSHV latency suggests an additional role for continued lytic replication in Kaposi sarcoma pathogenesis. *J Clin Invest* (2004) 113(1):124–36. doi: 10.1172/JCI200417803
11. Weidner-Glunde M, Kruminis-Kaszkiel E, Savanagouder M. Herpesviral Latency—Common Themes. *Pathogens* (2020) 9(2):125. doi: 10.3390/pathogens9020125
12. Ye L, Qian Y, Yu W, Guo G, Wang H, Xue X. Functional Profile of Human Cytomegalovirus Genes and Their Associated Diseases: A Review. *Front Microbiol* (2020) 11:2104. doi: 10.3389/fmicb.2020.02104
13. Khan KA, Coaquette A, Davrinche C, Herbein G. Bcl-3-Regulated Transcription from Major Immediate-Early Promoter of Human Cytomegalovirus in Monocyte-Derived Macrophages. *J Immunol* (2009) 182(12):7784–94. doi: 10.4049/jimmunol.0803800
14. Hall TA. BioEdit: a user-friendly biological sequence alignment editor and analysis program for Windows 95/98/NT. *Nucleic Acids Symposium Ser* (1999) 41:95–8.
15. Lepiller Q, Abbas W, Kumar A, Tripathy MK, Herbein G. HCMV Activates the IL-6-JAK-STAT3 Axis in HepG2 Cells and Primary Human Hepatocytes. *PloS One* (2013) 8(3):e59591. doi: 10.1371/journal.pone.0059591
16. Lischka P, Toth Z, Thomas M, Mueller R, Stamminger T. The UL69 Transactivator Protein of Human Cytomegalovirus Interacts with DEXD/H-Box RNA Helicase UAP56 To Promote Cytoplasmic Accumulation of Unspliced RNA. *Mol Cell Biol* (2006) 26(5):1631–43. doi: 10.1128/MCB.26.5.1631-1643.2006
17. Thomas M, Sonntag E, Müller R, Schmidt S, Zielke B, Fossen T, et al. pUL69 of Human Cytomegalovirus Recruits the Cellular Protein Arginine Methyltransferase 6 via a Domain That Is Crucial for mRNA Export and Efficient Viral Replication. *J Virol* (2015) 89(18):9601–15. doi: 10.1128/JVI.01399-15
18. Bikandi J, Millan RS, Rementeria A, Garaizar J. In silico analysis of complete bacterial genomes: PCR, AFLP-PCR and endonuclease restriction. *Bioinformatics* (2004) 20(5):798–9. doi: 10.1093/bioinformatics/btg491
19. Elston CW, Ellis IO. pathological prognostic factors in breast cancer. I. The value of histological grade in breast cancer: experience from a large study with long-term follow-up. *Histopathology* (1991) 19(5):403–10. doi: 10.1111/j.1365-2559.1991.tb00229.x
20. Antona D, Lepoutre A, Fonteneau L, Baudon C, Halftermeyer-Zhou F, Le Strat Y, et al. Seroprevalence of cytomegalovirus infection in France in 2010. *Epidemiol Infect* (2017) 145(7):1471–8. doi: 10.1017/S0950268817000103
21. Depledge DP, Palser AL, Watson SJ, Lai IY-C, Gray ER, Grant P, et al. Specific Capture and Whole-Genome Sequencing of Viruses from Clinical Samples. *PloS One* (2011) 6(11):e27805. doi: 10.1371/journal.pone.0027805
22. Kalejta RF. Functions of Human Cytomegalovirus Tegument Proteins Prior to Immediate Early Gene Expression. In: TE Shenk, MF Stinski, editors. *Human Cytomegalovirus*. Berlin, Heidelberg: Springer Berlin Heidelberg (2008). p. 101–15.
23. Winkler M, Rice SA, Stamminger T. UL69 of human cytomegalovirus, an open reading frame with homology to ICP27 of herpes simplex virus, encodes a transactivator of gene expression. *J Virol* (1994) 68(6):3943–54. doi: 10.1128/JVI.68.6.3943-3954.1994
24. Tunnicliffe RB, Collins RF, Ruiz Nivia HD, Sandri-Goldin RM, Golovanov AP. The ICP27 Homology Domain of the Human Cytomegalovirus Protein UL69 Adopts a Dimer-of-Dimers Structure. *mBio* (2018) 9(3):e01112–18. doi: 10.1128/mBio.01112-18
25. Herbein G, Nehme Z. Polyploid Giant Cancer Cells, a Hallmark of Oncoviruses and a New Therapeutic Challenge. *Front Oncol* (2020) 10:567116. doi: 10.3389/fonc.2020.567116
26. Winkler M, aus dem Siepen T, Stamminger T. Functional Interaction between Pleiotropic Transactivator pUL69 of Human Cytomegalovirus and the Human Homolog of Yeast Chromatin Regulatory Protein SPT6. *J Virol* (2000) 74(17):8053–64. doi: 10.1128/JVI.74.17.8053-8064.2000
27. Cygnar D, Hagemeier S, Kronemann D, Bresnahan WA. The Cellular Protein SPT6 Is Required for Efficient Replication of Human Cytomegalovirus. *J Virol* (2012) 86(4):2011–20. doi: 10.1128/JVI.06776-11
28. Thomas M, Müller R, Horn G, Bogdanow B, Imami K, Milbradt J, et al. Phosphosite Analysis of the Cytomegaloviral mRNA Export Factor pUL69 Reveals Serines with Critical Importance for Recruitment of Cellular Proteins Pin1 and UAP56/URH49. *J Virol* (2020) 94(8):e02151–19. doi: 10.1128/JVI.02151-19
29. Zielke B, Thomas M, Giede-Jeppe A, Muller R, Stamminger T. Characterization of the Betaherpesviral pUL69 Protein Family Reveals Binding of the Cellular mRNA Export Factor UAP56 as a Prerequisite for Stimulation of Nuclear mRNA Export and for Efficient Viral Replication. *J Virol* (2011) 85(4):1804–19. doi: 10.1128/JVI.01347-10
30. Aoyagi M, Gaspar M, Shenk TE. Human cytomegalovirus UL69 protein facilitates translation by associating with the mRNA cap-binding complex and excluding 4EBP1. *Proc Natl Acad Sci* (2010) 107(6):2640–5. doi: 10.1073/pnas.0914856107
31. Ogura T, Tanaka J, Kamiya S, Sato H, Ogura H, Hatano M. Human Cytomegalovirus Persistent Infection in a Human Central Nervous System Cell Line: Production of a Variant Virus with Different Growth Characteristics. *J Gen Virol* (1986) 67:2605–16. doi: 10.1099/0022-1317-67-12-2605
32. Cinatl J, Vogel J-U, Cinatl J, Weber B, Rabenau H, Novak M, et al. Long-Term Productive Human Cytomegalovirus Infection of a Human Neuroblastoma Cell Line. *Int J Cancer* (1996) 65:90–6. doi: 10.1002/(SICI)1097-0215(19960103)65:1<90::AID-IJC16>3.0.CO;2-M
33. Furukawa T. A variant of human cytomegalovirus derived from a persistently infected culture. *Virology* (1984) 137(1):191–4. doi: 10.1016/0042-6822(84)90023-0
34. Lu M, Shenk T. Human Cytomegalovirus UL69 Protein Induces Cells To Accumulate in G1 Phase of the Cell Cycle. *J Virol* (1999) 73(1):676–83. doi: 10.1128/JVI.73.1.676-683.1999
35. Hayashi ML, Blankenship C, Shenk T. Human cytomegalovirus UL69 protein is required for efficient accumulation of infected cells in the G1 phase of the cell cycle. *Proc Natl Acad Sci* (2000) 97(6):2692–6. doi: 10.1073/pnas.050587597
36. Cinatl J, Vogel J-U, Kotchetkov R, Wilhelm Doerr H. Oncomodulatory signals by regulatory proteins encoded by human cytomegalovirus: a novel role for viral infection in tumor progression. *FEMS Microbiol Rev* (2004) 28(1):59–77. doi: 10.1016/j.femsre.2003.07.005
37. Luo MH, Fortunato EA. Long-Term Infection and Shedding of Human Cytomegalovirus in T98G Glioblastoma Cells. *J Virol* (2007) 81(19):10424–36. doi: 10.1128/JVI.00866-07
38. Michaelis M, Doerr HW, Cinatl J. The Story of Human Cytomegalovirus and Cancer: Increasing Evidence and Open Questions. *Neoplasia* (2009) 11(1):1–9. doi: 10.1593/neo.81178
39. Eifler K, Vertegaal ACO. SUMOylation-Mediated Regulation of Cell Cycle Progression and Cancer. *Trends Biochem Sci* (2015) 40(12):779–93. doi: 10.1016/j.tibs.2015.09.006
40. Flotho A, Melchior F. Sumoylation: A Regulatory Protein Modification in Health and Disease. *Annu Rev Biochem* (2013) 82(1):357–85. doi: 10.1146/annurev-biochem-061909-093311
41. Hoellein A, Fallahi M, Schoeffmann S, Steidle S, Schaub FX, Rudelius M, et al. Myc-induced SUMOylation is a therapeutic vulnerability for B-cell lymphoma. *Blood* (2014) 124(13):2081–90. doi: 10.1182/blood-2014-06-584524
42. Rabellino A, Andreani C, Scaglioni PP. The Role of PIAS SUMO E3-Ligases in Cancer. *Cancer Res* (2017) 77(7):1542–7. doi: 10.1158/0008-5472.CAN-16-2958
43. Seeler J-S, Dejean A. SUMO and the robustness of cancer. *Nat Rev Cancer* (2017) 17(3):184–97. doi: 10.1038/nrc.2016.143
44. Bawa-Khalfe T, Yeh ETH. SUMO Losing Balance: SUMO Proteases Disrupt SUMO Homeostasis to Facilitate Cancer Development and Progression. *Genes Cancer* (2010) 1(7):748–52. doi: 10.1177/1947601910382555
45. Kessler JD, Kahle KT, Sun T, Meerbrey KL, Schlabach MR, Schmitt EM, et al. A SUMOylation-Dependent Transcriptional Subprogram Is Required for Myc-Driven Tumorigenesis. *Science* (2012) 335(6066):348–53. doi: 10.1126/science.1212728
46. De La Cruz-Herrera CF, Shire K, Siddiqi UZ, Frappier L. A genome-wide screen of Epstein-Barr virus proteins that modulate host SUMOylation identifies a SUMO E3 ligase conserved in herpesviruses. *PloS Pathog* (2018) 14(7):e1007176. doi: 10.1371/journal.ppat.1007176
47. Chang P-C, Izumiya Y, Wu C-Y, Fitzgerald LD, Campbell M, Ellison TJ, et al. Kaposi's Sarcoma-associated Herpesvirus (KSHV) Encodes a SUMO E3 ligase That Is SIM-dependent and SUMO-2/3-specific. *J Biol Chem* (2010) 285 (8):5266–73. doi: 10.1074/jbc.M109.088088

48. Poole EL, Kew VG, Lau JCH, Murray MJ, Stamminger T, Sinclair JH, et al. A Virally Encoded DeSUMOylase Activity Is Required for Cytomegalovirus Reactivation from Latency. *Cell Rep* (2018) 24(3):594–606. doi: 10.1016/j.celrep.2018.06.048
49. Almeida-Rios D, Graça I, Vieira FQ, Ramalho-Carvalho J, Pereira-Silva E, Martins AT, et al. Histone methyltransferase PRMT6 plays an oncogenic role of in prostate cancer. *Oncotarget* (2016) 7(33):53018–28. doi: 10.18632/oncotarget.10061
50. Christensen MH, Jensen SB, Miettinen JJ, Luecke S, Prabakaran T, Reinert LS, et al. HSV -1 ICP 27 targets the TBK 1-activated STING signalsome to inhibit virus-induced type I IFN expression. *EMBO J* (2016) 35(13):1385–99. doi: 10.15252/embj.201593458
51. Banete A, Seaver K, Bakshi D, Gee K, Basta S. On taking the STING out of immune activation. *J Leukoc Biol* (2018) 103(6):1189–95. doi: 10.1002/JLB.2MIR0917-383R
52. Valle Oseguera CA, Spencer JV. Human cytomegalovirus interleukin-10 enhances matrigel invasion of MDA-MB-231 breast cancer cells. *Cancer Cell Int* (2017) 17(1):24. doi: 10.1186/s12935-017-0399-5
53. Bishop RK, Valle Oseguera CA, Spencer JV. Human Cytomegalovirus interleukin-10 promotes proliferation and migration of MCF-7 breast cancer cells. *Cancer Cell Microenviron* (2015) 2(1):e678. doi: 10.14800/ccm.678
54. Rossetto CC, Tarrant-Elorza M, Pari GS. Cis and Trans Acting Factors Involved in Human Cytomegalovirus Experimental and Natural Latent Infection of CD14 (+) Monocytes and CD34 (+) Cells. *PloS Pathog* (2013) 9 (5):e1003366. doi: 10.1371/journal.ppat.1003366
55. Xu S, Schafer X, Munger J. Expression of Oncogenic Alleles Induces Multiple Blocks to Human Cytomegalovirus Infection. *J Virol* (2016) 90(9):4346–56. doi: 10.1128/JVI.00179-16
56. Nauclér CS, Geisler J, Vetvik K. The emerging role of human cytomegalovirus infection in human carcinogenesis: a review of current evidence and potential therapeutic implications. *Oncotarget* (2019) 10(42):4333–47. doi: 10.18632/oncotarget.27016

Conflict of Interest: The authors declare that the research was conducted in the absence of any commercial or financial relationships that could be construed as a potential conflict of interest.

Copyright © 2021 Haidar Ahmad, Al Moussawi, El Baba, Nehme, Pasquereau, Kumar, Molimard, Monnien, Algros, Karaky, Stamminger, Diab Assaf and Herbein. This is an open-access article distributed under the terms of the Creative Commons Attribution License (CC BY). The use, distribution or reproduction in other forums is permitted, provided the original author(s) and the copyright owner(s) are credited and that the original publication in this journal is cited, in accordance with accepted academic practice. No use, distribution or reproduction is permitted which does not comply with these terms.

11.3 Publication N°3

El Baba R, Herbein G. Immune Landscape of CMV Infection in Cancer Patients: From "Canonical" Diseases Toward Virus-Elicited Oncomodulation. Front Immunol 2021;12:730765. https://doi.org/10.3389/fimmu.2021.730765.

Human cytomegalovirus (HCMV) is a highly prevalent herpesvirus that persistently infects a significant portion of the global population. Despite robust host immune responses, HCMV has evolved multiple immune-modulatory strategies to replicate, evade host defenses, and establish lifelong latency. It achieves this by impairing the expression of HLA Class I and II molecules, evading natural killer cell-mediated cytotoxicity, interfering with cellular signaling, inhibiting apoptosis, escaping complement attack, and inducing immunosuppressive cytokines. HCMV also expresses various gene products that modulate the host immune response and affect non-coding RNA and regulatory proteins. These immune evasion strategies are associated with complications such as immunosenescence and malignant phenotypes, resulting in an immunosuppressive tumor microenvironment and oncomodulation. Consequently, HCMV's role in promoting tumor survival involves influencing cellular proliferation, survival, invasion, immune evasion, immunosuppression, and the production of angiogenic factors. Understanding HCMV's immune evasion mechanisms is crucial for developing adapted therapeutic approaches, particularly in the era of immunotherapy, which has transformed cancer treatment. By employing multimodal strategies that induce immunogenic tumor apoptosis and counteract the immune-suppressive microenvironment, it may be possible to enhance anti-tumor immunity.

frontiers in Immunology

REVIEW
published: 08 September 2021
doi: 10.3389/fimmu.2021.730765

Immune Landscape of CMV Infection in Cancer Patients: From "Canonical" Diseases Toward Virus-Elicited Oncomodulation

Ranim El Baba[1] *and Georges Herbein*[1,2*]

[1] Department Pathogens & Inflammation-EPILAB EA4266, University of Franche-Comté UBFC, Besançon, France,
[2] Department of Virology, Centre hospitalier régional universitaire de Besançon (CHRU) Besançon, Besancon, France

Human Cytomegalovirus (HCMV) is an immensely pervasive herpesvirus, persistently infecting high percentages of the world population. Despite the apparent robust host immune responses, HCMV is capable of replicating, evading host defenses, and establishing latency throughout life by developing multiple immune-modulatory strategies. HCMV has coexisted with humans mounting various mechanisms to evade immune cells and effectively win the HCMV-immune system battle mainly through maintaining its viral genome, impairing HLA Class I and II molecule expression, evading from natural killer (NK) cell-mediated cytotoxicity, interfering with cellular signaling, inhibiting apoptosis, escaping complement attack, and stimulating immunosuppressive cytokines (immune tolerance). HCMV expresses several gene products that modulate the host immune response and promote modifications in non-coding RNA and regulatory proteins. These changes are linked to several complications, such as immunosenescence and malignant phenotypes leading to immunosuppressive tumor microenvironment (TME) and oncomodulation. Hence, tumor survival is promoted by affecting cellular proliferation and survival, invasion, immune evasion, immunosuppression, and giving rise to angiogenic factors. Viewing HCMV-induced evasion mechanisms will play a principal role in developing novel adapted therapeutic approaches against HCMV, especially since immunotherapy has revolutionized cancer therapeutic strategies. Since tumors acquire immune evasion strategies, anti-tumor immunity could be prominently triggered by multimodal strategies to induce, on one side, immunogenic tumor apoptosis and to actively oppose the immune suppressive microenvironment, on the other side.

Keywords: HCMV, immunosuppression, immune evasion, immunosenescense, TME, oncomodulation, therapeutic approaches

OPEN ACCESS

Edited by:
Rebeca Alonso-Arias, Central University Hospital of Asturias, Spain

Reviewed by:
Sarah Elizabeth Jackson, University of Cambridge, United Kingdom
Jean-Pierre Routy, McGill University, Canada

***Correspondence:**
Georges Herbein
georges.herbein@univ-fcomte.fr

Specialty section:
This article was submitted to Viral Immunology, a section of the journal Frontiers in Immunology

Received: *25 June 2021*
Accepted: *23 August 2021*
Published: *08 September 2021*

Citation:
El Baba R and Herbein G (2021) Immune Landscape of CMV Infection in Cancer Patients: From "Canonical" Diseases Toward Virus-Elicited Oncomodulation. Front. Immunol. 12:730765. doi: 10.3389/fimmu.2021.730765

BACKGROUND

HCMV or human herpesvirus 5 (HHV-5) has co-evolved with mammalian hosts over millennia infecting almost 83% of the world's population, impending 100% in developing countries (1). After initial infection, HCMV can establish lifelong persistence within its corresponding host as well as possessing the reactivation potential; viral persistence depends on composite interactions among various

viral and host determinants. Such interactions mostly generate an equilibrium between the immunocompetent host and the virus itself. In the host, HCMV infrequently causes symptoms unless this balance is demolished by the minimized host immune proficiency (atypical settings) leading to substantial pathology (1, 2). Upon viewing several forms of viral-host interaction, the explicit HCMV reactivation in immunosuppressed patients (organ transplant recipients) and immunocompromised patients (septic patients, elderly, HIV-infected patients, etc.) is considered a well identifiable disease state (3, 4). Hence, in immunocompetent patients, HCMV is considered a multifaceted beta herpesvirus that is viewed as an asymptomatic and mildly pathogenic virus, but may nevertheless cause chronic infections along with acute and serious complications in immunocompromised individuals (5). HCMV persistence can also have a key influence on the host, even in healthy carriers, through the attenuation of innate and adaptive immune responses since HCMV starts to counteract several host immune response mechanisms required to control the infection (1, 2). HCMV potentially triggers the host immune responses starting by the mechanisms of innate immunity, including inflammatory cytokines resulting from virus/cell binding and NK cell induction which consequently drives adaptive immune responses, involving production of antibodies and the initiation of $CD4^+$ and $CD8^+$ T-cell responses. However, HCMV encodes various immune evasion mechanisms; hence, expressing several genes that influence both innate and adaptive immunity (5, 6).

HCMV, a leading viral cause of birth defects, has been linked to several mortality and morbidity conditions (7). The stage of HCMV acquisition may affect the range of associated clinical manifestations and the effectiveness of the immune responses exerted against HCMV (7, 8). Regarding congenital CMV infection, neurological defects might be experienced as mental retardation, cerebral palsy, and hearing impairment; newborns may experience either symptomatic or asymptomatic infections (7, 9, 10). Symptomatic infections might cause petechiae, low birth weight, jaundice, hepatosplenomegaly, seizures, and microcephaly; they appear to be more common in newborns infected during the first trimester of pregnancy (7). In case of premature birth, sepsis and respiratory distress can develop (11). Compared to adults, these observations indicate that controlling CMV replication is restricted during early stages of life and is associated with delayed immune responses and increased risk of symptomatic infection (7). Years later, persistent HCMV infection might be considered a potential risk factor exacerbating age-associated diseases and immunosenescence which is defined as the age-associated deterioration in overall immune condition (12–14) although some studies have indicated that the link between HCMV and immune aging is obscure (3, 15). Further, various stimuli can induce HCMV reactivation; it might be triggered in SARS-CoV-2 infected patients (16, 17) thus exacerbating the risk of coronavirus disease 2019 (COVID-19) (18, 19). Even if this interaction is still elusive and additional large scale studies are recommended (16), CMV testing and treatment should be taken into consideration in such critical conditions (18). CMV status must be taken into account for several vaccine responses, especially cancer despite the use of HCMV-based therapeutic cancer vaccines (20), since it has been suggested that with advanced age and due to CMV-associated altered immunity in both healthy and immunocompromised hosts, vaccine immunogenicity was modulated (21–23). Thus, recent studies are concerned about targeting HCMV to decrease the sensitivity to other infectious diseases and cancer, and to prevent poor responses to vaccination (21, 22).

The contribution of HCMV infection in late inflammatory complications highlights its potential association with chronic diseases, such as atherosclerosis, chronic rejection following solid-organ transplantation, and malignancies (24). Recent investigations have reported the prevalence of HCMV infection in tumoral tissues of malignancies such as malignant glioma, breast and colon cancer, negative Hodgkin's disease, Epstein-Barr virus (EBV), liver cancer, cervical cancer, and prostatic carcinoma (1, 25, 26). Despite the fact that HCMV is not yet included in the oncogenic viruses list, its possible contribution in carcinogenesis as initiator or promoter is significantly reported suggesting that HCMV and tumors express a symbiotic relationship (26–29). HCMV aids the tumor to escape immune surveillance by encoding viral proteins and inducing various cellular factors, in addition to the HCMV-induced immune tolerance which favors tumor growth. In return, HCMV harbors in the immunologically weak environment of the cancerous cells (6). This review accentuates the considerable influence of HCMV on the immune landscape and its oncomodulatory signals that might contribute to oncogenesis.

HOST IMMUNE RESPONSES AGAINST HCMV INFECTION

HCMV, a double-stranded DNA (dsDNA) genome beta-herpesvirus is considered the largest virus among the human herpesviruses (30). Upon HCMV infection and despite the counteracting host response, this virus powerfully adapts to the human immune system. HCMV is certainly not eradicated from the HCMV-positive immunocompetent patient, in whom the virus establishes latency (31). Thus, the human immune system is incompetent to clear the latent HCMV, however it mounts an immune defense targeting multiple viral proteins (8). Due to the existing coevolution between HCMV and the host immune system for millions of years, it's informative to study the immune defense strategies and pathogen counterstrategies (12). Innate immunity, in addition to adaptive humoral and cell-mediated immune responses, are induced by HCMV infection; such responses lead to the resolution of acute primary infection (5). Such immune responses differ during distinct life stages; throughout pregnancy, maternal anti-HCMV antibodies participate in preventing congenital fetal CMV infection (32). In addition, studies have shown that despite the detection of primary humoral and cellular immune responses in neonates, cell-mediated immune responses are delayed compared to adults which justifies the reason behind uncontrolled viremia and serious clinical harm in early life CMV infections (8, 32, 33). CMV-specific $CD8^+$ T-cell responses in congenitally infected newborns were characterized by lower IFN-γ levels and elevated

levels of IL-8 compared to adults (33). Finally, elderly people have increased sensitivity and susceptibility to serious infections and diseases most likely due to immunosenescence (14).

HCMV Entry

HCMV exhibits a wide host cell range, possessing the ability to infect several cell types for instance endothelial cells, epithelial cells, fibroblasts, smooth muscle cells, leukocytes, and dendritic cells (DCs) (8, 34). In healthy persons, HCMV initiates its replication in the mucosal epithelium; thereafter, it disperses to monocytes and CD34+ cells, where it institutes a latent infection. Upon differentiation of HCMV-infected monocytes into macrophages, a viral infection could be initiated (35). Infection of both hematopoietic and endothelial cells systemically eases the viral spread within the host (36), unlike prevalent cell types infection including smooth muscle cells and fibroblasts which enhances efficient proliferation of the virus (35).

Innate Immunity

As HCMV enters the cells, virions are firstly recognized by the host thus activating multiple pathways and strategies of innate immunity which is known as the primary host defense against HCMV infection (8). These involve inflammatory cytokines, type I interferon (IFN), and upregulation of CD80 and CD86 (37) that are essential for limiting pathogen's spread and thereafter priming the adaptive immune response (5, 8). The stimulation of the NF-κB pathway and predominant inflammatory cytokines production for example interleukin-6 (IL-6) and tumor necrosis factor-alpha (TNF-α) (38) result from the interaction of viral envelope glycoproteins B (gB) and glycoprotein H (gH) with the immune-sensor molecules namely, toll-like receptors 2 (TLR2) (5, 12, 39, 40). Such inflammatory cytokines are capable of inducing and triggering phagocytic cells, such as dendritic cells, which have the ability to clear HCMV-infected cells (5, 8, 38). In the initial infection sites, NK cells are activated to eradicate HCMV-infected cells by the liberation of cytotoxic proteins (38). Furthermore, studies have shown NK cells' role in inhibiting HCMV transmission in fibroblasts, epithelial, and endothelial cells and this through inducing IFN-β in target infected cells (41) and secretion of IFN-γ (42). NK cells, crucial guards of the immune system, produce a cytokine environment that triggers the consequential maturation of adaptive immune responses particularly T-cells (5, 8, 43).

Adaptive Immunity

The adaptive immunity which contributes to the control of HCMV infection is among the strongest responses in which it fully engages humoral and cellular immune responses. Adaptive immunity is necessary to fundamentally manage HCMV primary infection, afterwards HCMV will enter into a latent state (44). The development of a sustained adaptive immune response is essential to preserve HCMV latency, avert acute viremia, and avert lytic infection which, in contrast, is frequent in patients on immunosuppressive therapies and immunocompromised individuals often leading to unrestricted replication and clinically severe HCMV morbidity and mortality (45).

Humoral Responses

Following a primary HCMV infection, the initiation of a robust immune response to control HCMV is essentially required. Many evidences supported the role of humoral immunity in limiting viral propagation and HCMV severity through antibody production targeting multiple CMV proteins, envelope glycoproteins, and genes (8, 32). The key target for antibody neutralization against HCMV is gB since it is related to cellular adhesion and invasion; besides, gH is considered the secondary target as it is involved in the fusion of the host cell membrane with the viral envelope (37). Other targets include the structural tegument proteins (pp65 and pp150) and non-structural proteins (IE1) (8, 32). A study shows that pregnant women, primarily infected with HCMV, having HCMV specific IgM antibodies and missing neutralizing IgG antibodies are at greater risk of transmitting HCMV to their fetus in contrast to seropositive mothers experiencing a recurrent infection (45). Thus, underlying the critical role of humoral immunity, especially HCMV IgG, in controlling HCMV infection and spread.

T-Cell Mediated Immune Responses

Due to the fact that the immune response stimulated by primary infection does not eliminate HCMV, HCMV-specific $CD4^+$ T-cells, $CD8^+$ T-cells, and gamma delta (γδ) T-cells have been considered as critical players in restricting viral replication in hosts acquiring persistent infections (38, 46, 47). With regard to $CD8^+$ T-cells, the $CD8^+$ HCMV-specific T-cell response is targeted toward HCMV proteins which are being expressed at different stages of viral replication (IE, early, early-late, and late) in addition to other proteins possessing various functions (capsid, tegument, glycoprotein, DNA-regulatory, and immune escape) (37). It is worth noting that the most immunodominant antigens to which HCMV-specific $CD8^+$ T-cells react are addressed toward IE1 (UL123), IE2 (UL122), and pp65 (UL83) (37, 48). Even though the major histocompatibility complex (MHC) class I-restricted $CD8^+$ T-cell immune response role in targeting HCMV is evidently marked, there exists a significant indication that $CD4^+$ T-cells are as well fundamental in controlling HCMV infections (37). Further studies reveal the attainment of a cytolytic potential by pp65-specific $CD4^+$ T-cells and gB-specific $CD4^+$ CTL *in vivo* where $CD4^+$ T-cells released granzyme B in reaction to glia presenting endogenous gB (49). The recruitment of HCMV-specific T-cells into the memory compartment is stimulated by the relatively prolonged viral replication of HCMV since T-cells are mandatory to limit HCMV viral replication and impede certain diseases (50). HCMV-specific T-cell responses inflate throughout life leading to a significant fraction of memory T-cells in healthy seropositive individuals (50–52). Hence, HCMV-seropositive immunocompetent people maintain lifetime protection despite the insufficient or minimal HCMV-specific T-cell responses. Cellular responses from $CD4^+$ and $CD8^+$ T-cells vary among individuals (50). HCMV-positive serostatus has been associated with $CD8^+$ T-cell compartment expansion, reduced CD4:CD8 T-cell ratio as well as alterations in the expression of CD8+ T-cell senescence related markers (53, 54). These senescent cells are characterized by a progressive loss of CD28 and CD27,

upregulation of CD57 expression which is known as the classical immune senescence marker, replicative senescence, and shortened telomeres resulting in a limited cell proliferation capacity and finally the inability to eliminate the HCMV infection (14, 55). Other cellular responses include γδ T-cells and NK cells. Although the previously mentioned cells are not targeted specifically against HCMV, they can still successfully lyse HCMV-infected endothelial cells and fibroblasts in consequence of a cellular stress response that upregulates the endothelial protein C receptor (EPCR) in addition to CD54 (Intercellular adhesion molecule-1, *ICAM-1*) (56). γδ T-cells contribute to dual immune response, anti-infectious and antitumor. Activated γδ T-cells are essential immune effectors against HCMV in which they stimulate IFN-γ and TNF-α production that may synergize to inhibit HCMV replication (38).

HCMV PERSISTENCE DESPITE ANTIVIRAL IMMUNITY

In healthy individuals, the operative homeostatic equilibrium established between HCMV and the host prevents serious HCMV complications. Conversely, in an immunocompromised host, fetus, and neonates, HCMV infection can cause multiple forms of clinical harm (8). Disequilibrium in immunocompromised patients can result in unhindered viral replication followed by the reactivation of the latent virus, with subsequent morbidity and mortality (5). Despite a powerful immunity involving both arms of the immune system, HCMV establishes latency. In that context, HCMV-encoded determinants of tropism for endothelial cells, an imperative objective of the infection, were considered. It was stated that in endothelial cells the UL133-UL138 locus, encoded in the ULb′ region of the HCMV genome, is essential for the viral late-stage response (57). In infected cells, this locus was mandatory for preserving membrane organization and is required for the progeny viruses' maturation. However, it's not necessary for early/late gene expression or viral genome synthesis. Viruses missing the *UL133-UL138* region, produce progeny viruses that are deprived of tegument and envelopes, leading to deficient viral yields. *UL135* and *UL136* genes, encoded in the UL133-UL138 region, promote viral maturation. Additional recent data propose that this locus involves the main molecular switch among latency and reactivation, including the opposing roles of *UL135* and *UL138*. Moreover, a study reported that the outcome of antiviral immunity might be influenced by numerous viral determinants, including HCMV strain, virulence, MHC I downregulation, and other escape strategies elicited by HCMV during the early virus-host interaction (3).

HCMV ESCAPE MACHINERIES AND IMMUNOSUPPRESSION

HCMV has evolved manifold immune evasion strategies that modulate the host immune system and promotes more efficient infection and dissemination within the host. A chief evasion strategy depends on hindering the MHC class I-restricted antigen presentation (58). Throughout the immediate early HCMV infection phase, a cytotoxic T-lymphocyte (CTL) response counteract antigenic peptides resulting from the IE1 transcription factor (59, 60). The matrix protein, pp65, possessing a kinase activity, phosphorylates the IE1 protein and specifically inhibit the presentation of IE-derived antigenic peptides to escape immune recognition of the early produced viral proteins (59). Knowing that pp65 is delivered directly into the cells during the viral fusion phase, HCMV will instantly escape from immunological surveillance, till further immune evasion related proteins are secreted (61). HCMV-specific viral proteins and genes that are associated with the host interferon responses (pp65), inhibit NK cell detection or activation (37, 62), and inhibit the recognition of $CD4^+$ and $CD8^+$ T-cell by preventing MHC Class I and II antigen processing and appearance (1, 37, 61). HCMV infected cells produce viral IL-10 homolog which further suppresses $CD4^+$ and $C8^+$ T-cell responses (1, 61). The previously mentioned evasion mechanisms are summarized in **Figure 1**.

In the absence of MHC class expression, HCMV must be susceptible to NK cell-mediated lysis; however, HCMV donates a large proportion of its genome to down-regulate the NK cell activity (63). Consequently, the surface expression of HLA-E and HLA-G is stimulated by gpUL40 and CMV-IL10 respectively (64–66). In addition, the expression of UL16 supports HCMV to block natural killer group 2D (NKG2D)-mediated NK-cell activation and this is by adopting a blocking strategy that hinders the binding of NKG2D to UL16 binding proteins (ULBPs) namely, ULBP1 and ULBP2, and to the MHC class I chain-related gene B (MICB gene) (37, 61). HCMV US18 and US20 proteins stimulate the deterioration of a major stress protein namely, MHC class I polypeptide-related sequence A (MICA); hence, preventing the NK cell from recognizing infected cells' stress signals (67). Other machineries considered by HCMV to escape NK cell lysis involve the inhibition of NK cell-activating receptor (NKp30) by pp65 (37), UL122-encoded microRNA that represses *MICB* gene expression (68), and blocking of the expression of CD155 by HCMV-UL141 (37).

To counteract apoptosis and further evade the immune system, HCMV overexpresses anti-apoptotic proteins and inhibits pro-apoptotic molecules and death receptors. The former is achieved by upregulating B-cell lymphoma 2 (Bcl-2) in HCMV-infected cells (69) and expressing Fas-associated death-domain-like IL-1β-converting enzyme-inhibitory proteins (FLIP) by IE2 (70). On the other hand, pUL36 inhibits the induction of procaspase 8 to the death-inducing signaling complex (DISC) and pUL37 inhibits pro-apoptotic Bcl-2 members namely Bcl-2-associated X Protein (Bax) and Bcl-2 homologues antagonist/killer (Bak); thus, HCMV is hindering apoptosis through two distinct mechanisms (6, 61). Furthermore, HCMV has developed UL36 and UL37 proteins, which enhance the survival of infected cells; thus, stimulating viral dissemination within the host (37, 71). HCMV escapes complement attack by upregulating the host-encoded complement regulatory proteins (CRPs) (72) and by the ability of HCMV to integrate host cell-derived CRPs, CD55 and CD59 in its virions (6).

Lastly, HCMV produces the G-Protein-coupled receptors (GCRs) homologs US27, US28, UL33, and UL78 that might act as eliminators of chemotactic factors, thus hindering the inflammatory cells' accumulation at the viral infection site (61, 73). These viral approaches secure novel viral progeny production and facilitate the spread to other hosts (61). US28 is usually expressed in the early infection phase; it shows the highest homogeneity to the CC chemokine receptor CCR1. It also binds the CC chemokines RANTES, monocyte chemoattractant protein-1 (MCP-1), monocyte chemotactic protein-3 (MCP3), macrophage inflammatory protein-1 alpha (MIP-1α), and macrophage inflammatory protein-1 beta (MIP-1β), in addition to the membrane-associated CX3C chemokine, fractalkine (37, 61, 74). US28 expression results in the stimulation of phospholipase C and NF-κB signaling. The US28-fractalkine interaction has been involved in cell targeting and viral dissemination (61). The transcription of *US28* takes place during productive and latent HCMV infection, which might justify the dissemination of latent HCMV (75, 76). Moreover, HCMV encodes a homolog of the immunosuppressive cytokine IL-10 (UL111a) (62, 71); it likewise possesses potent immunosuppressive traits, including the inhibition of mitogen-stimulated peripheral blood mononuclear cells (PBMCs) proliferation in addition to the blockade of pro-inflammatory cytokine synthesis in PBMCs and monocyte (37, 61). CMV IL-10 binds to the cellular human receptor of IL-10 despite its minimal homology to the endogenous cellular IL-10 (61). In addition, HCMV establishes immune tolerance by inducing the transcription and release of TGF-β which inhibits anti-viral IFN-γ and TNF-α cytokine production and cytotoxic effector activities of HCMV specific Th1 cells (77). Further homologs encoded by HCMV are UL144 which is a viral TNF receptor and an effective IL-8-like chemokine (viral CXC-1) prompting the chemotaxis of peripheral blood neutrophils (UL146) (37). Lastly, HCMV strategies that modify the cellular infected environment to restrict immune identification are known to be widely expressed during lytic infection; however, recent evidence shows that viral genes' activity in preventing immune recognition is being remarkable even during latency phases (75). Recent data shows that the majority of the HCMV-encoded proteins and microRNAs (miRNAs) are expressed also during latent stages (75, 76) (**Table 1** and **Figure 1**).

HCMV COMPLICATIONS UNDER IMMUNOSUPPRESSION

The suppressive effects exerted by HCMV on the host immune system, HCMV persistence, dissemination, and reactivation result

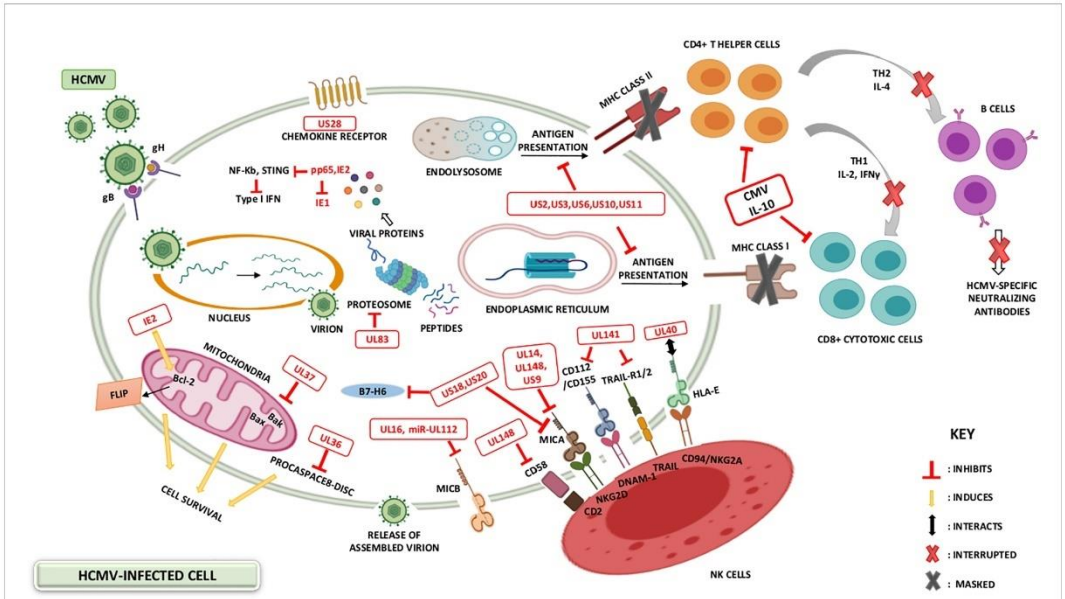

FIGURE 1 | HCMV-induced modulation of the host immune system. The battle between the host immunity and HCMV is permanent, with HCMV developing various mechanisms to evade the host immune system. Immunosuppression may be ascribed to the variety of immune modulators encoded by HCMV-specific gene products. HCMV viral genes prevent MHC Class I and II antigen presentation and thus interfere with interferon responses, NK cell recognition as well as $CD4^+$ and $CD8^+$ T-cell recognition. Additional HCMV genes for instance IL-10 homologue (UL111a), and viral proteins acting as receptors for host inflammatory cytokines (US28), further suppress the host immune responses.

in dire consequences. The severe and mortal complications resulting from HCMV reactivation mainly occur in immunosuppressed and seriously ill immunocompetent individuals in whom the HCMV infection is accompanied by prolonged hospitalization and/or mortality. Furthermore, the manipulation of the host immunity can result in superinfections with other herpesviruses or bacteria, and exacerbate SARS-CoV-2 infections that are benefiting from the weakened immune system (18, 19, 103, 104). Since HCMV infection is known as a prevalent congenital viral infection, it might generate viral hepatitis with jaundice in addition to long-lasting disabilities, including hearing and visual damage, neurological impairments, and mental retardation (103). Additionally, studies show that HCMV has been detected in tissue specimens from immunocompetent individuals with inflammatory diseases, including atherosclerosis, psoriasis (6, 105), rheumatoid arthritis (24), inflammatory bowel disease (IBD) (105), and systemic lupus erythematosus (SLE); it has been concerned in the development of these diseases (103). HCMV leads to the development of restenosis after coronary angioplasty, chronic rejection of organ transplantation, chronic graft-*versus*-host disease in recipients of bone marrow transplants (24). Such observations infer the presence of an association between HCMV and autoimmune diseases. Knowing that the HCMV chemokine receptor homolog, US28, is considered a major co-receptor for several HIV strains, it provokes cell fusion with several forms of viral envelope proteins in addition to stimulating HIV-1 entry into HCMV- infected cells (106). Several epidemiologic studies suggested that HCMV infection has been linked to an elevated risk of cardiovascular death, one of which revealed that CMV seropositivity has been significantly associated with cardiovascular mortality (*P-value*=0.007) (107). This association was confirmed by another study showing an "increased six-year cardiovascular mortality" (*P-value*=0.021) (108). Further findings showed that CMV seropositive elderly presented elevated cardiovascular mortality compared to CMV-negative ones; the subhazard ratio for cardiovascular mortality was 1.95 (95% CI: 1.29–2.96, *P-value*=0.002) (109). The association between HCMV and vascular diseases is verified by the transient presence of US28 in smooth muscle cells which induces chemokinesis and chemotaxis (61). Moreover, since HCMV infection has been involved in producing modifications among the total T-cell population and adversely affecting to the immune well-being of elderly, it stimulates the occurrence of numerous age-related syndromes, and decreases efficacy of vaccines (3, 12, 110). Additionally, in elderly, HCMV could contribute to inflammation-mediated vascular pathology which is evaluated by determining systemic inflammation markers (C-reactive protein, IL-6, and TNF) and it might also cause direct vascular damage (2).

HCMV ONCOMODULATION AND ITS SIGNIFICANCE IN TUMOR MICROENVIRONMENT

Alterations resulting from cancerous genetic and epigenetic instability provide recognizable antigens that are distinguished by the host immune system (111, 112). As cancer evolves, it can resist immune clearance by prompting tolerance in the presence of tumor-associated inflammatory cells (113). Consequently, a tumor microenvironment is generated and controlled by tumor-induced molecular and cellular interactions (114) in which immune cells not only fail to exert anti-tumor effector functions, but also promote tumor development (113). Since CMV possesses different cellular signaling pathways, encodes many genes that exhibit immunosuppressive effects, and may empower cancer hallmarks, it thus plays an essential role in generating cancerous cells and has a fundamental impact on the tumor microenvironment (1, 29, 115).

Some studies put extra emphasis on the indirect role of CMV in cancer (115, 116). For instance, Dey et al. suggested that the association between glioma and CMV is an "observational association" (117). However, the prevalence of HCMV is remarkably high in several cancer forms (26, 118). Several research groups showed that over 90% of breast, colon, and prostate cancer, rhabdomyosarcoma, hepatocellular cancer, salivary gland tumors, neuroblastoma and brain tumors were positive for HCMV nucleic acids and/or proteins (26). HCMV DNA was confirmed in 100% of breast cancer and 91% of sentinel lymph nodes samples from the metastatic group (119). Moreover, a study conducted by Taher et al., showed HCMV detection in 98% of breast cancer derived metastatic brain tumors, suggesting a potential link between HCMV and metastatic cancer (120). HCMV was considered as a potential therapeutic target in metastatic cancer due to the expression of HCMV-IE protein in 53% of breast cancer samples which therefore resulted in shorter overall survival, and the detection of HCMV DNA and transcripts in 92% and 80% of the used specimens respectively (120). Another study showed the inversely proportional relation between HCMV-IE1 presence and hormone receptor expression suggesting HCMV role in hormone receptor-negative breast cancer tumors (121). HCMV IE1 and pp65 were present in 82% and 78% of colorectal cancer samples, and in 80% and 92% of adenocarcinomas, respectively. In colon cancer cells, these HCMV-specific proteins contribute to the induction of Bcl-2 and COX-2 proteins thus promoting colon cancer progression (122). Cobbs et al. showed that HCMV-IE1 was expressed in all studied glioma biopsy specimens, in all grades (II-IV) (123). Over again, HCMV-IE and late proteins were expressed in 100% and 92% of primary neuroblastoma samples respectively; notably, HCMV proteins were detected in CD133 and CD44-positive neuroblastoma cells (118). HCMV DNA was detected in the peripheral blood of GBM patients (80%), suggesting either HCMV reactivation or viral DNA shedding from HCMV-tumor cells (124). In addition, HCMV was detected in all evaluated preneoplastic and neoplastic prostate lesions (125). In Hodgkin's disease cases, the HCMV infection frequency was 28.6% (126). Further, expression of HCMV was marked in the neoplastic epithelium of 97% of the carcinoma patients (127). 92% of the primary medulloblastoma cases expressed HCMV-IE protein while 73% expressed late viral proteins (128). Evident elevated survival rates were observed among HCMV positive glioblastoma patients who

TABLE 1 | HCMV gene products involved in immunomodulation and their oncogenic characteristics.

HCMV Gene Products	Mechanism of Action	Possible Oncogenic Characteristic
US2, US3, US6, US11	➢MHC class I expression impairment, reducing HCMV antigen presentation toward $CD8^+$ cells and evasion of $CD8^+$ T-cell immune responses, superinfection (60, 78) ➢US2 down regulates MHC class II and reduces HCMV antigen presentation to $CD4^+$ cells (79)	➢Preventing $CD8^+$ mediated cytotoxic tumor killing (80)
US18 and US20	➢Interfere with B7-H6 surface expression including endosomal degradation, evades NK cells' immune detection (81)	➢HCMV-immune evasion might indirectly affect tumor environment
***US28* (viral GPCR)**	➢Promotes chemotaxis (82, 83)	➢Cellular proliferation, tumor growth, enhanced angiogenesis and cell survival (84, 85)
UL16	➢Regulation of NK cell ligand NKG2D and impairing NK cells function (79)	➢Immune evasion, protects the cells from cytotoxic peptides-mediated lysis, and protects cancer cells from both NK and T-cells (80)
UL40	➢NK cell evasion (62) ➢HLA-E over expression (62), enhancing its interaction with the inhibitory receptor CD94/NKG2A (86)	➢HLA-E Over expression (1)
***UL83* (pp65)**	➢IE1 sequestration, repress proteasome processing, reduce NKp30 effect and delays antiviral gene expression (87)	➢Genomic mutation, immune evasion (84)
***UL122* (IE2)**	➢Overexpression of anti-apoptotic FLIP protein (60, 79)	➢Elevated immune suppression, cell proliferation, escaping growth suppressors and apoptosis (84)
***UL123* (IE1)**	➢Induction of TGF-β (82)	➢Cellular proliferation, genome instability and mutation, escaping growth suppressors, and ameliorated cell survival (84)
***UL82* (pp71)**	➢Inhibits antiviral response by binding to interferon stimulator gene (87, 88)	➢Cellular proliferation, escaping growth suppressors, and genomic mutation (84)
***UL111A* (cmvIL-10)**	➢Inhibits MHC class II expression and suppresses $CD4^+$ T-cell recognition (83, 89)	➢Immunosuppression, cellular proliferation, stimulates migration and metastasis, telomerase activation (84)
UL142	➢Inhibiting MICA (79, 90)	➢HCMV-immune evasion might indirectly affect tumor environment
UL36	➢Complexing with pro-caspase-8 thus suppressing its proteolytic stimulation and prompting its designation as viral inhibitor of caspase-8-induced apoptosis (vICA) (91, 92)	➢Enhanced cell survival
UL37	➢Inhibition of Bak and Bax protein, thus inhibiting apoptosis (79)	➢Enhanced cell survival
UL76	➢Activation of the DNA damage response thus inducing IL-8 expression (93)	➢Genome instability and mutation (84)
UL97	➢Forms a complex with pp65 and mediates immune evasion (5, 94)	➢Escaping growth suppressors (84)
UL141-UL144	➢Encodes for homolog of TNFR, hinders CD155 and CD112 expression (NK cell activating ligands) and the death receptor for the TNF family ligand TRAIL (5, 95)	➢HCMV-immune evasion might indirectly affect tumor environment
UL145	➢Depletion of helicase like transcription factor- (HLTF) through the recruitment of Cullin4/DDB ligase complex (96, 97)	➢Impeding innate immunity might indirectly affect tumor environment
UL146	➢Promotes neutrophil chemotaxis, immune escape (5, 98)	➢HCMV-immune evasion might indirectly affect tumor environment
UL148	➢CD58 Suppression; effective modulator of CTL function, amplify degranulation in cytotoxic T lymphocytes and NK cells against HCMV-infected cells (85)	➢HCMV-immune evasion might indirectly affect tumor environment
miR-UL112	➢Down regulation of MICB thus escaping NK cells, and decreased T-cell recognition (99, 100)	➢Exerts its oncogene function by directly targeting tumor suppressor candidate 3 (TUSC3) in GBM (101)
LncRNA	➢Function in both innate and adaptive immunity including the development, activation, and homeostasis of the immune system (102)	➢Cellular proliferation and transformation, facilitating signal transductions in cancer signaling pathways (84, 102), it's also involved in angiogenesis (85)

were on anti-viral therapy (valganciclovir) (120, 129). A 70% and 90% survival rate was proved with 6-month and continuous valganciclovir treatment, respectively (120). Despite the existing studies which describe the possible involvement of CMV in cancer, further large scale investigations are needed in addition to the necessity of novel epidemiologic studies knowing that the latter might be challenging to conduct especially among CMV-positive cancer patients.

HCMV infects multiple cell types including stem cells; referring to the fact that Thy-1 and platelet-derived growth factor receptor alpha (PDGFRα) stem cell markers enhance HCMV infection, stem cells are susceptible to HCMV infection (130, 131). Thus, stem cells serve as reservoirs for HCMV persistence and reactivation. The major stem cell regulator namely, Wnt tends to trigger HCMV transcriptional activation; hence, once HCMV disseminates to various body organs, viral expression occurs during patients' lifetime in stem cells (132). It is worth noting that the latter increases the chance of accumulation of genetic mutations; thus, stem cells lose control over their self-growth and renewal, act as a cancer source, and become susceptible to oncogenesis in the presence of inflammation and altered DNA repair pathways (133). In return, HCMV can support stem cells survival which would potentially elevate oncogenesis. Studies reveal the effect of

HCMV-IE1 protein in promoting the preservation of glioblastoma cancer stem cells through its induction of SRY-Box Transcription Factor 2 (SOX2), Nanog, Nestin, and octamer-binding transcription factor 4 (OCT3/4) where it's considered as a key regulator of glioblastoma stem-like phenotype (134). In GBM cells, the induction of transcription factors that are crucial for cancer stem cell persistence, cancer growth, and signaling pathways associated with the epithelial to mesenchymal (EMT) phenotype are stimulated by HCMV IE1 expression (134, 135). Many studies proved that cancer stem cells infected with HCMV possess a progression potential in contrast to HCMV-negative cancer stem cells. Some HCMV strains, for instance HCMV-DB and HCMV-BL, are capable of transforming human mammary epithelial cells and producing a "transcriptional profile" associated with DNA hypomethylation that resulted in enhanced proliferation, activation of cancer stem cell, and EMT process (136, 137). Likewise, HCMV was proven to induce an EMT phenotype in colorectal carcinoma cells accompanied with amplified tumor proliferation and cancer cell invasion (136). In addition, IE1 expression was detected in CMV transformed HMECs (CTH) cells which as well express embryonic stem cell markers (138). HCMV IE1 and IE2 gene expression in addition to UL76 genes prompt DNA mutagenesis, chromosome breakage, and genomic instability. Such expression of HCMV gene products could affect the pathways of p53 and Rb tumor suppressors, and other pathways that are responsible for DNA repair (27, 139, 140). Presuming the role of HCMV gene products in causing DNA damage directly and indirectly, and stimulating proliferation in stem cells, HCMV may have the potential to initiate and promote tumor formation. The oncomodulatory potential of HCMV catalyzes an oncogenic process by producing viral proteins, helping tumor cells to evade the immune system, and preventing and/or delaying cell death. The lack of HCMV specific cellular immune responses in these immune-privileged tumor sites would definitely enhance HCMV replication. On the other hand, cancer cells on their own can escape immune responses by diverse mechanisms. Thus, the combination of intrinsic cellular with viral immune escape machineries in cancer cells may offer an environment which enhances HCMV replication and boost cancer cells to evade from immune surveillance showing the bidirectional relationship between tumor cells and HCMV (25, 141). It's worth mentioning that HCMV can activate many of the tumor pathways' hallmarks including uncontrolled inflammation, myeloid cells' infiltration, immune modulation, angiogenesis, and metabolic reprogramming. Production of inflammatory cytokines including RANTES, MCP-1, MIP-1a, IFN-γ, TNF- α, IL-4, IL-18, and IL-8F is induced by HCMV (142, 143). The HCMV-US28 chemokine receptor strongly promotes the expression of the NF-kB, COX-2, IL-6, and p-STAT-3 which could initiate oncogenic pathways (144, 145). Upon HCMV infection of human cancer stem cells and in the presence of cmvIL-10, cancer stem cells can induce macrophage reprogramming "M2 phenotype" in the tumor microenvironment hence favoring the appearance of tumor-associated macrophages (TAMs) and enhancing other immunomodulatory, oncogenic, and angiogenic cytokines' expression such as STAT3 and vascular endothelial growth factor (VEGF) (146–148). Similar to US28, the cmvIL-10 chemokine which is known to be expressed in latency phase and tumor cells can enhance cancer cell invasion (149). In addition, HCMV can guarantee neutrophils and mononuclear cells survival, which can support a quick oncogenesis *via* the activation of an angiogenic switch (150, 151). Further, long non-coding RNAs (lncRNAs) were described as efficient players not only in facilitating signal transductions in tumor signaling pathways but also in promoting tumor evasion from immunosurveillance. It has been also shown that immune cells for instance, T-cells, B-cells, dendritic cells, macrophages, and myeloid cells control tumor immune responses *via* lncRNAs linked pathways (152, 153). In CTH cells, HCMV lncRNA4.9 was formerly detected in tumors isolated from xenograft NSG mice injected with CTH cells, as well as in human breast cancer biopsies (137). Moreover, several studies specified that modifications in gut permeability and intestinal microbiota translocation can stimulate chronic inflammation as well as causing auto-immune and neoplastic diseases (154, 155). Knowing that CMV presence was associated with upregulation of various cytokines, elevated epithelial gut damage, microbial translocation, and systemic inflammation (156, 157), it might play a part in eliciting carcinogenesis. All in all, these studies indicate that HCMV can be actively involved in enabling cancer progression and this is through inducing certain pathways that give rise to epigenetic modifications, and promoting the activation of cancer stem cell, angiogenesis, invasion, and an EMT phenotype (136, 158, 159). Certainly, one of the limitations for assessing the effect of HCMV on immunity and cancer progression is that the majority of the investigations were done on the high risk CMV-positive subpopulation which might involve diverse immunomodulation sociodemographic and environmental co-factors other than HCMV status as well as divergent lifestyles and medical history. Therefore, prospective studies are highly required to rule out other immunomodulatory factors and precisely evaluate the impact of CMV on host immunity.

Nonetheless, it is noteworthy that the oncogenic potency of HCMV clinical strains varies between low and high-risk strains. HCMV-DB and HCMV-BL have been classified as high-risk strains in which they possessed their oncogenic potentials in acutely infected human mammary epithelial cells (HMEC) *in vitro* showing sustained transformation. These high-risk strains were characterized by elevated *Myc* expression, PI3K/Akt pathway activation, and *p53* and *Rb* gene repression (138). With regard to immune responses, Myc suppresses immune surveillance by modulating the expression of the innate immune regulator (CD47, also known as integrin-associated protein) and the adaptive immune checkpoint namely, programmed death ligand 1 (PD-L1, also known as CD274 and B7-H1) (160–164). Further, Myc regulates thrombospondin-1 (161) and Type 1 IFN (165, 166). Hence, Myc initiates and maintains tumorigenesis through the modulation of immune regulatory molecules. PI3K/Akt activation induced inflammation and immunosuppression through nitric oxide synthase (NOS) overexpression; thus,

resulting in tumor initiation *via* the activated Notch pathway leading to tumor progression (167). On the other hand, suppression or mutation of p53 has been shown to decrease MHC-I presentation, increase STAT3 phosphorylation, upregulate PD-L1 *via* microRNA (miR34), elevate pro-inflammatory chemokine and cytokine production, and indirectly upregulate the expression of chemokine receptors (CXCR4 and CXCR5) (160, 168, 169). Loss of Rb leads to the increase in CCL2 and IL6 secretion and this is because of the elevated fatty acid oxidation (FAO) activity and enhanced mitochondrial superoxide (MS) production (170). Indeed, those molecular alterations have been linked to immune suppression in the tumor microenvironment indicating that only high-risk HCMV strains possessing oncomodulatory properties are potentially involved in the oncogenesis process as described previously (84, 138) (**Figure 2**). In line with the previously presented epidemiological studies, and since HCMV was confined within tumors correlating positively to poor prognosis, as well as the potential of HCMV gene products in regulating tumorigenic pathways and processes linked to cancer hallmarks, and finally the HCMV broad tissue tropism, we infer that HCMV possesses distinctive mechanisms in cancer progression (26, 29, 171).

THERAPEUTIC APPROACHES IN HIGH-RISK POPULATIONS

The fact that HCMV is highly prevalent in different cancer forms, opens up the possibility to manage such cancers with anti-HCMV medications. Currently, two major approaches are being chased; the first emphases on antiviral therapy while the other targets HCMV directed immunotherapy. The core approach to antiviral therapy involves the use of valganciclovir. The rationale behind using valganciclovir is suppressing HCMV replication in HCMV-positive glioblastoma (GBM) cells leading to the repression of virus-mediated tumor-promoting strategies. Despite its viral replication suppression, valganciclovir doesn't eradicate the virus. Thus, short-term valganciclovir treatment wouldn't be ideal for treating glioma patients, necessitating long-term treatment to maintain the tumor suppressive properties (116). Interestingly, valganciclovir treatment outcome was improved in combination with celecoxib (COX-2 specific inhibitor). Since glioblastoma, medulloblastoma, and neuroblastoma tumors show high expression of cyclooxygenase-2 (COX-2) and nonsteroidal anti-inflammatory drugs (NSAIDs) levels, COX-2 and PGE2 inhibitors possess a profound effect on tumor growth. The two inhibitors

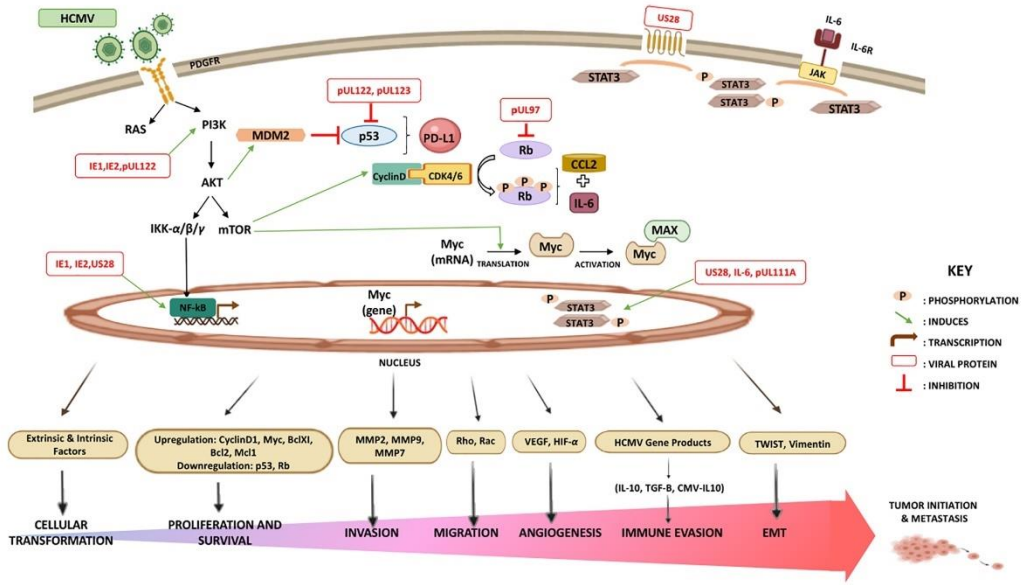

FIGURE 2 | Major signaling pathways stimulated by HCMV that modulate the immune landscape. HCMV-infected cells produce elevated levels of interleukin-6 (IL-6) that activates signal transduction *via* IL-6 receptor (IL6R)-STAT3 axis. US28, an active chemokine receptor, also plays a major role in activating STAT3 in cancer cells. The combination of STAT3 activation and the impact of HCMV on cancer cell apoptosis, invasion, migration, adhesion, angiogenesis, and immunogenicity significantly exacerbates malignancy. In contrast to p53 and Rb, the upregulation of Akt, Myc, PD-L1, and CCL2 strongly exerts immunosuppressive and oncomodulatory effects. HCMV-induced alterations in the TME may contribute to oncomodulation.

competently block HCMV replication and limiting the US28-expressing tumor cell growth. Therefore, the significant effects behind the use of aspirin and other NSAIDs in tumor prevention investigations could be somewhat due to the suppression of HCMV replication in pre-malignant lesions (80). The existing link between CMV and cancer creates a new avenue for immunotherapeutic strategies that target CMV such as, adoptive T-cell transfer and vaccine approaches (172). During adoptive lymphocyte transfer (ALT), autologous T-cells are expanded and activated *ex vivo* against the tumor. After that, they are transferred into patients where lymphodepletion stimulates a substantial proliferation of T-cells and intensifies tumor-specific immunity (173, 174). There exist various ongoing clinical studies assessing the effectiveness of adoptive T-cell therapy using HCMV-specific T-cells, or DCs with CMV-pp65 RNA in order to vaccinate GBM patients. CMV-specific T-cells, especially pp65-specific T-cells, favorably infiltrate glioblastoma tumors and were able to stimulate glioblastoma cells' killing (173). The fact that a high percentage of GMB samples were HCMV-positive has led to potential immunotherapy targets for GBM treatment. HCMV-specific proteins (IE1, pp65, and gB) are being investigated for the development of immunotherapy targets (116, 174). Interestingly, a study showed that CMV-stimulated NK cells and γδ-T-cells might have antineoplastic potential and CMV reactivation has been associated with minimal risk for relapsed leukemia in hematopoietic stem-cell transplantation (HSCT) patients (173). Since oncolytic virotherapy has been recognized as a promising approach for treating cancers in recent years, the use of "oncolytic CMV therapy" in combination with anti-tumor medications, immune checkpoint inhibitors (targeting CTLA4 and PD-L1), epigenetic therapeutics, or as "HCMV/HSV-1 oncolytic virus" could be regarded as one of the most intriguing antitumor approaches (175).

Major approaches used to target Myc are mostly targeting *Myc* gene transcription (JQ1, AZD5153, GSK525762, dBET1, THZ1, Roscovitine, Flavopiridol, QN-1, and APTO-253), inhibiting Myc mRNA translation (MLN0128, Silvestrol, eFT226, BTYNB, Rapamycin, MK2206, BEZ235), targeting Myc oncoprotein stability (Volasertib, TD19, P22077, MLN8237, BI 6727, and BI 2536), controlling Myc-Max interactions (Omomyc and MYCMI-6), and blocking Myc's accessibility to other genomic targets (Sulfopin) (176–178). Further, bromodomain and extraterminal protein (BET) inhibitor, JQ1, decreased expression of PD-L1 and CD47 resulting in the recruitment of T-cells. Hence, drugs targeting Myc-associated pathways may be used to modify the expression of immune checkpoints (179). Furthermore, the PI3K/AKT pathway is activated in cancer; thus, identifying AKT inhibitors that can block PI3K/AKT signaling could attenuate tumor growth and recover immune responses. AKT inhibitors are classified in Synthetic (MK-2206, AZD5363, GDC-0068, Perifosine) and natural AKT inhibitors (Resveratrol or grape powder, Ginger root extract, Sulforaphane) (180, 181). Few drugs in clinical use or preclinical assessment have been verified to directly or indirectly target PI3K signaling such as BEZ235, Ly294002, Rapamycin, CCI779, PX-866, SF1124, PX316, Miltefosine, and Perifosine (178, 181). Reactivating tumor suppressors is a substantial pharmacological challenge; restoring p-53 activity stimulated innate immunity particularly DC activation, and it also promoted adaptive immunity. Nutlin-3a, mouse double minute 2 homolog (MDM2) inhibitor, induces local p53 activation in the TME resulting in MDM2-mediated tumor cell apoptosis even in the presence of a sustained Notch activity (168, 182, 183). Re-expression of p53 was stimulated by Tamoxifen injections causing massive apoptosis (179). T-cell responses were driven by using p53 vaccines (ALVAC-p53 and MVAp53) or synthetic long peptides of p53 (169). Moreover, the highly selective cyclin-dependent kinases 4/6 (CDK4/6) inhibitors (Palbociclib, Ribociclib, and Abemaciclib) were proved to avert RB phosphorylation thus regulating MHC presentation, IFN-γ response, and IL-6 signaling (184–186). Carlumab, a human IgG1 monoclonal antibody, inhibited CCL2 and it consequently showed promising effects in both solid tumors and metastatic resistant prostate cancer. A distinct approach to CCL2/CCR2 interference, was hindering CCR2 using MLN1202 in bone metastasis (187). It has been shown that CCL2 knockout prompted marked suppression of TAMs-associated inflammatory cytokines (188); in addition, CCL2-CCR2 blockade exhibited tumor-suppressive function by blocking inflammatory monocyte recruitment within the tumor (170) (**Figure 3**).

Additionally, because of HCMV's ability to establish latency and reactivate, CMV vaccines are presently being developed for clinical use. To prevent HCMV infection in tumor-independent settings, the development of an effective HCMV vaccine has been investigated despite being a struggle for a couple of years. Few have already granted the approval to a phase III clinical trial thus possessing promising outcomes (189). The investigated anti-CMV vaccine types include the live-attenuated (phase 2), recombinant subunit (phase 2), virus vectored phase (1, 2), chimeric peptidic (phase 2), enveloped virus-like particles (phase 1), plasmid-based (phase 3), and mRNA (phase 2) vaccines (190). mRNA-1647, a CMV vaccine covering six mRNAs that encodes pentamer and gB protein, is designed for CMV prophylaxis; a phase 3 study will be initiated to assess the prevention of primary CMV infection in women of childbearing age (ClinicalTrials.gov Identifier: NCT04232280). Recent data showed that HCMV could perhaps induce transformation by enhancing the expression of viral genes (for example, *UL69* gene). The presence of *UL69* gene in CTH cell cultures and UL69 DNA in the majority of breast cancer biopsies indicates a potential significance of *UL69* as a target in developing HCMV-vaccine (191). The usage of HCMV vaccines for the treatment of cancer patients generally and GBM patients in specific might be of high therapeutic value especially that HCMV has been shown to express oncomodulatory functions. Letermovir, an FDA approved novel terminase inhibitor, is currently used for CMV prophylaxis as it selectively compromises CMV replication. It's characterized by its high potency compared to ganciclovir and limited toxicity profile (192). There exists an ongoing phase 2 clinical trial that aim to assess the anti-inflammatory potential of letermovir in adults with HIV and asymptomatic CMV being on

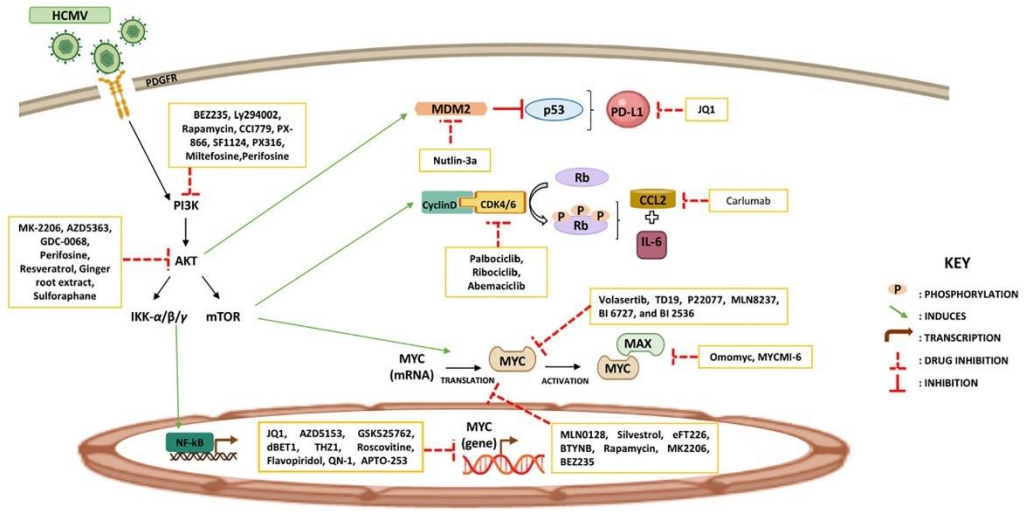

FIGURE 3 | Potential therapeutic approaches reinstating tumor immunity. Certain therapeutic strategies are used to increase tumor suppressor proteins and reduce oncoproteins' expression with the aim of restoring the immune response against tumors.

antiretroviral therapy-mediated suppression (ClinicalTrials.gov, Identifier: NCT04840199). Further investigations will be a welcome addition to evaluate the use of letermovir in averting CMV recurrence and treatment as well as to reverse letermovir resistance.

CONCLUSION

Overall, HCMV-induced amplification of immune evasion mechanisms mediates oncomodulation and enables tumors to further escape immune surveillance and develop immune tolerance favoring other malignant phenotypes. HCMV, infecting many cell types, induces a pro-inflammatory environment and conquers specific immune responses thus creating an immunosuppressive TME. Nevertheless, getting to know viral immune evasion mechanisms will aid in understanding aspects of cellular as well as immunological function, and contribute to the enhancement of immunotherapies' outcome and antiviral agents eliminating the virus from tumor tissues which could improve patient's immune responses and suppress tumor progression. Taking into consideration the profound effects of HCMV on the quality of life, there remain further experimental studies to be performed in order to design effective interventions including vaccines or other approaches that reinforce immune homeostasis and maintain the adapted immune response to aging.

AUTHOR CONTRIBUTIONS

All authors listed have made a substantial, direct, and intellectual contribution to the work and approved it for publication.

FUNDING

This work was supported by grants from the University of Franche-Comté, and the Région Franche-Comté (to GH). RB is a recipient of a doctoral scholarship from Hariri Foundation for Sustainable Human Development.

REFERENCES

1. Cox M, Kartikasari AER, Gorry PR, Flanagan KL, Plebanski M. Potential Impact of Human Cytomegalovirus Infection on Immunity to Ovarian Tumours and Cancer Progression. *Biomedicines* (2021) 9:351. doi: 10.3390/biomedicines9040351
2. Klenerman P, Oxenius A. T Cell Responses to Cytomegalovirus. *Nat Rev Immunol* (2016) 16:367–77. doi: 10.1038/nri.2016.38
3. Sansoni P, Vescovini R, Fagnoni FF, Akbar A, Arens R, Chiu Y-L, et al. New Advances in CMV and Immunosenescence. *Exp Gerontol* (2014) 55:54–62. doi: 10.1016/j.exger.2014.03.020
4. Foster H, Ulasov IV, Cobbs CS. Human Cytomegalovirus-Mediated Immunomodulation: Effects on Glioblastoma Progression. *Biochim Biophys Acta (BBA) - Rev Cancer* (2017) 1868:273–6. doi: 10.1016/j.bbcan.2017.05.006
5. Jackson SE, Mason GM, Wills MR. Human Cytomegalovirus Immunity and Immune Evasion. *Virus Res* (2011) 157:151–60. doi: 10.1016/j.virusres.2010.10.031

6. Lepiller Q, Aziz Khan K, Di Martino V, Herbein G. Cytomegalovirus and Tumors: Two Players for One Goal-Immune Escape. *TOVJ* (2011) 5:60–9. doi: 10.2174/1874357901105010060
7. Huygens A, Dauby N, Vermijlen D, Marchant A. Immunity to Cytomegalovirus in Early Life. *Front Immunol* (2014) 5:552. doi: 10.3389/fimmu.2014.00552
8. La Rosa C, Diamond DJ. The Immune Response to Human CMV. *Future Virol* (2012) 7:279–93. doi: 10.2217/fvl.12.8
9. Stagno S, Pass RF, Dworsky ME, Henderson RE, Moore EG, Walton PD, et al. Congenital Cytomegalovirus Infection: The Relative Importance of Primary and Recurrent Maternal Infection. *N Engl J Med* (1982) 306:945–9. doi: 10.1056/NEJM198204223061601
10. Dollard SC, Grosse SD, Ross DS. New Estimates of the Prevalence of Neurological and Sensory Sequelae and Mortality Associated With Congenital Cytomegalovirus Infection. *Rev Med Virol* (2007) 17:355–63. doi: 10.1002/rmv.544
11. Lanzieri TM, Dollard SC, Josephson CD, Schmid DS, Bialek SR. Breast Milk-Acquired Cytomegalovirus Infection and Disease in VLBW and Premature Infants. *PEDIATRICS* (2013) 131:e1937–45. doi: 10.1542/peds.2013-0076
12. Aiello A, Accardi G, Candore G, Caruso C, Colomba C, Di Bona D, et al. Role of Immunogenetics in the Outcome of HCMV Infection: Implications for Ageing. *IJMS* (2019) 20:685. doi: 10.3390/ijms20030685
13. Solana R, Tarazona R, Aiello AE, Akbar AN, Appay V, Beswick M, et al. CMV and Immunosenescence: From Basics to Clinics. *Immun Ageing* (2012) 9:23. doi: 10.1186/1742-4933-9-23
14. Pawelec G, Derhovanessian E. Role of CMV in Immune Senescence. *Virus Res* (2011) 157:175–9. doi: 10.1016/j.virusres.2010.09.010
15. Jergović M, Contreras NA, Nikolich-Žugich J. Impact of CMV Upon Immune Aging: Facts and Fiction. *Med Microbiol Immunol* (2019) 208:263–9. doi: 10.1007/s00430-019-00605-w
16. Moniz P, Brito S, Póvoa P. SARS-CoV-2 and Cytomegalovirus Co-Infections—A Case Series of Critically Ill Patients. *JCM* (2021) 10:2792. doi: 10.3390/jcm10132792
17. Le Balc'h P, Pinceaux K, Pronier C, Seguin P, Tadié J-M, Reizine F. Herpes Simplex Virus and Cytomegalovirus Reactivations Among Severe COVID-19 Patients. *Crit Care* (2020) 24:530. doi: 10.1186/s13054-020-03252-3
18. Söderberg-Nauclér C. Does Reactivation of Cytomegalovirus Contribute to Severe COVID-19 Disease? *Immun Ageing* (2021) 18:12. doi: 10.1186/s12979-021-00218-z
19. Xie L, Yi K, Li Y. SARS_CoV2 RBD Gene Transcription Cannot be Driven by CMV Promoter. *Virology* (2021) 558:22–7. doi: 10.1016/j.virol.2021.02.010
20. Wilski NA, Snyder CM. From Vaccine Vector to Oncomodulation: Understanding the Complex Interplay Between CMV and Cancer. *Vaccines* (2019) 7:62. doi: 10.3390/vaccines7030062
21. Aiello AE, Chiu Y-L, Frasca D. How Does Cytomegalovirus Factor Into Diseases of Aging and Vaccine Responses, and by What Mechanisms? *GeroScience* (2017) 39:261–71. doi: 10.1007/s11357-017-9983-9
22. Royston L, Isnard S, Lin J, Routy J-P. Cytomegalovirus as an Uninvited Guest in the Response to Vaccines in People Living With HIV. *Viruses* (2021) 13:1266. doi: 10.3390/v13071266
23. Poloni C, Szyf M, Cheishvili D, Tsoukas CM. Are the Healthy Vulnerable? Cytomegalovirus Seropositivity in Healthy Adults is Associated With Accelerated Epigenetic Age and Immune-Dysregulation. *J Infect Dis* (2021), jiab365. doi: 10.1093/infdis/jiab365
24. Soderberg-Naucler C. Does Cytomegalovirus Play a Causative Role in the Development of Various Inflammatory Diseases and Cancer? *J Intern Med* (2006) 259:219–46. doi: 10.1111/j.1365-2796.2006.01618.x
25. Cinatl J, Scholz M, Doerr HW. Role of Tumor Cell Immune Escape Mechanisms in Cytomegalovirus-Mediated Oncomodulation. *Med Res Rev* (2005) 25:167–85. doi: 10.1002/med.20018
26. Nauclêr CS, Geisler J, Vetvik K. The Emerging Role of Human Cytomegalovirus Infection in Human Carcinogenesis: A Review of Current Evidence and Potential Therapeutic Implications. *Oncotarget* (2019) 10:4333–47. doi: 10.18632/oncotarget.27016
27. Shen Y, Zhu H, Shenk T. Human Cytomegalovirus IE1 and IE2 Proteins are Mutagenic and Mediate "Hit-and-Run" Oncogenic Transformation in Cooperation With the Adenovirus E1A Proteins. *Proc Natl Acad Sci* (1997) 94:3341–5. doi: 10.1073/pnas.94.7.3341
28. Soroceanu L, Cobbs CS. Is HCMV a Tumor Promoter? *Virus Res* (2011) 157:193–203. doi: 10.1016/j.virusres.2010.10.026
29. Geisler J, Touma J, Rahbar A, Söderberg-Nauclér C, Vetvik K. A Review of the Potential Role of Human Cytomegalovirus (HCMV) Infections in Breast Cancer Carcinogenesis and Abnormal Immunity. *Cancers* (2019) 11:1842. doi: 10.3390/cancers11121842
30. Dolan A, Cunningham C, Hector RD, Hassan-Walker AF, Lee L, Addison C, et al. Genetic Content of Wild-Type Human Cytomegalovirus. *J Gen Virol* (2004) 85:1301–12. doi: 10.1099/vir.0.79888-0
31. Cook CH. Cytomegalovirus Reactivation in "Immunocompetent" Patients: A Call for Scientific Prophylaxis. *J Infect Dis* (2007) 196:1273–5. doi: 10.1086/522433
32. Gerna G, Sarasini A, Patrone M, Percivalle E, Fiorina L, Campanini G, et al. Human Cytomegalovirus Serum Neutralizing Antibodies Block Virus Infection of Endothelial/Epithelial Cells, But Not Fibroblasts, Early During Primary Infection. *J Gen Virol* (2008) 89:853–65. doi: 10.1099/vir.0.83523-0
33. Revello MG, Zavattoni M, Furione M, Fabbri E, Gerna G. Preconceptional Primary Human Cytomegalovirus Infection and Risk of Congenital Infection. *J Infect Dis* (2006) 193:783–7. doi: 10.1086/500509
34. Scrivano L, Sinzger C, Nitschko H, Koszinowski UH, Adler B. HCMV Spread and Cell Tropism are Determined by Distinct Virus Populations. *PloS Pathog* (2011) 7:e1001256. doi: 10.1371/journal.ppat.1001256
35. Cheung AKL, Abendroth A, Cunningham AL, Slobedman B. Viral Gene Expression During the Establishment of Human Cytomegalovirus Latent Infection in Myeloid Progenitor Cells. *Blood* (2006) 108:3691–9. doi: 10.1182/blood-2005-12-026682
36. Sinzger C, Digel M, Jahn G. Cytomegalovirus Cell Tropism. In: TE Shenk and MF Stinski, editors. *Human Cytomegalovirus Current Topics in Microbiology and Immunology*. Berlin, Heidelberg: Springer Berlin Heidelberg. (2008). p. 63–83. doi: 10.1007/978-3-540-77349-8_4
37. Crough T, Khanna R. Immunobiology of Human Cytomegalovirus: From Bench to Bedside. *Clin Microbiol Rev* (2009) 22:76–98. doi: 10.1128/CMR.00034-08
38. Khairallah C, Déchanet-Merville J, Capone M. γδ T Cell-Mediated Immunity to Cytomegalovirus Infection. *Front Immunol* (2017) 8:105. doi: 10.3389/fimmu.2017.00105
39. Compton T, Kurt-Jones EA, Boehme KW, Belko J, Latz E, Golenbock DT, et al. Human Cytomegalovirus Activates Inflammatory Cytokine Responses *via* CD14 and Toll-Like Receptor 2. *J Virol* (2003) 77:4588–96. doi: 10.1128/JVI.77.8.4588-4596.2003
40. Boehme KW, Guerrero M, Compton T. Human Cytomegalovirus Envelope Glycoproteins B and H Are Necessary for TLR2 Activation in Permissive Cells. *J Immunol* (2006) 177:7094–102. doi: 10.4049/jimmunol.177.10.7094
41. Iversen A-C, Norris PS, Ware CF, Benedict CA. Human NK Cells Inhibit Cytomegalovirus Replication Through a Noncytolytic Mechanism Involving Lymphotoxin-Dependent Induction of IFN-β. *J Immunol* (2005) 175:7568–74. doi: 10.4049/jimmunol.175.11.7568
42. Wu Z, Sinzger C, Reichel JJ, Just M, Mertens T. Natural Killer Cells Can Inhibit the Transmission of Human Cytomegalovirus in Cell Culture by Using Mechanisms From Innate and Adaptive Immune Responses. *J Virol* (2015) 89:2906–17. doi: 10.1128/JVI.03489-14
43. Moretta A, Marcenaro E, Parolini S, Ferlazzo G, Moretta L. NK Cells at the Interface Between Innate and Adaptive Immunity. *Cell Death Differ* (2008) 15:226–33. doi: 10.1038/sj.cdd.4402170
44. Picarda G, Benedict CA. Cytomegalovirus: Shape-Shifting the Immune System. *JI* (2018) 200:3881–9. doi: 10.4049/jimmunol.1800171
45. Manandhar, Hò, Pump, Blasczyk, Bade-Doeding. Battle Between Host Immune Cellular Responses and HCMV Immune Evasion. *IJMS* (2019) 20:3626. doi: 10.3390/ijms20153626
46. Lim EY, Jackson SE, Wills MR. The CD4+ T Cell Response to Human Cytomegalovirus in Healthy and Immunocompromised People. *Front Cell Infect Microbiol* (2020) 10:202. doi: 10.3389/fcimb.2020.00202
47. Jackson SE, Sedikides GX, Mason GM, Okecha G, Wills MR. Human Cytomegalovirus (HCMV)-Specific CD4+ T Cells Are Polyfunctional and Can Respond to HCMV-Infected Dendritic Cells *In Vitro*. *J Virol* (2017) 91:e02128–16. doi: 10.1128/JVI.02128-16

48. Manley TJ, Luy L, Jones T, Boeckh M, Mutimer H, Riddell SR. Immune Evasion Proteins of Human Cytomegalovirus do Not Prevent a Diverse CD8+ Cytotoxic T-Cell Response in Natural Infection. *Blood* (2004) 104:1075–82. doi: 10.1182/blood-2003-06-1937
49. Hegde NR, Dunn C, Lewinsohn DM, Jarvis MA, Nelson JA, Johnson DC. Endogenous Human Cytomegalovirus gB is Presented Efficiently by MHC Class II Molecules to CD4+ CTL. *J Exp Med* (2005) 202:1109–19. doi: 10.1084/jem.20050162
50. Sylwester AW, Mitchell BL, Edgar JB, Taormina C, Pelte C, Ruchti F, et al. Broadly Targeted Human Cytomegalovirus-Specific CD4+ and CD8+ T Cells Dominate the Memory Compartments of Exposed Subjects. *J Exp Med* (2005) 202:673–85. doi: 10.1084/jem.20050882
51. Northfield J, Lucas M, Jones H, Young NT, Klenerman P. Does Memory Improve With Age? CD85j (ILT-2/LIR-1) Expression on CD8+ T Cells Correlates With 'Memory Inflation' in Human Cytomegalovirus Infection. *Immunol Cell Biol* (2005) 83:182–8. doi: 10.1111/j.1440-1711.2005.01321.x
52. Pawelec G, Derhovanessian E, Larbi A. Immunosenescence and Cancer. *J Geriatric Oncol* (2010) 1:20–6. doi: 10.1016/j.jgo.2010.04.002
53. Poizot-Martin I, Allavena C, Duvivier C, Cano CE, Guillouet de Salvador F, Rey D, et al. CMV+ Serostatus Associates Negatively With CD4:CD8 Ratio Normalization in Controlled HIV-Infected Patients on cART. *PloS One* (2016) 11:e0165774. doi: 10.1371/journal.pone.0165774
54. Ballegaard V, Brændstrup P, Pedersen KK, Kirkby N, Stryhn A, Ryder LP, et al. Cytomegalovirus-Specific T-Cells are Associated With Immune Senescence, But Not With Systemic Inflammation, in People Living With HIV. *Sci Rep* (2018) 8:3778. doi: 10.1038/s41598-018-21347-4
55. Olsson J, Wikby A, Johansson B, Löfgren S, Nilsson B-O, Ferguson FG. Age-Related Change in Peripheral Blood T-Lymphocyte Subpopulations and Cytomegalovirus Infection in the Very Old: The Swedish Longitudinal OCTO Immune Study. *Mech Ageing Dev* (2001) 121:187–201. doi: 10.1016/S0047-6374(00)00210-4
56. Terrazzini N, Kern F. Cell-Mediated Immunity to Human CMV Infection: A Brief Overview. *F1000Prime Rep* (2014) 6. doi: 10.12703/P6-28
57. Bughio F, Elliott DA, Goodrum F. An Endothelial Cell-Specific Requirement for the UL133-UL138 Locus of Human Cytomegalovirus for Efficient Virus Maturation. *J Virol* (2013) 87:3062–75. doi: 10.1128/JVI.02510-12
58. Hewitt EW. The MHC Class I Antigen Presentation Pathway: Strategies for Viral Immune Evasion. *Immunology* (2003) 110:163–9. doi: 10.1046/j.1365-2567.2003.01738.x
59. Gilbert MJ, Riddell SR, Li CR, Greenberg PD. Selective Interference With Class I Major Histocompatibility Complex Presentation of the Major Immediate-Early Protein Following Infection With Human Cytomegalovirus. *J Virol* (1993) 67:3461–9. doi: 10.1128/jvi.67.6.3461-3469.1993
60. Gilbert MJ, Riddell SR, Plachter B, Greenberg PD. Cytomegalovirus Selectively Blocks Antigen Processing and Presentation of its Immediate–Early Gene Product. *Nature* (1996) 383:720–2. doi: 10.1038/383720a0
61. Vossen M, Westerhout E, Söderberg-Nauclér C, Wiertz E. Viral Immune Evasion: A Masterpiece of Evolution. *Immunogenetics* (2002) 54:527–42. doi: 10.1007/s00251-002-0493-1
62. Patel M, Vlahava V-M, Forbes SK, Fielding CA, Stanton RJ, Wang ECY. HCMV-Encoded NK Modulators: Lessons From *In Vitro* and *In Vivo* Genetic Variation. *Front Immunol* (2018) 9:2214. doi: 10.3389/fimmu.2018.02214
63. Sun J, Lanier L. The Natural Selection of Herpesviruses and Virus-Specific NK Cell Receptors. *Viruses* (2009) 1:362–82. doi: 10.3390/v1030362
64. Ulbrecht M, Martinozzi S, Grzeschik M, Hengel H, Ellwart JW, Pla M, et al. Cutting Edge: The Human Cytomegalovirus *UL40* Gene Product Contains a Ligand for HLA-E and Prevents NK Cell-Mediated Lysis. . *J Immunol* (2000) 164:5019–22. doi: 10.4049/jimmunol.164.10.5019
65. Tomasec P. Surface Expression of HLA-E, an Inhibitor of Natural Killer Cells, Enhanced by Human Cytomegalovirus Gpul40. *Science* (2000) 287:1031–3. doi: 10.1126/science.287.5455.1031
66. Spencer JV, Lockridge KM, Barry PA, Lin G, Tsang M, Penfold MET, et al. Potent Immunosuppressive Activities of Cytomegalovirus- Encoded Interleukin-10. *J Virol* (2002) 76:1285–92. doi: 10.1128/JVI.76.3.1285-1292.2002
67. Fielding CA, Aicheler R, Stanton RJ, Wang ECY, Han S, Seirafian S, et al. Two Novel Human Cytomegalovirus NK Cell Evasion Functions Target MICA for Lysosomal Degradation. *PloS Pathog* (2014) 10:e1004058. doi: 10.1371/journal.ppat.1004058
68. Stern-Ginossar N, Elefant N, Zimmermann A, Wolf DG, Saleh N, Biton M, et al. Host Immune System Gene Targeting by a Viral miRNA. *Science* (2007) 317:376–81. doi: 10.1126/science.1140956
69. Weller M, Malipiero U, Aguzzi A, Reed JC, Fontana A. Protooncogene Bcl-2 Gene Transfer Abrogates Fas/APO-1 Antibody-Mediated Apoptosis of Human Malignant Glioma Cells and Confers Resistance to Chemotherapeutic Drugs and Therapeutic Irradiation. *J Clin Invest* (1995) 95:2633–43. doi: 10.1172/JCI117965
70. Chiou S-H, Yang Y-P, Lin J-C, Hsu C-H, Jhang H-C, Yang Y-T, et al. The Immediate Early 2 Protein of Human Cytomegalovirus (HCMV) Mediates the Apoptotic Control in HCMV Retinitis Through Up-Regulation of the Cellular FLICE-Inhibitory Protein Expression. *J Immunol* (2006) 177:6199–206. doi: 10.4049/jimmunol.177.9.6199
71. Powers C, DeFilippis V, Malouli D, Früh K. Cytomegalovirus Immune Evasion. In: TE Shenk and MF Stinski, editors. *Human Cytomegalovirus Current Topics in Microbiology and Immunology*. Berlin, Heidelberg: Springer Berlin Heidelberg (2008). p. 333–59. doi: 10.1007/978-3-540-77349-8_19
72. Spiller OB, Morgan BP, Tufaro F, Devine DV. Altered Expression of Host-Encoded Complement Regulators on Human Cytomegalovirus-Infected Cells. *Eur J Immunol* (1996) 26:1532–8. doi: 10.1002/eji.1830260719
73. Margulies BJ, Browne H, Gibson W. Identification of the Human Cytomegalovirus G Protein-Coupled Receptor Homologue Encoded by UL33 in Infected Cells and Enveloped Virus Particles. *Virology* (1996) 225:111–25. doi: 10.1006/viro.1996.0579
74. Slinger E, Maussang D, Schreiber A, Siderius M, Rahbar A, Fraile-Ramos A, et al. HCMV-Encoded Chemokine Receptor US28 Mediates Proliferative Signaling Through the IL-6-STAT3 Axis. *Sci Signaling* (2010) 3:ra58–8. doi: 10.1126/scisignal.2001180
75. Jackson SE, Redeker A, Arens R, van Baarle D, van den Berg SPH, Benedict CA, et al. CMV Immune Evasion and Manipulation of the Immune System With Aging. *GeroScience* (2017) 39:273–91. doi: 10.1007/s11357-017-9986-6
76. Beisser PS, Laurent L, Virelizier J-L, Michelson S. Human Cytomegalovirus Chemokine Receptor Gene US28 Is Transcribed in Latently Infected THP-1 Monocytes. *J Virol* (2001) 75:5949–57. doi: 10.1128/JVI.75.13.5949-5957.2001
77. Michelson S, Alcami J, Kim SJ, Danielpour D, Bachelerie F, Picard L, et al. Human Cytomegalovirus Infection Induces Transcription and Secretion of Transforming Growth Factor Beta 1. *J Virol* (1994) 68:5730–7. doi: 10.1128/jvi.68.9.5730-5737.1994
78. Hansen SG, Powers CJ, Richards R, Ventura AB, Ford JC, Siess D, et al. Evasion of CD8+ T Cells Is Critical for Superinfection by Cytomegalovirus. *Science* (2010) 328:102–6. doi: 10.1126/science.1185350
79. Tortorella D, Gewurz BE, Furman MH, Schust DJ, Ploegh HL. Viral Subversion of the Immune System. *Annu Rev Immunol* (2000) 18:861–926. doi: 10.1146/annurev.immunol.18.1.861
80. Johnsen JI, Baryawno N, Söderberg-Nauclér C. Is Human Cytomegalovirus a Target in Cancer Therapy? *Oncotarget* (2011) 2:1329–38. doi: 10.18632/oncotarget.383
81. Charpak-Amikam Y, Kubsch T, Seidel E, Oiknine-Djian E, Cavaletto N, Yamin R, et al. Human Cytomegalovirus Escapes Immune Recognition by NK Cells Through the Downregulation of B7-H6 by the Viral Genes US18 and US20. *Sci Rep* (2017) 7:8661. doi: 10.1038/s41598-017-08866-2
82. Patro ARK. Subversion of Immune Response by Human Cytomegalovirus. *Front Immunol* (2019) 10:1155. doi: 10.3389/fimmu.2019.01155
83. McSharry B, Avdic S, Slobedman B. Human Cytomegalovirus Encoded Homologs of Cytokines, Chemokines and Their Receptors: Roles in Immunomodulation. *Viruses* (2012) 4:2448–70. doi: 10.3390/v4112448
84. Herbein G. The Human Cytomegalovirus, From Oncomodulation to Oncogenesis. *Viruses* (2018) 10:408. doi: 10.3390/v10080408
85. Ye L, Qian Y, Yu W, Guo G, Wang H, Xue X. Functional Profile of Human Cytomegalovirus Genes and Their Associated Diseases: A Review. *Front Microbiol* (2020) 11:2104. doi: 10.3389/fmicb.2020.02104
86. Rossini G, Cerboni C, Santoni A, Landini MP, Landolfo S, Gatti D, et al. Interplay Between Human Cytomegalovirus and Intrinsic/Innate Host

Responses: A Complex Bidirectional Relationship. *Mediators Inflamm* (2012) 2012:1–16. doi: 10.1155/2012/607276
87. Fu Y-Z, Su S, Gao Y-Q, Wang P-P, Huang Z-F, Hu M-M, et al. Human Cytomegalovirus Tegument Protein UL82 Inhibits STING-Mediated Signaling to Evade Antiviral Immunity. *Cell Host Microbe* (2017) 21:231–43. doi: 10.1016/j.chom.2017.01.001
88. Kalejta RF, Shenk T. The Human Cytomegalovirus UL82 Gene Product (Pp71) Accelerates Progression Through the G 1 Phase of the Cell Cycle. *J Virol* (2003) 77:3451–9. doi: 10.1128/JVI.77.6.3451-3459.2003
89. Cheung AKL, Gottlieb DJ, Plachter B, Pepperl-Klindworth S, Avdic S, Cunningham AL, et al. The Role of the Human Cytomegalovirus UL111A Gene in Down-Regulating CD4+ T-Cell Recognition of Latently Infected Cells: Implications for Virus Elimination During Latency. *Blood* (2009) 114:4128–37. doi: 10.1182/blood-2008-12-197111
90. Ashiru O, Bennett NJ, Boyle LH, Thomas M, Trowsdale J, Wills MR. NKG2D Ligand MICA Is Retained in the Cis-Golgi Apparatus by Human Cytomegalovirus Protein Ul142. *J Virol* (2009) 83:12345–54. doi: 10.1128/JVI.01175-09
91. McCormick AL, Roback L, Livingston-Rosanoff D, St. Clair C. The Human Cytomegalovirus UL36 Gene Controls Caspase-Dependent and -Independent Cell Death Programs Activated by Infection of Monocytes Differentiating to Macrophages. *J Virol* (2010) 84:5108–23. doi: 10.1128/JVI.01345-09
92. Skaletskaya A, Bartle LM, Chittenden T, McCormick AL, Mocarski ES. Goldmacher VS. A Cytomegalovirus-Encoded Inhibitor of Apoptosis That Suppresses Caspase-8 Activation. *Proc Natl Acad Sci* (2001) 98:7829–34. doi: 10.1073/pnas.141108798
93. Costa H, Nascimento R, Sinclair J, Parkhouse RME. Human Cytomegalovirus Gene UL76 Induces IL-8 Expression Through Activation of the DNA Damage Response. *PloS Pathog* (2013) 9: e1003609. doi: 10.1371/journal.ppat.1003609
94. Prichard MN, Britt WJ, Daily SL, Hartline CB, Kern ER. Human Cytomegalovirus UL97 Kinase Is Required for the Normal Intranuclear Distribution of Pp65 and Virion Morphogenesis. *J Virol* (2005) 79:15494–502. doi: 10.1128/JVI.79.24.15494-15502.2005
95. Benedict CA. A CMV Vaccine: TREATing Despite the TRICKs. *Expert Rev Vaccines* (2013) 12:1235–7. doi: 10.1586/14760584.2013.844653
96. Nightingale K, Lin K-M, Ravenhill BJ, Davies C, Nobre L, Fielding CA, et al. High-Definition Analysis of Host Protein Stability During Human Cytomegalovirus Infection Reveals Antiviral Factors and Viral Evasion Mechanisms. *Cell Host Microbe* (2018) 24:447–60.e11. doi: 10.1016/j.chom.2018.07.011
97. Le-Trilling VTK, Becker T, Nachshon A, Stern-Ginossar N, Schöler L, Voigt S, et al. The Human Cytomegalovirus Pul145 Isoforms Act as Viral DDB1-Cullin-Associated Factors to Instruct Host Protein Degradation to Impede Innate Immunity. *Cell Rep* (2020) 30:2248–60.e5. doi: 10.1016/j.celrep.2020.01.070
98. Hu L, Wen Z, Chen J, Chen Y, Jin L, Shi H, et al. The Cytomegalovirus UL146 Gene Product Vcxcl1 Promotes the Resistance of Hepatic Cells to CD8+ T Cells Through Up-Regulation of PD-L1. *Biochem Biophys Res Commun* (2020) 532:393–9. doi: 10.1016/j.bbrc.2020.08.060
99. De Pelsmaeker S, Romero N, Vitale M, Favoreel HW. Herpesvirus Evasion of Natural Killer Cells. *J Virol* (2018) 92:e02105–17. doi: 10.1128/JVI.02105-17
100. Nachmani D, Lankry D, Wolf DG, Mandelboim O. The Human Cytomegalovirus microRNA miR-UL112 Acts Synergistically With a Cellular microRNA to Escape Immune Elimination. *Nat Immunol* (2010) 11:806–13. doi: 10.1038/ni.1916
101. Liang Q, Wang K, Wang B, Cai Q. HCMV-Encoded miR-UL112-3p Promotes Glioblastoma Progression *via* Tumour Suppressor Candidate 3. *Sci Rep* (2017) 7:44705. doi: 10.1038/srep44705
102. Wu M, Fu P, Qu L, Liu J, Lin A. Long Noncoding RNAs, New Critical Regulators in Cancer Immunity. *Front Oncol* (2020) 10:550987. doi: 10.3389/fonc.2020.550987
103. Gredmark-Russ S, Söderberg-Nauclér C. Dendritic Cell Biology in Human Cytomegalovirus Infection and the Clinical Consequences for Host Immunity and Pathology. *Virulence* (2012) 3:621–34. doi: 10.4161/viru.22239
104. Handous I, Achour B, Marzouk M, Rouis S, Hazgui O, Brini I, et al. Co-Infections of Human Herpesviruses (CMV, HHV-6, HHV-7 and EBV) in non-Transplant Acute Leukemia Patients Undergoing Chemotherapy. *Virol J* (2020) 17:37. doi: 10.1186/s12985-020-01302-4
105. Rahbar A, Boström L, Lagerstedt U, Magnusson I, Söderberg-Naucler C, Sundqvist V-A. Evidence of Active Cytomegalovirus Infection and Increased Production of IL-6 in Tissue Specimens Obtained From Patients With Inflammatory Bowel Diseases. *Inflamm Bowel Dis* (2003) 9:154–61. doi: 10.1097/00054725-200305000-00002
106. Pleskoff O. Identification of a Chemokine Receptor Encoded by Human Cytomegalovirus as a Cofactor for HIV-1 Entry. *Science* (1997) 276:1874–8. doi: 10.1126/science.276.5320.1874
107. Wang H, Peng G, Bai J, He B, Huang K, Hu X, et al. Cytomegalovirus Infection and Relative Risk of Cardiovascular Disease (Ischemic Heart Disease, Stroke, and Cardiovascular Death): A Meta-Analysis of Prospective Studies Up to 2016. *JAHA* (2017) 6:e005025. doi: 10.1161/JAHA.116.005025
108. Spyridopoulos I, Martin-Ruiz C, Hilkens C, Yadegarfar ME, Isaacs J, Jagger C, et al. CMV Seropositivity and T-Cell Senescence Predict Increased Cardiovascular Mortality in Octogenarians: Results From the Newcastle 85 + Study. *Aging Cell* (2016) 15:389–92. doi: 10.1111/acel.12430
109. Savva GM, Pachnio A, Kaul B, Morgan K, Huppert FA, Brayne C, et al. The Medical Research Council Cognitive Function and Ageing Study. Cytomegalovirus Infection is Associated With Increased Mortality in the Older Population. *Aging Cell* (2013) 12:381–7. doi: 10.1111/acel.12059
110. Fülöp T, Larbi A, Pawelec G. Human T Cell Aging and the Impact of Persistent Viral Infections. *Front Immunol* (2013) 4:271. doi: 10.3389/fimmu.2013.00271
111. Macaluso M, Paggi MG, Giordano A. Genetic and Epigenetic Alterations as Hallmarks of the Intricate Road to Cancer. *Oncogene* (2003) 22:6472–8. doi: 10.1038/sj.onc.1206955
112. You JS, Jones PA. Cancer Genetics and Epigenetics: Two Sides of the Same Coin? *Cancer Cell* (2012) 22:9–20. doi: 10.1016/j.ccr.2012.06.008
113. Gonzalez H, Hagerling C, Werb Z. Roles of the Immune System in Cancer: From Tumor Initiation to Metastatic Progression. *Genes Dev* (2018) 32:1267–84. doi: 10.1101/gad.314617.118
114. Whiteside TL. The Tumor Microenvironment and its Role in Promoting Tumor Growth. *Oncogene* (2008) 27:5904–12. doi: 10.1038/onc.2008.271
115. Schuessler A, Walker DG, Khanna R. Cytomegalovirus as a Novel Target for Immunotherapy of Glioblastoma Multiforme. *Front Oncol* (2014) 4:275. doi: 10.3389/fonc.2014.00275
116. Hochhalter CB, Carr C, O'Neill BE, Ware ML, Strong MJ. The Association Between Human Cytomegalovirus and Glioblastomas: A Review. *NN* (2017) 4:96. doi: 10.20517/2347-8659.2017.10
117. Dey M, Ahmed AU, Lesniak MS. Cytomegalovirus and Glioma: Putting the Cart Before the Horse. *J Neurol Neurosurg Psychiatry* (2015) 86:191–9. doi: 10.1136/jnnp-2014-307727
118. Wolmer-Solberg N, Baryawno N, Rahbar A, Fuchs D, Odeberg J, Taher C, et al. Frequent Detection of Human Cytomegalovirus in Neuroblastoma: A Novel Therapeutic Target?: Human Cytomegalovirus in Neuroblastoma. *Int J Cancer* (2013) 133:2351–61. doi: 10.1002/ijc.28265
119. Taher C, de Boniface J, Mohammad A-A, Religa P, Hartman J, Yaiw K-C, et al. High Prevalence of Human Cytomegalovirus Proteins and Nucleic Acids in Primary Breast Cancer and Metastatic Sentinel Lymph Nodes. *PloS One* (2013) 8:e56795. doi: 10.1371/journal.pone.0056795
120. Taher C, Frisk G, Fuentes S, Religa P, Costa H, Assinger A, et al. High Prevalence of Human Cytomegalovirus in Brain Metastases of Patients With Primary Breast and Colorectal Cancers. *Trans Oncol* (2014) 7:732–40. doi: 10.1016/j.tranon.2014.09.008
121. Rahbar A, Touma J, Costa H, Davoudi B, Bukholm IR, Sauer T, et al. Low Expression of Estrogen Receptor-α and Progesterone Receptor in Human Breast Cancer Tissues Is Associated With High-Grade Human Cytomegalovirus Protein Expression. *Clin Breast Cancer* (2017) 17:526–35.e1. doi: 10.1016/j.clbc.2017.04.013
122. Harkins L, Volk AL, Samanta M, Mikolaenko I, Britt WJ, Bland KI, et al. Specific Localisation of Human Cytomegalovirus Nucleic Acids and Proteins in Human Colorectal Cancer. *Lancet* (2002) 360:1557–63. doi: 10.1016/S0140-6736(02)11524-8

123. Cobbs C, Harkins L, Samanta M, Gillespie GY, Bharara S, King PH, et al. Human Cytomegalovirus Infection and Expression in Human Malignant Glioma. *Cancer Res* (2002) 62:3347–50.
124. Mitchell DA, Xie W, Schmittling R, Learn C, Friedman A, McLendon RE, et al. Sensitive Detection of Human Cytomegalovirus in Tumors and Peripheral Blood of Patients Diagnosed With Glioblastoma. *Neuro-Oncology* (2008) 10:10–8. doi: 10.1215/15228517-2007-035
125. Samanta M, Harkins L, Klemm K, Britt WJ, Cobbs CS. High Prevalence of Human Cytomegalovirus in Prostatic Intraepithelial Neoplasia and Prostatic Carcinoma. *J Urol* (2003) 170:998–1002. doi: 10.1097/01.ju.0000080263.46164.97
126. Huang G, Yan Q, Wang Z, Chen X, Zhang X, Guo Y, et al. Human Cytomegalovirus in Neoplastic Cells of Epstein-Barr Virus Negative Hodgkin's Disease. *Int J Oncol* (2002) 21:31–6.
127. Harkins LE, Matlaf LA, Soroceanu L, Klemm K, Britt WJ, Wang W, et al. Detection of Human Cytomegalovirus in Normal and Neoplastic Breast Epithelium. *HerpesVi* (2010) 1:8. doi: 10.1186/2042-4280-1-8
128. Baryawno N, Rahbar A, Wolmer-Solberg N, Taher C, Odeberg J, Darabi A, et al. Detection of Human Cytomegalovirus in Medulloblastomas Reveals a Potential Therapeutic Target. *J Clin Invest* (2011) 121:4043–55. doi: 10.1172/JCI57147
129. Söderberg-Nauclér C, Rahbar A, Stragliotto G. Survival in Patients With Glioblastoma Receiving Valganciclovir. *N Engl J Med* (2013) 369:985–6. doi: 10.1056/NEJMc1302145
130. Li Q, Wilkie AR, Weller M, Liu X, Cohen JI. THY-1 Cell Surface Antigen (CD90) Has an Important Role in the Initial Stage of Human Cytomegalovirus Infection. *PloS Pathog* (2015) 11:e1004999. doi: 10.1371/journal.ppat.1004999
131. Soroceanu L, Akhavan A, Cobbs CS. Platelet-Derived Growth Factor-α Receptor Activation is Required for Human Cytomegalovirus Infection. *Nature* (2008) 455:391–5. doi: 10.1038/nature07209
132. Kapoor A, He R, Venkatadri R, Forman M, Arav-Boger R. Wnt Modulating Agents Inhibit Human Cytomegalovirus Replication. *Antimicrob Agents Chemother* (2013) 57:2761–7. doi: 10.1128/AAC.00029-13
133. Li J-W, Yang D, Yang D, Chen Z, Miao J, Liu W, et al. Tumors Arise From the Excessive Repair of Damaged Stem Cells. *Med Hypotheses* (2017) 102:112–22. doi: 10.1016/j.mehy.2017.03.005
134. Soroceanu L, Matlaf L, Khan S, Akhavan A, Singer E, Bezrookove V, et al. Cytomegalovirus Immediate-Early Proteins Promote Stemness Properties in Glioblastoma. *Cancer Res* (2015) 75:3065–76. doi: 10.1158/0008-5472.CAN-14-3307
135. Cobbs CS, Soroceanu L, Denham S, Zhang W, Kraus MH. Modulation of Oncogenic Phenotype in Human Glioma Cells by Cytomegalovirus IE1–Mediated Mitogenicity. *Cancer Res* (2008) 68:724–30. doi: 10.1158/0008-5472.CAN-07-2291
136. Teo WH, Chen H-P, Huang JC, Chan Y-J. Human Cytomegalovirus Infection Enhances Cell Proliferation, Migration and Upregulation of EMT Markers in Colorectal Cancer-Derived Stem Cell-Like Cells. *Int J Oncol* (2017) 51:1415–26. doi: 10.3892/ijo.2017.4135
137. Moussawi FA, Kumar A, Pasquereau S, Tripathy MK, Karam W, Diab-Assaf M, et al. The Transcriptome of Human Mammary Epithelial Cells Infected With the HCMV-DB Strain Displays Oncogenic Traits. *Sci Rep* (2018) 8:12574. doi: 10.1038/s41598-018-30109-1
138. Nehme Z, Pasquereau S, Haidar Ahmad S, Coaquette A, Molimard C, Monnien F, et al. Polyploid Giant Cancer Cells, Stemness and Epithelial-Mesenchymal Plasticity Elicited by Human Cytomegalovirus. *Oncogene* (2021) 40:3030–46. doi: 10.1038/s41388-021-01715-7
139. Fortunato EA, Spector DH. Viral Induction of Site-Specific Chromosome Damage. *Rev Med Virol* (2003) 13:21–37. doi: 10.1002/rmv.368
140. Siew V-K, Duh C-Y, Wang S-K. Human Cytomegalovirus UL76 Induces Chromosome Aberrations. *J BioMed Sci* (2009) 16:107. doi: 10.1186/1423-0127-16-107
141. Cinatl J, Scholz M, Kotchetkov R, Vogel J-U, Wilhelm Doerr H. Molecular Mechanisms of the Modulatory Effects of HCMV Infection in Tumor Cell Biology. *Trends Mol Med* (2004) 10:19–23. doi: 10.1016/j.molmed.2003.11.002
142. Clement M, Humphreys IR. Cytokine-Mediated Induction and Regulation of Tissue Damage During Cytomegalovirus Infection. *Front Immunol* (2019) 10:78. doi: 10.3389/fimmu.2019.00078
143. Streblow DN, Dumortier J, Moses AV, Orloff SL, Nelson JA. Mechanisms of Cytomegalovirus-Accelerated Vascular Disease: Induction of Paracrine Factors That Promote Angiogenesis and Wound Healing. In: TE Shenk and MF Stinski, editors. *Human Cytomegalovirus Current Topics in Microbiology and Immunology*. Berlin, Heidelberg: Springer Berlin Heidelberg (2008). p. 397–415. doi: 10.1007/978-3-540-77349-8_22
144. de Wit RH, Mujić-Delić A, van Senten JR, Fraile-Ramos A, Siderius M, Smit MJ. Human Cytomegalovirus Encoded Chemokine Receptor US28 Activates the HIF-1α/PKM2 Axis in Glioblastoma Cells. *Oncotarget* (2016) 7:67966–85. doi: 10.18632/oncotarget.11817
145. Maussang D, Langemeijer E, Fitzsimons CP, Stigter-van Walsum M, Dijkman R, Borg MK, et al. The Human Cytomegalovirus–Encoded Chemokine Receptor US28 Promotes Angiogenesis and Tumor Formation *via* Cyclooxygenase-2. *Cancer Res* (2009) 69:2861–9. doi: 10.1158/0008-5472.CAN-08-2487
146. Zheng X, Turkowski K, Mora J, Brüne B, Seeger W, Weigert A, et al. Redirecting Tumor-Associated Macrophages to Become Tumoricidal Effectors as a Novel Strategy for Cancer Therapy. *Oncotarget* (2017) 8:48436–52. doi: 10.18632/oncotarget.17061
147. Hollon TC, Price RL, Kwon C-H, Chiocca EA. Mutations in Glioblastoma Oncosuppressive Pathways Pave the Way for Oncomodulatory Activity of Cytomegalovirus. *OncoImmunology* (2013) 2:e25620. doi: 10.4161/onci.25620
148. Korbecki J, Gutowska I, Kojder I, Jeżewski D, Goschorska M, Łukomska A, et al. New Extracellular Factors in Glioblastoma Multiforme Development: Neurotensin, Growth Differentiation Factor-15, Sphingosine-1-Phosphate and Cytomegalovirus Infection. *Oncotarget* (2018) 9:7219–70. doi: 10.18632/oncotarget.24102
149. Valle Oseguera CA, Spencer JV. cmvIL-10 Stimulates the Invasive Potential of MDA-MB-231 Breast Cancer Cells. *PloS One* (2014) 9:e88708. doi: 10.1371/journal.pone.0088708
150. Nozawa H, Chiu C, Hanahan D. Infiltrating Neutrophils Mediate the Initial Angiogenic Switch in a Mouse Model of Multistage Carcinogenesis. *Proc Natl Acad Sci* (2006) 103:12493–8. doi: 10.1073/pnas.0601807103
151. Rahbar A, Cederarv M, Wolmer-Solberg N, Tammik C, Stragliotto G, Peredo I, et al. Enhanced Neutrophil Activity is Associated With Shorter Time to Tumor Progression in Glioblastoma Patients. *OncoImmunology* (2016) 5:e1075693. doi: 10.1080/2162402X.2015.1075693
152. Tai-Schmiedel J, Karniely S, Lau B, Ezra A, Eliyahu E, Nachshon A, et al. Human Cytomegalovirus Long Noncoding RNA4.9 Regulates Viral DNA Replication. *PloS Pathog* (2020) 16:e1008390. doi: 10.1371/journal.ppat.1008390
153. Denaro N, Merlano MC, Lo Nigro C. Long Noncoding RNAs as Regulators of Cancer Immunity. *Mol Oncol* (2019) 13:61–73. doi: 10.1002/1878-0261.12413
154. Tlaskalová-Hogenová H, Štěpánková R, Kozáková H, Hudcovic T, Vannucci L, Tučková L, et al. The Role of Gut Microbiota (Commensal Bacteria) and the Mucosal Barrier in the Pathogenesis of Inflammatory and Autoimmune Diseases and Cancer: Contribution of Germ-Free and Gnotobiotic Animal Models of Human Diseases. *Cell Mol Immunol* (2011) 8:110–20. doi: 10.1038/cmi.2010.67
155. Francescone R, Hou V, Grivennikov SI. Microbiome, Inflammation, and Cancer. *Cancer J* (2014) 20:181–9. doi: 10.1097/PPO.0000000000000048
156. Ramendra R, Isnard S, Lin J, Fombuena B, Ouyang J, Mehraj V, et al. Cytomegalovirus Seropositivity Is Associated With Increased Microbial Translocation in People Living With Human Immunodeficiency Virus and Uninfected Controls. *Clin Infect Dis* (2020) 71:1438–46. doi: 10.1093/cid/ciz1001
157. Gianella S, Chaillon A, Mutlu EA, Engen PA, Voigt RM, Keshavarzian A, et al. Effect of Cytomegalovirus and Epstein–Barr Virus Replication on Intestinal Mucosal Gene Expression and Microbiome Composition of HIV-Infected and Uninfected Individuals. *AIDS* (2017) 31:2059–67. doi: 10.1097/QAD.0000000000001579
158. Al-Koussa H, Atat OE, Jaafar L, Tashjian H, El-Sibai M. The Role of Rho GTPases in Motility and Invasion of Glioblastoma Cells. *Analytical Cell Pathol* (2020) 2020:1–9. doi: 10.1155/2020/9274016
159. Shimamura M, Murphy-Ullrich JE, Britt WJ. Human Cytomegalovirus Induces TGF-β1 Activation in Renal Tubular Epithelial Cells After Epithelial-To-Mesenchymal Transition. *PloS Pathog* (2010) 6:e1001170. doi: 10.1371/journal.ppat.1001170

160. Casey SC, Baylot V, Felsher DW. MYC: Master Regulator of Immune Privilege. *Trends Immunol* (2017) 38:298–305. doi: 10.1016/j.it.2017.01.002
161. Rakhra K, Bachireddy P, Zabuawala T, Zeiser R, Xu L, Kopelman A, et al. CD4+ T Cells Contribute to the Remodeling of the Microenvironment Required for Sustained Tumor Regression Upon Oncogene Inactivation. *Cancer Cell* (2010) 18:485–98. doi: 10.1016/j.ccr.2010.10.002
162. Soucek L, Lawlor ER, Soto D, Shchors K, Swigart LB, Evan GI. Mast Cells are Required for Angiogenesis and Macroscopic Expansion of Myc-Induced Pancreatic Islet Tumors. *Nat Med* (2007) 13:1211–8. doi: 10.1038/nm1649
163. Majeti R, Chao MP, Alizadeh AA, Pang WW, Jaiswal S, Gibbs KD, et al. CD47 Is an Adverse Prognostic Factor and Therapeutic Antibody Target on Human Acute Myeloid Leukemia Stem Cells. *Cell* (2009) 138:286–99. doi: 10.1016/j.cell.2009.05.045
164. Casey SC, Tong L, Li Y, Do R, Walz S, Fitzgerald KN, et al. MYC Regulates the Antitumor Immune Response Through CD47 and PD-L1. *Science* (2016) 352:227–31. doi: 10.1126/science.aac9935
165. Schlee M, Hölzel M, Bernard S, Mailhammer R, Schuhmacher M, Reschke J, et al. C-MYC Activation Impairs the NF-κb and the Interferon Response: Implications for the Pathogenesis of Burkitt's Lymphoma. *Int J Cancer* (2007) 120:1387–95. doi: 10.1002/ijc.22372
166. Stark GR, Kerr IM, Williams BRG, Silverman RH, Schreiber RD. How Cells Respond To Interferons. *Annu Rev Biochem* (1998) 67:227–64. doi: 10.1146/annurev.biochem.67.1.227
167. Villegas SN, Gombos R, García-López L, Gutiérrez-Pérez I, García-Castillo J, Vallejo DM, et al. PI3K/Akt Cooperates With Oncogenic Notch by Inducing Nitric Oxide-Dependent Inflammation. *Cell Rep* (2018) 22:2541–9. doi: 10.1016/j.celrep.2018.02.049
168. Cui Y, Guo G. Immunomodulatory Function of the Tumor Suppressor P53 in Host Immune Response and the Tumor Microenvironment. *IJMS* (2016) 17:1942. doi: 10.3390/ijms17111942
169. Blagih J, Buck MD, Vousden KH. P53, Cancer and the Immune Response. *J Cell Sci* (2020) 133:jcs237453. doi: 10.1242/jcs.237453
170. Li F, Kitajima S, Kohno S, Yoshida A, Tange S, Sasaki S, et al. Retinoblastoma Inactivation Induces a Protumoral Microenvironment *via* Enhanced CCL2 Secretion. *Cancer Res* (2019) 79:3903–15. doi: 10.1158/0008-5472.CAN-18-3604
171. Vishnu P, Aboulafia DM. The Oncogenicity of Human Cytomegalovirus. In: P Price, Makwana N and S Brunt, editors. *Manifestations of Cytomegalovirus Infection* (2013). doi: 10.5772/55051
172. Mitchell DA, Sampson JH. Toward Effective Immunotherapy for the Treatment of Malignant Brain Tumors. *Neurotherapeutics* (2009) 6:527–38. doi: 10.1016/j.nurt.2009.04.003
173. Quinn M, Erkes DA, Snyder CM. Cytomegalovirus and Immunotherapy: Opportunistic Pathogen, Novel Target for Cancer and a Promising Vaccine Vector. *Immunotherapy* (2016) 8:211–21. doi: 10.2217/imt.15.110
174. Rahman M, Dastmalchi F, Karachi A, Mitchell D. The Role of CMV in Glioblastoma and Implications for Immunotherapeutic Strategies. *OncoImmunology* (2019) 8:e1514921. doi: 10.1080/2162402X.2018.1514921
175. Herbein G, Nehme Z. Tumor Control by Cytomegalovirus: A Door Open for Oncolytic Virotherapy? *Mol Ther - Oncolytics* (2020) 17:1–8. doi: 10.1016/j.omto.2020.03.004
176. Wang C, Zhang J, Yin J, Gan Y, Xu S, Gu Y, et al. Alternative Approaches to Target Myc for Cancer Treatment. *Sig Transduct Target Ther* (2021) 6:117. doi: 10.1038/s41392-021-00500-y
177. Hashiguchi T, Bruss N, Best S, Lam V, Danilova O, Paiva CJ, et al. Cyclin-Dependent Kinase-9 Is a Therapeutic Target in MYC-Expressing Diffuse Large B-Cell Lymphoma. *Mol Cancer Ther* (2019) 18:1520–32. doi: 10.1158/1535-7163.MCT-18-1023
178. Chen H, Liu H, Qing G. Targeting Oncogenic Myc as a Strategy for Cancer Treatment. *Sig Transduct Target Ther* (2018) 3:5. doi: 10.1038/s41392-018-0008-7
179. Lozano G. Restoring P53 in Cancer: The Promises and the Challenges. *J Mol Cell Biol* (2019) 11:615–9. doi: 10.1093/jmcb/mjz063
180. Song M, Bode AM, Dong Z, Lee M-H. AKT as a Therapeutic Target for Cancer. *Cancer Res* (2019) 79:1019–31. doi: 10.1158/0008-5472.CAN-18-2738
181. Hennessy BT, Smith DL, Ram PT, Lu Y, Mills GB. Exploiting the PI3K/AKT Pathway for Cancer Drug Discovery. *Nat Rev Drug Discov* (2005) 4:988–1004. doi: 10.1038/nrd1902
182. Guo G, Yu M, Xiao W, Celis E, Cui Y. Local Activation of P53 in the Tumor Microenvironment Overcomes Immune Suppression and Enhances Antitumor Immunity. *Cancer Res* (2017) 77:2292–305. doi: 10.1158/0008-5472.CAN-16-2832
183. Beverly LJ, Felsher DW, Capobianco AJ. Suppression of P53 by Notch in Lymphomagenesis: Implications for Initiation and Regression. *Cancer Res* (2005) 65:7159–68. doi: 10.1158/0008-5472.CAN-05-1664
184. Finn RS, Dering J, Conklin D, Kalous O, Cohen DJ, Desai AJ, et al. PD 0332991, a Selective Cyclin D Kinase 4/6 Inhibitor, Preferentially Inhibits Proliferation of Luminal Estrogen Receptor-Positive Human Breast Cancer Cell Lines *In Vitro*. *Breast Cancer Res* (2009) 11:R77. doi: 10.1186/bcr2419
185. Knudsen ES, Wang JYJ. Targeting the RB-Pathway in Cancer Therapy. *Clin Cancer Res* (2010) 16:1094–9. doi: 10.1158/1078-0432.CCR-09-0787
186. Hutcheson J, Witkiewicz AK, Knudsen ES. The RB Tumor Suppressor at the Intersection of Proliferation and Immunity: Relevance to Disease Immune Evasion and Immunotherapy. *Cell Cycle* (2015) 14:3812–9. doi: 10.1080/15384101.2015.1010922
187. Lim SY, Yuzhalin AE, Gordon-Weeks AN, Muschel RJ. Targeting the CCL2-CCR2 Signaling Axis in Cancer Metastasis. *Oncotarget* (2016) 7:28697–710. doi: 10.18632/oncotarget.7376
188. Yang H, Zhang Q, Xu M, Wang L, Chen X, Feng Y, et al. CCL2-CCR2 Axis Recruits Tumor Associated Macrophages to Induce Immune Evasion Through PD-1 Signaling in Esophageal Carcinogenesis. *Mol Cancer* (2020) 19:41. doi: 10.1186/s12943-020-01165-x
189. Zhong J, Khanna R. Vaccine Strategies Against Human Cytomegalovirus Infection. *Expert Rev Anti-Infect Ther* (2007) 5:449–59. doi: 10.1586/14787210.5.3.449
190. Scarpini S, Morigi F, Betti L, Dondi A, Biagi C, Lanari M. Development of a Vaccine Against Human Cytomegalovirus: Advances, Barriers, and Implications for the Clinical Practice. *Vaccines* (2021) 9:551. doi: 10.3390/vaccines9060551
191. Haidar Ahmad S, Al Moussawi F, El Baba R, Nehme Z, Pasquereau S, Kumar A, et al. Identification of UL69 Gene and Protein in Cytomegalovirus-Transformed Human Mammary Epithelial Cells. *Front Oncol* (2021) 11:627866. doi: 10.3389/fonc.2021.627866
192. Shigle TL, Handy VW, Chemaly RF. Letermovir and its Role in the Prevention of Cytomegalovirus Infection in Seropositive Patients Receiving an Allogeneic Hematopoietic Cell Transplant. *Ther Adv Hematol* (2020) 11:204062072093715. doi: 10.1177/2040620720937150

Conflict of Interest: The authors declare that the research was conducted in the absence of any commercial or financial relationships that could be construed as a potential conflict of interest.

Publisher's Note: All claims expressed in this article are solely those of the authors and do not necessarily represent those of their affiliated organizations, or those of the publisher, the editors and the reviewers. Any product that may be evaluated in this article, or claim that may be made by its manufacturer, is not guaranteed or endorsed by the publisher.

Copyright © 2021 El Baba and Herbein. This is an open-access article distributed under the terms of the Creative Commons Attribution License (CC BY). The use, distribution or reproduction in other forums is permitted, provided the original author(s) and the copyright owner(s) are credited and that the original publication in this journal is cited, in accordance with accepted academic practice. No use, distribution or reproduction is permitted which does not comply with these terms.

GLOSSARY

ALT	Adoptive lymphocyte transfer
BAK	Bcl-2 homologues antagonist/killer
BAX	BCL2-Associated X Protein
Bcl-2	B-cell lymphoma 2
BET	Bromodomain and extraterminal protein
CDK	Cyclin-dependent kinases
COVID-19	Coronavirus disease 2019
COX-2	Cyclooxygenase-2
CRPs	Complement regulatory proteins
CTH	CMV transformed HMECs
CTLs	Cytotoxic T lymphocytes
DCs	Dendritic cells
DISC	Death-inducing signaling complex
dsDNA	Double-stranded DNA
EBV	Epstein-Barr virus
EMT	Epithelial to mesenchymal transition
EPCR	Endothelial protein C receptor
FAO	Fatty acid oxidation
FLIP	Fas-associated death-domain-like IL-1β-converting enzyme-inhibitory proteins
gB	Glycoproteins B
GBM	Glioblastoma
GCRs	G-Protein-coupled receptors
gH	Glycoprotein H
HCC	Hepatocellular carcinoma
HCMV	Human Cytomegalovirus
HHV-5	Human herpesvirus 5
HLTF	Helicase like transcription factor
HMEC	Human mammary epithelial cells
HSCT	Hematopoietic stem-cell transplantation
IBD	Inflammatory bowel disease
ICAM-1	Intercellular adhesion molecule-1
IFNs	Type I interferons
IL	Interleukin
IL6R	IL-6 receptor
JAK	Janus kinase
lncRNAs	Long non-coding RNAs
MCP-1	Monocyte chemoattractant protein-1
MCP3	Monocyte chemotactic protein-3
MDM2	Mouse double minute 2 homolog
MHC	Major histocompatibility complex
MICA	MHC Class I Polypeptide-Related Sequence A
MICB	MHC class I chain-related gene B
MIP-1α	Macrophage inflammatory protein-1 alpha
MIP-1β	Macrophage inflammatory protein-1 beta
miRNAs	microRNAs
MS	Mitochondrial superoxide
NK	Natural killer
NKG2D	Natural Killer Group 2D
NOS	Nitric oxide synthase
NSAIDs	Nonsteroidal anti-inflammatory drugs
Oct-4	Octamer-binding transcription factor 4
PBMCs	Peripheral blood mononuclear cells
PDGFRα	Platelet-derived growth factor receptor alpha
PD-L1	Programmed death-ligand 1
PI3K/AKT	Phosphatidylinositol-3-kinase and protein kinase B
SLE	Systemic lupus erythematosus
SOX2	SRY-Box Transcription Factor 2
STAT	Signal transducer and activator of transcription
TAMS	Tumor-associated macrophages
Th	T-helper
TLR2	Toll-like receptors 2
TME	Tumor microenvironment
TNFR	Tumor necrosis factor receptor
TNF-α	Tumor necrosis factor-alpha
TUSC3	Tumor suppressor candidate 3
UL	Unique long
ULBPs	UL16 binding proteins
US	Unique short
VEGF	Vascular endothelial growth factor
vICA	Viral inhibitor of caspase-8-induced apoptosis
γδ T-cells	Gamma-delta T-cells

11.4 Publication N°4

Haidar Ahmad S, Pasquereau S, **El Baba R**, Nehme Z, Lewandowski C, Herbein G. Distinct Oncogenic Transcriptomes in Human Mammary Epithelial Cells Infected With Cytomegalovirus. Front Immunol 2021;12:772160. https://doi.org/10.3389/fimmu.2021.772160.

Human cytomegalovirus (HCMV) is increasingly recognized as a potential oncovirus, beyond its oncomodulatory role. The study isolated two high-risk HCMV strains, HCMV-DB and HCMV-BL, which promoted oncogenic pathways and tumorigenicity in human mammary epithelial cells. In contrast, low-risk strains like HCMV-FS, KM, and SC did not induce these traits. When comparing high-risk and low-risk strains, high-risk HCMV-BL exhibited numerous pro-oncogenic features, including enhanced expression of oncogenes and genes associated with cell survival, proliferation, and epithelial-mesenchymal transition. Furthermore, mammosphere formation was observed only with high-risk strains. The Ki67 gene proved useful for distinguishing between high-risk and low-risk strains in vitro and in HCMV-positive breast cancer biopsies, primarily in basal tumors, potentially associated with high-risk HCMV strains. Overall, the transcriptome of human mammary epithelial cells infected with HCMV clinical isolates demonstrates an "oncogenic gradient," with high-risk strains creating a pro-oncogenic environment that may contribute to breast cancer development.

frontiers in Immunology

ORIGINAL RESEARCH
published: 22 December 2021
doi: 10.3389/fimmu.2021.772160

Distinct Oncogenic Transcriptomes in Human Mammary Epithelial Cells Infected With Cytomegalovirus

Sandy Haidar Ahmad[1†], *Sébastien Pasquereau*[1†], *Ranim El Baba*[1], *Zeina Nehme*[1], *Clara Lewandowski*[1] *and Georges Herbein*[1,2*]

[1] Pathogens & Inflammation/EPILAB Laboratory, EA4266, Université de Franche-Comté, Université Bourgogne Franche-Comté (UBFC), Besançon, France, [2] Department of Virology, Centre Hospitalier Universitaire (CHU) Besançon, Besançon, France

Human cytomegalovirus is being recognized as a potential oncovirus beside its oncomodulation role. We previously isolated two clinical isolates, HCMV-DB (KT959235) and HCMV-BL (MW980585), which in primary human mammary epithelial cells promoted oncogenic molecular pathways, established anchorage-independent growth *in vitro*, and produced tumorigenicity in mice models, therefore named high-risk oncogenic strains. In contrast, other clinical HCMV strains such as HCMV-FS, KM, and SC did not trigger such traits, therefore named low-risk oncogenic strains. In this study, we compared high-risk oncogenic HCMV-DB and BL strains (high-risk) with low-risk oncogenic strains HCMV-FS, KM, and SC (low-risk) additionally to the prototypic HCMV-TB40/E, knowing that all strains infect HMECs *in vitro*. Numerous pro-oncogenic features including enhanced expression of oncogenes, cell survival, proliferation, and epithelial-mesenchymal transition genes were observed with HCMV-BL. *In vitro*, mammosphere formation was observed only in high-risk strains. HCMV-TB40/E showed an intermediate transcriptome landscape with limited mammosphere formation. Since we observed that Ki67 gene expression allows us to discriminate between high and low-risk HCMV strains *in vitro*, we further tested its expression *in vivo*. Among HCMV-positive breast cancer biopsies, we only detected high expression of the Ki67 gene in basal tumors which may correspond to the presence of high-risk HCMV strains within tumors. Altogether, the transcriptome of HMECs infected with HCMV clinical isolates displays an "oncogenic gradient" where high-risk strains specifically induce a prooncogenic environment which might participate in breast cancer development.

Keywords: HCMV, cytomegalovirus, oncogenesis, breast cancer, high-risk, low-risk

OPEN ACCESS

Edited by:
Wen-Wei Chang, Chung Shan Medical University, Taiwan

Reviewed by:
Juliet Spencer, Texas Woman's University, United States
Yong Du, Hospital for Special Surgery, United States

***Correspondence:**
Georges Herbein
georges.herbein@univ-fcomte.fr

[†]*These authors have contributed equally to this work*

Specialty section:
This article was submitted to Viral Immunology, a section of the journal Frontiers in Immunology

Received: *08 September 2021*
Accepted: *24 November 2021*
Published: *22 December 2021*

Citation:
Haidar Ahmad S, Pasquereau S, El Baba R, Nehme Z, Lewandowski C and Herbein G (2021) Distinct Oncogenic Transcriptomes in Human Mammary Epithelial Cells Infected With Cytomegalovirus. Front. Immunol. 12:772160. doi: 10.3389/fimmu.2021.772160

INTRODUCTION

Breast cancer is the most common cancer diagnosed among women and recognized as one of the main causes of death in women (1). Etiologic factors of breast cancer are classified into genetic and environmental risk factors (2), and among these latter viruses could be involved (3, 4). Furthermore, the DNA and gene products of several viruses have been identified in breast cancer biopsies (5). Human cytomegalovirus (HCMV), a ubiquitous pathogen belonging to the *Herpesviridae* family,

has been detected in 90% of early and metastatic breast cancers (6–8). Likewise, HCMV DNA or antigens have been found in other malignancies including brain (glioblastoma, medulloblastoma), colon, prostate, and liver (7, 9–13). HCMV causes asymptomatic to mild infection in immunocompetent host, but it can lead to serious complications in the immunocompromised host and cancer patients (14, 15).

Although the growth of laboratory HCMV strains is restricted to fibroblasts, the clinical HCMV isolates infect a broad range of cells including epithelial cells, endothelial cells, monocytes, macrophages, fibroblasts, stromal cells, hepatocytes, smooth muscle cells, and neural stem/progenitor cells (16–19). Despite its known onco- and immunomodulatory effects, HCMV can transform primary human mammary epithelial cells (HMECs) *in vitro* as previously reported for the HCMV-DB and HCMV-BL strains (20, 21) in addition to the human embryonal lung fibroblasts (22). Moreover, blood monocyte, tissue macrophages, CD34+, and neural stem/progenitor are identified as HCMV reservoirs harboring latent virus (17, 23–28).

The different oncogenic abilities, cellular and molecular characteristics allowed us to classify HCMV strains into high or low-risk oncogenic strains. The high-risk strains promoted oncogenic molecular pathways, induced the expression of stemness markers, transformed epithelial cells, induced the appearance of polyploid giant cancer cells (PGCCs) in culture, established anchorage-independent growth *in vitro*, and produced tumorigenicity in mice models (20, 21). In contrast, the low-risk strains did not display such oncogenic features (21).

Herein, we compared six clinical HCMV strains for their oncogenic potential in HMECs using soft agar assay and transcriptomic analysis. Therefore, we compared the transcriptome profile of HMECs infected with the high-risk HCMV-BL strain versus the low-risk HCMV-FS, KM and SC strains. The transcriptome of HMECs infected with HCMV-BL presents oncogenic traits, favors cell cycling, cell proliferation, and epithelial-to-mesenchymal transition (EMT). However, the transcriptome of the HCMV-FS, KM and SC low-risk strains did not show any of the previously mentioned characteristics. HMECs infected with HCMV-TB40/E displayed a transcriptome phenotype similar to that of the HCMV-FS low-risk strain. In agreement with these distinct transcriptome profiles observed, we noticed the highest transformation and mammosphere formation in HMECs infected with the HCMV-BL high-risk strain, but not with the HCMV-FS, HCMV-KM and HCMV-SC low-risk ones. In line with the transcriptome phenotype observed in acutely infected HMECs, we perceived the preferential detection of high-risk HCMV strains along with the high expression of Ki67 in breast cancer biopsies, especially in the basal-like ones.

MATERIALS AND METHODS

Cell Cultures

HMECs were purchased from Life Technologies (Carlsbad, CA, USA). MDA-MB231 and MCF7 cells were provided by Institut Hiscia (Arlesheim, Switzerland). Human embryonic lung fibroblasts (MRC5) were purchased from RD-Biotech (Besançon, France). HMECs were cultivated in HMEC medium (Life Technologies) supplemented with HMEC supplement and bovine pituitary extract (Life Technologies). MDA-MB231, MCF7, and MRC5 were maintained in Dulbecco's modified Eagle medium (PAN- Biotech) supplemented with fetal bovine serum (Dutscher) and penicillin- streptomycin (Life Technologies). Cultures were free of mycoplasma (VenorGem classic mycoplasma detection, Minerva biolabs).

HMECs Infection With HCMV

HMECs were infected with HCMV-DB (KT959235), HCMV-BL (MW980585), HCMV-TB40/E (KF297339), HCMV-FS, HCMV-KM, and HCMV-SC. The HCMV clinical isolates were previously isolated in our laboratory (20, 21), except for HCMV-TB40/E (29). Cell-free virus stocks of HCMV were grown in HMECs as described previously (21). Virus titers were determined through the quantification of HCMV load by real-time qPCR detection using KAPA SYBR FAST Master Mix, Omega Bio-TEK) and *IE1* gene primers (sense, 5'-CGACGT TCCTGCAGACTATG-3'; anti-sense, 5'-TCCTCGGTCA CTTGTTCAAA-3') according to the manufacturer's protocol. Results were collected and analyzed using MxPro qPCR software.

Soft Agar Colony Formation Assay

Colony formation in soft agar seeded with HMECs uninfected, infected with the six strains listed above, MCF7 cells and MDA-MB231 cells were assayed using Cell Biolabs Cytosolic Cell Transformation Assay kit (Colorimetric assay, CB135; Cell Biolabs Inc., San Diego, CA) as per the manufacturer's protocol. The detection and quantification of colony formation was assessed by MTT assay (Cayman Chemical, Ann Arbor, MI). Colonies were observed under an Olympus microscope (Olympus Corporation, Tokyo, Japan)

Confocal Microscopy and Immunohistochemistry

Confocal microscopy was performed as described previously (21). Cells were washed using 1X PBS then fixed and permeabilized using BD Cytofix/Cytoperm, and finally stained with anti-IE1 (pp72) antibody (ab53495, Abcam). To visualize the nucleus, DAPI (4′, 6′-diamidino-2- phenylindole) staining was performed according to the manufacturer's protocol. Post-staining, confocal images were taken using 63X oil immersion objective lens with a LSM800 Carl-Zeiss confocal microscope 95 (Germany). The Ki67 immunohistochemistry (IHC) evaluation on breast biopsies was assessed using the monoclonal antibody MIB1 (Invitrogen).

Flow Cytometry Analysis

Uninfected HMECs and HCMV-infected HMECs were fixed and permeabilized for 20 minutes at 4°C using 100 µl Cytofix/Cytoperm solution (BD Biosciences), washed twice with 1X PBS supplemented with 3% FBS and 0.1% Triton-X, and then re-suspended in 100ul of staining buffer (1X PBS, 3% FBS, and

0.1% Triton-X). Cell staining was done using the anti-IE1 (CMV-pp72) antibody conjugated to PE (sc-69834, Santa Cruz Biotechnology). HMECs were incubated in the dark for 60 minutes at 4°C. Cells were washed twice with 1X PBS supplemented with 3% FBS and 0.1% Triton-X and subjected to cytofluorometric analysis on a BD LSRFortessa X-20 (BD Biosciences) flow cytometer. Data obtained was analyzed and processed using FACSDiva software (BD Biosciences).

Phylogenetic Analysis

Phylogenetic analysis was performed on several HCMV strains [BL (accession number: MW980585); DB (accession number: KT959235); TB40/E (accession number: KF297339); and Davis (accession number: JX512198.1)]. Multi-sequence alignments (MSA) were implemented using CLUSTAL W. Phylogenetic tree was constructed by means of the neighbor-joining method. The conducted analysis was done using MEGA7 software (http://www.megasoftware.net/).

RT^2 Profiler™ PCR Arrays Experiment

Total RNA was extracted from uninfected HMECs and HMECs infected with HCMV-BL, HCMV-TB40/E, HCMV-FS, HCMV-KM and HCMV-SC at MOI of 1 at day 1 post-infection using an RNA extraction kit (EZNA Total kit I, Omega BIO-TEK). Then, the cDNA was synthesized using the RT^2 First Strand Kit (Qiagen, Germantown, MD, USA) following the manufacturer's instructions. Two RT^2 Profiler™ PCR Arrays for human breast cancer (PAHS-131ZA) and human oncogenes & tumor suppressor genes (PAHS-502ZR) (both from Qiagen, Germantown, MD, USA) were performed using Mx3005P real-time PCR system as per manufacturer's instructions. These microarrays allow the quantification of mRNA from 84 cellular genes, using qPCR with premixed primer sets and SybrGreen qPCR MasterMix. DNA contamination control, housekeeping genes, reverse transcription control, and positive control were included in each PCR array. Data were analyzed using the manufacturer web-based analysis software (http://pcrdataanalysis.sabiosciencescom/pcr/arrayanalysis.php). The analysis was done based on three independent biological experiments for each of the HCMV strains.

Mammosphere Assay

Mammosphere formation by uninfected HMECs and HMECs infected with HCMV-BL, HCMV-TB40/E, HCMV-FS, and HCMV-KM at MOI of 1 was assayed as described previously (19). MCF7 and MDA-MB231 were used as positive controls. Mammospheres larger than 60 microns were counted.

Western Blotting

Cellular extracts of uninfected and infected HMECs with HCMV-DB and HCMV-TB40/E were prepared at 1 hour, 5 hours, days 1 and 3 post-infection and used to assess the expression of Rb, pRb, Akt, pAkt-Th308, pAkt-Ser473, STAT3, pSTAT3, CyclinD1, and ATM as described previously (20). Protein levels were quantified using ImageJ 1.40 software (National Institutes of Health, Bethesda, MA, USA). β-actin was used as loading control to normalize sample loading. Anti-Rb, anti-pRb, anti-Akt, anti-pAktThr308, anti-pAktSer473, anti-cyclin D1, and anti-ATM antibodies were purchased from Cell signaling (Danvers, MA, USA). Anti-pSTAT3 and anti-STAT3 antibodies were purchased from Santa Cruz Biotechnology (Santa Cruz, CA). Anti-β-actin antibody was purchased from Sigma-Aldrich (St. Louis, MO, USA).

Breast Biopsies

Nineteen frozen tumor breast biopsies (ten luminal tumor biopsies and nine basal tumor biopsies) and eight adjacent healthy breast biopsies were provided by the regional tumor bank (BB0033-00024 Tumorothèque Régionale de Franche-Comté). Healthy breast biopsies were numbered from one to eight, luminal tumor biopsies from nine to eighteen, and basal tumor biopsies from nineteen to twenty-seven. A detailed histopathological biopsy data including the histologic biopsy type, Elston-Ellis grading system, hormone percentages (estrogen and progesterone), presence or absence of the human epidermal growth factor receptor 2 (HER2) protein, vascular emboli, and TNM staging was provided as a supplementary data (**Supplementary Table 1**). Additionally, using twenty different breast tumor biopsies, we assessed the Ki67 mRNA and Ki67 protein levels measured by RT-qPCR and IHC, respectively, on the same biopsy sample. A written informed consent for participation was obtained from all patients. The study was authorized by the local ethics committees of Besançon University Hospital (Besançon, France) and the French Research Ministry (AC-2015-2496, CNIL n°1173545, NF-S-138 96900 n°F2015). The presence of HCMV, within all the biopsies, was assessed by qPCR using IE1 and UL69 primers as mentioned above and described previously (30). For Ki67 and GAPDH mRNA quantification, RNA was extracted from the biopsies using E.Z.N.A.® Total RNA Kit I (Omega BIO-TEK, GA, USA). Reverse transcription was performed using the SuperScript IV First-Strand Synthesis kit (Invitrogen, Carlsbad, CA, USA). The expression of Ki67 and GAPDH was assessed by real-time qPCR using KAPA SYBR FAST Master mix (KAPA BIOSYSTEMS, KK4601) and specific primer for Ki67 (sense, 5'TCCTTTGGTGGGCACCTAA GACCTG3'; anti-sense, 5'TGATGGTTGAGGTCGTTCCTTG ATG3') and GAPDH (sense, 5'CCCCTCTTCAAGGCCTC TAC3'; anti-sense, 5'CGACCACTTTGTCAAGCTCA3') according to the manufacturer's protocol. The fold change expression was calculated using the delta-delta Ct method (31). Biopsies having a fold change for Ki67 gene expression <30, from 30 to 100, and >100 were considered to have a low, intermediate, and high Ki67 mRNA absolute level respectively. The Ki67 mRNA cut-off was set based on the state of healthy biopsies (32).

Statistical Analysis

Statistical analysis was performed using the Wilcoxon test with the help of the Mathematics Department of the University of Franche-Comté. *p-value* ≤ *0.05* were considered statistically significant. In data analysis, Microsoft Excel was used to prepare the plots with

standard deviation and p-values. Statistical significance was represented on figures by stars, with the following code *p-value<0.05; **p-value<0.01; ***p-value<0.001.

RESULTS

Growth and Transforming Capacity of Six HCMV Clinical Strains in HMECs

A phylogenetic analysis was performed to analyse the genomic sequences of four HCMV strains, namely HCMV-DB, HCMV-BL, HCMV-TB40/E, and HCMV-Davis. Since the clinical isolates FS, KM and SC genomes were not sequenced, we selected the strain Davis for its similar clinical characteristics (33). The phylogenetic analysis showed that HCMV-BL is close to HCMV-DB, and HCMV-TB40/E is close to the genomes of HCMV-Davis (**Supplementary Figure 1**). The two observable brackets illustrate a high-risk group including DB and BL strains, and a low-risk group including TB40/E and Davis strains (**Supplementary Figure 1**).

We assessed the replication of six HCMV clinical isolates in HMECs, namely the HCMV-BL and HCMV-DB high-risk strains, the HCMV-FS, HCMV-KM and HCMV-SC low-risk strains, and the prototypic TB40/E strain (20, 21, 29). We evaluated the expression of the immediate early protein IE1 by immunofluorescence and flow cytometry. We observed strong IE1 expression in HMECs infected with the five strains (HCMV-DB, BL, TB40/E, FS and KM) at day 1 post-infection compared to the uninfected HMECs by confocal microscopy (**Figure 1A**). Moreover, the expression of IE1 protein in HMECs infected with the different HCMV strains was confirmed by flow cytometric analysis (**Figure 1B**). Further, we noticed productive replication of all six HCMV strains in infected HMECs as assayed by *IE1* detection in culture supernatants using qPCR (**Figure 1C** and **Supplementary Figure 2A**). An early and transient peak of viral replication was observed at day 1 post-infection for HMECs infected with HCMV-DB, HCMV-BL, and HCMV-TB40/E unlike the delayed peaks at day 3 and 5 post-infection for HMECs infected with HCMV-KM and HCMV-FS respectively. To further assess the oncogenic status of all six HCMV strains, we performed a soft agar assay. HMECs infected with the six HCMV strains were seeded in soft agar at day 1 post-infection. Cancer cell lines, MCF7 and MDA-MB231, were used as positive controls. Uninfected HMECs were used as negative control. Colony formation was detected at day 15 post-infection only with HCMV-DB and HCMV-BL compared to the uninfected HMECs (p-value $_{(\text{HCMV-DB : UI HMEC})}$ =0.03, p-value $_{(\text{HCMV-BL : UI HMEC})}$ =0.03, p-value $_{(\text{HCMV-DB : HCMV-TB40/E})}$ =0.03; p-value $_{(\text{HCMV-DB : HCMV-FS})}$ =0.03; p-value $_{(\text{HCMV-DB : HCMV-KM})}$ =0.03; p-value $_{(\text{HCMV-BL : HCMV-TB40/E})}$ =0.03; p-value $_{(\text{HCMV-BL : HCMV-FS})}$ =0.03; p-value $_{(\text{HCMV-BL : HCMV-KM})}$ =0.03). In contrast, no significant colony formation was observed with HCMV-FS, HCMV-KM, HCMV-SC, and HCMV-TB40/E infected HMECs (**Figure 1D** and **Supplementary Figure 2B**). Our results indicate that HMECs infected with the high-risk strains BL and DB have an anchorage-independent growth ability.

Distinct Transcriptome Profiles in HMECs Infected With Low-Risk and High-Risk HCMV Strains

We decided to compare the transcriptome profile of the high-risk BL strain, the low-risk FS, KM and SC strains, and the prototypic TB40/E strain. Human breast cancer along with human oncogenes and tumor suppressor genes RT^2 profiler PCR arrays were used to screen the infected HMECs with the four strains at MOI of 1 at day 1 post-infection and the uninfected HMECs. The expression of genes that are involved in signal transduction, cell cycle, cell survival, adhesion, angiogenesis, DNA repair, were examined by the RT^2 Profiler PCR arrays (**Supplementary Tables 2**, **3**).

The individual gene expression of the oncogenes *Myc* (MYC), *Fos* (FOS), *Jun* (JUN), *KRas* (KRAS), and *E2F1* was assessed in HMECs infected with the five strains HCMV-BL, TB40/E, FS, KM and SC compared to uninfected HMECs (**Figures 2A**, **3A** and **Supplementary Figure 2C**). Values for individual genes were pooled to constitute the overall expression of the oncogenes group **(Figure 2A)**. In HMECs infected with HCMV-BL, the expression of the oncogenes group was 5.8-fold higher compared to HMECs infected with the TB40/E strain (p-value $_{(\text{HCMV-BL: HCMV-TB40/E})}$ = 0.02), 8.5-fold higher compared to HMECs infected with FS strain (p-value $_{(\text{HCMV-BL: HCMV-FS})}$ = 0.004) (**Figure 2A**). However, the expression of these oncogenes was downregulated in HMECs infected with the KM strain (p-value $_{(\text{HCMV-BL: HCMV-KM})}$ = 0.0001) (**Figure 2A**). Among the oncogenes, Myc and E2F1 were mostly increased in HMECs infected with HCMV-BL compared to HCMV-TB40/E (p-value $_{(\text{Myc- HCMV-BL: HCMV-TB40/E})}$ = 0.12; p-value $_{(\text{E2F1- HCMV-BL: HCMV-TB40/E})}$= 0.04), HCMV-FS ($p$-value $_{(\text{Myc- HCMV-BL: HCMV-FS})}$ = 0.12; p-value $_{(\text{E2F1- HCMV-BL: HCMV-FS})}$ = 0.27) and HCMV-KM (p-value $_{(\text{Myc- HCMV-BL: HCMV-KM})}$ = 0.04; p-value $_{(\text{E2F1- HCMV-BL: HCMV-KM})}$ = 0.12) infected HMECs (**Figure 3A**). Furthermore, the expression of other oncogenes was tested for HMECs infected with the high-risk strain BL and the low-risk strain FS versus uninfected HMECs. We observed an upregulation of the transcripts of numerous other oncogenes such as KITLG, MYB, RARA, ROS1, and RUNX1 in HMECs infected with HCMV-BL and HCMV-FS (**Table 1**). The upregulation of KITLG, RARA, and ROS1 genes expression was at least 2-fold higher in HMECs infected with HCMV-BL compared to HMECs infected with HCMV-FS **(Table 1).** In HMECs infected with HCMV-SC, the oncogenes' expression (MYC, FOS, KRAS, JUN, E2F1) was low, likewise in HMECs infected with HCMV-FS (**Supplementary Figure 2C**).

The individual gene expression of the tumor suppressor genes coding for p53 protein (TP53), retinoblastoma protein (Rb), p73 protein (TP73), SMAD4, VHL, TSC1, and MDM2 was also assessed in the previously mentioned five strains compared to uninfected HMECs (**Figures 2B**, **3B** and **Supplementary Figure 2C**). Values for individual genes were pooled to constitute the overall expression of the tumor suppressor genes group (**Figure 2B**). The upregulation of tumor suppressor genes' expression was higher in HMECs infected with the BL strain compared to HMECs infected with the TB40/E and FS by 2

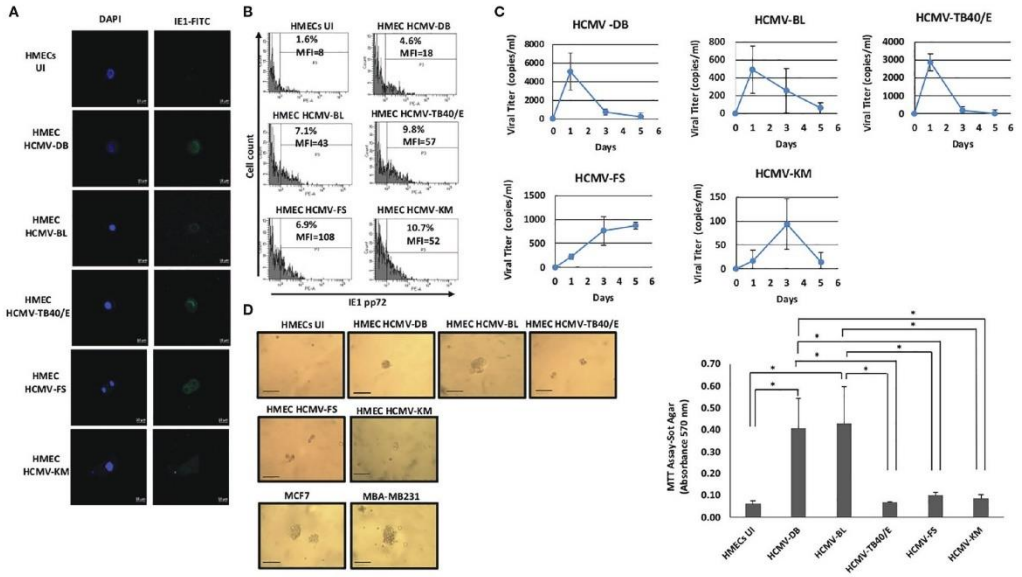

FIGURE 1 | Replication and transforming capacities of five HCMV strains in HMEC cultures. **(A)** Confocal microscopic images of DAPI and IE1 staining in HMECs infected with HCMV-DB, HCMV-BL, HCMV-TB40/E, HCMV-FS, and HCMV-KM. Uninfected HMECs (UI) was used as negative control. Magnification X63, scale bar 10 µm. Data shown are representative of three independent experiments. **(B)** Detection of IE1 (pp72) protein in HMECs infected with HCMV-DB, HCMV-BL, HCMV-TB40/E, HCMV-FS, and HCMV-KM. Uninfected HMECs (UI) was used as negative control. Data are represented as mean ± SD of two independent experiments. **(C)** Growth kinetics of the five HCMV strains in HMECs up to day 5 post-infection. Measurement of IE1 by qPCR in order to assess the viral growth. Data are represented as mean ± SD of three independent experiments. **(D)** Colony formation in soft agar seeded with HMECs infected with HCMV-DB, HCMV-BL, HCMV-TB40/E, HCMV-FS, and HCMV-KM at MOI of 1. MDA-MB231 and MCF7 were used as positive controls. Uninfected HMECs were used as negative control. Colonies were observed under an inverted light microscope (magnification ×100, scale bar 100µm). *Right panel.* Quantification was performed at day 15 post-seeding. Histogram represents mean ± SD of three independent experiments. *p-values* were determined by Wilcoxon test. **p-value* < 0.05.

(*p-value* (HCMV-BL: HCMV-TB40/E) = 0.02) and 3.8 fold (*p-value* (HCMV-BL: HCMV-FS) = 0.002) respectively (**Figures 2B**). Nevertheless, the expression of these tumor suppressor genes was downregulated in HMECs infected with HCMV-KM (*p-value* (HCMV-BL: HCMV-KM) = 0.00001) (**Figure 2B**). Among the tumor suppressor genes, TP53, VHL, Rb, and TSC1 expression was mainly increased in HMECs infected with HCMV-BL compared to HCMV-TB40/E (*p-value* (TP53- HCMV-BL: HCMV-TB40/E) = 0.04; *p-value* (SMAD4- HCMV-BL: HCMV-TB40/E) = 0.82; *p-value* (VHL- HCMV-BL: HCMV-TB40/E) = 0.27; *p-value* (Rb- HCMV-BL: HCMV-TB40/E) = 0.04; *p-value* (TSC1- HCMV-BL: HCMV-TB40/E) =0.51), HCMV-FS (*p-value* (TP53- HCMV-BL: HCMV-FS) = 0.04; *p-value* (SMAD4- HCMV-BL: HCMV-FS) = 0.12; *p-value* (VHL- HCMV-BL: HCMV-FS) = 0.51; *p-value* (Rb- HCMV-BL: HCMV-FS)= 0.04; *p-value* (TSC1- HCMV-BL: HCMV-FS) =0.51), and HCMV-KM (*p-value* (TP53- HCMV-BL: HCMV-KM) = 0.04; *p-value* (SMAD4- HCMV-BL: HCMV-KM)= 0.04; *p-value* (VHL- HCMV-BL: HCMV-KM) = 0.12; *p-value* (Rb- HCMV-BL: HCMV-KM)= 0.04; *p-value* (TSC1- HCMV-BL: HCMV-KM) =0.12) (**Figure 3B**). In HMECs infected with HCMV-SC, the tumor suppressor genes (TP53, VHL, TSC1) were slightly expressed, similarly in HMECs infected with HCMV-FS (**Supplementary Figure 2C**). The expression of TP73, a tumor suppressor gene, was markedly increased in HMECs infected with low-risk HCMV strains (KM and SC) and to a lower extent with FS and TB40/E strains compared to HMECs infected with high-risk BL strain (**Figure 3B** and **Supplementary Figure 2C**).

We then analyzed the individual expression of genes involved in cell proliferation namely STAT3, cyclin D1 (CCND1), and Ki67 antigen (MKI67). Interestingly, the STAT3/Cyclin D1 axis is activated in several cancer types including breast cancer (34). Values for individual genes were pooled to constitute the overall expression of the genes involved in cell proliferation group (**Figure 2C**). The expression of "proliferation" genes all together was 2.81 times more upregulated in the HMECs infected with the BL strain compared to HMECs infected with the TB40/E strain (*p-value* (HCMV-BL: HCMV-TB40/E) = 0.05) (**Figure 2C**). While the expression of "proliferation" genes was almost unchanged in HMECs infected with HCMV-FS compared to uninfected HMECs (*p-value* (HCMV-BL: HCMV-FS) = 0.005), it was downregulated in HMECs infected with HCMV-

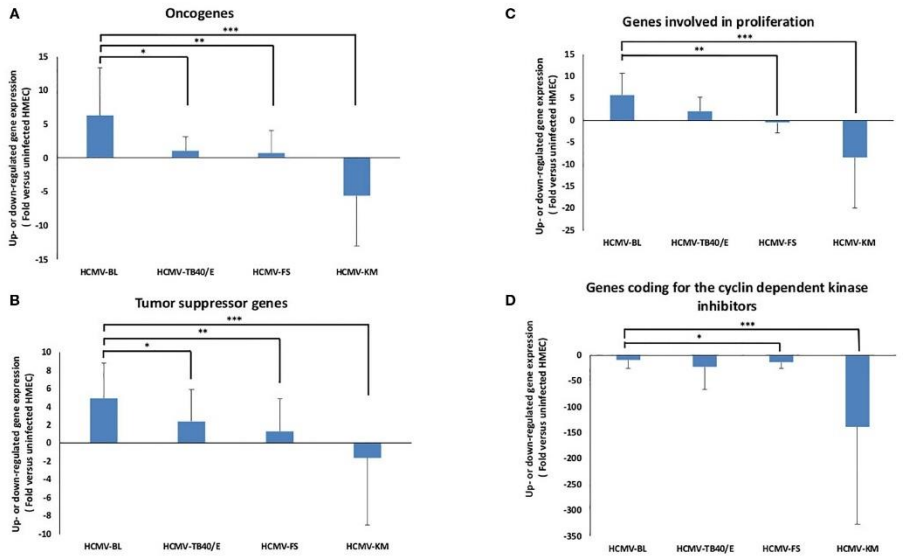

FIGURE 2 | Bulk analysis of the transcriptome differences in oncogenes, tumor suppressor genes, genes involved in cell proliferation and genes coding for cyclin dependent kinase inhibitors in HMECs infected with low-risk and high-risk HCMV strains. **(A)** Assessment of the bulk oncogene expression (based on MYC, FOS, KRAS, JUN, and E2F1 analysis). **(B)** Assessment of the bulk expression of tumor suppressor genes (based on TP53, TP73, SMAD4, VHL, RB, TSC1, and MDM2 analysis). **(C)** Assessment of the bulk expression of genes involved in cell proliferation (based on STAT3, CCND1, and MKI67 analysis). **(D)** Assessment of the bulk expression of genes coding for the cyclin-dependent kinase inhibitors (based on CDKN1A, CDKN2A, CDKN2B, and CDKN3 analysis). The gene expression was measured in HMECs infected with HCMV-BL, HCMV-TB40/E, HCMV-FS and HCMV-KM (MOI = 1) and compared to uninfected HMECs. Histograms represent mean ± SD of three independent experiments. *p-values* were determined by Wilcoxon test. **p-value* < 0.05; ***p-value* < 0.01; ****p-value* < 0.001.

KM (*p-value* $_{(HCMV\text{-}BL:\ HCMV\text{-}KM)}$ = 0.0007) (**Figure 2C**). The *STAT3* gene expression was up-regulated in HMECs infected with HCMV-BL in contrast to HMECs infected with HCMV-TB40/E (*p-value* $_{(HCMV\text{-}BL:\ HCMV\text{-}TB40/E)}$ = 0.04) and HCMV-FS (*p-value* $_{(HCMV\text{-}BL:\ HCMV\text{-}FS)}$ = 0.04) noting that it was substantially down-regulated in HMECs infected with HCMV-KM (*p-value* $_{(HCMV\text{-}BL:\ HCMV\text{-}KM)}$ = 0.04) (**Figure 3C**). The gene expression of cyclin D1 was up-regulated in HMECs infected with HCMV-BL compared to uninfected controls. In HMECs infected with HCMV-BL, cyclin D1 gene expression was 2 times more increased when compared to HMECs infected with HCMV-TB40/E (*p-value* $_{(HCMV\text{-}BL:\ HCMV\text{-}TB40/E)}$ = 0.12). In contrast, the expression of cyclin D1 was almost unchanged in HMECs infected with HCMV- FS compared to uninfected HMECs (*p-value* $_{(HCMV\text{-}BL:\ HCMV\text{-}FS)}$ = 0.12), and down-regulated with in HMECs infected with HCMV-KM (*p-value* $_{(HCMV\text{-}BL:\ HCMV\text{-}KM)}$ = 0.04) (**Figure 3C**). In agreement with the highest expression of cyclin D1 in HMECs infected with HCMV-BL and the lowest expression in HMECs infected with HCMV-KM strain, we observed the highest expression of the proliferation marker Ki67 gene (MKI67) in the former and very low expression in the latter (3-fold versus 0.6-fold increase compared to uninfected cells) (**Figure 3C**). HMECs infected with HCMV-SC showed a low expression of the genes involved in proliferation (CCDN1, MKI67) likewise in HMECs infected with the low-risk strains (**Supplementary Figure 2C**). We also assessed the expression of CDK inhibitors CDKN1A, CDKN2A, CDKN2B and CDKN3. Values for individual genes were pooled to constitute the overall expression of CDK inhibitors group (**Figure 2D**). The expression of CDK inhibitors genes was slightly decreased in HMECs infected with HCMV-BL compared to the other three strains TB40/E (*p-value* $_{(HCMV\text{-}BL:\ HCMV\text{-}TB40/E)}$ =0.81), FS (*p-value* $_{(HCMV\text{-}BL:\ HCMV\text{-}FS)}$ =0.02) and KM (*p-value* $_{(HCMV\text{-}BL:\ HCMV\text{-}KM)}$ = 0.001) (**Figures 2D**, **3D**). HMECs infected with HCMV-SC showed a minimal expression of the genes coding for the cyclin dependent kinase inhibitors (**Supplementary Figure 2C**).

HMECs Infected With Low-Risk and High-Risk HCMV Clinical Strains Display Distinct Expression of Cell Survival, Cell Adhesion, Angiogenesis, and EMT Genes

The expression of genes involved in cell survival, such as *AKT*, was upregulated in HMECs infected with BL, and TB40/E strains unlike in HMECs infected with FS and KM strains (*p-value* $_{(HCMV\text{-}BL:\ HCMV\text{-}FS)}$ = 0.12 and *p-value* $_{(HCMV\text{-}BL:\ HCMV\text{-}KM)}$ =0.04) (**Figure 4A**). In addition, REL was upregulated more in

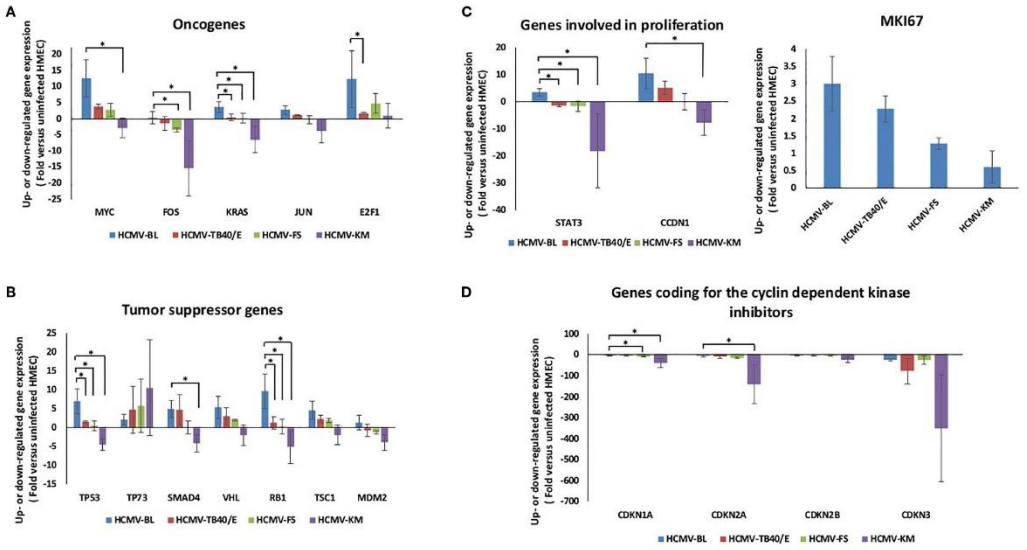

FIGURE 3 | Detailed transcriptome differences in oncogenes, tumor suppressor genes, genes involved in cell proliferation, and genes coding for the cyclin dependent kinase inhibitors in HMECs infected with low-risk and high-risk HCMV strains. **(A)** Assessment of the individual oncogenes expression including MYC, FOS, KRAS, JUN, and E2F1. **(B)** Assessment of the individual expression of tumor suppressor genes: TP53, TP73, SMAD4, VHL, RB, TSC1, and MDM2. **(C)** Assessment of the individual expression of genes involved in cell proliferation such as STAT3, CCDN1, and MKI67. **(D)** Assessment of the individual expression of genes coding for the cyclin-dependent kinase inhibitors: CDKN1A, CDKN2A, CDKN2B, and CDKN3. The gene expression was measured in HMECs infected with HCMV-BL, HCMV-TB40/E, HCMV-FS and HCMV-KM (MOI = 1) and compared to uninfected HMECs. Results represent mean ± SD of three independent experiments. *p-values* were determined by Wilcoxon test. *p-value < 0.05.

TABLE 1 | The fold change of several oncogenes' expression in HMECs infected with HCMV-BL and HCMV-FS versus uninfected HMECs.

Gene expression in HMECs infected with(Fold versus uninfected HMECs)		
Gene	**HCMV-BL**	**HCMV-FS**
KITLG	5.04*	1.93
MYB	11.10	6.15
RARA	74.67*	36.28
ROS1	29.50*	14.04
RUNX1	3.49	2.45

*Upregulated gene expression at least two times more in HMEC infected with HCMV-BL compared to HCMV-FS.

HCMV-BL than in HCMV-TB40/E (p-value (HCMV-BL: HCMV-TB40/E) =0.04) and HCMV-FS (p-value (HCMV-BL: HCMV-FS)=0.04) and was downregulated in HCMV-KM (p-value (HCMV-BL: HCMV-KM) =0.04) (**Figure 4A**). The expression of genes involved in DNA reparation (*ATM and MLH*) was downregulated in HMECs infected with HCMV-TB40/E, FS and KM compared to HMEC infected with HCMV-BL (p-value (ATM-HCMV-BL: HCMV-KM) =0.04 and p-value (ATM-HCMV-BL: HCMV-FS) =0.04) (**Figure 4B**). The gene expression of the molecules involved in cell adhesion such as E-cadherin (CDH1) and beta-catenin (CTNNB1) was minimal in HMECs infected with the four strains (BL, TB40/E, FS and KM) noting that it was mostly downregulated in HCMV-KM (p-value (CDH1-HCMV-BL: HCMV-KM) =0.04 and (p-value (CTNNB1-HCMV-BL: HCMV-KM) =0.04) (**Figure 4C**). The genes involved in angiogenesis regulation *S100A4 and EGF* were highly expressed in HMECs infected with HCMV-BL compared to HMECs infected with HCMV-FS and HCMV-KM (p-value (S100A4-HCMV-BL: HCMV-KM) =0.1; p-value (S100A4-HCMV-BL: HCMV-FS) =0.5; p-value (S100A4-HCMV-BL: HCMV-TB40/E) =0.1; p-value (EGF-HCMV-BL: HCMV-KM) =0.2; p-value (EGF-HCMV-BL: HCMV-FS) =0.05 p-value (EGF-HCMV-BL: HCMV-TB40/E) =0.5) (**Figure 4D**). Furthermore, the expression of genes involved in proteolysis including matrix metallopeptidase 9 (MMP9) and cathepsin D (CTSD) was 7-fold and 2.4-fold higher respectively, in HMECs infected with HCMV-BL compared to HMECs infected with HCMV-FS (**Supplementary Table 4**). The expression of the EMT markers for instance the

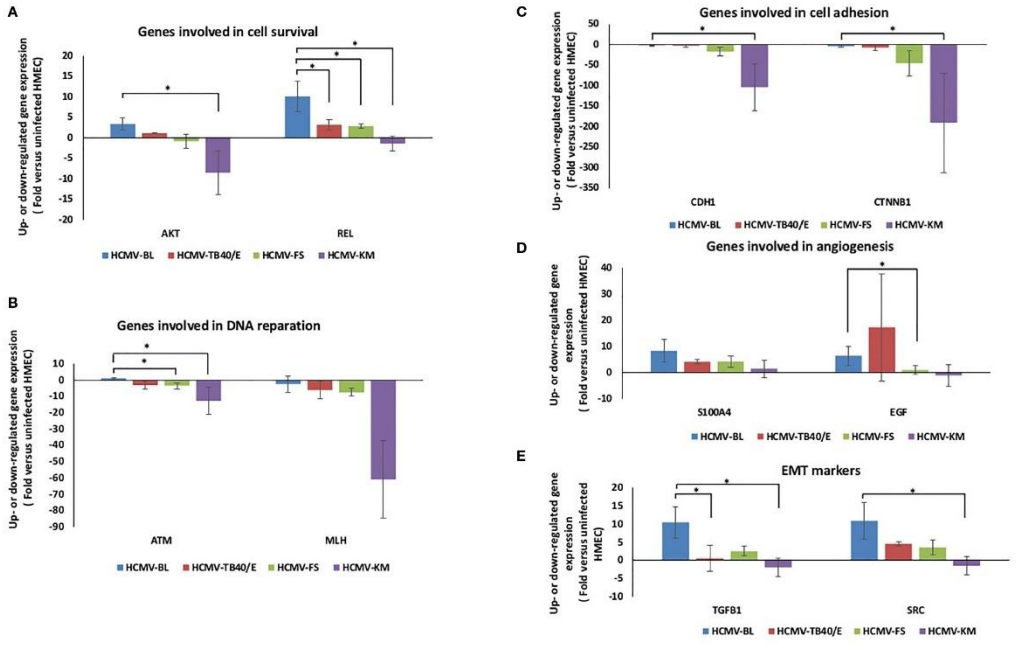

FIGURE 4 | Transcriptome differences in genes involved in cell survival, DNA reparation, cell adhesion, angiogenesis, and EMT markers in HMECs infected with low-risk and high-risk HCMV strains. Up- and downregulation of the expression of genes involved in **(A)** cell survival such as AKT and REL, **(B)** in DNA reparation (ATM and MLH), **(C)** in cell adhesion such as E-cadherin (CDH1) and beta-catenin (CTNNB1), **(D)** in angiogenesis (S100A4 and EGF) and **(E)** of the EMT markers (TGFB1 and SRC). The gene expression was measured in HMECs infected with HCMV-BL, HCMV-TB40/E, HCMV-FS and HCMV-KM (MOI = 1) and compared to uninfected HMECs. Data are represented as mean ± SD of three independent experiments. *p-values* were determined by Wilcoxon test. **p-value* < 0.05.

transforming growth factor-beta 1 (TGFB1) and the proto-oncogene tyrosine-protein kinase (SRC) was enhanced in HMECs infected with HCMV-BL compared to cells infected with HCMV-TB40/E (*p-value* $_{(TGFB1\text{- HCMV-BL: HCMV-TB40/E})}$ = 0.04; *p-value* $_{(SRC\text{- HCMV-BL: HCMV-TB40/E})}$ = 0.27), FS (*p-value* $_{(TGFB1\text{- HCMV-BL: HCMV-FS})}$ = 0.12; *p-value* $_{(SRC\text{- HCMV-BL: HCMV-FS})}$ = 0.12) and KM (*p-value* $_{(TGFB1\text{- HCMV-BL: HCMV-KM})}$ = 0.04; *p-value* $_{(SRC\text{- HCMV-BL: HCMV-KM})}$= 0.04) (**Figure 4E**). In HMECs infected with HCMV-SC, the genes involved in cell survival (AKT, REL), DNA reparation (MLH), and angiogenesis (S100A4) as well as the EMT marker (SRC) were regulated in a similar manner compared to HMECs infected with the FS strain (**Supplementary Figure 2C**).

Mammosphere Formation in HMECs Infected With Low-risk and High-Risk HCMV Clinical Strains

We previously observed that the high-risk strains (HCMV-BL and DB) favor the appearance of stemness in chronically infected HMECs and CMV-transformed HMECs (CTH cells) (21), further suggesting that HCMV strains that trigger cellular transformation could also promote stemness. Therefore, HMECs were infected with the high-risk strain HCMV-BL, the low-risk strains HCMV-FS and HCMV-KM, and the prototypic HCMV-TB40/E. At day 1 post-infection, mammosphere formation assay was performed as previously described (35, 36). When we challenged these HCMV-infected cultures to form mammospheres, we detected numerous mammospheres in HCMV-BL infected HMECs as previously reported for HCMV-DB infected cells (*p-value* $_{(HCMV\text{-BL: HMEC UI})}$ =0.03) (37), whereas HCMV-TB40/E displayed a limited number of mammospheres (*p-value* $_{(HCMV\text{-TB40/E: HMEC UI})}$ = 0.07); only few mammospheres were observed in HMECs infected with HCMV-FS and HCMV-KM (**Figure 5**). The breast cancer cell lines MCF7 and MDA-MB231 generated mammospheres as previously reported (37) (**Figure 5**). Moreover, few mammospheres were observed in uninfected HMECs as previously described (38) (**Figure 5**). Altogether, we noticed a preferential formation of mammospheres in HMECs infected with the high-risk HCMV-BL strain in opposition to the low-risk HCMV-TB40E (*p-value* $_{(HCMV\text{-BL: HCMV-TB40/E})}$ = 0.03), HCMV-

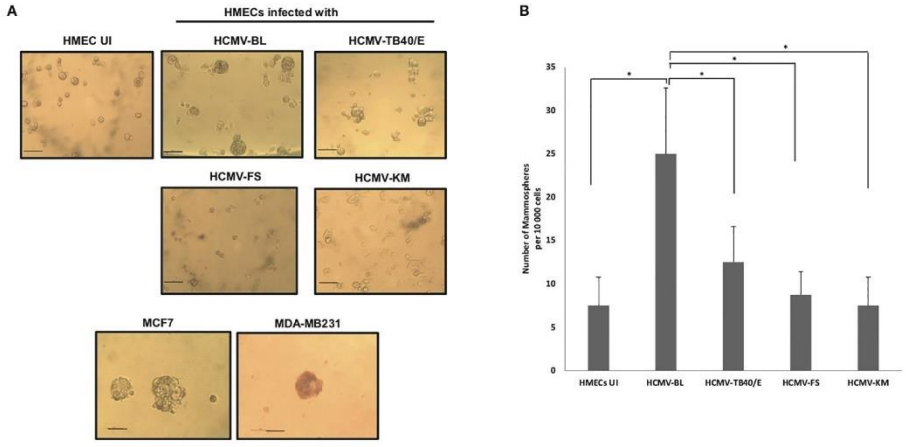

FIGURE 5 | Mammosphere formation in HMEC cultures infected with low-risk (HCMV-TB40/E, FS, and KM) and high-risk (HCMV-BL) strains. **(A)** Mammospheres were observed under an inverted light microscope (Magnification ×100, scale bare 100μm). MCF7 and MDA-MB231 cells were used as positive controls. Uninfected HMECs were used as a negative control. **(B)** The histogram represents the number of mammospheres per 10 000 cells in uninfected and infected HMECs. Data are represented as mean ± SD of three independent experiments. *p-values* were determined by Wilcoxon test. **p-value* < 0.05.

FS (*p-value* $_{(HCMV\text{-}BL:\ HCMV\text{-}FS)}$ = 0.03) and HCMV-KM (*p-value* $_{(HCMV\text{-}BL:\ HCMV\text{-}KM)}$ = 0.03) strains.

Side-By-Side Comparison of the Prototypic Strain TB40/E and the High-Risk DB Strain for Some Specific Phenotypic and Functional Traits

Since we observed limited mammospheres in HMECs infected with HCMV-TB40/E (**Figure 5**) and a slight increase in telomerase activity which has been previously reported (20), we decided to compare side by side the activation of oncogenic molecular pathways in HMECs infected with HCMV-TB40/E and the high-risk HCMV-DB strain. The productive HCMV-DB and TB40/E infection was confirmed in HMECs where both confocal microscopy imaging and flow cytometry data showed the IE1 staining (**Figures 1A, B**). At the protein expression level (day 3 post-infection), Rb was diminished whereas pRb was highly expressed in HMEC-HCMV-DB (*p-value* $_{(HCMV\text{-}DB:\ HMEC\text{-}UI)}$ = 0.04) and to a lesser extent in HMEC-HCMV-TB40/E (*p-value* $_{(HCMV\text{-}TB40/E:\ HMEC\text{-}UI)}$ = 0.04, *p-value* $_{(HCMV\text{-}TB40/E:\ HCMV\text{-}DB)}$ = 0.8) (**Figures 6A, B**). At the same time point, pSTAT3 expression was higher in HMEC-HCMV-DB (*p-value* $_{(HCMV\text{-}DB:\ HMEC\text{-}UI)}$ = 0.03) compared to HMEC-HCMV-TB40/E (*p-value* $_{(HCMV\text{-}TB40/E:\ HMEC\text{-}UI)}$ = 0.06) and STAT3 expression was further increased in HMEC-HCMV-DB compared to HMEC-HCMV-TB40/E (**Figures 6A, C**). Further, Akt expression was highly increased in HMEC-HCMV-DB (*p-value* $_{(HCMV\text{-}DB:\ HMEC\text{-}UI)}$ = 0.03), compared to HMEC-HCMV-TB40/E at day 3 post-infection (*p-value* $_{(HCMV\text{-}TB40/E:\ HMEC\text{-}UI)}$ = 0.06), and an increase in its phosphorylation on both serine 473 and threonine 308 in HMEC-HCMV-DB was observed (**Figures 6A, D**). At day 1 post-infection, cyclin D1 expression was increased in HEMC-HCMV-DB (*p-value* $_{(HCMV\text{-}DB:\ HMEC\text{-}UI)}$ = 0.03) compared to HMEC-HCMV-TB40/E (*p-value* $_{(HCMV\text{-}TB40/E:\ HMEC\text{-}UI)}$ = 0.06) (**Figures 6A, E**). The protein expression of ATM was elevated in HMECs infected with HCMV-DB in comparison to HCMV-TB40/E (**Figures 6A, F**). Our results indicate that the HCMV-TB40/E strain does not induce significant activation of the molecular oncogenic pathways, especially when compared to the high-risk strain HCMV-DB, and therefore should be classified as a low-risk HCMV strain consistent with the absence of colony formation in soft agar in HMEC cultures seeded with TB40/E.

Detection of HCMV in Breast Cancer Biopsies

To assess the impact of HCMV strains on cellular gene expression *in vivo*, Ki67 expression was quantified by RT-qPCR in breast tumor biopsies, including luminal and basal-like tumors compared to healthy breast tissues. First, we measured the percentage of healthy and tumor biopsies with low (<30), intermediate (30–100) or high (>100) Ki67 mRNA expression (**Figures 7A, B**). Basal-like biopsies accounted for the highest percentage of biopsies with high Ki67 mRNA expression level (% of basal-like: 44%) compared to healthy (2%) and luminal biopsies (20%) (*p-value* $_{(High\ Ki67\ -\ Basal\ :\ Healthy)}$ = 0.02) (**Figure 7A**). To further study the role of HCMV associated with Ki67 transcript expression, we assessed the presence of HCMV in the biopsies by quantifying *IE1* and *UL69* genes using qPCR (21, 30). In HCMV-positive biopsies, basal-like biopsies showed the

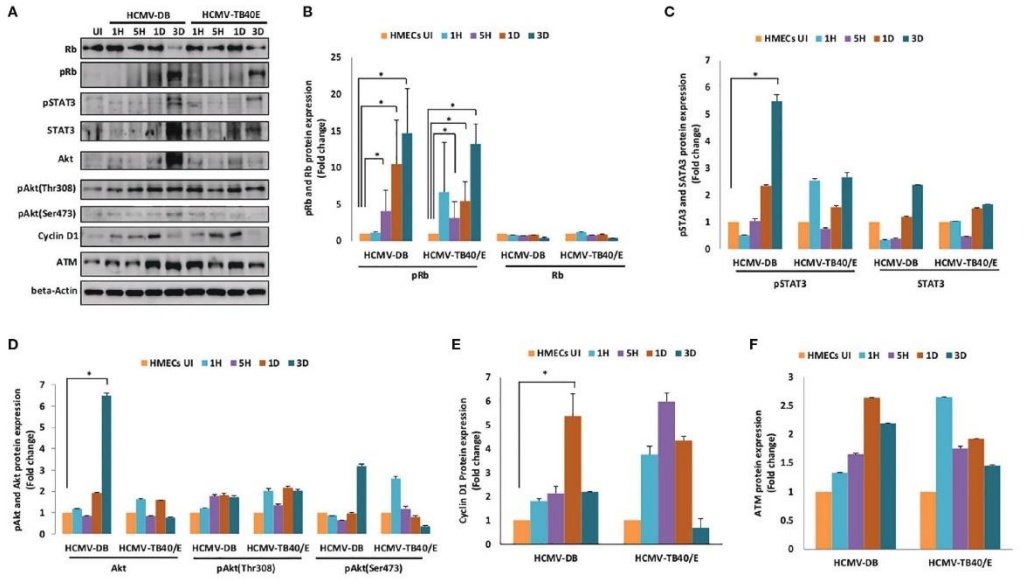

FIGURE 6 | Distinct activation of oncogenic pathways in HMECs infected with the high-risk DB strain and the prototypic TB40/E strain. **(A)** Immunoblotting data of Rb, pRb, STAT3, pSTAT3, Akt, pAkt-Thr308, pAkt-Ser473, cyclin D1 and ATM in uninfected HMECs and HMECs infected with HCMV-DB and HCMV-TB40/E (MOI = 1) at 1H, 5H, D1 and D3 post-infection. β-actin was used as loading control. Results are representative of three independent experiments. Histograms representing **(B)** Rb, pRb, **(C)** STAT3, pSTAT3 **(D)** Akt, pAkt-Thr308, pAkt-Ser473, **(E)** cyclin D1, and **(F)** ATM expression in HMECs infected with HCMV-DB and HCMV-TB40/E (MOI = 1) at 1H, 5H, D1 and D3 post-infection; protein expression is shown based on quantification by ImageJ 1.40 software. Data are represented as mean ± SD of three independent experiments. *p-values* were determined by Wilcoxon test. **p-value* < 0.05.

highest percentage of biopsies with high levels of Ki67 mRNA (40%) in contrast to the healthy (0%) and luminal (0%) biopsies (**Figure 7B**). Second, we assessed the absolute level of Ki67 mRNA per biopsy of healthy tissues, luminal and basal-like tumors taking into account the presence or absence of HCMV (**Figure 7C**). Healthy biopsies showed low absolute levels of Ki67 mRNA compared to tumor biopsies independent of HCMV status (presence or absence) (*p-value* = 0.02). In tumor biopsies, the absolute level of Ki67 mRNA was enhanced by 2.5-fold in HCMV-positive biopsies compared to HCMV-negative biopsies (*p-value* = 0.2). In HCMV-positive biopsies, the absolute level of Ki67 mRNA in basal tumors was enhanced by 31.45-fold compared to luminal tumors (*p-value* = 0.17) (**Figure 7C**). The absolute level of Ki67 mRNA was shown separately for each biopsy where cutoff lines were set to differentiate between low and high Ki67 expression and allow a closer look on the variability of Ki67 mRNA expression per sample (**Supplementary Figure 3**). Thus, when we independently measured the absolute level of Ki67 mRNA in each HCMV-positive biopsy, we detected two basal biopsies (biopsies #20 and #21) showing the highest absolute levels of Ki67 mRNA with 315 and 4015-fold increase versus the mean value of healthy tissue, respectively (**Figure 7D**). Meanwhile, much lower absolute levels of Ki67 mRNA were detected in the other HCMV-positive tumor and healthy biopsies. Low absolute levels of Ki67 mRNA were detected in HCMV-positive luminal biopsies (less than 30-fold increase versus mean value of healthy tissue) except for one biopsy (biopsy #15 with 108-fold increase) (**Figure 7D**).

Within our data, we were able to identify two biopsies, namely biopsies #20 and #21 (**Figure 7D**, arrows), that could harbor high-risk HCMV strains. Given the total number of biopsies, we might not be able to properly identify all the high-risk strains, which effect might be partially masked in the overall HCMV-positive biopsies. To confirm the high-risk status of biopsies #20 and #21, we isolated the strains for each biopsy and used it to infect HMECs (**Supplementary Figure 4A**). After few weeks in culture, we observed dense structures (**Supplementary Figure 4B**), similar to the morphology of the previously reported CTH cells (20, 21). These emerging structures were not present in HMECs infected with low-risk strains that were isolated from other biopsies in which we observed cell lysis. Overall, we identified two high-risk strains (n=2; 15%) out of the HCMV-positive biopsies (n=13); upon assessing the proportion of high-risk strain within tumor biopsies only, we identified two high-risk strains (n=2; 20%) out of the total HCMV-positive tumors (n=10).

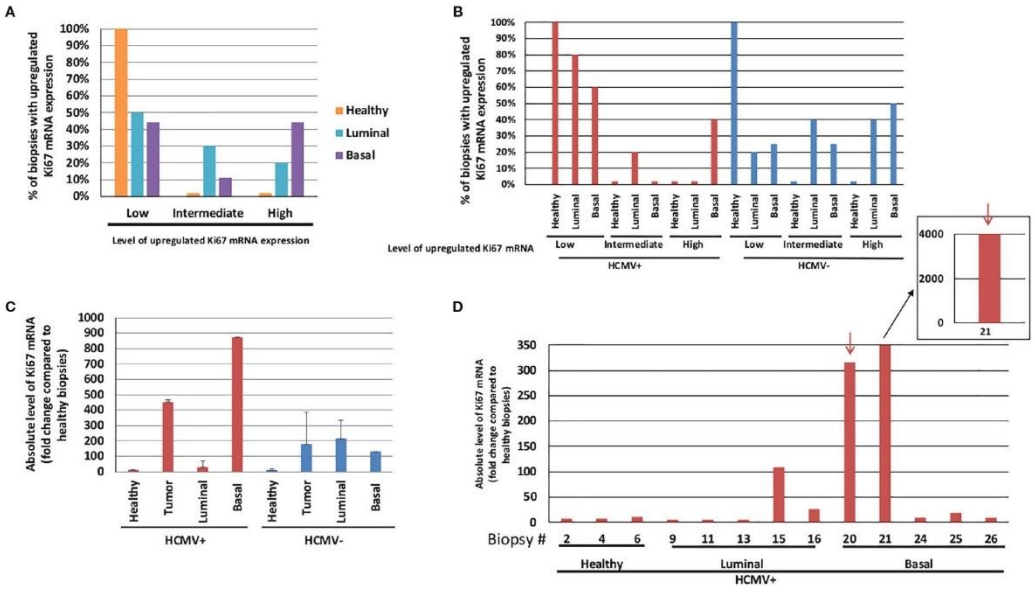

FIGURE 7 | Ki67 gene expression parallel to HCMV detection in healthy and tumor (luminal and basal) breast biopsies. **(A)** Histograms representing the percentage of healthy and tumor (luminal and basal) biopsies with an upregulated Ki67 mRNA expression compared to healthy tissue **(B)** in the presence/absence of HCMV. (Level of upregulated Ki67 mRNA expression: Low<30, 30<Intermediate <100, and High >100) **(C)** Histogram showing the mean ± SD of absolute levels of Ki67 mRNA in healthy, tumor (luminal + basal), luminal, and basal biopsies which were grouped into HCMV-positive and HCMV-negative biopsies. **(D)** Detailed absolute levels of Ki67 mRNA in HCMV-positive biopsies (healthy, luminal, and basal biopsies). *Red arrows*, two HCMV strains detected in basal tumors which expressed high Ki67 levels. Each number on the X-axis represents one healthy, luminal or basal biopsy. Biopsy details can be found in **Supplementary Table 1** and in *Materials and Methods*.

Finally, using twenty different breast tumor biopsies, we aimed at evaluating the value of Ki67 expression as an index for increased proliferation in breast cancer. Ki67 mRNA and protein levels were measured by RT-qPCR and IHC, respectively, on the same biopsy sample. A correlation was observed between Ki67 protein and mRNA levels (**Supplementary Figure 5**). This data indicates that Ki67 mRNA expression could be considered as a reliable marker for the measurement of increased proliferation in breast cancer.

DISCUSSION

We previously isolated the two clinical isolates, HCMV-DB and HCMV-BL, which in primary human mammary epithelial cells (HMECs) promoted oncogenic molecular pathways, established anchorage-independent growth *in vitro*, and produced tumorigenicity in mice models (20, 21), therefore named high-risk oncogenic strains. In contrast, other clinical HCMV strains such as HCMV-FS, KM and SC did not trigger such traits (21), therefore named low-risk oncogenic strains. TB40/E strain did not induce significant activation of the molecular oncogenic pathways in HMECs, especially when compared to the high-risk strain HCMV-DB, and therefore should be classified as a low-risk HCMV strain consistent with the absence of colony formation in soft agar. In contrast to the other HCMV low-risk strains, HCMV-KM was isolated from a two-year old infant with HCMV congenital infection which might explain the different observed transcriptome profile compared to other low-risk HCMV strains (39). Our results indicate the capacity of the six tested HCMV clinical strains to replicate efficiently in HMEC cells allowing the comparison of their transcriptome profile. The transcriptome of HMECs infected with HCMV-BL strain exhibits a pro-oncogenic cellular environment with enhanced expression of several oncogenes, proliferation markers, cell survival genes, and EMT traits (**Figure 8**). Moreover, these pro-oncogenic characteristics were accompanied with stemness traits as assessed *in vitro* by mammosphere formation. In contrast, based on the transcriptome analysis, the HCMV-FS, KM and SC strains were less prone to favor an oncogenic environment (**Figure 8**). The prototypic TB40/E strain displays mostly low-oncogenic traits as assessed by its proteomic profile in infected HMECs (**Figure 8**). Finally, we observed a potential link between the presence of HCMV in the breast tumor,

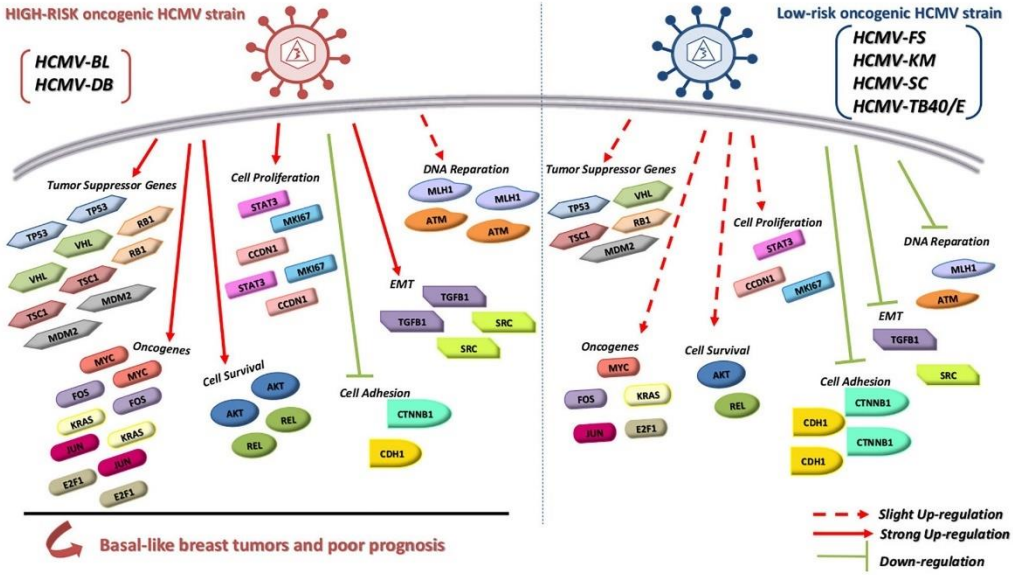

FIGURE 8 | A hypothetical model to summarize the transcriptome differences between low-risk and high-risk HCMV strains based on the modulation of cellular pathways involved in oncogenesis. In contrast to the low-risk HCMV strains (e.g. HCMV-FS, HCMV-KM and HCMV-TB40/E), the high-risk HCMV strains (e.g. HCMV-DB and HCMV-BL) strongly upregulate the expression of oncogenes, cell proliferation genes, genes involved in cell survival and EMT genes, thereby they might favor the initiation and/or the progression of basal breast tumors with poor prognosis.

especially the basal tumors, and high levels of Ki67 mRNA further suggesting the presence of high-risk HCMV strains in some of the basal tumors. Altogether, the transcriptome profiles of HCMV-infected HMECs and the analysis of Ki67 mRNA levels in breast tumors might allow for the classification of high and low-risk HCMV strains based on their oncogenic potential.

Although HCMV clinical isolates display a broad cellular tropism, the growth of laboratory HCMV strains is restricted to fibroblasts (16). Furthermore, several clinical HCMV strains can generate distinct inflammatory (M1) and immunosuppressive (M2) macrophage polarization after infection of blood monocytes and tissue macrophage and can establish latency in these latter (17, 23, 25, 40). The preferential tropism of clinical HCMV strains might favor their long-lasting low-level viral replication in HMECs and ultimately promote breast cancer (41–43). Taking into account its tropism for mammary epithelial cells and its transcriptome oncogenic environment, the HCMV-BL strain is close to the previously described HCMV-DB strain (37). Based on their transforming capacity *in vitro* (soft agar), the activation of oncogenic and proliferation pathways including Myc and Ki67 overexpression, and the development of tumors when injected in NSG mice (20, 21) the HCMV-DB and HCMV-BL strains are classified as high-risk strains.

Inactivation of tumor suppressor proteins such as retinoblastoma protein (Rb) and p53 and activation of pro-oncogenes such as Myc and Ras are critical events involved in HMEC cells transformation and immortalization (44, 45) and are known to favor breast cancer progression (46). Intriguingly, the expression of p53 was 7-fold higher in HMECs infected with high-risk strain HCMV-BL compared to uninfected HMECs. Enhanced expression of p53 has been described in human mammary epithelial cells infected with HCMV-DB (20, 37) and in fibroblasts infected with numerous HCMV strains (47, 48). To explain the functional inactivation of p53 needed for cell transformation, a potential inhibitory effect of IE2 on p53 transcriptional activity has been previously reported (49). In addition, we previously described p53 protein binding to IE2 in HCMV-DB infected HMECs, leading to its functional inactivation parallel to p53 transcript upregulation (20, 37). A similar mechanism might be in action in HMECs infected with HCMV-BL.

Likewise, the expression of Rb gene is increased in HMECs infected with HCMV-BL by 10-fold compared to the uninfected HMECs. Several small DNA tumor viruses such as adenovirus, human papillomavirus, and polyomavirus were described to abolish the function of Rb protein (50). In addition, it was reported that Rb inactivation mediated by viral proteins through the E2F transcriptional factor is necessary for viral replication and mammalian cells transformation (50, 51). Also, the inactivation of Rb protein could be caused by post-translation phosphorylation (52). For HCMV, manipulation of

the cell cycle through Rb inactivation could favor cell transformation (53). First, the viral protein pp71 degrades the hypophosphorylated Rb protein earlier during infection, then Rb protein reaccumulates later during infection (54–56). Second, the viral protein UL97 phosphorylates Rb protein on several CDK target sites and deactivates it. Third, the viral proteins IE1 and IE2 were described to activate E2F-responsive promoters and most probably induce Rb inactivation (57–59). Interestingly, parallel to enhanced Rb gene expression we observed high levels of E2F1 transcript in HMECs infected with the high-risk BL strain. Thus, the inactivation of both p53 and Rb proteins is mandatory for cell transformation in HCMV-BL and HCMV-DB infected HMECs which might explain that even under enhanced p53 and Rb gene expression, their protein activity will be abolished.

In agreement with our previous results (21), the overexpression of Myc and KRas could participate in the transformation process of HMEC cells infected with HCMV-BL. In addition, the enhanced expression of other oncogenes such as Jun and E2F1 observed in HMECs infected with HCMV-BL could stimulate transformation (60, 61). Interestingly, the viral proteins IE1 and IE2 induce Myc activation (62). We observed previously a similar activation of Myc and Ras protein and gene expression in HMECs infected with the HCMV-DB strain (20, 37).

Furthermore, one of the mechanisms described to transform HMECs is the link of Myc overexpression to PI3K/Akt pathway activation (63, 64). We observed mostly enhanced expression of Akt gene in HMECs infected with HCMV-BL compared to HCMV-FS, KM and TB40/E in agreement with our previous results (21), and an upregulation of serine-473 phosphorylation of Akt in HMECs infected with HCMV-DB compared to HCMV-TB40/E. The PI3K/Akt activation in HCMV infected cells is in line with previous findings (65). In addition, several studies have pointed the role of REL in cell growth and oncogenesis (66). The overexpression of REL was associated with cell transformation *in vitro* and/or *in vivo*. Epstein-Barr virus (EBV) activates REL/NF-kB during malignant transformation (67). Thus, the overexpression of REL in HMECs infected with HCMV-BL is consistent with its high oncogenic potential.

In agreement with the HCMV-DB transcriptome study (37), an enhanced expression of proliferation markers such as STAT3, cyclin D1, and especially Ki67 was observed in HMEC cells infected with HCMV-BL but not with HCMV- FS, KM, SC and TB40/E. The proliferation and invasion of several cancers could be explained by STAT3 activation and cyclin D1 overexpression (68). Moreover, the overexpression of pSTAT3 and STAT3 at day 3 post-infection was observed mainly in HMECs infected with HCMV-DB, but to a lesser extent with HCMV-TB40/E. These findings confirm that the high-risk HCMV strains such as BL and DB have high proliferation capacities compared to the low-risk HCMV strains, such as TB40/E, FS, KM and SC.

Studies have reported that ataxia telangiectasia mutated (ATM) is required for efficient viral replication of numerous viruses including HCMV, HSV-1, HPV, and HIV (69–73). Indeed, HCMV infection leads to host DNA damage responses (DDRs) with activation of the DNA reparation pathway (74–76). Enhanced expression of ATM gene was observed in infected HMECs with HCMV-BL and with HCMV-DB as reported previously (37). Lower levels of ATM expression were detected in HMECs infected with HCMV-TB40/E, FS, and KM. The enhanced expression of ATM can promote genome instability resulting in cellular transformation. MLH expression is necessary for efficient HSV-1 viral replication (77) and its enhanced expression has been linked to high levels of genomic instability, cancer progression, and aggressiveness (78, 79). Likewise, the overexpression of MMP9 and CTSD observed in HMECs infected with HCMV-BL was associated with the most aggressive subtype of breast cancer (80), tumor cell invasion, and metastasis (81–84).

The expression of genes involved in EMT such as the proto-oncogene tyrosine-protein kinase Src (85) and the transforming growth factor-beta 1 (TGFB1) (86, 87) was higher in HMECs infected with HCMV-BL than with HCMV-TB40/E, FS, KM and SC. Our findings are in accordance with our previous analysis of HCMV-DB transcriptome (37).

Altogether the transcriptome analysis of HMECs infected with the high-risk strain HCMV-BL underlines the potential capacity of the emergence of cancer stem cells (CSCs) compared to the HMECs infected with low-risk strains (HCMV-FS, KM and SC). In line with our transcriptome data and with the previously reported enhanced mammosphere formation in HMECs infected with HCMV-DB (37), we observed that the number of mammospheres detected in HMECs infected with HCMV-BL was 2-fold, 2.8-fold and 3-fold higher compared to HMECs infected with HCMV-TB40/E, HCMV-FS and KM, respectively

The distinct oncogenic potential of HCMV strains observed at the transcriptome level *in vitro* was then assessed *in vivo* in breast tumors. The nuclear protein Ki67 is not required only for cell proliferation in tumor but also for tumor initiation, growth, and metastasis. Moreover, Ki67 inactivation leads to transcriptome remodeling that alters mesenchymal-epithelial balance and suppresses stemness (88). Ki67 is highly expressed in malignant tissues with poorly differentiated tumor cells (89). High Ki67, possessing high proliferation potential, was reported to worsen the survival of triple negative breast cancer patients and to trigger quick tumor recurrence within a short period of time (90). Remarkably, enhanced expression of Ki67 gene and upregulation of Ki67 protein was observed in HMECs infected with the HCMV-DB and BL strains (20, 21). Therefore, we assessed the link between HCMV presence and Ki67 gene overexpression in breast tumor biopsies. Basal-like biopsies revealed the highest percentage of biopsies with high levels of Ki67 mRNA compared to the healthy and luminal biopsies. Only tumor biopsies were impacted by HCMV status; the highest level of Ki67 mRNA was detected in HCMV-positive tumor biopsies compared to HCMV-negative tumor biopsies. Among the HCMV-positive biopsies, the absolute level of Ki67 was low in all healthy and most of the luminal biopsies except for one luminal biopsy (#15 with limited increase in Ki67 absolute level). In contrast, among the tested basal-like HCMV-positive biopsies, we observed augmented absolute levels of Ki67 mRNA in two biopsies (biopsies #20 and #21) despite the low absolute levels of Ki67 mRNA that were detected in some biopsies.

The HCMV strains that were isolated from biopsies #20 and 21, transformed the freshly uninfected HMECs resulting in the appearance of CMV-transformed HMECs (CTH cells) *in vitro* indicating their high-risk profile **(Supplementary Figure 4)**. Since high-risk HCMV strains strongly enhanced the expression of Ki67Ag (20, 21), the majority of the HCMV strains detected in the breast tumor biopsies or in the adjacent tested healthy tissues might be non-oncogenic or low-risk HCMV strains. The detection of very high expression of Ki67 mRNA in two basal tumor biopsies concomitant with the presence of HCMV suggests a potential link between high-risk HCMV strains present in the tumor tissue, highly enhanced Ki67 expression, and the initiation and/or progression of basal breast tumors. In agreement with our results, Ki67 was described as a key marker associated with poor prognosis in triple-negative breast cancer (91). We are currently studying a larger cohort of breast cancer biopsies and assessing additional "oncogenic" markers such as c-Myc to further highlight the exact role of HCMV strains in breast oncogenesis.

CONCLUSION

In conclusion, our data indicate the capacity of high-risk HCMV strains to induce a pro-oncogenic cellular environment in contrast to the low-risk strains. Similar to the HCMV-DB strain, HCMV-BL was able to induce enhanced expression of various oncogenes, genes involved in proliferation, cell survival, DNA reparation, and EMT. Additionally, high-risk HCMV strains present stemness traits with enhanced mammosphere formation *in vitro* compared to the low-risk strains. *In vivo*, we detected the concomitant presence of a very high Ki67 gene expression in two HCMV-positive basal breast tumors, indicating a potential link between high-risk HCMV strains present in the tumoral tissue and the development of aggressive tumors of poor prognosis. The discrimination between HCMV clinical strains based on their distinct oncogenic potential will pave the way for understanding their respective role in breast cancer and open the door to new therapeutic approaches.

DATA AVAILABILITY STATEMENT

The original contributions presented in the study are included in the article/**Supplementary Material**. Further inquiries can be directed to the corresponding author.

ETHICS STATEMENT

The studies involving human participants were reviewed and approved by local ethics committees of Besançon University Hospital (Besançon, France) and the French Research Ministry (AC-2015-2496, CNIL n°1173545, NF-S-138 96900 n°F2015). The patients/participants provided their written informed consent to participate in this study.

AUTHOR CONTRIBUTIONS

Conceptualization, GH. Formal analysis, SH, SP, and GH. Investigation, SH, SP, RE, ZN, and CL. Writing—original draft preparation, SH and GH. Writing—review and editing, SH, SP, RE, and GH. Visualization, SH and SP. Supervision, GH. Project administration, GH. Funding acquisition, GH. All authors contributed to the article and approved the submitted version.

FUNDING

This work was supported by grants from the University of Franche-Comté (UFC) (CR3300), the Région Franche-Comté (2021-Y-08292 and 2021-Y-08290) and the Ligue contre le Cancer (CR3304) to GH. SH is recipient of a doctoral scholarship from Lebanese municipality. RE is a recipient of a doctoral scholarship from Hariri foundation for sustainable human development.

ACKNOWLEDGMENTS

We are grateful to Franck Monnien, Chloé Molimard and Marie-Paule Algros from the Pathology Department at the Besançon University Hospital for providing breast biopsies. We thank Dr. Davit Varron from the Mathematics Department of the University of Franche-Comté for the statistical analyses.

SUPPLEMENTARY MATERIAL

The Supplementary Material for this article can be found online at: https://www.frontiersin.org/articles/10.3389/fimmu.2021.772160/full#supplementary-material

REFERENCES

1. Lehmann BD, Bauer JA, Chen X, Sanders ME, Chakravarthy AB, Shyr Y, et al. Identification of Human Triple-Negative Breast Cancer Subtypes and Preclinical Models for Selection of Targeted Therapies. *J Clin Invest* (2011) 121:2750–67. doi: 10.1172/JCI45014
2. Hüsing A, Canzian F, Beckmann L, Garcia-Closas M, Diver WR, Thun MJ, et al. Prediction of Breast Cancer Risk by Genetic Risk Factors, Overall and by Hormone Receptor Status. *J Med Genet* (2012) 49:601–8. doi: 10.1136/jmedgenet-2011-100716
3. Alibek K, Kakpenova A, Mussabekova A, Sypabekova M, Karatayeva N. Role of Viruses in the Development of Breast Cancer. *Infect Agent Cancer* (2013) 8:32. doi: 10.1186/1750-9378-8-32
4. Zur Hausen H. The Search for Infectious Causes of Human Cancers: Where and Why. *Virology* (2009) 392:1–10. doi: 10.1016/j.virol.2009.06.001
5. Geisler J, Touma J, Rahbar A, Söderberg-Nauclér C, Vetvik K. A Review of the Potential Role of Human Cytomegalovirus (HCMV) Infections in Breast Cancer Carcinogenesis and Abnormal Immunity. *Cancers* (2019) 11:1842. doi: 10.3390/cancers11121842
6. Taher C, Frisk G, Fuentes S, Religa P, Costa H, Assinger A, et al. High Prevalence of Human Cytomegalovirus in Brain Metastases of Patients With Primary Breast and Colorectal Cancers. *Transl Oncol* (2014) 7:732–40. doi: 10.1016/j.tranon.2014.09.008
7. Taher C, de Boniface J, Mohammad A-A, Religa P, Hartman J, Yaiw K-C, et al. High Prevalence of Human Cytomegalovirus Proteins and Nucleic Acids

in Primary Breast Cancer and Metastatic Sentinel Lymph Nodes. *PloS One* (2013) 8:e56795. doi: 10.1371/journal.pone.0056795
8. El Shazly DF, Bahnassey AA, Omar OS, Elsayed ET, Al-Hindawi A, El-Desouky E, et al. Detection of Human Cytomegalovirus in Malignant and Benign Breast Tumors in Egyptian Women. *Clin Breast Cancer* (2018) 18: e629–42. doi: 10.1016/j.clbc.2017.10.018
9. Samanta M, Harkins L, Klemm K, Britt WJ, Cobbs CS. High Prevalence of Human Cytomegalovirus in Prostatic Intraepithelial Neoplasia and Prostatic Carcinoma. *J Urol* (2003) 170:998–1002. doi: 10.1097/01.ju.0000080263.46164.97
10. Harkins LE, Matlaf LA, Soroceanu L, Klemm K, Britt WJ, Wang W, et al. Detection of Human Cytomegalovirus in Normal and Neoplastic Breast Epithelium. *Herpesviridae* (2010) 1:8. doi: 10.1186/2042-4280-1-8
11. Baryawno N, Rahbar A, Wolmer-Solberg N, Taher C, Odeberg J, Darabi A, et al. Detection of Human Cytomegalovirus in Medulloblastomas Reveals a Potential Therapeutic Target. *J Clin Invest* (2011) 121:4043–55. doi: 10.1172/JCI57147
12. Bhattacharjee B, Renzette N, Kowalik TF. Genetic Analysis of Cytomegalovirus in Malignant Gliomas. *J Virol* (2012) 86:6815–24. doi: 10.1128/JVI.00015-12
13. Banerjee S, Wei Z, Tan F, Peck KN, Shih N, Feldman M, et al. Distinct Microbiological Signatures Associated With Triple Negative Breast Cancer. *Sci Rep* (2015) 5:15162. doi: 10.1038/srep15162
14. Coaquette A, Bourgeois A, Dirand C, Varin A, Chen W, Herbein G. Mixed Cytomegalovirus Glycoprotein B Genotypes in Immunocompromised Patients. *Clin Infect Dis Off Publ Infect Dis Soc Am* (2004) 39:155–61. doi: 10.1086/421496
15. El Baba R, Herbein G. Immune Landscape of CMV Infection in Cancer Patients: From "Canonical" Diseases Toward Virus-Elicited Oncomodulation. *Front Immunol* (2021) 12:730765. doi: 10.3389/fimmu.2021.730765
16. Wang D, Shenk T. Human Cytomegalovirus Virion Protein Complex Required for Epithelial and Endothelial Cell Tropism. *Proc Natl Acad Sci* (2005) 102:18153–8. doi: 10.1073/pnas.0509201102
17. Khan KA, Coaquette A, Davrinche C, Herbein G. Bcl-3-Regulated Transcription From Major Immediate-Early Promoter of Human Cytomegalovirus in Monocyte-Derived Macrophages. *J Immunol Baltim Md 1950* (2009) 182:7784–94. doi: 10.4049/jimmunol.0803800
18. Belzile J-P, Stark TJ, Yeo GW, Spector DH. Human Cytomegalovirus Infection of Human Embryonic Stem Cell-Derived Primitive Neural Stem Cells is Restricted at Several Steps But Leads to the Persistence of Viral DNA. *J Virol* (2014) 88:4021–39. doi: 10.1128/JVI.03492-13
19. Lepiller Q, Abbas W, Kumar A, Tripathy MK, Herbein G. HCMV Activates the IL-6-JAK-STAT3 Axis in HepG2 Cells and Primary Human Hepatocytes. *PloS One* (2013) 8:e59591. doi: 10.1371/journal.pone.0059591
20. Kumar A, Tripathy MK, Pasquereau S, Al Moussawi F, Abbas W, Coquard L, et al. The Human Cytomegalovirus Strain DB Activates Oncogenic Pathways in Mammary Epithelial Cells. *EBioMedicine* (2018) 30:167–83. doi: 10.1016/j.ebiom.2018.03.015
21. Nehme Z, Pasquereau S, Haidar Ahmad S, Coaquette A, Molimard C, Monnien F, et al. Polyploid Giant Cancer Cells, Stemness and Epithelial-Mesenchymal Plasticity Elicited by Human Cytomegalovirus. *Oncogene* (2021) 40:3030–46. doi: 10.1038/s41388-021-01715-7
22. Geder KM, Lausch R, O'Neill F, Rapp F. Oncogenic Transformation of Human Embryo Lung Cells by Human Cytomegalovirus. *Science* (1976) 192:1134–7. doi: 10.1126/science.179143
23. Hargett D, Shenk TE. Experimental Human Cytomegalovirus Latency in CD14+ Monocytes. *Proc Natl Acad Sci USA* (2010) 107:20039–44. doi: 10.1073/pnas.1014509107
24. Noriega VM, Haye KK, Kraus TA, Kowalsky SR, Ge Y, Moran TM, et al. Human Cytomegalovirus Modulates Monocyte-Mediated Innate Immune Responses During Short-Term Experimental Latency *In Vitro*. *J Virol* (2014) 88:9391–405. doi: 10.1128/JVI.00934-14
25. Smith MS, Bentz GL, Alexander JS, Yurochko AD. Human Cytomegalovirus Induces Monocyte Differentiation and Migration as a Strategy for Dissemination and Persistence. *J Virol* (2004) 78:4444–53. doi: 10.1128/jvi.78.9.4444-4453.2004
26. Zhuravskaya T, Maciejewski JP, Netski DM, Bruening E, Mackintosh FR, St Jeor S. Spread of Human Cytomegalovirus (HCMV) After Infection of Human Hematopoietic Progenitor Cells: Model of HCMV Latency. *Blood* (1997) 90:2482–91. doi: 10.1182/blood.V90.6.2482
27. Taylor-Wiedeman J, Sissons JG, Borysiewicz LK, Sinclair JH. Monocytes are a Major Site of Persistence of Human Cytomegalovirus in Peripheral Blood Mononuclear Cells. *J Gen Virol* (1991) 72(Pt 9):2059–64. doi: 10.1099/0022-1317-72-9-2059
28. Movassagh M, Gozlan J, Senechal B, Baillou C, Petit JC, Lemoine FM. Direct Infection of CD34+ Progenitor Cells by Human Cytomegalovirus: Evidence for Inhibition of Hematopoiesis and Viral Replication. *Blood* (1996) 88:1277–83. doi: 10.1182/blood.V88.4.1277.bloodjournal8841277
29. Sinzger C, Schmidt K, Knapp J, Kahl M, Beck R, Waldman J, et al. Modification of Human Cytomegalovirus Tropism Through Propagation In Vitro is Associated With Changes in the Viral Genome. *J Gen Virol* (1999) 80 (Pt 11):2867–77. doi: 10.1099/0022-1317-80-11-2867
30. Haidar Ahmad S, Al Moussawi F, El Baba R, Nehme Z, Pasquereau S, Kumar A, et al. Identification of UL69 Gene and Protein in Cytomegalovirus-Transformed Human Mammary Epithelial Cells. *Front Oncol* (2021) 11:627866. doi: 10.3389/fonc.2021.627866
31. Schmittgen TD, Livak KJ. Analyzing Real-Time PCR Data by the Comparative C(T) Method. *Nat Protoc* (2008) 3:1101–8. doi: 10.1038/nprot.2008.73
32. Bustreo S, Osella-Abate S, Cassoni P, Donadio M, Airoldi M, Pedani F, et al. Optimal Ki67 Cut-Off for Luminal Breast Cancer Prognostic Evaluation: A Large Case Series Study With a Long-Term Follow-Up. *Breast Cancer Res Treat* (2016) 157:363–71. doi: 10.1007/s10549-016-3817-9
33. Wilkinson GWG, Davison AJ, Tomasec P, Fielding CA, Aicheler R, Murrell I, et al. Human Cytomegalovirus: Taking the Strain. *Med Microbiol Immunol (Berl)* (2015) 204:273–84. doi: 10.1007/s00430-015-0411-4
34. Banerjee K, Resat H. Constitutive Activation of STAT3 in Breast Cancer Cells: A Review. *Int J Cancer* (2016) 138:2570–8. doi: 10.1002/ijc.29923
35. Lombardo Y, de Giorgio A, Coombes CR, Stebbing J, Castellano L. Mammosphere Formation Assay From Human Breast Cancer Tissues and Cell Lines. *J Vis Exp JoVE* (2015) 97:52671. doi: 10.3791/52671
36. Manuel Iglesias J, Beloqui I, Garcia-Garcia F, Leis O, Vazquez-Martin A, Eguiara A, et al. Mammosphere Formation in Breast Carcinoma Cell Lines Depends Upon Expression of E-Cadherin. *PloS One* (2013) 8:e77281. doi: 10.1371/journal.pone.0077281
37. Moussawi FA, Kumar A, Pasquereau S, Tripathy MK, Karam W, Diab-Assaf M, et al. The Transcriptome of Human Mammary Epithelial Cells Infected With the HCMV-DB Strain Displays Oncogenic Traits. *Sci Rep* (2018) 8:12574. doi: 10.1038/s41598-018-30109-1
38. Klopp AH, Lacerda L, Gupta A, Debeb BG, Solley T, Li L, et al. Mesenchymal Stem Cells Promote Mammosphere Formation and Decrease E-Cadherin in Normal and Malignant Breast Cells. *PloS One* (2010) 5:e12180. doi: 10.1371/journal.pone.0012180
39. Renzette N, Gibson L, Bhattacharjee B, Fisher D, Schleiss MR, Jensen JD, et al. Rapid Intrahost Evolution of Human Cytomegalovirus Is Shaped by Demography and Positive Selection. *PloS Genet* (2013) 9:e1003735. doi: 10.1371/journal.pgen.1003735
40. Chan G, Nogalski MT, Yurochko AD. Activation of EGFR on Monocytes is Required for Human Cytomegalovirus Entry and Mediates Cellular Motility. *Proc Natl Acad Sci USA* (2009) 106:22369–74. doi: 10.1073/pnas.0908787106
41. Grivennikov SI, Greten FR, Karin M. Immunity, Inflammation, and Cancer. *Cell* (2010) 140:883–99. doi: 10.1016/j.cell.2010.01.025
42. Teng MW, Bolovan-Fritts C, Dar RD, Womack A, Simpson ML, Shenk T, et al. An Endogenous Accelerator for Viral Gene Expression Confers a Fitness Advantage. *Cell* (2012) 151:1569–80. doi: 10.1016/j.cell.2012.11.051
43. McKinney C, Zavadil J, Bianco C, Shiflett L, Brown S, Mohr I. Global Reprogramming of the Cellular Translational Landscape Facilitates Cytomegalovirus Replication. *Cell Rep* (2014) 6:9–17. doi: 10.1016/j.celrep.2013.11.045
44. Dimri G, Band H, Band V. Mammary Epithelial Cell Transformation: Insights From Cell Culture and Mouse Models. *Breast Cancer Res BCR* (2005) 7:171–9. doi: 10.1186/bcr1275
45. Abba MC, Laguens RM, Dulout FN, Golijow CD. The C-Myc Activation in Cervical Carcinomas and HPV 16 Infections. *Mutat Res* (2004) 557:151–8. doi: 10.1016/j.mrgentox.2003.10.005
46. Lee EYHP, Muller WJ. Oncogenes and Tumor Suppressor Genes. *Cold Spring Harb Perspect Biol* (2010) 2:a003236. doi: 10.1101/cshperspect.a003236

47. Hannemann H, Rosenke K, O'Dowd JM, Fortunato EA. The Presence of P53 Influences the Expression of Multiple Human Cytomegalovirus Genes at Early Times Postinfection. *J Virol* (2009) 83:4316–25. doi: 10.1128/JVI.02075-08
48. Muganda P, Mendoza O, Hernandez J, Qian Q. Human Cytomegalovirus Elevates Levels of the Cellular Protein P53 in Infected Fibroblasts. *J Virol* (1994) 68:8028–34. doi: 10.1128/JVI.68.12.8028-8034.1994
49. Hsu C-H, Chang MDT, Tai K-Y, Yang Y-T, Wang P-S, Chen C-J, et al. HCMV IE2-Mediated Inhibition of HAT Activity Downregulates P53 Function. *EMBO J* (2004) 23:2269–80. doi: 10.1038/sj.emboj.7600239
50. Helt A-M, Galloway DA. Mechanisms by Which DNA Tumor Virus Oncoproteins Target the Rb Family of Pocket Proteins. *Carcinogenesis* (2003) 24:159–69. doi: 10.1093/carcin/24.2.159
51. Cress WD, Nevins JR. Use of the E2F Transcription Factor by DNA Tumor Virus Regulatory Proteins. In: Farnham PJ, editor. *Transcriptional Control of Cell Growth: The E2F Gene Family Current Topics in Microbiology and Immunology*. Berlin, Heidelberg: Springer (1996). p. 63–78. doi: 10.1007/978-3-642-79910-5_3
52. Elenbaas B, Spirio L, Koerner F, Fleming MD, Zimonjic DB, Donaher JL, et al. Human Breast Cancer Cells Generated by Oncogenic Transformation of Primary Mammary Epithelial Cells. *Genes Dev* (2001) 15:50–65. doi: 10.1101/gad.828901
53. Soroceanu L, Cobbs CS. Is HCMV a Tumor Promoter? *Virus Res* (2011) 157:193–203. doi: 10.1016/j.virusres.2010.10.026
54. Kalejta RF, Bechtel JT, Shenk T. Human Cytomegalovirus Pp71 Stimulates Cell Cycle Progression by Inducing the Proteasome-Dependent Degradation of the Retinoblastoma Family of Tumor Suppressors. *Mol Cell Biol* (2003) 23:1885–95. doi: 10.1128/MCB.23.6.1885-1895.2003
55. Kalejta RF, Shenk T. Proteasome-Dependent, Ubiquitin-Independent Degradation of the Rb Family of Tumor Suppressors by the Human Cytomegalovirus Pp71 Protein. *Proc Natl Acad Sci USA* (2003) 100:3263–8. doi: 10.1073/pnas.0538058100
56. Hume AJ, Finkel JS, Kamil JP, Coen DM, Culbertson MR, Kalejta RF. Phosphorylation of Retinoblastoma Protein by Viral Protein With Cyclin-Dependent Kinase Function. *Science* (2008) 320:797–9. doi: 10.1126/science.1152095
57. Poma EE, Kowalik TF, Zhu L, Sinclair JH, Huang ES. The Human Cytomegalovirus IE1-72 Protein Interacts With the Cellular P107 Protein and Relieves P107-Mediated Transcriptional Repression of an E2F-Responsive Promoter. *J Virol* (1996) 70:7867–77. doi: 10.1128/JVI.70.11.7867-7877.1996
58. Wiebusch L, Asmar J, Uecker R, Hagemeier C. Human Cytomegalovirus Immediate-Early Protein 2 (IE2)-Mediated Activation of Cyclin E Is Cell-Cycle-Independent and Forces S-Phase Entry in IE2-Arrested Cells. *J Gen Virol* (2003) 84:51–60. doi: 10.1099/vir.0.18702-0
59. Song Y-J, Stinski MF. Effect of the Human Cytomegalovirus IE86 Protein on Expression of E2F-Responsive Genes: A DNA Microarray Analysis. *Proc Natl Acad Sci USA* (2002) 99:2836–41. doi: 10.1073/pnas.052010099
60. Boldogh I, AbuBakar S, Deng CZ, Albrecht T. Transcriptional Activation of Cellular Oncogenes Fos, Jun, and Myc by Human Cytomegalovirus. *J Virol* (1991) 65:1568–71. doi: 10.1128/JVI.65.3.1568-1571.1991
61. Boldogh I, AbuBakar S, Albrecht T. Activation of Proto-Oncogenes: An Immediate Early Event in Human Cytomegalovirus Infection. *Science* (1990) 247:561–4. doi: 10.1126/science.1689075
62. Hagemeier C, Walker SM, Sissons PJ, Sinclair JH. The 72k IE1 and 80K IE2 Proteins of Human Cytomegalovirus Independently Trans-Activate the C-Fos, C-Myc and Hsp70 Promoters via Basal Promoter Elements. *J Gen Virol* (1992) 73(Pt 9):2385–93. doi: 10.1099/0022-1317-73-9-2385
63. Altomare DA, Testa JR. Perturbations of the AKT Signaling Pathway in Human Cancer. *Oncogene* (2005) 24:7455–64. doi: 10.1038/sj.onc.1209085
64. Zhao JJ, Gjoerup OV, Subramanian RR, Cheng Y, Chen W, Roberts TM, et al. Human Mammary Epithelial Cell Transformation Through the Activation of Phosphatidylinositol 3-Kinase. *Cancer Cell* (2003) 3:483–95. doi: 10.1016/s1535-6108(03)00088-6
65. Cojohari O, Peppenelli MA, Chan GC. Human Cytomegalovirus Induces an Atypical Activation of Akt To Stimulate the Survival of Short-Lived Monocytes. *J Virol* (2016) 90:6443–52. doi: 10.1128/JVI.00214-16
66. Gilmore TD, Koedood M, Piffat KA, White DW. Rel/NF-Kappab/IkappaB Proteins and Cancer. *Oncogene* (1996) 13:1367–78.
67. Luque I, Gélinas C. Rel/NF-Kappa B and I Kappa B Factors in Oncogenesis. *Semin Cancer Biol* (1997) 8:103–11. doi: 10.1006/scbi.1997.0061
68. Luo J, Yan R, He X, He J. Constitutive Activation of STAT3 and Cyclin D1 Overexpression Contribute to Proliferation, Migration and Invasion in Gastric Cancer Cells. *Am J Transl Res* (2017) 9:5671–7.
69. Lilley CE, Carson CT, Muotri AR, Gage FH, Weitzman MD. DNA Repair Proteins Affect the Lifecycle of Herpes Simplex Virus 1. *Proc Natl Acad Sci USA* (2005) 102:5844–9. doi: 10.1073/pnas.0501916102
70. Tarakanova Vl, Leung-Pineda V, Hwang S, Yang Cw, Matatall K, Basson M, et al. Gamma-Herpesvirus Kinase Actively Initiates a DNA Damage Response by Inducing Phosphorylation of H2AX to Foster Viral Replication. *Cell Host Microbe* (2007) 1:275–86. doi: 10.1016/j.chom.2007.05.008
71. Moody CA, Laimins LA. Human Papillomaviruses Activate the ATM DNA Damage Pathway for Viral Genome Amplification Upon Differentiation. *PloS Pathog* (2009) 5:e1000605. doi: 10.1371/journal.ppat.1000605
72. Xiaofei E, Pickering MT, Debatis M, Castillo J, Lagadinos A, Wang S, et al. An E2F1-Mediated DNA Damage Response Contributes to the Replication of Human Cytomegalovirus. *PloS Pathog* (2011) 7:e1001342. doi: 10.1371/journal.ppat.1001342
73. Perfettini J-L, Nardacci R, Bourouba M, Subra F, Gros L, Séror C, et al. Critical Involvement of the ATM-Dependent DNA Damage Response in the Apoptotic Demise of HIV-1-Elicited Syncytia. *PloS One* (2008) 3:e2458. doi: 10.1371/journal.pone.0002458
74. Castillo JP, Frame FM, Rogoff HA, Pickering MT, Yurochko AD, Kowalik TF. Human Cytomegalovirus IE1-72 Activates Ataxia Telangiectasia Mutated Kinase and a P53/P21-Mediated Growth Arrest Response. *J Virol* (2005) 79:11467–75. doi: 10.1128/JVI.79.17.11467-11475.2005
75. Xiaofei E, Savidis G, Chin CR, Wang S, Lu S, Brass AL, et al. A Novel DDB2-ATM Feedback Loop Regulates Human Cytomegalovirus Replication. *J Virol* (2014) 88:2279–90. doi: 10.1128/JVI.03423-13
76. Shirata N, Kudoh A, Daikoku T, Tatsumi Y, Fujita M, Kiyono T, et al. Activation of Ataxia Telangiectasia-Mutated DNA Damage Checkpoint Signal Transduction Elicited by Herpes Simplex Virus Infection. *J Biol Chem* (2005) 280:30336–41. doi: 10.1074/jbc.M500976200
77. Mohni KN, Mastrocola AS, Bai P, Weller SK, Heinen CD. DNA Mismatch Repair Proteins Are Required for Efficient Herpes Simplex Virus 1 Replication∇. *J Virol* (2011) 85:12241–53. doi: 10.1128/JVI.05487-11
78. Chakraborty U, Dinh TA, Alani E. Genomic Instability Promoted by Overexpression of Mismatch Repair Factors in Yeast: A Model for Understanding Cancer Progression. *Genetics* (2018) 209:439–56. doi: 10.1534/genetics.118.300923
79. Wilczak W, Rashed S, Hube-Magg C, Kluth M, Simon R, Büscheck F, et al. Up-Regulation of Mismatch Repair Genes MSH6, PMS2 and MLH1 Parallels Development of Genetic Instability and is Linked to Tumor Aggressiveness and Early PSA Recurrence in Prostate Cancer. *Carcinogenesis* (2017) 38:19–27. doi: 10.1093/carcin/bgw116
80. Yousef EM, Tahir MR, St-Pierre Y, Gaboury LA. MMP-9 Expression Varies According to Molecular Subtypes of Breast Cancer. *BMC Cancer* (2014) 14:609. doi: 10.1186/1471-2407-14-609
81. Ballin M, Gomez DE, Sinha CC, Thorgeirsson UP. Ras Oncogene Mediated Induction of a 92kda Metalloproteinase; Strong Correlation With the Malignant Phenotype. *Biochem Biophys Res Commun* (1988) 154:832–8. doi: 10.1016/0006-291X(88)90215-X
82. Bernhard EJ, Gruber SB, Muschel RJ. Direct Evidence Linking Expression of Matrix Metalloproteinase 9 (92-kDa Gelatinase/Collagenase) to the Metastatic Phenotype in Transformed Rat Embryo Cells. *Proc Natl Acad Sci* (1994) 91:4293–7. doi: 10.1073/pnas.91.10.4293
83. Björklund M, Koivunen E. Gelatinase-Mediated Migration and Invasion of Cancer Cells. *Biochim Biophys Acta* (2005) 1755:37–69. doi: 10.1016/j.bbcan.2005.03.001
84. Shay G, Lynch CC, Fingleton B. Moving Targets: Emerging Roles for MMPs in Cancer Progression and Metastasis. *Matrix Biol J Int Soc Matrix Biol* (2015) 44–46:200–6. doi: 10.1016/j.matbio.2015.01.019
85. Diaz N, Minton S, Cox C, Bowman T, Gritsko T, Garcia R, et al. Activation of Stat3 in Primary Tumors From High-Risk Breast Cancer Patients Is Associated With Elevated Levels of Activated Src and Survivin Expression. *Clin Cancer Res* (2006) 12:20–8. doi: 10.1158/1078-0432.CCR-04-1749
86. Xu J, Lamouille S, Derynck R. TGF-β-Induced Epithelial to Mesenchymal Transition. *Cell Res* (2009) 19:156–72. doi: 10.1038/cr.2009.5

87. Wendt MK, Allington TM, Schiemann WP. Mechanisms of Epithelial-Mesenchymal Transition by TGF-β. *Future Oncol Lond Engl* (2009) 5:1145–68. doi: 10.2217/fon.09.90
88. Mrouj K, Andrés-Sánchez N, Dubra G, Singh P, Sobecki M, Chahar D, et al. Ki-67 Regulates Global Gene Expression and Promotes Sequential Stages of Carcinogenesis. *Proc Natl Acad Sci* (2021) 118:e2026507118. doi: 10.1073/pnas.2026507118
89. Li LT, Jiang G, Chen Q, Zheng JN. Ki67 is a Promising Molecular Target in the Diagnosis of Cancer (Review). *Mol Med Rep* (2015) 11:1566–72. doi: 10.3892/mmr.2014.2914
90. Keam B, Im S-A, Lee K-H, Han S-W, Oh D-Y, Kim JH, et al. Ki-67 can be Used for Further Classification of Triple Negative Breast Cancer Into Two Subtypes With Different Response and Prognosis. *Breast Cancer Res* (2011) 13:R22. doi: 10.1186/bcr2834
91. Li H, Han X, Liu Y, Liu G, Dong G. Ki67 as a Predictor of Poor Prognosis in Patients With Triple−Negative Breast Cancer. *Oncol Lett* (2015) 9:149–52. doi: 10.3892/ol.2014.2618

Conflict of Interest: The authors declare that the research was conducted in the absence of any commercial or financial relationships that could be construed as a potential conflict of interest.

Publisher's Note: All claims expressed in this article are solely those of the authors and do not necessarily represent those of their affiliated organizations, or those of the publisher, the editors and the reviewers. Any product that may be evaluated in this article, or claim that may be made by its manufacturer, is not guaranteed or endorsed by the publisher.

Copyright © 2021 Haidar Ahmad, Pasquereau, El Baba, Nehme, Lewandowski and Herbein. This is an open-access article distributed under the terms of the Creative Commons Attribution License (CC BY). The use, distribution or reproduction in other forums is permitted, provided the original author(s) and the copyright owner(s) are credited and that the original publication in this journal is cited, in accordance with accepted academic practice. No use, distribution or reproduction is permitted which does not comply with these terms.

11.5 Publication N°5

Nehme Z, Pasquereau S, Haidar Ahmad S, **El Baba R**, Herbein G. Polyploid giant cancer cells, EZH2 and Myc upregulation in mammary epithelial cells infected with high-risk human cytomegalovirus. EBioMedicine 2022;80:104056. https://doi.org/10.1016/j.ebiom.2022.104056.

Human cytomegalovirus (HCMV) infection has been associated with complex cancer processes. Herein, we explored the molecular mechanisms underlying HCMV-induced oncogenesis. We have identified EZH2 as a downstream target for HCMV-induced Myc upregulation during acute and chronic infection with high-risk strains. This leads to the development of giant cells and acquisition of embryonic stemness markers in CMV-transformed cells. We also found that EZH2 inhibitors can mitigate the malignant properties of these cells. Breast biopsies with HCMV were characterized by elevated EZH2 and Myc expression, and this correlated with the presence of giant cancer cells. Further, we isolated two oncogenic HCMV strains from basal-like tumors with high EZH2 and Myc levels. This study suggests a connection between HCMV-induced Myc activation, EZH2 upregulation, and the development of polyploidy, supporting the idea that EZH2 and Myc play a role in tumorigenesis. Additionally, EZH2 is identified as a potential therapeutic target for breast cancer, especially in the presence of HCMV infection.

Polyploid giant cancer cells, EZH2 and Myc upregulation in mammary epithelial cells infected with high-risk human cytomegalovirus

Zeina Nehme,[a] Sébastien Pasquereau,[a] Sandy Haidar Ahmad,[a] Ranim El Baba,[a] and Georges Herbein [a,b]*

[a]Department Pathogens and Inflammation-EPILAB, EA4266, Université de Franche-Comté, Université Bourgogne Franche-Comté (UBFC), 16 route de Gray, Besançon F-25030, France
[b]Department of Virology, CHU Besançon, Besançon, France

Summary

Background Human cytomegalovirus (HCMV) infection has been actively implicated in complex neoplastic processes. Beyond oncomodulation, the molecular mechanisms that might underlie HCMV-induced oncogenesis are being extensively studied. Polycomb repressive complex 2 (PRC2) proteins, in particular enhancer of zeste homolog 2 (EZH2) are associated with cancer progression. Nevertheless, little is known about EZH2 activation in the context of HCMV infection and breast oncogenesis.

Methods Herein, we identified EZH2 as a downstream target for HCMV-induced Myc upregulation upon acute and chronic infection with high-risk strains using a human mammary epithelial model.

Findings We detected polyploidy and CMV-transformed HMECs (CTH) cells harboring HCMV and dynamically undergoing the giant cells cycle. Acquisition of embryonic stemness markers positively correlated with EZH2 and Myc expression. EZH2 inhibitors curtail sustained CTH cells' malignant phenotype. Besides harboring polyploid giant cancer cells (PGCCs), tumorigenic breast biopsies were characterized by an enhanced EZH2 and Myc expression, with a strong positive correlation between EZH2 and Myc expression, and between PGCC count and EZH2/Myc expression in the presence of HCMV. Further, we isolated two HCMV strains from $EZH2^{High}Myc^{High}$ basal-like tumors which replicate in MRC5 cells and transform HMECs toward CTH cells after acute infection.

Interpretation Our data establish a potential link between HCMV-induced Myc activation, the subsequent EZH2 upregulation, and polyploidy induction. These data support the proposed tumorigenesis properties of EZH2/Myc, and allow the isolation of two oncogenic HCMV strains from $EZH2^{High}Myc^{High}$ basal breast tumors while identifying EZH2 as a potential therapeutic target in the management of breast cancer, particularly upon HCMV infection.

Funding This work was supported by grants from the University of Franche-Comté (UFC) (CR3300), the Région Franche-Comté (2021-Y-08292 and 2021-Y-08290) and the Ligue contre le Cancer (CR3304) to Georges Herbein. Zeina Nehme is a recipient of a doctoral scholarship from the municipality of Habbouch. Sandy Haidar Ahmad is recipient of a doctoral scholarship from Lebanese municipality. Ranim El Baba is a recipient of a doctoral scholarship from Hariri foundation for sustainable human development.

Copyright © 2022 The Author(s). Published by Elsevier B.V. This is an open access article under the CC BY-NC-ND license (http://creativecommons.org/licenses/by-nc-nd/4.0/)

Keywords: Cytomegalovirus; Polyploid giant cancer cells; EZH2; Myc; Breast cancer; CTH cells

eBioMedicine 2022;80: 104056
Published online xxx
https://doi.org/10.1016/j.ebiom.2022.104056

Introduction

Human cytomegalovirus (HCMV), or human herpesvirus 5 (HHV-5), is a ubiquitous DNA virus with a mid to high seroprevalence, reaching up to 95% of the adult population worldwide.[1] Beyond the paradigm of oncomodulation, HCMV infection and viral products fulfill the criteria of cancer hallmarks updated by Hanahan and Weinberg to rationalize the complexities of neoplastic disease,[2,3] with viral proteins and/or nucleic acids

*Corresponding author at: Department Pathogens and Inflammation-EPILAB, EA4266, Université de Franche-Comté, Université Bourgogne Franche-Comté (UBFC), 16 route de Gray, Besançon F-25030, France.
E-mail address: georges.herbein@univ-fcomte.fr (G. Herbein).

Research in context

Evidence before this study

Beside the fact that the majority of the adult population worldwide are human cytomegalovirus (HCMV)-seropositive, HCMV infection and viral products meet the criteria of cancer hallmarks in which HCMV-viral products are being detected in multiple cancers. Most importantly, recent evidence reveals that HCMV gene products are found in more than 90% of tumors and metastases of breast cancers, and their augmented expression can be linked to a more aggressive phenotype. To intervene in the development and implementation of effective diagnostic, preventive, and therapeutic measures, we must imperatively identify HCMV's mechanism of action in breast cancer. Recent data demonstrated that polyploidy giant cancer cells play a critical role in breast cancer pathophysiology. Polyploid giant cancer cells (PGCCs) or tumorigenesis drivers were mostly detected in poorly differentiated and therapy resistant cancers. Previously, we showed that the infection with the two clinical strains HCMV-DB (KT959235) and HCMV-BL (MW980585) induces HMECs transformation into CMV-Transformed HMECs (CTH cells). CTH cells presented a polyploid phenotype, stemness, epithelial-to-mesenchymal plasticity which resulted in fast growing breast tumors in NSG mice.

Added value of this study

Given the oncogenic properties of enhancer of zeste homolog 2 (EZH2) and Myc especially in high-grade breast cancer, in the present study, we intended to assess the link between HCMV, PGCCs, EZH2, and Myc in the context of breast cancer development and progression. Originally, our findings show that high-risk HCMV strains can promote a polyploid phenotype and reveal the existence of a potential link between HCMV infection, Myc/EZH2 upregulation and polyploidy generation *in vitro* and in basal breast tumors. Altogether, our findings confirm the proposed tumorigenic properties of EZH2 and Myc in the context of HCMV infection.

Implications of all the available evidence

A better understanding of the potential link between HCMV and breast cancer will pave the way for new targeted therapies thus increasing the overall survival of breast cancer patients.

being detected in a multitude of cancer types.[4] For instance, in the context of breast cancer, HCMV proteins were confined to neoplastic cells in primary tumors, sentinel lymph node[5,6] and brain metastases, with shorter overall survival and time to tumor progression in patients having the highest expression of HCMV immediate early (IE) proteins.[7] Recently, productive HCMV infection in breast tumor cells has been reported and could indicate that HCMV replication may play a role in breast cancer progression.[8] This rationalizes the urgent need to actively dissect the exact etiological role of HCMV in the relevance of breast cancer in order to contribute to the development of novel diagnostic, preventive, or therapeutic strategies.

On the other hand, polyploid giant cancer cells (PGCCs) are recognized as a cancerous cellular subpopulation endowed with an enhanced tumorigenic properties, tumor maintenance and recurrence, as well as therapy resistance, the latter accentuated by tumor heterogeneity.[9–11] Giant cancerous cells were described in a wide range of high-grade cancers, chemoresistant tumors and cancer cell lines, for instance glioma, breast, lung, prostate and colorectal cancer.[12] Being greatly dedifferentiated with embryonic stem-like traits, PGCCs are able to replicate through an asymmetric division pattern, resulting in the establishment of a mitotically-competent progeny population.[13] Remarkably, a shared characteristic among all malignancies triggered by oncoviruses is the presence of polyploidy, highlighting PGCCs as keystone phenotype in virally-induced tumors.[14]

Being the enzymatic subunit of polycomb repressive complex 2 (PRC2), enhancer of zeste homolog 2 (EZH2) is a histone-lysine N-methyltransferase responsible of transcriptional silencing.[15] EZH2 aberrations are associated with the development and progression of a variety of cancers.[16,17] Indeed, high EZH2 levels, notably in triple-negative breast cancer,[18] are strongly associated with poor clinical outcome[19] and correlate with aggressive pathologic features, including high nuclear grade and proliferative index.[18] In parallel, EZH2 was shown to expand the stem cell pool and the breast tumor initiating cells, including luminal progenitor cells, hence enhancing accelerated breast cancer initiation, metastasis and growth.[20–22] Interestingly, *EZH2* is identified as a downstream target of Myc oncogene, the latter coordinately regulating *EZH2* through transcriptional and post-transcriptional mechanisms during tumor initiation and disease progression.[23,24] On the other hand, EZH2 was shown to be recruited to the major immediate early promoter (MIEP) in CD14+ monocytes where HCMV establishes latent infection *in vivo*.[25] Further, EZH2 was demonstrated to be overexpressed in glioblastoma multiforme tissues harboring HCMV.[26] Intriguingly, EZH2 is overexpressed in PGCCs,[27,28] the latter being also triggered by HCMV infection,[29] which points toward a potential link between HCMV, PGCCs, and EZH2.

Previously, we demonstrated that the infection with the clinical strains HCMV-DB (KT959235) and HCMV-BL (MW980585) induces HMECs transformation into CMV-Transformed HMECs (CTH), the latter displaying a polyploid phenotype, stemness, epithelial-to-mesenchymal (EMT) plasticity, and resulting in the appearance of fast growing breast tumors in NSG mice.[29,30] Given the stated EZH2 oncogenic functions, we aimed to evaluate the presence of a potential link between the

triad of HCMV, PGCCs and EZH2, as well as the potential interrelation with Myc in the context of breast carcinogenesis. Subsequently, in the present study, we assessed the activation of Myc, EZH2 and SUZ12 expression, as well as polyploidy levels following acute infection with low- or high-risk HCMV strains.[31] This was complemented by deciphering the morphological and phenotypic characteristics of CTH cells undergoing the giant cell cycle and the potential implication of Myc and PRC2 proteins in both CTH cells and breast cancer biopsies.

Materials and methods

Cell lines and culture

Human primary mammary epithelial cells (HMECs, A10565) and embryonic lung fibroblasts (MRC5, 84002) were purchased from Life Technologies (Carlsbad, CA, USA) and RD-Biotech (Besançon, France), respectively. Human breast cancer cell lines MDA-MB231 and MCF7 were obtained from Institut Hiscia (Arlesheim, Switzerland). MRC5, MDA-MB231 and MCF7 cells were grown in Dulbecco's modified Eagle medium (DMEM) (PAN-Biotech) supplemented with fetal bovine serum (Dutscher) and penicillin/streptomycin (Life Technologies) (10% and 1% final concentration, respectively). HMECs were cultured in HMEC medium (Life Technologies) supplemented with HMEC supplement and bovine pituitary extract (Life Technologies) at 37 °C, 5% CO_2 and 95% humidity. CTH cells emerging following chronic infection with HCMV-BL and HCMV-DB isolates were cultured in the same condition as HMECs. Mycoplasma monthly screening was performed to certify mycoplasma free cultures (VenorGem classic mycoplasma detection, Minerva biolabs).

HCMV clinical isolates growth and detection

HCMV-FS, HCMV-KM, HCMV-BL, and HCMV-DB clinical strains were isolated from patients hospitalized at Besançon University Hospital (France). The clinical and biological data for the four hospitalized patients from whom we isolated the HCMV-DB, BL, FS and KM strains were provided (Suppl. Table 1). Viral stocks were prepared and stored at -80°C as detailed previously.[29] The presence of ULb' region was detected in all the four strains as well as in the B544 and B693 strains isolated from the triple negative breast cancer (TNBC) tissues (see below), as measured by the detection of UL128/UL130/UL131 by qPCR (Suppl. Fig. 1). Infection of HMECs or MRC5 (1×10^6) cells with the clinical isolates was carried out at a multiplicity of infection (MOI) of 1. Briefly, cells were incubated at 37°C for 2 h, after which the inoculum was discarded, and the cellular monolayer was washed thoroughly three times with 1X PBS and covered with fresh medium. To determine viral kinetics, infectious cell-free supernatant was harvested at the indicated time points post-infection, DNA was isolated (EZNA Blood DNA Kit, D3392-02, Omega BIO-TEK) and real-time IE1 quantitative PCR (qPCR) was performed using a Stratagene Mx3005P thermocycler (Agilent), using IE1 primers (Suppl. Table 2). qPCR was performed using KAPA SYBR FAST Master Mix (KAPA BIOSYSTEMS, KK4601) and reactions were activated at 95°C for 10 min, followed by 50 cycles (15 s at 95°C and 1 min at 60°C). Results were collected and analyzed using MxPro qPCR software. Where indicated, HCMV lncRNA4.9 was determined by PCR assay by using DreamTaq DNA polymerase (EP0701, Thermo Scientific). PCR products were resolved by agarose gel electrophoresis and SYBR Green I (Roche) was used for visualization.

Microscopy

CTH cells were monitored using an Olympus optical microscope (Japan) and OPTIKA microscopy digital camera (Opticam, Italy). To study the giant cell cycle, confocal microscopy was used and DAPI (4′, 6′-diamidino-2- phenylindole) staining was performed according to the manufacturer's protocol. To assess the expression of EZH2, SUZ12, Myc, pp65, and HCMV late Ag, uninfected HMECs and CTH cells were washed with 1X PBS, fixed and permeabilized (BD Cytofix/Cytoperm, 554722). Primary antibodies targeting EZH2, SUZ12, Myc, pp65, and HCMV late Ag (Suppl. Table 3) were used in parallel to DAPI staining. After staining, slides were evaluated using 63X oil immersion objective lens with a Carl-Zeiss confocal microscope (Germany). Images were analyzed using ZenBlue Software (Carl-Zeiss Microscopy GmbH).

Western blotting

Western blotting was performed as described previously.[30,32] Lysates from uninfected HMECs, CTH cells, MDA-MB231 and MCF7 were used to examine the expression of EZH2 and SUZ12. Lysates from uninfected HMECs and CTH cells were used to determine Myc expression. Antibodies used are listed in supplementary Table 3. Densitometry using ImageJ 1.40 software (National Institutes of Health, Bethesda, MA, USA) was employed to quantify protein levels. β-actin (A5316, St. Louis, MO, USA) was used as control to normalize sample loading.

Flow cytometry analysis

Uninfected HMECs and CTH cells collection, fixation, permeabilization, staining, and incubation were performed as described previously.[29] Cytofluorometric analysis was performed using a BD LSRFortessa X-20 (BD Biosciences) flow cytometer. FACSDiva software (BD Biosciences) was used to collect and analyze data.

Staining was performed for EZH2, SUZ12, Oct4, SSEA4, Nanog, Tra-1-60, SOX2, Akt, pAkt(Ser473), STAT3, pSTAT3, EpCAM, CD49f, Vimentin, E-Cadherin, CD24 and CD44. Antibodies used are listed in supplementary Table 3. Proliferation of CTH cells left untreated or treated with EZH2 inhibitors was assessed by measuring Ki67 antigen (Ag) expression by intracellular flow cytometry as described previously.[33] For cell cycle analysis, uninfected HMECs or HCMV-infected HMECs were washed in 1X PBS, fixed in 70% ethanol and resuspended in 50 µg/ml propidium iodide (P3566, life technologies, Eugene, USA) with 0.1 mg/ml RNase (R4642, Sigma-Aldrich, Saint-Louis, MO, USA), then incubated at 37°C for 30 min as described previously.[34]

RNA cross-linking immunoprecipitation (RNA CLIP) assay

RNA Cross-linking Immunoprecipitation (RNA CLIP) was performed on CTH cells as previously reported.[25]

Semi-quantitative reverse-transcriptase polymerase chain reaction (RT-PCR)

Total RNA was extracted using E.Z.N.A.® Total RNA Kit I (Omega Bio-Tech, GA, USA) according to the manufacturer's instructions. SuperScript IV First-Strand Synthesis kit (Invitrogen, Carlsbad, CA, USA) was used for reverse transcription. Semi-quantitative PCR was performed for Oct4, SSEA-4 synthase, Nanog, Tra-1-60, SOX2 and β-globin expression. Primers used are listed in supplementary Table 2. Two μl target cDNA conversion mixture was amplified using DreamTaq DNA polymerase (EP0701, 83 Thermo Scientific). RT-PCR products were electrophoresed on a 2% agarose gel stained with SYBR Green I (Roche).

EZH2 inhibition assay

The EZH2 inhibitors EPZ6438 and GSK343 (Cayman Chemical, Ann Arbor, MI, USA) were dissolved in Dimethyl Sulfoxide (DMSO) (Sigma-Aldrich). CTH cells were left untreated or treated by EZH2 inhibitors at 0.1µM and fresh drugs were added every two days.

Soft agar colony formation and colorimetric MTT assays

CTH cells left untreated or treated with EZH2 inhibitors at 0.1µM and HMECs infected with HCMV-B544 and HCMV-B693 strains were seeded in soft agar (Colorimetric assay, CB135; Cell Biolabs Inc., San Diego, CA) as described previously.[35] After 15 days of incubation, colonies quantification was performed using MTT (3-(4,5- dimethylthiazol-2-yl)-2,5-diphenyl tetrazolium bromide) assay as described previously[30] and soft agar colonies were observed under an Olympus microscope (magnification 200×).

Mammosphere assay

CTH cells untreated or treated with EZH2 inhibitors were cultured in 2 mL of mammosphere media (CCM012, R&D Systems, Minneapolis, MN, USA) supplemented with 2U/ml heparin (2812, Bio-Techne, Minneapolis, MN, USA) and 0.5 µg/ml hydrocortisone (4093, Bio-Techne, Minneapolis, MN, USA), in an ultra-low attachment surface 96-well plate. Mammospheres were observed using an Olympus optical microscope (Japan).

Chromatin immunoprecipitation (ChIP) assay

ChIP was performed using a Chromatin Immunoprecipitation assay kit (Millipore, cat no. 17-295) as previously described.[36] Chromatin cross-linking was achieved via a 10-min treatment of nuclear extracts with 1% formaldehyde at 37°C. Cross-linked lysates were sonicated to shear the DNA to an average length of 300 to 1000 base pairs. Following sonication, the lysates were pre-cleared via incubation with a 50% slurry of salmon sperm DNA/Protein A Agarose for 30 min. The pre-cleared supernatants were incubated with the primary antibodies anti-H3K27me3, anti-H3K4me3, and total anti-H3 (1:50 dilution, Suppl. Table 3) overnight and then with salmon sperm DNA/Protein A agarose beads at 4°C for 1 h. Following multiple washes, the DNA-protein complexes were eluted and the DNA was recovered by reversing the cross-linking with NaCl and proteinase K. The DNA was then extracted using the Qiaquick PCR Purification Kit (Qiagen, cat. no 28106) and analyzed by SYBR-Green real-time qPCR. The immunoprecipitated samples, along with the input DNA, were amplified for the HCMV MIEP enhancer (Enh) (Suppl. Table 3).

Genomic analysis of HCMV strains

The analysis of HCMV-DB and BL genomes and their comparison to other HCMV strains including the two laboratory adapted strains AD-169 and Towne in addition to Merlin, Toledo, TR, PH, VR1814, Davis, JP, and TB40/E (clinical strains with low passages in culture) was done using the NCBI nucleotide blast tool (https://blast. ncbi.nlm.nih.gov/BlastAlign.cgi). The phylogenetic analysis was performed as previously reported.[37]

Breast cancer biopsies

Tumor breast biopsies (luminal tumor biopsies n=10 and basal tumor biopsies n=9) and adjacent healthy breast biopsies (n=8) were provided by the Regional tumor bank (BB0033-00024 Tumorothèque Régionale de Franche-Comté). A written informed consent for participation was obtained from all patients. The study was authorized by the local ethics committees of Besançon University Hospital (Besançon, France) and the French Research Ministry (AC-2015-2496, CNIL n°1173545, NF-S-138 96900 n°F2015). Hematoxylin and eosin

slides were used to detect PGCCs presence based on Zhang et al. description, with PGCCs being defined as a cancer cell with a nucleus at least three times larger than that of a diploid cancer cell.[38] RNA was extracted from the biopsies using E.Z.N.A.® Total RNA Kit I (Omega Bio-Tech, GA, USA). Reverse transcription was performed using the SuperScript IV First-Strand Synthesis kit (Invitrogen, Carlsbad, CA, USA). Expression of EZH2, Myc, and GAPDH was assessed by real-time qPCR using KAPA SYBR FAST Master mix (KAPA BIOSYSTEMS, KK4601) and specific primers for EZH2, Myc and GAPDH (Suppl. Table 2) according to the manufacturer's protocol. Fold change expression was calculated using the delta-delta Ct method.[39]

The two strains, B544 and B693, were isolated from patients with TNBC. The treatment, clinical outcome and pathological data for these two TNBC patients were provided (Suppl. Table 4). HCMV strains, B544 and B693, were isolated by mechanical tissue disruption and filtration of the frozen biopsy through a 0.45 µm filter and initially grown on MRC5 cells. The supernatant from MRC5 culture was filtrated through a 0.45 µm filter and used to infect HMECs. The purity of our HCMV cultures was confirmed by ruling out the presence of other viruses (Epstein-Barr virus, human papillomavirus, Kaposi sarcoma herpesvirus and adenovirus).

Statistical analysis

All quantitative results are reported as mean ± SD of independent experiments and analyzed by using statistical software SPSS 23. Statistical analyses were performed using Mann-Whitney U test, and correlation analyses were done using Pearson and Spearman correlation tests. Differences with p-value≤0·05 were considered significant and all exact p-values were provided in each figure. Microsoft Excel was used to construct the plots and histogram data.

Role of funding source

The funders had no role in the study design, data collection, data analyses or interpretation, manuscript writing, or publication decisions.

Reagent validation

Relevant documentation on reagent validation (antibody, cell lines, viruses) has been provided in the Supplemental Data Reagent Validation file.

Results

Myc and EZH2 activation parallels polyploidy induction in HMECs acutely infected with high-risk HCMV

We previously reported the replication of the clinical strain HCMV-DB in HMECs *in vitro*.[30] In the present study, we infected HMECs with three newly isolated HCMV clinical isolates that we previously sorted into low- (HCMV-KM, HCMV-FS) and high- (HCMV-DB, HCMV-BL) risk oncogenic strains,[29,31] as well as the already described HCMV-DB strain. All strains productively replicated in HMECs with the peak viral titer detected between day 1 and 8 post-infection (Figure 1a) due to the conservation of an intact ULb' region[29] required for infection of epithelial/endothelial cells.[40] As control, productive infection peak level was lower by 1 to 3 logs in HMECs compared to MRC5 fibroblasts (Figure 1b).

Previously, activation of proto-oncogenes, including Myc was reported as an early event upon HCMV infection.[41] We detected higher expression levels of Myc and EZH2 in HMECs infected with high-risk strains compared to low-risk ones (p-value=0·03 and 0·03, respectively; [Mann-Whitney U test]) (Figures 1c and d, Suppl. 2). No distinct pattern of SUZ12 expression variances was noted between low- and high-risk strains (Figures 1e, Suppl. 2). In parallel, we detected a higher percentage of <2N population in HMECs infected with HCMV-FS and HCMV-KM, versus a higher percentage of >4N population in HMECs infected with HCMV-BL and HCMV-DB (Figure 1f), pointing toward a higher polyploidy induction with the high-risk strains.

As we have previously demonstrated the activation of JAK/STAT3 axis in primary human hepatocytes and HepG2 cells infected with HCMV,[33] we observed an increase in STAT3 phosphorylation and STAT3 protein in HMECs infected with the four strains at day 1 post-infection (Figure 1g). EZH2 inhibitors and ganciclovir partially blocked the upregulation of P-STAT3 and STAT3 observed in HMECs acutely infected with HCMV, mostly in cultures infected with the high-risk DB strain (Suppl. Figure 3).

CTH cells and giant cells cycling in HMECs chronically infected with high-risk HCMV strains

HMECs cultures were individually infected with the four isolates to monitor long-term cultures.[30] As control, uninfected cells were used, the latter being discontinued after 50 days due to cellular senescence, as well as for HMECs infected with the low-risk HCMV-FS and HCMV-KM strains. Notably, CTH cells emerged only with HMECs infected with HCMV-BL and HCMV-DB isolates, with cells being heterogeneous in terms of shape and size (Figure 2). Compared to uninfected cultures that displayed typical epithelial-like morphology (Figure 2a1), we observed a mixture of spheroids and giant cells dispersed among small cells, with morphological heterogeneity raging from mesenchymal, epithelial, and fibroblastic-like structures to small spore-like cells (Figure 2). We were able to cluster the detected shapes into elongated cells, round dark cells, and big flat cells.

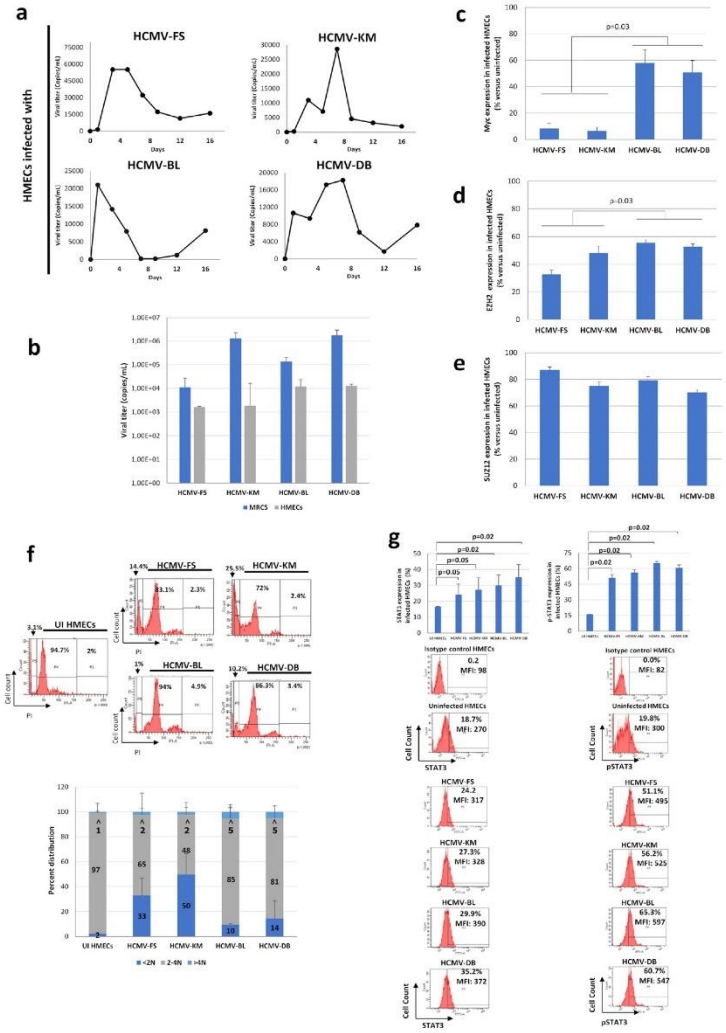

Figure 1. Replication of HCMV clinical strains in HMECs with activation of oncogenic pathways and increased polyploidy. a. Time-course of the viral titer in supernatant of HMECs infected with the strains HCMV-FS, HCMV-KM, HCMV-BL and HCMV-DB, as measured by IE1 qPCR. b. Comparison of peak viral titer in supernatant of HMECs and MRC5 cells infected with the strains HCMV-FS, HCMV-KM, HCMV-BL and HCMV-DB, as measured by IE1 qPCR. c, d, e. Comparison of the expression of (c) Myc, (d) EZH2 and (e) SUZ12, in HMECs infected with the strains HCMV-FS, HCMV-KM, HCMV-BL and HCMV-DB. Histograms represent mean values ± SD of 3 independent experiments. f. Cell population repartition based on DNA content, as marked by PI staining of HMECs infected with the strains HCMV-FS, HCMV-KM, HCMV-BL and HCMV-DB. Cells are classified between <2N, 2-4N and >4N populations. Histograms represent the mean ±SD of 3 independent experiments. g. STAT3 and pSTAT3 expression in HMECs infected with HCMV-FS, HCMV-KM, HCMV-BL, and HCMV-DB strains, as measured by FACS. Histograms represent mean ±SD of 3 independent experiments. p-values were determined by Mann-Whitney U test.

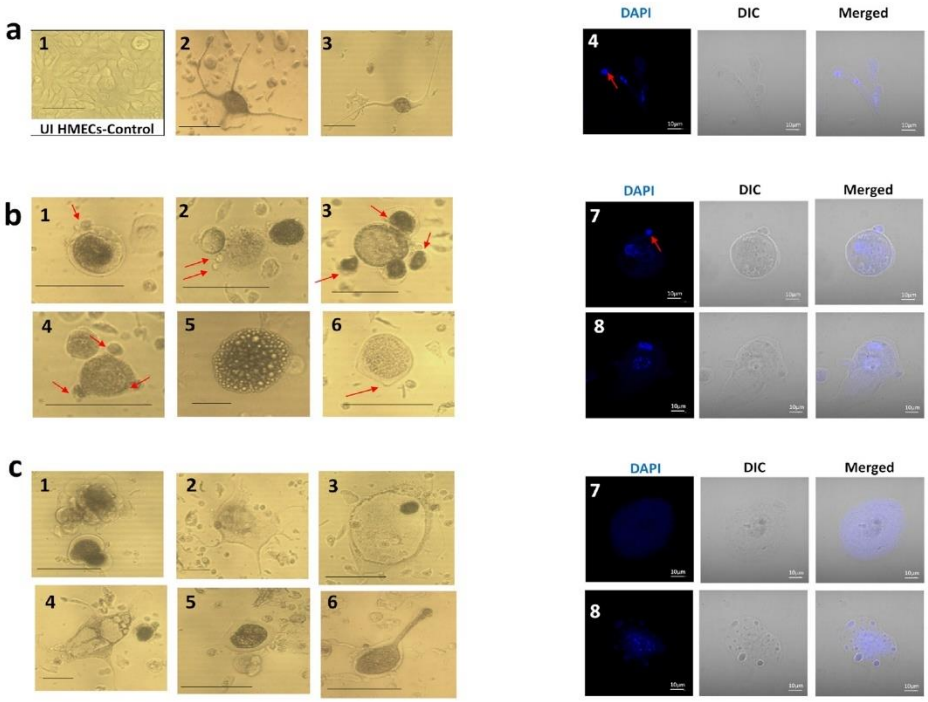

Figure 2. Appearance of CTH and polyploid giant cancer cells following infection of HMECs with HCMV-DB and HCMV-BL strains. a. Presence of neuron-like elongated cells, displaying multiple nuclei, as observed under an inverted light microscope (1-3) and a fluorescence confocal microscope (4) using DAPI staining. Uninfected HMECs (1), CTH-DB (3 and 4) and CTH-BL (2). b. Presence of dense bodied cells, showing morula-like or blastomere-like structures, as observed under an inverted light microscope (1-6) and a fluorescence confocal microscope (7-8) using DAPI staining. CTH-DB (3, 5, 6, 7) and CTH-BL (1, 2, 4, 8). c. Presence of giant cells, showing granular appearance and blastocyst-like shapes and displaying intense polyploidy, as observed under an inverted light microscope (1-6) and a fluorescence confocal microscope (7-8) using DAPI staining. CTH-DB (1, 5) and CTH-BL (2, 3, 4, 6, 7, 8). Inverted light microscope scale bar represents 100µm; Confocal microscope scale bar represents 10µm.

Elongated spindle-like cells displayed neuron-like shapes, with some cells forming coral-like structures, long microvilli, and filopodia (Figure 2a2-3). Upon observation by confocal microscopy, multiple nuclei were detected within bodies and branches of elongated cells, from where small mononucleated daughter cells were budding (Figure 2a4, red arrow). In parallel, densely packed bodies with smooth edges were also detected (Figure 2b1-6). Some cells exhibited morula-like structure (Figure 2b5), while others were morphologically indistinguishable from blastomeres (Figure 2b1-4). Round cells with short microvilli and some small budding spherical bodies were also present (Figure 2b1, red arrows). Figure 2b7, 8 show asymmetric cell division pattern represented by budding of daughter cells from either mononucleated or multinucleated cells. On the other hand, giant cells appeared to be hypertrophic, irregular in shape with small apophyses and granular appearance (Figure 2c). Cells displayed ruffle shape (Figure 2c1) and multiple microvilli (Figure 2c2) with some cells exhibiting a blastocyst-like morphology (Figure 2c3). Intensive polyploidization with nuclei displaying irregular contours was detected, parallel to cells displaying a single giant nucleus (Figure 2c7, 8).

The described morphological heterogenicity confirmed the presence of PGCCs in our culture. As the latter are described to undergo the "giant cell cycle", we monitored by confocal microscopy the fate of infected cells (Suppl. Figure 4). In response to HCMV infection (red arrow), a subset of cells enters the "giant cell cycle" (1), as evidenced by a nucleus size increase, possibly due to endoreplication. Some cells directly bud from giant mononucleated cells (2), whereas others form elongated

ones (3), where DNA migrates horizontally into adjacent cells via the branch of cytoplasm, followed by budding (7). On the other hand, some cells continue endoreplication (4) to generate mononucleated or multinucleated PGCCs (5), followed by depolyploidization, as illustrated by daughter cells budding from multinucleated (6) or mononucleated (7) giant cells. Taken together, our data suggest that infected cells can enter a self-renewal state and grow as PGCCs, followed by depolyploidization, thus fulfilling the steps of the "giant cell cycle".

CTH cells display upregulated EZH2 and Myc expression, EMT traits and stemness

As the deregulation of PRC2 proteins, particularly EZH2, has been linked to the initiation of tumorigenesis, and that Myc is identified as an EZH2 regulator during tumor initiation and progression[23], we assessed the expression of EZH2, SUZ12 and Myc proteins in CTH cells. EZH2 and Myc expression was upregulated in CTH cells compared to uninfected HMECs (p-value=0·03 and 0·02, respectively; [Mann-Whitney U test]), with a slight increase in SUZ12 expression (p-value=0·11; [Mann-Whitney U test]) (Figure 3a). EZH2, SUZ12, and Myc proteins were positively stained in CTH cells as demonstrated by confocal microscopy imaging (Figure 3b). According to CTH cells subpopulation analysis on the basis of their size (FSC) and ploidy (N) (Figure 3a),[29] PGCCs were shown to highly express EZH2, SUZ12 and Myc proteins, in contrast to small cells (SC). This upregulation was further confirmed by western blot, with a parallel enhanced expression of EZH2, SUZ12, and Myc in CTH cells (p-value=0·07, 0·07 and 0·02, respectively; [Mann-Whitney U test]) (Figure 3c).

PGCCs and SCs undergoing the giant cell cycle are described to have differential expression of proliferation, epithelial, mesenchymal and stemness markers.[27,42] Hence, we assessed the expression of a panel of markers in PGCCs and SCs (Suppl. Figure 5). Compared to uninfected HMECs and SCs, PGCCs are highly proliferative, with high levels of Ki67 Ag, along with a high expression of the mesenchymal marker vimentin and the stemness markers CD49f and CD44, as well CD24, a marker overexpressed in breast cancer (Suppl. Figure 5). EpCAM downregulation was observed in both PGCCs and SCs, compared to uninfected HMECs (Suppl. Figure 5). A slight increase was seen with the epithelial marker E-cadherin in PGCCs, with a remarkable upregulation in SCs (Suppl. Figure 5).

As the acquisition of embryonic-like traits is activated in PGCCs,[38,42] we detected the expression of the embryonic markers Oct4 and Nanog in CTH cells (Figure 4a). This was further confirmed by RT-PCR (Figure 4b) and flow cytometric analysis (Figure 4c), where an upregulation of Oct4, SSEA-4, Nanog, Tra-1-60, and SOX2 in CTH cells compared to uninfected HMECs was further demonstrated (p-value=0·03; [Mann-Whitney U test]), with PGCCs expressing the highest level of embryonic stemness compared to SCs (Figures 4d and Suppl. 6). Interestingly, high EZH2 and Myc expression in PGCCs positively correlated with embryonic stemness expression (Figure 4e and f), reinforcing the link between EZH2/Myc upregulation and stemness.

EZH2 upregulation regulates proliferation, transformation, stemness, and HCMV replication in CTH cells

Viral presence in CTH cells was confirmed by detecting HCMV pp65 antigen (Figure 5a), which could indicate a potential link between the observed phenotype and HCMV. In addition to pp65 detection, HCMV-DB infected CTH cells were positive for HCMV late antigens (Figure 5a) and IE1 antigen as previously reported.[29]

As long non-coding RNAs (lncRNAs), in particular HCMV lncRNA4.9, interact with components of the polycomb repression complex and shape chromatin structure,[25] lncRNA4.9 presence and interaction with EZH2 in CTH cells were confirmed by using conventional PCR and RNA cross-linking immunoprecipitation assay, respectively (Figure 5b and c). An increase in HCMV titer with EZH2 blockage was also detected, compared to untreated CTH cells (p-value=0·03; [Mann-Whitney U test]) (Figure 5d). The viral replication was upregulated in CTH cells treated with EZH2 inhibitors parallel to enhanced $H3K4Me3$ chromatin mark in the enhancer region of IE gene as measured by chromatin immunoprecipitation (Suppl. Figure 7).

Previously, it has been shown that PRC2 increases breast cancer proliferation and migration, with EZH2 being related to increased tumor cell proliferation[43] and expansion of breast tumor-initiating cells while promoting a stem cell-like phenotype. Upon treatment with the EZH2 inhibitors (EPZ6438 and GSK343), EZH2 blockade significantly decreased the proliferation of treated CTH cells compared to untreated cells as assessed by Ki67 Ag expression levels (p-value=0·02; [Mann-Whitney U test]) (Figure 6a). In addition, EPZ6438 and GSK343 treatment significantly diminished CTH cells colony formation in soft agar (p-value=0·03; [Mann-Whitney U test]) (Figure 6b). Mammospheres formation was described to be inhibited upon EZH2 depletion.[44] Unexpectedly, treatment with EZH2 inhibitors (EPZ6438 and GSK343) did not inhibit mammospheres formation in CTH cells with larger spheres formed with EZH2 inhibitors treatment (Figure 6c). Finally, EZH2, SUZ12, and Myc were highly expressed in HMECs infected with the supernatant which was harvested from CTH-DB cells as demonstrated by confocal microscopy imaging (Suppl. Figure 8).

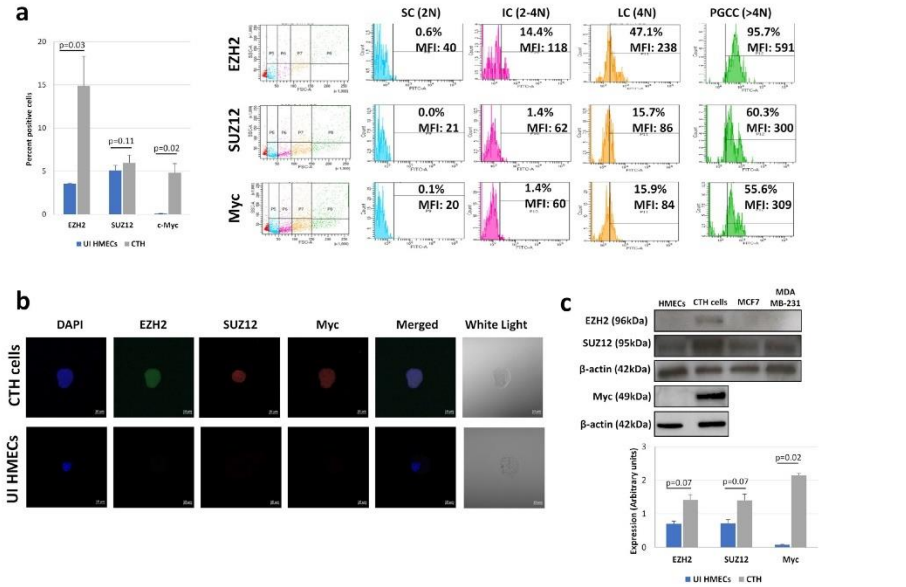

Figure 3. Myc, EZH2 and SUZ12 activation in CTH cells. a. Myc, EZH2, and SUZ12 expression in CTH cells and subpopulations, as measured by FACS. Histogram represents the mean ±SD of 3 independent experiments. PGCCs: polyploid giant cancer cells; LC: large cells; IC: intermediate cell; SC: small cells. b. Myc, EZH2 and SUZ12 expression in CTH cells as observed by fluorescence confocal microscope. Scale bar represents 10μm. c. Myc, EZH2, and SUZ12 expression in CTH cells as measured by western blot. Protein expression was measured by densitometry using ImageJ software; histogram represents the mean ±SD of 3 independent experiments. p-values were determined by Mann-Whitney U test.

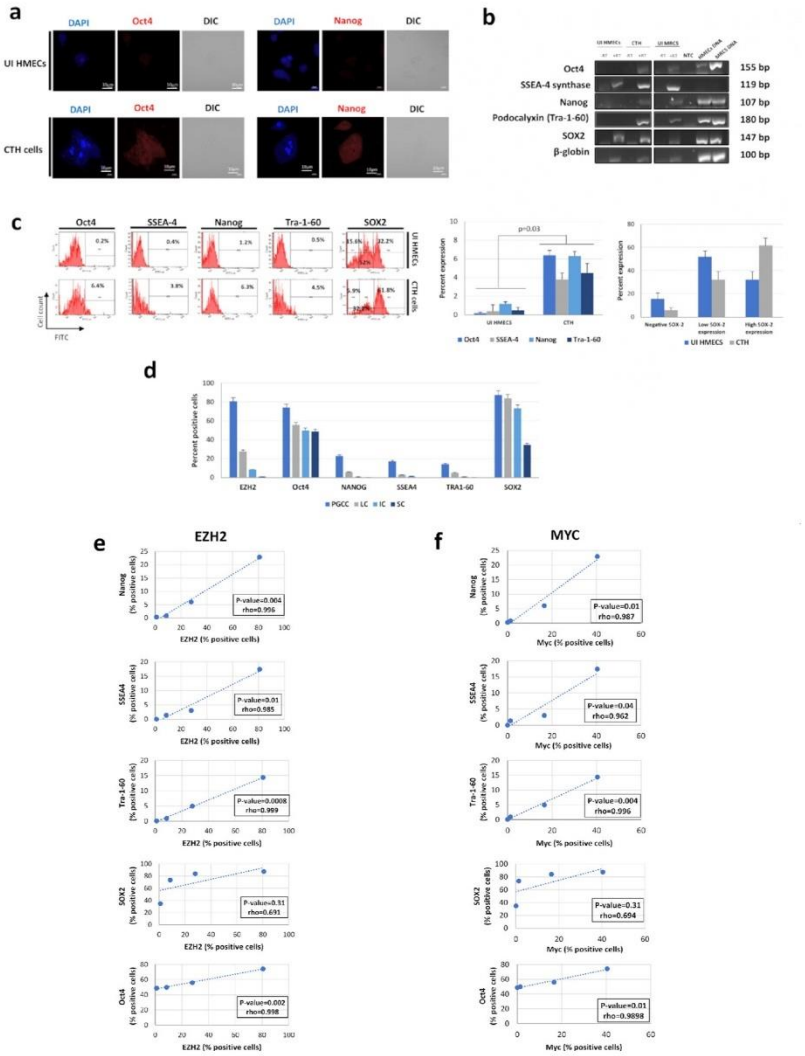

Figure 4. Increased expression of embryonic markers in CTH cells compared to HMECs. a. Oct4 and Nanog expression in CTH cells and HMECs, observed by fluorescence confocal microscopy. b. Expression of Oct4, SSEA-4 synthase, Nanog, Tra-1-60 and SOX2 at mRNA levels in CTH cells and HMECs. Cellular DNA was used as positive control. Beta-globin was used as housekeeping control gene. RT: reverse transcriptase; NTC: non-treated control. c. Embryonic markers expression in CTH cells and HMECs, as measured by FACS. Histograms represent mean values ±SD of 3 independent experiments. p-values were determined by Mann-Whitney U test. d. EZH2 and embryonic markers expression for CTH cells subpopulations. Histograms represent mean ±SD of 3 independent experiments. PGCCs: polyploid giant cancer cells; LC: large cells; IC: intermediate cell; SC: small cells. e, f. Correlation between (e) EZH2 and (f) Myc expression and embryonic markers expression in subpopulations of CTH cells. p-values were determined by Spearman's correlation test.

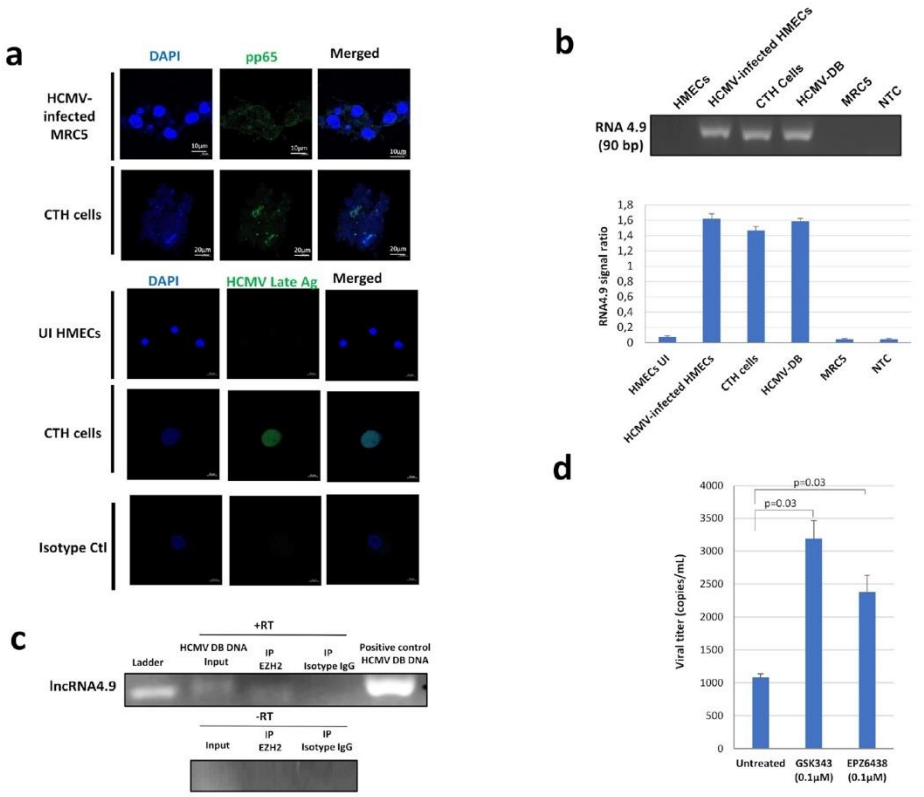

Figure 5. Presence of HCMV in CTH cells and enhanced viral replication upon EZH2 inhibition. a. HCMV pp65 protein and HCMV late Ag expression in CTH-DB cells, observed in fluorescence confocal microscopy. HCMV-infected cells were used as positive control. DAPI was used for nuclear staining. b. RNA4.9 gene presence in CTH-DB cells, as detected by conventional PCR. HCMV-infected HMECs and HCMV-DB genomic DNA were used as positive controls; MRC5 genomic DNA was used as negative control. Histogram represents the ratio of RNA4.9 signal to beta-globin signal as mean ±SD of 3 independent experiments. c. RNA-Immunoprecipitation of lncRNA4.9 using EZH2 antibody. d. Viral titer in supernatant of CTH-DB cells untreated or treated with EZH2 inhibitors GSK343 and EPZ6438, as quantified by IE1 qPCR. Histogram represents mean ±SD of 3 independent experiments. p-values were determined by Mann-Whitney U test.

PGCCs, EZH2 and Myc upregulation are detected in breast cancer tissues that are HCMV-positive

Previously, PGCCs number in breast cancer was linked to invasion and metastasis.[45] PGCCs with giant or multiple nuclei were present in human breast cancer biopsies, in particular triple negative breast cancer biopsies (Figure 7a). As expected, triple negative biopsies displayed higher tumor grade (p-value<0·001; [Mann-Whitney U test]), tubule formation (p-value=0·02; [Mann-Whitney U test]), nuclear pleomorphism (p-value<0·001; [Mann-Whitney U test]), and mitotic count (p-value=0·0017; [Mann-Whitney U test]) compared to luminal biopsies (Figure 7b). On the other hand, and compared to healthy biopsies (mean=2·4), tumor biopsies displayed an enhanced EZH2 expression (mean=31, p-value=0·02; [Mann-Whitney U test]), notably in the basal ones (mean=35·8) (Figure 7c). In this latter subset, EZH2 expression was prominent in biopsies harboring HCMV (mean=47·2) (Figure 7c), pointing toward a potential correlation between EZH2 upregulation and HCMV presence. Similar results were observed for Myc expression; Myc was highly expressed in HCMV-positive basal tumors (mean=17·9) compared to luminal ones (mean=2·2) (Figure 7d). High expression levels of EZH2 and Myc were measured in HCMV-positive basal biopsies compared to HCMV-negative basal biopsies

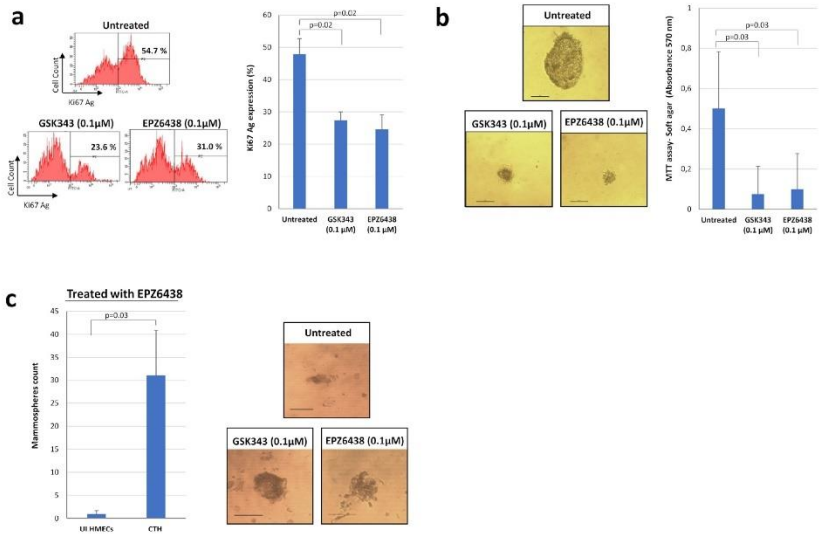

Figure 6. EZH2 inhibitors block CTH cell proliferation, colony formation in soft agar and enhance mammosphere formation. a. Ki-67 Ag expression in CTH untreated and treated with EZH2 inhibitors (GSK343 and EPZ6438), as measured by FACS. Histogram represents mean ±SD of 3 independent experiments. b. Soft-agar assay on CTH cells untreated and treated with EZH2 inhibitors (GSK343 and EPZ6438). Colony formation was assessed by inverted light microscope observation and quantified by MTT assay. Scale bar represents 100μm. Histogram represents mean ±SD of 3 independent experiments. c. Mammosphere formation assay on CTH cells untreated and treated with EZH2 inhibitors (GSK343 and EPZ6438). Mammospheres were observed under an inverted light microscope. Scale bar represents 100μm. p-values were determined by Mann-Whitney U test.

and to all luminal biopsies independent of HCMV status (Figure 7c and d). This was further confirmed by the presence of a strong positive correlation between EZH2 and Myc expression in tumor biopsies, exclusively in the presence of HCMV (r=0·929, p-value <0·001; [Pearson's correlation test]) and particularly in basal samples (r=0·914, p-value=0·03; [Pearson's correlation test]) (Figure 7e). Further, PGCC count strongly correlated with EZH2 expression only in tumor biopsies harboring HCMV (r=0·750, p-value=0·012; [Pearson's correlation test]), notably in luminal ones (r=0·946, p-value=0·015; [Pearson's correlation test]) (Figure 7f). On the other hand, PGCC count strongly correlated with Myc expression in HCMV-positive tissues (r=0·733, p-value=0·009; [Pearson's correlation test]), remarkably in basal ones (r=0·757, p-value=0·13; [Pearson's correlation test]) (Figure 7g). All in all, two HCMV strains, namely B544 and B693, where detected in biopsies with high expression levels of EZH2 and Myc, and were classified as $EZH2^{High}Myc^{High}$ basal breast tumors (Figure 7c and d).

Isolation of two oncogenic HCMV strains from $EZH2^{High}Myc^{High}$ basal breast tumors

Two HCMV strains, B544 and B693, were isolated from $EZH2^{High}Myc^{High}$ basal breast tumors by tissue disruption and filtration (Suppl. Figure 9a), and subsequently grown in MRC5 cells, showing a peak of viral load at day 20 and 19 post-infection, respectively (Suppl. Figure 9b). We measured the expression of EZH2, SUZ12, and Myc by FACS analysis, and lncRNA4.9 and IE1 transcripts by RT-PCR assay in HMECs acutely infected with B544 and B693 strains at day 1 post infection. We observed the upregulation of EZH2, SUZ12 and Myc expression in infected cells versus uninfected controls (Figure 8a). In parallel, lncRNA4.9 and IE1 transcripts were detected in HMECs acutely infected with the two strains (Figure 8a). Both B544 and B693 isolates of HCMV transformed infected HMECs toward CTH cells (Figure 8b). Thus, in the culture of CTH-B544 and CTH-B693, at day 105 post-infection, we detected large cells with blastomere-like morphology, numerous small round cells along with mesenchymal cells (Figure 8c). The previously described cell features are similar to that of CTH which were observed in HMEC cultures acutely infected with high-risk oncogenic strains DB and BL (Figure 2); these features could denote transformed cells which undergo different stages of the giant cell cycling. In agreement with the transformation of HMECs infected with B544 and B693 strains towards CTH cells, we observed the formation of colonies in soft agar seeded with HMECs infected with B544 and B693 strains (Figure 8d) indicating that they favor an anchorage-independent growth as previously observed for the high-risk DB and BL strains.[29] Finally, we observed the upregulation of Myc and EZH2 expression in CTH-B693 and CTH-B544 cells (Figure 8e). Also, we detected lncRNA4.9 transcripts in CTH-B6544 and CTH-B693 cells (Figure 8e). In both CTH-B544 and CTH-B693 cells, we detected the IE1 and late HCMV Ag protein using confocal microscopy (Figure 8f).

Discussion

We previously reported the classification of HCMV clinical isolates into low- or high-risk transforming strains.[29,31] Herein, we show that differential expression of Myc, EZH2 and SUZ12 proteins parallels polyploidy induction upon acute infection with low- or high-risk transforming strains. The activation of Myc/EZH2/PGCCs axis upon chronic infection with high-risk strains was further confirmed in CTH cultures, the latter being morphologically heterogeneous upon undergoing the "giant cell cycle", with stemness and EMT traits. Further, CTH cells were shown to harbor HCMV, with a direct physical interaction between HCMV lncRNA4.9 and EZH2, the latter being implicated in proliferation, transformation potential, mammospheres formation and HCMV replication. Breast tumor biopsies were found to harbor PGCCs with enhanced EZH2 expression, a strong positive correlation between EZH2 and Myc expression on one hand, and a high correlation between PGCC count and EZH2/Myc expression on the other hand, exclusively in the presence of HCMV. Finally, two HCMV strains were isolated from $EZH2^{High}Myc^{High}$ basal breast tumors which acutely transformed infected HMECs toward CTH cells, thereby indicating a direct link between high-risk HCMV strains and basal-like breast cancer.

Accumulated evidence highlight Myc and EZH2 as key players in both oncogenesis and stemness.[46–49] Upon acute infection with high-risk strains, a slight activation of Myc, EZH2 and polyploidy induction was noted (Figure 1). The activation of the described axis was further accentuated in CTH cells with a substantial upregulation of Myc and EZH2 proteins (Figure 3), and the appearance of PGCCs in culture (Figure 2). EZH2 overexpression was described to play a crucial role in breast cancer pathogenesis, where it represses early growth response 1 (EGR1) expression, resulting in the inhibition of EGR1-mediated tumor-suppressive signals.[50] Furthermore, EZH2 mediates ribosomal DNA stability via silencing of PHACTR2-AS1, inducing genomic instability and promoting growth and metastasis in breast cancer,[51] in line with the reduction in CTH cells proliferation observed upon EZH2 blockage (Figure 6a). Our results are also consistent with the reported GSK343-induced reduction in glioma cells proliferation.[52] In this sense, one of the molecular mechanisms reported to trigger EZH2 overexpression is through transcriptional regulation by Myc.[23] Indeed, Myc was shown to stimulate EZH2 expression by binding and activating the promoter of the latter,[53,54] by

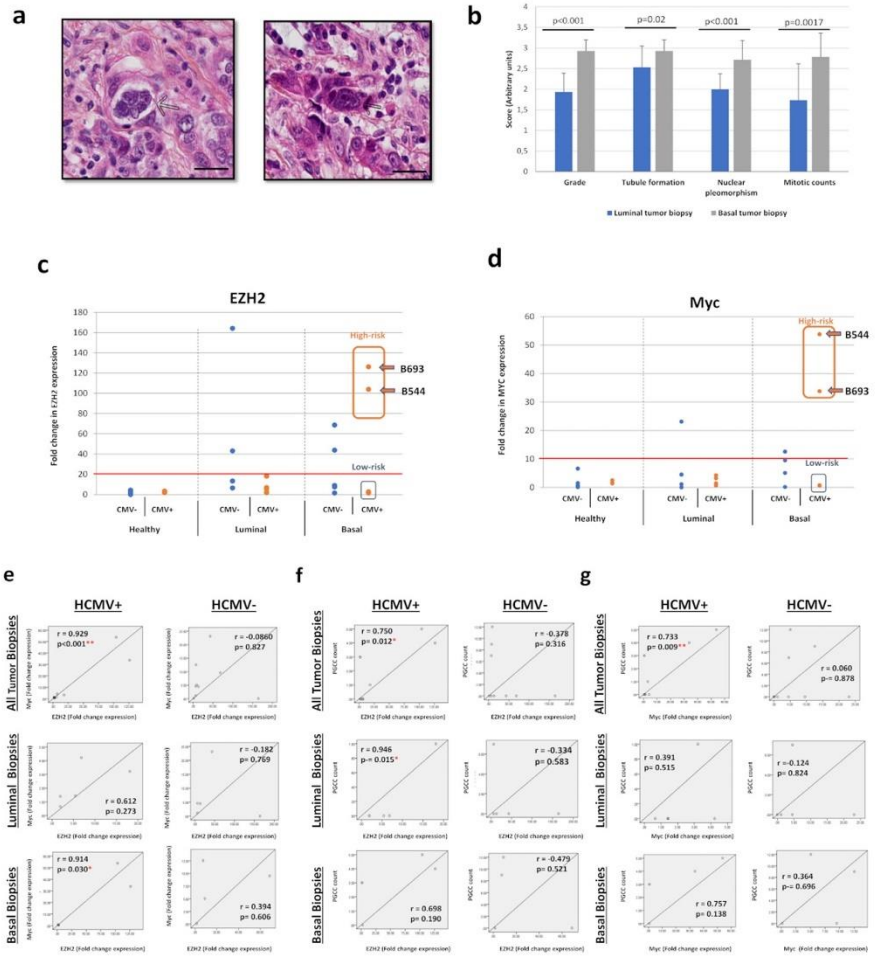

Figure 7. Detection of PGCCs in breast cancer biopsies and EZH2/Myc expression in healthy, tumor, luminal and basal biopsies. a. Presence of PGCCs in breast tumor biopsies (arrows). Tissue was stained using HES. Magnification: 80X. Scale bars are 25 µm. b. Comparison of histological characteristics of luminal and basal tumor biopsies. p-values were determined by Mann-Whitney U test. c, d. Scattered plots showing (c) EZH2 and (d) Myc expression in individual healthy, luminal, and basal HCMV-positive and negative biopsies. The cut-off for classifying high- and low-risk strains is represented by the horizontal red line. p-values were determined by Mann-Whitney U test. e, f, g. Correlation between the expression EZH2, Myc, and PGCC count in tumor biopsies in the presence or absence of HCMV. Correlation test between (e) EZH2 and Myc expression, (f) EZH2 expression and PGCC count, (g) Myc expression and PGCC count in all tumor, luminal and basal biopsies in the presence or absence of HCMV. *p-value≤0·05; ** p-value ≤0·01; p-values were determined by Pearson's correlation test.

alternatively repressing its negative regulator miR-26a,[55] or by directly suppressing miR-137, where Myc-miR-137-EZH2 pathway was linked to cisplatin resistance in ovarian cancer.[56] Further, bromodomain-4 protein (BRD4) was shown to positively regulate EZH2 transcription through Myc upregulation.[57] Intriguingly, Myc activation was widely reported in breast cancer progression, particularly in triple-

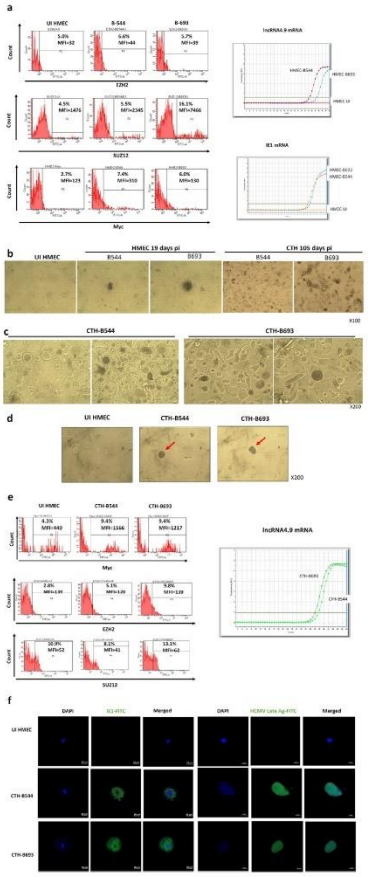

Figure 8. The acute transformation of HMECs infected with two HCMV strains which were isolated from EZH2^{High}Myc^{High} basal breast tumors toward CTH cells. a. *Left Panel.* Upregulation of EZH2, SUZ12 and Myc expression in HMECs infected with HCMV-B544 and HCMV-B693 strains at day 1 post infection versus uninfected controls, as measured by FACS. *Right Panel.* Detection of lncRNA4.9 and IE1 transcripts in HMECs infected with HCMV-B544 and HCMV-B693 strains at day 1 post infection, as measured by RT-qPCR. b. Time-course of appearance of CTH cells in HMEC cultures acutely infected with B544 and B693 HCMV strains. c. PGCCs structures obtained in CTH cells following the acute infection of HMECs with the two HCMV strains B544 and B693. d. Colony formation in soft agar seeded with HMECs infected with HCMV-B544 and HCMV-B693 strains. After 14 days in soft agar (day 15 post infection), colonies were observed under an Olympus microscope (magnification 200×). Results are representative of three independent experiments. e. *Left Panel.* Expression of Myc, EZH2 and SUZ12 in CTH-B693 and CTH-B544 cells, as measured by FACS. *Right Panel.* Detection of the lncRNA4.9 transcript in CTH-B544 and CTH-693 cells, as measured by RT-qPCR. f. HCMV IE1 protein and HCMV late Ag expression in CTH-B544 and CTH-B693 cells observed by fluorescence confocal microscopy. DAPI was used for nuclear staining.

negative breast cancer and in tumors displaying drug resistant phenotype,[11,47,58] similarly to aggressive medulloblastoma tumors where higher Myc levels were associated with increased EZH2 expression.[59] On the other hand, by uncoupling DNA replication from mitosis, Myc overexpression can induce DNA replication, thus opening the door toward polyploidy.[60] In this context, an intricate relationship between Myc, polyploidy and cancer was demonstrated,[61] with Myc being correlated with nuclear pleomorphism in primary and metastatic renal cell carcinomas.[62] Interestingly, we previously showed that the high-risk HCMV-BL robustly induced Myc expression, along with low p53 levels,[29] which can enhance stem cells replicative potential and reprogramming of progenitors in breast cancer, as Myc was identified as a transcriptional target of p53 in mammary stem cells and is activated upon p53 loss.[63] Besides, HCMV-DB strongly increased pRb expression,[29] with the pRB-E2F pathway being described to regulate the expression of EZH2.[64] Finally, we infected MCF-7 cells with HCMV-DB, BL, and TB40/E strains. We observed the upregulation of Myc expression following infection of MCF7 cells with the high-risk DB and BL strains, but not with TB40E (Suppl. Figure 10). The three strains slightly upregulated EZH2 and SUZ12 in MCF7 cells (Suppl. Figure 10). Previously, following the infection of HMECs with TB40/E strain, neither a significant activation of the molecular oncogenic pathways was observed in acutely infected HMEC nor CTH cells were detected in culture,[31] especially when compared to the high-risk HCMV-DB and BL strains. Therefore, TB40/E strain should be classified as a low-risk HCMV strain. This data is consistent with the absence of colony formation in soft agar that had been seeded with HMECs infected with TB40/E strain.[31] In addition, the phylogenetic analysis which was done using the whole genomic sequences of several HCMV strains corroborated the similarity of HCMV-DB and BL strains' genomes; genomes of DB and BL strains were dissimilar to the genome of TB40-E strain (Suppl. Figure 11). This emphasizes the hypothesis that high-risk strains DB and BL differentially induce Myc upregulation, and consequently stimulate EZH2 overexpression as well as polyploidy induction, pointing toward the presence Myc/EZH2/PGCCs axis underlying the described results.

Though, the interrelationship between HCMV and EZH2 is further complexed by the detection of HCMV lncRNA4.9 gene in CTH cells (Figure 5b and c). Indeed, cellular lncRNAs such as HOX antisense intergenic

RNA (HOTAIR) were described to interact with the PRC2 complex in breast cancer, and to increase cancer invasiveness and metastasis.[65] In our present study, it was shown that HCMV-lncRNA4.9 interacts with EZH2 (Figure 5c), which is in line with Rossetto et al. report describing lncRNA4.9 interaction with EZH2 and SUZ12 proteins, suggesting a role of lncRNA4.9 in mediating gene suppression at the MIEP during latency.[25] This is consistent with the increase in viral titer following EZH2 inhibition, possibly due to latency reversal (Figure 5d). In fact, the reactivation of HCMV under EZH2 inhibitors could be explained by at least two distinct mechanisms. First, EZH2 inhibitors could directly block the repressive H3K27 trimethylation in the HCMV promoter/enhancer and favor IE expression followed by viral reactivation.[66] Second, the promoter of the MIEP transcriptional repressor, growth factor independence 1 (GFI1), is controlled by the EZH2-NDY1/KDM2B-JARID2 axis, therefore EZH2 inhibitors might result in an enhanced GFI1 expression which could block viral reactivation.[36] To discriminate between the respective effects of EZH2 on GFI1/MIEP axis and histone methylation (H3K27, H3K4), we performed a ChIP assay. The repressive H3K27Me3 and activator H3K4Me3 marks on the enhancer of the MIEP were studied. The H3K4Me3 mark was shown to be strongly enhanced compared to a very limited increase in the H3K27Me3 chromatin mark on its enhancer at 24 hrs post treatment of CTH-DB (Suppl. Figure 7), consistent with an active transcriptional promoter. Interestingly, although the promoter of the MIEP transcriptional repressor GFI1 is controlled by the EZH2-NDY1/KDM2B-JARID2 axis and EZH2 inhibitors might therefore result in an enhanced GFI1 expression which could block viral replication in human foreskin fibroblasts acutely infected with HCMV,[36] this was not observed in our CTH model. In fact, promoters occupied by GFI1 showed higher levels of the marks associated with active transcription such as H3K4me3.[67] In addition, GFI1 associates with the chromodomain helicase DNA binding protein 4 (CHD4); GFI1/CHD4 complexes occupy active or bivalent promoters as well as active enhancers. These sites have a more closed chromatin configuration when CHD4 is present and a more open chromatin conformation when GFI1 is present.[67] Thus, in CTH cells treated with EZH2 inhibitors, GFI1 might occupy an active transcriptional promoter MIEP with enhanced H3K4Me3 mark or a bivalent promoter, and thereby could stimulate the expression of the IE gene and viral replication. Further, the role of GFI1 on IE transcription and viral replication could depend on the type of HCMV infection (acutely infected cells versus "chronically-infected" CTH cells), the cell type involved (fibroblasts versus epithelial-derived CTH cells) and the differentiation state and lineage commitment of the infected cells.[68] Altogether, the enhanced viral replication observed in CTH cells treated with EZH2 inhibitors could be mostly explained by the enhanced presence of GFI1 on the MIEP parallel to the enhanced H3K4Me3 rather than the decreased H3K27Me3 chromatin marks (Suppl. Figure 7). Finally, GFI1 may have additional non-transcriptional functions and interacts with a number of proteins involved in DNA repair.[68] An E2F1-mediated DNA damage response contributes to the replication of HCMV[69] making the role of GFI1 even more complex in HCMV replication. The role of GFI1 on HCMV replication definitively needs further studies.

Besides oncogenesis, recent studies have reinforced the importance of EZH2 in maintaining embryonic stemness,[70,71] as well as its implication in cancer stem cells.[72] This evidence correlates with the previously reported up-regulation of the stemness marker CD44 and mammospheres formation in CTH cells.[29] Further, EZH2 was shown to promote breast tumor initiating cells expansion, including mammary stem and luminal progenitor cells,[21,22,73] possibly through the activation of NOTCH1 signaling,[20] prompting the hypothesis that EZH2 facilitates transformation by blocking differentiation.[16] Interestingly, Myc controls the expression of developmental regulators in embryonic stem cells via the upregulation of the PRC2 complex.[74] Myc inhibition depletes cancer stem-like cells in a dose-dependent manner in triple-negative breast cancer.[75] Indeed, EZH2-mediated stemness could underlie not only the maintenance and expansion of PGCCs expressing high degree of embryonic stemness (Figure 4), but also their appearance in culture, as EZH2 expression in astrocytes induced their dedifferentiation toward stem-like cells expressing nestin, SOX2, and CD133.[76] Contrary to the loss and compromised self-renewal of stem cells upon EZH2 deletion,[71,77] we did not observe an inhibition of mammospheres formation upon EPZ6438 treatment; larger mammospheres were detected upon EZH2 blockage (Figure 6c). Indeed, this is in line with some reports describing an expansion of the stem and progenitor cell compartments upon EZH2 loss, coupled to JAK2-V617F axis activation.[78] As EPZ6438 is a selective EZH2 inhibitor,[79] the observed mammospheres expansion could be due to the expression of EZH1, a close homologue of EZH2 that can form an alternative PRC2 complex that partially compensates for the loss of EZH2.[80] To note that, it would be possible that EZH2 depletion in luminal breast cancer cells such as MCF7 cells[44] inhibits stemness and limits mammospheres formation by blocking the appearance of progenitor luminal cells. In this context, given the role of EZH2 in shifting progenitor luminal cells towards basal-like breast cancer cells, its blockade can result in the maintenance of progenitor cells, ultimately increasing mammospheres formation.[81]

A complex interrelation exists between Akt, STAT3 and EZH2. Certainly, STAT3 was described to act as a transcriptional factor that induces EZH2 upregulation by binding to the relative promoter region,[82] justifying

the higher EZH2 expression levels detected in HMECs infected with the high-risk strains compared to the low-risk ones (Figure 1d). In turn, EZH2 overexpression is sufficient for Akt activation, which can mediate breast cancer gene 1 (BRCA1) inhibition, aberrant mitoses with extra centrosomes, and genomic instability[83]. Alternatively, Akt phosphorylation of EZH2 was also reported, where the phosphorylation of the latter may exert pro-tumorigenic functions in a trimethylation-independent manner, as suggested by Xu et al.[84] Phosphorylated EZH2 binds to and methylates STAT3, leading to enhanced STAT3 activity, highlighting the Akt-EZH2-STAT3 axis as a positive regulator of tumor malignancy.[85] Interestingly, E2F8, an atypical transcription factor regulated by STAT3 signaling, was shown to be essential for polyploidization in mammalian cells,[86] potentially participating in the induction of >4N population observed upon infection with the high-risk strains (Figure 1f). We previously described an increase in Akt activation in HCMV-DB and HCMV-BL infected HMECs which is consistent with the observed increase in EZH2 and STAT3 activation.[29,30,87] Detection of a heterogeneous population in CTH cultures (Figure 2) is in line with the previous reports describing the evolution of mononuclear cells upon radio- or chemotherapy treatment into enlarged giant cells with single or multiple nuclei, followed by budding of small daughter cells that actively divide to generate their own progeny cells.[88,89] The detection of asymmetric division in CTH cells confirmed previous reports' findings in which they describe the return of PGCCs into non-polyploid state via the mechanisms of growth and division of simple organisms such as yeasts and other unicellular organisms.[42,90] Indeed, this process of slow self-renewal (Suppl. Figure 4) that was referred to as the "giant cell cycle"[9,38] not only coordinates the morphological dynamics observed in our cultures, but also explains the differential expression of proliferation, stemness and EMT markers between PGCCs and SCs (Suppl. Figure 5). In particular, the activation of embryonic-like stemness in CTH cells (Figure 4) points toward reprogramming and dedifferentiation as we and other researchers previously described.[29,42,91]

Further, we reported the detection of PGCCs in tumor biopsies displaying high EZH2 expression (Figure 7). Our results are in line with other findings describing strong EZH2 expression in the nucleus of invading stem-like PGCCs,[28] as well as in cancer stem-cells population isolated from human breast cancer, xenograft tumor cells, and primary breast tumor cells.[21] It is worth mentioning that the positive correlation detected between PGCC count and EZH2 or Myc expression in tumor biopsies is only established in the presence of HCMV (Figure 7), which indicates a potential role of the latter in the induction and/or maintenance of the observed phenotype. In fact, as our results are in accordance with a described significant positive correlation between Myc and EZH2 mRNA expression in primary prostate cancer specimens,[23] it has been shown that the infection with Epstein-Barr virus (EBV), a closely related herpesvirus, markedly induced expression of both Myc, and EZH2 mRNA levels in the same experimental model.[92] Since we did not detect EBV in our biopsy samples, this could emphasize a parallel role of HCMV in our model, where further experimental studies are certainly needed to comprehensively understand the exact role played by HCMV in the context of mammary tumors, in particular breast cancer molecular subtypes.

Using distinct methodological approaches, we detected the viral genes IE1 and lncRNA4.9, their transcripts, and most importantly viral proteins such as IE1, pp65, and the late HCMV antigens in CTH cells.[29,31] The detection of early and late viral genes, transcripts and proteins in CTH cells suggested that a lytic cycle is taking place even at a low-level and that the whole genome (or at least most of it) of HCMV high-risk strains might be present in CTH cells. The lytic viral replication could be necessary, even if limited, as well as the viral latency, to maintain/favor the transformed state of CTH cells in culture. In fact, the other two oncogenic herpesviruses, namely EBV and Kaposi's sarcoma-associated herpesvirus (KSHV), require the presence of both lytic and latent viral stages to be oncogenic. Indeed, in addition to the role played by viral latency in EBV and KSHV-induced malignancies, lytic replication might also contribute to EBV-induced oncogenesis and KSHV-induced sarcoma, respectively.[93,94] Further studies are required to clarify the role of HCMV lytic replication and latent dormancy in the described model and the potential contribution of individual lytic or latent HCMV genes to oncogenesis.

Lastly, since EZH2 and Myc have been implicated in tumor initiation, two HCMV strains (HCMV-B544 and HCMV-B693) were isolated from $EZH2^{High}Myc^{High}$ basal tumors to assess their transforming potential. After infection of HMECs cells with these HCMV isolates, we were able to obtain CTH cells, with morphological features matching those of PGCC, giant cell cycling and the previously described CTH cells obtained with HCMV-DB and HCMV-BL strains.[29–31] The detection of IE1 and HCMV late antigen proteins parallel to upregulated Myc, EZH2 expression and lncRNA4.9 transcript in cultures of CTH-B693 and CTH-B544 cells recapitulates the molecular phenotype observed in CTH-DB and CTH-BL cells. As a result, some high-risk HCMV strains are present in basal breast tumors in which they possess tumor-promoting abilities and therefore are considered as oncogenic strains.

In conclusion, our data indicate that high-risk HCMV strains can induce a polyploid phenotype with a distinctive cell cycle, tumor heterogeneity, epithelial to mesenchymal plasticity and embryonic-like stemness. Our findings highlight the presence of a potential link

between HCMV infection, Myc/EZH2 upregulation and polyploidy induction *in vitro* and in human breast cancer biopsies, supporting the proposed tumorigenesis properties of EZH2 and providing new prospect of using EZH2 inhibitors in the context of breast cancer.[95] A more detailed analysis of PRC2 target genes within CTH cells and their corresponding response to inhibitors may establish new avenues to understand the complex pathogenesis of breast cancer and open the door for targeted therapies in the future.

Contributors

Conceptualization, G.H.; formal analysis, S.H.A., S.P., Z.N., R.E.B, G.H.; investigation, S.H.A., S.P., R.E.B, Z.N.; writing—original draft preparation, Z.N., S.P., S.H.A., G.H.; writing—review and editing, Z.N., G.H.; directly accessed and verified the underlying data: Z.N., S.P., S.H.A., R.E.B., G.H.; visualization, S.H.A., S.P., Z.N.; supervision, G.H.; project administration, G.H.; funding acquisition, G.H. All authors have read and agreed to the published version of the manuscript.

Funding

This work was supported by grants from the University of Franche-Comté (UFC) (CR3300), the Région Franche-Comté (2021-Y-08292 and 2021-Y-08290) and the Ligue contre le Cancer (CR3304) to Georges Herbein. Zeina Nehme is a recipient of a doctoral scholarship from the municipality of Habbouch. Sandy Haidar Ahmad is recipient of a doctoral scholarship from Lebanese municipality. Ranim El Baba is a recipient of a doctoral scholarship from Hariri foundation for sustainable human development.

Data availability statement

The datasets used and/or analyzed during the present study are available from the corresponding author on reasonable request.

Declaration of interests

The authors declare no conflict of interest.

Acknowledgments

We are grateful to the Pathology Department at the Besançon University Hospital for providing breast biopsies and data. We thank DImaCell Imaging Ressource Center, University of Bourgogne Franche-Comté, Faculty of Health Sciences, 25000 Besançon, France for technical support. This work was supported by grants from the University of Franche-Comté (UFC) (CR3300), the Région Franche-Comté (2021-Y-08292 and 2021-Y-08290) and the Ligue contre le Cancer (CR3304) to Georges Herbein. Zeina Nehme is a recipient of a doctoral scholarship from the municipality of Habbouch. Sandy Haidar Ahmad is recipient of a doctoral scholarship from Lebanese municipality. Ranim El Baba is a recipient of a doctoral scholarship from Hariri foundation for sustainable human development.

Supplementary materials

Supplementary material associated with this article can be found in the online version at doi:10.1016/j.ebiom.2022.104056.

References

1 Schottstedt V, Blümel J, Burger R, et al. Human cytomegalovirus (HCMV) – revised*. *Transfus Med Hemother*. 2010;37:365–375. https://doi.org/10.1159/000322141.
2 Hanahan D, Weinberg RA. Hallmarks of cancer: the next generation. *Cell*. 2011;144:646–674. https://doi.org/10.1016/j.cell.2011.02.013.
3 Herbein G. The human cytomegalovirus, from oncomodulation to oncogenesis. *Viruses*. 2018;10:408. https://doi.org/10.3390/v10080408.
4 Michaelis M, Doerr HW, Cinatl J. The story of human cytomegalovirus and cancer: increasing evidence and open questions. *Neoplasia*. 2009;11:1–9. https://doi.org/10.1593/neo.81178.
5 Taher C, de Boniface J, Mohammad AA, et al. High prevalence of human cytomegalovirus proteins and nucleic acids in primary breast cancer and metastatic sentinel lymph nodes. *PLoS ONE*. 2013;8:e56795. https://doi.org/10.1371/journal.pone.0056795.
6 El Shazly DF, Bahnassey AA, Omar OS, et al. Detection of human cytomegalovirus in malignant and benign breast tumors in egyptian women. *Clin Breast Cancer*. 2018;18:e629–e642. https://doi.org/10.1016/j.clbc.2017.10.018.
7 Taher C, Frisk G, Fuentes S, Religa P, et al. High prevalence of human cytomegalovirus in brain metastases of patients with primary breast and colorectal cancers. *Transl Oncol*. 2014;7:732–740. https://doi.org/10.1016/j.tranon.2014.09.008.
8 Branch KM, Garcia EC, Chen YM, et al. Productive infection of human breast cancer cell lines with human cytomegalovirus (HCMV). *Pathogens*. 2021;10:641. https://doi.org/10.3390/pathogens10060641.
9 Liu J. The dualistic origin of human tumors. *Semin Cancer Biol*. 2018;53:1–16. https://doi.org/10.1016/j.semcancer.2018.07.004.
10 Zhao Q, Zhang K, Li Z, et al. High migration and invasion ability of PGCCs and their daughter cells associated with the nuclear localization of S100A10 modified by SUMOylation. *Front Cell Dev Biol*. 2021;9: 696871. https://doi.org/10.3389/fcell.2021.696871.
11 Liu Y, Zhu C, Tang L, et al. MYC dysfunction modulates stemness and tumorigenesis in breast cancer. *Int J Biol Sci*. 2021;17:178–187. https://doi.org/10.7150/ijbs.51458.
12 White-Gilbertson S, Voelkel-Johnson C. Giants and monsters: unexpected characters in the story of cancer recurrence. *Adv Cancer Res*. 2020;148:201–232. https://doi.org/10.1016/bs.acr.2020.03.001.
13 Amend SR, Torga G, Lin KC, et al. Polyploid giant cancer cells: Unrecognized actuators of tumorigenesis, metastasis, and resistance. *Prostate*. 2019;79:1489–1497. https://doi.org/10.1002/pros.23877.
14 Herbein G, Nehme Z. Polyploid giant cancer cells, a hallmark of oncoviruses and a new therapeutic challenge. *Front Oncol*. 2020;10: 567116. https://doi.org/10.3389/fonc.2020.567116.
15 Cao R, Wang L, Wang H, et al. Role of histone H3 lysine 27 methylation in polycomb-group silencing. *Science*. 2002;298:1039–1043. https://doi.org/10.1126/science.1076997.
16 Kim KH, Roberts CWM. Targeting EZH2 in cancer. *Nat Med*. 2016;22:128–134. https://doi.org/10.1038/nm.4036.
17 Veneti Z, Gkouskou K, Eliopoulos A. Polycomb repressor complex 2 in genomic instability and cancer. *Int J Mol Sci*. 2017;18:1657. https://doi.org/10.3390/ijms18081657.
18 Guo S, Li X, Rohr J, et al. EZH2 overexpression in different immunophenotypes of breast carcinoma and association with clinicopathologic features. *Diagn Pathol*. 2016;11:41. https://doi.org/10.1186/s13000-016-0491-5.

19 Kleer CG, Cao Q, Varambally S, et al. EZH2 is a marker of aggressive breast cancer and promotes neoplastic transformation of breast epithelial cells. *Proc Natl Acad Sci U S A*. 2003;100:11606–11611. https://doi.org/10.1073/pnas.1933744100.

20 Gonzalez ME, Moore HM, Li X, et al. EZH2 expands breast stem cells through activation of NOTCH1 signaling. *PNAS*. 2014;111:3098–3103. https://doi.org/10.1073/pnas.1308953111.

21 Chang CJ, Yang JY, Xia W, et al. EZH2 promotes expansion of breast tumor initiating cells through activation of RAF1-β-catenin signaling. *Cancer Cell*. 2011;19:86–100. https://doi.org/10.1016/j.ccr.2010.10.035.

22 Wu J, Crowe DL. The histone methyltransferase EZH2 promotes mammary stem and luminal progenitor cell expansion, metastasis and inhibits estrogen receptor-positive cellular differentiation in a model of basal breast cancer. *Oncol Rep*. 2015;34:455–460. https://doi.org/10.3892/or.2015.4003.

23 Koh CM, Iwata T, Zheng Q, Bethel C, Yegnasubramanian S, De Marzo AM. Myc enforces overexpression of EZH2 in early prostatic neoplasia via transcriptional and post-transcriptional mechanisms. *Oncotarget*. 2011;2:669–683. https://doi.org/10.18632/oncotarget.327.

24 Kuser-Abali G, Alptekin A, Cinar B. Overexpression of MYC and EZH2 cooperates to epigenetically silence MST1 expression. *Epigenetics*. 2014;9:634–643. https://doi.org/10.4161/epi.27957.

25 Rossetto CC, Tarrant-Elorza M, Pari GS. Cis and trans acting factors involved in human cytomegalovirus experimental and natural latent infection of CD14 (+) Monocytes and CD34 (+) cells. *PLoS Pathog*. 2013;9: e1003366. https://doi.org/10.1371/journal.ppat.1003366.

26 Ahani N, Shirkoohi R, Rokouei M, Alipour Eskandani M, Nikravesh A. Overexpression of enhancer of zeste human homolog 2 (EZH2) gene in human cytomegalovirus positive glioblastoma multiforme tissues. *Med Oncol*. 2014;31:252. https://doi.org/10.1007/s12032-014-0252-9.

27 Zhang S, Mercado-Uribe I, Hanash S, Liu J. iTRAQ-based proteomic analysis of polyploid giant cancer cells and budding progeny cells reveals several distinct pathways for ovarian cancer development. *PLOS ONE*. 2013;8:e80120. https://doi.org/10.1371/journal.pone.0080120.

28 Zhang L, Ding P, Lv H, et al. Number of polyploid giant cancer cells and expression of EZH2 are associated with VM formation and tumor grade in human ovarian tumor. *BioMed Res Int*. 2014;2014: e903542. https://doi.org/10.1155/2014/903542.

29 Nehme Z, Pasquereau S, Haidar Ahmad S, et al. Polyploid giant cancer cells, stemness and epithelial-mesenchymal plasticity elicited by human cytomegalovirus. *Oncogene*. 2021;40:3030–3046. https://doi.org/10.1038/s41388-021-01715-7.

30 Kumar A, Tripathy MK, Pasquereau S, et al. The human cytomegalovirus strain DB activates oncogenic pathways in mammary epithelial cells. *EBioMedicine*. 2018;30:167–183. https://doi.org/10.1016/j.ebiom.2018.03.015.

31 Haidar Ahmad S, Pasquereau S, El Baba R, Nehme Z, Lewandowski C, Herbein G. Distinct oncogenic transcriptomes in human mammary epithelial cells infected with cytomegalovirus. *Front Immunol*. 2021;12: 772160. https://doi.org/10.3389/fimmu.2021.772160.

32 Khan KA, Coaquette A, Davrinche C, Herbein G. Bcl-3-regulated transcription from major immediate-early promoter of human cytomegalovirus in monocyte-derived macrophages. *J Immunol*. 2009;182:7784–7794. https://doi.org/10.4049/jimmunol.0803800.

33 Lepiller Q, Abbas W, Kumar A, Tripathy MK, Herbein G. HCMV activates the IL-6-JAK-STAT3 Axis in HepG2 cells and primary human hepatocytes. *PLOS ONE*. 2013;8:e59591. https://doi.org/10.1371/journal.pone.0059591.

34 Basheer F, Giotopoulos G, Meduri E, et al. Contrasting requirements during disease evolution identify EZH2 as a therapeutic target in AML. *J Exp Med*. 2019;216:966–981. https://doi.org/10.1084/jem.20181276.

35 Borowicz S, Van Scoyk M, Avasarala S, et al. The soft agar colony formation assay. *J Vis Exp*. 2014:51998. https://doi.org/10.3791/51998.

36 Sourvinos G, Morou A, Sanidas I, et al. The downregulation of GFI1 by the EZH2-NDY1/KDM2B-JARID2 axis and by human cytomegalovirus (HCMV) associated factors allows the activation of the HCMV major IE promoter and the transition to productive infection. *PLoS Pathog*. 2014;10: e1004136. https://doi.org/10.1371/journal.ppat.1004136.

37 Moussawi FA, Kumar A, Pasquereau S, et al. The transcriptome of human mammary epithelial cells infected with the HCMV-DB strain displays oncogenic traits. *Sci Rep*. 2018;8:12574. https://doi.org/10.1038/s41598-018-30109-1.

38 Zhang S, Mercado-Uribe I, Xing Z, Sun B, Kuang J, Liu J. Generation of cancer stem-like cells through the formation of polyploid giant cancer cells. *Oncogene*. 2014;33:116–128. https://doi.org/10.1038/onc.2013.96.

39 Schmittgen TD, Livak KJ. Analyzing real-time PCR data by the comparative C T method. *Nat Protoc*. 2008;3:1101–1108. https://doi.org/10.1038/nprot.2008.73.

40 Gerna G, Kabanova A, Lilleri D. Human cytomegalovirus cell tropism and host cell receptors. *Vaccines (Basel)*. 2019;7:70. https://doi.org/10.3390/vaccines7030070.

41 Boldogh I, AbuBakar S, Albrecht T. Activation of proto-oncogenes: an immediate early event in human cytomegalovirus infection. *Science*. 1990;247:561–564. https://doi.org/10.1126/science.1689075.

42 Niu N, Mercado-Uribe I, Liu J. Dedifferentiation into blastomere-like cancer stem cells via formation of polyploid giant cancer cells. *Oncogene*. 2017;36:4887–4900. https://doi.org/10.1038/onc.2017.72.

43 Fluge Ä, Gravdal K, Carlsen E, et al. Expression of EZH2 and Ki-67 in colorectal cancer and associations with treatment response and prognosis. *Br J Cancer*. 2009;101:1282–1289. https://doi.org/10.1038/sj.bjc.6605333.

44 Li J, Xi Y, Li W, et al. TRIM28 interacts with EZH2 and SWI/SNF to activate genes that promote mammosphere formation. *Oncogene*. 2017;36:2991–3001. https://doi.org/10.1038/onc.2016.453.

45 Fei F, Zhang D, Yang Z, et al. The number of polyploid giant cancer cells and epithelial-mesenchymal transition-related proteins are associated with invasion and metastasis in human breast cancer. *J Exp Clin Cancer Res*. 2015;34:158. https://doi.org/10.1186/s13046-015-0277-8.

46 Chang CJ, Hung MC. The role of EZH2 in tumour progression. *Br J Cancer*. 2012;106:243–247. https://doi.org/10.1038/bjc.2011.551.

47 Xu J, Chen Y, Olopade OI. MYC and breast cancer. *Genes Cancer*. 2010;1:629–640. https://doi.org/10.1177/1947601910378691.

48 Kumari K, Das B, Adhya AK, Rath AK, Mishra SK. Genome-wide expression analysis reveals six contravened targets of EZH2 associated with breast cancer patient survival. *Sci Rep*. 2019;9:1974. https://doi.org/10.1038/s41598-019-39122-4.

49 Gao B, Liu X, Li Z, Zhao L, Pan Y. Overexpression of EZH2/NSD2 histone methyltransferase axis predicts poor prognosis and accelerates tumor progression in triple-negative breast cancer. *Front Oncol*. 2020;10: 600514. https://doi.org/10.3389/fonc.2020.600514.

50 Guan X, Deng H, Choi UL, et al. EZH2 overexpression dampens tumor-suppressive signals via an EGR1 silencer to drive breast tumorigenesis. *Oncogene*. 2020;39:7127–7141. https://doi.org/10.1038/s41388-020-01484-9.

51 Chu W, Zhang X, Qi L, et al. The EZH2–PHACTR2–AS1–ribosome axis induces genomic instability and promotes growth and metastasis in breast cancer. *Cancer Res*. 2020;80:2737–2750. https://doi.org/10.1158/0008-5472.CAN-19-3326.

52 Yu T, Wang Y, Hu Q, et al. The EZH2 inhibitor GSK343 suppresses cancer stem-like phenotypes and reverses mesenchymal transition in glioma cells. *Oncotarget*. 2017;8:98348–98359. https://doi.org/10.18632/oncotarget.21311.

53 Nie Z, Guo C, Das SK, et al. Dissecting transcriptional amplification by MYC. *Elife*. 2020;9:e52483. https://doi.org/10.7554/eLife.52483.

54 Nie Z, Hu G, Wei G, et al. c-Myc is a universal amplifier of expressed genes in lymphocytes and embryonic stem cells. *Cell*. 2012;151:68–79. https://doi.org/10.1016/j.cell.2012.08.033.

55 Sander S, Bullinger L, Klapproth K, et al. MYC stimulates EZH2 expression by repression of its negative regulator miR-26a. *Blood*. 2008;112:4202–4212. https://doi.org/10.1182/blood-2008-03-147645.

56 Sun J, Cai X, Yung MM, et al. miR-137 mediates the functional link between c-Myc and EZH2 that regulates cisplatin resistance in ovarian cancer. *Oncogene*. 2019;38:564–580. https://doi.org/10.1038/s41388-018-0459-x.

57 Wu X, Liu D, Tao D, et al. BRD4 regulates EZH2 transcription through upregulation of C-MYC and represents a novel therapeutic target in bladder cancer. *Mol Cancer Ther*. 2016;15:1029–1042. https://doi.org/10.1158/1535-7163.MCT-15-0750.

58 Fallah Y, Brundage J, Allegakoen P, Shajahan-Haq AN. MYC-driven pathways in breast cancer subtypes. *Biomolecules*. 2017;7:53. https://doi.org/10.3390/biom7030053.

59 Natsumeda M, Liu Y, Nakata S, et al. Inhibition of enhancer of zest homologue 2 is a potential therapeutic target for high-MYC

medulloblastoma. *Neuropathology*. 2019;39:71–77. https://doi.org/10.1111/neup.12534.
60 Li Q, Dang CV. c-Myc overexpression uncouples DNA replication from mitosis. *Mol Cell Biol*. 1999;19:5339–5351. https://doi.org/10.1128/mcb.19.8.5339.
61 Vazquez-Martin A, Anatskaya OV, Giuliani A, et al. Somatic polyploidy is associated with the upregulation of c-MYC interacting genes and EMT-like signature. *Oncotarget*. 2016;7:75235–75260. https://doi.org/10.18632/oncotarget.12118.
62 Kinouchi T, Saiki S, Naoe T, et al. Correlation of c-myc expression with nuclear pleomorphism in human renal cell carcinoma. *Cancer Res*. 1989;49:3627–3630.
63 Santoro A, Vlachou T, Luzi L, et al. p53 Loss in breast cancer leads to myc activation, increased cell plasticity, and expression of a mitotic signature with prognostic value. *Cell Reports*. 2019;26:624–638. https://doi.org/10.1016/j.celrep.2018.12.071. e8.
64 Bracken AP, Pasini D, Capra M, Prosperini E, Colli E, Helin K. EZH2 is downstream of the pRB-E2F pathway, essential for proliferation and amplified in cancer. *EMBO J*. 2003;22:5323–5335. https://doi.org/10.1093/emboj/cdg542.
65 Gupta RA, Shah N, Wang KC, et al. Long non-coding RNA HOTAIR reprograms chromatin state to promote cancer metastasis. *Nature*. 2010;464:1071–1076. https://doi.org/10.1038/nature08975.
66 Dooley AL, O'Connor CM. Regulation of the MIE locus during HCMV latency and reactivation. *Pathogens*. 2020;9:E869. https://doi.org/10.3390/pathogens9110869.
67 Helness A, Fraszczak J, Joly-Beauparlant C, et al. GFI1 tethers the NuRD complex to open and transcriptionally active chromatin in myeloid progenitors. *Commun Biol*. 2021;4:1356. https://doi.org/10.1038/s42003-021-02889-2.
68 Beauchemin H, Möröy T. Multifaceted actions of GFI1 and GFI1B in hematopoietic stem cell self-renewal and lineage commitment. *Front Genet*. 2020;11: 591099. https://doi.org/10.3389/fgene.2020.591099.
69 E X, Pickering MT, Debatis M, et al. An E2F1-mediated DNA damage response contributes to the replication of human cytomegalovirus. *PLoS Pathog*. 2011;7: e1001342. https://doi.org/10.1371/journal.ppat.1001342.
70 Ezhkova E, Pasolli HA, Parker JS, et al. EZH2 orchestrates gene expression for the stepwise differentiation of tissue-specific stem cells. *Cell*. 2009;136:1122–1135. https://doi.org/10.1016/j.cell.2008.12.043.
71 Huang XJ, Wang X, Ma X, et al. EZH2 is essential for development of mouse preimplantation embryos. *Reprod Fertil Dev*. 2014;26:1166–1175. https://doi.org/10.1071/RD13169.
72 Yu J, Yu J, Rhodes DR, et al. A polycomb repression signature in metastatic prostate cancer predicts cancer outcome. *Cancer Res*. 2007;67:10657–10663. https://doi.org/10.1158/0008-5472.CAN-07-2498.
73 Stefansson OA, Esteller M. EZH2-mediated epigenetic repression of DNA repair in promoting breast tumor initiating cells. *Breast Cancer Res*. 2011;13:309. https://doi.org/10.1186/bcr2871.
74 Neri F, Zippo A, Krepelova A, Cherubini A, Rocchigiani M, Oliviero S. Myc regulates the transcription of the PRC2 gene to control the expression of developmental genes in embryonic stem cells. *Mol Cell Biol*. 2012;32:840–851. https://doi.org/10.1128/MCB.06148-11.
75 Yang A, Qin S, Schulte BA, Ethier SP, Tew KD, Wang GY. MYC inhibition depletes cancer stem-like cells in triple-negative breast cancer. *Cancer Res*. 2017;77:6641–6650. https://doi.org/10.1158/0008-5472.CAN-16-3452.
76 Sher F, Boddeke E, Copray S. EZH2 expression in astrocytes induces their dedifferentiation toward neural stem cells. *Cell Reprogr*. 2010;13:1–6. https://doi.org/10.1089/cell.2010.0052.
77 Collinson A, Collier AJ, Morgan NP, et al. Deletion of the polycomb-group protein EZH2 leads to compromised self-renewal and differentiation defects in human embryonic stem cells. *Cell Rep*. 2016;17:2700–2714. https://doi.org/10.1016/j.celrep.2016.11.032.
78 Shimizu T, Kubovcakova L, Nienhold R, et al. Loss of Ezh2 synergizes with JAK2-V617F in initiating myeloproliferative neoplasms and promoting myelofibrosis. *J Exp Med*. 2016;213:1479–1496. https://doi.org/10.1084/jem.20151136.
79 Knutson SK, Kawano S, Minoshima Y, et al. Selective inhibition of EZH2 by EPZ-6438 leads to potent antitumor activity in EZH2-mutant non-hodgkin lymphoma. *Mol Cancer Ther*. 2014;13:842–854. https://doi.org/10.1158/1535-7163.MCT-13-0773.
80 Xie H, Xu J, Hsu JH, et al. Polycomb repressive complex 2 regulates normal hematopoietic stem cell function in a developmental-stage-specific manner. *Cell Stem Cell*. 2014;14:68–80. https://doi.org/10.1016/j.stem.2013.10.001.
81 Granit RZ, Gabai Y, Hadar T, et al. EZH2 promotes a bi-lineage identity in basal-like breast cancer cells. *Oncogene*. 2013;32:3886–3895. https://doi.org/10.1038/onc.2012.390.
82 Pan YM, Wang CG, Zhu M, et al. STAT3 signaling drives EZH2 transcriptional activation and mediates poor prognosis in gastric cancer. *Mol Cancer*. 2016;15:79. https://doi.org/10.1186/s12943-016-0561-z.
83 Gonzalez ME, DuPrie ML, Krueger H, et al. Histone methyltransferase EZH2 induces akt-dependent genomic instability and BRCA1 inhibition in breast cancer. *Cancer Res*. 2011;71:2360–2370. https://doi.org/10.1158/0008-5472.CAN-10-1933.
84 Xu K, Wu ZJ, Groner AC, et al. EZH2 oncogenic activity in castration-resistant prostate cancer cells is polycomb-independent. *Science*. 2012;338:1465–1469. https://doi.org/10.1126/science.1227604.
85 Kim E, Kim M, Woo DH, et al. Phosphorylation of EZH2 activates STAT3 signaling via STAT3 methylation and promotes tumorigenicity of glioblastoma stem-like cells. *Cancer Cell*. 2013;23:839–852. https://doi.org/10.1016/j.ccr.2013.04.008.
86 Pandit SK, Westendorp B, Nantasanti S, et al. E2F8 is essential for polyploidization in mammalian cells. *Nat Cell Biol*. 2012;14:1181–1191. https://doi.org/10.1038/ncb2585.
87 Liao Y, Hung MC. Physiological regulation of Akt activity and stability. *Am J Transl Res*. 2010;2:19–42.
88 Niu N, Zhang J, Zhang N, et al. Linking genomic reorganization to tumor initiation via the giant cell cycle. *Oncogenesis*. 2016;5:e281. https://doi.org/10.1038/oncsis.2016.75.
89 Lin KC, Torga G, Sun Y, et al. The role of heterogeneous environment and docetaxel gradient in the emergence of polyploid, mesenchymal and resistant prostate cancer cells. *Clin Exp Metastasis*. 2019;36:97–108. https://doi.org/10.1007/s10585-019-09958-1.
90 Zhang D, Wang Y, Zhang S. Asymmetric cell division in polyploid giant cancer cells and low eukaryotic cells. *Biomed Res Int*. 2014;2014:1–8. https://doi.org/10.1155/2014/432652.
91 Díaz-Carballo D, Saka S, Klein J, et al. A distinct oncogenerative multinucleated cancer cell serves as a source of stemness and tumor heterogeneity. *Cancer Res*. 2018;78:2318–2331. https://doi.org/10.1158/0008-5472.CAN-17-1861.
92 Ichikawa T, Okuno Y, Sato Y, et al. Regulation of epstein-barr virus life cycle and cell proliferation by histone H3K27 methyltransferase EZH2 in Akata cells. *MSphere*. 2018;3. https://doi.org/10.1128/mSphere.00478-18. e00478-18.
93 Münz C. Latency and lytic replication in Epstein–Barr virus-associated oncogenesis. *Nat Rev Microbiol*. 2019;17:691–700. https://doi.org/10.1038/s41579-019-0249-7.
94 Ganem D. KSHV and the pathogenesis of Kaposi sarcoma: listening to human biology and medicine. *J Clin Investig*. 2010;120:939–949. https://doi.org/10.1172/JCI40567.
95 Lehmann BD, Colaprico A, Silva TC, et al. Multi-omics analysis identifies therapeutic vulnerabilities in triple-negative breast cancer subtypes. *Nat Commun*. 2021;12:6276. https://doi.org/10.1038/s41467-021-26502-6.

11.6 Publication N°6

El Baba R, Pasquereau S, Haidar Ahmad S, Diab-Assaf M, Herbein G. Oncogenic and Stemness Signatures of the High-Risk HCMV Strains in Breast Cancer Progression. Cancers 2022;14:4271. https://doi.org/10.3390/cancers14174271.

Lately, human cytomegalovirus (HCMV) has been progressively implicated in carcinogenesis alongside its oncomodulatory impact. CMV-Transformed Human mammary epithelial cells (CTH) phenotype might be defined by giant cell cycling, whereby the generation of polyploid giant cancer cells (PGCCs) could expedite the acquisition of malignant phenotypes. Herein, the main study objectives were to assess the transformation potential in vitro and evaluate the obtained cellular phenotype, the genetic and molecular features, and the activation of cellular stemness programs of HCMV strains, B544 and B693, which were previously isolated from triple-negative breast cancer (TNBC) biopsies. The strains' sensitivity to paclitaxel and ganciclovir combination therapy was evaluated. A unique molecular landscape was unveiled in the tumor microenvironment of TNBC harboring high-risk HCMV. Overall, the explicit oncogenic and stemness signatures highlight HCMV potential in breast cancer progression thus paving the way for targeted therapies and clinical interventions which prolong the overall survival of breast cancer patients.

cancers

MDPI

Article

Oncogenic and Stemness Signatures of the High-Risk HCMV Strains in Breast Cancer Progression

Ranim El Baba [1], Sébastien Pasquereau [1], Sandy Haidar Ahmad [1], Mona Diab-Assaf [2] and Georges Herbein [1,3,*]

[1] Pathogens & Inflammation/EPILAB Laboratory, EA 4266, Université de Franche-Comté, Université Bourgogne Franche-Comté (UBFC), 25030 Besançon, France
[2] Molecular Cancer and Pharmaceutical Biology Laboratory, Lebanese University, Beirut 1500, Lebanon
[3] Department of Virology, CHU Besançon, 25030 Besançon, France
* Correspondence: georges.herbein@univ-fcomte.fr; Tel.: +33-381-665-616; Fax: +33-381-665-695

Simple Summary: Lately, human cytomegalovirus (HCMV) has been progressively implicated in carcinogenesis alongside its oncomodulatory impact. CMV-Transformed Human mammary epithelial cells (CTH) phenotype might be defined by giant cell cycling, whereby the generation of polyploid giant cancer cells (PGCCs) could expedite the acquisition of malignant phenotypes. Herein, the main study objectives were to assess the transformation potential in vitro and evaluate the obtained cellular phenotype, the genetic and molecular features, and the activation of cellular stemness programs of HCMV strains, B544 and B693, which were previously isolated from triple-negative breast cancer (TNBC) biopsies. The strains' sensitivity to paclitaxel and ganciclovir combination therapy was evaluated. A unique molecular landscape was unveiled in the tumor microenvironment of TNBC harboring high-risk HCMV. Overall, the explicit oncogenic and stemness signatures highlight HCMV potential in breast cancer progression thus paving the way for targeted therapies and clinical interventions which prolong the overall survival of breast cancer patients.

Abstract: Background: Human cytomegalovirus (HCMV) oncomodulation, molecular mechanisms, and ability to support polyploid giant cancer cells (PGCCs) generation might underscore its contribution to oncogenesis, especially breast cancers. The heterogeneity of strains can be linked to distinct properties influencing the virus-transforming potential, cancer types induced, and patient's clinical outcomes. Methods: We evaluated the transforming potential in vitro and assessed the acquired cellular phenotype, genetic and molecular features, and stimulation of stemness of HCMV strains, B544 and B693, isolated from $EZH2^{High}Myc^{High}$ triple-negative breast cancer (TNBC) biopsies. Therapeutic response assessment after paclitaxel (PTX) and ganciclovir (GCV) treatment was conducted in addition to the molecular characterization of the tumor microenvironment (TME). Findings: HCMV-B544 and B693 transformed human mammary epithelial cells (HMECs). We detected multinucleated and lipid droplet-filled PGCCs harboring HCMV. Colony formation was detected and Myc was overexpressed in CMV-Transformed-HMECs (CTH cells). CTH-B544 and B693 stimulated stemness and established an epithelial/mesenchymal hybrid state. HCMV-IE1 was detected in CTH long-term cultures indicating a sustained viral replication. Biopsy B693 unveiled a tumor signature predicting a poor prognosis. CTH-B544 cells were shown to be more sensitive to PTX/GCV therapy. Conclusion: The oncogenic and stemness signatures of HCMV strains accentuate the oncogenic potential of HCMV in breast cancer progression thereby leading the way for targeted therapies and innovative clinical interventions that will improve the overall survival of breast cancer patients.

Keywords: human cytomegalovirus; CTH cells; PGCCs; HCMV strains; TNBC; paclitaxel; ganciclovir; oncogenesis

check for updates

Citation: El Baba, R.; Pasquereau, S.; Haidar Ahmad, S.; Diab-Assaf, M.; Herbein, G. Oncogenic and Stemness Signatures of the High-Risk HCMV Strains in Breast Cancer Progression. *Cancers* **2022**, *14*, 4271. https://doi.org/10.3390/cancers14174271

Academic Editors: Maria G. Isaguliants, Alexander Ivanov, Franco M. Buonaguro and Christoph F. A. Vogel

Received: 29 June 2022
Accepted: 25 August 2022
Published: 1 September 2022

Publisher's Note: MDPI stays neutral with regard to jurisdictional claims in published maps and institutional affiliations.

Copyright: © 2022 by the authors. Licensee MDPI, Basel, Switzerland. This article is an open access article distributed under the terms and conditions of the Creative Commons Attribution (CC BY) license (https://creativecommons.org/licenses/by/4.0/).

1. Introduction

Globally, breast cancer poses a formidable health challenge as it is the most prevalent malignancy accounting for a high number of cancer deaths in women [1]. Breast cancer

consists of a group of heterogeneous diseases driven by a multifactorial etiology involving genetic predisposition, hormones, and environmental factors; viruses are considered indisputable causal factors for nearly 10% of all human malignancies [2].

Human cytomegalovirus (HCMV), a member of the family Herpesviridae subfamily Betaherpesvirinae, is a ubiquitous host-restricted virus with a seroprevalence between 40% and 95% in the adult population [3]. Growing evidence suggests a link between persistent HCMV infection and malignancy [4–7]. Beyond oncomodulation, several studies implicate HCMV as a viral promoter of oncogenesis due to the presence of its nucleic acids and/or proteins in common tumor types [8,9]. Furthermore, HCMV promotes the acquisition of cancer hallmarks such as sustaining proliferative signaling, inducing angiogenesis, evading growth suppressors, avoiding immune destruction and apoptosis, facilitating replicative immortality, activating invasion, and metastasis as well as contributing to therapeutic resistance [8].

Recently, polyploidy, a major hallmark of cancer, was found to be present in approximately 37% of human tumors [10]. Dormant polyploid giant cancer cells (PGCCs) are associated with the induction of quiescence and increased storage capacity through the presence of vacuoles and accumulation of lipid droplets, increased metabolic capacity, and elevated energy production [11–13]. PGCCs could be triggered by radiotherapy, chemotherapeutics, hypoxia, oxidative stress, hyperthermia, and oncoviruses [14–18]. Beside therapy resistance, PGCCs were associated with metastasis and cancer relapse [18]. A recent study revealed the potential of HCMV in inducing the dedifferentiation of mature HMECs and generating PGCC's phenotype as well as showing a significant correlation between the presence of PGCCs and HCMV in breast cancer biopsies [4].

Between 15% and 20% of all human cancers possess a direct infectious origin [19]. To start with, human papillomavirus (HPV) strains were classified into high- and low-risk strains after being isolated from different lesions. These discoveries were shown to radically alter the tumor diagnosis, prognosis, and prevention approaches [20,21]. Various Epstein–Barr virus (EBV) strains are associated with properties that influence their transforming capacities and the type of induced tumor [22,23]. Additionally, Kaposi's sarcoma-associated herpesvirus (KSHV) isolates were identified in patients of different geographical regions, indicating the importance of these newly isolated strains [24,25] in developing better diagnostic procedures and novel treatment approaches in the context of KSHV-associated malignancies as well as enriching potential vaccine studies [26].

Triple-negative breast cancer (TNBC) comprises 15% of breast cancers globally [27]. Despite its susceptibility to standard chemotherapy, TNBC is highly invasive, has a high relapse tendency, and is associated with a poor overall prognosis [28]. Recently, more significant advances include characterizing the molecular features of TNBC which will maximize the efficacy of certain chemotherapeutic agents and aid in actively exploring novel therapeutic targets [29].

Previous studies demonstrated the ability of HCMV-DB and HCMV-BL strains in transforming primary HMECs into CMV-Transformed HMECs (CTH) cells in vitro [4,30]. CTH cells, which are slow self-renewing cells, undergo diverse stages of the giant cell cycle. They were shown to be heterogeneous, generate PGCCs, exhibit dedifferentiation, and display stemness and EMT/MET features [4]. Herein, we originally isolated two HCMV strains, B544 and B693, from TNBC biopsies to assess their transformation potential in vitro and evaluate the obtained cellular phenotype, the genetic and molecular features, and the activation of cellular stemness programs. We examined the sensitivity of these strains to paclitaxel (PTX) and ganciclovir (GCV) combination therapy. Further, a specific molecular landscape was disclosed in the tumor microenvironment (TME) of TNBC harboring high-risk HCMV.

2. Materials and Methods

2.1. Cell Lines and Culture

HMECs (A10565, Life Technologies, Carlsbad, CA, USA), CTH cells, MDA-MB231 as well as MCF7 (Institut Hiscia, Arlesheim, Switzerland), and MRC5 (RD-Biotech, Besançon, France) were cultured as previously described [5]. HCMV-B544 and HCMV-B693 cultures used in this study were maintained for at least 9 months in culture.

2.2. HCMV Isolates Growth and Detection

Data corresponding to TNBC biopsies and other HCMV strains were reported previously [5]. To prepare cell-free virus stocks, the two strains were propagated in MRC5 cells for a few passages to avoid losing the ULb' region. Infections of HMECs and MRC5 cells, viral quantification, and replication including assessment of HCMV existence were performed as described previously [4]. Briefly, infection of HMECs or MRC5 (1×10^6) cells with the clinical isolates was performed at a multiplicity of infection (MOI) of 1. Cells were incubated at 37 °C for two hours, after which the inoculum was discarded, and the cell monolayer was washed three times using 1X PBS and afterwards covered with fresh medium. For viral quantification, infectious supernatant (cell-free) was harvested, DNA was isolated (EZNA Blood DNA Kit, D3392-02, Omega BIO-TEK) and real-time IE1 quantitative PCR (qPCR) was carried out using a Stratagene Mx3005P thermocycler (Agilent, Santa Clara, CA, USA) and IE1 primers. qPCR was performed using a KAPA SYBR FAST Master Mix (KAPA BIOSYSTEMS, KK4601, Potters Bar, UK); reactions were activated at 95 °C for 10 min, followed by 50 cycles (15 s at 95 °C and 1 min at 60 °C). Results were collected and analyzed using MxPro qPCR software. The primers used are listed in Supplementary Table S1.

2.3. Microscopy

CTH cell cultures were monitored and confocal microscopy imaging for HMECs and CTH cells was performed as described previously [5,31]. Primary antibodies targeting IE1, pp65, Myc, Ki67 Ag, Oct4, Nanog, SOX2, and SSEA4 are listed in Supplementary Table S2. Post-staining, the slides were assessed using a 63× oil immersion objective lens with a Carl-Zeiss confocal microscope (Jena, Germany); images were analyzed using ZenBlue Software (Carl-Zeiss Microscopy GmbH).

2.4. Soft Agar Colony Formation Assay

Colony formation in soft agar seeded with uninfected HMECs, B544, B693, DB, and BL-infected HMECs, as well as untreated and PTX/GCV-treated CTH cells, was carried out as mentioned previously [5]. MCF7 and MDA-MB231 were used as positive controls.

2.5. Tumorsphere Assay

Tumorsphere formation by uninfected HMECs and HMECs infected with HCMV-B544 and HCMV-B693 was evaluated as described in detail previously [6].

2.6. Flow Cytometry Analysis

Cells (1×10^5) were collected from uninfected HMECs and CTH cells, fixed, permeabilized, and stained as previously reported [5,6]. Cytofluorometric analysis was achieved using a BD LSRFortessa X-20 (BD Biosciences) flow cytometer. FACSDiva software (BD Biosciences) was used for data collection and analysis. Primary antibodies and their corresponding secondary antibodies are detailed in Supplementary Table S2.

2.7. Quantitative Reverse Transcription PCR (RT-qPCR)

Reverse transcription was performed as mentioned previously [6]. In brief, RNA was extracted from the biopsies using the EZNA® Total RNA Kit I (Omega BIO-TEK, Norcross, GA, USA). Reverse transcription was carried out using the SuperScript IV First-Strand Synthesis kit (Invitrogen, Carlsbad, CA, USA). The expression of markers was assessed by

performing real-time qPCR using a KAPA SYBR FAST Master mix (KAPA BIOSYSTEMS, KK4601) and specific primers according to the manufacturer's protocol. The fold change expression was calculated by adopting the delta-delta Ct method. The primers used are provided in Supplementary Table S1.

2.8. CTH Treatment

CTH cells were treated with 12-O-45 tetradecanoylphorbol-13-acetate (TPA) (100 nM, P8139, Sigma-Aldrich, Burlington, MA, USA), ganciclovir (20 µM, SML2346 Sigma-Aldrich), and paclitaxel (20 nM, Paclitaxel Arrow 6 mg/mL). Treatment was renewed every day.

2.9. Statistical Analysis

All quantitative results are reported as mean ± SD of the independent experiments. Statistical analyses were performed using Mann–Whitney test; a p-value ≤ 0.05 was considered significant. Microsoft Excel was used to construct the plots and histogram data.

3. Results

3.1. Growth of Two HCMV Clinical Strains Isolated from TNBC in HMECs and the Emergence of Morphologically Distinct Cells

To assess the cellular environment achieved by HCMV, B544 and B693 were isolated from TNBC biopsies and grown in MRC5 cells, revealing a viral growth at days 3 and 5 post-infection (PI) (Figure 1A). At day 1 post-HMECs infection, HCMV-IE1 and pp65 were detected with confocal microscopy (Figure 1B). HCMV-B544 and B693 promoted the transformation of the infected HMECs toward CTH cells as previously reported [5]. Uninfected HMECs were used as controls which underwent cellular senescence in long-term cultures. At day 110 PI, we detected a wide variety of spheroids and giant cells distributed between round dense cells, flat, and elongated spindle-like cells. Afterwards, lipid droplet-packed cells, multinucleated giant cells, cell budding, and filopodium protrusions were observed in CTH cultures (Figure 1C,D). Hence, this population displayed mesenchymal and fibroblastic-like structures in addition to epithelial and small cells. The above-mentioned detailed cell morphology is close to that of CTH cells which were previously detected in HMEC cultures acutely infected with high-risk BL and DB strains [5]. Thus, the CTH-B544 and CTH-B693 heterogeneous cell population represent transformed and self-renewing cells that are engaged in distinct phases of the giant cell cycle [12,13].

3.2. Transformation Capacity of CTH Cells and the Induction of an Oncogenic Environment

To evaluate the transformation of HCMV-B544 and B693 immortalized infected HMECs, cells were seeded in soft agar. Colony formation was detected at day 14 post-seeding in CTH-B544 and CTH-B693 cells (p-value ≤ 0.05) in contrast to uninfected HMECs which showed no changes (Figure 2A). The resulting anchorage-independent growth in CTH cells is a crucial phase in the acquisition of malignancies. With regard to oncogenes, the expression of c-Myc was assessed by performing confocal microscopy imaging where large and elongated CTH cells showed remarkable c-Myc staining compared to uninfected HMECs (Figure 2B). Using flow cytometry, a slightly higher expression of the proliferation marker (Ki67Ag) was detected in CTH-B693 compared to CTH-B544 cells with a limited expression in the uninfected HMECs. Only CTH-B544 and B693 cells were positively stained with Ki67 Ag as detected by confocal microscopy imaging (Figure 3A). On the other hand, a slight increase in the expression of phosphorylated Akt (pAkt-ser473) along with a limited to nonexistent increase in Akt expression levels was shown in all CTH cells compared to uninfected HMECs (Figure 3B and Supplementary Figure S1). Overall, the acquisition of an immortal phenotype in CTH-B544 and B693 cells reflects their transformation potential.

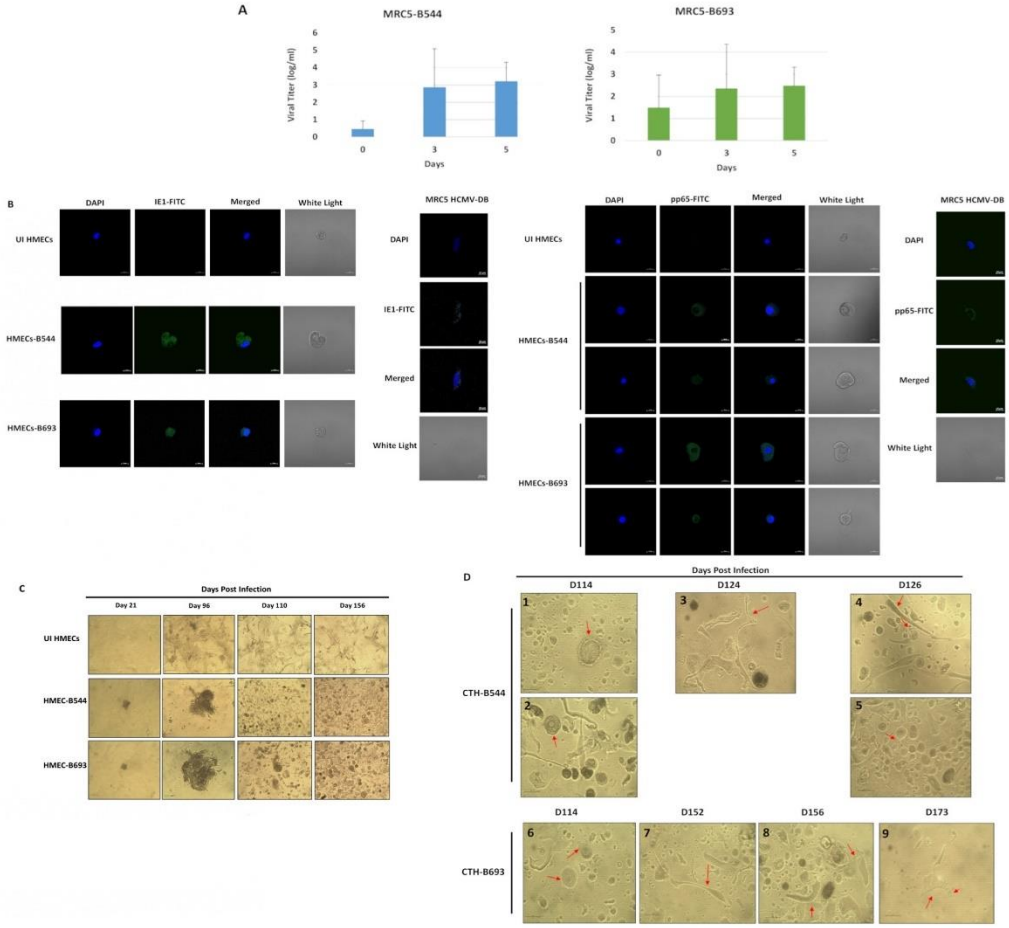

Figure 1. Replication of B544 and B693 strains in MRC5 cultures, and the appearance of morphologically distinct cells following the infection of HMECs with these high-risk strains. (**A**) Time-course of the viral titer in the supernatant of MRC5 infected with the strains HCMV-B544 and HCMV-B693, as measured by IE1-qPCR. (**B**) Confocal microscopic images of HCMV-IE1 and pp65 staining in HMECs infected with HCMV-B544 and HCMV-B693 (day 1 post-infection). Uninfected HMECs were used as controls. Nuclei were counterstained with DAPI; magnification ×63, scale bar 10 µm. (**C**) HMECs time-course infection with HCMV-B544 and HCMV-B693 strains (MOI = 1). Magnification ×100, scale bar 100 µm. Uninfected HMECs were used as a control. (**D**) Presence of giant cells with blastomere-like morphology (1 and 6), mesenchymal cells (4 and 7), lipid droplet-packed cells (3, 8, and 9), cells displaying multiple nuclei (2) as well as cell budding (4, 5, and 6), and cells with filopodia protrusions (9) in CTH-B544 and CTH-B693 cells. The inverted light microscope scale bar represents 100 µm; magnification ×200.

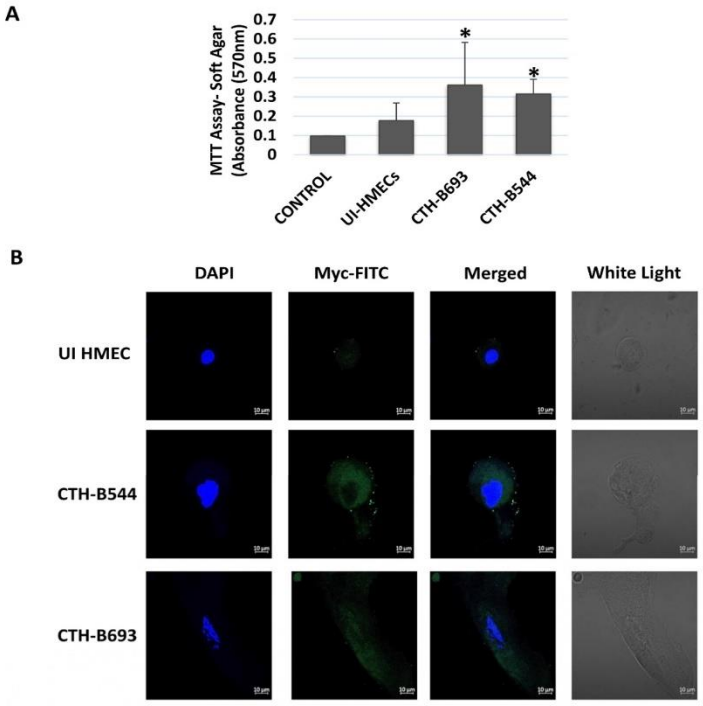

Figure 2. Colony formation in soft agar and Myc expression in CTH-B544 and B693 cells. (**A**) Colony formation in soft agar seeded with uninfected HMECs, CTH-B544 and CTH-B693 cells. At day 15 post-seeding, quantification of colonies was performed; Histogram represents the mean data ± SD of three independent experiments. * p-value ≤ 0.05, (**B**) Confocal microscopic images of Myc and DAPI staining in CTH cells. Magnification ×63, scale bar 10 μm.

3.3. CTH Cells Promote Embryonic Stemness and Develop an Epithelial/Mesenchymal Hybrid State

When cultured in serum-free tumorsphere medium, CTH-B544 and B693 cells gave rise to mammospheres at day 14 and expressed stemness markers versus uninfected HMECs (Figure 4A). CTH cells revealed a rise in CD44 and CD24 expression when compared to uninfected HMECs (Figure 4B), in line with CTH-DB and BL data (Supplementary Figure S1). Activated expression of the embryonic stem cell markers, SSEA-4 and Nanog, was recognized in CTH-B544, CTH-B693, CTH-DB, and CTH-BL cells by performing flow cytometry (Figure 5A and Supplementary Figure S1) and confocal microscopy imaging (Figure 5B,C). Moreover, CTH-B544 and B693 cells gained embryonic stem-like properties by highly expressing Oct4 and SOX2 as demonstrated by confocal microscopy imaging (Figure 5D,E). Similar to CTH-DB and BL, the newly discovered CTH cells showed an elevated expression of the stemness marker CD49f or Integrin alpha-6, and a limited EpCAM expression (Figure 6 and Supplementary Figure S1). CTH-B544 and B693 as well as CTH-DB and BL cells were positive for both vimentin and E-cadherin staining (Figure 6 and Supplementary Figure S1) thereby signifying their ability to dynamically oscillate between the epithelial-hybrid-mesenchymal spectrum as reported previously in tumors with poor prognosis [32,33]. As a result, CTH-B544 and B693 cells exhibited the following two phenotypes: stemness and hybrid epithelial/mesenchymal phenotypes.

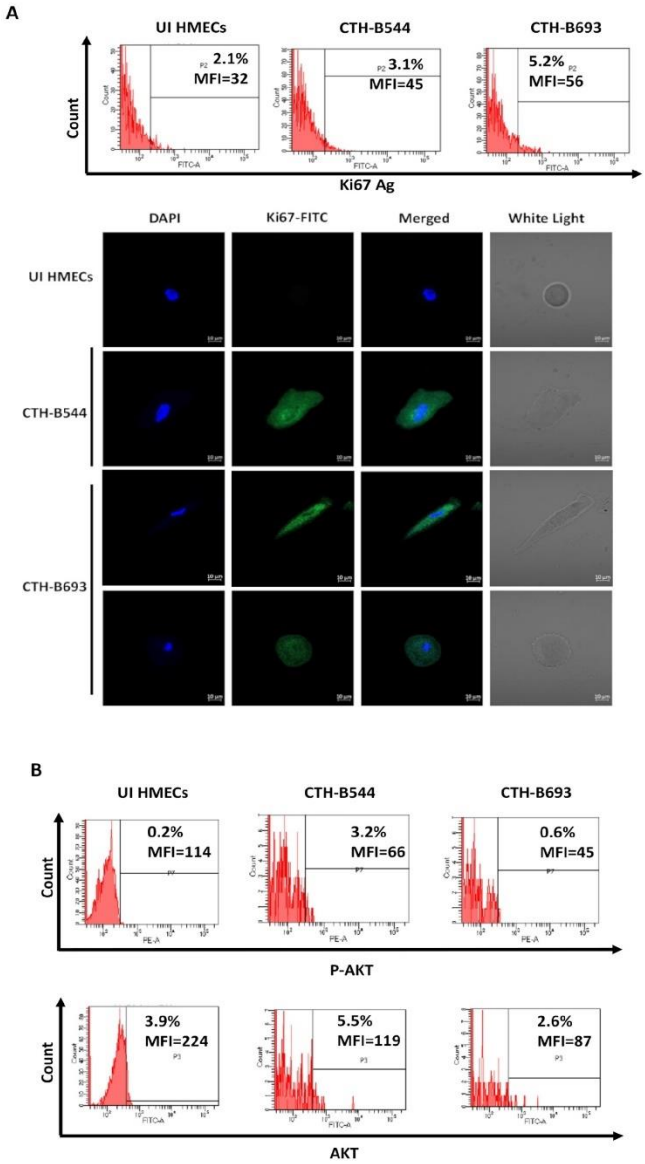

Figure 3. CTH proliferation capacities and AKT activation. (**A**) Proliferation assessment by FACS and confocal microscopy; UI HMECs, CTH-B544 and CTH-B693 cells were stained for Ki67 Ag and DAPI. Magnification ×63, scale bar 10 µm. (**B**) P-AKT, and AKT expression in UI HMECs and CTH cells, as measured by FACS. Results are representative of three independent experiments.

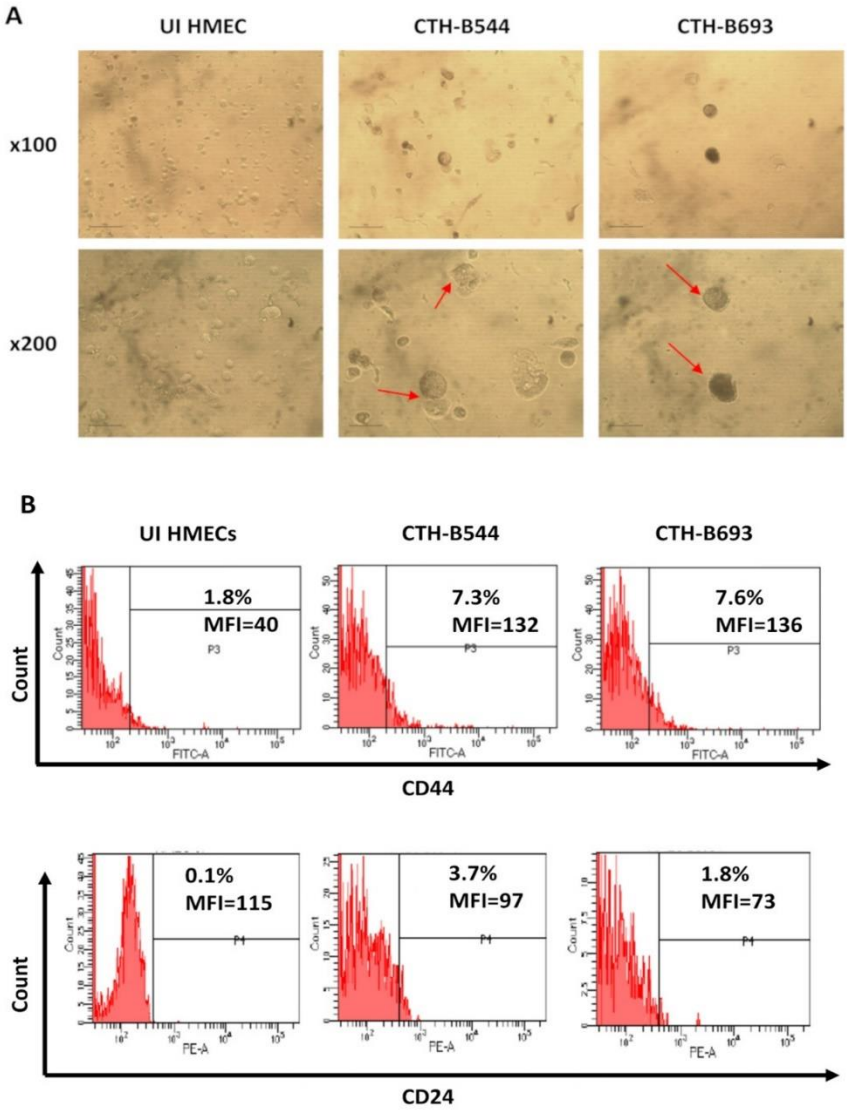

Figure 4. Tumorspheres formation and the expression of stemness markers in CTH cells. (**A**) Tumorspheres were observed under an inverted light microscope in CTH-B544 and CTH-B693 cells. Magnification ×100 and ×200, scale bare 100 µm. Uninfected HMECs were used as a negative control. (**B**) FACS staining of CD44 and CD24 was performed in CTH cells. Results are representative of three independent experiments.

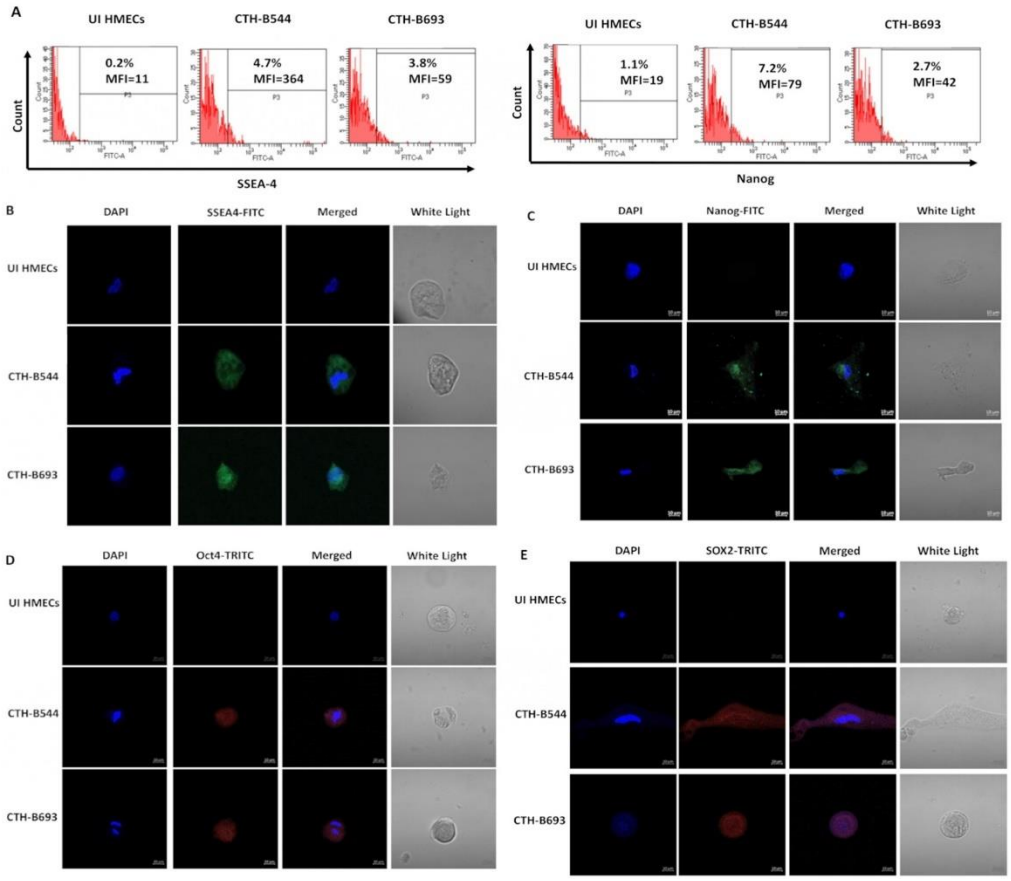

Figure 5. Expression of embryonic stem cell markers in CTH-B544 and B693 cells. (**A**) Detection of SSEA4 and Nanog in CTH cells by FACS. Results are representative of three independent experiments. Confocal microscopy imaging demonstrating the expression of (**B**) SSEA-4, (**C**) Nanog, (**D**) Oct4, and (**E**) SOX2. Nuclei were counterstained with DAPI; magnification ×63, scale bar 10 µm.

3.4. Persistent HCMV Replication in CTH-B544 and CTH-B693 Long-Term Cultures

To determine the sustained HCMV presence, HCMV-IE1 antigen was detected using flow cytometric analysis. IE1 was strongly expressed in CTH-B544 and CTH-B693; uninfected HMECs showed no staining for IE1 (Figure 7A). Using qPCR, we detected HCMV (IE1 DNA) in the supernatant of CTH-B544 and CTH-B693 cultures (Figure 7B). Further, CTH cells were positively stained for HCMV-pp65 antigen versus uninfected HMECs (Figure 7C). CTH cells were treated with TPA to assess latency relevance (Figure 7D,E). Post TPA treatment, the proliferation of CTH-B544 and CTH-B693 cells was promoted (Figure 7D). IE1 detection was elevated at day 1 and day 2 post-treatment in CTH-B544 and CTH-B693, respectively (p-value= 0.33), and subsequently decreased (Figure 7E).

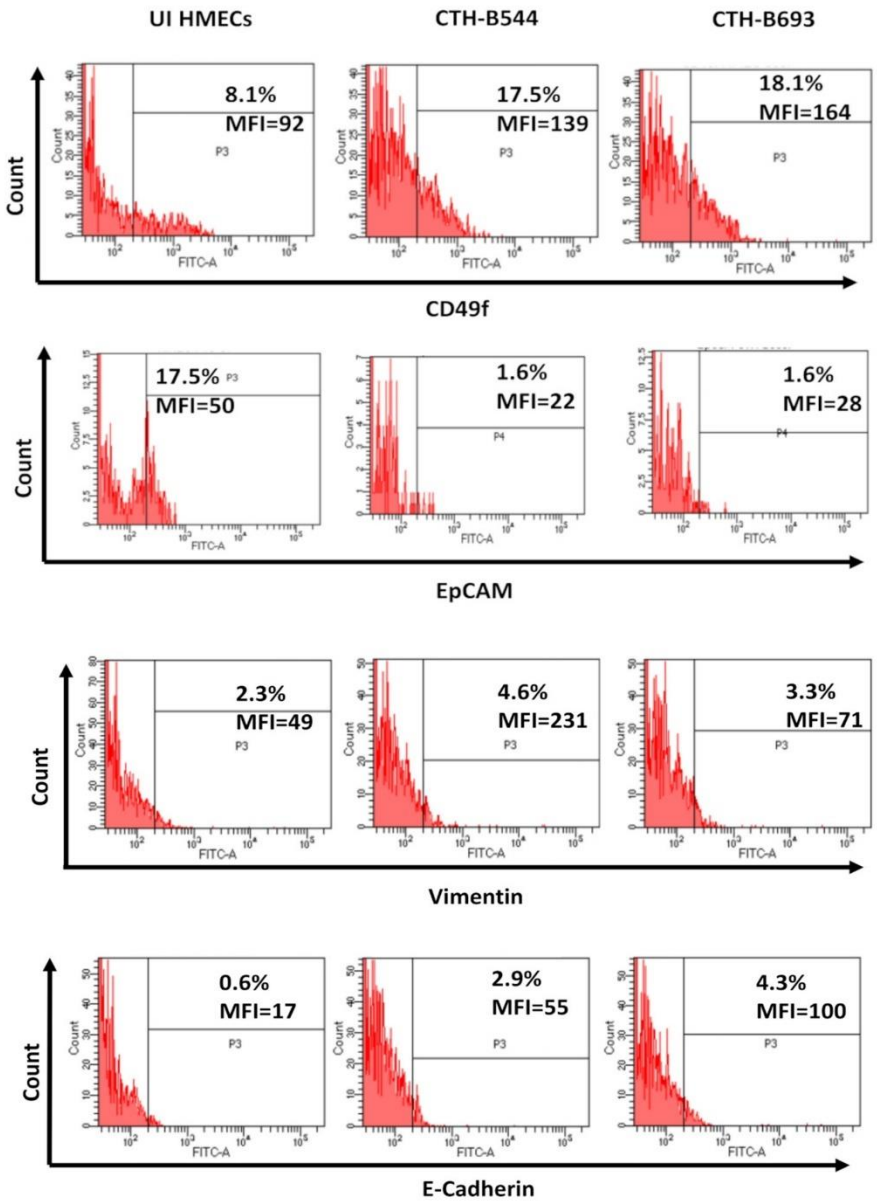

Figure 6. Phenotypic analysis of CTH cells. Detection of a panel of cell markers through FACS staining of CD49f, EpCAM, Vimentin, and E-cadherin in CTH-B544 and CTH-B693 versus UI HMECs. Results are representative of three independent experiments.

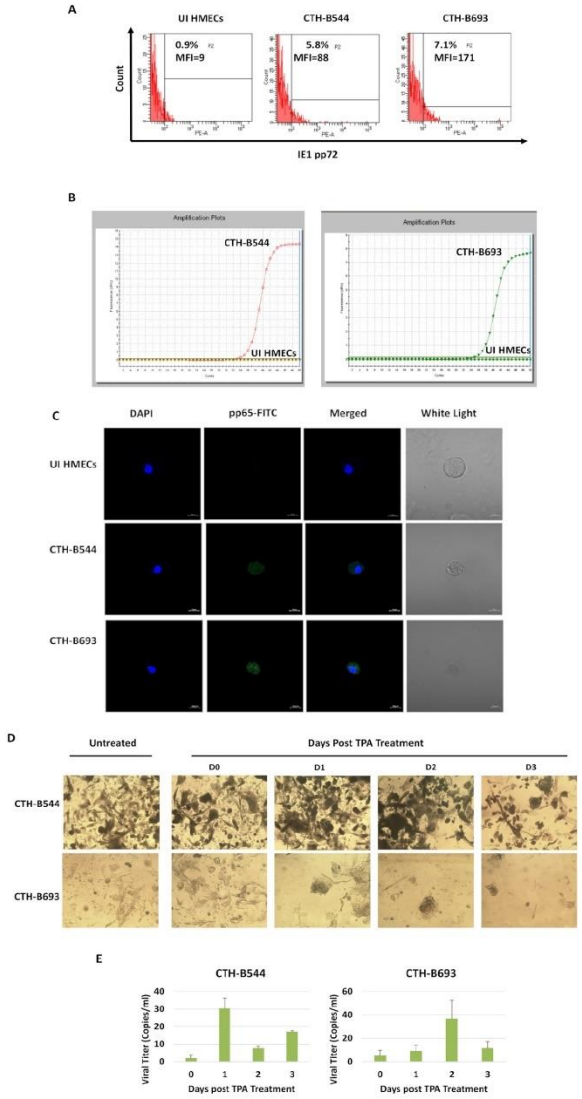

Figure 7. Sustained viral replication in CTH cells. IE1 expression in CTH cells was assessed by (**A**) FACS and (**B**) qPCR. (**C**) pp65 detection in CTH-B544 and B693 cells as demonstrated by confocal microscopy imaging. As a negative control, uninfected HMECs were used; nuclei were counterstained with DAPI; magnification ×63, scale bar 10 µm. (**D**,**E**) Determination of viral reactivation from latency in CTH cells through the treatment of TPA. (**D**) Representative images of CTH cultures treated with TPA (100 nM). Untreated cells were used as a control. Magnification ×100, scale bar 100 µm. (**E**) HCMV lytic replication was induced by TPA in CTH cultures. Histograms represent the mean data ± SD of three independent experiments.

3.5. A Specific Molecular Landscape Unveiled in the Tumor Microenvironment of TNBC Harboring High-Risk HCMV

To evaluate the variation in strains' aggressiveness, we compared the transcriptomic profile corresponding to the two high-risk biopsies. The absolute mRNA level of epidermal growth factor receptor (EGFR), cyclin dependent kinase inhibitor 2A (CNDK2A), cyclin D1 (CCND1), SOX2, Oct4, and Nanog was assessed by RT-qPCR. EGFR, a proto-oncogene that enhances cell proliferation and survival, the cell cycle regulator CNDK2A, the proliferation marker CCND1, and the three embryonic markers were overexpressed in biopsy 693 compared to biopsy 544 (p-value ≤ 0.05 for all markers) (Figure 8A). Our results indicated that biopsy 693, from which we isolated the HCMV-B693 strain, is associated with higher tumor aggressiveness and poor prognosis.

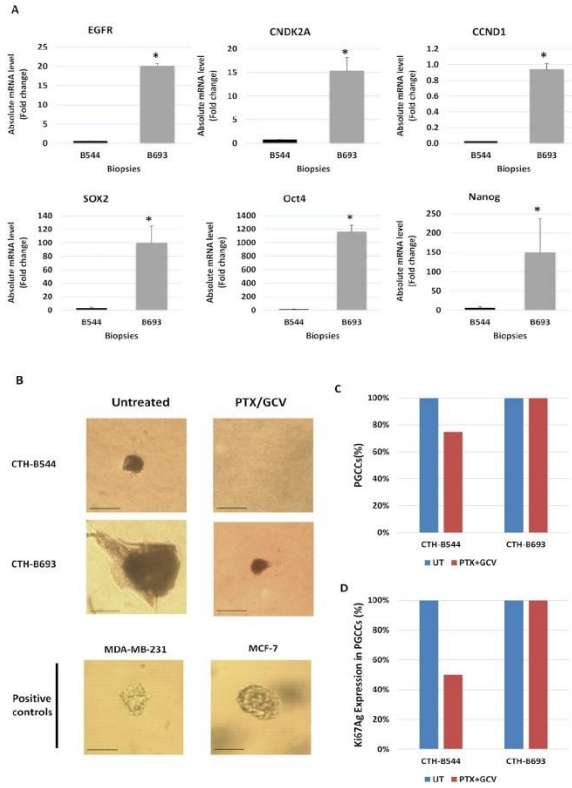

Figure 8. Distinct responses of CTH cells to paclitaxel/ganciclovir (PTX/GCV) treatment in vitro recapitulates distinct TNBC molecular signatures in vivo. (**A**) EGFR, CNDK2A, CCND1, SOX2, Oct4, and Nanog mRNA expression was measured by RT-qPCR in TNBC biopsies B544 and B693. Histograms represent the mean ± SD of three independent experiments. * $p \leq 0.05$, determined by Mann–Whitney U test. (**B**) Soft agar seeded with CTH-B544 and CTH-B693 cells treated with PTX (20 nM)/GCV (20 µM) combination therapy. Untreated cells were used as negative controls; MCF7 and MDA-MB231 cells were used as positive controls. Magnification ×200, scale bar 100 µm. (**C**) Propidium iodide (PI) staining for detection of PGCCs in untreated and treated CTH cells by FACS analysis. (**D**) Ki67 Ag expression in PGGCs of untreated and treated CTH cells.

3.6. Restricting Soft Agar Colony Formation, Controlling PGCCs Count and Proliferation by Paclitaxel and Ganciclovir Therapy

To assess the colony formation in soft agar, CTH cells were treated by PTX/GCV combination therapy to target the oncogenic cellular environment as well as HCMV. Breast cancer cell lines, MDAMB231 and MCF7 were used as positive controls. PTX/GCV treatment of CTH-B544 cells resulted in the disappearance of colonies; however, colony formation was restricted in treated CTH-B693 cells versus untreated cells (Figure 8B). Post therapy, the PGCCs count was reduced by 25% in CTH-B544 while it remained constant in CTH-B693 as measured by FACS (Figure 8C). Further, the proliferation of PGCCs was assessed by Ki67 Ag measurement using flow cytometric analysis; Ki67 Ag expression was reduced in PTX/GCV-treated CTH-B544, but not in CTH-B693 (Figure 8D). Our outcomes revealed that CTH-B544 cells are more responsive to PTX/GCV therapy compared to CTH-B693 cells implying that the latter exhibits aggressive behavior.

4. Discussion

To the best of our knowledge, the present study demonstrated the oncogenic transformation and stemness potential of HCMV-B544 and B693 strains that were isolated from TNBC biopsies and indicated a differential treatment response depending on the HCMV strain present in the tumor.

CTH-B544 and CTH-B693 cells are heterogeneous cellular populations that give rise to PGCCs, and display dedifferentiating phenotypes with stemness features as well as hybrid epithelial/mesenchymal phenotypes, resembling the morphological features found in aggressive cancers [13,14,17]. PGCCs formation was promoted in hypoxic environments [12,17]. It is worth noting that hypoxia inducible factor 1 alpha (HIF-1α) expression is induced by HCMV infection [34]. In PGCCs, the evaluation of metabolic reprogramming revealed the presence of PLIN4, a perilipin covering the lipid droplets especially in chemoresistant tumors [13]; the Warburg effect [35] and the involvement of the glycolytic pathway were also found to be induced in cancer environments and upon HCMV infection [12].

Myc activation has been widely described in breast cancer progression and can be used as a predictive marker for cancer staging, therapy resistance, and prognosis [36]. It is noteworthy that both B544 and B693 HCMV strains were isolated from $EZH2^{High}Myc^{High}$-expressing TNBC, further [5] indicating a potential link between the presence of these HCMV strains and cancer progression. The coupling of c-Myc overexpression with Akt pathway activation observed in CTH cells is in line with previous findings [4]. Moreover, colony formation was detected in CTH-B544 and CTH-B693 cells associated with a high expression level of Ki67 Ag and c-Myc overexpression, thus revealing cellular transformation and their oncogenic potential which is consistent with the previously reported CTH data [4]. Ki67, a prognostic biomarker in invasive breast cancer, is not only required for cell proliferation in tumors but is also strongly linked to tumor initiation, growth, and metastasis [37].

PGCC-bearing CTH cells acquired embryonic-like stemness and an epithelial-mesenchymal hybrid phenotype. Studies have shown that the acquisition of the EMT and stemness properties lead to an increase in the invasiveness and the metastatic potential of cancer cells within tumors [32]. The embryonic stem cells transcriptional network is based on the presence of master pluripotency regulators, Oct4, SSEA-4, SOX2, and Nanog [38]. Besides mammosphere generation, CTH-B544 and CTH-B693 gained a stemness phenotype with increased expression of Oct4, SOX2, and Nanog promoting tumor progression; CTH cells were positively stained for SSEA4 which is associated with EMT and drug resistance [38]. SOX2, Nanog, and Oct4 expression was associated with poor differentiation, advanced cancer stages, and the worst outcomes in breast cancer patients [39].

Studies have implicated CD44 in breast cancer cell adhesion, proliferation, motility and migration, angiogenesis, and metastasis. Limited CD24 expression in breast cancer cells was shown to augment their growth and metastatic potential through a chemokine receptor response [38]. The CD44high/CD24low phenotype was recognized in CTH-B544 and B693

cells indicating a tumor-initiating phenotype similar to that of the highly tumorigenic breast cancer cells [40]. The existence of an intermediate state between epithelial and mesenchymal phenotypes is considered a hybrid E/M state which is associated with elevated cellular plasticity, migration, stem-cell-like properties, metastatic potential, and therapy resistance [32]. In CTH cells, the co-existence of vimentin and E-cadherin resembled a partial EMT hence ensuring their plasticity while preserving the same tumor-propagating potential [4]. Since in breast tumors CD49f was considered a marker for distant metastasis and recurrence, CD49f+/CD44high/CD24low CTH cells represented an aggressive phenotype which is associated with an increased risk for disease recurrence with poor clinical outcomes [41].

The initiation of KSHV and EBV lytic cycles has been shown to support malignancies driven by the aforementioned oncogenic viruses [42,43]. HCMV persistence was established in CTH cells by detecting IE1 and pp65 throughout long-term cultures [4,5,30]. High-risk strains express immediate-early (IE), early (E), and late (L) viral antigens including IE1 in agreement with a viral lytic cycle following the acute infection of permissive cells such as MCR5 cells. High-risk strains are detected in chronically infected cells, for instance CTH cells in our study, which is in line with the HCMV latency observed in Hodgkin's disease and Non-Hodgkin's lymphoma revealing the latent viral UL138 protein expression [44]. Nonetheless, a dynamic state of latency is recommended by novel transcriptomic studies. Since HCMV develops a complex relationship with the host, to define lytic and latency phases, several studies used the ratio of replicative and latency genes as a phase indicator [45,46]. To further highlight the role of the HCMV-IE1 gene, a study showed the potential of HCMV in regulating stemness in glioblastoma cells by specifically increasing SOX2 and Nestin, thus upregulating stemness and proliferation markers [47].

Studies have suggested that the polymorphism of oncoviruses' strains plays a vital role in explaining their association with distinct pathogenic and tumor properties [22,42]. Certain HPV strains were isolated from invasive cervical cancer biopsies and have thus been acknowledged as oncogenic/high-risk HPV strains [42]. EBV strains cloned and rescued from nasopharyngeal carcinoma (NPC) and gastric carcinomas potentially infect epithelial cells compared to strains originating from infectious mononucleosis (IM) or B lymphoma [22,48]. The existence of diverse strains expressing potential biomarkers and possessing various replication potentials in different tissues and/or cell types explain the distinct oncogenicity [22,23]. The variability of oncogenic and pathogenic KSHV potential was indicated to be dependent on KSHV different subtypes [42]. Overall, discovering distinct viral strains will adjust the different adopted approaches to tumor diagnosis, prognosis, prevention, advanced treatment, as well as therapy monitoring and will enrich potential vaccine studies [21,26,49]. Likewise, the diversity of HCMV strains was validated by our data and the previously published data in which only few clinical HCMV strains conserve the potential to transform HMECs [6] and fit with a "blastomere-like" model of oncogenesis [4]. When HCMV-B544 and B693 were isolated from IE1/Myc/Ki67/EZH2-positive TNBC biopsies [5], the findings revealed a phenotype similar to the already described HCMV-DB and BL phenotype.

On the transcriptomic level, biopsy 693 overexpressed EGFR, CNDK2A, CCND1, SOX2, Oct4, and Nanog. It is known that EGFR promotes TNBC progression through JAK/STAT3 signaling [50], CNDK2A drives TNBC tumorigenesis [51], CCND1 has a prognostic significance in TNBC [52], and the three embryonic markers correlate with stemness, metastasis, tumor relapse, and poor clinical outcomes of TNBC [53]; therefore, we propose that biopsy 693 maintains a tumor signature that is associated with an aggressive behavior which predicts poor clinical outcome.

A study revealed the potential of combining GCV with certain chemotherapeutic agents to suppress EBV-positive NPC tumor growth [54]. In HPV-infected cervical cancer cells, cidofovir and cisplatin inhibited cellular proliferation, reduced E6 protein expression, and restored the activity of p53 [55]. A third study showed the effectiveness of anti-herpetic drugs, GCV and cidofovir, as single therapies or in combination with chemotherapy in

treating KSHV-associated primary effusion lymphoma (PEL) [56]. Based on our results, the heterogeneity of HCMV strains including their distinct behavioral aspects had a major impact on CTH cells' response post-therapy. CTH-B544 cells were therapy sensitive whereas CTH-B693 cells displayed an aggressive behavior with lower sensitivity to PTX/GCV combination therapy. Generally, isolating distinct HCMV strains from tumors that possess potential prognostic biomarkers and behave differently depending on their own heterogeneity and various cell types may improve the diagnostic process and treatment options, provide effective follow-up strategies, and may be essentially pertinent in breast cancer pathophysiology and other adenocarcinomas, particularly of poor prognosis.

5. Conclusions

Our outcomes originally revealed the oncogenic and stemness potential of two HCMV strains, namely B544 and B693 where HCMV generated PGCCs, displayed dedifferentiating phenotypes with stemness features as well as hybrid epithelial/mesenchymal phenotypes. Large-scale experiments are highly encouraged to further validate our findings. Meanwhile, the presented data provides new insights into the oncogenic role of HCMV in breast cancer progression, thereby uncovering novel targeted therapeutic approaches and assisting in the development of advanced clinical interventions.

Supplementary Materials: The following supporting information can be downloaded at: https://www.mdpi.com/article/10.3390/cancers14174271/s1, Supplementary Figure S1: Activation of oncogenic pathways, expression of embryonic markers, and phenotypic characterization of CTH cells. Flow cytometric analysis of CTH-DB cells, CTH-BL cells, MRC5 cells infected with HCMV-DB, and MRC5 cells infected with HCMV-BL for (A) Ki67 (B) pAKT and AKT, (C) CD44 and CD24, (D) SSEA4 and Nanog, (E) CD49f, vimentin, E-cadherin, and EpCAM, and (F) IE1. Results are representative of three independent experiments; Supplementary Table S1: List of Primers Used; Supplementary Table S2: List of Antibodies Used.

Author Contributions: Conceptualization, G.H.; formal analysis, R.E.B., S.P., S.H.A., G.H.; investigation, S.P., R.E.B., S.H.A.; writing—original draft preparation, R.E.B., S.P., M.D.-A., G.H.; writing—review and editing, R.E.B., S.P., M.D.-A., G.H.; directly accessed and verified the underlying data: S.P., S.H.A., R.E.B., G.H.; visualization, R.E.B., S.H.A., S.P.; supervision, G.H.; project administration, G.H.; funding acquisition, G.H. All authors have read and agreed to the published version of the manuscript.

Funding: This work was supported by grants from the University of Franche-Comté (UFC) (CR3300), the Région Franche-Comté (2021-Y-08292 and 2021-Y-08290) and the Ligue contre le Cancer (CR3304) to Georges Herbein. Ranim El Baba is a recipient of a doctoral scholarship from Hariri foundation for sustainable human development.

Institutional Review Board Statement: The study was conducted according to the guidelines of the Declaration of Helsinki. The study was authorized by the local ethics committees of Besançon University Hospital (Besançon, France) and the French Research Ministry (AC-2015-2496, CNIL n°1173545, NF-S-138 96900 n°F2015).

Informed Consent Statement: Written informed consent for participation was obtained from all patients.

Data Availability Statement: The datasets used and/or analyzed during the present study are available from the corresponding author on reasonable request.

Acknowledgments: The authors are grateful to the Pathology Department at the Besançon University Hospital for providing breast biopsies and data. The authors thank DImaCell Imaging Resource Center, University of Bourgogne Franche-Comté, Faculty of Health Sciences, Besançon, France for technical support.

Conflicts of Interest: The authors declare no conflict of interest.

References

1. Sung, H.; Ferlay, J.; Siegel, R.L.; Laversanne, M.; Soerjomataram, I.; Jemal, A.; Bray, F. Global Cancer Statistics 2020: GLOBOCAN Estimates of Incidence and Mortality Worldwide for 36 Cancers in 185 Countries. *CA Cancer J. Clin.* **2021**, *71*, 209–249. [CrossRef] [PubMed]
2. Schiller, J.T.; Lowy, D.R. An Introduction to Virus Infections and Human Cancer. *Recent Results Cancer Res.* **2021**, *217*, 1–11. [CrossRef] [PubMed]
3. Silva, J.D.M.; Pinheiro-Silva, R.; de Oliveira, R.C.; Alves, C.E.D.C.; Barbosa, A.N.; Pontes, G.S. Prevalence and Recurrence Rates of Cytomegalovirus Infection Among Patients with Hematological Diseases in the Western Brazilian Amazon: A Cross-Sectional Study. *Front. Public Health* **2021**, *9*, 692226. [CrossRef] [PubMed]
4. Nehme, Z.; Pasquereau, S.; Ahmad, S.H.; Coaquette, A.; Molimard, C.; Monnien, F.; Algros, M.-P.; Adotevi, O.; Assaf, M.D.; Feugeas, J.-P.; et al. Polyploid giant cancer cells, stemness and epithelial-mesenchymal plasticity elicited by human cytomegalovirus. *Oncogene* **2021**, *40*, 3030–3046. [CrossRef]
5. Nehme, Z.; Pasquereau, S.; Ahmad, S.H.; El Baba, R.; Herbein, G. Polyploid giant cancer cells, EZH2 and Myc upregulation in mammary epithelial cells infected with high-risk human cytomegalovirus. *eBioMedicine* **2022**, *80*, 104056. [CrossRef]
6. Ahmad, S.H.; Pasquereau, S.; El Baba, R.; Nehme, Z.; Lewandowski, C.; Herbein, G. Distinct Oncogenic Transcriptomes in Human Mammary Epithelial Cells Infected with Cytomegalovirus. *Front. Immunol.* **2021**, *12*, 772160. [CrossRef]
7. Branch, K.; Garcia, E.; Chen, Y.; McGregor, M.; Min, M.; Prosser, R.; Whitney, N.; Spencer, J. Productive Infection of Human Breast Cancer Cell Lines with Human Cytomegalovirus (HCMV). *Pathogens* **2021**, *10*, 641. [CrossRef]
8. Herbein, G. The Human Cytomegalovirus, from Oncomodulation to Oncogenesis. *Viruses* **2018**, *10*, 408. [CrossRef]
9. El Baba, R.; Herbein, G. Immune Landscape of CMV Infection in Cancer Patients: From "Canonical" Diseases Toward Virus-Elicited Oncomodulation. *Front. Immunol.* **2021**, *12*, 730765. [CrossRef]
10. Matsumoto, T.; Wakefield, L.; Peters, A.; Peto, M.; Spellman, P.; Grompe, M. Proliferative polyploid cells give rise to tumors via ploidy reduction. *Nat. Commun.* **2021**, *12*, 646. [CrossRef]
11. Pienta, K.J.; Hammarlund, E.U.; Brown, J.S.; Amend, S.R.; Axelrod, R.M. Cancer recurrence and lethality are enabled by enhanced survival and reversible cell cycle arrest of polyaneuploid cells. *Proc. Natl. Acad. Sci. USA* **2021**, *118*, e2020838118. [CrossRef]
12. Liu, J.; Niu, N.; Li, X.; Zhang, X.; Sood, A.K. The life cycle of polyploid giant cancer cells and dormancy in cancer: Opportunities for novel therapeutic interventions. *Semin. Cancer Biol.* **2022**, *81*, 132–144. [CrossRef] [PubMed]
13. Liu, J.; Erenpreisa, J.; Sikora, E. Polyploid giant cancer cells: An emerging new field of cancer biology. *Semin. Cancer Biol.* **2021**, *81*, 1–4. [CrossRef]
14. Zhang, J.; Qiao, Q.; Xu, H.; Zhou, R.; Liu, X. Human cell polyploidization: The good and the evil. *Semin. Cancer Biol.* **2021**, *81*, 54–63. [CrossRef] [PubMed]
15. Herbein, G.; Nehme, Z. Polyploid Giant Cancer Cells, a Hallmark of Oncoviruses and a New Therapeutic Challenge. *Front. Oncol.* **2020**, *10*, 567116. [CrossRef]
16. Dittmar, T.; Weiler, J.; Luo, T.; Hass, R. Cell-Cell Fusion Mediated by Viruses and HERV-Derived Fusogens in Cancer Initiation and Progression. *Cancers* **2021**, *13*, 5363. [CrossRef]
17. Zhang, S.; Mercado-Uribe, I.; Xing, Z.; Sun, B.; Kuang, J.; Liu, J. Generation of cancer stem-like cells through the formation of polyploid giant cancer cells. *Oncogene* **2014**, *33*, 116–128. [CrossRef]
18. Mirzayans, R.; Andrais, B.; Murray, D. Roles of Polyploid/Multinucleated Giant Cancer Cells in Metastasis and Disease Relapse Following Anticancer Treatment. *Cancers* **2018**, *10*, 118. [CrossRef]
19. Alizon, S.; Bravo, I.G.; Farrell, P.J.; Roberts, S. Towards a multi-level and a multi-disciplinary approach to DNA oncovirus virulence. *Philos. Trans. R. Soc. B Biol. Sci.* **2019**, *374*, 20190041. [CrossRef] [PubMed]
20. Reddout, N.; Christensen, T.; Bunnell, A.; Jensen, D.; Johnson, D.; O'Malley, S.; Kingsley, K. High risk HPV types 18 and 16 are potent modulators of oral squamous cell carcinoma phenotypes in vitro. *Infect. Agents Cancer* **2007**, *2*, 21. [CrossRef] [PubMed]
21. Pešut, E.; Đukić, A.; Lulić, L.; Skelin, J.; Šimić, I.; Gašperov, N.M.; Tomaić, V.; Sabol, I.; Grce, M. Human Papillomaviruses-Associated Cancers: An Update of Current Knowledge. *Viruses* **2021**, *13*, 2234. [CrossRef]
22. Tsai, M.-H.; Lin, X.; Shumilov, A.; Bernhardt, K.; Feederle, R.; Poirey, R.; Kopp-Schneider, A.; Pereira, B.; Almeida, R.; Delecluse, H.-J. The biological properties of different Epstein-Barr virus strains explain their association with various types of cancers. *Oncotarget* **2017**, *8*, 10238–10254. [CrossRef] [PubMed]
23. Delecluse, S.; Poirey, R.; Zeier, M.; Schnitzler, P.; Behrends, U.; Tsai, M.-H.; Delecluse, H.-J. Identification and Cloning of a New Western Epstein-Barr Virus Strain That Efficiently Replicates in Primary B Cells. *J. Virol.* **2020**, *94*, e01918-19. [CrossRef] [PubMed]
24. Pérez, C.L.; Tous, M.I. Diversity of human herpesvirus 8 genotypes in patients with AIDS and non-AIDS associated Kaposi's sarcoma, Castleman's disease and primary effusion lymphoma in Argentina. *J. Med. Virol.* **2017**, *89*, 2020–2028. [CrossRef] [PubMed]
25. Bhutani, M.; Polizzotto, M.N.; Uldrick, T.S.; Yarchoan, R. Kaposi Sarcoma–Associated Herpesvirus-Associated Malignancies: Epidemiology, Pathogenesis, and Advances in Treatment. *Semin. Oncol.* **2015**, *42*, 223–246. [CrossRef] [PubMed]
26. Moorad, R.; Juarez, A.; Landis, J.T.; Pluta, L.J.; Perkins, M.; Cheves, A.; Dittmer, D.P. Whole-genome sequencing of Kaposi sarcoma-associated herpesvirus (KSHV/HHV8) reveals evidence for two African lineages. *Virology* **2022**, *568*, 101–114. [CrossRef]
27. Guarneri, V.; Dieci, M.V.; Conte, P. Relapsed Triple-Negative Breast Cancer: Challenges and Treatment Strategies. *Drugs* **2013**, *73*, 1257–1265. [CrossRef] [PubMed]

28. Yin, L.; Duan, J.-J.; Bian, X.-W.; Yu, S.-C. Triple-negative breast cancer molecular subtyping and treatment progress. *Breast Cancer Res.* **2020**, *22*, 61. [CrossRef]
29. Yao, H.; He, G.; Yan, S.; Chen, C.; Song, L.; Rosol, T.J.; Deng, X. Triple-negative breast cancer: Is there a treatment on the horizon? *Oncotarget* **2017**, *8*, 1913–1924. [CrossRef]
30. Kumar, A.; Tripathy, M.K.; Pasquereau, S.; Al Moussawi, F.; Abbas, W.; Coquard, L.; Khan, K.A.; Russo, L.; Algros, M.-P.; Valmary-Degano, S.; et al. The Human Cytomegalovirus Strain DB Activates Oncogenic Pathways in Mammary Epithelial Cells. *EBioMedicine* **2018**, *30*, 167–183. [CrossRef]
31. Kumar, A.; Abbas, W.; Colin, L.; Khan, K.A.; Bouchat, S.; Varin, A.; Larbi, A.; Gatot, J.-S.; Kabeya, K.; VanHulle, C.; et al. Tuning of AKT-pathway by Nef and its blockade by protease inhibitors results in limited recovery in latently HIV infected T-cell line. *Sci. Rep.* **2016**, *6*, 24090. [CrossRef] [PubMed]
32. Liao, T.-T.; Yang, M.-H. Hybrid Epithelial/Mesenchymal State in Cancer Metastasis: Clinical Significance and Regulatory Mechanisms. *Cells* **2020**, *9*, 623. [CrossRef] [PubMed]
33. Grosse-Wilde, A.; D'Hérouël, A.F.; McIntosh, E.; Ertaylan, G.; Skupin, A.; Kuestner, R.E.; del Sol, A.; Walters, K.-A.; Huang, S. Stemness of the hybrid Epithelial/Mesenchymal State in Breast Cancer and Its Association with Poor Survival. *PLoS ONE* **2015**, *10*, e0126522. [CrossRef] [PubMed]
34. McFarlane, S.; Nicholl, M.J.; Sutherland, J.S.; Preston, C.M. Interaction of the human cytomegalovirus particle with the host cell induces hypoxia-inducible factor 1 alpha. *Virology* **2011**, *414*, 83–90. [CrossRef]
35. Warburg, O. On the Origin of Cancer Cells. *Science* **1956**, *123*, 309–314. [CrossRef]
36. Fallah, Y.; Brundage, J.; Allegakoen, P.; Shajahan-Haq, A.N. MYC-Driven Pathways in Breast Cancer Subtypes. *Biomolecules* **2017**, *7*, 53. [CrossRef] [PubMed]
37. Davey, M.G.; Hynes, S.O.; Kerin, M.J.; Miller, N.; Lowery, A.J. Ki-67 as a Prognostic Biomarker in Invasive Breast Cancer. *Cancers* **2021**, *13*, 4455. [CrossRef]
38. Hadjimichael, C.; Chanoumidou, K.; Papadopoulou, N.; Arampatzi, P.; Papamatheakis, J.; Kretsovali, A. Common stemness regulators of embryonic and cancer stem cells. *World J. Stem Cells* **2015**, *7*, 1150–1184. [CrossRef]
39. Sridharan, S.; Howard, C.M.; Tilley, A.M.C.; Subramaniyan, B.; Tiwari, A.K.; Ruch, R.J.; Raman, D. Novel and Alternative Targets Against Breast Cancer Stemness to Combat Chemoresistance. *Front. Oncol.* **2019**, *9*, 1003. [CrossRef]
40. Velasco-Velázquez, M.A.; Popov, V.M.; Lisanti, M.P.; Pestell, R.G. The Role of Breast Cancer Stem Cells in Metastasis and Therapeutic Implications. *Am. J. Pathol.* **2011**, *179*, 2–11. [CrossRef]
41. Ye, F.; Zhong, X.; Qiu, Y.; Yang, L.; Wei, B.; Zhang, Z.; Bu, H. CD49f Can Act as a Biomarker for Local or Distant Recurrence in Breast Cancer. *J. Breast Cancer* **2017**, *20*, 142–149. [CrossRef] [PubMed]
42. Jary, A.; Veyri, M.; Gothland, A.; Leducq, V.; Calvez, V.; Marcelin, A.-G. Kaposi's Sarcoma-Associated Herpesvirus, the Etiological Agent of All Epidemiological Forms of Kaposi's Sarcoma. *Cancers* **2021**, *13*, 6208. [CrossRef] [PubMed]
43. Münz, C. Latency and lytic replication in Epstein–Barr virus-associated oncogenesis. *Nat. Rev. Genet.* **2019**, *17*, 691–700. [CrossRef]
44. Mehravaran, H.; Makvandi, M.; Zade, A.S.; Neisi, N.; Kiani, H.; Radmehr, H.; Shahani, T.; Hoseini, S.Z.; Ranjbari, N.; Samiei, R.N. Association of Human Cytomegalovirus with Hodgkin's Disease and Non-Hodgkin's lymphomas. *Asian Pac. J. Cancer Prev.* **2017**, *18*, 593–597. [PubMed]
45. Collins-McMillen, D.; Kamil, J.; Moorman, N.; Goodrum, F. Control of Immediate Early Gene Expression for Human Cytomegalovirus Reactivation. *Front. Cell. Infect. Microbiol.* **2020**, *10*, 476. [CrossRef] [PubMed]
46. Forte, E.; Zhang, Z.; Thorp, E.B.; Hummel, M. Cytomegalovirus Latency and Reactivation: An Intricate Interplay with the Host Immune Response. *Front. Cell. Infect. Microbiol.* **2020**, *10*, 130. [CrossRef]
47. Soroceanu, L.; Matlaf, L.; Khan, S.; Akhavan, A.; Singer, E.; Bezrookove, V.; Decker, S.; Ghanny, S.; Hadaczek, P.; Bengtsson, H.; et al. Cytomegalovirus Immediate-Early Proteins Promote Stemness Properties in Glioblastoma. *Cancer Res.* **2015**, *75*, 3065–3076. [CrossRef] [PubMed]
48. Shannon-Lowe, C.; Rickinson, A. The Global Landscape of EBV-Associated Tumors. *Front. Oncol.* **2019**, *9*, 713. [CrossRef]
49. Peng, R.-J.; Han, B.-W.; Cai, Q.-Q.; Zuo, X.-Y.; Xia, T.; Chen, J.-R.; Feng, L.-N.; Lim, J.Q.; Chen, S.-W.; Zeng, M.; et al. Genomic and transcriptomic landscapes of Epstein-Barr virus in extranodal natural killer T-cell lymphoma. *Leukemia* **2018**, *33*, 1451–1462. [CrossRef]
50. Song, X.; Liu, Z.; Yu, Z. EGFR Promotes the Development of Triple Negative Breast Cancer Through JAK/STAT3 Signaling. *Cancer Manag. Res.* **2020**, *12*, 703–717. [CrossRef]
51. Nie, L.; Wei, Y.; Zhang, F.; Hsu, Y.-H.; Chan, L.-C.; Xia, W.; Ke, B.; Zhu, C.; Deng, R.; Tang, J.; et al. CDK2-mediated site-specific phosphorylation of EZH2 drives and maintains triple-negative breast cancer. *Nat. Commun.* **2019**, *10*, 5114–5115. [CrossRef] [PubMed]
52. A Velasco-Velázquez, M.; Li, Z.; Casimiro, M.; Loro, E.; Homsi, N.; Pestell, R.G. Examining the role of cyclin D1 in breast cancer. *Futur. Oncol.* **2011**, *7*, 753–765. [CrossRef] [PubMed]
53. Fultang, N.; Chakraborty, M.; Peethambaran, B. Regulation of cancer stem cells in triple negative breast cancer. *Cancer Drug Resist* **2021**, *4*, 321–342. [CrossRef] [PubMed]
54. Feng, W.-H.; Israel, B.; Raab-Traub, N.; Busson, P.; Kenney, S.C. Chemotherapy induces lytic EBV replication and confers ganciclovir susceptibility to EBV-positive epithelial cell tumors. *Cancer Res.* **2002**, *62*, 1920–1926. [PubMed]

55. Yang, J.; Dai, L.-X.; Chen, M.; Li, B.; Ding, N.; Li, G.; Liu, Y.-Q.; Li, M.-Y.; Wang, B.-N.; Shi, X.-L.; et al. Inhibition of antiviral drug cidofovir on proliferation of human papillomavirus-infected cervical cancer cells. *Exp. Ther. Med.* **2016**, *12*, 2965–2973. [CrossRef]
56. Coen, N.; Duraffour, S.; Snoeck, R.; Andrei, G. KSHV Targeted Therapy: An Update on Inhibitors of Viral Lytic Replication. *Viruses* **2014**, *6*, 4731–4759. [CrossRef]

11.7 Publication N°7

Bouezzedine F, **El Baba R**, Morot-Bizot S, Diab-Assaf M, Herbein G. Cytomegalovirus at the crossroads of immunosenescence and oncogenesis. Explor Immunol 2023:17–27. https://doi.org/10.37349/ei.2023.00086.

Human cytomegalovirus (HCMV) is a common herpesvirus infecting a significant portion of the population. While it often causes mild symptoms, HCMV can trigger strong immune responses and persist for life. In individuals with weakened immune systems, such as those with AIDS or transplant recipients, HCMV can lead to severe diseases. Immunosenescence, associated with aging and inflammation (inflammaging), has received increased attention. HCMV is closely linked to accelerated aging of the immune system and age-related diseases, contributing to mortality, reduced vaccine efficacy, serious illnesses, and cancer, particularly in the elderly. HCMV can both initiate and worsen immunosenescence, and its reactivation, involving different viral cycles, adds to its genetic diversity. In addition to its oncogenic role, the immune-privileged tumor microenvironment plays a significant part in tumor progression. Understanding the interplay between HCMV, immunosenescence, and cancer could lead to novel therapeutic approaches, particularly for challenging cancers in older individuals.

Exploration of Immunology

Open Exploration

Open Access Review

Cytomegalovirus at the crossroads of immunosenescence and oncogenesis

Fidaa Bouezzedine[1,2†], Ranim El Baba[1,2†], Stéphanie Morot-Bizot[3], Mona Diab-Assaf[2], Georges Herbein[1,4*]

[1]Department of Pathogens & Inflammation-EPILAB EA4266, University of Franche-Comté, F-25030 Besançon, France
[2]Molecular Cancer and Pharmaceutical Biology Laboratory, Lebanese University, Beirut 1500, Lebanon
[3]Apex Biosolutions, 25000 Besançon, France
[4]Department of Virology, CHRU Besançon, 25000 Besançon, France

[†]These authors contributed equally to this work.
[*]**Correspondence:** Georges Herbein, Department of Pathogens & Inflammation-EPILAB EA4266, University of Franche-Comté, 16 route de Gray, F-25030 Besançon, France. georges.herbein@univ-fcomte.fr
Academic Editor: Roberto Paganelli, G. d'Annunzio University, Italy

Received: November 15, 2022 **Accepted:** December 27, 2022 **Published:** February 24, 2023

Cite this article: Bouezzedine F, El Baba R, Morot-Bizot S, Diab-Assaf M, Herbein G. Cytomegalovirus at the crossroads of immunosenescence and oncogenesis. Explor Immunol. 2023;3:17–27. https://doi.org/10.37349/ei.2023.00086

Abstract

Human cytomegalovirus (HCMV), whose genome is around 235 kb, is a ubiquitous human herpesvirus that infects between 40% and 95% of the population. Though HCMV infection is commonly asymptomatic and leads to subtle clinical symptoms, it can promote robust immune responses and establish lifelong latency. In addition, in immunocompromised hosts, including individuals with acquired immunodeficiency syndrome (AIDS), transplant recipients, and developing fetuses it can lead to severe diseases. Immunosenescence, well-defined as the alterations in the immune system, is linked mainly to aging and has been recently gathering considerable attention. Senescence was characterized by an elevated inflammation and hence considered a powerful contributor to "inflammaging" that is measured mainly by tumor necrosis factor-α (TNF-α), interleukin-6 (IL-6), and C-reactive protein (CRP) levels as well as latent viral infections, for instance, cytomegalovirus (CMV). Inflammaging resulted in a senescence-associated secretory phenotype (SASP). HCMV is markedly associated with accelerated aging of the immune system as well as several age-associated diseases that accumulate and subsequently deteriorate the immune responses, thus have been linked to mortality, declined vaccine efficacy, serious diseases, and tumors in the elderly. HCMV triggers or exacerbates immunosenescence; on the other hand, the weakened immune responses and inflammaging favor viral reactivation and highlight the role of HCMV in aging as well as viral-associated tumors. HCMV reactivation resulting in sequential lytic and latent viral cycles could contribute to HCMV genomic variability. Besides the oncomodulatory role and transforming capacities of HCMV, the immune-privileged tumor microenvironment has been considered the main element in tumor progression and aggressiveness. Therefore, the interplay between HCMV, immunosenescence, and cancer will aid in discovering new therapeutic approaches that target HCMV and act as immune response boosters mainly to fight cancers of poor prognosis, particularly in the elderly population.

© **The Author(s) 2023.** This is an Open Access article licensed under a Creative Commons Attribution 4.0 International License (https://creativecommons.org/licenses/by/4.0/), which permits unrestricted use, sharing, adaptation, distribution and reproduction in any medium or format, for any purpose, even commercially, as long as you give appropriate credit to the original author(s) and the source, provide a link to the Creative Commons license, and indicate if changes were made.

Keywords

Cytomegalovirus, immunosenescence, oncomodulation, oncogenesis, inflammaging, tumor microenvironment

Introduction

Human cytomegalovirus (HCMV) belongs to the β-herpesvirus family and is a prevalent human pathogen infecting 40% to 95% of the world's population [1]. Following primary infection, cytomegalovirus (CMV) possesses the capacity to induce both lytic and latent infections to establish lifelong persistence in human hosts [2]. The clinical course of HCMV infection is widely variable, it depends on the age and is highly influenced by the immune fitness of the host. While the immunocompetent healthy individuals are asymptomatic, the congenitally infected infants could be symptomatic at birth and suffer long-term neurologic sequelae [3]. However, over time pronounced changes occur in the human immune system, known as immunosenescence. These age-related changes decrease immune protection and have been linked to mortality, decreased vaccine responsiveness, cardiovascular diseases, and cancer in the elderly [4, 5]. Importantly, while some studies implicate HCMV in driving immunosenescence and disease risk, others suggest it enhances immune function [6, 7]. Recently, HCMV has been reported to induce oncomodulation and even oncogenesis in some cases [2]. In this review, the role of HCMV in driving immunosenescence and its impact on oncogenesis were highlighted.

Concepts and hallmarks of immunosenescence

Immunosenescence is a normal physiologic process in which immune system function slowly changes with age. In fact, immunosenescence is regulated by many factors including aging, particularly the degeneration of the thymus resulting in a decrease of the T cell population and decrease of $CD8^+$ naive T cells, one of the main manifestations of immunosenescence [8]; as well the inflammation which produces senescence-associated secretory phenotype (SASP) wherein aging cells secrete soluble factors such as growth factors, cytokines, chemokines, and extracellular matrix inducing several senescence-related diseases, including various malignancies [9] in addition to the overlooking of intrinsic and extrinsic factors of the immune system [10]. Moreover, the characterization of the hallmarks of immunosenescence is essential, especially for understanding its impact on the disease risk and tumor progression. With aging, the cytotoxic effect of immune cells as well as the expression of interferon γ (IFN-γ) and cytotoxic molecules such as granzyme B and perforin decrease [11, 12]. In addition, memory T cells which differentiate from naive T cells upon primary antigenic stimulation play a crucial role in the adaptive immune system and enable a robust immune response over the human lifespan. Nevertheless, pronounced age-associated changes occur in the composition of T cell populations (naive *versus* memory cells). Despite the increased number of memory cells during early life, it shows senescent changes after 65 years [13]. One of the most prominent markers of T cell senescence is the loss of the costimulatory molecule CD28 and the accumulation of highly differentiated effector memory T cell [$CD27^-CD28^-CD57^+$ killer cell lectin-like receptor G1 (KLRG1)$^+$], which are hallmarks of immunosenescence [14]. Another hallmark of senescent T cells is telomerase shortening [15]. It should be noted that, in the process of immunosenescence, there is remodeling of mature natural killer (NK) cells and reduced expression of the activated receptors which may affect the immune monitoring effect of NK cells in the elderly [16]. Age-related modifications also occur in naive/memory B cell subsets. Indeed, in the elderly, there is a reduction of naive B cells, accompanied by the expansion of memory B cells that show a senescence-associated phenotype [17]. While the functions of dendritic cells (DCs) such as antigen presentation, endocytosis, and IFN production are reduced in elderly individuals [18], the phagocytic ability of neutrophils decreases [19]. Aged macrophages reduce their functional activity leading to the accumulation of unphagocytosed debris, increased senescent-associated markers, increased inflammatory cytokine production, reduced autophagy, and a decrease in Toll-like receptor (TLR) expression [20].

HCMV infection driving immunosenescence

Following primary infection, HCMV has the capacity to induce both lytic and latent infection to establish lifelong persistence in human hosts. Despite the extensive innate and adaptive response elicited by HCMV infection during both lytic and latent infection, the virus develops diverse immune evasion strategies to alter the host immune recognition [21]. The clinical presentation of HCMV infection is highly influenced by the immune response of the host during distinct life stages. In healthy immunocompetent hosts, viral reactivation which occurs throughout life induces the establishment of immune memory leading to the control of viral replication. However, in immunocompromised hosts, the loss of CMV-specific $CD4^+CD8^+$ T cells favors uncontrolled viral replication and dissemination leading to serious clinical diseases and even death [22]. In addition, long-term HCMV persistence will modulate the immune system composition and function even in healthy HCMV-infected individuals (Figure 1). Many epidemiologic studies on aging indicate that HCMV seropositivity is associated with immunosenescence and increased mortality in the elderly [23, 24]. Moreover, HCMV seropositive older individuals have a reduced response to vaccination [25]. Reactivation of HCMV triggered in severe acute respiratory syndrome coronavirus 2 (SARS-CoV-2) infected patients exacerbates the risk of coronavirus disease [26]. Although, the link between HCMV and immunosenescence request more investigation, HCMV persistence is thought to be a driver of immunosenescence in humans [7]. It was postulated that inflation of HCMV-specific T cells during viral persistence compromised host immunity. In HCMV-infected elderly individuals, the $CD8^+$ T cells response to HCMV antigens constitutes 50% of the entire memory $CD8^+$ T cells compartment in peripheral blood, while around 30% of total circulating $CD4^+$ T cells can be HCMV responsive [27]. The majority of this terminally differentiated inflationary HCMV-specific $CD8^+$ T cell subset has a typical age-related senescent T cell phenotype [$CD57^+CD28^-$ C-C motif chemokine receptor 7 $(CCR7)^-$], lacking CD28 expression which is a major characteristic of T cell aging [28]. This finding is supported by the fact that this large population of HCMV-specific $CD8^+CD28^-$ T cells is absent in seronegative elderly individuals [29]. Moreover, in elderly hosts, impairment of T cell immunity is also linked to memory inflation in HCMV infection. Despite the diverse $CD8^+$ T cells repertoire to recognize different viral epitopes soon after HCMV primary infection, this diversity starts to decrease with age often manifested as large clonal expansions of cells of limited antigen specificity together with a marked shrinkage of the T cell antigen receptor repertoire [7]. In elderly hosts, more than 25% of total $CD8^+$ T cells show a specific response to an individual immunodominant HCMV epitope such as p65 tumor suppressor protein (p65) and immediate early 1 (IE1) [30]. This limited diversity of HCMV-specific T cell clones during memory inflation may affect the immune protection to novel and vaccine antigens through decreased T cell receptors (TCRs) diversity in the elderly and thereby exposing them to the risk of life-threatening diseases [31]. Additionally, in older adults, most inflationary $CD4^+$ T cells induce T-helper 1 (Th1) responses by producing IFN-γ which explains the poor humoral responses seen in the elderly [32]. Although HCMV has a more immunologic impact on memory T cells than naive T cells, it also alters naive T cells. Thus, mainly and exclusively in older subjects with elevated anti-CMV antibody titers, there is a significant decrease in $CD4^+$ naive T cells parallel to an absolute increase in effector/effector memory $CD4^+CD8^+$ T cells [33].

Moreover, cell exhaustion, another form of T cell dysfunction, can arise during chronic infection which is often associated with inefficient control of persisting infections due to the loss of proliferative potential, decreased cytotoxicity, impaired cytokines secretions, and high expression of several inhibitory receptors [programmed death 1 (PD1), KLRG1, and CD57]. HCMV-specific $CD8^+$ T cells are characterized by a low proliferative capacity and expression of senescent markers such as KLRG1 and CD57. These cells are not totally exhausted since they are still highly cytotoxic and produce Th1 cytokines in response to viral replication [31]. It's worth mentioning that HCMV infection leads to the accumulation of functional exhausted cells that could accelerate immunosenescence in immunocompromised and immunosuppressed individuals [34].

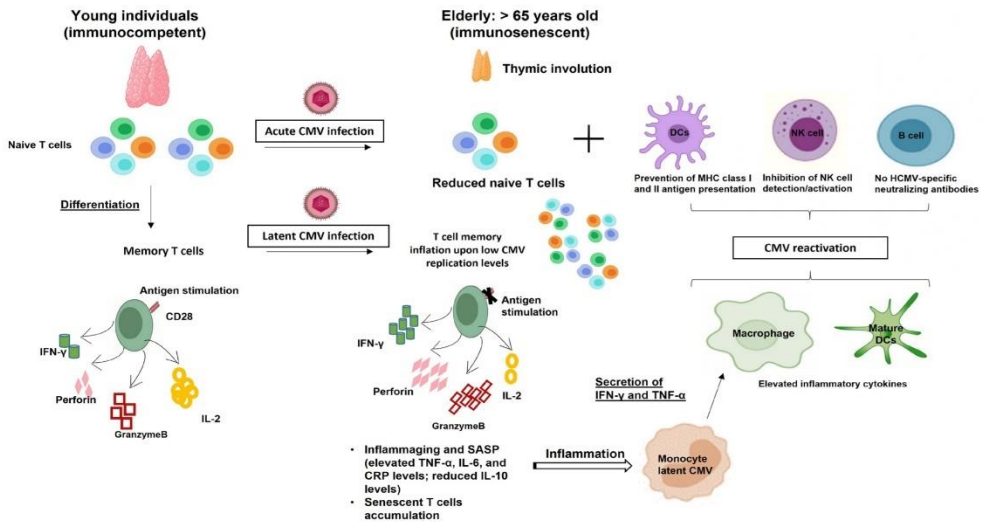

Figure 1. HCMV-induced immunosenescence. Acute and chronic HCMV infections modulate the host immune system resulting in naive T cell pool depletion and memory inflation, respectively which further drive/accelerate immunosenescence. The weakened immune responses and inflammaging favor HCMV reactivation which is the key to the accumulated HCMV-specific immune responses. IL-2: interleukin-2; TNF-α: tumor necrosis factor-α; CRP: C-reactive protein; MHC: major histocompatibility complex

Immunosenescence—a key player in cancer

Due to the increased rates of mortality and morbidity of various tumors with age, cancers are generally defined as aging diseases. The immunosenescence features and mechanisms were described as an important player in the tumoral process resulting in a high-risk of tumors in elderly groups [35]. Immunosenescence in the tumorogenesis process reflects the senescence of both innate (NK cells and macrophages) and acquired immune cells (B cells and T cells) affected on one side by the age-related change and the other side by the factors of the tumor microenvironment (TME). In acute myeloid leukaemia (AML) in elderly patients, NK cells harbor diminished levels of several activating receptors that contribute to impairing NK function and thereby favoring disease progression and decreased survival [36]. Age-modified changes in tissue-specific macrophages and neutrophils cause chronic low inflammation that is associated with a macrophage pro-tumorigenic phenotype [19]. Cytotoxic T lymphocytes (CTLs) are critical in eliminating tumor cells as well as virally infected cells. Thus, alterations of CTL function observed during aging could favor both viral infection and cancer. In patients with HCMV-positive glioblastoma multiforme (GBM), the signs of immunosenescence in the $CD4^+$ T cells compartment are associated with poor prognosis which may reflect the activity of HCMV [37]. Aging can also alter the TME. Thus, the increased presence of tumor-associated macrophages (TAMs) and tumor-derived γδ regulatory T cells (Tregs) in TME has been reported to decrease both innate and adaptive immunity; TAMs produce cytokines that promote T cell inactivation and inhibition of DCs activity thus increasing cancer cell proliferation [38, 39]. In hypoxic TME, tumor-derived cyclic adenosine monophosphate (cAMP) activates DNA damage and induces T cell senescence [40]. Similarly, glucose deprivation triggers DNA damage and activates the p38 pathway leading to cell cycle arrest and inhibition of T cell proliferation [41]. Moreover, the TME oncogenic stress activates signaling pathways including nuclear factor-kB (NF-kB), p38, CCAAT/enhancer binding protein β (C/EBPβ), and mechanistic target of rapamycin complex 1 (mTORC1) which play a role in regulating T cell SASP [42]. Furthermore, in aging, secretion of SASP molecules, such as IL-6, IL-8, and IL-10 in TME favors tumor progression through an inflammaging mechanism [43, 44]. Finally, HCMV favors immunosenescence with decreased immune defenses and inflammaging that could trigger viral reactivation from latency and further supports its role in aging as well as viral-driven malignancies.

Oncomodulatory and oncogenic properties of HCMV

Besides HCMV-induced immunosenescence, presented evidence reveals HCMV presence in numerous solid tumors [45, 46]. HCMV proteins have been found in 90–100% of breast, ovarian, colon, and prostate tumors, in sarcomas as well as in neural-derived tumors such as neuroblastoma, glioblastoma, and medulloblastoma [47]. Taking into account the broader concept of cancer hallmarks, the TME and cancer progression are considered essential oncomodulatory mechanisms relating tumor initiation to viral infections caused by oncoviruses [48]. HCMV mediates both oncomodulation and oncogenesis (Figure 2) [49]. During HCMV infection, the virus expresses viral gene products possessing potential transforming capacities and activating specific molecular pro-oncogenic pathways. HCMV key products involves IE1, IE2, unique short 28 protein (pUS28), viral IL-10 (vIL-10), unique long 76 protein (pUL76), pUL97, pUL82, pUS2, pUL16, 65-kDa tegument protein (pp65), pUL36, pUL37x1, and long non-coding RNA4.9 (lncRNA4.9) [49]. Early HCMV proteins regulate main cellular factors, for instance, retinoblastoma protein family, p53, cyclins, Wnt, phosphoinositide 3-kinase (PI3K)/protein kinase B (Akt), and NF-kB, hence affecting the cell cycle, differentiation, cellular proliferation, apoptosis, and metabolism [50–52]. HCMV-unique short 28 (US28) stimulates signaling pathways that are well-known to interfere with proliferation as well as survival, migration, angiogenesis, and inflammation [53–56]. pp65 tends to incapacitate the intrinsic cellular immune responses [57]. By expressing CMV IL-10 (cmvIL-10), HCMV displays a potent immunosuppressive effect thereby promoting the maturation of protumoral M2 macrophages TAM [58]. Thus, HCMV can entirely promote the steps of classical hallmarks of cancer through the expression of many gene products [49]. Furthermore, a direct oncogenic outcome was revealed by a few HCMV strains, namely, high-risk strains [59], that could promote cellular stress, polyploid giant cancer cells (PGCCs) generation, stemness, and epithelial-to-mesenchymal transition (EMT) plasticity explaining the appearance of aggressive tumor phenotypes, particularly adenocarcinomas, having poor prognosis, metastasis, therapy resistance, and relapse [46, 60]. HCMV-DB and BL, isolated high-risk clinical strains, displayed oncogenic potential in human mammary epithelial cells (HMECs) and replicated in epithelial cells with the interchange of lytic and latent viral cycles promoting the appearance of CMV-transformed HMECs (CTH cells) [60–62]. Two additional high-risk HCMV strains, namely biopsy 544 (B544) and B693, recently isolated from enhancer of zeste homolog 2 $(EZH2)^{High}$ Myc^{High} triple-negative breast cancer (TNBC) biopsies revealed oncogenic and stemness potential [63, 64]. EZH2 was identified as a downstream target for HCMV-induced Myc upregulation upon HMECs infection with high-risk HCMV strains [64]. In GBM tissues harboring HCMV, EZH2 overexpression was detected [65]. EZH2 is overexpressed in PGCCs highlighting the presence of a potential link between HCMV infection, Myc/EZH2 upregulation, and PGCC generation [64]. Hence, this evidence suggests that some HCMV strains may not only possess an oncomodulatory role but in a certain cellular context, it unveils direct tumor-promoting strategies. Besides the transforming capacities of HCMV, the TME has increasingly been recognized as a key element in tumor progression and metastasis [2]. Restricted immune control against HCMV will favor the productive viral infection in the immune-privileged TME thereby supporting a stem-cell-like state of cancer cells and promoting cancer aggressiveness [66, 67]. HCMV reactivation in M1 macrophages promotes an M2/TAM shift, thus driving the neoplastic progression [21, 68]. Tumor cells evade immune responses promoting EMT, metastasis, and relapse. Therefore, in tumor cells, the association of cellular machinery and viral immune evasion mechanisms may give rise to an environment that enhances limited HCMV replication and triggers cancer cells to evade immune surveillance revealing the bidirectional association between cancer cells and HCMV [21, 69]. Persistent HCMV infection markedly alters the host immune system and has been suggested to trigger or exacerbate age-associated diseases as well as immunosenescence (Figure 3) [70, 71].

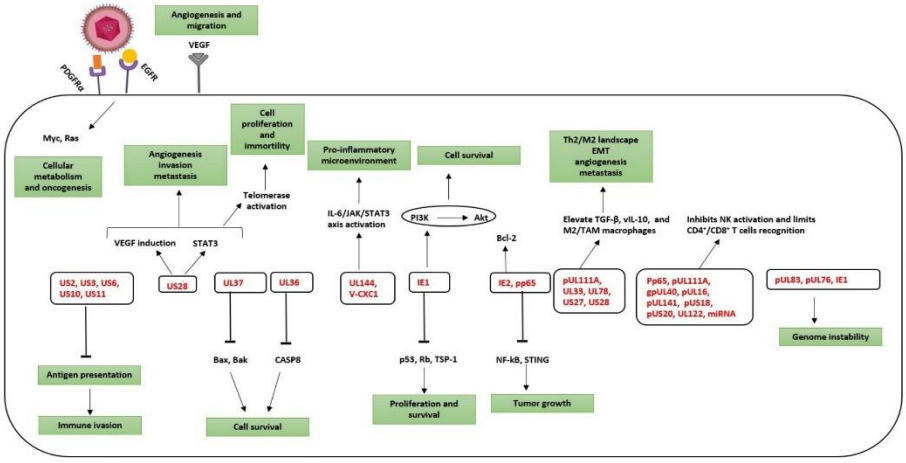

Figure 2. HCMV from oncomodulation to oncogenesis. Activation of specific molecular pathways that are implicated in oncomodulation and cellular transformation. Oncomodulation, which favors the growth and spread of tumor cells, as well as oncogenesis are mainly targeted by HCMV gene products (in red). PDGFRα: platelet-derived growth factor receptor α; EGFR: epidermal growth factor receptor; VEGF: vascular endothelial growth factor; STAT3: signal transducer and activator of transcription 3; JAK: Janus kinase; TGF-β: transforming growth factor β; UL37: unique long 37; V-CXC1: viral chemokine (C-X-C motif) ligand 1; gpUL40: glycoprotein unique long 40; miRNA: microRNA; STING: stimulator of interferon genes; TSP-1: thrombospondin 1; CASP8: caspase 8; Bcl-2: B-cell lymphoma 2; Bax: Bcl-2-associated X protein; Bak: Bcl-2 homologous antagonist/killer; Rb: retinoblastoma protein

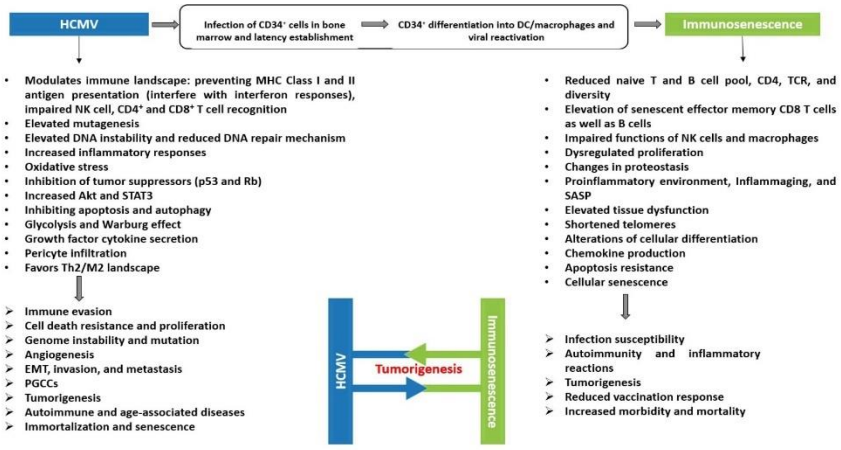

Figure 3. The interplay between HCMV-induced immunosenescence and oncogenesis. A scheme showing the potential association between HCMV, immunosenescence, and tumorigenesis. Persistent HCMV infection fulfills all the cancer hallmarks and is associated with enhanced aging of the immune system. Immunosenescence and inflammaging play a substantial role in the pathogenesis of several serious diseases in the elderly. Both players, HCMV and immunosenescence, have been associated with high mortality rates, chronic diseases, and tumors

Conclusions

HCMV infection and immunosenescence in clinical conditions such as organ transplantation, cancer, immunodeficiency, as well as autoimmune and inflammatory illnesses, support the concept that HCMV can affect their progression by inducing immunosenescence. In return, immunosenescence favors HCMV reactivation from latency in an inflammatory microenvironment (inflammaging). Viral reactivation will trigger

HCMV-driven oncomodulation by low- and high-risk HCMV strains, and could also promote the initiation of tumorigenesis, particularly by high-risk HCMV strains, thus directly favoring the appearance of tumors especially adenocarcinoma and glioblastoma in an immunocompromised TME with immunosenescence and inflammaging traits. A better understanding of the complex interaction between HCMV, immunosenescence, and tumors will open new perspectives to explore novel therapeutic approaches that will reverse immunosenescence and boost the immune system to fight viral infections, especially HCMV, and tumor development in the elderly.

Abbreviations

Akt: protein kinase B

CMV: cytomegalovirus

DCs: dendritic cells

EMT: epithelial-to-mesenchymal transition

EZH2: enhancer of zeste homolog 2

HCMV: human cytomegalovirus

HMECs: human mammary epithelial cells

IE1: immediate early 1

IFN-γ: interferon γ

IL-6: interleukin-6

KLRG1: killer cell lectin-like receptor G1

NF-kB: nuclear factor-kB

NK: natural killer

p65: p65 tumor suppressor protein

PGCCs: polyploid giant cancer cells

pp65: 65-kDa tegument protein

pUL76: unique long 76 protein

pUS28: unique short 28 protein

SASP: senescence-associated secretory phenotype

TAMs: tumor-associated macrophages

Th1: T-helper 1

TME: tumor microenvironment

UL37: unique long 37

US28: unique short 28

Declarations

Author contributions

FB, REB, SMB, MDA, and GH: Writing—original draft, Writing—review & editing. GH: Conceptualization, Supervision.

Conflicts of interest

The authors declare that they have no conflicts of interest.

Ethical approval

Not applicable.

Consent to participate

Not applicable.

Consent to publication

Not applicable.

Availability of data and materials

Not applicable.

Funding

GH received grants from the University of Franche-Comté [3300]. The funders had no role in study design, data collection and analysis, decision to publish, or preparation of the manuscript.

Copyright

© The Author(s) 2023.

References

1. Zuhair M, Smit GSA, Wallis G, Jabbar F, Smith C, Devleesschauwer B, et al. Estimation of the worldwide seroprevalence of cytomegalovirus: a systematic review and meta-analysis. Rev Med Virol. 2019;29:e2034.
2. Herbein G. Tumors and cytomegalovirus: an intimate interplay. Viruses. 2022;14:812.
3. Ehlinger EP, Webster EM, Kang HH, Cangialose A, Simmons AC, Barbas KH, et al. Maternal cytomegalovirus-specific immune responses and symptomatic postnatal cytomegalovirus transmission in very low-birth-weight preterm infants. J Infect Dis. 2011;204:1672–82. Erratum in: J Infect Dis. 2012;205:1767.
4. Olsson J, Wikby A, Johansson B, Löfgren S, Nilsson BO, Ferguson FG. Age-related change in peripheral blood T-lymphocyte subpopulations and cytomegalovirus infection in the very old: the Swedish longitudinal OCTO immune study. Mech Ageing Dev. 2000;121:187–201.
5. Wang H, Peng G, Bai J, He B, Huang K, Hu X, et al. Cytomegalovirus infection and relative risk of cardiovascular disease (ischemic heart disease, stroke, and cardiovascular death): a meta-analysis of prospective studies up to 2016. J Am Heart Assoc. 2017;6:e005025.
6. Picarda G, Benedict CA. Cytomegalovirus: shape-shifting the immune system. J Immunol. 2018;200:3881–9.
7. Koch S, Larbi A, Özcelik D, Solana R, Gouttefangeas C, Attig S, et al. Cytomegalovirus infection: a driving force in human T cell immunosenescence. Ann N Y Acad Sci. 2007;1114:23–35.
8. Thomas R, Wang W, Su DM. Contributions of age-related thymic involution to immunosenescence and inflammaging. Immun Ageing. 2020;17:2.
9. Accardi G, Caruso C. Immune-inflammatory responses in the elderly: an update. Immun Ageing. 2018;15:11.
10. Masters AR, Haynes L, Su DM, Palmer DB. Immune senescence: significance of the stromal microenvironment. Clin Exp Immunol. 2017;187:6–15.
11. Crespo J, Sun H, Welling TH, Tian Z, Zou W. T cell anergy, exhaustion, senescence, and stemness in the tumor microenvironment. Curr Opin Immunol. 2013;25:214–21.
12. Yang OO, Lin H, Dagarag M, Ng HL, Effros RB, Uittenbogaart CH. Decreased perforin and granzyme B expression in senescent HIV-1-specific cytotoxic T lymphocytes. Virology. 2005;332:16–9.
13. Farber DL, Yudanin NA, Restifo NP. Human memory T cells: generation, compartmentalization and homeostasis. Nat Rev Immunol. 2014;14:24–35.

14. Huff WX, Kwon JH, Henriquez M, Fetcko K, Dey M. The evolving role of $CD8^+CD28^-$ immunosenescent T cells in cancer immunology. Int J Mol Sci. 2019;20:2810.
15. Bernadotte A, Mikhelson VM, Spivak IM. Markers of cellular senescence. Telomere shortening as a marker of cellular senescence. Aging (Albany NY). 2016;8:3–11.
16. Manser AR, Uhrberg M. Age-related changes in natural killer cell repertoires: impact on NK cell function and immune surveillance. Cancer Immunol Immunother. 2016;65:417–26.
17. Bulati M, Caruso C, Colonna-Romano G. From lymphopoiesis to plasma cells differentiation, the age-related modifications of B cell compartment are influenced by "inflamm-ageing". Ageing Res Rev. 2017;36:125–36.
18. Agrawal A, Agrawal S, Gupta S. Role of dendritic cells in inflammation and loss of tolerance in the elderly. Front Immunol. 2017;8:896.
19. Jackaman C, Tomay F, Duong L, Abdol Razak NB, Pixley FJ, Metharom P, et al. Aging and cancer: the role of macrophages and neutrophils. Ageing Res Rev. 2017;36:105–16.
20. De Maeyer RPH, Chambers ES. The impact of ageing on monocytes and macrophages. Immunol Lett. 2021;230:1–10.
21. El Baba R, Herbein G. Immune landscape of CMV infection in cancer patients: from "canonical" diseases toward virus-elicited oncomodulation. Front Immunol. 2021;12:730765.
22. Sansoni P, Vescovini R, Fagnoni FF, Akbar A, Arens R, Chiu YL, et al. New advances in CMV and immunosenescence. Exp Gerontol. 2014;55:54–62.
23. Roberts ET, Haan MN, Dowd JB, Aiello AE. Cytomegalovirus antibody levels, inflammation, and mortality among elderly Latinos over 9 years of follow-up. Am J Epidemiol. 2010;172:363–71.
24. Pawelec G, Gouttefangeas C. T-cell dysregulation caused by chronic antigenic stress: the role of CMV in immunosenescence? Aging Clin Exp Res. 2006;18:171–3.
25. Trzonkowski P, Myśliwska J, Szmit E, Wieckiewicz J, Lukaszuk K, Brydak LB, et al. Association between cytomegalovirus infection, enhanced proinflammatory response and low level of anti-hemagglutinins during the anti-influenza vaccination—an impact of immunosenescence. Vaccine. 2003;21:3826–36.
26. Söderberg-Nauclér C. Does reactivation of cytomegalovirus contribute to severe COVID-19 disease? Immun Ageing. 2021;18:12.
27. Li H, Margolick JB, Bream JH, Nilles TL, Langan S, Bui HT, et al. Heterogeneity of $CD4^+$ and $CD8^+$ T-cell responses to cytomegalovirus in HIV-infected and HIV-uninfected men who have sex with men. J Infect Dis. 2014;210:400–4.
28. Kuijpers TW, Vossen MT, Gent MR, Davin JC, Roos MT, Wertheim-van Dillen PM, et al. Frequencies of circulating cytolytic, $CD45RA^+CD27^-$, $CD8^+$ T lymphocytes depend on infection with CMV. J Immunol. 2003;170:4342–8.
29. Derhovanessian E, Maier AB, Beck R, Jahn G, Hähnel K, Slagboom PE, et al. Hallmark features of immunosenescence are absent in familial longevity. J Immunol. 2010;185:4618–24.
30. Sylwester AW, Mitchell BL, Edgar JB, Taormina C, Pelte C, Ruchti F, et al. Broadly targeted human cytomegalovirus-specific $CD4^+$ and $CD8^+$ T cells dominate the memory compartments of exposed subjects. J Exp Med. 2005;202:673–85.
31. Klenerman P, Oxenius A. T cell responses to cytomegalovirus. Nat Rev Immunol. 2016;16:367–77.
32. van Leeuwen EM, Remmerswaal EB, Heemskerk MH, ten Berge IJ, van Lier RA. Strong selection of virus-specific cytotoxic $CD4^+$ T-cell clones during primary human cytomegalovirus infection. Blood. 2006;108:3121–7.
33. Wertheimer AM, Bennett MS, Park B, Uhrlaub JL, Martinez C, Pulko V, et al. Aging and cytomegalovirus infection differentially and jointly affect distinct circulating T cell subsets in humans. J Immunol. 2014;192:2143–55.

34. Chou JP, Effros RB. T cell replicative senescence in human aging. Curr Pharm Des. 2013;19:1680–98.
35. DeSantis CE, Miller KD, Dale W, Mohile SG, Cohen HJ, Leach CR, et al. Cancer statistics for adults aged 85 years and older, 2019. CA Cancer J Clin. 2019;69:452–67.
36. Sanchez-Correa B, Campos C, Pera A, Bergua JM, Arcos MJ, Bañas H, et al. Natural killer cell immunosenescence in acute myeloid leukaemia patients: new targets for immunotherapeutic strategies? Cancer Immunol Immunother. 2016;65:453–63.
37. Fornara O, Odeberg J, Wolmer Solberg N, Tammik C, Skarman P, Peredo I, et al. Poor survival in glioblastoma patients is associated with early signs of immunosenescence in the CD4 T-cell compartment after surgery. Oncoimmunology. 2015;4:e1036211.
38. Ye J, Ma C, Hsueh EC, Eickhoff CS, Zhang Y, Varvares MA, et al. Tumor-derived γδ regulatory T cells suppress innate and adaptive immunity through the induction of immunosenescence. J Immunol. 2013;190:2403–14.
39. Wang D, Yang L, Yue D, Cao L, Li L, Wang D, et al. Macrophage-derived CCL22 promotes an immunosuppressive tumor microenvironment via IL-8 in malignant pleural effusion. Cancer Lett. 2019;452:244–53.
40. Vang T, Torgersen KM, Sundvold V, Saxena M, Levy FO, Skålhegg BS, et al. Activation of the COOH-terminal Src kinase (Csk) by cAMP-dependent protein kinase inhibits signaling through the T cell receptor. J Exp Med. 2001;193:497–507.
41. Lanna A, Henson SM, Escors D, Akbar AN. The kinase p38 activated by the metabolic regulator AMPK and scaffold TAB1 drives the senescence of human T cells. Nat Immunol. 2014;15:965–72.
42. Goronzy JJ, Weyand CM. Mechanisms underlying T cell ageing. Nat Rev Immunol. 2019;19:573–83.
43. Fane M, Weeraratna AT. How the ageing microenvironment influences tumour progression. Nat Rev Cancer. 2020;20:89–106.
44. Fulop T, Larbi A, Pawelec G, Khalil A, Cohen AA, Hirokawa K, et al. Immunology of aging: the birth of inflammaging. Clin Rev Allergy Immunol. 2021;[Epub ahead of print].
45. Rahbar A, Orrego A, Peredo I, Dzabic M, Wolmer-Solberg N, Stråat K, et al. Human cytomegalovirus infection levels in glioblastoma multiforme are of prognostic value for survival. J Clin Virol. 2013;57:36–42.
46. Cobbs C. Cytomegalovirus is a tumor-associated virus: armed and dangerous. Curr Opin Virol. 2019;39:49–59.
47. Söderberg-Nauclér C. New mechanistic insights of the pathogenicity of high-risk cytomegalovirus (CMV) strains derived from breast cancer: hope for new cancer therapy options. EBioMedicine. 2022;81:104103.
48. Hanahan D, Weinberg RA. Hallmarks of cancer: the next generation. Cell. 2011;144:646–74.
49. Herbein G. The Human cytomegalovirus, from oncomodulation to oncogenesis. Viruses. 2018;10:408.
50. Cinatl J Jr, Vogel JU, Kotchetkov R, Wilhelm Doerr H. Oncomodulatory signals by regulatory proteins encoded by human cytomegalovirus: a novel role for viral infection in tumor progression. FEMS Microbiol Rev. 2004;28:59–77.
51. Yurochko AD, Kowalik TF, Huong SM, Huang ES. Human cytomegalovirus upregulates NF-kappa B activity by transactivating the NF-kappa B p105/p50 and p65 promoters. J Virol. 1995;69:5391–400.
52. Söderberg-Nauclér C. Does cytomegalovirus play a causative role in the development of various inflammatory diseases and cancer? J Intern Med. 2006;259:219–46.
53. Heukers R, Fan TS, de Wit RH, van Senten JR, De Groof TWM, Bebelman MP, et al. The constitutive activity of the virally encoded chemokine receptor US28 accelerates glioblastoma growth. Oncogene. 2018;37:4110–21.
54. de Wit RH, Mujić-Delić A, van Senten JR, Fraile-Ramos A, Siderius M, Smit MJ. Human cytomegalovirus encoded chemokine receptor US28 activates the HIF-1α/PKM2 axis in glioblastoma cells. Oncotarget. 2016;7:67966–85.

55. Soroceanu L, Matlaf L, Bezrookove V, Harkins L, Martinez R, Greene M, et al. Human cytomegalovirus US28 found in glioblastoma promotes an invasive and angiogenic phenotype. Cancer Res. 2011;71:6643–53.
56. Maussang D, Langemeijer E, Fitzsimons CP, Stigter-van Walsum M, Dijkman R, Borg MK, et al. The human cytomegalovirus-encoded chemokine receptor US28 promotes angiogenesis and tumor formation via cyclooxygenase-2. Cancer Res. 2009;69:2861–9.
57. Crough T, Khanna R. Immunobiology of human cytomegalovirus: from bench to bedside. Clin Microbiol Rev. 2009;22:76–98.
58. Bellone G, Turletti A, Artusio E, Mareschi K, Carbone A, Tibaudi D, et al. Tumor-associated transforming growth factor-β and interleukin-10 contribute to a systemic Th2 immune phenotype in pancreatic carcinoma patients. Am J Pathol. 1999;155:537–47.
59. Herbein G. High-risk oncogenic human cytomegalovirus. Viruses. 2022;14:2462.
60. Nehme Z, Pasquereau S, Haidar Ahmad S, Coaquette A, Molimard C, Monnien F, et al. Polyploid giant cancer cells, stemness and epithelial-mesenchymal plasticity elicited by human cytomegalovirus. Oncogene. 2021;40:3030–46.
61. Haidar Ahmad S, Pasquereau S, El Baba R, Nehme Z, Lewandowski C, Herbein G. Distinct oncogenic transcriptomes in human mammary epithelial cells infected with cytomegalovirus. Front Immunol. 2021;12:772160.
62. Kumar A, Tripathy MK, Pasquereau S, Al Moussawi F, Abbas W, Coquard L, et al. The human cytomegalovirus strain DB activates oncogenic pathways in mammary epithelial cells. EBioMedicine. 2018;30:167–83.
63. El Baba R, Pasquereau S, Haidar Ahmad S, Diab-Assaf M, Herbein G. Oncogenic and stemness signatures of the high-risk HCMV strains in breast cancer progression. Cancers (Basel). 2022;14:4271.
64. Nehme Z, Pasquereau S, Haidar Ahmad S, El Baba R, Herbein G. Polyploid giant cancer cells, EZH2 and Myc upregulation in mammary epithelial cells infected with high-risk human cytomegalovirus. EBioMedicine. 2022;80:104056.
65. Ahani N, Shirkoohi R, Rokouei M, Alipour Eskandani M, Nikravesh A. Overexpression of enhancer of zeste human homolog 2 (*EZH2*) gene in human cytomegalovirus positive glioblastoma multiforme tissues. Med Oncol. 2014;31:252.
66. Nauclér CS, Geisler J, Vetvik K. The emerging role of human cytomegalovirus infection in human carcinogenesis: a review of current evidence and potential therapeutic implications. Oncotarget. 2019;10:4333–47.
67. Wang ECY, Pjechova M, Nightingale K, Vlahava VM, Patel M, Ruckova E, et al. Suppression of costimulation by human cytomegalovirus promotes evasion of cellular immune defenses. Proc Natl Acad Sci U S A. 2018;115:4998–5003.
68. Chen Y, Song Y, Du W, Gong L, Chang H, Zou Z. Tumor-associated macrophages: an accomplice in solid tumor progression. J Biomed Sci. 2019;26:78.
69. Lepiller Q, Aziz Khan K, Di Martino V, Herbein G. Cytomegalovirus and tumors: two players for one goal-immune escape. Open Virol J. 2011;5:60–9.
70. Solana R, Tarazona R, Aiello AE, Akbar AN, Appay V, Beswick M, et al. CMV and immunosenescence: from basics to clinics. Immun Ageing. 2012;9:23.
71. Goodrum F, Caviness K, Zagallo P. Human cytomegalovirus persistence. Cell Microbiol. 2012;14:644–55.

11.8 Publication N°8

El Baba R, Pasquereau S, Haidar Ahmad S, Monnien F, Abad M, Bibeau F, et al. EZH2-Myc driven glioblastoma elicited by cytomegalovirus infection of human astrocytes. Oncogene 2023;42:2031–45. https://doi.org/10.1038/s41388-023-02709-3.

Increasing evidence suggests that human cytomegalovirus (HCMV) may have oncogenic potential, particularly in malignant gliomas. Notably, the presence of the EZH2 and Myc genes correlates with the severity of gliomas. This study provides the first experimental proof that HCMV can reprogram mature human astrocytes, leading to the creation of CMV-Elicited Glioblastoma Cells (CEGBCs) with traits resembling glioblastoma cells. HCMV mimics the cellular and molecular processes associated with transformation and invasion, with CEGBCs exhibiting spheroid formation and invasiveness. Glioblastoma multiforme (GBM) biopsies were characterized by elevated EZH2 and Myc expression, with a strong positive correlation when HCMV was present. Eleven clinical HCMV strains were isolated from GBM tissues, transforming astrocytes into CEGBCs with increased EZH2 and Myc expression. These CEGBC-derived spheroids displayed invasive potential and were responsive to treatment with an EZH2 inhibitor, ganciclovir, and temozolomide. This research establishes a model for HCMV-induced glioblastoma and underscores the significance of Myc and EZH2 in astrocytic brain tumor pathophysiology, offering potential avenues for novel therapeutic strategies.

ARTICLE OPEN

Check for updates

EZH2-Myc driven glioblastoma elicited by cytomegalovirus infection of human astrocytes

Ranim El Baba[1], Sébastien Pasquereau[1,4], Sandy Haidar Ahmad[1,4], Franck Monnien[2], Marine Abad[2], Frédéric Bibeau[2] and Georges Herbein[1,3]✉

© The Author(s) 2023

Mounting evidence is identifying human cytomegalovirus (HCMV) as a potential oncogenic virus. HCMV has been detected in malignant gliomas. EZH2 and Myc play a potential oncogenic role, correlating with the glioma grade. Herewith, we present the first experimental evidence for HCMV as a reprogramming vector, straight through the dedifferentiation of mature human astrocytes, and generation of *CMV-Elicited Glioblastoma Cells* (CEGBCs) possessing glioblastoma-like traits. HCMV counterparts the progression of the perceived cellular and molecular mechanisms succeeding the transformation and invasion processes with CEGBCs involved in spheroid formation and invasiveness. Glioblastoma multiforme (GBM) biopsies were characterized by an elevated EZH2 and Myc expression, possessing a strong positive correlation between the aforementioned markers in the presence of HCMV. From GBM tissues, we isolated HCMV clinical strains that transformed HAs toward CEGBCs exhibiting upregulated EZH2 and Myc. Spheroids generated from CEGBCs possessed invasion potential and were sensitive to EZH2 inhibitor, ganciclovir, and temozolomide triple therapy. HCMV clinical strains transform HAs and fit with an HCMV-induced glioblastoma model of oncogenesis, and supports the tumorigenic properties of Myc and EZH2 which might be highly pertinent in the pathophysiology of astrocytic brain tumors and thereby paving the way for new therapeutic strategies.

Oncogene (2023) 42:2031–2045; https://doi.org/10.1038/s41388-023-02709-3

INTRODUCTION

Glioblastoma multiforme (GBM), a subtype of adult diffuse glioma, is a primary central nervous system (CNS) tumor presumed to arise from neuroglial stem cells or their progenitors in the subventricular zone [1, 2]. There has been a recent paradigm shift, with increasing reliance on molecular information for diagnostic classification and prognostication within gliomas, as seen in the most recent World Health Organization (WHO) classification of CNS tumors [2]. Despite the molecular evolution of GBM, it continues to be an incurable disease with poor survival.

Cancer etiological factors are assorted into genetic or environmental risk factors of which viruses are estimated to contribute to 20% of all cancer cases [3]. Human cytomegalovirus (HCMV) is a ubiquitous pathogen belonging to *Herpesviridae* family that is often detected in cancer patients [4]. It exhibits a broad cellular tropism providing an advantageous platform for efficient viral proliferation and inter-host transmission, with a prominent role of blood monocytes in viral dissemination [5]. The establishment of viral reservoirs and latency in monocytes, tissue macrophages, and myeloid lineage $CD34^+$ hematopoietic progenitor cells could further promote disease progression. Potential interrelation between HCMV and cancer has been explored and oncomodulation paradigm was used to explain HCMV genome and/or antigens detection in a multitude of malignancies including breast cancer, colorectal, prostate, and GBM [4, 6–8]. HCMV infects neural stem/progenitor cells, and human astrocytes [9–12]. Going beyond oncomodulation, previous studies demonstrated HCMV ability to induce the transformation of human embryonal lung fibroblasts [13] and human mammary epithelial cells (HMECs) in vitro [7, 14, 15]. Although HCMV DNA and antigens, especially IE1, have been detected in GBM tissue [16], there is no conclusive evidence about HCMV oncogenicity in GBM, and the mechanisms by which the virus might contribute/induce oncogenesis remain elusive.

Being the enzymatic subunit of polycomb repressive complex 2 (PRC2), enhancer of zeste homolog 2 (EZH2) is a histone-lysine N-methyltransferase responsible of transcriptional silencing. EZH2 was shown to expand the stem cell pool and the tumor-initiating cells in glioma, breast and prostate cancer, hence enhancing accelerated initiation, metastasis and growth [17–19]. It was identified as a downstream target of Myc oncogene, the latter coordinately regulating EZH2 through transcriptional and post-transcriptional mechanisms during tumor initiation and disease progression [20]. EZH2 was shown to be recruited to the major immediate early promoter (MIEP) in $CD14+$ monocytes where HCMV establishes latent infection in vivo [21]. Further, EZH2 was demonstrated to be overexpressed in GBM tissues harboring HCMV [22]. EZH2 was overexpressed in polyploid giant cancer cells (PGCCs) [23, 24], the latter being also triggered by HCMV infection in breast cancer [15] which points toward a

[1]Department of Pathogens & Inflammation-EPILAB Laboratory EA4266, University of Franche-Comté, Besançon, France. [2]Department of Pathology, CHU Besançon, Besançon, France. [3]Department of Virology, CHU Besançon, Besançon, France. [4]These authors contributed equally: Sébastien Pasquereau, Sandy Haidar Ahmad.
✉email: georges.herbein@univ-fcomte.fr

Received: 16 March 2023 Revised: 20 April 2023 Accepted: 21 April 2023
Published online: 5 May 2023

potential link between HCMV, PGCCs, and EZH2. Myc has been found overexpressed in GBM; its expression correlates with glioma grade where 60–80% of GBM reveal elevated Myc levels [25]. In glioma cells, EZH2 knockdown depleted Myc expression [19]. Further, Myc direct transcriptional regulation by EZH2 may establish a new mechanism underlying glioma cancer stem cell maintenance [17].

Although the mainstay of treatment for GBMs is surgery, followed by radiation and chemotherapy especially temozolomide (TMZ), new therapeutic strategies are needed. The development of checkpoint inhibitors has opened new possibilities to fight GBM [26]. In addition, some EZH2 inhibitors have been proven efficient in some poor prognosis cancers [27]. The detection of HCMV in GBM biopsies could suggest the use of anti-HCMV therapies [28]. Immunotherapies directed against HCMV antigens [29, 30] seem to show that curtailing HCMV infection contributes to a positive outcome in GBM patients.

To assess the HCMV oncogenic potential in human astrocytes (HAs), HAs were infected with HCMV-DB and BL clinical strains that were previously isolated in our laboratory and shown to elicit the transformation of human mammary epithelial cells [7, 24]. Herein, we screened the two HCMV clinical strains for their transforming potential and analyzed for the first time the molecular and cellular features of CMV-elicited glioblastoma cells, CEGBCs, which appeared in long-term cultures. Moreover, we assessed the impact of TMZ, the antiviral drug GCV, and EZH2 inhibitor (GSK 343) in vitro within this glioblastoma model. Given the stated EZH2 oncogenic functions, we aimed to evaluate the presence of a potential link between the triad of HCMV, CEGBCs and EZH2, as well as the potential interrelation with Myc in the context of glioblastoma carcinogenesis. This was complemented by deciphering the morphological and phenotypic characteristics of CEGBCs and the potential implication of Myc and PRC2 proteins in both CEGBCs and GBM biopsies. In the latter, we isolated eleven clinical HCMV strains that displayed oncogenic, stemness, and invasiveness features when cultivated on HAs with enhanced EZH2/Myc expression that could be curtailed by combination therapy including TMZ, GCV, and EZH2 inhibitors.

RESULTS

HCMV clinical isolates permissively infect HAs inducing increased Myc and EZH2 expression

The cellular environment induced by HCMV infection was assessed by studying the tropism of DB and BL high-risk HCMV strains (Fig. 1) as well as KM and FS low-risk HCMV strains (Supplementary Fig. 1) to HAs. HCMV-DB and BL strains replicated in HAs with a burst of viral growth (6 logs for DB and 3 logs for BL) followed by occasional blips (Fig. 1a and Supplementary Fig. 2). Acute infection was then confirmed through immediate early gene (IE1), pp65, and the late HCMV antigens detection (Fig. 1b, c and Supplementary Fig. 1). In addition, IE1 and early/late gene (UL69) transcripts were detected in HAs infected with HCMV-DB and BL compared to controls (Fig. 1d). At day 3 post-infection, Myc was overexpressed in HAs-DB and BL compared to controls (p-value = 0.09), mostly in HAs-DB. Elevated EZH2 expression was detected in HAs-DB and BL compared to uninfected HAs (p-value = 0.02) (Fig. 1e). Myc and EZH2 transcripts were detected in HAs-DB and BL compared to controls (Fig. 1f). Lower apoptosis levels were recognized with the two strains (Fig. 1g) in line with Akt and pAkt-Ser473 upregulation as confirmed by western blot and FACS, particularly with HCMV-DB (Fig. 1h). In contrast to the high-risk DB and BL strains, the low-risk FS and KM strains did not elicit any of the above-mentioned behavior (Supplementary Fig. 1). Taken together, a Myc^{High} $EZH2^{High}$ molecular profile was observed with both high-risk strains, preferentially with HCMV-DB.

Emergence of a glioblastoma-like phenotype with CEGBCs in HAs chronically infected with high-risk HCMV strains that display dedifferentiation, embryonic stemness, PMT traits and spheroid-forming capacity

In contrast to the low-risk HCMV strains that didn't allow long-term replication in HA cultures and were senescent (Supplementary Fig. 1), HAs infected with HCMV-DB and BL were maintained in culture for an extended period of time (Supplementary Fig. 2). Around day 80–90 post-infection, dense cellular aggregates appeared in HCMV-BL and DB cultures with invasive-like cells irradiating from the main cellular structures resembling the formerly described "go or growth" phenotype of glioblastoma cells [31] (Fig. 2a, b). Cells with a glioblastoma-like phenotype were termed *"CMV-Elicited GlioBlastoma Cells"* or CEGBCs similar to the previously reported "CMV-Transformed Human mammary epithelial cells" or CTH cells [7, 15].

We next assessed the protein expression of EZH2 and Myc in CEGBCs in which increased expression levels were observed compared to controls (Fig. 2c). CEGBCs characterization was achieved by assessing oncogenes, tumor suppressor genes and cell cycle genes. Oncogenes and cell cycle genes were mainly upregulated in CEGBCs-DB; however, tumor suppressor genes were down-regulated mostly in CEGBCs-BL (Fig. 2d, e). CEGBCs-DB and BL were seeded on a soft agar to evaluate their tumorigenic potential and colony formation was detected; uninfected HAs and HAs infected with herpes simplex virus (HSV) showed no colony formation (Fig. 2f). Primary GBM experiences the subtype switch during relapse, shifting from the proneural (PN) subtype to the mesenchymal (MES) one namely the proneural-mesenchymal transition (PMT), thus acquiring a therapy-resistant phenotype [32]. With regards to PMT markers, vimentin was elevated mostly in CEGBCs-DB, and to a lesser extent in CEGBCs-BL (Fig. 2g). CD44, a widely accepted marker for cancer stem cells and a mesenchymal marker regulating both stemness and epithelial-mesenchymal plasticity, was shown to be predominantly upregulated in CEGBCs-DB (Fig. 2h). EMT genes were mostly upregulated in CEGBCs-DB compared to CEGBCs-BL (Fig. 2i). CEGBCs-DB were shown to be close to the transcriptome profile of mesenchymal glioblastoma (mGB) whereas CEGBCs-BL expressed more PN traits (mesenchymal markers: p-value $_{(CEGBCs\text{-}DB:CEGBCs\text{-}BL)} = 0.002$; proneural markers: p-value $_{(CEGBCs\text{-}DB:CEGBCs\text{-}BL)} = 0.06$) (Fig. 2j). Taking into account the proteomic and transcriptome data, CEGBCs-DB mostly displayed a mesenchymal phenotype compared to CEGBCs-BL. High levels of SOX2, Oct4, and SSEA4 were detected in CEGBCs (Fig. 3a and Supplementary Fig. 5a, b). Hence, the identified stemness features in CEGBCs indicated their relevance to glioblastoma stem cells (GSCs). Assessing the spheroid formation potential of CEGBCs, spheroids were generated 24–48 hours post-seeding; no spheroid formation was detected in HAs infected with HSV (Fig. 3b). Nestin and IE1 were concomitantly expressed in CEGBCs-DB and BL spheroids (Fig. 3c).

CEGBCs productively infected with high-risk HCMV display invasiveness

CEGBCs from spheroids readily invaded astrocyte scaffolds, by aligning along and intercalating between astrocytes and penetrating all scaffold layers as measured by nestin detection. After 7 days, nestin was present in the spheroids' core and invasive part; cells were IE1 and nestin-positive. HCMV-IE1 was predominantly located in the spheroid core and present in the individual cells detaching from the core (Fig. 3d). Uninfected HAs expressed GFAP in the absence of nestin (Supplementary Fig. 13). PGCCs and neural progenitor cell (NPC)-like cells, positive for nestin and IE1, were also present (Fig. 3e, f); supernatants were positive for HCMV-IE1 indicating ongoing viral replication (Supplementary Fig. 8). Further, using a 3D collagen-invasion assay, invasiveness was noticed for CEGBCs-DB and to a lesser extent for CEGBCs-BL as measured by the invasion area (Fig. 3g, h); the protrusions'

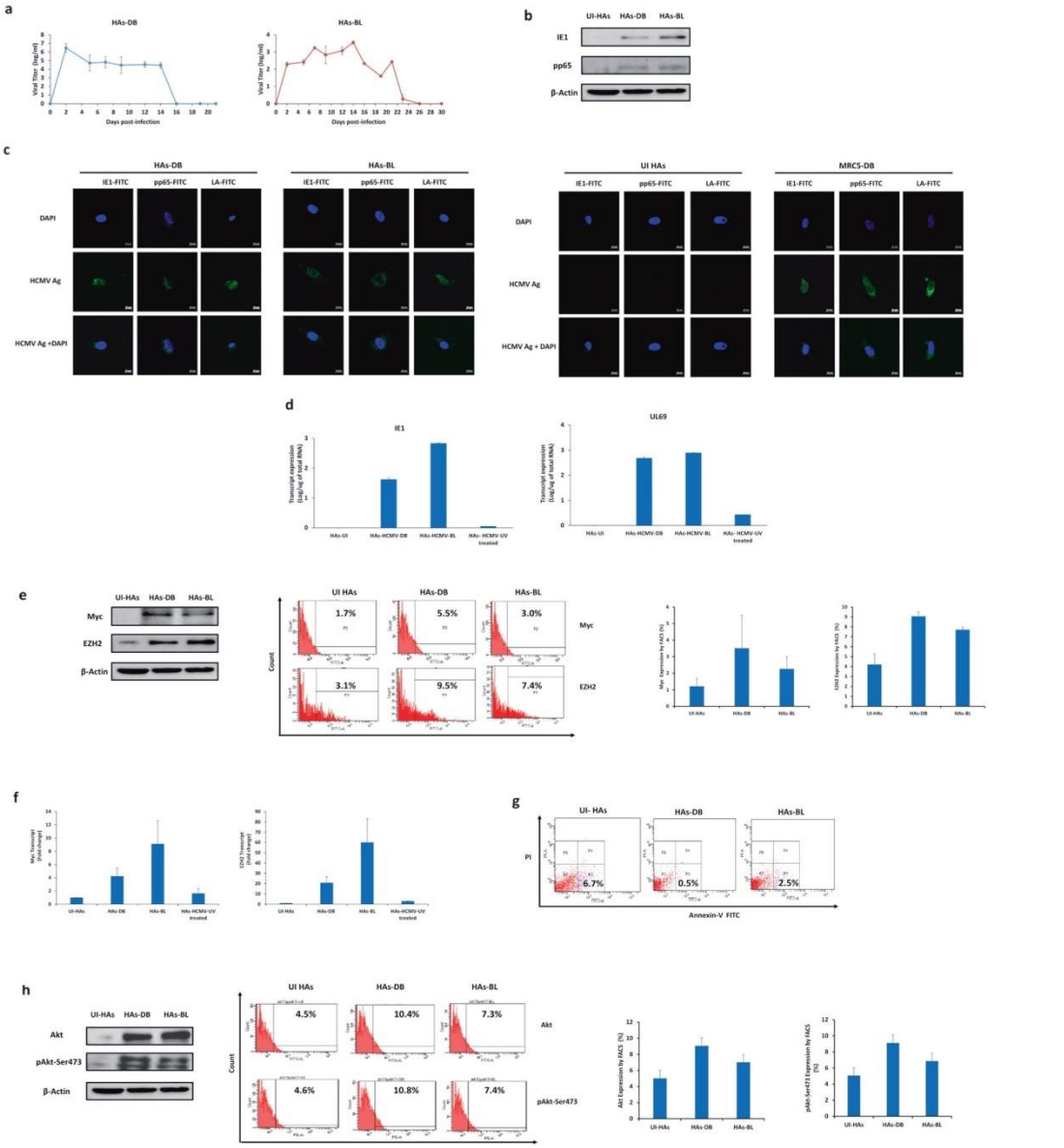

Fig. 1 Replication of two high-risk oncogenic HCMV strains in HAs cultures, the activation of oncogenic pathways, and reduced apoptosis rates. a Time-course of the viral titer in the supernatant of HAs infected with HCMV-DB and BL as measured by IE1-qPCR. **b** Immunoblotting data of IE1 and pp65 in uninfected HAs lysates and HAs infected with HCMV-DB and BL (day 5 post-infection). β-actin was used as loading control. **c** Confocal microscopic images of HCMV-IE1, pp65, and late antigen staining in HAs infected with HCMV-DB and BL (day 1 post-infection). Uninfected HAs and MRC5-DB cells were used as negative and positive controls, respectively. Nuclei were counterstained with DAPI; magnification ×63, scale bar 10 μm. **d** IE1 and UL69 transcripts detection by RT-qPCR in uninfected HAs, HAs-DB and BL as well as HAs infected with UV-treated HCMV. **e** Myc and EZH2 protein expression as measured by western blot (day 5 post-infection) and FACS (day 3 post-infection) in uninfected HAs and HAs infected with HCMV-DB and BL. β-actin was used as loading control. **f** Myc and EZH2 transcripts detection by RT-qPCR. **g** Early apoptosis assessment in HAs-DB and BL (MOI = 1). UI HAs were used as a control. **h** Akt, and pAkt-Ser473 protein expression as measured by western blot and FACS in uninfected HAs and HAs infected with HCMV-DB and BL. β-actin was used as loading control. Data are represented as mean ± SD of two independent experiments.

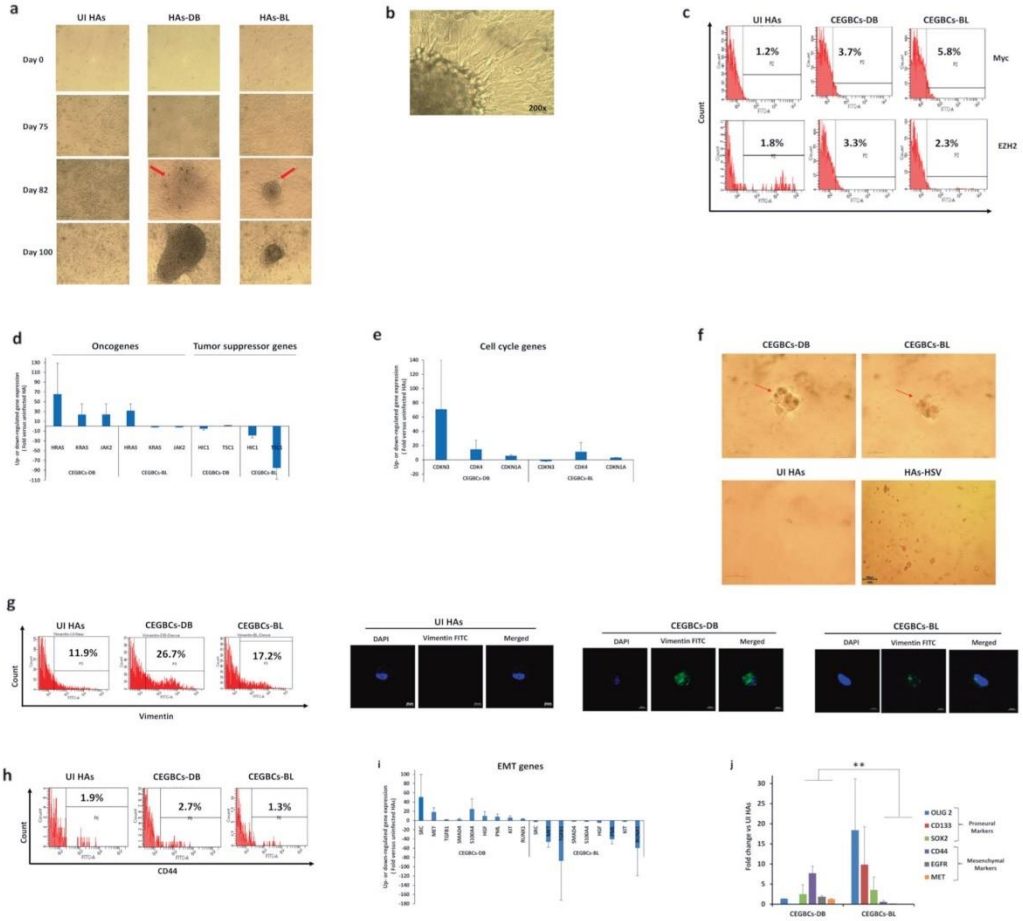

Fig. 2 Chronic infection of HAs with HCMV clinical isolates, the appearance of CEGBCs as well as colony formation in soft agar, and the phenotypic characterization of CEGBCs. a HAs time-course infection with HCMV-DB and BL strains (MOI = 1). Red arrows showing the generated CEGBCs. Magnification ×100, scale bar 100 µm. Uninfected HAs were used as a control. **b** An inverted light microscope was used to closely follow up the chronic CEGBCs-DB and BL cultures and the appearance of several structures; magnification 200x, scale bar 100 µm. **c** FACS staining of Myc and EZH2 in HAs infected with HCMV-DB and BL; uninfected HAs were used as a negative control. The fold regulation of oncogenes and tumor suppressor genes (**d**) as well as cell cycle genes (**e**) was assessed in uninfected HAs and HAs infected with HCMV-DB and BL using RT^2 Profiler PCR Arrays. **f** Colony formation in soft agar seeded with CEGBCs-DB and BL (MOI = 1); UI HAs and HAs-HSV were used as controls. Formed colonies were observed under an inverted light microscope (Magnification 200x, scale bar 100 µm). **g** Vimentin expression by FACS and confocal microscopy in CEGBCs-DB and BL; uninfected HAs were used as a control. Nuclei were counterstained with DAPI; magnification ×63, scale bar 10 µm. **h** FACS staining of CD44 in CEGBCs-DB and BL. Uninfected HAs were used as controls. **i** The fold regulation of EMT genes was assessed in UI HAs and HAs infected with HCMV-DB and BL using RT^2 Profiler PCR Arrays. **j** Histogram depicting the expression of PN markers (OLIG2, CD133, and SOX2), MES markers (CD44, EGFR, and MET), as quantified by RT-qPCR in CEGBCs-DB and BL. ***p*-value ≤ 0.01. Data are represented as mean ± SD of two independent experiments.

number and length were also recorded (Supplementary Fig. 7). Within the CEGBCs-DB cultures, the majority of invading cells adopted a neural progenitor-like phenotype with a round small cell body and a long leading process characterized by high cell motility (Supplementary Fig. 9, left panel). Cellular heterogeneity occurred among the invasive cells with random morphology in which low motility cells co-existed with highly motile cells (Supplementary Fig. 9). Three mechanisms of invasiveness were detected in CEGBCs-DB and BL cultures as recently reported [33] (Supplementary Fig. 10a–c). Filopodia and lamellipodia were also observed (Supplementary Fig. 10d).

Detection of lncRNA4.9/EZH2 and HOTAIR/EZH2 complexes in CEGBCs cultures

HCMV latency in CEGBCs cultures was established by IE1 expression that was observed at day 1 post-TPA treatment

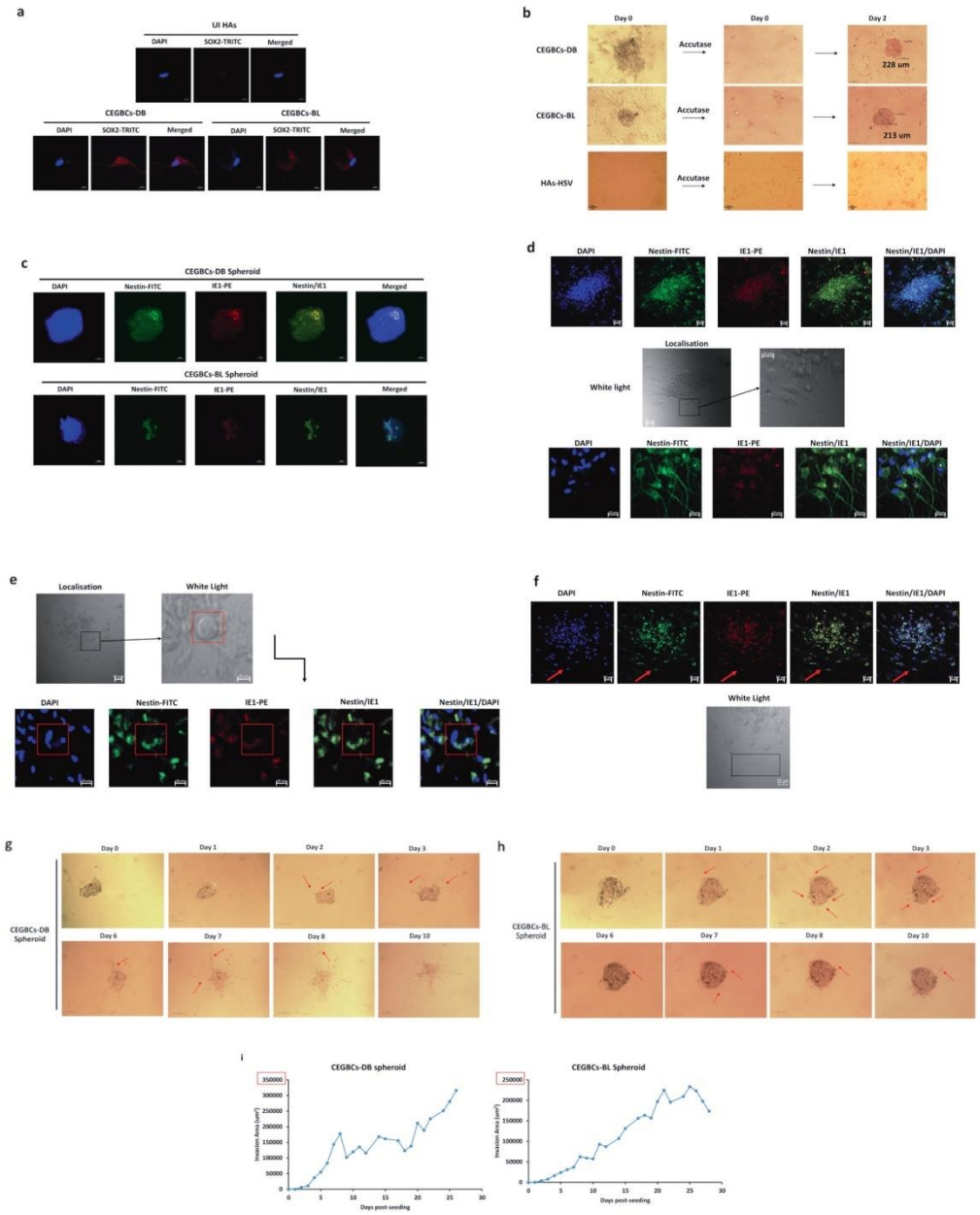

(Fig. 4a and Supplementary Fig. 6) parallel to the detection of HCMV gene (lncRNA4.9) (Fig. 4b). In agreement with the presence of the lncRNA4.9 gene in EZH2-expressing CEGBCs, we observed the interaction of HCMV lncRNA4.9 and cellular lncRNA HOX antisense intergenic RNA (HOTAIR) transcripts with EZH2 using RNA CLIP assay (Fig. 4c, d). Cellular lncRNA HOTAIR transcript, reported as a poor prognostic factor in cancers [34] was detected particularly in the EZH2 immunoprecipitated samples corresponding to CEGBCs-DB compared to CEGBCs-BL (Fig. 4d).

Fig. 3 Spheroid-forming potentials of CEGBCs as well as invasiveness and migration. a Confocal microscopic images of SOX2 and DAPI staining in CEGBCs-DB and BL. UI HAs were used as controls; magnification ×63, scale bar 10 µm. **b** Schematic for spheroid generation from the chronically infected DB and BL astrocytes (day 222 post-infection); magnification 100x, scale bar 100 µm. HAs-HSV were used as a negative control. **c** Concomitant staining of IE1 and Nestin in CEGBCs-DB and BL spheroids. Nuclei were counterstained with DAPI; magnification ×63, scale bar 10 µm. **d** HCMV-IE1 and Nestin staining in 3D-scaffolds formed by CEGBCs in confluent culture and seeded with CEGBCs-DB and BL spheroids using confocal microscopy; magnification x20, scale bar 20 µm. Confocal microscopic images of Nestin and IE1 staining in PGCCs (**e**) and isolated cells (**f**) present in CEGBCs-BL culture (red arrows). Nuclei were counterstained with DAPI; magnification ×20, scale bar 20 and 50 µm. Time-course of the 3D-invasion assay where CEGBCs-DB (**g**) and BL (**h**) spheroids were embedded into type-1 collagen in the presence of HCl; red arrows showing cell invasion. Magnification x100, scale bar 100 µm. **i** Graphs showing the variation in the invasion area of CEGBCs-DB and BL spheroids. Measurements were taken using ImageJ; data are represented as mean ± SD of two independent experiments.

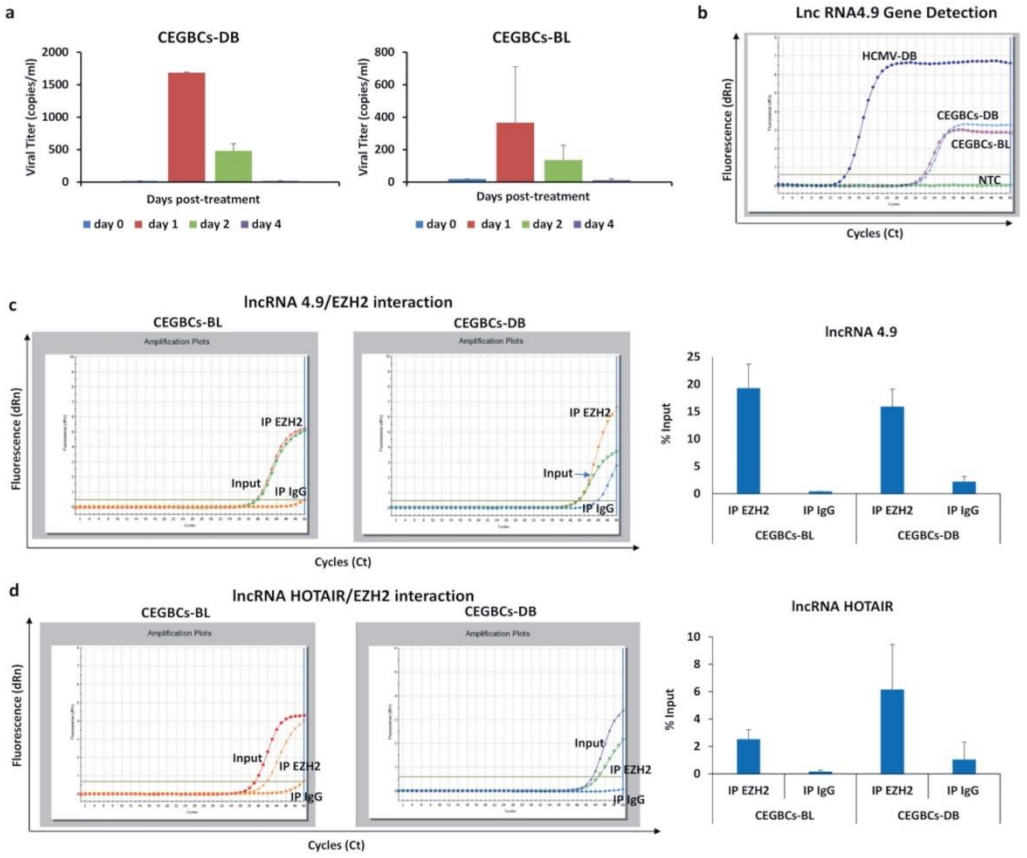

Fig. 4 Detection of replicative HCMV and identification of the lncRNA4.9 and HOTAIR/EZH2 complex in CEGBCs cultures. a Histograms representing the viral load post-TPA treatment (100 nM) in CEGBCs-DB and BL cultures as measured by IE1-qPCR. **b** lncRNA 4.9 gene detection in CEGBCs-DB and BL using RT-qPCR. HCMV-DB sample was used as a positive control. NTC: no template control. lncRNA 4.9 (**c**) and lncRNA HOTAIR (**d**) transcript detection in the EZH2 IP samples of CEGBCs-DB and BL, as measured by RT-qPCR. Mouse anti-IgG was used as an isotype control. Data are represented as mean ± SD of two independent experiments.

Upregulation of EZH2 and Myc in HCMV-positive GBM tissues

To further decipher the role of HCMV and EZH2-Myc pathway in vivo, we analyzed 37 GBM biopsies (MGMT promoter methylated $n = 17$ and MGMT promoter unmethylated $n = 20$) for the presence of HCMV as well as EZH2 and Myc expression. Tumor biopsies displayed an enhanced EZH2 and Myc expression in both MGMT promoter methylated and unmethylated tissues, particularly in MGMT promoter unmethylated ones (Fig. 5b). HCMV was detected in all GBM samples (100%) (Supplementary Table 3). In all GBM biopsies, there was a statistically significant strong correlation between Myc and EZH2 expression (Fig. 5c). A significant strong correlation was found between HCMV presence (IE1 gene)

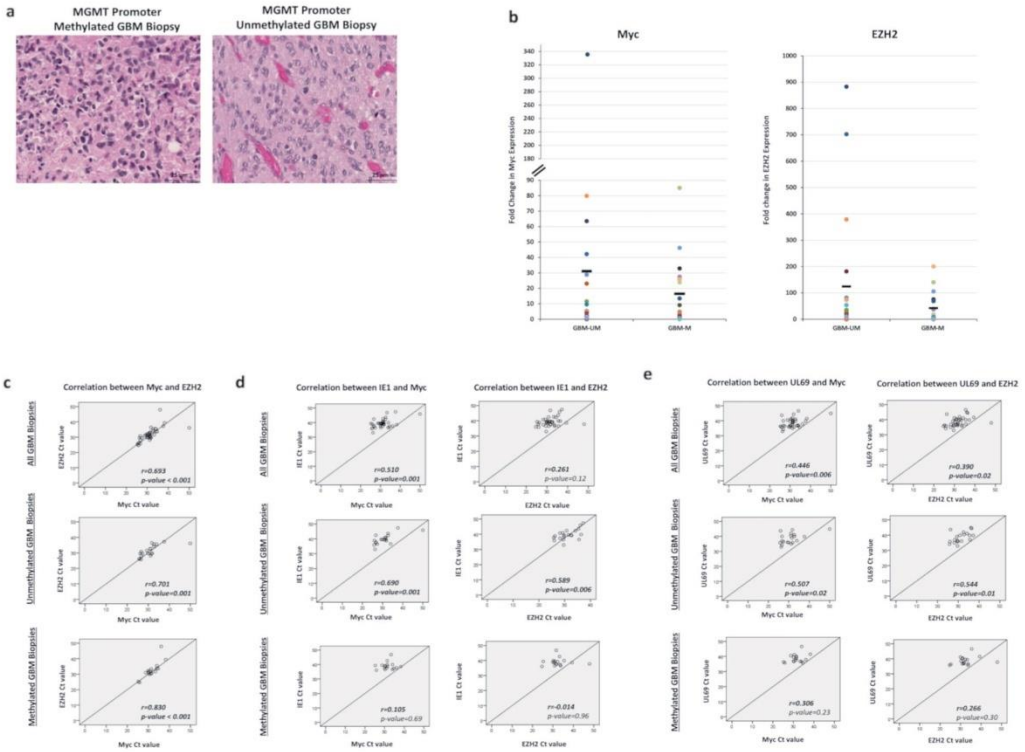

Fig. 5 HCMV detection as well as EZH2, and Myc expression in glioblastoma biopsies. a Glioblastoma multiforme tissue was stained using HES; magnification x40, scale bar 25 µm. **b** Scattered plots showing Myc, and EZH2 expression in individual methylated, and unmethylated HCMV-positive GBM biopsies. Mean values are indicated. **c** Correlation test between Myc and EZH2 expression in all GBM biopsies, methylated, and unmethylated HCMV-positive GBM biopsies. Correlation test between IE1 (**d**) and UL69 (**e**) presence and the expression of Myc and EZH2. *p*-values were determined by Pearson's correlation test.

and Myc/EZH2 expression in unmethylated GBM biopsies ($r = 0.690$, p-value $= 0.001$; $r = 0.589$, p-value $= 0.006$; respectively) (Fig. 5d). In unmethylated GBM biopsies, HCMV presence (UL69 gene) strongly correlated with Myc/EZH2 expression ($r = 0.507$, p-value $= 0.02$ and $r = 0.544$, p-value $= 0.01$, respectively) (Fig. 5e). On the other hand, a weak to moderate correlation was detected between HCMV presence and Myc/EZH2 expression in methylated GBM biopsies (Fig. 5d, e).

Isolation of oncogenic HCMV strains from GBM tumors

Among the thirty-seven GBM biopsies, eleven GBM biopsies were considered for HCMV isolation. Eleven HCMV-GBM strains were isolated from MGMT promoter methylated ($n = 4$) and MGMT promoter unmethylated ($n = 7$) GBM tumors by tissue disruption and filtration, and were subsequently grown in MRC5 cells showing a peak of viral load (1–3 log) around day 20 post-infection (Fig. 6a and Supplementary Table 4). Following HAs infection with the eleven HCMV-GBM strains, we detected cell clusters with irradiating low and high motility cells displaying a neural progenitor-like phenotype (Fig. 6b) parallel to the sustained viral replication confirmed by FACS (Fig. 6c) and IE1 gene detection by qPCR (Fig. 6d). Viral transcripts (IE1 and UL69) were detected in HAs infected with methylated and unmethylated HCMV-GBM strains compared to uninfected HAs (Fig. 6e). Upregulated Myc and EZH2 proteins and transcripts were detected in HAs infected with methylated and unmethylated HCMV-GBM strains, unlike uninfected HAs (Fig. 6f–h and Supplementary Table 4). All HCMV-GBM isolates transformed HAs as measured by soft agar colony formation assay (p-value $_{(\text{UI HAs: HCMV-GBM})} = 0.02$; p-value $_{(\text{UI HAs: HCMV-GBM-M})} = 0.04$, p-value $_{(\text{UI HAs: HCMV-GBM-UM})} = 0{\cdot}03$) (Fig. 6i).

Spheroids were generated 24–48 hours post-seeding the HAs infected with the clinical HCMV-GBM strains (p-value $_{(\text{UI HAs: HCMV-GBM})} = 0.02$; p-value $_{(\text{UI HAs: HCMV-GBM-M})} = 0.04$, p-value $_{(\text{UI HAs: HCMV-GBM-UM})} = 0.03$) (Fig. 7a). High SOX2 levels were detected in spheroids generated from the eleven HCMV-GBM strains (Fig. 7b and Supplementary Table 4). Nestin and IE1 were concomitantly expressed in spheroids generated from all HCMV-GBM strains (Fig. 7c). Spheroids generated from the HCMV-GBM strains did not express GFAP unlike uninfected HAs (Supplementary Fig. 13). Further, a 3D collagen-invasion assay was performed to evaluate the invasiveness potential of the spheroids generated from HCMV-GBM strains (Fig. 7d). The lncRNA4.9 gene was detected in CEGBCs derived from HCMV-GBM strains (Fig. 7e). Viral lncRNA4.9 and cellular lncRNA HOTAIR transcripts were detected in the EZH2

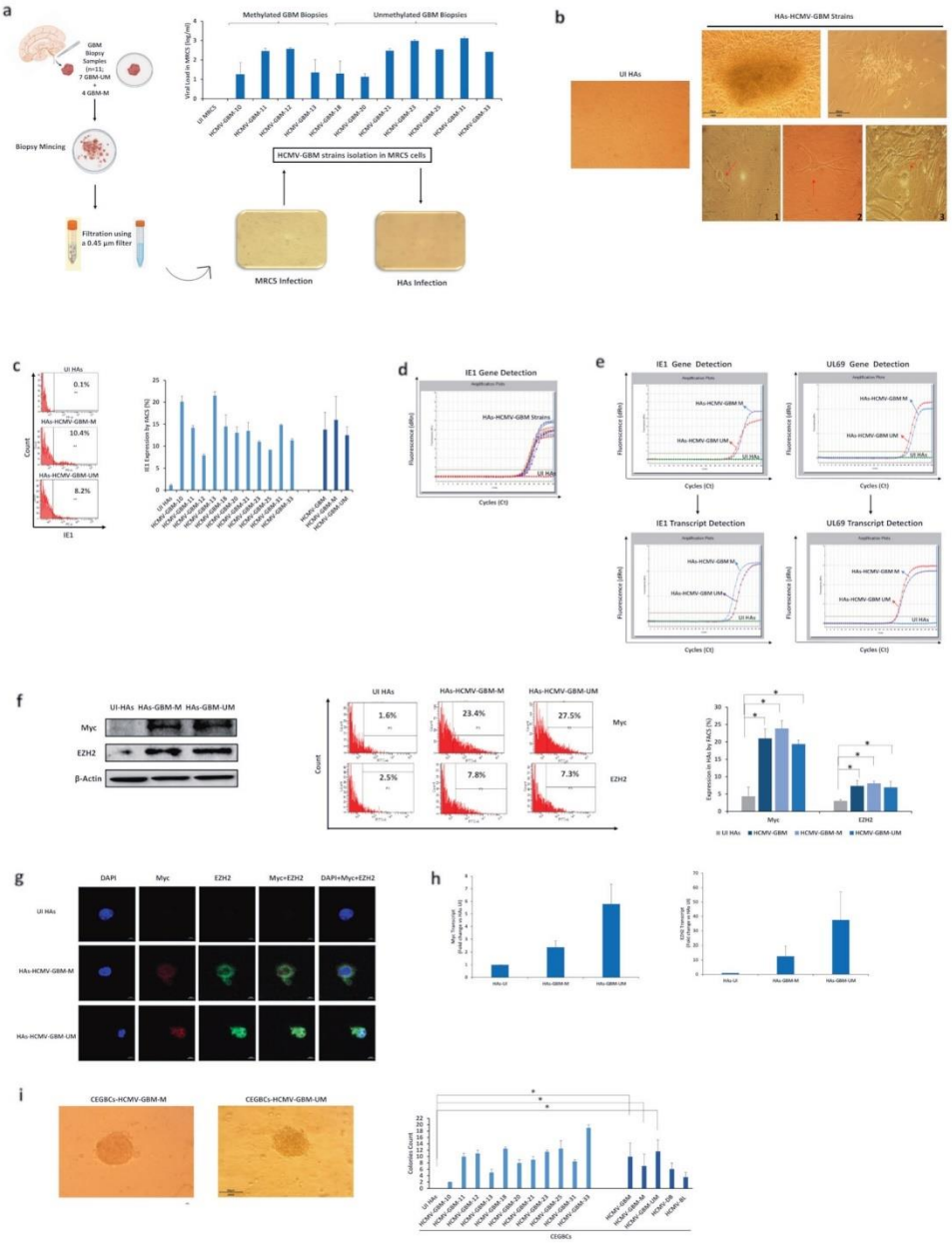

immunoprecipitated samples corresponding to CEGBCs derived from all HCMV-GBM strains, mostly from MGMT promoter unmethylated HCMV-GBM strains, using RNA CLIP assay (p-value $_{(UI\ HAs:GBM)} = 0.03$; p-value $_{(UI\ HAs:\ GBM\text{-}M)} = 0.07$; p-value $_{(UI\ HAs:\ GBM\text{-}UM)} = 0.04$) (Fig. 7f).

EZH2 inhibitor, TMZ, and GCV tritherapy curtails CEGBCs growth

Although TMZ is known as the first-choice chemotherapeutic agent in glioblastoma, TMZ resistance often becomes a limiting factor in effective glioblastoma treatment [35, 36]. Herein, we

Fig. 6 Isolation of oncogenic HCMV strains from GBM biopsies. a Isolation protocol of eleven HCMV-GBM strains from GBM tissues; seven unmethylated and four methylated GBM biopsies. Histogram representing the viral replication of the isolated HCMV strains in MRC5 cultures. UI MRC5 cells were used as control. **b** The subsequent infection of HAs generating CEGBCs. Microscopic images showing the different cellular morphology (red arrows) generated in human astrocytes infected with the eleven isolated GBM HCMV strains; (1) neural progenitor cell (NPC)-like cells; (2) dendritic-like cells with cytoplasmic prolongation, and (3) PGCCs; magnification x100, scale bar 100 µm. IE1 protein and gene expression in the isolated methylated and unmethylated promoter HCMV-GBM strains as measured by FACS (**c**) and qPCR (**d**), respectively; UI HAs were used as a control. **e** IE1 and UL69 gene and transcript detection in HAs infected with the isolated methylated and unmethylated promoter HCMV-GBM strains as measured by qPCR and RT-qPCR, respectively. **f** Myc and EZH2 expression in the isolated methylated and unmethylated GBM strains, as measured by western blot and FACS; uninfected HAs were used as a control. β-actin was used as loading control. Histogram representing Myc and EZH2 expression in uninfected HAs, the total isolated HCMV-GBM strains, methylated and unmethylated HCMV-GBM strains as measured by FACS. **g** Confocal microscopic images of Myc and EZH2 staining in HAs infected with the isolated methylated and unmethylated promoter HCMV-GBM strains. Nuclei were counterstained with DAPI; magnification ×63, scale bar 10 µm. **h** Myc and EZH2 transcripts detection by RT-qPCR. **i** Colony formation in soft agar seeded with CEGBCs generated from HAs infection with the isolated methylated and unmethylated promoter HCMV-GBM strains; UI HAs were used as a control. Formed colonies were observed under an inverted light microscope (Magnification 200x, scale bar 100 µm). Histograms representing the number of colonies generated in all GBM strains as well as methylated and unmethylated HCMV-GBM strains. Data are represented as mean ± SD of two independent experiments. *p-value ≤ 0.05.

evaluated EZH2 inhibitor GSK343, GCV and TMZ efficacy as single therapies, as well as bi- or tri-combination therapy on CEGBCs-DB, BL, and GBM spheroids (Fig. 8). TMZ reduced spheroids' size by 23% only in CEGBCs-BL cultures, unlike CEGBCs-DB which displayed more mesenchymal traits (p-value $_{(CEGBCs\text{-}DB:CEGBCs\text{-}BL)} = 0.03$). GCV reduced the spheroids' size by 21% and 24% in CEGBCs-DB and BL, respectively (p-value $_{(CEGBCs\text{-}DB:CEGBCs\text{-}BL)} = 0.35$). On the other hand, GCV/TMZ combination therapy lead to a 27% size reduction of CEGBCs-BL spheroids, meanwhile having a very limited effect in CEGBCs-DB in which the spheroids' size was reduced by 9% (p-value $_{(CEGBCs\text{-}DB:CEGBCs\text{-}BL)} < 0.01$) (Fig. 8a). Spheroids of CEGBCs-DB and BL were treated by GSK343, GSK343/GCV, GSK343/TMZ, and GSK343/GCV/TMZ. CEGBCs-DB were resistant to mostly all therapies except the triple therapy (p-value $_{(CEGBCs\text{-}DB:CEGBCs\text{-}BL)} = 0.06$) unlike CEGBCs-BL that were mainly responsive to GSK343/TMZ (p-value $_{(CEGBCs\text{-}DB:CEGBCs\text{-}BL)} < 0.001$) and triple treatment ($p$-value $_{(CEGBCs\text{-}DB:CEGBCs\text{-}BL)} = 0.06$) (Fig. 8a). Under triple therapy (GSK343/GCV/TMZ), spheroids' size was reduced by around 90% in CEGBCs-DB and BL at day 10 post-treatment (p-value $_{(triple\ therapy:\ TMZ)} = 0.02$) (Fig. 8b). Spheroids' size was reduced by around 60% with all the eleven HCMV-GBM strains at day 10 post-triple treatment (GSK343/GCV/TMZ) (p-value $_{(triple\ therapy:\ TMZ)} < 0.001$) (Fig. 8c), similar to that reported for DB and BL strains.

DISCUSSION

In the present study, we assessed the potential transforming capacities of HCMV-DB and BL following the HAs infection, previously classified into high-risk transforming strains [15, 24, 37, 38]. HAs infection with the high-risk HCMV-DB and BL strains resulted in a pro-oncogenic cellular environment and sustained growth of CEGBCs with soft agar colonies formation, unlike HAs infected with the low-risk HCMV-KM and FS strains that showed no transforming potentials and resulted in cell death in the long term cultures. CEGBCs displayed a "go and growth" phenotype in 2D monolayer cultures, dedifferentiated and displayed stemness as well as PMT features, and finally resulted in spheroid formation and invasion in 3D cultures (Supplementary Fig. 14). PGCCs appearance as well as cellular heterogeneity were previously allied to cultures of mammary epithelial cells infected with the high-risk HCMV strains [15, 39]. Similar to HMECs transformed with the high-risk HCMV strains, around day 80 post-infection, we observed the appearance of dense cell aggregates, followed by the emergence of a wide array of morphologically distinct cells in HCMV-DB and BL cultures (Fig. 2a and Supplementary Fig. 4). We named these cells CMV-elicited glioblastoma cells (CEGBCs) with reference to the CMV-transformed HMECs (CTH) cells. PGCCs, NPC-like, neuron-like and mesenchymal-like cells were detected as well as filopodia, lamellipodia, and asymmetric cell division patterns (Fig. 3, Supplementary Fig. 10, and Supplementary Fig. 15). The described patterns could be representative of self-renewing cells undergoing diverse stages of the previously described giant cell cycle [15, 39], although blastomere-like structures weren't so far detected as reported previously in CTH cells [15]. A replication-competent virus susceptible to reactivation from latency upon TPA treatment has been detected in CEGBC cultures. Activation of the Myc/EZH2 axis was observed in acute and sustained chronic infection with both high-risk HCMV strains. In agreement with EZH2 activation by HCMV, we observed a direct interaction between EZH2 and HCMV lncRNA4.9 transcript, likewise between EZH2 and cellular lncRNA HOTAIR transcript, a poor prognosis oncogenic factor for glioma patients. In line with EZH2 and HCMV involvement in our glioblastoma model, combination triple therapy (GSK343/GCV/TMZ) curtailed the growth of CEGBCs-derived spheroids. In vivo, all GBM tumor biopsies were found to harbor HCMV with enhanced EZH2 and Myc expression, possessing a strong positive correlation between EZH2 and Myc expression as well as a strong correlation between EZH2/Myc and HCMV presence. Eleven HCMV-GBM strains were isolated from GBM tumors which acutely transformed HAs toward CEGBCs with increased EZH2/Myc expression that undergo dedifferentiation towards glioblastoma stem cells with spheroid formation and invasiveness capacities that could be curtailed by GSK343/GCV/TMZ triple therapy.

Among the mechanisms studied to transform HAs and promote disease progression in addition to poor prognosis in GBM, is the coupling of Myc and EZH2 overexpression as well as the depletion of retinoblastoma protein (Rb) (Fig. 1 and Supplementary Fig. 3) which was observed in our study [17, 40]. Although limited Myc upregulation and Rb downregulation were observed, none of the two low-risk HCMV-KM and FS strains transformed HAs as measured by soft agar colony formation in addition to the cell death observed in prolonged cultures (Supplementary Fig. 1). On the other hand, the high-risk clinical isolates HCMV-DB and BL can drive HAs towards oncogenic transformation in vitro. Our findings conform to the "astrocyte dedifferentiation theory" corresponding to glioblastoma origin [41–43]. In contrast to uninfected HAs, the distinct transcriptome profile including oncogenes, tumor suppressor genes and cell cycle genes facilitated the characterization of CEGBCs that possess a glioblastoma-like phenotype [44, 45]. Stemness acquisition, commonly described in metastasis and poorly differentiated tumors [46–48], is in accordance with previous findings where GB-generated spheroids are composed of glioma stem cells (GSCs). The concomitant presence of the stemness marker nestin and HCMV-IE1 was detected in the spheroid structures generated from CEGBCs, as reported for nestin in the cell lines derived from GBM [49]. Highly motile Nestin/IE1-

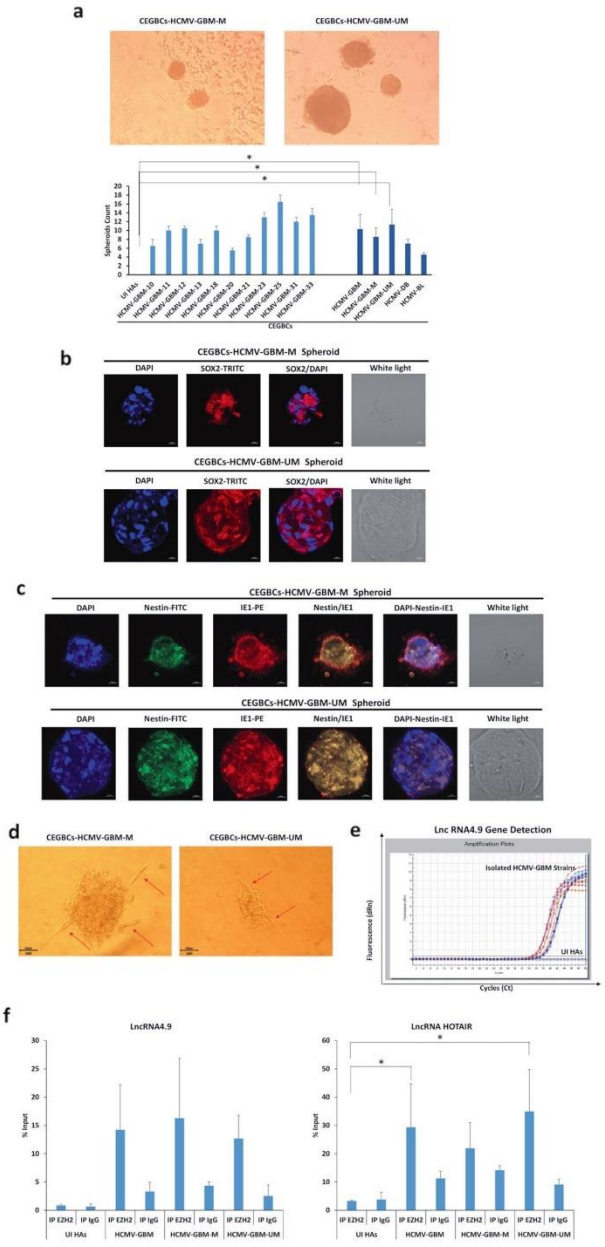

Fig. 7 Spheroid forming and invasion potentials of the HCMV-GBM strains and the detection of lncRNA 4.9 and HOTAIR transcripts. **a** Microscopic images of the spheroids generated from the isolated GBM HCMV strains; magnification ×100, scale bar 20 µm. Histograms representing the number of spheroids generated in all HCMV GBM strains as well as methylated and unmethylated HCMV-GBM strains; UI HAs were used as a control. Confocal microscopic images of SOX2 (**b**) and concomitant Nestin/IE1 (**c**) staining in spheroids generated from the isolated HCMV-GBM strains. Nuclei were counterstained with DAPI; magnification ×63, scale bar 10 µm. **d** Microscopic images showing the invasion potential of CEBGCs through protrusions and cell migration (red arrows); magnification ×200, scale bar 20 µm. **e** lncRNA 4.9 gene detection in the supernatants of HAs infected with the isolated HCMV-GBM strains using qPCR; UI HAs were used as a control. **f** Interaction of lncRNA4.9 and HOTAIR transcripts with EZH2 in CEGBCs-GBM using RNA cross-linking immunoprecipitation (CLIP) assay.

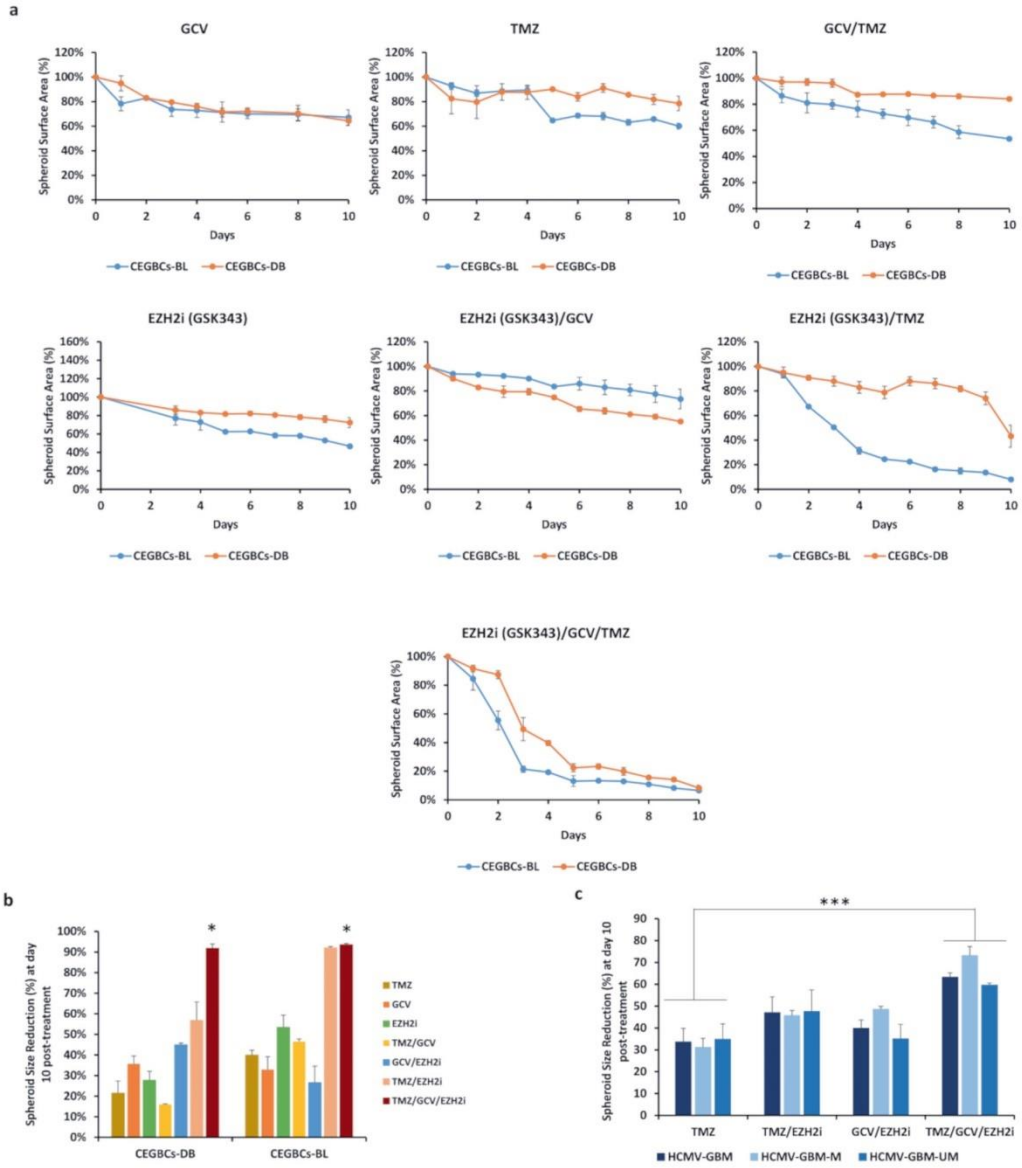

Fig. 8 The effect of diverse single and combination therapies on CEGBCs' growth. a Curves representing the spheroid surface area corresponding to CEGBCs-DB and BL under GCV(20 μM), TMZ(50 μM), GCV(20 μM)/TMZ(50 μM), GSK343 (0.1 μM), GSK343 (0.1 μM)/ GCV(20 μM), GSK343 (0.1 μM)/TMZ(50 μM), and GSK343 (0.1 μM)/GCV(20 μM)/TMZ(50 μM) therapies. **b** Histogram representing the CEGBCs-DB and BL spheroids size reduction 10 days post-treatment. Data are represented as mean ± SD of two independent experiments. *p-value ≤ 0.05. **c** Histogram representing the CEGBCs-GBM spheroids size reduction at day 10 post-treatment. Data are represented as mean ± SD of two independent experiments. *p-value ≤ 0.05; ***p-value ≤ 0.001.

positive cells were spotted leaving the core which are similar to the neural-progenitor-like tumor cells detected in glioblastoma, especially the ones adopting the Lévy-like movement patterns [1, 33]. The concomitant presence of viral proteins and nestin within transformed cells has been reported for the two herpes oncoviruses EBV and KSHV [50, 51]. In agreement with enhanced CD44 and CD133 expression in CEGBCs, their expression in glioblastoma stem cells correlates with cell proliferation, intra-

tumor heterogeneity, invasion and poor prognosis in CD44-expressing glioma [46, 52]. The presence of vimentin^{+}/CD44^{+} cells in CEGBC cultures as well as the detection of stem cells expressing SOX2 and nestin confirms the PMT plasticity. In agreement with the proneural-mesenchymal plasticity described upon oncogenic stress activation highlighting astrocyte plasticity/reactivity during tumorigenesis [32, 53, 54], a high invasive potential was observed in CEGBCs-DB compared to BL with increased mesenchymal traits indicating a more aggressive behavior that might drive therapeutic resistance.

Accumulated evidence highlighted Myc and EZH2 as key players in both oncogenesis and stemness. Myc stimulates EZH2 expression by activating the EZH2 promoter [55], repressing miR-26a [20], or directly suppressing miR-137. Bromodomain-4 protein (BRD4) positively regulates EZH2 transcription through Myc upregulation [56]. Myc activation was reported in glioblastoma progression, particularly in poor prognosis and therapy resistant-tumors [55, 57]. EZH2 mediates proliferation, migration, and invasion in GBM. High-risk HCMV clinical strains DB and BL differentially induce Myc upregulation, and consequently stimulate EZH2 overexpression as well as CEGBCs induction, pointing toward the presence of Myc/EZH2/CEGBCs axis underlying the described results. Though, the interrelationship between HCMV and EZH2 is further complexed by the detection of HCMV lncRNA4.9 gene in CEGBCs which is in line with Rossetto et al. report [21]. Consistent with our data, the cellular lncRNA HOTAIR was described to interact with EZH2 in glioblastoma, thus linked to tumor dissemination, PMT, and drug resistance [57, 58]. The noticeable detection of high lncRNA HOTAIR in the EZH2 IP samples corresponding to CEGBCs-DB explicates the aggressiveness of this particular high-risk HCMV strain, predicting poor prognosis. Indeed, EZH2-mediated stemness could underlie the appearance and maintenance of CEGBCs expressing a high degree of embryonic stemness, as EZH2 expression in astrocytes induced their dedifferentiation toward stem-like cells expressing nestin, SOX2, and CD133 [43]. Further, we reported the detection of HCMV in GBM tumor biopsies displaying enhanced EZH2, Myc, and Akt expression (Fig. 5 and Supplementary Fig. 11). HCMV-induced Myc and EZH2 expression along with the embryonic stem-like phenotype in the IE1-expressing CEGBCs could establish a significant model in the context of GBM.

Since EZH2 and Myc have been implicated in tumor initiation and proven to impact glioblastoma appearance and development with the two high-risk HCMV DB and BL strains isolated from biological fluids (cervical swab and urine respectively), we evaluated EZH2/Myc expression and recovered HCMV strains directly from GBM biopsies thereby assessing their oncogenic potential. Eleven HCMV strains were isolated from GBM tumors (with unmethylated and methylated MGMT promoters). After HAs infection, CEGBCs were generated with morphological features matching the previously described CEGBCs-DB and BL and led to the appearance of spheroids with invasiveness potential. HCMV-IE1 protein detection parallel to stemness markers and the upregulated Myc and EZH2 expression parallel to the detection of lncRNA4.9 gene, lncRNA4.9 and HOTAIR transcripts in cultures infected with the eleven HCMV-GBM strains recapitulates the previously observed molecular phenotype induced by HCMV-DB and BL strains. The expression of Myc was predominantly elevated in IE1-positive HAs (Supplementary Fig. 12). Altogether, HCMV strains are present in GBM tumors retaining tumor-promoting abilities, therefore considered as oncogenic strains.

Highlighting the critical role of EZH2 and HCMV in our glioblastoma model, the impact of EZH2 inhibitor (GSK343) and anti-HCMV drug ganciclovir (GCV) alone and in combination with TMZ was assessed. TMZ possessed a very limited effect on the growth of CEGBCs spheroids derived from HCMV-DB, HCMV-BL and the eleven HCMV-GBM strains. In agreement with our results, valganciclovir possessed a positive effect on glioblastoma tumors with an unmethylated or methylated MGMT promoter gene [28], potentially through its antiproliferative effect [59, 60]. Although GSK343 single therapy had a limited effect on the growth of CEGBCs spheroids, its combination with TMZ enhanced the restriction of the CEGBCs spheroids growth derived from DB and BL, and to a lesser extent HCMV-GBM strains. EZH2 may modulate TMZ resistance where blocking EZH2 reverses TMZ chemosensitivity in GBM patients; an increased number of apoptotic cells were detected by knocking down EZH2 [61]. Although encouraging responses were detected post-dual therapy (GSK343/TMZ) in CEGBCs-DB and BL, and to a lesser extent from the eleven GBM HCMV strains, the triple therapy (TMZ/GSK343/GCV) was the most effective in CEGBCs derived from DB, BL, and the eleven GBM HCMV strains. Hence, triple therapy provides the foundation for a combinational therapeutic strategy to improve overall patient survival, reduce viral resistance, and lower drug toxicity.

In conclusion, our data indicated that high-risk HCMV strains and more importantly all the HCMV-GBM strains isolated directly from GBM biopsies can induce a CEGBCs phenotype with tumor heterogeneity, proneural to mesenchymal plasticity, and embryonic-like stemness leading to spheroid formation and invasiveness. Our findings highlight the presence of a potential link between HCMV infection, Myc/EZH2 upregulation and CEGBCs induction in vitro and in GBM biopsies. A more detailed analysis of target genes within CEGBCs and their corresponding response to inhibitors may establish new avenues to understand the complex pathogenesis of glioblastoma and open the door for targeted therapies.

MATERIALS AND METHODS

Cell cultures

Primary human astrocytes (HAs) and human embryonic lung fibroblasts (MRC5) were cultured as described in "Supplementary Materials and Methods".

Viruses

Clinical HCMV strains, namely HCMV-DB (GenBank KT959235), BL (GenBank MW980585), KM, and FS were isolated from patients that were hospitalized at Besançon University Hospital (France) as described previously [7, 15]. Cell-free virus stocks and infections were performed as previously detailed [15]. Careful screening of our viral stocks was conducted to rule out the presence of other oncoviruses [15]. Infections of HAs and MRC5 cells, quantification of viral replication, and HCMV detection were performed as described previously [15] and in "Supplementary Materials and Methods". Primers used are listed in Supplementary Table 1.

Isolation and growth of CEGBCs

Upon the appearance of large cellular clusters/structures in HAs cultures that were infected with HCMV-DB and BL isolates, clusters were gently detached, cultured in astrocytes medium (Innoprot), and maintained in culture for more than 10 months. CEGBCs were cultured as described in "Supplementary Materials and Methods".

Western blotting

Expression of IE1, pp65, Myc, EZH2, Akt, and pAkt in uninfected HCMV-infected HAs was assessed as described previously [7]. β-actin was used as loading control. Antibodies used are supplied in Supplementary Table 2.

Flow cytometry analysis

Cells (1×10^5) were collected from uninfected HAs, HCMV-infected HAs, and CEGBCs, fixed, permeabilized, and stained as previously reported [15]. The antibodies used are provided in Supplementary Table 2.

RT^2 profiler PCR array

The RT^2 profiler PCR array was performed as detailed previously [62] and in "Supplementary Materials and Methods".

RNA cross-linking immunoprecipitation (RNA CLIP) assay

RNA CLIP assay was performed on CEGBCs and uninfected HAs as previously reported [21, 24]. qPCR analysis of EZH2 immunoprecipitated samples (IP EZH2) and negative control (IP IgG) were normalized with respect to each input and expressed as ($2^{(-\Delta Ct)}$) x 100 (% Input) as previously reported [63]. The antibodies used are provided in Supplementary Table 2.

Reverse transcription quantitative polymerase chain reaction (RT-qPCR)

The detection of transcripts was assessed by RT-qPCR as detailed previously [62] and in "Supplementary Materials and Methods". Primers used are listed in Supplementary Table 1.

Confocal microscopy

Confocal microscopy of infected human astrocytes, MRC5 cells, CEGBCs, and spheroids was performed as previously detailed [15]. The antibodies used are provided in Supplementary Table 2.

Soft agar colony formation assay

Colony formation in soft agar (Colorimetric assay, CB135; Cell Biolabs Inc., San Diego, CA) seeded with uninfected HAs or CEGBCs was performed as described previously [15].

Spheroid formation assay

Spheroids of CEGBCs were prepared as described previously [64, 65]. Detailed description is provided in "Supplementary Materials and Methods".

Invasion assays

Detailed description of the invasion assays is provided in "Supplementary Materials and Methods".

Glioblastoma multiforme biopsies and HCMV isolation

GBM biopsies [$n = 37$; O (6)-methylguanine DNA methyltransferase (MGMT) promoter methylated GBM biopsies $n = 17$, and MGMT promoter unmethylated GBM biopsies $n = 20$] as well as healthy brain biopsies ($n = 4$) were provided by the Regional tumor bank (BB0033-00024 Tumorothèque Régionale de Franche-Comté). A written informed consent for participation was obtained from all patients. The study was authorized by the local ethics committees of Besançon University Hospital (Besançon, France) and the French Research Ministry (AC-2015-2496, CNIL n°1173545, NF-S-138 96900 n°F2015). Detailed description of biopsies analysis is provided in "Supplementary Materials and Methods". Briefly, genomic DNA was isolated from patient biopsies, and HCMV presence was identified by qPCR using specific primers against IE1 and UL69 genes. RNA was extracted from the biopsies, and following reverse transcription the expression of EZH2, Myc, and GAPDH was assessed by real-time qPCR. Eleven HCMV-GBM strains were isolated from MGMT promoter methylated ($n = 4$) and promoter unmethylated ($n = 7$) GBM biopsies. Primers used are listed in Supplementary Table 1.

Statistical analysis

Detailed description of the statistical tests used is provided in "Supplementary Materials and Methods".

DATA AVAILABILITY

The data supporting the findings of this study are available within the article and its Supplementary Information files and from the corresponding authors on request.

REFERENCES

1. Lee JH, Lee JE, Kahng JY, Kim SH, Park JS, Yoon SJ. et al. Human glioblastoma arises from subventricular zone cells with low-level driver mutations. Nature. 2018;560:243–7. https://doi.org/10.1038/s41586-018-0389-3.
2. Louis DN, Perry A, Wesseling P, Brat DJ, Cree IA, Figarella-Branger D. et al. The 2021 WHO Classification of Tumors of the Central Nervous System: a summary. Neuro-Oncol. 2021;23:1231–51. https://doi.org/10.1093/neuonc/noab106.
3. zur Hausen H. Cancers in Humans: A Lifelong Search for Contributions of Infectious Agents, Autobiographic Notes. Annu Rev Virol. 2019;6:1–28. https://doi.org/10.1146/annurev-virology-092818-015907.
4. El Baba R, Herbein G. Immune Landscape of CMV Infection in Cancer Patients: From "Canonical" Diseases Toward Virus-Elicited Oncomodulation. Front Immunol. 2021;12:730765. https://doi.org/10.3389/fimmu.2021.730765.
5. Perera MR, Wills MR, Sinclair JH. HCMV Antivirals and Strategies to Target the Latent Reservoir. Viruses. 2021;13:817. https://doi.org/10.3390/v13050817.
6. Cobbs C, Harkins L, Samanta M, Gillespie GY, Bharara S, King PH, et al. Human cytomegalovirus infection and expression in human malignant glioma. Cancer Res. 2002;62:3347–50.
7. Kumar A, Tripathy MK, Pasquereau S, Al Moussawi F, Abbas W, Coquard L. et al. The Human Cytomegalovirus Strain DB Activates Oncogenic Pathways in Mammary Epithelial Cells. EBioMedicine. 2018;30:167–83. https://doi.org/10.1016/j.ebiom.2018.03.015.
8. Xu S, Schafer X, Munger J. Expression of Oncogenic Alleles Induces Multiple Blocks to Human Cytomegalovirus Infection. J Virol. 2016;90:4346–56. https://doi.org/10.1128/JVI.00179-16.
9. Belzile J-P, Stark TJ, Yeo GW, Spector DH. Human Cytomegalovirus Infection of Human Embryonic Stem Cell-Derived Primitive Neural Stem Cells Is Restricted at Several Steps but Leads to the Persistence of Viral DNA. J Virol. 2014;88:4021–39. https://doi.org/10.1128/JVI.03492-13.
10. Odeberg J, Wolmer N, Falci S, Westgren M, Seiger Å, Söderberg-Nauclér C. Human Cytomegalovirus Inhibits Neuronal Differentiation and Induces Apoptosis in Human Neural Precursor Cells. J Virol. 2006;80:8929–39. https://doi.org/10.1128/JVI.00676-06.
11. Kossmann T, Morganti-Kossmann MC, Orenstein JM, Britt WJ, Wahl SM, Smith PD. Cytomegalovirus Production by Infected Astrocytes Correlates with Transforming Growth Factor-β Release. J INFECT DIS. 2003;187:534–41. https://doi.org/10.1086/373995.
12. Luo MH, Hannemann H, Kulkarni AS, Schwartz PH, O'Dowd JM, Fortunato EA. Human Cytomegalovirus Infection Causes Premature and Abnormal Differentiation of Human Neural Progenitor Cells. J Virol. 2010;84:3528–41. https://doi.org/10.1128/JVI.02161-09.
13. Geder L, Lausch R, O'Neill F, Rapp F. Oncogenic Transformation of Human Embryo Lung Cells by Human Cytomegalovirus. Science. 1976;192:1134–7. https://doi.org/10.1126/science.179143.
14. Herbein G. The Human Cytomegalovirus, from Oncomodulation to Oncogenesis. Viruses. 2018;10:408. https://doi.org/10.3390/v10080408.
15. Nehme Z, Pasquereau S, Haidar Ahmad S, Coaquette A, Molimard C, Monnien F. et al. Polyploid giant cancer cells, stemness and epithelial-mesenchymal plasticity elicited by human cytomegalovirus. Oncogene. 2021;40:3030–46. https://doi.org/10.1038/s41388-021-01715-7.
16. Peredo-Harvey I, Rahbar A, Söderberg-Nauclér C. Presence of the Human Cytomegalovirus in Glioblastomas—A Systematic Review. Cancers. 2021;13:5051. https://doi.org/10.3390/cancers13205051.
17. Suvà M-L, Riggi N, Janiszewska M, Radovanovic I, Provero P, Stehle J-C. et al. EZH2 Is Essential for Glioblastoma Cancer Stem Cell Maintenance. Cancer Res. 2009;69:9211–8. https://doi.org/10.1158/0008-5472.CAN-09-1622.
18. Liu H, Sun Y, Qi X, Gordon RE, O'Brien JA, Yuan H. et al. EZH2 Phosphorylation Promotes Self-Renewal of Glioma Stem-Like Cells Through NF-κB Methylation. Front Oncol. 2019;9:641. https://doi.org/10.3389/fonc.2019.00641.
19. Yu T, Wang Y, Hu Q, Wu W, Wu Y, Wei W. et al. The EZH2 inhibitor GSK343 suppresses cancer stem-like phenotypes and reverses mesenchymal transition in glioma cells. Oncotarget. 2017;8:98348–59. https://doi.org/10.18632/oncotarget.21311.
20. Sander S, Bullinger L, Klapproth K, Fiedler K, Kestler HA, Barth TFE. et al. MYC stimulates EZH2 expression by repression of its negative regulator miR-26a. Blood. 2008;112:4202–12. https://doi.org/10.1182/blood-2008-03-147645.
21. Rossetto CC, Tarrant-Elorza M, Pari GS. Cis and Trans Acting Factors Involved in Human Cytomegalovirus Experimental and Natural Latent Infection of CD14 (+) Monocytes and CD34 (+) Cells. PLoS Pathog. 2013;9:e1003366. https://doi.org/10.1371/journal.ppat.1003366.
22. Ahani N, Shirkoohi R, Rokouei M, Alipour Eskandani M, Nikravesh A. Overexpression of enhancer of zeste human homolog 2 (EZH2) gene in human cytomegalovirus positive glioblastoma multiforme tissues. Med Oncol. 2014;31:252. https://doi.org/10.1007/s12032-014-0252-9.
23. Zhang S, Mercado-Uribe I, Xing Z, Sun B, Kuang J, Liu J. Generation of cancer stem-like cells through the formation of polyploid giant cancer cells. Oncogene. 2014;33:116–28. https://doi.org/10.1038/onc.2013.96.
24. Nehme Z, Pasquereau S, Haidar Ahmad S, El Baba R, Herbein G. Polyploid giant cancer cells, EZH2 and Myc upregulation in mammary epithelial cells infected with high-risk human cytomegalovirus. EBioMedicine. 2022;80:104056. https://doi.org/10.1016/j.ebiom.2022.104056.

25. Annibali D, Whitfield JR, Favuzzi E, Jauset T, Serrano E, Cuartas I. et al. Myc inhibition is effective against glioma and reveals a role for Myc in proficient mitosis. Nat Commun. 2014;5:4632. https://doi.org/10.1038/ncomms5632.
26. Arrieta VA, Dmello C, McGrail DJ, Brat DJ, Lee-Chang C, Heimberger AB. et al. Immune checkpoint blockade in glioblastoma: from tumor heterogeneity to personalized treatment. J Clin Investig. 2023;133:e163447. https://doi.org/10.1172/JCI163447.
27. Eich M-L, Athar M, Ferguson JE, Varambally S. EZH2-Targeted Therapies in Cancer: Hype or a Reality. Cancer Res. 2020;80:5449–58. https://doi.org/10.1158/0008-5472.CAN-20-2147.
28. Pantalone MR, Rahbar A, Söderberg-Naucler C, Stragliotto G. Valganciclovir as Add-on to Second-Line Therapy in Patients with Recurrent Glioblastoma. Cancers. 2022;14:1958. https://doi.org/10.3390/cancers14081958.
29. Daubon T, Hemadou A, Romero Garmendia I, Saleh M. Glioblastoma Immune Landscape and the Potential of New Immunotherapies. Front Immunol. 2020;11:585616. https://doi.org/10.3389/fimmu.2020.585616.
30. Schuessler A, Smith C, Beagley L, Boyle GM, Rehan S, Matthews K. et al. Autologous T-cell Therapy for Cytomegalovirus as a Consolidative Treatment for Recurrent Glioblastoma. Cancer Res. 2014;74:3466–76. https://doi.org/10.1158/0008-5472.CAN-14-0296.
31. Engwer C, Knappitsch M, Surulescu C. A multiscale model for glioma spread including cell-tissue interactions and proliferation. Math Biosci Eng. 2016;13:443–60. https://doi.org/10.3934/mbe.2015011.
32. Fedele M, Cerchia L, Pegoraro S, Sgarra R, Manfioletti G. Proneural-Mesenchymal Transition: Phenotypic Plasticity to Acquire Multitherapy Resistance in Glioblastoma. IJMS. 2019;20:2746. https://doi.org/10.3390/ijms20112746.
33. Venkataramani V, Yang Y, Schubert MC, Reyhan E, Tetzlaff SK, Wißmann N. et al. Glioblastoma hijacks neuronal mechanisms for brain invasion. Cell. 2022;185:2899–2917.e31. https://doi.org/10.1016/j.cell.2022.06.054.
34. Xin X, Li Q, Fang J, Zhao T. LncRNA HOTAIR: A Potential Prognostic Factor and Therapeutic Target in Human Cancers. Front Oncol. 2021;11:679244. https://doi.org/10.3389/fonc.2021.679244.
35. Singh N, Miner A, Hennis L, Mittal S. Mechanisms of temozolomide resistance in glioblastoma - a comprehensive review. CDR. 2021;4:17–43. https://doi.org/10.20517/cdr.2020.79.
36. Virrey JJ, Golden EB, Sivakumar W, Wang W, Pen L, Schönthal AH. et al. Glioma-associated endothelial cells are chemoresistant to temozolomide. J Neurooncol. 2009;95:13–22. https://doi.org/10.1007/s11060-009-9891-7.
37. El Baba R, Pasquereau S, Haidar Ahmad S, Diab-Assaf M, Herbein G. Oncogenic and Stemness Signatures of the High-Risk HCMV Strains in Breast Cancer Progression. Cancers. 2022;14:4271. https://doi.org/10.3390/cancers14174271.
38. Herbein G. High-Risk Oncogenic Human Cytomegalovirus. Viruses. 2022;14:2462. https://doi.org/10.3390/v14112462.
39. Liu J. The dualistic origin of human tumors. Semin Cancer Biol. 2018;53:1–16. https://doi.org/10.1016/j.semcancer.2018.07.004.
40. Furnari FB, Fenton T, Bachoo RM, Mukasa A, Stommel JM, Stegh A. et al. Malignant astrocytic glioma: genetics, biology, and paths to treatment. Genes Dev. 2007;21:2683–710. https://doi.org/10.1101/gad.1596707.
41. Stiles CD, Rowitch DH. Glioma Stem Cells: A Midterm Exam. Neuron. 2008;58:832–46. https://doi.org/10.1016/j.neuron.2008.05.031.
42. Beiriger J, Habib A, Jovanovich N, Kodavali CV, Edwards L, Amankulor N. et al. The Subventricular Zone in Glioblastoma: Genesis, Maintenance, and Modeling. Front Oncol. 2022;12:790976. https://doi.org/10.3389/fonc.2022.790976.
43. Sher F, Boddeke E, Copray S. Ezh2 Expression in Astrocytes Induces Their Dedifferentiation Toward Neural Stem Cells. Cell Reprogramming. 2011;13:1–6. https://doi.org/10.1089/cell.2010.0052.
44. Sasmita AO, Wong YP, Ling APK. Biomarkers and therapeutic advances in glioblastoma multiforme. Asia-Pac J Clin Oncol. 2018;14:40–51. https://doi.org/10.1111/ajco.12756.
45. Senhaji N, Squalli Houssaini A, Lamrabet S, Louati S, Bennis S. Molecular and Circulating Biomarkers in Patients with Glioblastoma. IJMS. 2022;23:7474. https://doi.org/10.3390/ijms23137474.
46. Guerra-Rebollo M, Garrido C, Sánchez-Cid L, Soler-Botija C, Meca-Cortés O, Rubio N. et al. Targeting of replicating CD133 and OCT4/SOX2 expressing glioma stem cells selects a cell population that reinitiates tumors upon release of therapeutic pressure. Sci Rep. 2019;9:9549. https://doi.org/10.1038/s41598-019-46014-0.
47. Ben-Porath I, Thomson MW, Carey VJ, Ge R, Bell GW, Regev A. et al. An embryonic stem cell–like gene expression signature in poorly differentiated aggressive human tumors. Nat Genet. 2008;40:499–507. https://doi.org/10.1038/ng.127.
48. Lou Y-W, Wang P-Y, Yeh S-C, Chuang P-K, Li S-T, Wu C-Y. et al. Stage-specific embryonic antigen-4 as a potential therapeutic target in glioblastoma multiforme and other cancers. Proc Natl Acad Sci USA. 2014;111:2482–7. https://doi.org/10.1073/pnas.1400283111.
49. Veselska R, Kuglik P, Cejpek P, Svachova H, Neradil J, Loja T. et al. Nestin expression in the cell lines derived from glioblastoma multiforme. BMC Cancer. 2006;6:32. https://doi.org/10.1186/1471-2407-6-32.
50. Li Y, Zhong C, Liu D, Yu W, Chen W, Wang Y. et al. Evidence for Kaposi Sarcoma Originating from Mesenchymal Stem Cell through KSHV-induced Mesenchymal-to-Endothelial Transition. Cancer Res. 2018;78:230–45. https://doi.org/10.1158/0008-5472.CAN-17-1961.
51. Kondo S, Wakisaka N, Muramatsu M, Zen Y, Endo K, Murono S. et al. Epstein-Barr Virus Latent Membrane Protein 1 Induces Cancer Stem/Progenitor-Like Cells in Nasopharyngeal Epithelial Cell Lines. J Virol. 2011;85:11255–64. https://doi.org/10.1128/JVI.00188-11.
52. Xiao Y, Yang K, Wang Z, Zhao M, Deng Y, Ji W. et al. CD44-Mediated Poor Prognosis in Glioma Is Associated With M2-Polarization of Tumor-Associated Macrophages and Immunosuppression. Front Surg. 2022;8:775194. https://doi.org/10.3389/fsurg.2021.775194.
53. Yabo YA, Niclou SP, Golebiewska A. Cancer cell heterogeneity and plasticity: A paradigm shift in glioblastoma. Neuro-Oncol. 2022;24:669–82. https://doi.org/10.1093/neuonc/noab269.
54. Li F, Liu X, Sampson JH, Bigner DD, Li C-Y. Rapid Reprogramming of Primary Human Astrocytes into Potent Tumor-Initiating Cells with Defined Genetic Factors. Cancer Res. 2016;76:5143–50. https://doi.org/10.1158/0008-5472.CAN-16-0171.
55. Nie Z, Guo C, Das SK, Chow CC, Batchelor E, Simons SS. et al. Dissecting transcriptional amplification by MYC. ELife. 2020;9:e52483. https://doi.org/10.7554/eLife.52483.
56. Wu X, Liu D, Tao D, Xiang W, Xiao X, Wang M. et al. BRD4 Regulates EZH2 Transcription through Upregulation of C-MYC and Represents a Novel Therapeutic Target in Bladder Cancer. Mol Cancer Therap. 2016;15:1029–42. https://doi.org/10.1158/1535-7163.MCT-15-0750.
57. Chen X, Guo Z-Q, Cao D, Chen Y, Chen J. MYC-mediated upregulation of PNO1 promotes glioma tumorigenesis by activating THBS1/FAK/Akt signaling. Cell Death Dis. 2021;12:244. https://doi.org/10.1038/s41419-021-03532-y.
58. Yadav B, Pal S, Rubstov Y, Goel A, Garg M, Pavlyukov M. et al. LncRNAs associated with glioblastoma: From transcriptional noise to novel regulators with a promising role in therapeutics. Mol Ther Nucleic Acids. 2021;24:728–42. https://doi.org/10.1016/j.omtn.2021.03.018.
59. Ding Z, Mathur V, Ho PP, James ML, Lucin KM, Hoehne A. et al. Antiviral drug ganciclovir is a potent inhibitor of microglial proliferation and neuroinflammation. J Exp Med. 2014;211:189–98. https://doi.org/10.1084/jem.20120696.
60. Zhang S, Mu Z, He C, Zhou M, Liu D, Zhao X-F. et al. Antiviral Drug Ganciclovir Is a Potent Inhibitor of the Proliferation of Müller Glia–Derived Progenitors During Zebrafish Retinal Regeneration. Investig Ophthalmol Vis Sci. 2016;57:1991. https://doi.org/10.1167/iovs.15-18669.
61. Fan T-Y, Wang H, Xiang P, Liu Y-W, Li H-Z, Lei B-X, et al. Inhibition of EZH2 reverses chemotherapeutic drug TMZ chemosensitivity in glioblastoma. Int J Clin Exp Pathol. 2014;7:6662–70.
62. Haidar Ahmad S, Pasquereau S, El Baba R, Nehme Z, Lewandowski C, Herbein G. Distinct Oncogenic Transcriptomes in Human Mammary Epithelial Cells Infected With Cytomegalovirus. Front Immunol. 2021;12:772160. https://doi.org/10.3389/fimmu.2021.772160.
63. Battistelli C, Cicchini C, Santangelo L, Tramontano A, Grassi L, Gonzalez FJ. et al. The Snail repressor recruits EZH2 to specific genomic sites through the enrollment of the lncRNA HOTAIR in epithelial-to-mesenchymal transition. Oncogene. 2017;36:942–55. https://doi.org/10.1038/onc.2016.260.
64. Daubon T, Guyon J, Raymond A-A, Dartigues B, Rudewicz J, Ezzoukhry Z. et al. The invasive proteome of glioblastoma revealed by laser-capture microdissection. Neuro-Oncol Adv. 2019;1:1–12. https://doi.org/10.1093/noajnl/vdz029.
65. Guyon J, Andrique L, Pujol N, Røsland GV, Recher G, Bikfalvi A. et al. A 3D Spheroid Model for Glioblastoma. JoVE. 2020;158:e60998. https://doi.org/10.3791/60998.

ACKNOWLEDGEMENTS

This work was supported by grants from the University of Franche-Comté (UFC) (CR3300), the Région Franche-Comté (2021-Y-08292 and 2021-Y-08290) and the Ligue contre le Cancer (CR3304) to Georges Herbein. REB is a recipient of a doctoral scholarship from Hariri foundation for sustainable human development. SHA is supported by ANR (Agence Nationale pour la Recherche) grant. The funders had no role in the data collection, analysis, patient recruitment, or decision to publish. The authors thank DImaCell Imaging Ressource Center, University of Bourgogne Franche-Comté, Faculty of Health Sciences, 25000 Besançon, France for technical support.

AUTHOR CONTRIBUTIONS

Conceptualization, GH; formal analysis, REB, SP, SHA, FB, GH; investigation, REB, SP, SHA, FM, MA; writing—original draft preparation, REB, SHA, GH; writing—review and editing, REB, SHA, GH; directly accessed and verified the underlying data: REB, SP, SHA, GH; visualization, REB, SP, SHA, GH; supervision, GH; project administration, GH; funding acquisition, GH. All authors have read and agreed to the published version of the manuscript.

COMPETING INTERESTS

The authors declare no competing interests.

INSTITUTIONAL REVIEW BOARD STATEMENT

The study was conducted according to the guidelines of the Declaration of Helsinki. A written informed consent for participation was obtained from all patients. The study was authorized by the local ethics committees of Besançon University Hospital (Besançon, France) and the French Research Ministry (AC-2015-2496, CNIL n°1173545, NF-S-138 96900 n°F2015).

ADDITIONAL INFORMATION

Supplementary information The online version contains supplementary material available at https://doi.org/10.1038/s41388-023-02709-3.

Correspondence and requests for materials should be addressed to Georges Herbein.

Reprints and permission information is available at http://www.nature.com/reprints

Publisher's note Springer Nature remains neutral with regard to jurisdictional claims in published maps and institutional affiliations.

Open Access This article is licensed under a Creative Commons Attribution 4.0 International License, which permits use, sharing, adaptation, distribution and reproduction in any medium or format, as long as you give appropriate credit to the original author(s) and the source, provide a link to the Creative Commons license, and indicate if changes were made. The images or other third party material in this article are included in the article's Creative Commons license, unless indicated otherwise in a credit line to the material. If material is not included in the article's Creative Commons license and your intended use is not permitted by statutory regulation or exceeds the permitted use, you will need to obtain permission directly from the copyright holder. To view a copy of this license, visit http://creativecommons.org/licenses/by/4.0/.

© The Author(s) 2023

11.9 Publication N°9

Haidar Ahmad S, **El Baba R**, Herbein G. Polyploid giant cancer cells, cytokines and cytomegalovirus in breast cancer progression. Cancer Cell Int 2023;23:119. https://doi.org/10.1186/s12935-023-02971-1.

This study investigates the connection between human cytomegalovirus (HCMV) and breast cancer, focusing on high-risk HCMV strains. It finds that high-risk HCMV strains contribute to oncogenic effects leading to aggressive breast cancer. We examined cytokine expression in HCMV-transformed cells and breast cancer biopsies, revealing a correlation between cytokine production and the presence of polyploid giant cancer cells (PGCCs) in both in vitro and in vivo settings. This suggests the potential for novel therapies, particularly cytokine-based immunotherapy, in treating aggressive basal-like breast cancer associated with high-risk HCMV strains.

Haidar Ahmad *et al. Cancer Cell International* (2023) 23:119
https://doi.org/10.1186/s12935-023-02971-1

Cancer Cell International

RESEARCH Open Access

Polyploid giant cancer cells, cytokines and cytomegalovirus in breast cancer progression

Sandy Haidar Ahmad[1], Ranim El Baba[1] and Georges Herbein[1,2*]

Abstract

Background Breast cancer is the most common cancer among women. Accumulated evidence over the past decades indicates a very high prevalence of human cytomegalovirus (HCMV) in breast cancer. High-risk HCMV strains possess a direct oncogenic effect displayed by cellular stress, polyploid giant cancer cells (PGCCs) generation, stemness, and epithelial-to-mesenchymal transition (EMT) leading to cancer of aggressive phenotype. Breast cancer development and progression have been regulated by several cytokines where the latter can promote cancer cell survival, help in tumor immune evasion, and initiate the EMT process, thereby resulting in invasion, angiogenesis, and breast cancer metastasis. In the present study, we screened cytokines expression in cytomegalovirus-transformed HMECs (CTH cells) cultures infected with HCMV high-risk strains namely, HCMV-DB and BL, as well as breast cancer biopsies, and analyzed the association between cytokines production, PGCCs count, and HCMV presence in vitro and in vivo.

Methods In CTH cultures and breast cancer biopsies, HCMV load was quantified by real-time qPCR. PGCCs count in CTH cultures and breast cancer biopsies was identified based on cell morphology and hematoxylin and eosin staining, respectively. CTH supernatants were evaluated for the production of TGF-β, IL-6, IL1-β, and IL-10 by ELISA assays. The above-mentioned cytokines expression was assessed in breast cancer biopsies using reverse transcription-qPCR. The correlation analyses were performed using Pearson correlation test.

Results The revealed PGCCs/cytokine profile in our in vitro CTH model matched that of the breast cancer biopsies, in vivo. Pronounced cytokine expression and PGCCs count were detected in particularly CTH-DB cultures and basal-like breast cancer biopsies.

Conclusions The analysis of cytokine profiles in PGCCs present mostly in basal-like breast cancer biopsies and derived from CTH cells chronically infected with the high-risk HCMV strains might have the potential to provide novel therapies such as cytokine-based immunotherapy which is a promising field in cancer treatments.

Keywords Human cytomegalovirus, High-risk HCMV strains, CTH cells, PGCCs, Cytokines, Breast cancer biopsies

Introduction

Polyploid giant cancer cells (PGCCs) play an important role in tumor heterogeneity; they are implicated in tumor initiation, progression, metastasis, and therapy resistance in breast, ovarian, and prostate cancers [1, 2]. PGCCs count was associated with tumor grade and metastasis degree in patients with breast cancer (BC) [3]. PGCCs promote BC metastasis and

*Correspondence:
Georges Herbein
georges.herbein@univ-fcomte.fr
[1] Department Pathogens and Inflammation-EPILAB, EA4266, University of France-Comté, 16 Route de Gray, 25030 Besançon Cedex, France
[2] Department of Virology, CHRU Besancon, Besancon, France

© The Author(s) 2023. **Open Access** This article is licensed under a Creative Commons Attribution 4.0 International License, which permits use, sharing, adaptation, distribution and reproduction in any medium or format, as long as you give appropriate credit to the original author(s) and the source, provide a link to the Creative Commons licence, and indicate if changes were made. The images or other third party material in this article are included in the article's Creative Commons licence, unless indicated otherwise in a credit line to the material. If material is not included in the article's Creative Commons licence and your intended use is not permitted by statutory regulation or exceeds the permitted use, you will need to obtain permission directly from the copyright holder. To view a copy of this licence, visit http://creativecommons.org/licenses/by/4.0/. The Creative Commons Public Domain Dedication waiver (http://creativecommons.org/publicdomain/zero/1.0/) applies to the data made available in this article, unless otherwise stated in a credit line to the data.

chemoresistance by modulating the tumor microenvironment (TME) [1, 4]. The presence of polyploidy was identified as a common characteristic among all the tumors initiated by oncoviruses [5]. Human cytomegalovirus (HCMV), a ubiquitous beta-herpesvirus, exhibits a broad cellular tropism [6]. HCMV genome and/or antigens were detected in numerous malignancies including breast, ovarian, prostate, and colon cancer, as well as in neural-derived cancers such as glioblastoma, neuroblastoma, and medulloblastoma. The potential relation between HCMV and cancer was explained by the oncomodulation paradigm [7–12]. Besides the oncomodulation paradigm, our research group highlighted a direct oncogenic effect of high-risk HCMV strains [13–17]. Following human mammary epithelial cells (HMECs) infection, high-risk strains namely, HCMV-DB and HCMV-BL transformed HMECs into cytomegalovirus-transformed HMECs (CTH cells) [16, 17]. PGCCs appearance was described in CTH cultures and associated with enhanced cell proliferation, activation of epithelial-to-mesenchymal transition (EMT), and stemness processes [17, 18]. Moreover, the expression of HCMV-IE1 was identified in PGCCs-CTH cells [17, 18]. These studies highlighted the emergence of PGCCs as a critical factor following HCMV infection.

Numerous studies have described the capacity of cytokines to regulate the induction and progression of breast cancer. Several interleukins including IL-1, IL-6, IL-11, IL-19, and transforming-growth factor β (TGF-β) promoted breast cancer cell proliferation and/or invasion [19, 20]. TGF-β, the most studied cytokine in breast cancer, plays a dual role in tumor progression. At an early stage of tumorigenesis, TGF-β acts as a tumor suppressor due to its anti-proliferative effects. At late stages, TGF-β induces tumor progression by enhancing cancer cell invasion, survival, and immune evasion [21–24]. Furthermore, the presence of TGF-β in the microenvironment correlates with tumor progression and poor prognosis [22]. IL-6 is capable to convert non-stem cancer cells to cancer stem-like cells in breast and prostate cell lines [25]. IL-1 and IL-10 are highly expressed in high grade breast cancer [26–28]. Further, the IL-1 was associated with cancer cells' proliferation, invasion, angiogenesis, and breast cancer metastasis [29, 30]. IL-6, and IL-1 activate NF-kB and increase cyclin D1 in the normal breast cells causing a neoplastic phenotype [31]. Furthermore, IL-6 and TGF-β initiate the epithelial-to-mesenchymal transition (EMT) process [24, 32–35] leading to cancer progression and metastasis [34, 36, 37]. Additionally, some cytokines including TGF-β, IL-10 and IL-6 were described to facilitate tumor escape [38–41]. Herein, we screened cytokines expression in CTH cultures as well as breast cancer biopsies, and analyzed the link between cytokines production, PGCCs, and HCMV presence in vitro and in vivo.

Materials and methods

Cells cultures

Human primary mammary cells (HMECs) were purchased from Life Technologies (Carlsbad, CA, USA). HMECs were cultured in HMEC medium supplemented with HMEC supplement, bovine pituitary extract, and penicillin/streptomycin (Life Technologies) at 37 °C, 5% CO2, and 95% humidity. HMECs were infected with high-risk strains HCMV-DB (KT959235) and HCMV-BL (MW980585) at MOI of 1 as previously described [17, 42]. Following chronic infection, CMV-Transformed HMECs (CTH) cells were emerging and cultured in the same conditions as HMECs. CTH cells were maintained in culture for more than 12 months. Mycoplasma contamination status was monitored on a monthly basis for all cultures (VenorGem classic mycoplasma detection, Minerva biolabs).

Breast biopsies

Healthy breast biopsies (n = 4) and breast cancer biopsies (n = 16: luminal tumor biopsies n = 8 and basal tumor biopsies n = 8) were provided by the Regional Tumor Bank (BB0033-00024 Tumorothéque Régionale de Franche-Comté). The local ethics committees of Besançon University Hospital (Besançon, France) and the French Research Ministry (AC-2015-2496, CNIL n°1173545, NF-S-96900 n ° F2015) permitted the study. All patients provide their written informed consent to participate in the study.

Viral detection

Real-time qPCR was used to assess the presence of HCMV in CTH cultures and breast cancer biopsies. DNA

(See figure on next page.)

Fig. 1 PGCCs detection in CTH cultures. **a** An inverted light microscope was used to monitor the chronic CMV-transformed-HMECs (CTH)-BL and CTH-DB cultures, Magnification × 100, scale bar 100 µm. **b** Curves representing the PGCCs count detected in CTH cultures. The Y-axis represents the PGCCs count /well, and the X-axis represents the days post-infection. **c.** Time-course of the viral load in the CTH-DB and BL culture as measured by IE1-qPCR. Data are represented as mean ± SD of two independent experiments. Blue and orange curves represent the viral load (copies/ml) as measured by IE1-qPCR (Left Y-axis) and PGCCs count/well (Right Y-axis), respectively. The X-axis represents the days post-infection

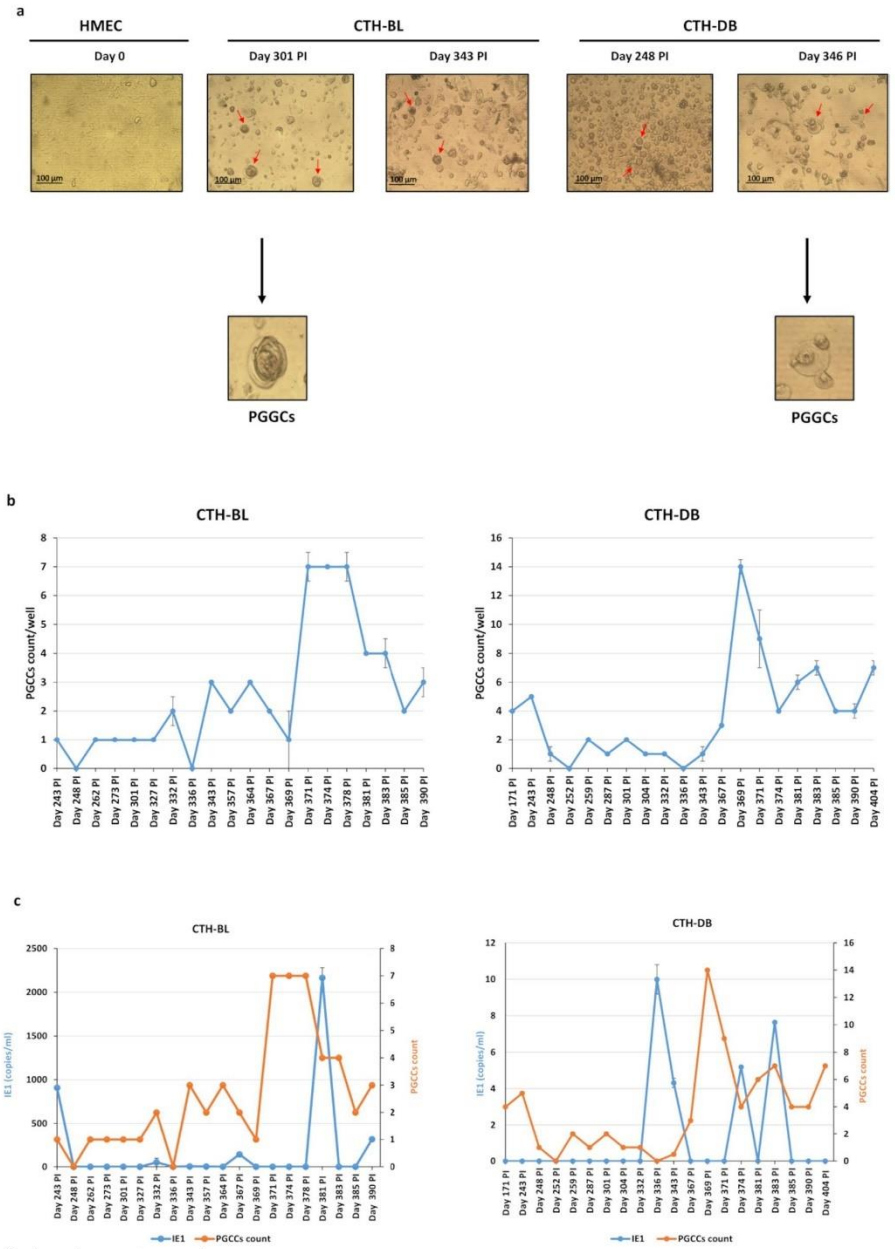

Fig. 1 (See legend on previous page.)

was extracted from CTH supernatants using E.Z.N.A. Blood DNA Kit, D3392-02, Omega BIO-TEK). Genomic DNA isolated from patient breast tumor biopsies and healthy human breast tissue was provided by the Regional Tumor Bank (BB0033-00024 Tumorothèque Régionale de Franche-Comté). Viral load was quantified by qPCR using KAPA SYBR FAST Master Mix (KAPA BIOSYSTEMS, KK4601) and IE1 primers (Forward 5'-CGACGT TCCTGCAGACTATG-3' and reverse 5'-TCCTCGGTC ACTTGTTCAAA-3') according to the manufacturer's protocol. Reactions were activated at 95 °C for 10 min, followed by 50 cycles (15 s at 95 °C and 1 min at 60 °C). Real-time qPCR reactions were conducted using a Stratagene Mx3005P thermocycler (Agilent). Results were analyzed using MxPro qPCR software.

PGCCs detection and count in CTH cultures and biopsies

CTH cells were monitored by an Olympus optical microscope (Japan) and OPTIKA microscopy digital camera (Opticam, Italy). PGCCs present in CTH cultures were identified and counted based on cell morphology as previously reported [18]. PGCCs presence in BC biopsies was confirmed by hematoxylin and eosin staining based on Zhang et al. PGCCs description [43]. PGCCs quantification was similarly performed for all breast cancer biopsies. Briefly, PGCCs were counted in five hot spots of each tumor sample in hematoxylin and eosin slides (magnification 400X, field diameter 0.45 mm).

Cytokines production and expression in CTH cultures and biopsies

Supernatants from CTH cultures were harvested on different days post-infection and evaluated for the presence of cytokines. ELISA kits were used for the detection of Human TGF-β (kit reference 650.010.096, Diaclone, France), human IL-6 (kit reference 851.520.001, Diaclone, France), human IL-1β (kit reference 851.610.001, Diaclone, France), and human IL-10 (kit reference 851.540.005, Diaclone, France) in CTH supernatants. ELISA assays were performed according to the manufacturer's protocol.

Cytokines expression in breast cancer biopsies was evaluated by reverse transcription-quantitative polymerase chain reaction (RT-qPCR). Total RNA was extracted from BC biopsies using E.Z.N.A. Total RNA Kit I (Omega Bio-Tech, GA, USA). Following DNase I treatment (ThermoFisher), reverse transcription was performed using the SuperScript IV First-Strand Synthesis kit (Invitrogen, Carlsbad, CA, USA). Expression of TGF-β, IL-6, IL1-β, and IL-10 was measured by real-time qPCR using KAPA SYBR FAST Master Mix (KAPA BIOSYSTEMS, KK4601) and specific primers (listed in Additional file 1: Table S1) according to the manufacturer's protocol. The cytokines analyzed in the tissue samples were normalized to the housekeeping gene GAPDH. The GAPDH primers used are listed in Additional file 1: Table S1.

Statistics

The statistic software SPSS 23 was used to analyze the data. Correlation analyses were performed using Pearson correlation test. p-value ≤ 0.05 was considered significant. Plots and histograms were executed using Microsoft Excel. Data are presented as mean $\pm$ SD of two independent experiments.

Results

Kinetics of PGCCs appearance in CTH cultures

CTH cells were maintained in culture for more than 12 months as previously reported [17, 18]. After chronic infection, CTH cells exhibit an extremely heterogeneous population. Compared to uninfected HMECs, we identified the presence of large cells with morphological heterogeneity in chronic CMV-transformed-HMECs (CTH)-BL and CTH-DB (Fig. 1a, red arrows). Besides the presence of small-sized cells, giant cells with large nuclei, as well as giant cells with blastomere-like morphology and mesenchymal cells, were identified in CTH cultures parallel to the asymmetric cell division patterns; these giant cells were named PGCCs as previously reported [17, 18]. The PGCCs count was monitored from day 171 to 404 and from day 243 to 390 in chronically infected CTH-DB and CTH-BL cultures, respectively. The PGCCs count in CTH-BL cultures increased slightly at day 343 post-infection and reached a peak at days 371, 374, and 378 post-infection. A higher PGCCs count was observed in CTH-DB cultures, especially at day 369 post-infection (Fig. 1b). Furthermore, we assessed the presence of HCMV in CTH cultures using real-time qPCR. HCMV viral load was higher in CTH-BL compared to CTH-DB cultures. Viral replication was noticed in the presence of low PGCCs count in CTH cultures (Fig. 1c).

(See figure on next page.)

Fig. 2 Cytokines production in CTH cultures. Cytokines TGF-β (**a**), IL-10 (**b**), IL-1β (**c**), and IL-6 (**d**) were measured in supernatants of CTH cultures by ELISA kits. Remarkably, TGF-β concentration was enhanced along with the PGCCs count in the CTH-DB culture. IL-10 concentration was reduced in the CTH-BL culture with the presence of a high PGCCs count. The higher IL-6 expression was detected in CTH-DB culture. Data are represented as mean $\pm$ SD of two independent experiments. Blue and orange curves represent the cytokine concentration (pg/ml) (Left Y-axis) and PGCCs count/well (Right Y-axis), respectively. The X-axis represents the days post-infection

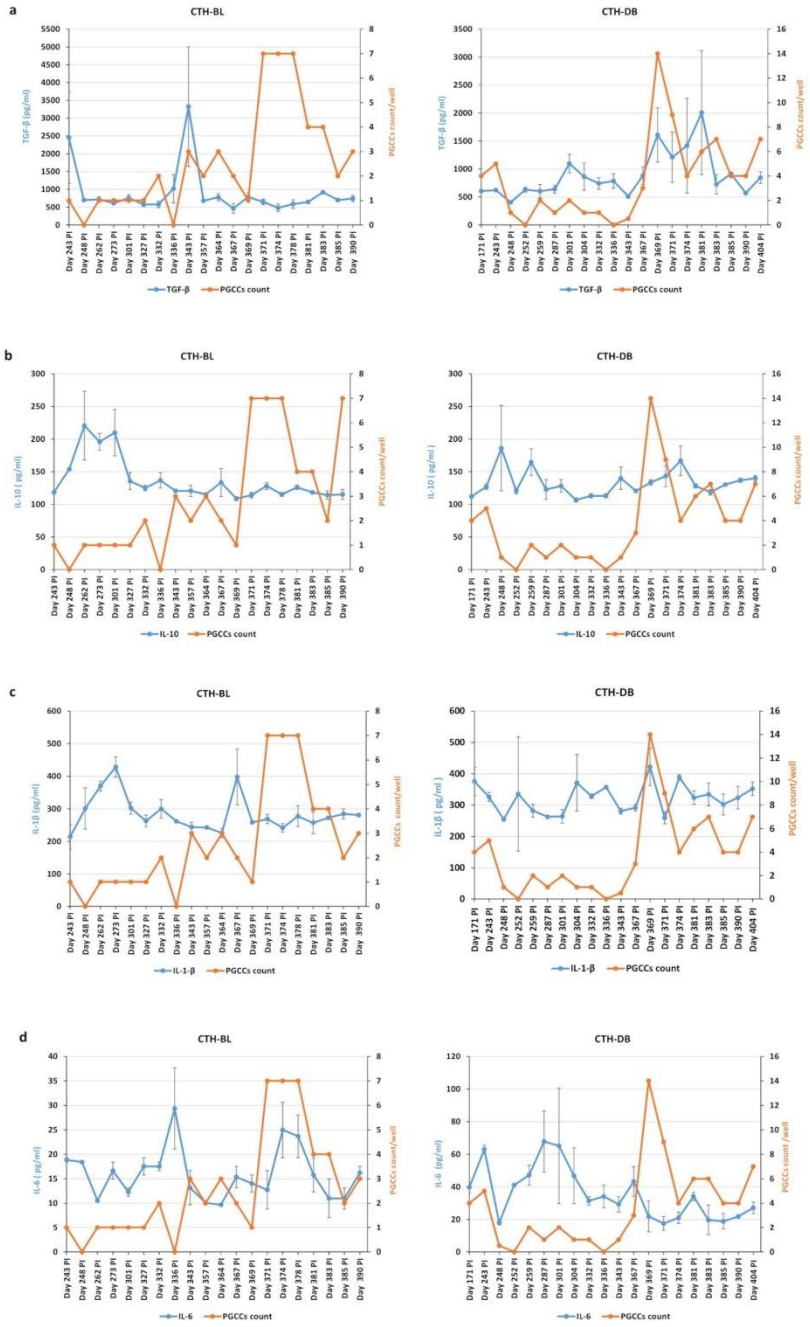

Fig. 2 (See legend on previous page.)

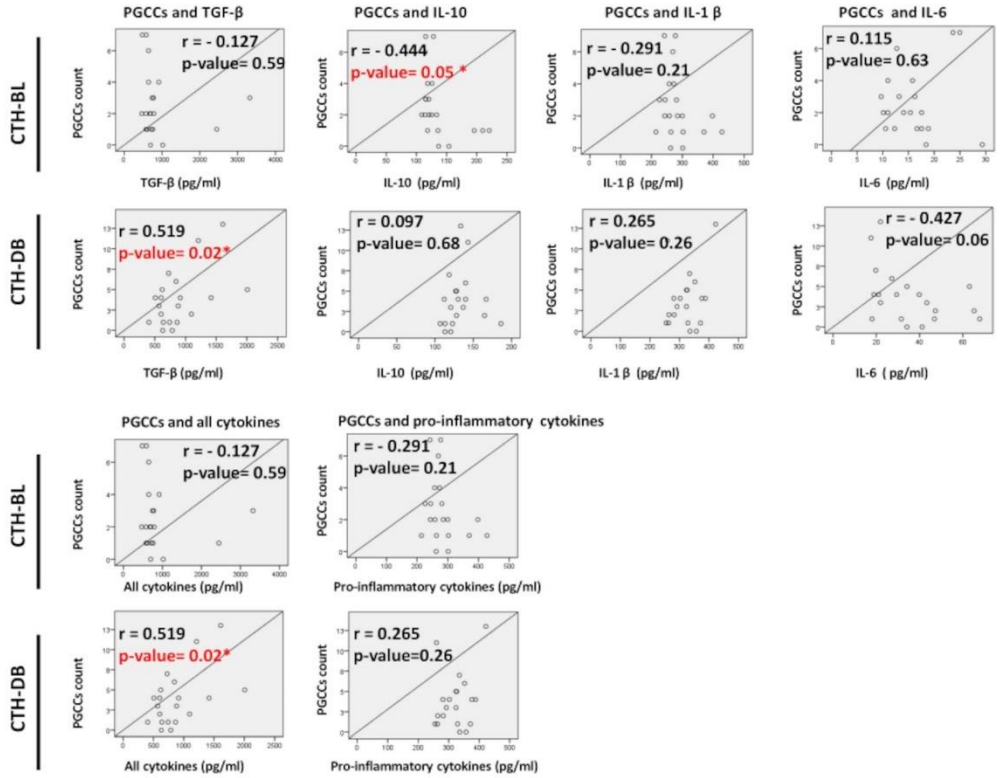

Fig. 3 Correlation between PGCCs count and cytokines production in CTH cultures. Pearson's correlation between PGCCs count and cytokine production was conducted in CTH cultures. A statistically significant negative correlation was detected between IL-10 expression and PGCCs count in CTH-BL culture. Moreover, a significant strong positive correlation was observed between PGCCs count and TGF-β or all cytokines production in CTH-DB cultures. The X-axis represents cytokine concentration (pg/ml), and the Y-axis represents PGCCs count. All cytokines: TGF-β, IL-6, IL10, IL-1β, Pro-inflammatory cytokines: IL-1β and IL-6. (r) stands for correlation coefficient and (*) shows significant p-value ≤ 0.05

Kinetics of cytokines production (TGF-β, IL-1β, IL-6, and IL-10) in CTH cultures

We assessed cytokines production in CTH cultures using ELISA assays (Fig. 2). The cytokine TGF-β was detected in CTH-BL and DB cultures at a concentration ranging between 500 and 3400 pg/ml. The highest TGF-β concentration was noticed at day 343 post-infection in CTH-BL culture. Remarkably, the TGF-β concentration was increased along with the PGCCs count in the CTH-DB culture (Fig. 2a). The production of IL-10 and IL-1β slightly varied between CTH-BL and CTH-DB cultures (Fig. 2b and c). Particularly, IL-10 concentration was decreased in the CTH-BL culture with the presence of a high PGCCs count (Fig. 2b). Higher expression of IL-6 was induced in CTH-DB compared to CTH-BL (Fig. 2d).

Correlation between PGCCs/cytokine production depends on the HCMV strain (DB versus BL)

We analyzed the link between viral load or PGCCs presence and cytokines production using Pearson's correlation test. We noticed a statistically significant negative correlation between IL-10 expression and PGCCs count in CTH-BL (r = -0.444, p-value = 0.05) (Fig. 3 and Table 1). Furthermore, TGF-β or all cytokines production were strongly and positively correlated with PGCCs count in CTH-DB culture (r = 0.519, p-value = 0.02, and r = 0.519, p-value = 0.02, respectively) (Fig. 3). No other statistically significant correlation was detected between the remaining cytokines and PGCCs count (Table 1. For example, a non-significant negative correlation was detected

Table 1 Correlation between PGCCs count and cytokines production in CTH cultures

	Correlation between PGCCs and the cytokines below	r	p-value
CTH-BL	TGF-β	− 0.127	0.59
CTH-DB		0.519	0.02*
CTH-BL	IL-10	− 0.444	0.05*
CTH-DB		0.097	0.68
CTH-BL	IL-1β	− 0.291	0.21
CTH-DB		0.265	0.26
CTH-BL	IL-6	0.115	0.63
CTH-DB		− 0.427	0.06
CTH-BL	All cytokines	− 0.127	0.59
CTH-DB		0.519	0.02*
CTH-BL	Pro-inflammatory cytokines	− 0.291	0.21
CTH-DB		0.265	0.26

All cytokines: TGF-β, IL-6, IL10, IL-1β, Pro-inflammatory cytokines: IL-1β and IL-6. (r) stands for correlation coefficient and (*) shows significant p-value ≤ 0.05. *PGCCs* Polyploid giant cancer cells, *CTH* Cytomegalovirus-Transformed HMECs, *TGF-β* Transforming growth factor beta, *IL* Interleukin

between PGCCs count and IL-6 production in CTH-DB culture (r = -0.427, p-value = 0.06) (Fig. 3). No significant correlation was found between HCMV presence (IE1 gene) and cytokines production (Fig. 4).

Detection of PGCCs and cytokines, as well as the correlation between PGCCs/cytokine expression in BC biopsies

To further decipher the relation between PGCCs count and cytokine production in vivo, we analyzed sixteen breast cancer biopsies (luminal n = 8 and basal-like n = 8) parallel to four healthy mammary biopsies for the presence of PGCCs, HCMV, as well as cytokine expression. The pathological data for the sixteen breast cancer biopsies were provided in Table 2. PGCCs with giant or multiple nuclei were detected in human breast cancer biopsies, in particular basal-like breast cancer biopsies (Fig. 5, arrows). Compared to healthy biopsies, high expression of TGF-β, IL-1β, and IL-10 was reported in BC biopsies, notably in basal-like biopsies; a slight variation in IL-6 expression was noticed in BC biopsies (Fig. 6). Hence, all cytokines as well as pro-inflammatory cytokines were highly expressed in basal-like BC biopsies compared to healthy biopsies (Fig. 6). As we previously confirmed the positive correlation between PGCCs count and HCMV presence in basal-like breast cancer, we assessed the expression of cytokines in these PGCCs-positive basal-like biopsies. A statistically significant strong positive correlation was identified between HCMV presence and IL-10, IL-6, all cytokines, and pro-inflammatory cytokines in PGCCs-positive basal-like biopsies (r = 0.899 p-value = 0.04, and r = 0.924, p-value = 0.03, r = 0.961, p-value = 0.009, and r = 0.882, p-value = 0.05, respectively) (Fig. 7).

Discussion

Polyploid giant cancer cells (PGCCs) were previously found in vitro and in vivo, and are especially noticeable in poorly differentiated, late-stage, and treatment-resistant cancers [44–46]. PGCCs count is increased in high breast tumor grade and lymph node metastases which suggests a relation between PGCCs and tumor recurrence potential [3]. Moreover, PGCCs were found in MDA-MB-231 and MCF7 breast cancer cell lines [43, 47, 48]. PGCCs induced a mesenchymal phenotype and displayed stem-like properties [3, 43, 46]. In line with these studies, PGCCs were mainly detected in basal-like compared to luminal biopsies. Further, our CTH cells that exhibit PGCCs following chronic HCMV infection were described to display mesenchymal and embryonic-like stemness features [17, 18]. As oncoviruses might trigger PGCCs formation [5], it is worth mentioning the absence of any other oncovirus in our viral stocks and CTH culture, thus confirming that the detected PGCCs phenotype is due to HCMV.

Furthermore, cytokines were described to regulate the induction and protection in breast cancer [31]; overexpression of several cytokines was described in estrogen receptor-negative breast carcinoma [26]. We mainly detected high expression of TGF-β, IL-1β, and IL-10 in basal-like breast cancer compared to healthy and luminal biopsies. In agreement with our data, TGF-β and IL-6 were described to promote epithelial to mesenchymal transition by downregulating the expression of cell adhesion genes and upregulating the cell motility genes and genes associated with the mesenchymal phenotype [24, 32–34, 49]. This regulation could lead to a complete mesenchymal process (C-EMT) which was strongly associated with basal-like tumors [50, 51]. Additionally, ER-positive breast tumor cells were described to produce lower levels of IL-6 than ER-negative breast tumor cells [52]. Overexpression of IL-6 exhibits an epithelial-to-mesenchymal transition (EMT) phenotype in MCF7 cells and promotes their invasiveness [53]. In line with this study, higher IL-6 production was detected in CTH-DB cultures that previously exhibited more EMT features compared to CTH-BL cultures [17, 18]. However, the inhibition of IL-6 and IL-8 in TNBC cell lines decreased cell survival as well as colony formation, and prevented tumor growth in vivo [54]. Likewise, the expression of IL-1β was mainly reported in a highly malignant invasive mammary cell line (such as MDA-MB-231) [28, 55,

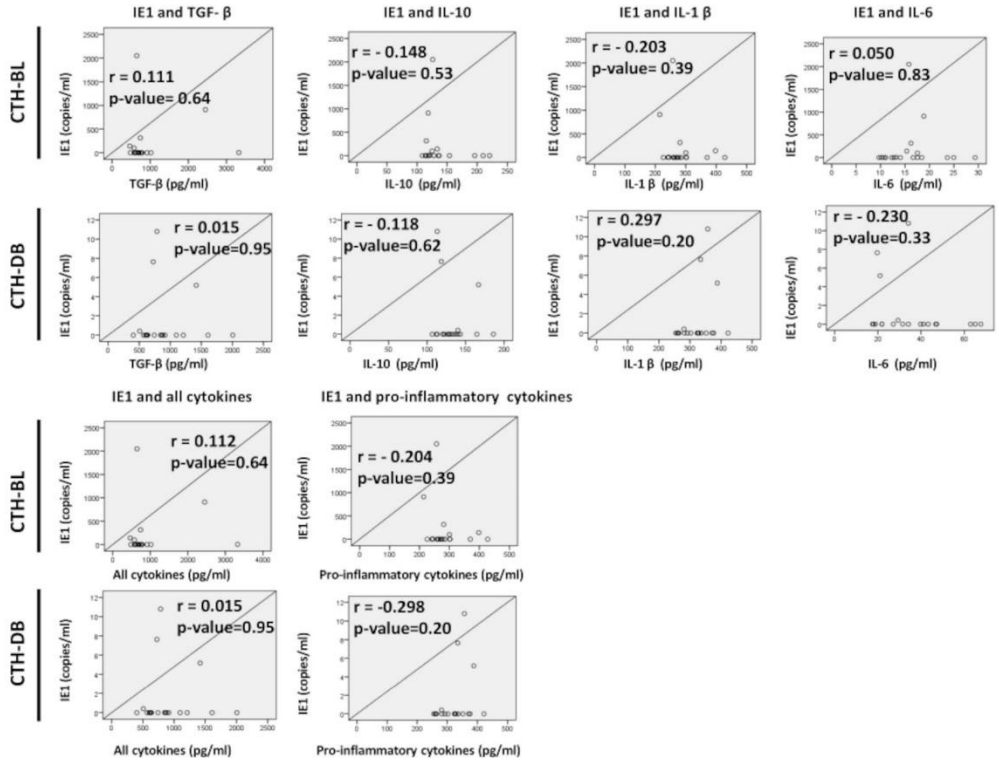

Fig. 4 Correlation between HCMV presence and cytokines production in CTH cultures. Pearson's correlation between viral load and cytokine production was conducted in CTH cultures. No significant correlation was identified between IE1 gene expression and cytokines production. The X-axis represents cytokine concentration (pg/ml), and the Y-axis represents viral load as measured by IE1 detection using qPCR (copies/ml). All cytokines: TGF-β, IL-6, IL10, IL-1β, Pro-inflammatory cytokines: IL-1β and IL-6. (r) stands for correlation coefficient

56]. In agreement with our in vivo outcomes, high levels of IL1-β were linked to breast cancer aggressiveness and poor prognosis [26, 57]. In addition, high expression of IL-10 was reported in breast tumors [26, 58].

Cytokines play a critical role not only in tumor growth and metastases but also in tumor evasion.

For instance, the anti-inflammatory cytokine IL-10 inhibits cytokine production and antigen presentation by T cells and macrophages [38, 39]. TGF-β was described to suppress natural killer cells (NK) and promote regulatory T-cell activity through a neuropilin-1-mediated mechanism [24, 59, 60]. This could explain the high IL-10 and TGF-β expression detected in the poor prognosis basal-like breast cancer biopsies compared to the luminal and healthy breast biopsies. Additionally, HCMV-infected tumor cells produce immunosuppressive cytokines such as IL-10 to escape the immune responses and counteract the pro-inflammatory cytokines production [8, 61]. This might be in line with the significant strong correlation detected between HCMV replication (IE1 expression) and IL-10 production in PGCCs-positive basal-like biopsies.

The HCMV-encoded IL-10, a homolog of the potent human interleukin 10 (hIL-10), possesses a range of immunomodulatory functions, including suppression of pro-inflammatory cytokine production. [62–64]. During viral latency, the expression of latency-associated cmvIL-10 (LAcmvIL-10), another isoform of the virus-encoded IL-10, modulates the microenvironment of infected cells and allows immunity evasion [65]. Furthermore, the immune suppressive cytokine TGF-β was reported to stimulate HCMV replication in fibroblast cultures [66]. HCMV produces TGF-β in different tumor cell types including glioblastoma, leukemia, and osteosarcoma cells

Table 2 Pathological data of breast cancer biopsies

	Biopsies #	ER	PR	HER2	Histo Type	Elston Ellis Grade	Vascular emboli	TNM
Luminal biopsies	#1	95	10	0	Lobular	II (3,2,1)	No	T2N0Mx
	#2	100	95	0	Ductal	II (2,2,2)	No	T2N0Mx
	#3	95	90	0	Ductal	II (3,2,1)	No	T1cN0Mx
	#4	95	70	0	Ductal	II (3,2,2)	No	T2N1Mx
	#5	100	100	0	Ductal	I (2,1,1)	No	ND
	#6	80	90	0	Lobular	II (3,2,1)	No	T2N1Mx
	#7	95	95	0	Ductal	I (2,2,1)	No	T1cN1mi
	#8	99	15	0	Ductal	III (3,2,3)	No	T3N1miMx
Basal biopsies	#9	0	0	0	Ductal	III (3,3,3)	No	T2N2aMx
	#10	0	0	0	Ductal	III (3,2,3)	ND	ND
	#11	0	0	0	Ductal	III (3,3,3)	Yes	ND
	#12	0	0	0	Ductal	III (3,3,3)	Yes	ND
	#13	0	0	0	Ductal	III (3,3,3)	Yes	ND
	#14	0	0	0	Ductal	III (3,3,2)	Yes	ND
	#15	0	0	0	Ductal	III (3,3,3)	Yes	T2N1mi
	#16	0	0	0	Ductal	III (3,2,3)	ND	T2N0

ND Not determined

[67, 68]. The HCMV IE2 protein enhances TGF-β gene transcription by interacting with the Egr-1 DNA-binding protein [69]. Moreover, a comparative study showed that HCMV-IE proteins activated the TGF-β promoter in the absence and presence of HCMV infection [68]. Hence, the production of TGF-β by HCMV could influence the infected cells, neighboring tissues and immune responses to benefit from the stimulating viral replication and avoid immune responses through the negative regulatory effects of TGF-β on lymphocytes functions [9, 70, 71]. This could further explain the enhanced expression of TGF-β detected in CTH cultures and basal-like biopsies.

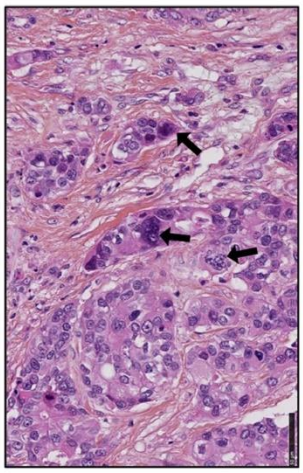

Fig. 5 PGCCs detection in breast cancer biopsies. Presence of PGCCs in breast cancer biopsies (arrows). The tissue was stained using HES. Magnification: 40X. Scale bars are 50 µm

Latency was reported to be essential for transformation induced by oncogenic herpesviruses [17, 72]. HCMV persistence was described in tubular epithelial cells [73], neural stem cells [74], and osteogenic sarcoma-derived cells [75]. Furthermore, the detection of some lytic blips suggests that both lytic viral replication and viral latency are essential to promote and maintain CTH transformation as previously reported for the other two oncogenic herpesviruses, namely EBV and Kaposi's sarcoma-associated herpesvirus (KSHV) [76, 77]. In addition, the detection of different PGCCs count and cytokine concentrations in CTH cultures suggests that the diversity of HCMV strains could affect the exhibition of PGCCs and cytokines production. Several studies showed that HCMV disease and pathogenesis could be related to HCMV genome diversity [78, 79]. Increasing evidence suggests an association between HCMV genetic diversity and HCMV pathogenesis that could also modulate oncomodulation/oncogenesis [80, 81].

PGCCs detection and cytokines expression depend not only on breast cancer type but also on the tumor microenvironment (TME). The composition of TME is modified by PGCCs through the recruitment of diploid cancer cells from adjacent zones; these diploid cells can

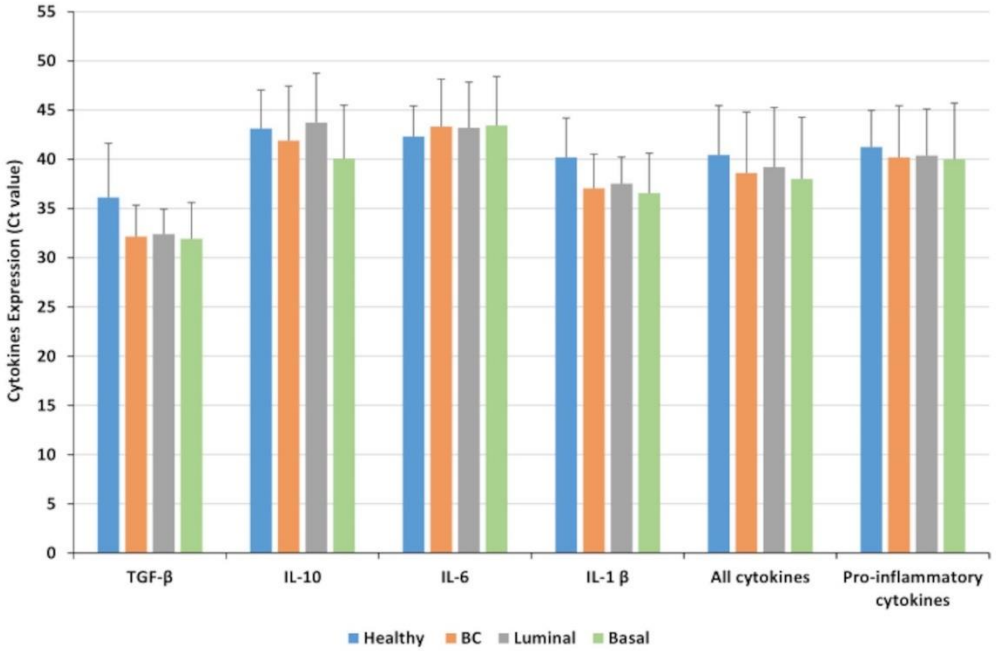

Fig. 6 Cytokines expression in breast biopsies. Histogram representing the expression of TGF-β, IL-10, IL-6, IL-1β, all cytokines and pro-inflammatory cytokines in healthy breast biopsies, all breast cancer biopsies (BC), as well as luminal and basal biopsies. Cytokines expression in biopsies was assessed by reverse transcription-quantitative polymerase chain reaction (RT-qPCR). Data are represented as mean ± SD of two independent experiments

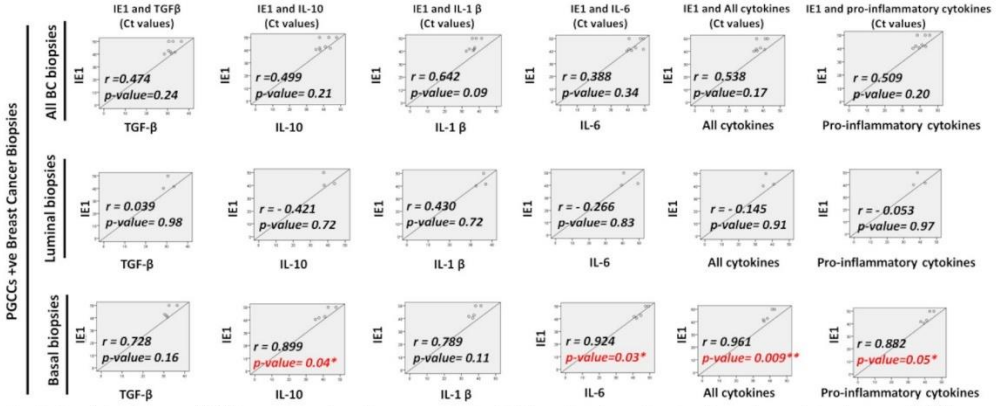

Fig. 7 Correlation between HCMV presence and cytokines expression in PGCCs-positive breast biopsies. Pearson's correlation between HCMV load and cytokines expression was conducted in luminal and basal breast cancer biopsies. A statistically significant strong positive correlation was observed between HCMV presence and IL-10, IL-6, all cytokines, and pro-inflammatory cytokines in PGCCs-positive basal-like biopsies. The X-axis represents cytokine expression (Ct value), and the Y -axis represents viral load as measured by IE1 qPCR (Ct value). All cytokines: TGF-β, IL-6, IL10, IL-1β, Pro-inflammatory cytokines: IL-1β and IL-6. (r) stands for correlation coefficient. *p-value ≤ 0.05; **p-value ≤ 0.01

ultimately become PGCCs [82]. Additionally, PGCCs progeny formation was described to be a part of the TME. PGCCs stemness, metastasis, vasculogenic mimicry and chemoresistance were recognized as the outcomes of the dynamic relationship between PGCCs and the TME [1]. Tumor cells secrete cytokines that recruit and activate other cells in the TME. Moreover, cytokines induce a tumor-supportive immune microenvironment by inhibiting anti-tumor immunity [83]. The inactivation of NF-kB in myeloid cells was described to reduce cytokines expression and tumor size [84]. The inflammatory cytokines including IL-1β, IL-6, IL-8, and CCL-5 that are induced by NF-kB promote tumor growth through the induction of cell proliferation [85]. The tumor-associated macrophage (TAMs), tumor-associated neutrophils (TANs), myeloid-derived suppressor cells (MDSC), and regulatory cells (Tregs) present in the TME are associated with poor prognosis. They produce IL-10 and TGF-β that suppress the activity of NK cells, T and B lymphocytes in the TME, allowing the proliferation and survival of cancer cells [85]. Also, TAMs, endothelial cells, and fibroblasts in the TME induce angiogenesis via IL-6, IL-8, and TGF-β [86–88]. TAMs promote metastasis and invasion in breast cancer through the secretion of IL-1β [31, 89]. TAMs, the most abundant cells in the TME, were associated with poor prognosis, especially in basal-like breast cancer [90, 91]. Furthermore, the pro-metastatic microenvironmental factor S100A4 was described to stimulate basal-like breast cancer cells to secrete pro-inflammatory cytokines that convert monocytes into TAM-like cells [92]. In line with this data, we detected the highest expression of the pro-inflammatory cytokines, IL-1β and IL-6, in basal-like breast cancer. Moreover, the abundant presence of TAMs in basal-like breast cancer could explain the high expression of TGF-β and IL-10 detected in basal biopsies compared to luminal ones. Hence, we highlighted the critical relationship between PGCCs/cytokines present in the TME and the basal-like breast cancer. Furthermore, the significant strong correlation identified between HCMV presence and the expression of IL-10, IL-6, all cytokines and pro-inflammatory cytokines suggested that HCMV presence could regulate cytokines expression in basal-like BC biopsies. High HCMV load might favor EMT features and immune evasion in basal-like BC biopsies by upregulating the expression of cytokines, particularly IL-10 and IL-6. Thus, our outcomes underline the strong link between HCMV load, PGCCs presence and cytokines expression in basal-like breast cancer that displays the most aggressive phenotype.

The in vitro PGCCs/cytokine profile present in our CTH model matched the in vivo PGCCs/cytokine profile identified in breast cancer biopsies. The highest IL-6 expression usually linked to EMT and PGCCs count was identified in CTH-DB culture and basal-like biopsies that harbor the most malignant phenotype [17, 18, 93]. Finally, telomere dysfunction-driven polyploidization is a universal source of tumor evolution that occurs continuously during neoplastic cell growth [94]. Oncoviruses deregulate telomerase activity and telomere length and promote cancer development [95]. Interestingly, HCMV activates telomerase [96], and favors the appearance of PGCCs which are considered as hallmarks of oncoviruses [5]. Further studies are needed to investigate the relationship and underlying mechanisms between polyploid cancer cells, cytokines production, and cytomegalovirus.

Our study has some limitations to address. To start with, the limited sample size; higher sample size enhances the significance level of our findings. Furthermore, the restricted cytokine evaluation; assessing more cytokines in CTH cultures and breast cancer biopsies might highlight the potential role of HCMV in cytokine production and cancer progression. Additionally, the absence of characterization of inflammatory cells that might underline the link between HCMV, cytokine production and cancer progression.

Conclusion

In conclusion, our findings revealed for the first time an association between high-risk HCMV strains, PGCCs formation, and cytokines production in vitro and in vivo. Our study presents a proof-of-concept for highlighting the cytokine profile in breast cancer, particularly the basal-like breast cancer, parallel to the presence of PGCCs and HCMV detection, thereby opening the door toward new therapeutic approaches in breast cancer patients with poor prognostic characteristics.

Supplementary Information

The online version contains supplementary material available at https://doi.org/10.1186/s12935-023-02971-1.

Additional file 1: Table S1. List of primers used.

Acknowledgements
The authors thank the Pathology Department of Besançon University Hospital for providing the breast cancer biopsies.

Author contributions
SHA, REB performed experiments. GH, SHA, REB participated to the data analysis. GH conceived and designed the project. SHA, REB, GH wrote the manuscript.

Funding
This work was supported by grants from the University of Franche-Comté, and the Région Franche-Comté to G.H. S.H.A was supported by ANR (Agence Nationale pour la Recherche) grant. R.EB. is a recipient of a doctoral scholarship from Apex Biosolutions company. The funders had no role in the data collection, analysis, patient recruitment, or decision to publish.

Availability of data and materials
The data supporting the findings of this study are available within the article and its Supplementary Information files and from the corresponding authors on request.

Declarations

Ethics approval and consent to participate
The local ethics committees of Besançon University Hospital (Besançon, France) and the French Research Ministry (AC-2015-2496, CNIL n°1173545, NF-S-96900 n ° F2015) permitted the study. All patients provide their written informed consent to participate in the study.

Consent for publication
Not applicable.

Competing interests
The authors declare that they have no competing interests.

Received: 11 February 2023 Accepted: 12 June 2023
Published online: 20 June 2023

References

1. Chen J, Niu N, Zhang J, Qi L, Shen W, Donkena KV, et al. Polyploid giant cancer cells (PGCCs): the evil roots of cancer. Curr Cancer Drug Targets. 2019;19:360–7. https://doi.org/10.2174/1568009618666180703154233.
2. White-Gilbertson S, Voelkel-Johnson C. Giants and monsters: unexpected characters in the story of cancer recurrence. Adv Cancer Res. 2020;148:201–32. https://doi.org/10.1016/bs.acr.2020.03.001.
3. Fei F, Zhang D, Yang Z, Wang S, Wang X, Wu Z, et al. The number of polyploid giant cancer cells and epithelial-mesenchymal transition-related proteins are associated with invasion and metastasis in human breast cancer. J Exp Clin Cancer Res. 2015;34:158. https://doi.org/10.1186/s13046-015-0277-8.
4. Amend SR, Torga G, Lin K-C, Kostecka LG, de Marzo A, Austin RH, et al. Polyploid giant cancer cells: unrecognized actuators of tumorigenesis, metastasis, and resistance. Prostate. 2019;79:1489–97. https://doi.org/10.1002/pros.23877.
5. Herbein G, Nehme Z. Polyploid giant cancer cells, a hallmark of oncoviruses and a new therapeutic challenge. Front Oncol. 2020;10:567116. https://doi.org/10.3389/fonc.2020.567116.
6. Sinzger C, Digel M, Jahn G. Cytomegalovirus cell tropism. Curr Top Microbiol Immunol. 2008;325:63–83. https://doi.org/10.1007/978-3-540-77349-8_4.
7. Cobbs CS, Harkins L, Samanta M, Gillespie GY, Bharara S, King PH, et al. Human cytomegalovirus infection and expression in human malignant glioma. Cancer Res. 2002;62:3347–50.
8. Cox M, Kartikasari AER, Gorry PR, Flanagan KL, Plebanski M. Potential impact of human cytomegalovirus infection on immunity to ovarian tumours and cancer progression. Biomedicines. 2021;9:351. https://doi.org/10.3390/biomedicines9040351.
9. Michaelis M, Doerr HW, Cinatl J. The story of human cytomegalovirus and cancer: increasing evidence and open questions. Neoplasia. 2009;11:1–9. https://doi.org/10.1593/neo.81178.
10. Samanta M, Harkins L, Klemm K, Britt WJ, Cobbs CS. High prevalence of human cytomegalovirus in prostatic intraepithelial neoplasia and prostatic carcinoma. J Urol. 2003;170:998–1002. https://doi.org/10.1097/01.ju.0000080263.46164.97.
11. Taher C, de Boniface J, Mohammad A-A, Religa P, Hartman J, Yaiw K-C, et al. High prevalence of human cytomegalovirus proteins and nucleic acids in primary breast cancer and metastatic sentinel lymph nodes. PLoS ONE. 2013;8:e56795. https://doi.org/10.1371/journal.pone.0056795.
12. Taher C, Frisk G, Fuentes S, Religa P, Costa H, Assinger A, et al. High prevalence of human cytomegalovirus in brain metastases of patients with primary breast and colorectal cancers. Transl Oncol. 2014;7:732–40. https://doi.org/10.1016/j.tranon.2014.09.008.
13. Haidar Ahmad S, Al Moussawi F, El Baba R, Nehme Z, Pasquereau S, Kumar A, et al. Identification of UL69 gene and protein in cytomegalovirus-transformed human mammary epithelial cells. Front Oncol. 2021;11:627866. https://doi.org/10.3389/fonc.2021.627866.
14. Herbein G. The human cytomegalovirus, from oncomodulation to oncogenesis. Viruses. 2018;10:408. https://doi.org/10.3390/v10080408.
15. Herbein G. High-risk oncogenic human cytomegalovirus. Viruses. 2022;14:2462. https://doi.org/10.3390/v14112462.
16. Kumar A, Tripathy MK, Pasquereau S, Al Moussawi F, Abbas W, Coquard L, et al. The Human cytomegalovirus strain DB activates oncogenic pathways in mammary epithelial cells. EBioMedicine. 2018;30:167–83. https://doi.org/10.1016/j.ebiom.2018.03.015.
17. Nehme Z, Pasquereau S, Haidar Ahmad S, Coaquette A, Molimard C, Monnien F, et al. Polyploid giant cancer cells, stemness and epithelial-mesenchymal plasticity elicited by human cytomegalovirus. Oncogene. 2021;40:3030–46. https://doi.org/10.1038/s41388-021-01715-7.
18. Nehme Z, Pasquereau S, Haidar Ahmad S, El Baba R, Herbein G. Polyploid giant cancer cells, EZH2 and Myc upregulation in mammary epithelial cells infected with high-risk human cytomegalovirus. EBioMedicine 2022;80:104056. https://doi.org/10.1016/j.ebiom.2022.104056.
19. Hsing C-H, Cheng H-C, Hsu Y-H, Chan C-H, Yeh C-H, Li C-F, et al. Upregulated IL-19 in breast cancer promotes tumor progression and affects clinical outcome. Clin Cancer Res. 2012;18:713–25. https://doi.org/10.1158/1078-0432.CCR-11-1532.
20. Nicolini A, Carpi A, Rossi G. Cytokines in breast cancer. Cytokine Growth Factor Rev. 2006;17:325–37. https://doi.org/10.1016/j.cytogfr.2006.07.002.
21. Band AM, Laiho M. Crosstalk of TGF-β and estrogen receptor signaling in breast cancer. J Mammary Gland Biol Neoplasia. 2011;16:109–15. https://doi.org/10.1007/s10911-011-9203-7.
22. Joshi A, Cao D. TGF-beta signaling, tumor microenvironment and tumor progression: the butterfly effect. Front Biosci. 2010;15:180–94. https://doi.org/10.2741/3614.
23. Meulmeester E, Ten Dijke P. The dynamic roles of TGF-β in cancer. J Pathol. 2011;223:205–18. https://doi.org/10.1002/path.2785.
24. Zu X, Zhang Q, Cao R, Liu J, Zhong J, Wen G, et al. Transforming growth factor-β signaling in tumor initiation, progression and therapy in breast cancer: an update. Cell Tissue Res. 2012;347:73–84. https://doi.org/10.1007/s00441-011-1225-3.
25. Iliopoulos D, Hirsch HA, Wang G, Struhl K. Inducible formation of breast cancer stem cells and their dynamic equilibrium with non-stem cancer cells via IL6 secretion. Proc Natl Acad Sci U S A. 2011;108:1397–402. https://doi.org/10.1073/pnas.1018898108.
26. Chavey C, Bibeau F, Gourgou-Bourgade S, Burlinchon S, Boissière F, Laune D, et al. Oestrogen receptor negative breast cancers exhibit high cytokine content. Breast Cancer Res. 2007;9:R15. https://doi.org/10.1186/bcr1648.
27. Pantschenko AG, Pushkar I, Anderson KH, Wang Y, Miller LJ, Kurtzman SH, et al. The interleukin-1 family of cytokines and receptors in human breast cancer: implications for tumor progression. Int J Oncol. 2003;23:269–84.
28. Singer CF, Kronsteiner N, Hudelist G, Marton E, Walter I, Kubista M, et al. Interleukin 1 system and sex steroid receptor expression in human breast cancer: interleukin 1alpha protein secretion is correlated with malignant phenotype. Clin Cancer Res. 2003;9:4877–83.
29. Apte RN, Krelin Y, Song X, Dotan S, Recih E, Elkabets M, et al. Effects of micro-environment- and malignant cell-derived interleukin-1 in carcinogenesis, tumour invasiveness and tumour-host interactions. Eur J Cancer. 2006;42:751–9. https://doi.org/10.1016/j.ejca.2006.01.010.
30. Wolf JS, Chen Z, Dong G, Sunwoo JB, Bancroft CC, Capo DE, et al. IL (interleukin)-1alpha promotes nuclear factor-kappaB and AP-1-induced IL-8 expression, cell survival, and proliferation in head and neck squamous cell carcinomas. Clin Cancer Res. 2001;7:1812–20.
31. Esquivel-Velázquez M, Ostoa-Saloma P, Palacios-Arreola MI, Nava-Castro KE, Castro JI, Morales-Montor J. The role of cytokines in breast cancer development and progression. J Interferon Cytokine Res. 2015;35:1–16. https://doi.org/10.1089/jir.2014.0026.
32. Allington TM, Schiemann WP. The cain and Abl of epithelial-mesenchymal transition and transforming growth factor-β in mammary epithelial cells. Cells Tissues Organs. 2010;193:98–113. https://doi.org/10.1159/000320163.
33. Heldin C-H, Landström M, Moustakas A. Mechanism of TGF-beta signaling to growth arrest, apoptosis, and epithelial-mesenchymal transition. Curr Opin Cell Biol. 2009;21:166–76. https://doi.org/10.1016/j.ceb.2009.01.021.

34. Wendt MK, Allington TM, Schiemann WP. Mechanisms of epithelial-mesenchymal transition by TGF-β. Future Oncol. 2009;5:1145–68. https://doi.org/10.2217/fon.09.90.
35. Xu J, Lamouille S, Derynck R. TGF-β-induced epithelial to mesenchymal transition. Cell Res. 2009;19:156–72. https://doi.org/10.1038/cr.2009.5.
36. Voulgari A, Pintzas A. Epithelial-mesenchymal transition in cancer metastasis: mechanisms, markers and strategies to overcome drug resistance in the clinic. Biochim Biophys Acta. 2009;1796:75–90. https://doi.org/10.1016/j.bbcan.2009.03.002.
37. Xie G, Yao Q, Liu Y, Du S, Liu A, Guo Z, et al. IL-6-induced epithelial-mesenchymal transition promotes the generation of breast cancer stem-like cells analogous to mammosphere cultures. Int J Oncol. 2012;40:1171–9. https://doi.org/10.3892/ijo.2011.1275.
38. Hamidullah, Changkija B, Konwar R. Role of interleukin-10 in breast cancer. Breast Cancer Res Treat 2012;133:11–21. https://doi.org/10.1007/s10549-011-1855-x.
39. Moore KW, O'Garra A, de Waal MR, Vieira P, Mosmann TR. Interleukin-10. Annu Rev Immunol. 1993;11:165–90. https://doi.org/10.1146/annurev.iy.11.040193.001121.
40. Salazar-Onfray F, López MN, Mendoza-Naranjo A. Paradoxical effects of cytokines in tumor immune surveillance and tumor immune escape. Cytokine Growth Factor Rev. 2007;18:171–82. https://doi.org/10.1016/j.cytogfr.2007.01.015.
41. Toutirais O, Chartier P, Dubois D, Bouet F, Lévêque J, Catros-Quemener V, et al. Constitutive expression of TGF-bêta1, interleukin-6 and interleukin-8 by tumor cells as a major component of immune escape in human ovarian carcinoma. Eur Cytokine Netw. 2003;14:246–55.
42. Haidar Ahmad S, Pasquereau S, El Baba R, Nehme Z, Lewandowski C, Herbein G. Distinct oncogenic transcriptomes in human mammary epithelial cells infected with cytomegalovirus. Front Immunol. 2021;12:772160. https://doi.org/10.3389/fimmu.2021.772160.
43. Zhang S, Mercado-Uribe I, Xing Z, Sun B, Kuang J, Liu J. Generation of cancer stem-like cells through the formation of polyploid giant cancer cells. Oncogene. 2014;33:116–28. https://doi.org/10.1038/onc.2013.96.
44. Lv H, Shi Y, Zhang L, Zhang D, Liu G, Yang Z, et al. Polyploid giant cancer cells with budding and the expression of cyclin E, S-phase kinase-associated protein 2, stathmin associated with the grading and metastasis in serous ovarian tumor. BMC Cancer. 2014;14:576. https://doi.org/10.1186/1471-2407-14-576.
45. Niu N, Mercado-Uribe I, Liu J. Dedifferentiation into blastomere-like cancer stem cells via formation of polyploid giant cancer cells. Oncogene. 2017;36:4887–900. https://doi.org/10.1038/onc.2017.72.
46. Sirois I, Aguilar-Mahecha A, Lafleur J, Fowler E, Vu V, Scriver M, et al. A unique morphological phenotype in chemoresistant triple-negative breast cancer reveals metabolic reprogramming and PLIN4 expression as a molecular vulnerability. Mol Cancer Res. 2019;17:2492–507. https://doi.org/10.1158/1541-7786.MCR-19-0264.
47. Lopez-Sánchez LM, Jimenez C, Valverde A, Hernandez V, Peñarando J, Martinez A, et al. CoCl2, a mimic of hypoxia, induces formation of polyploid giant cells with stem characteristics in colon cancer. PLoS ONE. 2014;9:e99143. https://doi.org/10.1371/journal.pone.0099143.
48. Xuan B, Ghosh D, Cheney EM, Clifton EM, Dawson MR. Dysregulation in actin cytoskeletal organization drives increased stiffness and migratory persistence in polyploidal giant cancer cells. Sci Rep. 2018;8:11935. https://doi.org/10.1038/s41598-018-29817-5.
49. Culig Z. Cytokine disbalance in common human cancers. Biochim Biophys Acta. 2011;1813:308–14. https://doi.org/10.1016/j.bbamcr.2010.12.010.
50. Aiello NM, Maddipati R, Norgard RJ, Balli D, Li J, Yuan S, et al. EMT subtype influences epithelial plasticity and mode of cell migration. Dev Cell. 2018;45:681-695.e4. https://doi.org/10.1016/j.devcel.2018.05.027.
51. Sørlie T, Perou CM, Tibshirani R, Aas T, Geisler S, Johnsen H, et al. Gene expression patterns of breast carcinomas distinguish tumor subclasses with clinical implications. Proc Natl Acad Sci U S A. 2001;98:10869–74. https://doi.org/10.1073/pnas.191367098.
52. Sasser AK, Sullivan NJ, Studebaker AW, Hendey LF, Axel AE, Hall BM. Interleukin-6 is a potent growth factor for ER-alpha-positive human breast cancer. FASEB J. 2007;21:3763–70. https://doi.org/10.1096/fj.07-8832com.
53. Sullivan N, Sasser A, Axel A, Vesuna F, Raman V, Ramirez N, et al. Interleukin-6 induces an epithelial–mesenchymal transition phenotype in human breast cancer cells. Oncogene. 2009;28:2940–7. https://doi.org/10.1038/onc.2009.180.
54. Hartman ZC, Poage GM, den Hollander P, Tsimelzon A, Hill J, Panupinthu N, et al. Growth of triple-negative breast cancer cells relies upon coordinate autocrine expression of the proinflammatory cytokines IL-6 and IL-8. Cancer Res. 2013;73:3470–80. https://doi.org/10.1158/0008-5472.CAN-12-4524-T.
55. Escobar P, Bouclier C, Serret J, Bièche I, Brigitte M, Caicedo A, et al. IL-1β produced by aggressive breast cancer cells is one of the factors that dictate their interactions with mesenchymal stem cells through chemokine production. Oncotarget. 2015;6:29034–47. https://doi.org/10.18632/oncotarget.4732.
56. Holen I, Lefley DV, Francis SE, Rennicks S, Bradbury S, Coleman RE, et al. IL-1 drives breast cancer growth and bone metastasis in vivo. Oncotarget. 2016;7:75571–84. https://doi.org/10.18632/oncotarget.12289.
57. Jin L, Yuan RQ, Fuchs A, Yao Y, Joseph A, Schwall R, et al. Expression of interleukin-1beta in human breast carcinoma. Cancer. 1997;80:421–34. https://doi.org/10.1002/(sici)1097-0142(19970801)80:3%3c421::aid-cncr10%3e3.0.co;2-z.
58. Kozłowski L, Zakrzewska I, Tokajuk P, Wojtukiewicz MZ. Concentration of interleukin-6 (IL-6), interleukin-8 (IL-8) and interleukin-10 (IL-10) in blood serum of breast cancer patients. Rocz Akad Med Bialymst. 2003;48:82–4.
59. Glinka Y, Prud'homme GJ. Neuropilin-1 is a receptor for transforming growth factor beta-1, activates its latent form, and promotes regulatory T cell activity. J Leukoc Biol. 2008;84:302–10. https://doi.org/10.1189/jlb.0208090.
60. Yoshimura A, Wakabayashi Y, Mori T. Cellular and molecular basis for the regulation of inflammation by TGF-beta. J Biochem (Tokyo). 2010;147:781–92. https://doi.org/10.1093/jb/mvq043.
61. Herbein G. Tumors and cytomegalovirus: an intimate interplay. Viruses. 2022;14:812. https://doi.org/10.3390/v14040812.
62. Jenkins C, Garcia W, Godwin MJ, Spencer JV, Stern JL, Abendroth A, et al. Immunomodulatory properties of a viral homolog of human interleukin-10 expressed by human cytomegalovirus during the latent phase of infection. J Virol. 2008;82:3736–50. https://doi.org/10.1128/JVI.02173-07.
63. Kotenko SV, Saccani S, Izotova LS, Mirochnitchenko OV, Pestka S. Human cytomegalovirus harbors its own unique IL-10 homolog (cmvIL-10). Proc Natl Acad Sci U S A. 2000;97:1695–700. https://doi.org/10.1073/pnas.97.4.1695.
64. Spencer JV, Lockridge KM, Barry PA, Lin G, Tsang M, Penfold MET, et al. Potent immunosuppressive activities of cytomegalovirus-encoded interleukin-10. J Virol. 2002;76:1285–92. https://doi.org/10.1128/jvi.76.3.1285-1292.2002.
65. Poole E, Avdic S, Hodkinson J, Jackson S, Wills M, Slobedman B, et al. Latency-associated viral interleukin-10 (IL-10) encoded by human cytomegalovirus modulates cellular IL-10 and CCL8 secretion during latent infection through changes in the cellular microRNA hsa-miR-92a. J Virol. 2014;88:13947–55. https://doi.org/10.1128/JVI.02424-14.
66. Alcami J, Paya CV, Virelizier JL, Michelson S. Antagonistic modulation of human cytomegalovirus replication by transforming growth factor beta and basic fibroblastic growth factor. J Gen Virol. 1993;74:269–74. https://doi.org/10.1099/0022-1317-74-2-269.
67. Kwon YJ, Kim D-J, Kim JH, Park C-G, Cha C-Y, Hwang E-S. Human cytomegalovirus (HCMV) infection in osteosarcoma cell line suppresses GM-CSF production by induction of TGF-beta. Microbiol Immunol. 2004;48:195–9. https://doi.org/10.1111/j.1348-0421.2004.tb03505.x.
68. Michelson S, Alcami J, Kim SJ, Danielpour D, Bachelerie F, Picard L, et al. Human cytomegalovirus infection induces transcription and secretion of transforming growth factor beta 1. J Virol. 1994;68:5730–7. https://doi.org/10.1128/JVI.68.9.5730-5737.1994.
69. Yoo YD, Chiou CJ, Choi KS, Yi Y, Michelson S, Kim S, et al. The IE2 regulatory protein of human cytomegalovirus induces expression of the human transforming growth factor beta1 gene through an Egr-1 binding site. J Virol. 1996;70:7062–70. https://doi.org/10.1128/JVI.70.10.7062-7070.1996.
70. Kehrl JH, Taylor A, Kim SJ, Fauci AS. Transforming growth factor-beta is a potent negative regulator of human lymphocytes. Ann N Y Acad Sci. 1991;628:345–53. https://doi.org/10.1111/j.1749-6632.1991.tb17267.x.
71. Wahl SM, Allen JB, Wong HL, Dougherty SF, Ellingsworth LR. Antagonistic and agonistic effects of transforming growth factor-beta and IL-1 in rheumatoid synovium. J Immunol. 1990;145:2514–9.

72. Soroceanu L, Matlaf L, Khan S, Akhavan A, Singer E, Bezrookove V, et al. Cytomegalovirus immediate-early proteins promote stemness properties in glioblastoma. Cancer Res. 2015;75:3065–76. https://doi.org/10.1158/0008-5472.CAN-14-3307.
73. Heieren MH, Kim YK, Balfour HH. Human cytomegalovirus infection of kidney glomerular visceral epithelial and tubular epithelial cells in culture. Transplantation. 1988;46:426–32. https://doi.org/10.1097/00007890-198809000-00019.
74. Belzile J-P, Stark TJ, Yeo GW, Spector DH. Human cytomegalovirus infection of human embryonic stem cell-derived primitive neural stem cells is restricted at several steps but leads to the persistence of viral DNA. J Virol. 2014;88:4021–39. https://doi.org/10.1128/JVI.03492-13.
75. Furukawa T. A variant of human cytomegalovirus derived from a persistently infected culture. Virology. 1984;137:191–4. https://doi.org/10.1016/0042-6822(84)90023-0.
76. Ganem D. KSHV and the pathogenesis of Kaposi sarcoma: listening to human biology and medicine. J Clin Invest. 2010;120:939–49. https://doi.org/10.1172/JCI40567.
77. Münz C. Latency and lytic replication in Epstein-Barr virus-associated oncogenesis. Nat Rev Microbiol. 2019;17:691–700. https://doi.org/10.1038/s41579-019-0249-7.
78. Renzette N, Bhattacharjee B, Jensen JD, Gibson L, Kowalik TF. Extensive genome-wide variability of human cytomegalovirus in congenitally infected infants. PLOS Pathog. 2011;7:e1001344. https://doi.org/10.1371/journal.ppat.1001344.
79. Renzette N, Gibson L, Jensen JD, Kowalik TF. Human cytomegalovirus intrahost evolution-a new avenue for understanding and controlling herpesvirus infections. Curr Opin Virol. 2014;8:109–15. https://doi.org/10.1016/j.coviro.2014.08.001.
80. Coaquette A, Bourgeois A, Dirand C, Varin A, Chen W, Herbein G. Mixed cytomegalovirus glycoprotein B genotypes in immunocompromised patients. Clin Infect Dis Off Publ Infect Dis Soc Am. 2004;39:155–61. https://doi.org/10.1086/421496.
81. Leach CT, Detels R, Hennessey K, Liu Z, Visscher BR, Dudley JP, et al. A longitudinal study of cytomegalovirus infection in human immunodeficiency virus type 1-seropositive homosexual men: molecular epidemiology and association with disease progression. J Infect Dis. 1994;170:293–8. https://doi.org/10.1093/infdis/170.2.293.
82. Saini G, Joshi S, Garlapati C, Li H, Kong J, Krishnamurthy J, et al. Polyploid giant cancer cell characterization: new frontiers in predicting response to chemotherapy in breast cancer. Semin Cancer Biol. 2022;81:220–31. https://doi.org/10.1016/j.semcancer.2021.03.017.
83. Binnewies M, Roberts EW, Kersten K, Chan V, Fearon DF, Merad M, et al. Understanding the tumor immune microenvironment (TIME) for effective therapy. Nat Med. 2018;24:541–50. https://doi.org/10.1038/s41591-018-0014-x.
84. Xia Y, Shen S, Verma IM. NF-κB, an active player in human cancers. Cancer Immunol Res. 2014;2:823–30. https://doi.org/10.1158/2326-6066.CIR-14-0112.
85. Kartikasari AER, Huertas CS, Mitchell A, Plebanski M. Tumor-induced inflammatory cytokines and the emerging diagnostic devices for cancer detection and prognosis. Front Oncol. 2021;11:692142. https://doi.org/10.3389/fonc.2021.692142.
86. Gopinathan G, Milagre C, Pearce OMT, Reynolds LE, Hodivala-Dilke K, Leinster DA, et al. Interleukin-6 stimulates defective angiogenesis. Cancer Res. 2015;75:3098–107. https://doi.org/10.1158/0008-5472.CAN-15-1227.
87. Levy L, Hill CS. Alterations in components of the TGF-beta superfamily signaling pathways in human cancer. Cytokine Growth Factor Rev. 2006;17:41–58. https://doi.org/10.1016/j.cytogfr.2005.09.009.
88. Waugh DJJ, Wilson C. The interleukin-8 pathway in cancer. Clin Cancer Res. 2008;14:6735–41. https://doi.org/10.1158/1078-0432.CCR-07-4843.
89. Coffelt SB, Kersten K, Doornebal CW, Weiden J, Vrijland K, Hau C-S, et al. IL-17-producing γδ T cells and neutrophils conspire to promote breast cancer metastasis. Nature. 2015;522:345–8. https://doi.org/10.1038/nature14282.
90. Zhang Y, Cheng S, Zhang M, Zhen L, Pang D, Zhang Q, et al. High-infiltration of tumor-associated macrophages predicts unfavorable clinical outcome for node-negative breast cancer. PLoS ONE. 2013;8:e76147. https://doi.org/10.1371/journal.pone.0076147.
91. Zhao X, Qu J, Sun Y, Wang J, Liu X, Wang F, et al. Prognostic significance of tumor-associated macrophages in breast cancer: a meta-analysis of the literature. Oncotarget. 2017;8:30576–86. https://doi.org/10.18632/oncotarget.15736.
92. Prasmickaite L, Tenstad EM, Pettersen S, Jabeen S, Egeland EV, Nord S, et al. Basal-like breast cancer engages tumor-supportive macrophages via secreted factors induced by extracellular S100A4. Mol Oncol. 2018;12:1540–58. https://doi.org/10.1002/1878-0261.12319.
93. Kvokačková B, Remšík J, Jolly MK, Souček K. Phenotypic heterogeneity of triple-negative breast cancer mediated by epithelial-mesenchymal plasticity. Cancers. 2021;13:2188. https://doi.org/10.3390/cancers13092188.
94. Christodoulidou A, Raftopoulou C, Chiourea M, Papaioannou GK, Hoshiyama H, Wright WE, et al. The roles of telomerase in the generation of polyploidy during neoplastic cell growth. Neoplasia. 2013;15:156–68. https://doi.org/10.1593/neo.121398.
95. Tornesello ML, Cerasuolo A, Starita N, Tornesello AL, Bonelli P, Tuccillo FM, et al. The molecular interplay between human oncoviruses and telomerase in cancer development. Cancers. 2022;14:5257. https://doi.org/10.3390/cancers14215257.
96. Strååt K, Liu C, Rahbar A, Zhu Q, Liu L, Wolmer-Solberg N, et al. Activation of telomerase by human cytomegalovirus. J Natl Cancer Inst. 2009;101:488–97. https://doi.org/10.1093/jnci/djp031.

Publisher's Note

Springer Nature remains neutral with regard to jurisdictional claims in published maps and institutional affiliations.

Ready to submit your research? Choose BMC and benefit from:

- fast, convenient online submission
- thorough peer review by experienced researchers in your field
- rapid publication on acceptance
- support for research data, including large and complex data types
- gold Open Access which fosters wider collaboration and increased citations
- maximum visibility for your research: over 100M website views per year

At BMC, research is always in progress.

Learn more biomedcentral.com/submissions

11.10 Publication N°10

El Baba R, Haidar Ahmad S, Monnien F, Mansar R, Bibeau F, Herbein G. Polyploidy, EZH2 upregulation, and transformation in cytomegalovirus-infected human ovarian epithelial cells. Oncogene 2023. https://doi.org/10.1038/s41388-023-02813-4.

The present study investigates the connection between human cytomegalovirus (HCMV) infection and epithelial ovarian cancer (OC), particularly high-grade serous ovarian carcinoma (HGSOC). Herein, we identified the presence of polyploid giant cancer cells (PGCCs) with stem cell-like characteristics in HGSOC. Additionally, we highlighted the role of the oncogene EZH2, which correlates with OC tumor grade and proliferation. Our study presents evidence of HCMV's involvement in transforming human ovarian epithelial cells, leading to the creation of "CMV-transformed Ovarian cells" (CTO). High-risk clinical HCMV strains, including the three strains isolated from HGSOC biopsies, induced distinct cellular and molecular changes, including EZH2 upregulation and increased cell proliferation. These findings support the notion of an HCMV-induced model for epithelial ovarian cancer and suggest the tumorigenic properties of EZH2. This research may have implications for targeted therapeutics in the treatment of ovarian tumors.

ARTICLE OPEN

Check for updates

Polyploidy, EZH2 upregulation, and transformation in cytomegalovirus-infected human ovarian epithelial cells

Ranim El Baba[1], Sandy Haidar Ahmad[1], Franck Monnien[2], Racha Mansar[2], Frédéric Bibeau[2] and Georges Herbein[1,3]✉

© The Author(s) 2023

Human cytomegalovirus (HCMV) infection has been implicated in epithelial ovarian cancer (OC). Polyploidy giant cancer cells (PGCCs) have been observed in high-grade serous ovarian carcinoma (HGSOC); they possess cancer stem cell-like characteristics and give rise to progeny cells expressing epithelial-mesenchymal transition (EMT) markers. EZH2 plays a potential oncogenic role, correlating with high proliferative index and tumor grade in OC. Herein, we present the experimental evidence for HCMV as a reprogramming vector that elicited human ovarian epithelial cells (OECs) transformation leading to the generation of "*CMV-transformed Ovarian cells*" (CTO). The infection with the two high-risk clinical strains, namely HCMV-DB and BL provoked a distinct cellular and molecular mechanisms in infected OECs. EZH2 upregulation and cellular proliferation were curtailed by using EZH2 inhibitors. The HGSOC biopsies were characterized by an elevated EZH2 expression, possessing a strong positive correlation between the aforementioned marker and HCMV. From HGSOC biopsies, we isolated three HCMV clinical strains that transformed OECs generating CTO cells which displayed proliferative potentials in addition to EZH2 upregulation and PGCCs generation; these features were reduced upon EZH2 inhibition. High-risk HCMV strains transformed OECs confirming an HCMV-induced epithelial ovarian cancer model and highlighting EZH2 tumorigenic properties. Our findings might be highly relevant in the pathophysiology of ovarian tumors thereby nominating new targeted therapeutics.

Oncogene (2023) 42:3047–3061; https://doi.org/10.1038/s41388-023-02813-4

INTRODUCTION

Epithelial ovarian cancer (OC), the most common and life-threatening cancer amongst gynecologic malignancies, has a 5-year age-standardized survival rate of 30–40%. Nearly 75% of all OC cases are diagnosed at late stages [1]. Despite the advances in treatment modalities, the overall survival remains low for stage III and stage IV accounting for 40 and 20%, respectively. Optimal surgery and platinum-based chemotherapy (such as carboplatin and cisplatin) remain the mainstay of treatment often combined with paclitaxel, gemcitabine, a humanized monoclonal antibody targeting vascular endothelial growth factor (VEGF) bevacizumab, pegylated liposomal doxorubicin, cyclophosphamide, topotecan, poly-ADP-ribose- polymerase (PARP) inhibitors, and immune check point inhibitors especially for recurrent OC [2–4]. In some cases, due to the poor blood supply to the peritoneal surface, hyperthermic intraperitoneal chemotherapy (HIPEC) has been used as a therapeutic alternative [5].

Human cytomegalovirus (HCMV) is a herpesvirus that infects between 40 and 95% of the worldwide population [6]. In healthy individuals, primary HCMV infection is asymptomatic. HCMV establishes a life-long chronic latency primarily in monocytes, tissue macrophages, and myeloid lineage $CD34^+$ hematopoietic progenitor cells, with periodic reactivation [7]. HCMV genomic variability could contribute to its oncomodulatory role where HCMV will encourage the development and spread of tumor cells [8, 9]. Lately, an oncogenic role of HCMV has been underlined where the high-risk HCMV strains directly transform primary cells [10].

Polyploidy, a condition in which a normally diploid cell acquires additional sets of chromosomes, is formed via cell-cell fusion or endoreplication [11]. Polyploidy giant cancer cells (PGCCs) have been confirmed to possess cancer stem cell (CSC)-like characteristics, and give rise to progeny cells through asymmetric division which express epithelial-mesenchymal transition (EMT)-related markers thereby promoting invasion and migration [12–14]. Studies have shown that PGCCs generation was induced by anti-cancer therapies where the latter convert proliferating tumor into dormant cells [15]. The presence of PGCCs in OC has been preferentially reported in poor prognosis cancers participating in tumor relapse and therapy resistance [16]. Moreover, previous studies revealed the detection of PGCCs harboring HCMV; a significant correlation was shown between PGCCs presence and HCMV in breast cancer biopsies [17–20]. Besides PGCCs, tetraploidy has been reported in approximately 26% of solid tumors [21]; it's usually formed through cell fusion, endoreduplication, mitotic slippage, or cytokinetic failure, the latter two being the main mechanisms [21, 22]. It has been reported that tetraploid cells induce aneuploidy and transformation of mouse ovarian surface epithelial cells [23]. Aneuploidy post-tetraploidization is observed mainly in p53-inactivated cells [21]. p53 and telomerase depletion generates a state of chronic DNA damage, therefore, resulting in tetraploidization [21, 24].

[1]Department of Pathogens & Inflammation-EPILAB Laboratory EA4266, University of Franche-Comté, Besançon, France. [2]Department of Pathology, CHU Besançon, Besançon, France. [3]Department of Virology, CHU Besançon, Besançon, France. ✉email: georges.herbein@univ-fcomte.fr

Received: 10 July 2023 Revised: 10 August 2023 Accepted: 15 August 2023
Published online: 26 August 2023

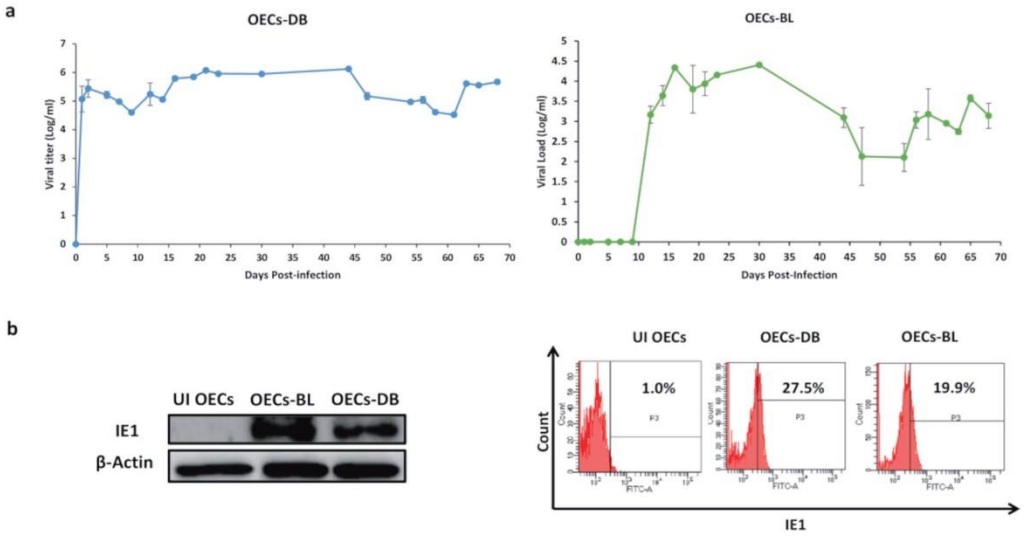

Fig. 1 Replication of high-risk HCMV strains in OECs cultures. a Time-course of the viral titer in the supernatant of OECs infected with HCMV-DB and BL as measured by IE1-qPCR. **b** Immunoblotting data of IE1 in uninfected OECs lysates and OECs infected with HCMV-DB and BL (day 5 post-infection). β-actin was used as loading control. IE1 expression by FACS in acutely infected OECs-DB and BL; UI OECs were used as a control.

Classical OC risk factors including age, family history, epigenetic as well as genetic alterations might generate a tumor-supporting cellular environment, where some oncogenic viruses reside and advance their oncogenic potential [1]. EZH2 dysregulation was associated with the development, progression, and therapeutic resistance of many tumors, particularly OC [25]. Several studies showed that EZH2 overexpression is associated with high-grade serous ovarian carcinoma (HGSOC) [25, 26]. Another study revealed that invading PGCCs possess strong EZH2 expression [27]. All in all, EZH2 potentially serves as an effective therapeutic target [25]. Moreover, there exists a strong emerging evidence showing HCMV infection prevalence in breast, cervical, colon, liver, prostate, and brain cancer patients [28–30]. HCMV-IE and pp65 proteins were detected in 82 and 97% of epithelial ovarian cancer, respectively [31]. Prominent HCMV-IE protein expression was linked to a higher stage of OC [31]. Further, CMV DNA was detected in 70% of cancerous ovarian tissues and was significantly higher compared to benign tumor cases [32]. Recent studies have identified high HCMV expression in OC biopsies that were associated with poor survival outcomes [33].

To investigate the potential role of HCMV infection in epithelial ovarian cancer, especially in HGSOC, human ovarian epithelial cells (OECs) were infected with low (KM and FS) and high-risk (DB and BL) oncogenic HCMV clinical strains; the latter previously transformed human astrocytes and human mammary epithelial cell [17, 30, 34]. In this study, we assessed the transforming potential of the two high-risk clinical strains, HCMV-DB and HCMV-BL, and investigated their molecular and cellular features that appeared in the long-term "*CMV-transformed Ovarian cells*" (CTO) cultures. Additionally, from HGSOC biopsies that revealed high EZH2 expression, we isolated three clinical HCMV strains that displayed oncogenic and stemness features when cultivated on OECs with enhanced EZH2 expression that could be curtailed by EZH2 inhibitors.

RESULTS

OECs chronically infected with HCMV-DB and BL strains generated CTO cells with PGCCs

Upon studying the tropism exhibited by HCMV in OECs, all HCMV clinical strains replicated showing a peak viral replication at day 21, 16, 16, and 19 post-infection in OECs infected with HCVM-DB, HCMV-BL, HCMV-KM, and HCMV-FS, respectively (Fig. 1a and Supplementary Fig. 1a). The peak level of HCMV productive infection was 6 and 4 logs in OECs-DB and BL, respectively (Fig. 1a). HCMV-IE1 and pp65 proteins were detected in OECs-DB and BL (Fig. 1b and Supplementary Fig. 2).

We noticed the existence of large-sized cells having large nuclei that were detected only in OECs chronically infected with the high-risk HCMV-DB and BL strains compared to uninfected OECs (Fig. 2a) and OECs chronically infected with HCMV-KM and FS strains (Supplementary Fig. 1b). Further, around three months post-infection, cellular survival was noted only in the chronically infected OECs-DB and BL compared to OECs-KM and FS (Supplementary Fig. 3). The emerging cells were termed *"CMV-Transformed Ovarian epithelial cells"* or CTO similar to the transformed cells that were previously reported by our group, namely, "CMV-Transformed Human mammary epithelial cells" or CTH cells and "CMV-Elicited GlioBlastoma Cells" or CEGBCs [30, 34].

After applying a morphology-based classification, cellular heterogeneity was detected in CTO-DB and BL cultures including giant cells, blastomeres, blastocytes, multinucleated, mesenchymal, budding, and lipid droplets-rich cells as well as cells exhibiting filopodia and cytoplasmic vacuolization (Fig. 2b). Some of the aforementioned morphologies were further confirmed by confocal microscopy showing mainly multinucleated and mesenchymal cells, asymmetric division, budding, and cells with giant nuclei (Fig. 2c). A high percentage of tetraploidization and polyploidy cells was detected in CTO-DB and BL compared to UI OECs (Fig. 2d). CTO-DB and BL populations were classified into PGCCs (≥4 N), intermediate cells (ICs of 2–4 N), and small cells (SCs of 2 N) (Fig. 2d). As a positive control, cobalt chloride ($CoCl_2$) was

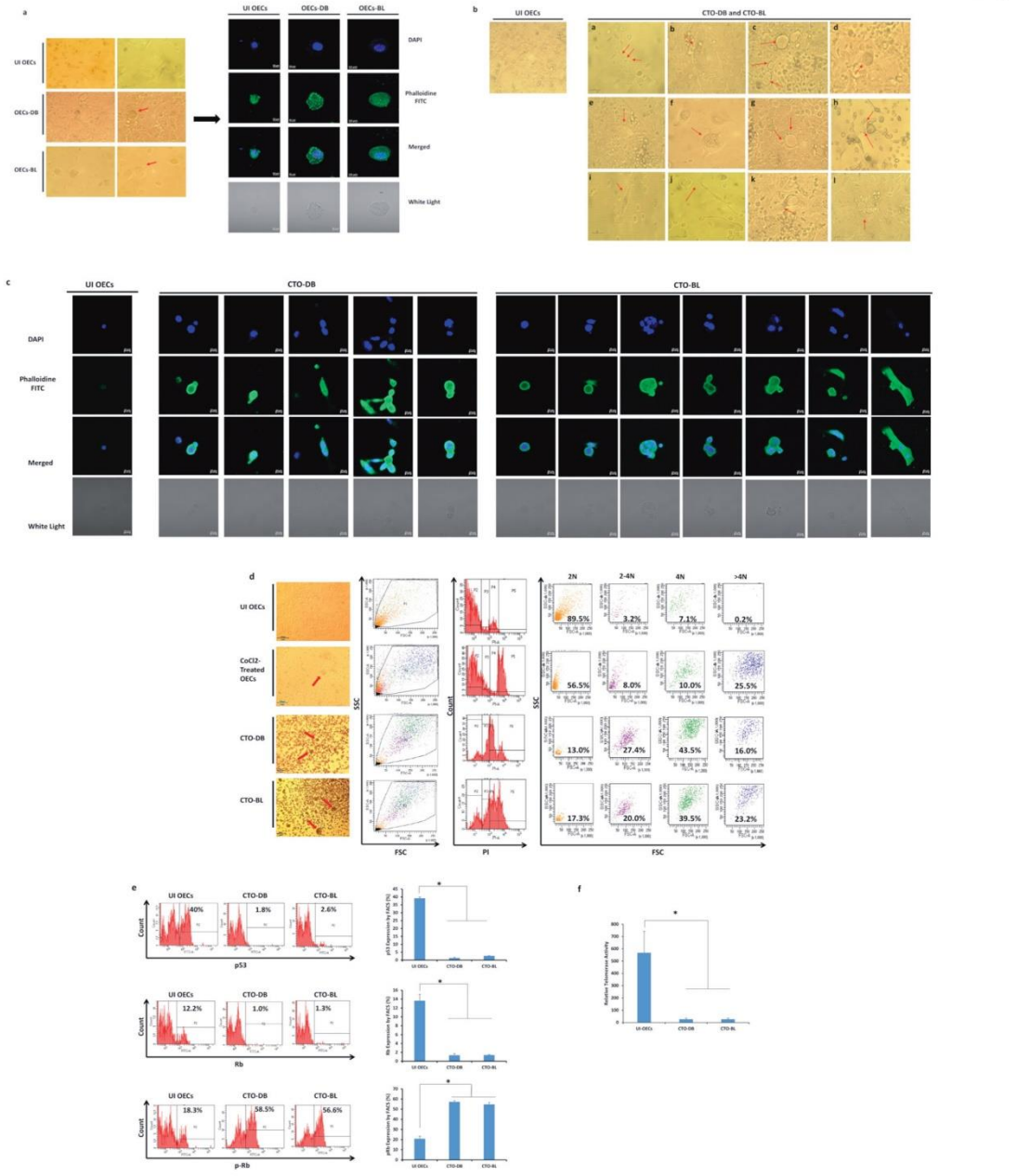

used to induce PGCCs formation in OECs cultures (Fig. 2d, Supplementary Fig. 4).

Since the blockade of tumor suppressors and decreased telomerase activity have been correlated with tetraploidization in several human cancers [24], p53 and Rb expression as well as telomerase activity were assessed in uninfected OECs, CTO-DB, and CTO-BL (Fig. 2e, f). Downregulation of p53 and Rb proteins was noticed in CTO-DB and BL compared to controls

Fig. 2 Chronic infection of OECs with the high-risk HCMV clinical isolates and polyploidy detection in OECs cultures. a Microscopic images including confocal images of DAPI and phalloidine staining in OECs infected with HCMV-DB and BL; uninfected OECs were used as a negative control. Left panel: magnification ×100 and ×200, scale bar 100 and 50 μm; Right panel: magnification ×63, scale bar 10 μm. Red arrows showing the PGCCs detected in OECs cultures. **b** The appearance of distinct cellular morphologies of the giant cell cycle including (**a**) filopodia, (**b**, **c**, **d**) blastomeres and blastocytes, (**e**) lipid droplets-filled cells, (**f**) multinucleated, (**g**, **h**) budding, (**i**) mesenchymal cells as well as (**j**, **k**, **l**) few atypical morphologies; magnification ×100, scale bar 100 μm. Uninfected OECs were used as a control. **c** Confocal microscopic images of DAPI and phalloidine staining in CTO-DB and BL. Uninfected OECs were used as a negative control; magnification ×63, scale bar 10 μm. **d** Propidium iodide (PI) staining for polyploidy detection in HCMV-transformed OECs. Cobalt chloride (CoCl2)-treated OECs (450 μM) were used as a positive control. Microscopic images of uninfected OECs as well as the PGCCs generated in CTO-DB and BL cultures and post-CoCl2 treatment; magnification ×100, scale bar 100 μm. **e** p53, Rb, and p-Rb expression in uninfected OECs and CTO-DB and BL by FACS. **f** Histograms representing the relative telomerase activity in uninfected OECs as well as CTO-DB and BL. Data are represented as mean ± SD of two independent experiments. *p-value ≤ 0·05.

(p-value $_{(UI\ OECs:CTO\text{-}HCMV)} = 0·03$), unlike pRb which was upregulated in CTO-DB and BL (p-value $_{(UI\ OECs:CTO\text{-}HCMV)} = 0·03$) (Fig. 2e). Notably, telomerase activity was relatively low or undetectable in CTO-DB and BL compared to uninfected OECs (p-value = 0·03) (Fig. 2f). Hence, p53 and Rb downregulation along with decreased telomerase activity are sufficient to drive polyploidization in CTO-DB and BL, as previously reported [24].

CTO cells display dedifferentiation, stemness, and EMT characteristics

CTO-DB and BL were seeded in soft agar to assess their oncogenic transforming potential. Colony formation was detected in the cultures seeded with CTO-DB and BL, compared to uninfected OECs (Fig. 3a). On the proteomic level, EZH2 and Myc upregulation was detected in CTO-DB and BL compared to uninfected OECs (p-value $_{(UI\ OECs:CTO\text{-}HCMV)} = 0·03$) (Fig. 3b–d); on the contrary, a limited EZH2 and Myc upregulation was observed in OECs-KM and FS (p-value $_{(UI\ OECs:OECs\text{-}HCMV)} = 0·02$) (Supplementary Fig. 1c). A significant positive correlation between EZH2 and Myc protein expression was detected in CTO cells ($r = 0.983$, p-value < 0·001) (Supplementary Fig. 5). Further, EZH2 and Myc transcripts were upregulated in CTO-DB and BL compared to uninfected controls (p-value $_{(UI\ OECs:CTO\text{-}HCMV)} = 0·03$) (Fig. 3e). Altogether, a remarkable EZH2 upregulation parallel to the limited increase in Myc expression was noticed in CTO infected with the high-risk HCMV-DB and BL strains. EZH2 and Myc were expressed mainly in the PGCCs subpopulation of CTO-DB and BL (Fig. 3g). A limited increase in SUZ12 expression was observed in CTO-DB and BL compared to uninfected OECs (p-value $_{(UI\ OECs:CTO\text{-}HCMV)} = 0·03$) (Supplementary Fig. 6a, b). Upon assessing the proliferative potential of OECs chronically infected with HCMV high-risk strains, Ki67Ag was highly prominent in CTO-DB and BL compared to uninfected OECs (p-value $_{(UI\ OECs:CTO\text{-}HCMV)} = 0·03$) (Fig. 3f). High Ki67Ag expression was detected in the large cells (Fig. 3g).

CTO-DB and BL displayed an embryonic stemness phenotype. The key regulatory genes maintaining the pluripotency and self-renewal properties of embryonic stem cells, Nanog, Sox2, and Oct4 were shown to be highly expressed in CTO-DB and BL compared to uninfected OECs (Fig. 4a, b, and Supplementary Fig. 7a). Additionally, transcripts of Nanog, Sox2, and Oct4 were elevated in CTO-DB and BL (Nanog, p-value $_{(UI\ OECs:CTO\text{-}HCMV)} = 0·06$; Sox2 and Oct4, p-value $_{(UI\ OECs:CTO\text{-}HCMV)} = 0·03$) (Fig. 4c and Supplementary Fig. 7b). Besides PGCCs appearance in CTO-DB and BL cultures, it's worth mentioning the appearance of spontaneous spheroids in CTO-BL cultures (Fig. 4d). Further, in the presence of methylcellulose, spheroids were generated in CTO-DB and BL cultures (Fig. 4e). Finally, CD44, a marker of stemness and invasiveness, was upregulated in CTO-DB and BL cultures compared to uninfected OECs (Supplementary Fig. 8).

EMT fuels cancer progression, tumor cell invasion, and therapy resistance [35]. PGCCs gain strong invasiveness and migration ability after they undergo EMT [36]. Vimentin was strongly upregulated in DB and BL-infected OECs (p-value $_{(UI\ OECs:CTO\text{-}HCMV)} = 0·03$), whereas a slight decrease in E-cadherin was noticed compared to uninfected OECs (p-value $_{(UI\ OECs:CTO\text{-}HCMV)} = 0·06$) (Fig. 5a–c). Vimentin and E-cadherin were expressed mainly in the PGCCs and ICs subpopulations of CTO-DB and BL (Fig. 5d). Altogether, the co-existence of vimentin and E-cadherin was detected in CTO-DB and BL, indicating a mesenchymal/epithelial hybrid state that was also accompanied with occasionally existing small cells possessing an elevated E-cadherin expression (Fig. 5 and Supplementary Fig. 9). The co-existence of mesenchymal and epithelial phenotypes confirms the cellular plasticity of CTO-DB and BL. As a control, EZH2, Myc, Ki67Ag, Vimentin, E-cadherin, and CD44 protein expression in the subpopulations of uninfected OECs was provided in Supplementary Fig. 10.

Lytic and latent HCMV replication in transformed OECs

Sustained HCMV replication was confirmed in OECs chronically infected with HCMV-DB and BL, namely CTO-DB and BL (Fig. 6). IE1 protein was remarkably detected in CTO-DB and BL versus uninfected OECs (Fig. 6a, b); elevated IE1 expression was detected mainly in the PGCCs subpopulation compared to ICs and SCs (Supplementary Fig. 11). IE1 and UL69 genes and transcripts were detected in CTO-DB and BL compared to uninfected OECs (Fig. 6c, d), indicating lytic HCMV replication. In addition, HCMV latency in CTO-DB and BL cultures was established by IE1 reactivation that was observed post-TPA treatment (p-value $_{(CTO:TPA\ treated\ CTO)} = 0·02$) (Fig. 6e and Supplementary Fig. 12).

Given that EZH2 is considered a major tumor marker and an effective therapeutic target for OC, herein, we evaluated the impact of two EZH2 inhibitors (GSK343 and EPZ6438) on CTO proliferation and polyploidization. Upon EZH2 blockade (Supplementary Fig. 13), detection of HCMV-IE1 gene was suppressed (Fig. 6f). Ki67Ag protein expression was decreased post-EZH2 inhibitor treatment of CTO-DB and BL compared to untreated CTO cells (p-value $_{(CTO:EZH2\ inhibitors\ treated\ CTO)} = 0·004$) (Fig. 6g). Upon assessing the PI expression in the subpopulations of CTO cells, GSK343 and EPZ6438 reduced tetraploidization and polyploidization in treated CTO cells compared to controls (p-value $_{(CTO:EZH2\ inhibitors\ treated\ CTO)} = 0·007$ and 0·004, respectively) (Fig. 6h).

EZH2 upregulation in HCMV-positive HGSOC biopsies and the isolation of three oncogenic HCMV strains from EZH2^{High} HGSOC biopsies

To further assess the role of HCMV, EZH2, and PGCCs induction in vivo, we analyzed 25 OC biopsies (HGSOC biopsies $n = 18$ and adjacent non-tumoral biopsies $n = 7$) (Supplementary Table 3) for the presence of HCMV, PGCCs count, as well as EZH2, Myc, and Akt expression (Fig. 7, Supplementary Fig. 14, and Supplementary Fig. 15). PGCCs with giant or multiple nuclei were detected in the HGSOC biopsies (Fig. 7a). HCMV was detected in 72% of HGSOC biopsies (Fig. 7b). Elevated PGCCs count was mainly detected in HCMV-positive HGSOC biopsies (Fig. 7c). HCMV-positive tumor biopsies displayed mostly an enhanced EZH2 and Akt with a limited Myc expression (Fig. 7d, Supplementary Fig. 14, and Supplementary Fig. 15a). A significant positive correlation was found between HCMV presence and EZH2 as well as Akt expression ($r = -0.598$, p-value = 0·009 and $r = -0.466$, p-value =

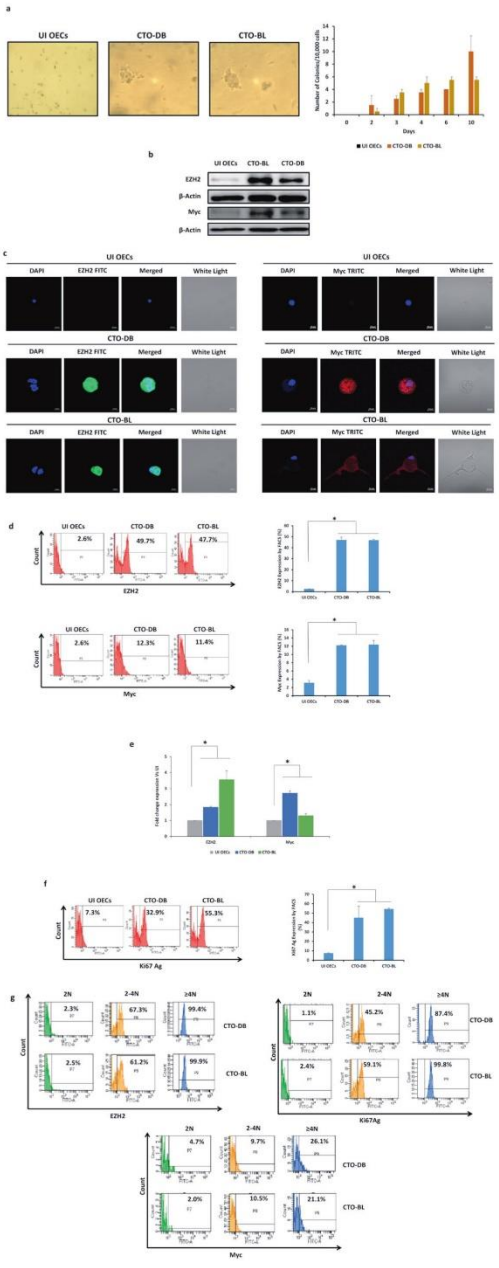

Fig. 3 Colony formation in soft agar and the phenotypic characterization of HCMV-transformed OECs. a Colony formation in soft agar seeded with CTO-DB and BL (MOI = 1); UI OECs were used as a negative control. Formed colonies were observed under an inverted light microscope (Magnification ×200, scale bar 50 µm). Histogram representing the colony quantification/10,000 cells over days. **b** Immunoblotting data of EZH2 and Myc in uninfected OECs lysates and CTO-DB and BL. β-actin was used as loading control. **c** Confocal microscopic images of EZH2, Myc, and DAPI staining in CTO-DB and BL. UI OECs were used as controls; magnification ×63, scale bar 10 µm. **d** FACS staining of EZH2 and Myc in uninfected OECs as well as CTO-DB and BL. **e** EZH2 and Myc transcripts detection by RT-qPCR. **f** FACS staining of Ki67Ag in uninfected OECs as well as CTO-DB and BL. **g** EZH2, Myc, and Ki67Ag expression in CTO-DB and BL subpopulations (2 N, 2–4 N, and ≥4 N). Data are represented as mean ± SD of two independent experiments. *p-value ≤ 0·05.

0·05, respectively, based on Ct values) (Fig. 7e and Supplementary Fig. 15b). A significant positive correlation was detected between Akt expression and EZH2 as well as Myc expression ($r = 0.420$, p-value = 0·015 and $r = 0.620$, p-value = 0·006, respectively) (Supplementary Fig. 15b). Among the eighteen HCMV-positive HGSOC biopsies, three biopsies with the highest EZH2 expression were considered for HCMV isolation. The three HCMV-OC strains were isolated by tissue disruption and filtration, and were subsequently grown in MRC5 cells showing a peak of viral load of 3 logs around day 7 post-infection (Fig. 7f). Following OECs infection with the three HCMV-OC strains, HCMV presence was confirmed by the detection of IE1 gene in addition to the morphological changes that appeared in the OECs infected cultures, for instance, giant and multinucleated cells showing cell budding as well as mesenchymal cells (Fig. 7f, g). Post-EZH2 inhibition, using GSK343, no HCMV replication was detected in addition to the absence of morphological heterogeneity in the infected cultures (Fig. 7g, h). Upregulation of Ki67Ag, EZH2, and Myc expression was observed in CTO-HCMV-OC compared to uninfected OECs and GSK-treated CTO-HCMV-OC cells (Ki67Ag p-value $_{(CTO:GSK343\text{-}CTO)}$ = 0·01; EZH2 p-value $_{(CTO:GSK343\text{-}CTO)}$ = 0·002; Myc p-value $_{(CTO:GSK343\text{-}CTO)}$ = 0·002) (Fig. 7i). GSK343 reduced Ki67Ag, EZH2, and Myc expression by 56%, 79%, and 63%, respectively (Fig. 7i). EZH2 inhibition reduced PGCCs percentage in infected cultures compared to untreated CTO cells (p-value = 0·002) (Fig. 7j).

DISCUSSION

In the present study, we assessed the potential transforming capacities of the high-risk HCMV-DB and BL strains, following the OECs infection. The OECs infection with the high-risk HCMV-DB and BL strains resulted in a pro-oncogenic cellular environment and sustained growth of CMV-transformed OECs with soft agar colonies formation. The CTO cells dedifferentiated, displayed stemness as well as EMT-MET hybrid phenotype, and finally resulted in PGGCs generation (Fig. 8) and spheroid formation. HCMV presence accompanied by polyploidy, EZH2 upregulation, and malignant phenotype potentially confirm the transformation process. In vivo, 72% of HGSOC biopsies were found to harbor HCMV with elevated PGCCs count as well as enhanced EZH2 expression, revealing a strong correlation between HCMV, PGCCs, and EZH2 expression. Three HCMV-OC strains were isolated from $EZH2^{high}$ OC tumors that transformed OECs toward CTO possessing increased EZH2, Ki67Ag, and Myc expression parallel to polyploidy induction. The expression of the aforementioned markers and polyploidy were curtailed by EZH2 inhibitors therapy.

PGCCs play a fundamental role in tumor progression and in regulating tumor heterogeneity [37, 38]. Accumulating evidence reveals the presence of PGCCs in OC, particularly the HGSOC, where PGCCs act as stem-like, self-renewing cells that are considered prognostic factors for OC [38, 39]. In our study, CTO cells generated PGCCs, and were heterogeneous showing distinct

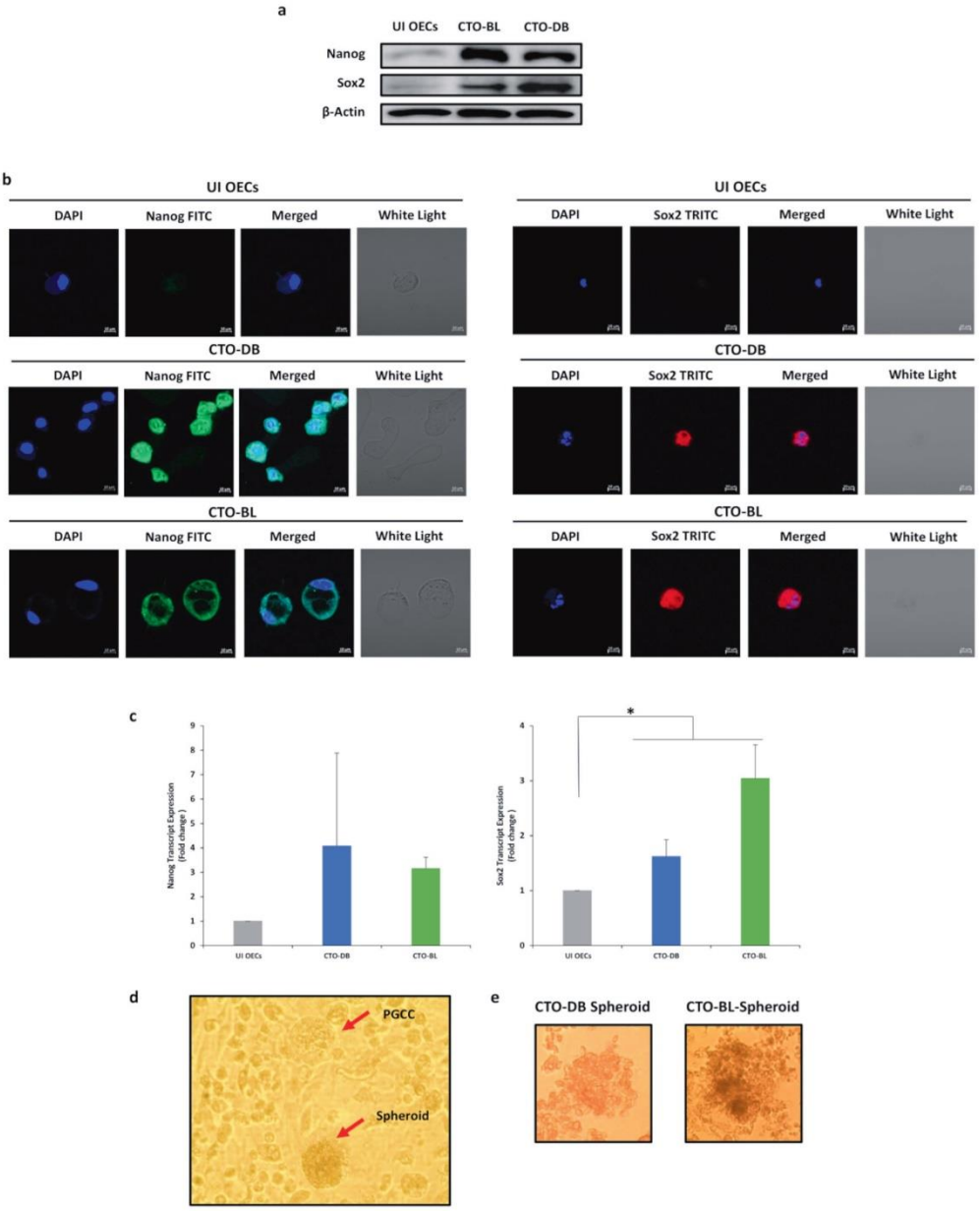

Fig. 4 HCMV-transformed OECs display an embryonic stemness phenotype and possess spheroid-forming potential. a Immunoblotting data of Nanog and Sox2 in uninfected OECs lysates and CTO-DB and BL. β-actin was used as loading control. **b** Confocal microscopic images of Nanog, Sox2, and DAPI staining in CTO-DB and BL. UI OECs were used as controls; magnification ×63, scale bar 10 µm. **c** Nanog and Sox2 transcripts detection by RT-qPCR. Data are represented as mean ± SD of two independent experiments. **d** Spontaneous spheroid formation and PGCCs were detected under an inverted light microscope in HCMV-transformed OECs cultures. Magnification ×100, scale bar 100 µm. **e** Spheroid generation from the chronically infected DB and BL OECs in methyl-cellulose assay; magnification ×100, scale bar 100 µm. *p-value ≤ 0·05.

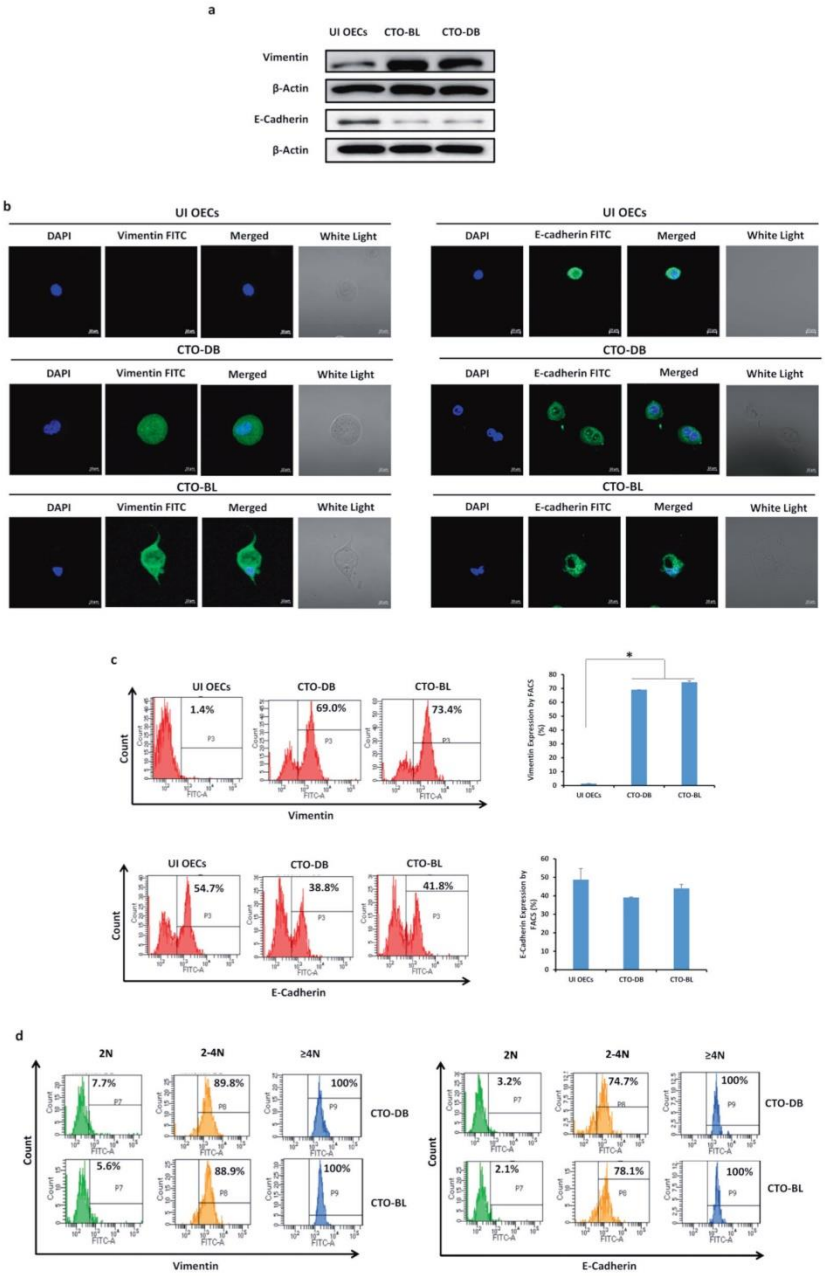

Fig. 5 HCMV infection of OECs enhances EMT/MET hybrid traits. Vimentin and E-cadherin expression by western blot (**a**), confocal microscopy (**b**), and FACS (**c**) in CTO-DB and BL. Uninfected OECs were used as controls. **d** Vimentin and E-cadherin expression in CTO-DB and BL subpopulations (2 N, 2–4 N, and ≥4 N). Data are represented as mean ± SD of two independent experiments. *p-value ≤ 0·05.

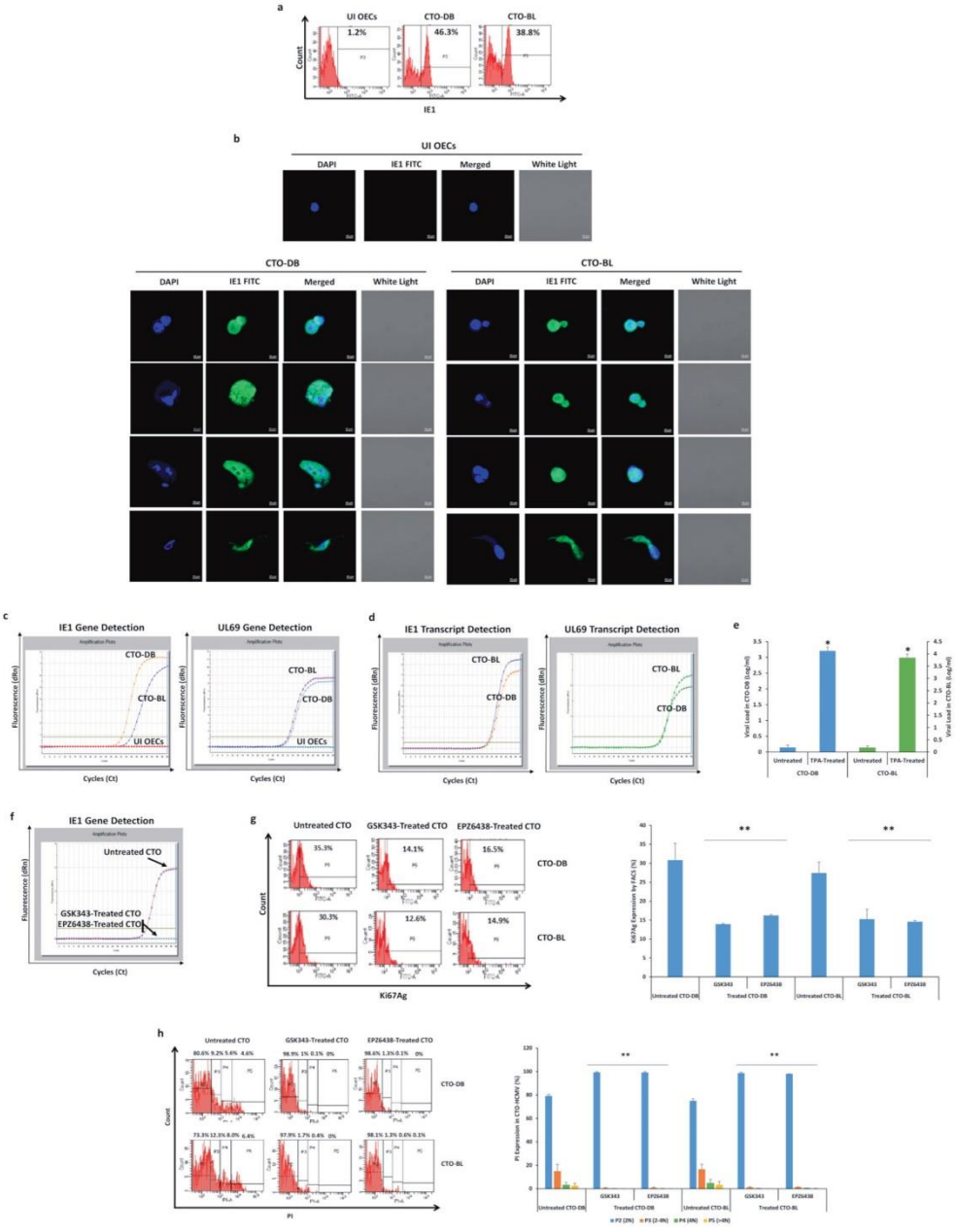

morphological features including budding, filopodia, lipid droplets-filled cells, blastomere-like cells, and multinucleated cells that were previously detected in OC especially HGSOC [13, 37, 40–44] and reported upon HCMV infection of human mammary epithelial cells [17–19]. Our findings indicated that polyploidy harboring HCMV might induce the acquisition of a malignant phenotype via the giant cell cycling [14]. p53 and Rb inactivation have been correlated with tetraploidization in human

Fig. 6 Sustained HCMV replication in chronically HCMV-infected OECs. a IE1 expression by FACS in chronically infected OECs-DB and BL cultures. **b** IE1 expression by confocal microscopy in CTO-DB and BL; uninfected OECs were used as a control. Nuclei were counterstained with DAPI; magnification ×63, scale bar 10 µm. **c** IE1 and UL69 gene detection in chronically infected OECs-DB and BL as measured by qPCR. Uninfected OECs were used as a negative control. **d** IE1 and UL69 transcripts detection as measured by RT-qPCR. **e** Histogram representing the viral load post-TPA treatment in CTO-DB and BL cultures as measured by IE1-qPCR. **f** IE1 gene detection by qPCR in untreated CTO-DB, and CTO-DB treated with two EZH2 inhibitors (0.1 µM of GSK34 and EPZ6438). Ki67Ag expression (**g**) and PI staining (**h**) in untreated CTO-DB/BL and CTO-DB/BL treated with 0.1 µM of GSK34 and EPZ6438 by FACS. Data are represented as mean ± SD of two independent experiments. **p*-value ≤ 0·05; ***p*-value ≤ 0·01.

tumors [22]. Indeed, p53 was shown to be mutated in more than 50% of human tumors, especially HGSOC; most of the p53 mutations acquired an oncogenic function. It's worth mentioning that tumor-promoting viruses reduce p53 activity [45]. Studies have shown that the incidence of tetraploidy occurs in p53-deficient cells possessing prolonged DNA damage due to persistent telomere dysfunction [46]. p53 and Rb expression was decreased in CTO-DB and BL that showed high percentages of tetraploidization and decreased telomerase activity, in line with the telomere-driven tetraploidization induced by critically short telomeres with the potential to promote tumorigenesis in early cancerous lesions [24]. Several HCMV products have been involved in the cellular transformation including IE1, IE2, pp65, US28, cmvIL-10, UL76, UL44, and UL84, etc. Such expression of HCMV gene products could impair the pathways of p53 and Rb [6, 8]. HCMV-IE1, IE2, and UL97 allow the evasion of p53 and Rb [8]. Hence, the impaired p53 and Rb pathways in CTO cells were due to the transforming potential of HCMV contrasting the Ras, human telomerase reverse transcriptase (hTERT), and SV40-mediated transformation of human ovarian cells [47].

Numerous biomarkers have become essential in characterizing and managing ovarian cancers [48]. EZH2, a downstream target of Myc oncogene, has been involved in regulating cell cycle progression [49]. Elevated EZH2 activity has been reported in approximately 85% of epithelial ovarian carcinomas [50]. Since EZH2 enhances cell proliferation, inhibits apoptosis, promotes angiogenesis, metastasis and therapy resistance in OC [50, 51], inhibiting EZH2 suggests an effectual strategy for developing OC therapies. A study reported that EZH2 degradation profoundly blocked ovarian tumor cell proliferation and tumorigenesis in vitro and in vivo [52]. Given the recent approval of the EZH2-targeting agent (tazemetostat) by the FDA as a treatment for follicular lymphoma, enhanced therapies may soon be available for suppressing ovarian cancers [50]. A combination of EZH2 inhibitor, PARP inhibitor, and/or immune checkpoint blockers might be synergistic in ovarian cancers [53, 54]. In line with the critical role of EZH2 in epithelial ovarian cancer [25], EZH2 overexpression was detected in CTO-DB and BL compared to uninfected OECs. EZH2 inhibition restricted the proliferation potential of CTO cells and limited tetraploidization. Moreover, Myc, as a transcription factor, plays an essential role in regulating multiple cellular processes. Enhanced Myc expression and/or mutated Myc have been reported in most human cancers and have been observed in 20–50% of ovarian carcinoma [55, 56]. A limited expression of Myc was detected in the PGCCs population of HCMV-infected OECs, reinforcing the emerging data on limited Myc expression in dormant cells [57]. EZH2 upregulation was shown to be the main feature in CTO cells and ovarian epithelial cancers. Anti-EZH2 treatment makes EZH2 a desirable therapeutic target, unlike anti-Myc therapeutics. Given the absence of enzymatic activity and the lack of surface domains specific for most pharmacological inhibitors, Myc is considered an "undruggable" protein [55], hence anti-Myc therapeutics might fall short of expectations in limiting ovarian cancers.

Cells possessing sphere-forming potentials were shown to reside in the malignant ascites of OC patients [58–60]. In OC, the aforementioned cells are strong contributors to tumor progression, metastasis, chemotherapy resistance, and disease relapse [59]. The spontaneous spheroid generation along with the high expression of Nanog and Oct4 in CTO-DB and BL is in line with the previously described OC cell phenotype [61]. Given their role in maintaining pluripotency and long-term self-renewal, the embryonic transcription factors Oct4 and Nanog are recognized as part of the stem cell signature that strongly correlates with spheroid formation, tumor initiation, and chemoresistance in ovarian cancer cells [61, 62]. CD44 was highly expressed in CTO-DB and BL cells; it has been previously shown to drive the progression of several tumors [63, 64], maintain stem cell quiescence, and promote EMT in OC [65]. Further, CD44 has been linked to the sphere-forming, self-renewing and tumor-initiating potential of OC cells [66]. The co-existence of vimentin and E-cadherin in CTO-DB and BL highlights the high cellular plasticity. EMT plasticity with EMT and MET alternately taking place was revealed during HGSOC progression where cells co-express epithelial and mesenchymal determinants [44, 67, 68]. Besides cellular plasticity, the hybrid E/M state promotes stem-like properties as well as metastatic and tumorigenic potential [69, 70].

Upon infecting OECs with HCMV-DB and BL strains, IE1 and pp65 proteins were detected which is in line with the recent studies that have identified high expressions of HCMV-IE or pp65 in ovarian tumor samples that were associated with poor survival outcomes [1, 33], suggesting that HCMV infection could potentially promote cancer progression. All in all, HCMV-induced EZH2 expression along with the embryonic stem-like phenotype and cellular plasticity in the IE1-expressing OECs/CTO cells could establish a significant model in the context of OC. Several studies shed light on the existence of herpesviruses DNA and proteins in ovarian tissues that may hold potential in the process of OC tumorigenesis [1, 33, 71]. Herein, we reported the detection of HCMV in HGSOC biopsies displaying elevated PGCCs count as well as enhanced EZH2 expression. It is worth mentioning that, neither HPV nor EBV was detected in the eighteen tested HGOSC biopsies.

Three HCMV strains with a strong transforming potential, so called high-risk strains, were isolated from $EZH2^{High}$ HGOSC biopsies. After OECs infection, CTO cells were generated with morphological features matching the previously described CTO-DB and BL. Additionally, we evaluated EZH2 expression in the high-risk HCMV strains that were recovered directly from HGSOC biopsies thereby assessing their oncogenic and stemness potential. Unlike GSK-treated CTO, the expression of EZH2, Myc, and Ki67Ag was predominantly elevated in untreated CTO-HCMV-OC cells parallel to the PGCCs appearance. In summary, HCMV clinical strains reside in HGOSC biopsies retaining cancer-promoting potentials.

The high-risk HCMV strains that were isolated from HGSOC, TNBC, and GBM patients shared the same transforming potential [17, 30, 34]. PGCCs were detected in the aforementioned cell cultures that were shown to highly express Myc and EZH2 pointing toward a potential link between HCMV, PGCCs, EZH2, and Myc. CTO and CTH cells dedifferentiated and revealed stemness as well as EMT traits [17, 19, 34]. On the other hand, CEGBCs dedifferentiated and displayed stemness, PMT as well as invasiveness features [30]. The phenotypic changes were similar in HCMV-infected ovarian and mammary epithelial cells. However, the difference was mainly the detection of high percentages of tetraploid cells in the CTO cultures compared to the >4 N population detected in CTH cells. In both models, a high degree of cellular plasticity was detected knowing that

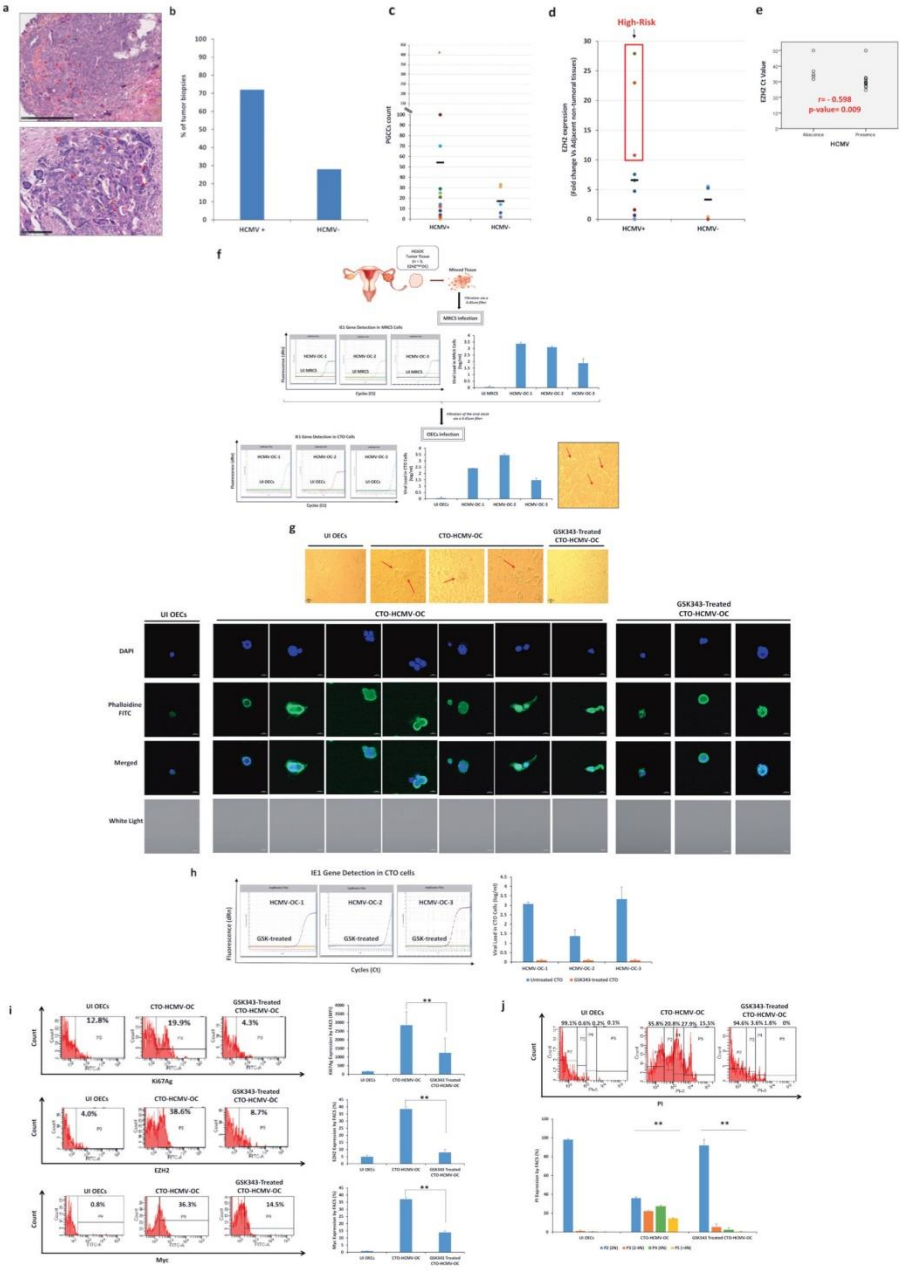

ovarian and mammary epithelial cells are isolated from human glandular organs.

Given that cancer patients with lower HCMV activity have a better prognosis, targeting HCMV might have a vital role in treating OC [33]. Post-anti-CMV therapy, a remarkably high extended survival was observed in both newly diagnosed and recurrent glioblastoma patients [72]. Current vaccine candidates have focused on several HCMV antigens/epitopes such as gB, gH, pentamer complex, pp65

Fig. 7 HCMV detection, PGCCs presence as well as EZH2 expression in ovarian cancer biopsies. a Ovarian cancer tissue HES staining; magnification ×400, scale bar 250 µm (upper panel) and 100 µm (lower panel). Red arrow representing the PGCCs while the yellow arrow represents the diploid carcinoma cells. **b** Histogram representing HCMV presence in the ovarian tumor biopsies. **c** Scattered plots showing the PGCCs count in HCMV-positive and negative ovarian tumor biopsies. **d** Scattered plots representing EZH2 expression in HCMV-positive and negative ovarian tumor biopsies by RT-qPCR. Red box indicates the high-risk HCMV strains with high EZH2 expression. **e** Correlation test between Ct value of EZH2 and HCMV presence *p*-values were determined by Spearman's correlation test. **f** Isolation protocol of the three high-risk HCMV-ovarian cancer strains from HGSOC tissues; histogram representing the viral replication of the isolated HCMV strains in MRC5 cells and CTO cultures by IE-qPCR. CTO cells were observed under an inverted light microscope (magnification ×200, scale bar 50 µm). **g** Light microscopic images (magnification ×200, scale bar 50 µm) as well as confocal images of DAPI and phalloidine staining in CTO-HCMV-OC and GSK343-treated CTO cells (magnification ×63, scale bar 10 µm); uninfected OECs were used as a negative control. **h** IE1 gene detection in CTO-HCMV-OC and GSK343-treated CTO cells by IE-qPCR. **i, j** Ki67Ag, EZH2, Myc expression (**i**) and PI staining (**j**) in CTO-HCMV-OC, GSK343-treated CTO cells, and uninfected OECs by FACS. Data are represented as mean ± SD of two independent experiments. ***p*-value ≤ 0·01.

and IE1 [73, 74]. Recently, CMV-specific immunotherapy including cytotoxic T lymphocyte (CTL) or dendritic cell (DC)-based vaccines has contributed to minimal successful outcomes in glioblastoma treatment [74, 75]. In addition, using EZH2 inhibitors to specifically target ovarian tumors could ultimately improve patients outcomes [25]. Two inhibitors triggering EZH2 degradation (DZNep and YM281) exhibited potent efficacy in OC cell lines and xenografts [52]. GSK343 significantly induced apoptosis and inhibited the invasion of ovarian epithelial cells in 3D cultures which more closely mimics the tumor microenvironment in vivo [76]. In patient-derived glioma stem cells, GSK343 was shown to suppress the stemness traits [77]. Interestingly, in the present study, EZH2 inhibitors totally blocked HCMV replication (Figs. 6f and 7h). It's worth noting that the HCMV major immediate early promoter (MIEP) transcriptional repressor, growth factor independence1 (GFI1), is controlled by the EZH2-NDY1/KDM2B-JARID2 axis. Therefore, EZH2 inhibitors might result in an enhanced GFI1 expression which could block viral replication [78]. Hence, combinational therapies including EZH2 inhibitors may prove to be a promising milestone in developing therapeutic strategies for ovarian cancer treatment.

CONCLUSION

In conclusion, our data indicated that the high-risk HCMV strains which triggered EZH2 upregulation can induce polyploidy, OECs dedifferentiation, stemness, and EMT/MET characteristics parallel to the existence of giant cell cycling. Future studies, with more detailed analyses, may establish new avenues to understand the complex pathogenesis of OC and might pave the way for novel targeted therapies.

MATERIAL AND METHODS

Cell cultures

Human ovarian surface epithelial cells (HOSE cells or OECs, as mentioned in our study) and human embryonic lung fibroblasts (MRC5 cells) were purchased from Innoprot (Derio, Spain) and RD-Biotech (Besançon, France), respectively. OECs were cultivated in ovarian epithelial cell medium (serum-free) supplemented with ovarian epithelial cell growth supplement (OEpiCGS) and penicillin/streptomycin solution (P60132, Innoprot). MRC5 cells were cultivated in Dulbecco's modified Eagle medium (Sigma-Aldrich, Saint-Louis, MO) supplemented with 10% fetal bovine serum (Dutscher, Bernolsheim, France) and penicillin (100 U/mL)-streptomycin (100 µg/mL) (Life Technologies, Eugene, OR). Cells were cultured under standard conditions (37 °C, 5% CO_2, 95% humidity). To note that, HOSE cells or OECs were isolated from healthy human ovaries, as mentioned in the technical data sheet (P10982, Innoprot). Cultures were verified as mycoplasma-free as determined by monthly screenings (VenorGem classic mycoplasma detection, Minerva Biolabs).

Characterization of HCMV clinical isolates

Clinical HCMV strains, namely HCMV-DB (GenBank KT959235), BL (GenBank MW980585), KM, and FS were isolated from patients that were hospitalized at Besançon University Hospital (France) as previously described [19, 34]. Cell-free virus stocks and infections were performed as previously detailed. It is worth mentioning that careful screening of our viral stocks was conducted to rule out the presence of other oncoviruses [19].

Viral growth and detection

Infections of OECs, quantification of viral replication, and HCMV detection were performed as previously described [19]. OECs (1×10^6) infection with the clinical isolates was performed at a multiplicity of infection (MOI) of 1. For HCMV quantification, cell-free infectious supernatant was collected, DNA was isolated (EZNA Blood DNA Kit, D3392-02, Omega BIO-TEK, Norcross, GA) and real-time IE1 quantitative PCR (qPCR) was performed using KAPA SYBR FAST Master Mix (KAPA BIOSYSTEMS, Potters Bar, UK) and IE1 and UL69 primers. Real-time qPCR reactions were activated at 95 °C for 10 min and then 50 cycles (15 s at 95 °C and 1 min at 60 °C) were conducted using a Stratagene Mx3005P thermocycler (Agilent Technologies, Santa Clara, CA). Results collection and analysis were done using MxPro qPCR software. Primers used are listed in Supplementary Table 1.

Western blotting

IE1, pp65, Myc, EZH2, Sox2, Nanog, E-cadherin, and vimentin expression in uninfected OECs, HCMV-infected OECs and CTO cells was assessed as described previously [34]. β-actin was used as a loading control. Antibodies used are supplied in Supplementary Table 2.

Flow cytometry analysis

Cells (1×10^5) were collected from uninfected OECs, HCMV-infected OECs and CTO cells. Cells were fixed, permeabilized, and stained as previously reported [19]. Cytofluorometric analysis was achieved using a BD LSRFortessa X-20 (BD Biosciences) flow cytometer. FACSDiva software (BD Biosciences) was used for data collection and analysis. The antibodies used are provided in Supplementary Table 2. For cell cycle analysis, uninfected OECs or CTO cells were washed in 1X PBS, fixed in 70% ethanol, and resuspended in 50 µg/ml propidium iodide (P3566, life technologies, Eugene, USA) with 0.1 mg/ml RNase (R4642, Sigma-Aldrich, Saint-Louis, MO, USA), then incubated at 37 °C for 30 min as described previously [17].

Assessment of telomerase activity

Uninfected OECs and CTO cells were collected, washed with PBS, and resuspended in RIPA lysis buffer and 4% protease inhibitor on ice for 30 min. Samples were then centrifuged at 16,000 g for 30 min at 4 °C and the protein concentration was determined using Bradford assay (DC Protein Assay kit, Bio-Rad Laboratories, Hercules, CA). Telomerase activity was assessed as described previously and according to the manufacturer's instructions [19].

Reverse transcription quantitative polymerase chain reaction (RT-qPCR)

The detection of IE1, UL69, EZH2, Myc, Sox2, Nanog, and Oct4 transcripts was assessed by RT-qPCR as detailed previously [79]. Briefly, total RNA was extracted using E.Z.N.A. Total RNA Kit I (Omega Bio-Tech, GA, USA), and reverse transcription was performed using the SuperScript IV First-Strand Synthesis kit (Invitrogen, Carlsbad, CA, USA). The expression of markers was measured by real-time qPCR using a KAPA SYBR FAST Master Mix (KAPA BIOSYSTEMS, KK4601) and specific primers according to the manufacturer's protocol. Primers used are listed in Supplementary Table 1.

Confocal microscopy

Confocal microscopy of uninfected and HCMV-infected OECs as well as spheroids was performed as previously detailed [19]. The antibodies used are provided in Supplementary Table 2.

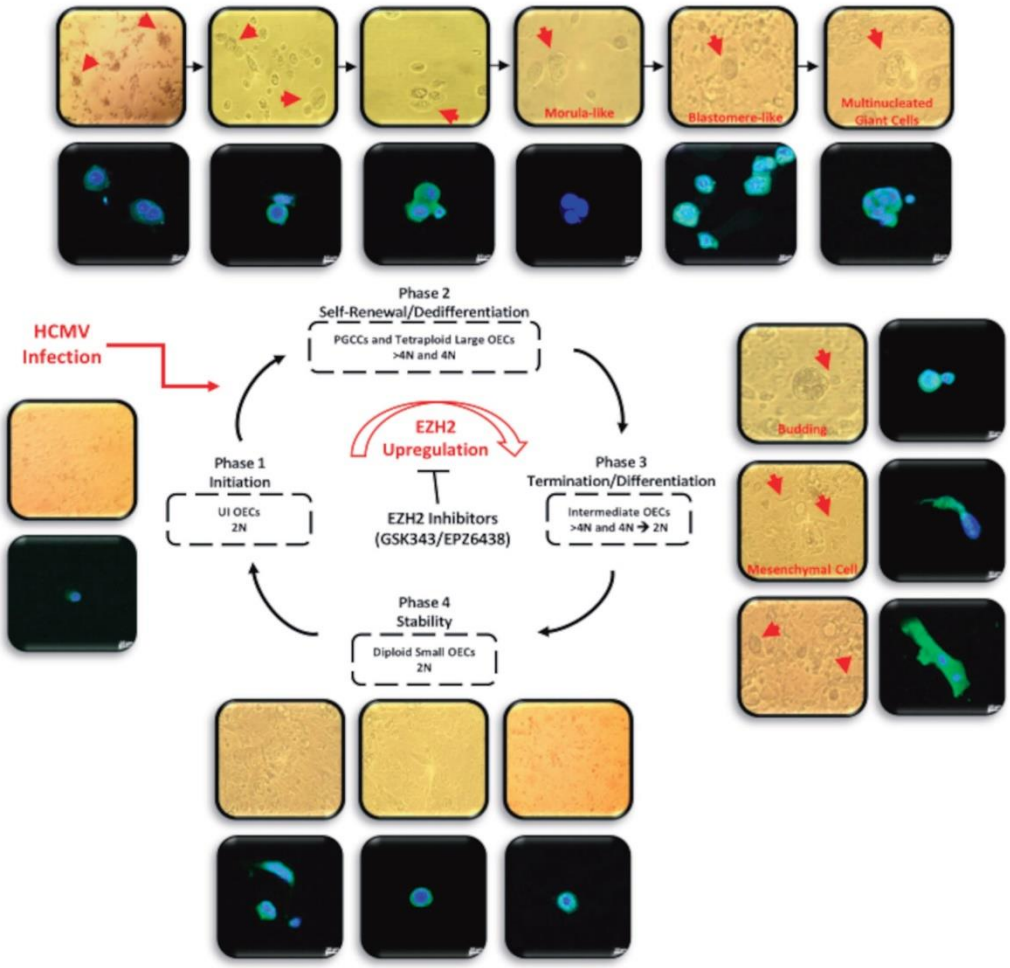

Fig. 8 A schematic representing the giant cell cycling following HCMV infection of OECs. Giant cell cycle representing four distinct phases including initiation, self-renewal, termination and stability. Upon HCMV infection, the 2 N OECs go into the initiation phase through endoreplication. Polyploid cells (> 4 N) and tetraploid cells (4 N) generate in the self-renewal/dedifferentiation stage due to HCMV infection and the subsequent EZH2 upregulation. Cell budding takes place from multinucleated or mononucleated giant cells generating intermediate 2–4 N OECs during the termination/differentiation phase. Intermediate OECs gradually reach stability and are converted into diploid small OECs (2 N).

Soft agar colony formation assay

Colony formation in soft agar (Colorimetric assay, CB135; Cell Biolabs Inc., San Diego, CA) seeded with uninfected and HCMV-infected OECs was performed as previously described [19].

Spheroid formation assay

Spheroids of OECs were prepared as described previously [80]. Single cells (1×10^4) isolated by accutase were seeded in a serum-free OECs medium containing methylcellulose.

EZH2 inhibition assay

CTO-DB and BL were treated with 0.1 µM of two EZH2 inhibitors (GSK343 and EPZ6438). Treatment was renewed every 2 days. Ki67Ag and EZH2 expression by FACS was assessed in treated and untreated CTO cells. HCMV-IE1 gene detection was detected in the supernatants of treated and untreated CTO cells.

Ovarian cancer biopsies

Ovarian biopsies ($n = 25$; HGSOC biopsies $n = 18$, and adjacent non-tumoral biopsies $n = 7$) were provided by the Regional tumor bank (BB0033-00024 Tumorothèque Régionale de Franche-Comté). Clinical data and treatments of the OC patients were provided in Supplementary Table 3. A written informed consent for participation was obtained from all patients. The study was authorized by the local ethics committees of Besançon University Hospital (Besançon, France) and the French Research Ministry (AC-2015-2496, CNIL n°1173545, NF-S-138 96900 n°F2015).

Genomic DNA was isolated from patient biopsies, and HCMV presence was identified by qPCR using specific primers against IE1 and UL69 genes. RNA was extracted from the biopsies and reverse transcription was performed as reported previously [17, 79]. Expression of EZH2, Myc, Akt, and β-2-Microglobulin was assessed by real-time qPCR using specific primers according to the manufacturer's protocol. Fold change expression in OC biopsies versus adjacent non-tumoral biopsies was calculated using the delta-delta Ct method [17, 79]. Neither human papillomavirus (HPV) nor Epstein-Barr virus (EBV) was detected in the ovarian cancer biopsies. Primers used are listed in Supplementary Table 1. PGCCs presence in HGSOC biopsies was confirmed by hematoxylin and eosin staining; briefly, PGCCs were counted in five hot spots of each tumor sample (magnification ×400, field diameter of 250 µm and 100 µm, Zeiss Axiostar). Three HCMV-OC strains were isolated from HGSOC biopsies.

Statistical analysis

Quantitative results are reported as mean ± SD of independent experiments. Statistical analyses were done using Wilcoxon and Mann-Whitney tests; a p-value ≤ 0·05 was considered to be statistically significant [*: ≤0·05; **: ≤0·01; ***: ≤0·001]. Correlation analysis was done using Spearman, Pearson, and Kendall's Tau correlation tests. Microsoft Excel was used to construct the plots and histogram data.

DATA AVAILABILITY

The data supporting the findings of this study are available within the article and its Supplementary Information files and from the corresponding authors on request.

REFERENCES

1. Cox M, Kartikasari AER, Gorry PR, Flanagan KL, Plebanski M. Potential Impact of Human Cytomegalovirus Infection on Immunity to Ovarian Tumours and Cancer Progression. Biomedicines. 2021;9:351. https://doi.org/10.3390/biomedicines9040351.
2. Dangaj Laniti D, Coukos G. Genetics and anatomy sculpt immune-cell partners of ovarian cancer. Nature. 2022;612:634–6. https://doi.org/10.1038/d41586-022-04169-3.
3. Leary A, Tan D, Ledermann J. Immune checkpoint inhibitors in ovarian cancer: where do we stand?. Ther Adv Med Oncol. 2021;13:175883592110398. https://doi.org/10.1177/17588359211039899.
4. Wysocki PJ, Łobacz M, Potocki P, Kwinta Ł, Michałowska-Kaczmarczyk A, Słowik A. et al. Metronomic Chemotherapy Based on Topotecan or Topotecan and Cyclophosphamide Combination (CyTo) in Advanced, Pretreated Ovarian Cancer. Cancers. 2023;15:1067. https://doi.org/10.3390/cancers15041067.
5. Lim P-Q, Han I-H, Seow K-M, Chen K-H. Hyperthermic Intraperitoneal Chemotherapy (HIPEC): An Overview of the Molecular and Cellular Mechanisms of Actions and Effects on Epithelial Ovarian Cancers. IJMS. 2022;23:10078. https://doi.org/10.3390/ijms231710078.
6. El Baba R, Herbein G. Immune Landscape of CMV Infection in Cancer Patients: From "Canonical" Diseases Toward Virus-Elicited Oncomodulation. Front Immunol. 2021;12:730765. https://doi.org/10.3389/fimmu.2021.730765.
7. Forte E, Zhang Z, Thorp EB, Hummel M. Cytomegalovirus Latency and Reactivation: An Intricate Interplay With the Host Immune Response. Front Cell Infect Microbiol. 2020;10:130. https://doi.org/10.3389/fcimb.2020.00130.
8. Herbein G. The Human Cytomegalovirus, from Oncomodulation to Oncogenesis. Viruses. 2018;10:408. https://doi.org/10.3390/v10080408.
9. Cinatl J, Vogel J-U, Kotchetkov R, Wilhelm Doerr H. Oncomodulatory signals by regulatory proteins encoded by human cytomegalovirus: a novel role for viral infection in tumor progression. FEMS Microbiol Rev. 2004;28:59–77. https://doi.org/10.1016/j.femsre.2003.07.005.
10. Herbein G. High-Risk Oncogenic Human Cytomegalovirus. Viruses. 2022;14:2462. https://doi.org/10.3390/v14112462.
11. Li X, Zhong Y, Zhang X, Sood AK, Liu J. Spatiotemporal view of malignant histogenesis and macroevolution via formation of polyploid giant cancer cells. Oncogene. 2023;42:665–78. https://doi.org/10.1038/s41388-022-02588-0.
12. Zhou X, Zhou M, Zheng M, Tian S, Yang X, Ning Y. et al. Polyploid giant cancer cells and cancer progression. Front Cell Dev Biol. 2022;10:1017588. https://doi.org/10.3389/fcell.2022.1017588.
13. Niu N, Mercado-Uribe I, Liu J. Dedifferentiation into blastomere-like cancer stem cells via formation of polyploid giant cancer cells. Oncogene. 2017;36:4887–900. https://doi.org/10.1038/onc.2017.72.
14. Liu J, Erenpreisa J, Sikora E. Polyploid giant cancer cells: An emerging new field of cancer biology. Semin Cancer Biol. 2022;81:1–4. https://doi.org/10.1016/j.semcancer.2021.10.006.
15. Mirzayans R. The Cellular Response to DNA Damage: From DNA Repair to Polyploidy and Beyond. IJMS. 2023;24:6852. https://doi.org/10.3390/ijms24076852.
16. Yart L, Bastida-Ruiz D, Allard M, Dietrich P-Y, Petignat P, Cohen M. Linking unfolded protein response to ovarian cancer cell fusion. BMC Cancer. 2022;22:622. https://doi.org/10.1186/s12885-022-09648-4.
17. Nehme Z, Pasquereau S, Haidar Ahmad S, El Baba R, Herbein G. Polyploid giant cancer cells, EZH2 and Myc upregulation in mammary epithelial cells infected with high-risk human cytomegalovirus. EBioMedicine. 2022;80:104056. https://doi.org/10.1016/j.ebiom.2022.104056.
18. El Baba R, Pasquereau S, Haidar Ahmad S, Diab-Assaf M, Herbein G. Oncogenic and Stemness Signatures of the High-Risk HCMV Strains in Breast Cancer Progression. Cancers. 2022;14:4271. https://doi.org/10.3390/cancers14174271.
19. Nehme Z, Pasquereau S, Haidar Ahmad S, Coaquette A, Molimard C, Monnien F. et al. Polyploid giant cancer cells, stemness and epithelial-mesenchymal plasticity elicited by human cytomegalovirus. Oncogene. 2021;40:3030–46. https://doi.org/10.1038/s41388-021-01715-7.
20. Herbein G, Nehme Z. Polyploid Giant Cancer Cells, a Hallmark of Oncoviruses and a New Therapeutic Challenge. Front Oncol. 2020;10:567116. https://doi.org/10.3389/fonc.2020.567116.
21. Tanaka K, Goto H, Nishimura Y, Kasahara K, Mizoguchi A, Inagaki M. Tetraploidy in cancer and its possible link to aging. Cancer Sci. 2018;109:2632–40. https://doi.org/10.1111/cas.13717.
22. Castedo M, Senovilla L, Vitale I, Kroemer G. Tetraploid cancer cell precursors in ovarian carcinoma. Cell Cycle. 2012;11:3157–8. https://doi.org/10.4161/cc.21722.
23. Lv L, Zhang T, Yi Q, Huang Y, Wang Z, Hou H. et al. Tetraploid cells from cytokinesis failure induce aneuploidy and spontaneous transformation of mouse ovarian surface epithelial cells. Cell Cycle. 2012;11:2864–75. https://doi.org/10.4161/cc.21196.
24. Davoli T, de Lange T. Telomere-Driven Tetraploidization Occurs in Human Cells Undergoing Crisis and Promotes Transformation of Mouse Cells. Cancer Cell. 2012;21:765–76. https://doi.org/10.1016/j.ccr.2012.03.044.
25. Jones BA, Varambally S, Arend RC. Histone Methyltransferase EZH2: A Therapeutic Target for Ovarian Cancer. Mol Cancer Ther. 2018;17:591–602. https://doi.org/10.1158/1535-7163.MCT-17-0437.
26. Leitner K, Tsibulak I, Wieser V, Knoll K, Reimer D, Marth C. et al. Clinical impact of EZH2 and its antagonist SMARCA4 in ovarian cancer. Sci Rep. 2020;10:20412. https://doi.org/10.1038/s41598-020-77532-x.
27. Zhang L, Ding P, Lv H, Zhang D, Liu G, Yang Z. et al. Number of Polyploid Giant Cancer Cells and Expression of EZH2 Are Associated with VM Formation and Tumor Grade in Human Ovarian Tumor. BioMed Res Int. 2014;2014:1–9. https://doi.org/10.1155/2014/903542.
28. Cobbs C, Harkins L, Samanta M, Gillespie G, Bharara S, King P, et al. Human cytomegalovirus infection and expression in human malignant glioma. Cancer Res. 2002;62:3347–50.
29. Nauclér CS, Geisler J, Vetvik K. The emerging role of human cytomegalovirus infection in human carcinogenesis: a review of current evidence and potential therapeutic implications. Oncotarget. 2019;10:4333–47. https://doi.org/10.18632/oncotarget.27016.
30. El Baba R, Pasquereau S, Haidar Ahmad S, Monnien F, Abad M, Bibeau F. et al. EZH2-Myc driven glioblastoma elicited by cytomegalovirus infection of human astrocytes. Oncogene. 2023;42:2031–45. https://doi.org/10.1038/s41388-023-02709-3.
31. Yin M, Chen A, Zhao F, Ji X, Li C, Wang G. Detection of human cytomegalovirus in patients with epithelial ovarian cancer and its impacts on survival. Infect Agents Cancer. 2020;15:23. https://doi.org/10.1186/s13027-020-00289-5.
32. Paradowska E, Jabłońska A, Studzińska M, Wilczyński M, Wilczyński JR. Detection and genotyping of CMV and HPV in tumors and fallopian tubes from epithelial ovarian cancer patients. Sci Rep. 2019;9:19935. https://doi.org/10.1038/s41598-019-56448-1.
33. Carlson JW, Rådestad AF, Söderberg-Naucler C, Rahbar A. Human cytomegalovirus in high grade serous ovarian cancer possible implications for patients survival. Medicine. 2018;97:e9685. https://doi.org/10.1097/MD.0000000000009685.
34. Kumar A, Tripathy MK, Pasquereau S, Al Moussawi F, Abbas W, Coquard L. et al. The Human Cytomegalovirus Strain DB Activates Oncogenic Pathways in Mammary Epithelial Cells. EBioMedicine. 2018;30:167–83. https://doi.org/10.1016/j.ebiom.2018.03.015.
35. Dudás J, Ladányi A, Ingruber J, Steinbichler TB, Riechelmann H. Epithelial to Mesenchymal Transition: A Mechanism that Fuels Cancer Radio/Chemoresistance. Cells. 2020;9:428. https://doi.org/10.3390/cells9020428.
36. Zhao Q, Zhang K, Li Z, Zhang H, Fu F, Fu J. et al. High Migration and Invasion Ability of PGCCs and Their Daughter Cells Associated With the Nuclear Localization of S100A10 Modified by SUMOylation. Front Cell Dev Biol. 2021;9:696871. https://doi.org/10.3389/fcell.2021.696871.

37. Richards JS, Candelaria NR, Lanz RB. Polyploid giant cancer cells and ovarian cancer: new insights into mitotic regulators and polyploidy. Biol Reprod. 2021;105:305–16. https://doi.org/10.1093/biolre/ioab102.
38. Zhang S, Mercado-Uribe I, Xing Z, Sun B, Kuang J, Liu J. Generation of cancer stem-like cells through the formation of polyploid giant cancer cells. Oncogene. 2014;33:116–28. https://doi.org/10.1038/onc.2013.96.
39. Bowers RR, Andrade MF, Jones CM, White-Gilbertson S, Voelkel-Johnson C, Delaney JR. Autophagy modulating therapeutics inhibit ovarian cancer colony generation by polyploid giant cancer cells (PGCCs). BMC Cancer. 2022;22:410. https://doi.org/10.1186/s12885-022-09503-6.
40. Iwahashi N, Ikezaki M, Fujimoto M, Komohara Y, Fujiwara Y, Yamamoto M. et al. Lipid Droplet Accumulation Independently Predicts Poor Clinical Prognosis in High-Grade Serous Ovarian Carcinoma. Cancers. 2021;13:5251. https://doi.org/10.3390/cancers13205251.
41. Yoshihara M, Yamakita Y, Kajiyama H, Senga T, Koya Y, Yamashita M. et al. Filopodia play an important role in the trans-mesothelial migration of ovarian cancer cells. Exp Cell Res. 2020;392:112011. https://doi.org/10.1016/j.yexcr.2020.112011.
42. Zhang S, Mercado-Uribe I, Hanash S, Liu J. iTRAQ-Based Proteomic Analysis of Polyploid Giant Cancer Cells and Budding Progeny Cells Reveals Several Distinct Pathways for Ovarian Cancer Development. PLoS ONE. 2013;8:e80120. https://doi.org/10.1371/journal.pone.0080120.
43. Lv H, Shi Y, Zhang L, Zhang D, Liu G, Yang Z. et al. Polyploid giant cancer cells with budding and the expression of cyclin E, S-phase kinase-associated protein 2, stathmin associated with the grading and metastasis in serous ovarian tumor. BMC Cancer. 2014;14:576. https://doi.org/10.1186/1471-2407-14-576.
44. Davidson B, Tropé CG, Reich R. Epithelial–Mesenchymal Transition in Ovarian Carcinoma. Front Oncol. 2012;2:33. https://doi.org/10.3389/fonc.2012.00033.
45. Aloni-Grinstein R, Charni-Natan M, Solomon H, Rotter V. p53 and the Viral Connection: Back into the Future ‡. Cancers. 2018;10:178. https://doi.org/10.3390/cancers10060178.
46. Davoli T, Denchi EL, De Lange T. Persistent Telomere Damage Induces Bypass of Mitosis and Tetraploidy. Cell. 2010;141:81–93. https://doi.org/10.1016/j.cell.2010.01.031.
47. Liu J, Yang G, Thompson-Lanza JA, Glassman A, Hayes K, Patterson A. et al. A Genetically Defined Model for Human Ovarian Cancer. Cancer Res. 2004;64:1655–63. https://doi.org/10.1158/0008-5472.CAN-03-3380.
48. Yadav G, Vashisht M, Yadav V, Shyam R. Molecular biomarkers for early detection and prevention of ovarian cancer—A gateway for good prognosis: A narrative review. Int J Prev Med. 2020;11:135. https://doi.org/10.4103/ijpvm.IJPVM_75_19.
49. Sander S, Bullinger L, Klapproth K, Fiedler K, Kestler HA, Barth TFE. et al. MYC stimulates EZH2 expression by repression of its negative regulator miR-26a. Blood. 2008;112:4202–12. https://doi.org/10.1182/blood-2008-03-147645.
50. Coughlan AY, Testa G. Exploiting epigenetic dependencies in ovarian cancer therapy. Int J Cancer. 2021;149:1732–43. https://doi.org/10.1002/ijc.33727.
51. Reid BM, Vyas S, Chen Z, Chen A, Kanetsky PA, Permuth JB. et al. Morphologic and molecular correlates of EZH2 as a predictor of platinum resistance in high-grade ovarian serous carcinoma. BMC Cancer. 2021;21:714. https://doi.org/10.1186/s12885-021-08413-3.
52. Chen J, Hong JH, Huang Y, Liu S, Yin J, Deng P. et al. EZH2 mediated metabolic rewiring promotes tumor growth independently of histone methyltransferase activity in ovarian cancer. Mol Cancer. 2023;22:85. https://doi.org/10.1186/s12943-023-01786-y.
53. Karakashev S, Zhang R. Targeting CARM1 in ovarian cancer with EZH2 and PARP inhibitors. Mol Cell Oncol. 2020;7:1760675. https://doi.org/10.1080/23723556.2020.1760675.
54. Kandalaft LE, Dangaj Laniti D, Coukos G. Immunobiology of high-grade serous ovarian cancer: lessons for clinical translation. Nat Rev Cancer. 2022;22:640–56. https://doi.org/10.1038/s41568-022-00503-z.
55. Reyes-González JM, Vivas-Mejía PE. c-MYC and Epithelial Ovarian Cancer. Front Oncol. 2021;11:601512. https://doi.org/10.3389/fonc.2021.601512.
56. Bast RC, Hennessy B, Mills GB. The biology of ovarian cancer: new opportunities for translation. Nat Rev Cancer. 2009;9:415–28. https://doi.org/10.1038/nrc2644.
57. Shichiri M, Hanson K, Sedivy J. Effects of c-myc expression on proliferation, quiescence, and the G0 to G1 transition in nontransformed cells. Cell Growth Differ. 1993;4:93–104.
58. Velletri T, Villa CE, Cilli D, Barzaghi B, Lo Riso P, Lupia M. et al. Single cell-derived spheroids capture the self-renewing subpopulations of metastatic ovarian cancer. Cell Death Differ. 2022;29:614–26. https://doi.org/10.1038/s41418-021-00878-w.
59. Liao J, Qian F, Tchabo N, Mhawech-Fauceglia P, Beck A, Qian Z. et al. Ovarian Cancer Spheroid Cells with Stem Cell-Like Properties Contribute to Tumor Generation, Metastasis and Chemotherapy Resistance through Hypoxia-Resistant Metabolism. PLoS ONE. 2014;9:e84941. https://doi.org/10.1371/journal.pone.0084941.
60. Shepherd TG, Dick FA. Principles of dormancy evident in high-grade serous ovarian cancer. Cell Div. 2022;17:2. https://doi.org/10.1186/s13008-022-00079-y.
61. Pease JC, Brewer M, Tirnauer JS. Spontaneous spheroid budding from monolayers: a potential contribution to ovarian cancer dissemination. Biol Open. 2012;1:622–8. https://doi.org/10.1242/bio.2012653.
62. Robinson M, Gilbert SF, Waters JA, Lujano-Olazaba O, Lara J, Alexander LJ. et al. Characterization of SOX2, OCT4 and NANOG in Ovarian Cancer Tumor-Initiating Cells. Cancers. 2021;13:262. https://doi.org/10.3390/cancers13020262.
63. Martincuks A, Li P-C, Zhao Q, Zhang C, Li Y-J, Yu H. et al. CD44 in Ovarian Cancer Progression and Therapy Resistance—A Critical Role for STAT3. Front Oncol. 2020;10:589601. https://doi.org/10.3389/fonc.2020.589601.
64. Gao Y, Foster R, Yang X, Feng Y, Shen JK, Mankin HJ. et al. Up-regulation of CD44 in the development of metastasis, recurrence and drug resistance of ovarian cancer. Oncotarget. 2015;6:9313–26. https://doi.org/10.18632/oncotarget.3220.
65. Zhou J, Du Y, Lu Y, Luan B, Xu C, Yu Y. et al. CD44 Expression Predicts Prognosis of Ovarian Cancer Patients Through Promoting Epithelial-Mesenchymal Transition (EMT) by Regulating Snail, ZEB1, and Caveolin-1. Front Oncol. 2019;9:802. https://doi.org/10.3389/fonc.2019.00802.
66. Lupia M, Cavallaro U. Ovarian cancer stem cells: still an elusive entity?. Mol Cancer. 2017;16:64. https://doi.org/10.1186/s12943-017-0638-3.
67. Loret N, Denys H, Tummers P, Berx G. The Role of Epithelial-to-Mesenchymal Plasticity in Ovarian Cancer Progression and Therapy Resistance. Cancers. 2019;11:838. https://doi.org/10.3390/cancers11060838.
68. Ricci F, Bernasconi S, Perego P, Ganzinelli M, Russo G, Bono F. et al. Ovarian carcinoma tumor-initiating cells have a mesenchymal phenotype. Cell Cycle. 2012;11:1966–76. https://doi.org/10.4161/cc.20308.
69. Tedja R, Alvero AB, Fox A, Cardenas C, Pitruzzello M, Chehade H. et al. Generation of Stable Epithelial–Mesenchymal Hybrid Cancer Cells with Tumorigenic Potential. Cancers. 2023;15:684. https://doi.org/10.3390/cancers15030684.
70. Liao T-T, Yang M-H. Hybrid Epithelial/Mesenchymal State in Cancer Metastasis: Clinical Significance and Regulatory Mechanisms. Cells. 2020;9:623. https://doi.org/10.3390/cells9030623.
71. Pathak S, Wilczyński JR, Paradowska E. Factors in Oncogenesis: Viral Infections in Ovarian Cancer. Cancers. 2020;12:561. https://doi.org/10.3390/cancers12030561.
72. Stragliotto G, Pantalone MR, Rahbar A, Bartek J, Söderberg-Naucler C. Valganciclovir as Add-on to Standard Therapy in Glioblastoma Patients. Clin Cancer Res. 2020;26:4031–9. https://doi.org/10.1158/1078-0432.CCR-20-0369.
73. Nelson CS, Herold BC, Permar SR. A new era in cytomegalovirus vaccinology: considerations for rational design of next-generation vaccines to prevent congenital cytomegalovirus infection. Npj Vaccines. 2018;3:38. https://doi.org/10.1038/s41541-018-0074-4.
74. Yu C, He S, Zhu W, Ru P, Ge X, Govindasamy K. Human cytomegalovirus in cancer: the mechanism of HCMV-induced carcinogenesis and its therapeutic potential. Front Cell Infect Microbiol. 2023;13:1202138. https://doi.org/10.3389/fcimb.2023.1202138.
75. Weller M, Roth P, Preusser M, Wick W, Reardon DA, Platten M. et al. Vaccine-based immunotherapeutic approaches to gliomas and beyond. Nat Rev Neurol. 2017;13:363–74. https://doi.org/10.1038/nrneurol.2017.64.
76. Amatangelo M, Garipov A, Li H, Conejo-Garcia JR, Speicher D, Zhang R. Three-dimensional culture sensitizes epithelial ovarian cancer cells to EZH2 methyltransferase inhibition. Cell Cycle. 2013;12:2113–9. https://doi.org/10.4161/cc.25163.
77. Yu T, Wang Y, Hu Q, Wu W, Wu Y, Wei W. et al. The EZH2 inhibitor GSK343 suppresses cancer stem-like phenotypes and reverses mesenchymal transition in glioma cells. Oncotarget. 2017;8:98348–59. https://doi.org/10.18632/oncotarget.21311.
78. Sourvinos G, Morou A, Sanidas I, Codruta I, Ezell SA, Doxaki C. et al. The Down-regulation of GFI1 by the EZH2-NDY1/KDM2B-JARID2 Axis and by Human Cytomegalovirus (HCMV) Associated Factors Allows the Activation of the HCMV Major IE Promoter and the Transition to Productive Infection. PLoS Pathog. 2014;10:e1004136. https://doi.org/10.1371/journal.ppat.1004136.
79. Haidar Ahmad S, Pasquereau S, El Baba R, Nehme Z, Lewandowski C, Herbein G. Distinct Oncogenic Transcriptomes in Human Mammary Epithelial Cells Infected With Cytomegalovirus. Front Immunol. 2021;12:772160. https://doi.org/10.3389/fimmu.2021.772160.
80. Bilandzic M, Stenvers KL. Assessment of Ovarian Cancer Spheroid Attachment and Invasion of Mesothelial Cells in Real Time. JoVE. 2014;51655. https://doi.org/10.3791/51655.

ACKNOWLEDGEMENTS

This work was supported by grants from the University of Franche-Comté (UFC) (CR3300), the Région Franche-Comté (2021-Y-08292 and 2021-Y-08290) and the Ligue contre le Cancer (CR3304) to Georges Herbein. REB is a recipient of a doctoral scholarship from Apex Biosolutions. SHA is supported by ANR (Agence Nationale pour la Recherche) grant. We thank Apex Biosolutions for financial support. The funders had no role in the data collection, analysis, patient recruitment, or decision to

publish. The authors thank DImaCell Imaging Ressource Center, University of Bourgogne Franche-Comté, Faculty of Health Sciences, 25000 Besançon, France for technical support.

AUTHOR CONTRIBUTIONS

Conceptualization, GH; formal analysis, REB, SHA, RM, FM, FB, GH; investigation, REB, SHA, FM, RM; writing—original draft preparation, REB, SHA, GH; writing—review and editing, REB, SHA, GH; directly accessed and verified the underlying data: REB, SHA, GH; visualization, REB, SHA, GH; supervision, GH; project administration, GH; funding acquisition, GH. All authors have read and agreed to the published version of the manuscript.

COMPETING INTERESTS

The authors declare no competing interests.

INSTITUTIONAL REVIEW BOARD STATEMENT

The study was conducted according to the guidelines of the Declaration of Helsinki. A written informed consent for participation was obtained from all patients. The study was authorized by the local ethics committees of Besançon University Hospital (Besançon, France) and the French Research Ministry (AC-2015-2496, CNIL n°1173545, NF-S-138 96900 n°F2015).

ADDITIONAL INFORMATION

Supplementary information The online version contains supplementary material available at https://doi.org/10.1038/s41388-023-02813-4.

Correspondence and requests for materials should be addressed to Georges Herbein.

Reprints and permission information is available at http://www.nature.com/reprints

Publisher's note Springer Nature remains neutral with regard to jurisdictional claims in published maps and institutional affiliations.

Open Access This article is licensed under a Creative Commons Attribution 4.0 International License, which permits use, sharing, adaptation, distribution and reproduction in any medium or format, as long as you give appropriate credit to the original author(s) and the source, provide a link to the Creative Commons license, and indicate if changes were made. The images or other third party material in this article are included in the article's Creative Commons license, unless indicated otherwise in a credit line to the material. If material is not included in the article's Creative Commons license and your intended use is not permitted by statutory regulation or exceeds the permitted use, you will need to obtain permission directly from the copyright holder. To view a copy of this license, visit http://creativecommons.org/licenses/by/4.0/.

© The Author(s) 2023

11.11 Publication N°11

Bouezzedine F, **El Baba R**, Haidar Ahmad S, Herbein G. Polyploid Giant Cancer Cells Generated from Human Cytomegalovirus-Infected Prostate Epithelial Cells. Cancers 2023;15:4994. https://doi.org/10.3390/cancers15204994.

Prostate cancer remains a leading cause of death in men worldwide. Polyploid giant cancer cells (PGCCs) and chromosomal instability have been proposed to drive the progression of cancer. Given that HCMV infection has been implicated in malignant diseases from different cancer entities, in the present study, we assessed its transformation potential in vitro and evaluated the obtained cellular and molecular phenotypes of prostate epithelial cells (PECs) using HCMV high-risk clinical strains, DB and BL, which were previously isolated in our laboratory. HCMV-induced PGCC formation, Myc and EZH2 upregulation, as well as the stemness and epithelial–mesenchymal transition features verified the transformation process of PECs. Our research work deserves to be distributed among the scientific community, as it paves the way for upcoming studies targeting the potential role of HCMV and PGCCs in prostate cancer development and treatment.

cancers

MDPI

Article

Polyploid Giant Cancer Cells Generated from Human Cytomegalovirus-Infected Prostate Epithelial Cells

Fidaa Bouezzedine [1], Ranim El Baba [1], Sandy Haidar Ahmad [1] and Georges Herbein [1,2,*]

[1] Pathogens & Inflammation/EPILAB Laboratory, EA 4266, University of Franche-Comté, 25000 Besançon, France; fidaa.bou_ezzeddine@univ-fcomte.fr (F.B.); ranim.elbaba@univ-fcomte.fr (R.E.B.); sandy.haydar_ahmad@univ-fcomte.fr (S.H.A.)
[2] Department of Virology, CHU Besançon, 25030 Besançon, France
* Correspondence: georges.herbein@univ-fcomte.fr; Tel.: +33-626-479-529; Fax: +33-381-665-695

Simple Summary: Prostate cancer remains a leading cause of death in men worldwide. Polyploid giant cancer cells (PGCCs) and chromosomal instability have been proposed to drive the progression of cancer. Given that HCMV infection has been implicated in malignant diseases from different cancer entities, in the present study, we assessed its transformation potential in vitro and evaluated the obtained cellular and molecular phenotypes of prostate epithelial cells (PECs) using HCMV high-risk clinical strains, DB and BL, which were previously isolated in our laboratory. HCMV-induced PGCC formation, Myc and EZH2 upregulation, as well as the stemness and epithelial–mesenchymal transition features verified the transformation process of PECs. Our research work deserves to be distributed among the scientific community, as it paves the way for upcoming studies targeting the potential role of HCMV and PGCCs in prostate cancer development and treatment.

Abstract: Background: Prostate cancer is the most commonly diagnosed malignancy and the sixth leading cause of cancer death in men worldwide. Chromosomal instability (CIN) and polyploid giant cancer cells (PGCCs) have been considered predominant hallmarks of cancer. Recent clinical studies have proven the association of CIN, aneuploidy, and PGCCs with poor prognosis of prostate cancer (PCa). Evidence of HCMV transforming potential might indicate that HCMV may be involved in PCa. Methods: Herein, we underline the role of the high-risk HCMV-DB and -BL clinical strains in transforming prostate epithelial cells and assess the molecular and cellular oncogenic processes associated with PCa. Results: Oncogenesis parallels a sustained growth of "*CMV-Transformed Prostate epithelial cells*" or CTP cells that highly express Myc and EZH2, forming soft agar colonies and displaying stemness as well as mesenchymal features, hence promoting EMT as well as PGCCs and a spheroid appearance. Conclusions: HCMV-induced Myc and EZH2 upregulation coupled with stemness and EMT traits in IE1-expressing CTP might highlight the potential role of HCMV in PCa development and encourage the use of anti-EZH2 and anti-HCMV in PCa treatment.

Keywords: human cytomegalovirus; CIN; PGCCs; high-risk HCMV strains; prostate cancer; oncogenesis; stemness

check for updates

Citation: Bouezzedine, F.; El Baba, R.; Haidar Ahmad, S.; Herbein, G. Polyploid Giant Cancer Cells Generated from Human Cytomegalovirus-Infected Prostate Epithelial Cells. *Cancers* **2023**, *15*, 4994. https://doi.org/10.3390/cancers15204994

Academic Editor: Henry H. Heng

Received: 29 August 2023
Revised: 12 October 2023
Accepted: 12 October 2023
Published: 15 October 2023

Copyright: © 2023 by the authors. Licensee MDPI, Basel, Switzerland. This article is an open access article distributed under the terms and conditions of the Creative Commons Attribution (CC BY) license (https://creativecommons.org/licenses/by/4.0/).

1. Introduction

Prostate cancer (PCa) is the most common solid tumor in men and the most prevalent tumor in the genitourinary system [1]. Based on the American Cancer Society's statistics in 2022, PCa was considered the most frequent malignancy and the second-ranked cause of death among men in the United States [2,3]. Variable risk factors may influence the risk of developing PCa; however, little evidence exists for PCa prevention strategies except for early diagnosis, which aids in reducing PCa mortality [2,3]. In asymptomatic early stages, PCa, also called localized PCa, is not detectable. This explains the severity of PCa in terminal stages, indicating the presence of metastatic sites or a castration-resistant cancer

form (CRPC), which are often difficult to treat. At that stage, the median survival is 9 to 30 months [4].

Chromosomal instability, or CIN, has long been viewed as a topic of choice in cancer research [5] and a predominant hallmark of cancer [6]. Studying CIN can be beneficial for patient management involving diagnosis, prognosis, therapy, and genetic counseling [7]. A study showed that therapy monitoring using CIN led to the reduction of genome chaos-mediated drug resistance [5]. It is worth noting that CIN and aneuploidy are not identical, as aneuploidy represents a state of imbalanced karyotype [8]. In PCa, clinical studies revealed that CIN and aneuploidy have been linked to aggressive lethal disease [8,9], where castration and chemotherapy-resistant tumors showed a high incidence of CIN [9]. Polyploid giant cancer cells, or PGCCs, are formed through endoreplication and are considered a special subpopulation of cancer cells that contribute to solid tumor heterogeneity [10,11]. Recently, urinary PGCCs were detected in prostate cancer tissues [12]. Further, these giant cells contributed to the production of mononucleated aneuploid cells via neosis and might result in clinical relapse and chemoresistance in CRPC [13].

Prostate cancer pathogenesis involves heritable and environmental factors. A possible viral etiology of prostate cancer progression has been suggested, and evidence for viral-mediated genetic changes and associated immune dysregulation has been explored for many viruses, especially those known for infection of the anogenital and urinary sites [14]. HCMV, or human herpesvirus 5 (HHV-5), is a ubiquitous DNA virus that is detected in the urine and prostate tissue of infected subjects [15,16]. It infects between 40% and 95% of the population worldwide [17]. In healthy individuals, HCMV infection is considered mild or asymptomatic; however, in immunocompromised patients, it causes life-threatening illness in addition to congenital infections [18]. HCMV of prostatic origin established a long-term persistent infection in human embryo lung cells (HEL cells) in vitro [19]. Further, HCMV-specific intracellular immunofluorescent antigens were detected in prostatic cancer cell cultures [20,21]. An HCMV isolate that transformed HEL cells in vitro was yielded from normal human prostatic tissue [21]. Upon transplantation to athymic nude mice, these cell transformants were highly oncogenic [20]. These complex findings constitute further evidence of HCMV transforming capacity and indicate that HCMV may be involved in the development of prostatic neoplasia [20–22].

In agreement with the research findings of Rapp and Geder around fifty years ago, beyond the oncomodulation model, the presence of HCMV nucleic acid and proteins in several tumors (for instance, glioblastoma, neuroblastoma, colon cancer, breast cancer, and ovarian cancer) promoted HCMV as an oncovirus and highlighted a strong link between persistent HCMV infection and malignancy [23]. Recently, our group confirmed a potential direct oncogenic feature of HCMV and highlighted the role of polyploid giant cancer cells (PGCCs) in the HCMV-mediated transformation process, in agreement with the giant cell cycling theory unveiled recently by Liu and colleagues [24,25]. The oncogenic processes associated with HCMV infection at the cellular and molecular levels involved the transformation of epithelial cells, sustained proliferative signaling, growth suppressor evasion and apoptosis, and generation of PGCCs, as well as invasion and metastasis [26–28].

In line with the oncogenic potential of HCMV in mammary epithelial cells, we investigated its link with PCa. First, by revealing a direct transformation of prostate epithelial cells infected by the high-risk HCMV clinical strains (DB and BL HCMV strains) already isolated in our laboratory. Second, by exploring the molecular and cellular oncogenic processes associated with PCa cancer—for instance, generation of PGCCs, formation of soft agar colonies, and spheroid formation, as well as the induction of stemness and EMT markers.

2. Materials and Methods

Cell cultures. Human prostate epithelial cells (PECs) (Ref: CC-2555) were purchased from Lonza (Basel, Switzerland). The cells were maintained in prostate epithelial cell growth medium BulletKit (CC-3166) and were cultured under standard conditions (37 °C,

5% CO_2, 95% humidity). Cultures were free of mycoplasma as determined by monthly screening (VenorGem classic mycoplasma detection, Minerva biolabs).

Viral growth and PEC infection. Clinical HCMV strains, namely HCMV-DB (GenBank KT959235), -BL (GenBank MW980585), -KM, and -FS, were isolated from patients who were hospitalized at Besançon University Hospital (Besançon, France) as previously described [26,29]. The human prostate epithelial cells were infected overnight with a multiplicity of infection (MOI) of 1. Screening of our viral stocks was conducted using real-time quantitative PCR to rule out the presence of other oncoviruses, namely EBV (sense, 5′-GATTTGGACCCGAAATCTGAT-3′; anti-sense, 5′-TCTGGGGGCTTATTCCTCTT-3′) and HPV (HPV16(E6) sense, 5′-GCACCAAAAGAGAACTGCAATGTT-3′; anti-sense, 5′-AGTCATATACCTCACGTCGCAGTA-3′). PEC infections, quantification of HCMV replication, and HCMV detection were performed as previously described [26]. For HCMV quantification, supernatants from infected PECs were harvested, DNA was isolated (EZNA Blood DNA Kit, D3392-02, Omega BIO-TEK, Norcross, GA, USA) and real-time IE1 quantitative PCR (qPCR) was performed using a Stratagene Mx3005P thermocycler (Agilent Technologies, Santa Clara, CA, USA) and IE1 primers (sense, 5′-CGACGTTCCTGCAGACTATG-3′; anti-sense, 5′-TCCTCGGTCACTTGTTCAAA-3′). qPCR was carried out using KAPA SYBR FAST Master Mix (KAPA BIOSYSTEMS, Potters Bar, UK). Results were collected and analyzed using MxPro qPCR software (Version 3.2).

Microscopy. Infected prostate cell cultures were monitored by an Olympus optical microscope (Olympus Corporation, Tokyo, Japan) and OPTIKA microscopy digital camera (Opticam, Romano d'Ezzelino, Italy). Confocal microscopy of prostate epithelial cells was performed as described previously [26]. Briefly, cells were washed with 1× PBS, fixed and permeabilized (BD Cytofix/Cytoperm, 554722) and subsequently stained with the following antibodies: anti-IE1 (pp72), anti-Myc, anti-EZH2, anti-Nestin, anti-Nanog, anti-SOX2, anti-vimentin, and anti-E-cadherin. For visualization of the nucleus and the cytoplasm, DAPI (4′, 6′-diamidino-2-phenylindole) and phalloidin staining, respectively, were performed according to the manufacturer's protocol. After staining, confocal imaging was performed using a 63× oil immersion objective lens with an LSM800 Carl-Zeiss confocal microscope (Germany). Images were analyzed by using ZenBlue Software (Version 3.6, Carl-Zeiss Microscopy GmbH, Oberkochen, Germany). The antibodies used are provided in Supplementary Table S1.

Flow cytometry analysis. 1×10^5 cells were collected from uninfected and infected PECs. Cells were fixed and permeabilized using 100 µL of BD Biosciences Cytofix/Cytoperm solution (554722) for 20 min at 4 °C and washed twice with 1× BD Perm wash. Cells were then stained using the respective primary and secondary antibodies, as reported previously [26]. Cells were then subjected to cytofluorometric analysis using a BD LSRFortessa X-20 (BD Biosciences, Franklin Lakes, NJ, USA) flow cytometer. Data obtained were analyzed and processed using FACSDiva software (BD FACSDiva 8.0.1, BD Biosciences). The antibodies used are provided in Supplementary Table S1.

Soft agar colony formation assay. Colony formation in soft agar seeded with uninfected PECs and DB- and BL-infected PECs was assayed using Cell Biolabs Cytosolic Cell Transformation Assay Kit (Colorimetric assay, CB 135; Cell Biolabs Inc., San Diego, CA, USA) as per the manufacturer's protocol. Colonies were observed under an Olympus microscope (Olympus Corporation, Tokyo, Japan).

Spheroid formation assay. Spheroids of PECs were prepared as described previously [30]. Single cells (2×10^3) isolated using accutase were seeded in a serum-free PEC medium containing methylcellulose.

Statistics. Quantitative results are reported as mean ± SD of independent experiments. Statistical analyses were done using the Mann–Whitney test; a p-value ≤ 0.05 was considered to be statistically significant [*: $\leq$0.05; **: $\leq$0.01; ***: $\leq$0.001]. Microsoft Excel v2309 was used to construct the plots and histogram data.

3. Results

3.1. HCMV-DB and -BL Clinical Strains Chronically Infected PECs Generating CTP Cells with PGCCs

In PECs, all HCMV clinical strains replicated, showing a peak viral replication at days 3, 3, 13, and 9 post-infection with HCVM-DB, HCMV-BL, HCMV-KM, and HCMV-FS, respectively (Figure 1A and Supplementary Figure S1). The peak of HCMV load was 3 and 5 logs in PEC-DB and -BL, respectively (Figure 1A). HCMV-IE1 protein was detected in PEC-DB and -BL (Figure 1B). HCMV replication was further detected in the chronically infected PEC-DB and -BL cells (Supplementary Figure S2).

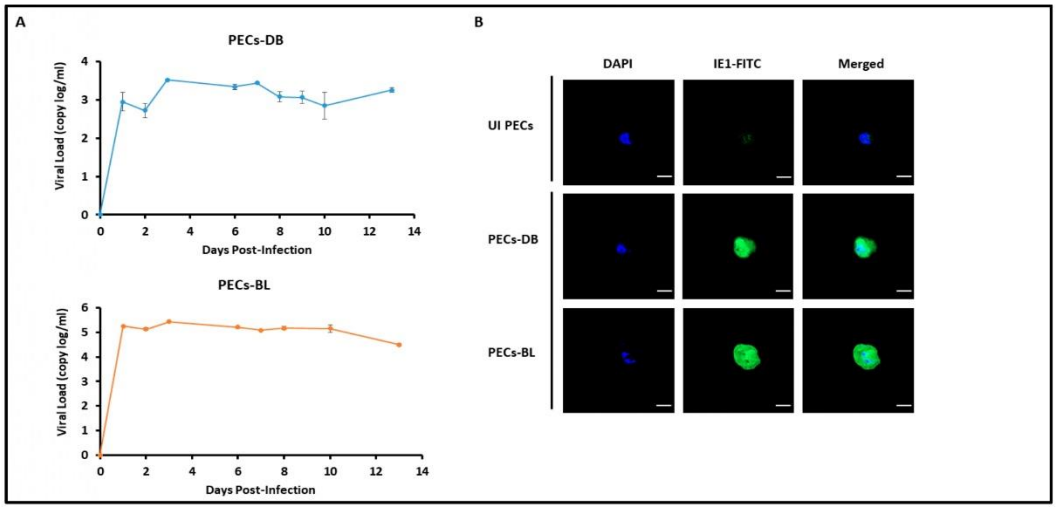

Figure 1. Replication of HCMV-DB and -BL strains in PEC cultures. (**A**) Time course of the viral titer in the supernatant of PECs infected with HCMV-DB and -BL as measured by IE1-qPCR. (**B**) Confocal microscopic images of IE1 staining in PEC-DB and -BL. UI PECs were used as controls; magnification ×63, scale bar 10 µm. Data are represented as mean ± SD of two independent experiments.

In chronically infected PEC cultures, we detected giant cells having large nuclei that were observed only in PECs chronically infected with the high-risk HCMV-DB and -BL strains, unlike uninfected PECs (Figure 2A) and PECs chronically infected with HCMV-KM and -FS strains. The emerging cells were termed "*CMV-Transformed Prostate epithelial cells*" or CTP cells, equivalent to the transformed cells that were previously reported by our group, namely, "CMV-Transformed Human mammary epithelial cells" or CTH cells, and "CMV-Elicited GlioBlastoma Cells" or CEGBCs [28,29]. Cellular heterogeneity, including giant cells, blastomeres, blastocytes, multinucleated, budding, and mesenchymal cells, as well as cells showing filopodia and lipid droplets (Figure 2A), were detected in CTP-DB and -BL cultures. The presence of PGCCs and budding cells was confirmed by confocal staining of CTP cells (Figure 2B). On evaluating the proliferation potential of CTP cells, Ki67Ag was assessed in CTP cells; Ki67Ag expression was elevated in CTP-DB and -BL cells compared to uninfected PECs (p-value $_{(UI\ PECs:CTP\text{-}HCMV)}$ = 0.02) (Figure 3A). Further, polyploidy was detected mainly in CTP-DB and -BL cells compared to UI PECs; cobalt chloride ($CoCl_2$) was used as a positive control to induce PGCC formation in PEC cultures (Figure 3B). CTP-DB and -BL cell populations were classified into PGCCs (>4 N), large cells (4 N), intermediate cells (ICs of 2–4 N), and small cells (SCs of 2 N) (Figure 3C). The percentage of PGCCs was significantly increased in CTP-DB and -BL cultures (p-value

(UI PECs:CTP-HCMV) = 0.02). Increased polyploidy observed in CTP-DB and -BL cultures is in line with an almost two-fold increase in the S-phase (2–4 N) cells compared to uninfected PECs. Further, a drastic two-fold reduction was noticed in the 2 N cells of CTP-DB and -BL cultures compared to uninfected PECs (Figure 3C). Altogether, increased DNA synthesis and polyploidy were observed in CTP-DB and -BL cells compared to uninfected PECs.

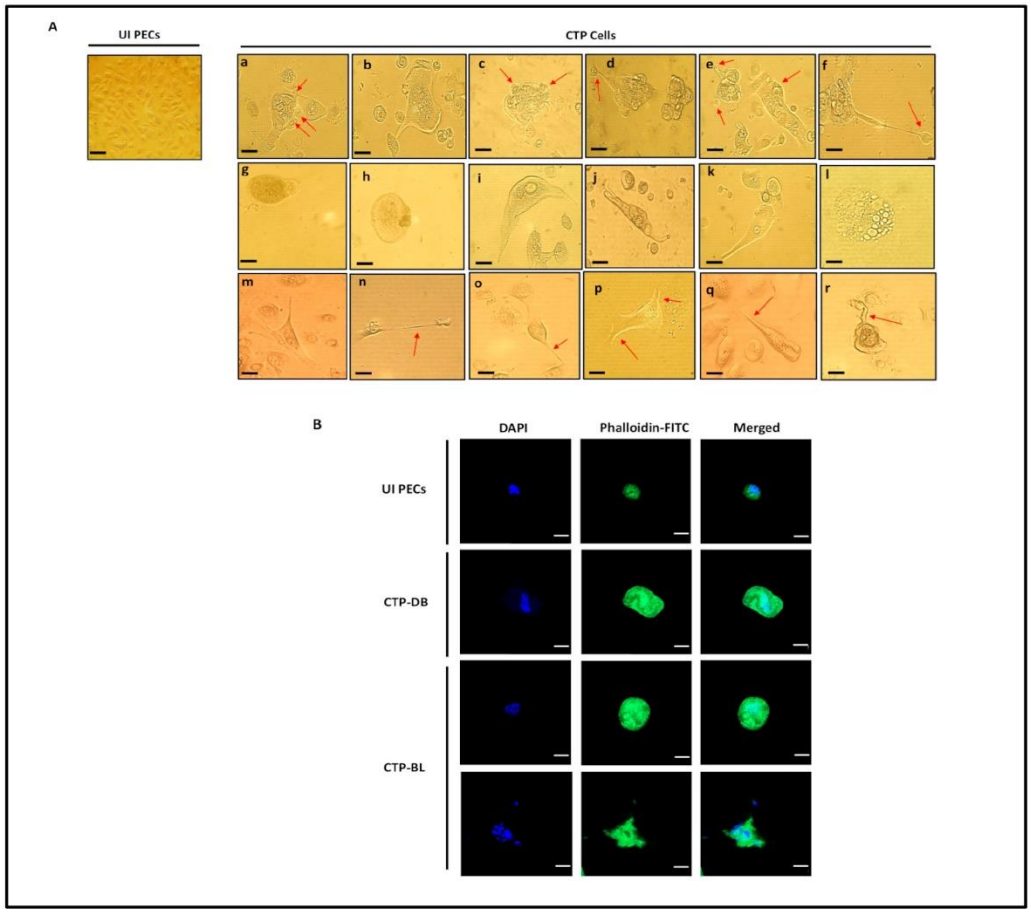

Figure 2. Chronic infection of PECs with the high-risk HCMV strains and detection of morphological heterogeneity in CTP cultures. (**A**) Microscopic images of distinct cellular morphologies of the giant cell cycle, including (**a**–**f**) budding, (**g**,**h**) blastomeres and blastocytes, (**i**–**k**) mesenchymal cells, (**l**) lipid droplet-filled cells, (**m**–**r**) filopodia; magnification ×100, scale bar 100 µm (for UI PECs) and ×200, scale bar 50 µm (for images **a**–**r**). Uninfected PECs were used as a control. (**B**) Confocal microscopic images of DAPI and phalloidine staining in CTP-DB and -BL cells. Uninfected PECs were used as a negative control; magnification ×63, scale bar 10 µm. Red arrows show the defined morphologies.

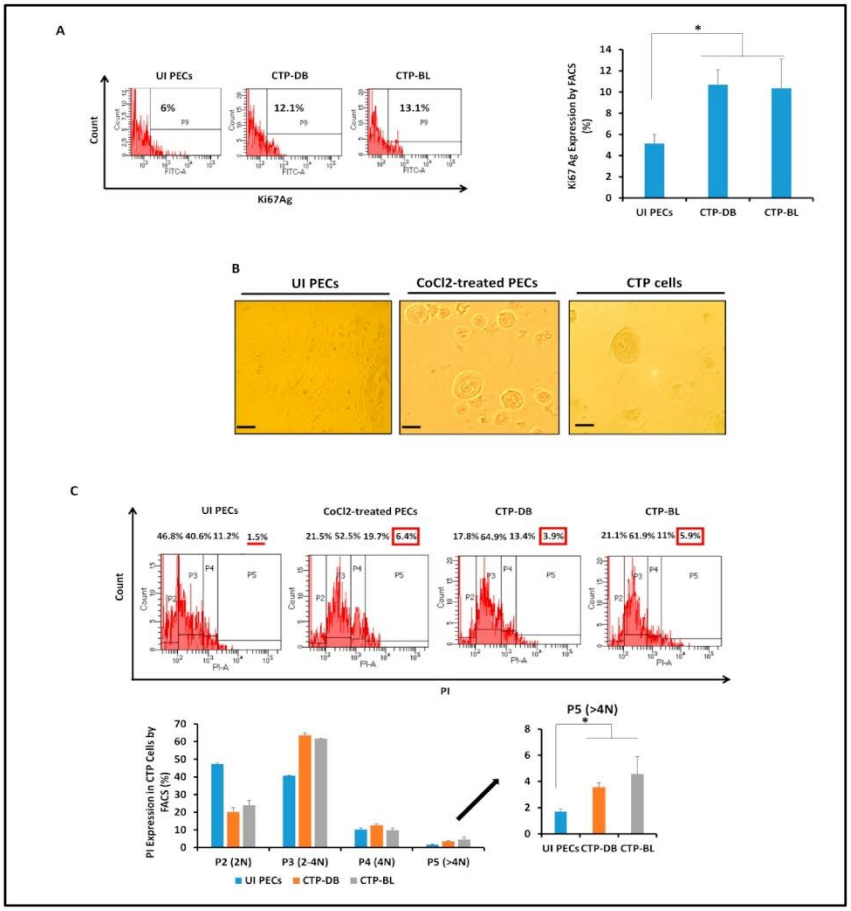

Figure 3. Assessing the proliferative potential and detecting polyploidy in CTP-DB and -BL cultures. (**A**) FACS staining of Ki67Ag in uninfected PECs as well as CTP-DB and -BL cells. (**B**) Microscopic images of polyploidy detected in CTP-DB and -BL cultures. Cobalt chloride ($CoCl_2$)-treated PECs (300 µM) were used as a positive control, while uninfected PECs were used as a negative control. Magnification ×200, scale bar 50 µm. (**C**) Propidium iodide (PI) staining for polyploidy detection in CTP-DB and -BL cells by FACS. CoCl2-treated PECs were used as a positive control, and uninfected PECs were used as a negative control. Data are represented as mean ± SD of two independent experiments. * p-value ≤ 0.05. The red line shows the low percentage of P5 (>4 N). Red boxes emphasizes the high percentages of p5 (>4 N).

3.2. CTP Cells Exhibited Dedifferentiation, Stemness, and EMT Traits Parallel to the Sustained HCMV Replication

CTP-DB and -BL cells were seeded in soft agar to assess their oncogenic transforming potential. Colony formation was detected in the cultures seeded with CTP-DB and -BL cells compared to uninfected PECs (Figure 4A). EZH2 and Myc upregulation was detected in CTP-DB and -BL cells compared to uninfected PECs (p-value $_{(\text{UI PECs:CTP-HCMV})}$ = 0.02)

(Figure 4B). In CTP cells, the elevated levels of EZH2 and Myc proteins were confirmed by confocal microscopy imaging (Figure 4C). Suz12 expression was decreased in CTP-DB and -BL cells compared to uninfected PECs (p-value $_{(UI\ PECs:CTP\text{-}HCMV)}$ = 0.02) (Supplementary Figure S3).

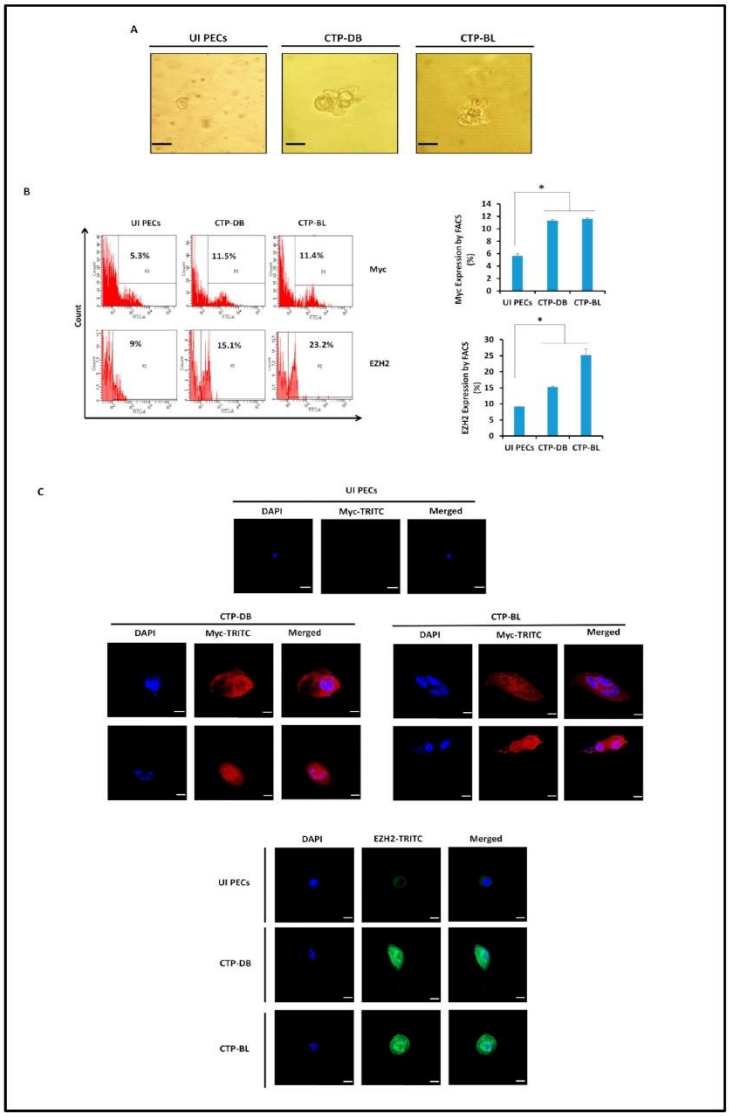

Figure 4. Transformation potential and phenotypic characterization of CTP-DB and -BL cells. (**A**) Colony formation in soft agar seeded with CTP-DB and -BL cells; uninfected PECs were used as a

negative control. Formed colonies were observed under an inverted light microscope (magnification 200×, scale bar 50 µm). (**B**) FACS staining of Myc and EZH2 in uninfected PECs as well as CTP-DB and -BL cells. Data are represented as mean ± SD of two independent experiments. (**C**) Confocal microscopic images of Myc, EZH2, and DAPI staining in CTP-DB and -BL cells. Uninfected PECs were used as controls; magnification ×63, scale bar 10 µm. * p-value ≤ 0.05.

In addition to PGCC presence in CTP cultures, spontaneous spheroids, as well as methylcellulose-induced spheroids, were detected in CTP-DB and -BL cultures (Figure 5A,B). Nestin, an intermediate filament protein and marker of undifferentiated cells [31], was upregulated in CTP-DB and -BL cultures compared to uninfected PECs (Figure 5C). Nanog and SOX2 expression in CTP-DB and -BL cells revealed an embryonic stemness phenotype within the aforementioned HCMV-transformed cells (Figure 5C).

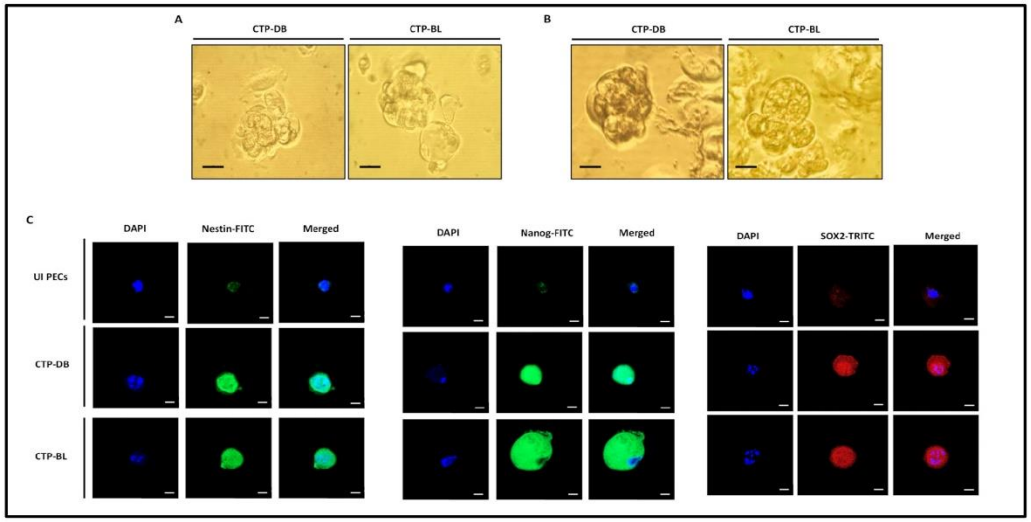

Figure 5. CTP-DB and -BL cells display a stemness phenotype. (**A**) Spontaneous spheroids were detected under an inverted light microscope in CTP-DB and -BL cultures. Magnification ×200, scale bar 50 µm. (**B**) Spheroids were observed in the chronically infected CTP-DB and -BL cell cultures in methylcellulose, scale bar 25 µm. (**C**) Confocal microscopic images of Nestin, Nanog, SOX2, and DAPI staining in CTP-DB and -BL cells. Uninfected PECs were used as controls; magnification ×63, scale bar 10 µm.

Through EMT, tumors can attain a mesenchymal phenotype close to cancer stem cell features that contribute to metastasis [32]. Vimentin expression was upregulated in CTP-DB and -BL cultures (p-value $_{(\text{UI PECs:CTP-HCMV})}$ = 0.02), whereas E-cadherin was downregulated compared to uninfected PECs (p-value $_{(\text{UI PECs:CTP-HCMV})}$ = 0.02) (Figure 6A,B).

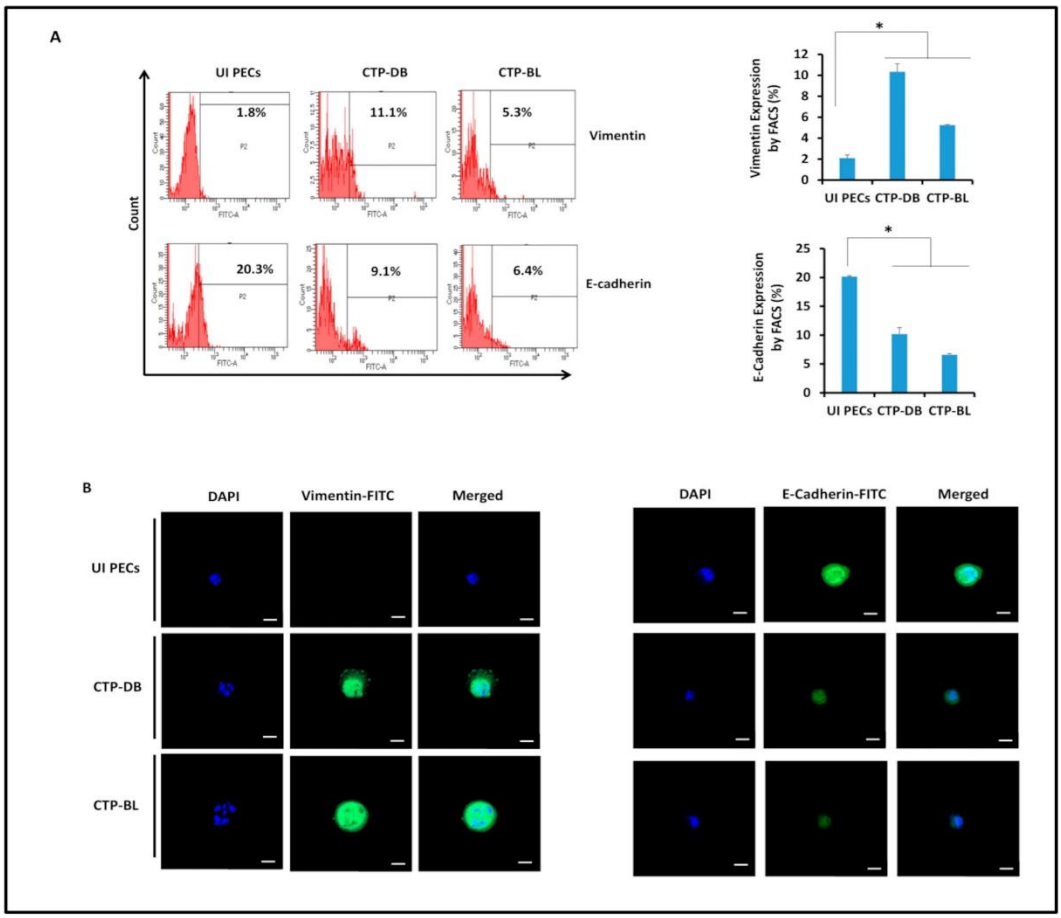

Figure 6. EMT in CTP-DB and -BL cultures. (**A**) Vimentin and E-cadherin expression by FACS in CTP-DB and -BL cells. Uninfected PECs were used as controls. Data are represented as mean ± SD of two independent experiments. (**B**) Confocal microscopic images of vimentin, E-cadherin, and DAPI staining in CTP-DB and -BL cells. Uninfected PECs were used as controls; magnification ×63, scale bar 10 µm. * p-value ≤ 0.05.

In PECs chronically infected with high-risk HCMV-DB and -BL, HCMV replication was sustained (Figure 7). IE1 protein and gene were remarkably detected in CTP-DB and -BL cells versus uninfected PECs (Figure 7A,B).

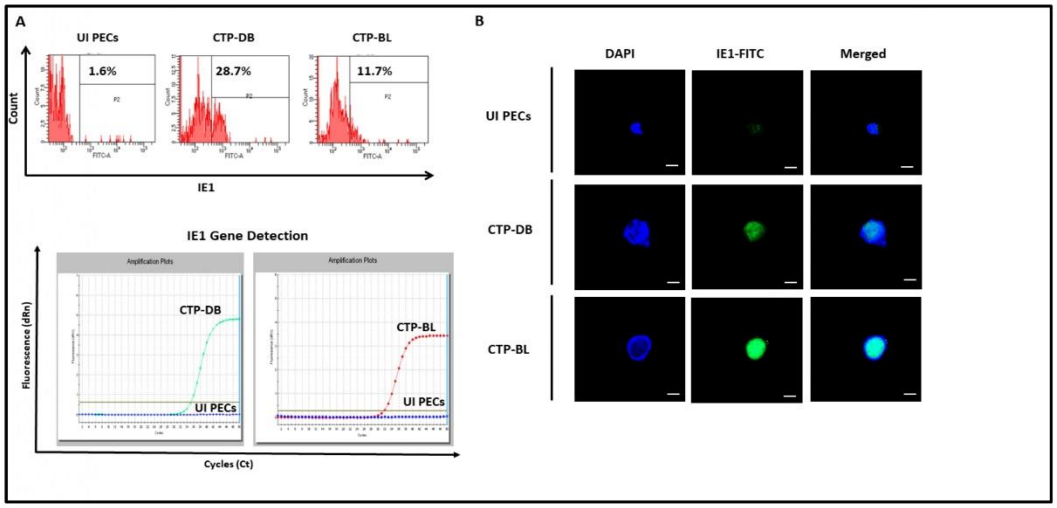

Figure 7. Sustained HCMV replication in CTP-DB and -BL cultures. (**A**) IE1 protein and gene expression in chronically infected CTP-DB and -BL cell cultures by FACS and qPCR, respectively. Uninfected PECs were used as a negative control. (**B**) Confocal microscopic images of IE1 and DAPI staining in CTP-DB and -BL cells. Uninfected PECs were used as controls; magnification ×63, scale bar 10 μm.

4. Discussion

Polyploidy, a feature of chromosomal instability, can be triggered by oncoviruses [33]. In our study, we evaluated the transforming capacities of the high-risk oncogenic HCMV-DB and -BL strains following PEC infection. An oncogenic environment, along with a sustained growth of CTP cells with soft agar colonies, was detected upon infecting PECs with HCMV-DB and -BL. The HCMV-transformed PECs or CTP cells dedifferentiated, displayed stemness traits, gained mesenchymal features promoting EMT, and yielded PGCCs (Figure 8 and Supplementary Figure S4), and they also possessed spheroid formation potential. HCMV detection, PGCC appearance, and Myc and EZH2 upregulation verified the transformation process in PECs.

CIN/aneuploidy is associated with tumor progression and is considered a poor prognostic biomarker in various tumor types, including prostate cancer [8,9]. Knowing that the exerted potential oncomodulatory effects of HCMV infection are through enhanced replication stress, subverted DNA damage response, and induced genomic instability [34], it is of high importance to maintain CIN/aneuploidy under a tolerable threshold; this is to prevent tumor aggressiveness [7,9]. PGCC presence has been described in multiple tumors—for instance, breast, ovarian, colon, melanoma, lung, pancreas, urinary bladder, renal, thyroid, and prostate [24,26,35,36]. Studies with human prostate cancer cell lines showed that PGCCs are more aggressive, metastatic, and highly resistant to common chemotherapies [25,37]. They constitute stem cell-like traits and express various embryonic stem cell markers facilitating cancer cell survival, therapy resistance, and tumor relapse [36,37]. In line with the previous studies, CTP cells showed various cellular morphologies, including multinucleated cells, cell budding, blastomeres, blastocytes, filopodia, and cells with lipid droplets. The aforementioned morphologies were previously detected in PCa [36,38–40]. In agreement with the blastomere-like stemness and giant cell life cycle reported previously by Niu et al. [41,42], we observed the PGCC appearance as well as cellular heterogeneity in HCMV-transformed prostate epithelial cell cultures (CTP cells). The CTP cell popula-

tion was highly heterogeneous, including PGCCs, blastomere-like cells, morula-like cells, mesenchymal cells, and small cells. The described patterns could be representative of self-renewing cells undergoing diverse stages of the previously described giant cell cycle. Thus, our outcomes revealed that PGCCs harboring HCMV might promote a malignant phenotype via giant cell cycling [24,25].

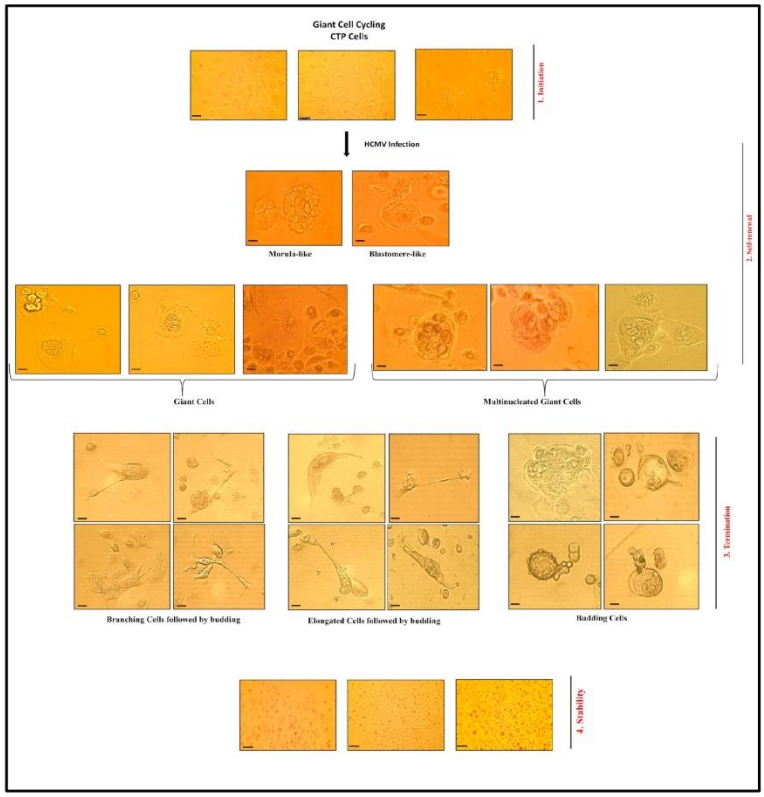

Figure 8. A schematic diagram illustrating giant cell cycling in CTP-DB and -BL cultures. Microscopic images of distinct cellular morphologies of the giant cell cycle; magnification ×200, scale bar 50 µm (initiation, self-renewal, and termination phases), and ×100, scale bar 100 µm (stability phase). Initiation, self-renewal, termination, and stability represent the four different stages of the giant cell cycle. Post-HCMV infection and via endoreplication, the 2 N PECs go into the initiation phase. Subsequently, polyploid cells (>4 N) and tetraploid cells (4 N) are produced in the self-renewal/dedifferentiation phase. During the termination/differentiation stage, the intermediate cells (2–4 N) will be generated from multinucleated or mononucleated giant cells through budding. Intermediate PECs enter the stability stage and are afterward replaced by diploid small PECs (2 N).

In addition to PGCCs, numerous other cellular and molecular mechanisms could account for the genome chaos observed in various solid tumor types, including, among others, chromothripsis [43], drug-tolerant persister (DTP) cancer cells [44], reversible senescence [45], treacherous apoptosis [46], oncogenic p21WAF1 expression [47,48], and anastasis [49]. Although we identified here the role of HCMV in PGCC formation, we cannot

exclude the role of HCMV in the appearance of other aspects of genome chaos. HCMV induces the generation of intracellular reactive oxygen intermediates (ROIs) within minutes after infection of the cell, and then it uses these ROIs to facilitate its own gene expression and replication. Conversely, antioxidants inhibit HCMV immediate early gene expression and viral replication [50]. Since there is an increasing consensus that disrupting redox homeostasis by intervening with redox signaling is theoretically a promising therapeutic strategy for targeting drug-tolerant persister cancer cells [51], it might be possible that HCMV will modulate redox signaling in infected cells and, thereby, play a role in the generation/maintenance of DTP cancer cells. Programmed cell death or apoptosis has generally been viewed as a protective mechanism that suppresses tumor growth and prevents tumor progression. However, recent studies have shown that apoptosis can also have a paradoxical pro-tumoral role by increasing genomic instability, creating an immunosuppressive microenvironment, or driving therapy resistance. Thus, recently, it has been shown that islands of apoptotic cell death are strongly associated with tumor heterogeneity in their special proximity in vivo and induce therapy resistance in vitro. Since apoptosis disorder is a key pathogenesis mechanism of HCMV-related diseases [52], we cannot exclude that HCMV infection could be involved in the foci of apoptotic cells, thereby leading to tumor heterogenicity/therapy resistance.

Recent advances in genomics and proteomics highlighted the essential role of certain biomarkers in several tumors, mainly PCa [53,54]. Myc overexpression contributed to prostate tumor initiation and progression by disrupting transcriptional pause release at androgen receptor-regulated genes [55]. Other studies highlighted the oncogenic function of the methyltransferase EZH2 in castration-resistant prostate cancer cells, where EZH2 acts as a coactivator for critical transcription factors, including the androgen receptor [56,57]. In line with the previously mentioned findings, Myc and EZH2 overexpression was detected in CTP-DB and -BL cells compared to uninfected PECs. The CTP stemness phenotype was confirmed by the spheroids detected in CTP-DB and -BL cultures in addition to the high expression of nestin, Nanog, and SOX2, which are shown to be linked to prostate cancer development, progression, invasion, and metastasis [31,58–60]. Prostate cancer cells acquire invasive and metastatic characteristics via EMT [61,62]. Increasing evidence indicates that EMT promotes prostate cancer metastatic progression, and it is mainly associated with increased stemness and drug resistance [63]. In our study, vimentin was highly expressed in CTP cells, unlike E-cadherin, which was downregulated in CTP-DB and -BL cells, in line with the EMT phenotype.

Several studies have revealed the presence of infectious agents in the prostate, including oncogenic viruses, such as HPV, EBV, and BK polyomavirus [64,65]. The strength of the viral etiology and the molecular events involved in the development of PCa are still unclear. Recent evidence concluded that the HPV high-risk types have a causal role in prostate cancer [66]. HPV oncogenic proteins (E6 and E7) exert their carcinogenic potential through interacting with and degrading tumor suppressors (p53 and Rb) [67]. The association between EBV and prostate cancer is still under debate [68]. Although herpes simplex virus (HSV) is not recognized as an oncovirus, a significant association between prostate cancer and serologic evidence of HSV-2 infection is probably due to a long latency period for prostate cancer progression after HSV-2 infection [69].

Infecting PECs with the high-risk HCMV strains, namely DB and BL, revealed a sustained viral replication through the detection of HCMV-IE1 in chronically infected cultures, suggesting that HCMV infection could potentially promote cancer progression. We believe that there is an alternation of productive and latent phases in the HCMV-transformed cells, as already reported for other herpes oncoviruses, namely KSHV and EBV [70,71].

In agreement with our results, several studies showed that HCMV may be directly involved in the development of prostatic intraepithelial neoplasia [16,22]. Nevertheless, the association between HCMV and PCa has been explored, in which two out of ten case-control studies revealed no significant association between HCMV and increased PCa

risk [66,72–78]. In fact, the observed discrepancies between these studies at the molecular and serological level may depend on the differences in techniques' sensitivity for detecting HCMV in prostate tissues. In addition to its direct oncogenic potential, an oncomodulatory effect of HCMV linked to the ability of HCMV to interfere with the transforming cell properties has been reported [79,80]. A study done by Blaheta et al. on the prostate cancer cell model (PC3) demonstrated that HCMV acts on the invasive properties of the prostatic cancerous cell line PC3, and this carcinogenic process is promoted by elevated c-Myc levels [81]. Also, androgen in the prostate could activate the HCMV major immediate early promoter (MIEP), leading to viral replication, which might contribute to oncomodulation in prostate cancers [82].

5. Conclusions

In conclusion, HCMV-induced Myc and EZH2 overexpression, along with the stemness and EMT cellular phenotypes in IE1-expressing PECs, led to the appearance of transformed CTP cells and might determine a significant model in the context of PCa. Furthermore, the use of anti-EZH2 and anti-HCMV therapies could open the door to new avenues that might be beneficial in the management of PCa, especially the more aggressive castration-resistant ones, such as hormone-refractory PCa with high metastatic potential.

Supplementary Materials: The following supporting information can be downloaded at: https://www.mdpi.com/article/10.3390/cancers15204994/s1, Figure S1. Replication of low-risk HCMV strains in PECs cultures; Figure S2. Sustained HCMV replication in CTP-DB and BL cultures; Figure S3. Expression of Suz12 in CTP-DB and BL cultures; Figure S4. A schematic diagram representing the giant cell cycling in CTP-BL cell cultures; Table S1. List of antibodies.

Author Contributions: Conceptualization, G.H.; formal analysis, F.B., R.E.B., S.H.A. and G.H.; investigation, F.B., R.E.B. and S.H.A.; writing—original draft preparation, F.B., R.E.B., S.H.A. and G.H.; writing—review and editing, F.B., R.E.B., S.H.A. and G.H.; directly accessed and verified the underlying data: F.B., R.E.B., S.H.A. and G.H.; visualization, F.B., R.E.B. and S.H.A.; supervision, G.H.; project administration, G.H.; funding acquisition, G.H. All authors have read and agreed to the published version of the manuscript.

Funding: This work was supported by grants from the University of Franche-Comté (UFC) (CR3300), the Région Franche-Comté (2021-Y-08292 and 2021-Y-08290), and the Ligue contre le Cancer (CR3304) to Georges Herbein. We thank Apex Biosolutions for financial support. Fidaa Bouezzeddine is a recipient of a postdoctoral scholarship from the Région Bourgogne Franche-Comté; Ranim El Baba is a recipient of a doctoral scholarship from Apex Biosolutions; Sandy Haidar Ahmad is a recipient of a postdoctoral fellowship from the Agence Nationale de la Recherche Médicale.

Institutional Review Board Statement: Not applicable.

Informed Consent Statement: Not applicable.

Data Availability Statement: The datasets used and/or analyzed during the present study are available from the corresponding author on reasonable request.

Acknowledgments: We thank DImaCell Imaging Ressource Center, University of Bourgogne Franche-Comté, Faculty of Health Sciences, 25000 Besançon, France, for technical support.

Conflicts of Interest: The authors declare no conflict of interest.

References

1. Wang, L.; Liu, X.; Liu, Z.; Wang, Y.; Fan, M.; Yin, J.; Zhang, Y.; Ma, Y.; Luo, J.; Li, R.; et al. Network Models of Prostate Cancer Immune Microenvironments Identify ROMO1 as Heterogeneity and Prognostic Marker. *Sci. Rep.* **2022**, *12*, 192. [CrossRef]
2. Siegel, R.L.; Miller, K.D.; Fuchs, H.E.; Jemal, A. Cancer Statistics, 2022. *CA Cancer J. Clin.* **2022**, *72*, 7–33. [CrossRef]
3. Gandaglia, G.; Leni, R.; Bray, F.; Fleshner, N.; Freedland, S.J.; Kibel, A.; Stattin, P.; Van Poppel, H.; La Vecchia, C. Epidemiology and Prevention of Prostate Cancer. *Eur. Urol. Oncol.* **2021**, *4*, 877–892. [CrossRef]
4. Liu, J.J.; Zhang, J. Sequencing Systemic Therapies in Metastatic Castration-Resistant Prostate Cancer. *Cancer Control* **2013**, *20*, 181–187. [CrossRef]

5. Ye, C.J.; Sharpe, Z.; Heng, H.H. Origins and Consequences of Chromosomal Instability: From Cellular Adaptation to Genome Chaos-Mediated System Survival. *Genes* **2020**, *11*, 1162. [CrossRef]
6. Heng, H.H.; Bremer, S.W.; Stevens, J.B.; Horne, S.D.; Liu, G.; Abdallah, B.Y.; Ye, K.J.; Ye, C.J. Chromosomal Instability (CIN): What It Is and Why It Is Crucial to Cancer Evolution. *Cancer Metastasis Rev.* **2013**, *32*, 325–340. [CrossRef]
7. Heng, E.; Thanedar, S.; Heng, H.H. Challenges and Opportunities for Clinical Cytogenetics in the 21st Century. *Genes* **2023**, *14*, 493. [CrossRef] [PubMed]
8. Stopsack, K.H.; Whittaker, C.A.; Gerke, T.A.; Loda, M.; Kantoff, P.W.; Mucci, L.A.; Amon, A. Aneuploidy Drives Lethal Progression in Prostate Cancer. *Proc. Natl. Acad. Sci. USA* **2019**, *116*, 11390–11395. [CrossRef]
9. Dhital, B.; Santasusagna, S.; Kirthika, P.; Xu, M.; Li, P.; Carceles-Cordon, M.; Soni, R.K.; Li, Z.; Hendrickson, R.C.; Schiewer, M.J.; et al. Harnessing Transcriptionally Driven Chromosomal Instability Adaptation to Target Therapy-Refractory Lethal Prostate Cancer. *Cell Rep. Med.* **2023**, *4*, 100937. [CrossRef] [PubMed]
10. Chen, J.; Niu, N.; Zhang, J.; Qi, L.; Shen, W.; Donkena, K.V.; Feng, Z.; Liu, J. Polyploid Giant Cancer Cells (PGCCs): The Evil Roots of Cancer. *CCDT* **2019**, *19*, 360–367. [CrossRef] [PubMed]
11. Zhou, X.; Zhou, M.; Zheng, M.; Tian, S.; Yang, X.; Ning, Y.; Li, Y.; Zhang, S. Polyploid Giant Cancer Cells and Cancer Progression. *Front. Cell Dev. Biol.* **2022**, *10*, 1017588. [CrossRef]
12. Garrido Castillo, L.N.; Anract, J.; Delongchamps, N.B.; Huillard, O.; BenMohamed, F.; Decina, A.; Lebret, T.; Dachez, R.; Paterlini-Bréchot, P. Polyploid Giant Cancer Cells Are Frequently Found in the Urine of Prostate Cancer Patients. *Cancers* **2023**, *15*, 3366. [CrossRef] [PubMed]
13. Mittal, K.; Donthamsetty, S.; Kaur, R.; Yang, C.; Gupta, M.V.; Reid, M.D.; Choi, D.H.; Rida, P.C.G.; Aneja, R. Multinucleated Polyploidy Drives Resistance to Docetaxel Chemotherapy in Prostate Cancer. *Br. J. Cancer* **2017**, *116*, 1186–1194. [CrossRef] [PubMed]
14. Abidi, S.H.; Bilwani, F.; Ghias, K.; Abbas, F. Viral Etiology of Prostate Cancer: Genetic Alterations and Immune Response. A Literature Review. *Int. J. Surg.* **2018**, *52*, 136–140. [CrossRef]
15. Coaquette, A.; Bourgeois, A.; Dirand, C.; Varin, A.; Chen, W.; Herbein, G. Mixed Cytomegalovirus Glycoprotein B Genotypes in Immunocompromised Patients. *Clin. Infect. Dis.* **2004**, *39*, 155–161. [CrossRef]
16. Samanta, M.; Harkins, L.; Klemm, K.; Britt, W.J.; Cobbs, C.S. High Prevalence of Human Cytomegalovirus in Prostatic Intraepithelial Neoplasia and Prostatic Carcinoma. *J. Urol.* **2003**, *170*, 998–1002. [CrossRef] [PubMed]
17. Herbein, G. High-Risk Oncogenic Human Cytomegalovirus. *Viruses* **2022**, *14*, 2462. [CrossRef]
18. Griffiths, P.; Reeves, M. Pathogenesis of Human Cytomegalovirus in the Immunocompromised Host. *Nat. Rev. Microbiol.* **2021**, *19*, 759–773. [CrossRef]
19. Rapp, F.; Geder, L.; Murasko, D.; Lausch, R.; Ladda, R.; Huang, E.S.; Webber, M.M. Long-Term Persistence of Cytomegalovirus Genome in Cultured Human Cells of Prostatic Origin. *J. Virol.* **1975**, *16*, 982–990. [CrossRef]
20. Geder, L.; Kreider, J.; Rapp, F. Human Cells Transformed In Vitro by Human Cytomegalovirus: Tumorigenicity in Athymic Nude Mice2. *JNCI J. Natl. Cancer Inst.* **1977**, *58*, 1003–1009. [CrossRef]
21. Geder, L.; Sanford, E.J.; Rohner, T.J.; Rapp, F. Cytomegalovirus and Cancer of the Prostate: In Vitro Transformation of Human Cells. *Cancer Treat. Rep.* **1977**, *61*, 139–146. [PubMed]
22. Geder, L.; Rapp, F. Herpesviruses and Prostate Carcinogenesis. *Arch. Androl.* **1980**, *4*, 71–78. [CrossRef]
23. Herbein, G. The Human Cytomegalovirus, from Oncomodulation to Oncogenesis. *Viruses* **2018**, *10*, 408. [CrossRef]
24. Liu, J.; Niu, N.; Li, X.; Zhang, X.; Sood, A.K. The Life Cycle of Polyploid Giant Cancer Cells and Dormancy in Cancer: Opportunities for Novel Therapeutic Interventions. *Semin. Cancer Biol.* **2022**, *81*, 132–144. [CrossRef]
25. Liu, J.; Erenpreisa, J.; Sikora, E. Polyploid Giant Cancer Cells: An Emerging New Field of Cancer Biology. *Semin. Cancer Biol.* **2022**, *81*, 1–4. [CrossRef]
26. Nehme, Z.; Pasquereau, S.; Haidar Ahmad, S.; Coaquette, A.; Molimard, C.; Monnien, F.; Algros, M.-P.; Adotevi, O.; Diab Assaf, M.; Feugeas, J.-P.; et al. Polyploid Giant Cancer Cells, Stemness and Epithelial-Mesenchymal Plasticity Elicited by Human Cytomegalovirus. *Oncogene* **2021**, *40*, 3030–3046. [CrossRef]
27. Haidar Ahmad, S.; Pasquereau, S.; El Baba, R.; Nehme, Z.; Lewandowski, C.; Herbein, G. Distinct Oncogenic Transcriptomes in Human Mammary Epithelial Cells Infected with Cytomegalovirus. *Front. Immunol.* **2021**, *12*, 772160. [CrossRef]
28. El Baba, R.; Pasquereau, S.; Haidar Ahmad, S.; Monnien, F.; Abad, M.; Bibeau, F.; Herbein, G. EZH2-Myc Driven Glioblastoma Elicited by Cytomegalovirus Infection of Human Astrocytes. *Oncogene* **2023**, *42*, 2031–2045. [CrossRef] [PubMed]
29. Kumar, A.; Tripathy, M.K.; Pasquereau, S.; Al Moussawi, F.; Abbas, W.; Coquard, L.; Khan, K.A.; Russo, L.; Algros, M.-P.; Valmary-Degano, S.; et al. The Human Cytomegalovirus Strain DB Activates Oncogenic Pathways in Mammary Epithelial Cells. *EBioMedicine* **2018**, *30*, 167–183. [CrossRef] [PubMed]
30. Jouberton, E.; Voissiere, A.; Penault-Llorca, F.; Cachin, F.; Miot-Noirault, E. Multicellular Tumor Spheroids of LNCaP-Luc Prostate Cancer Cells as in Vitro Screening Models for Cytotoxic Drugs. *Am. J. Cancer Res.* **2022**, *12*, 1116–1128.
31. Hyder, C.L.; Lazaro, G.; Pylvänäinen, J.W.; Roberts, M.W.G.; Rosenberg, S.M.; Eriksson, J.E. Nestin Regulates Prostate Cancer Cell Invasion by Influencing FAK and Integrin Localisation and Functions. *J. Cell Sci.* **2014**, *127*, 2161–2173. [CrossRef] [PubMed]
32. Chaves, L.P.; Melo, C.M.; Saggioro, F.P.; Reis, R.B.D.; Squire, J.A. Epithelial–Mesenchymal Transition Signaling and Prostate Cancer Stem Cells: Emerging Biomarkers and Opportunities for Precision Therapeutics. *Genes* **2021**, *12*, 1900. [CrossRef]

33. Herbein, G.; Nehme, Z. Polyploid Giant Cancer Cells, a Hallmark of Oncoviruses and a New Therapeutic Challenge. *Front. Oncol.* **2020**, *10*, 567116. [CrossRef] [PubMed]
34. Merchut-Maya, J.M.; Bartek, J.; Bartkova, J.; Galanos, P.; Pantalone, M.R.; Lee, M.; Cui, H.L.; Shilling, P.J.; Brøchner, C.B.; Broholm, H.; et al. Human Cytomegalovirus Hijacks Host Stress Response Fueling Replication Stress and Genome Instability. *Cell Death Differ.* **2022**, *29*, 1639–1653. [CrossRef]
35. Nehme, Z.; Pasquereau, S.; Haidar Ahmad, S.; El Baba, R.; Herbein, G. Polyploid Giant Cancer Cells, EZH2 and Myc Upregulation in Mammary Epithelial Cells Infected with High-Risk Human Cytomegalovirus. *eBioMedicine* **2022**, *80*, 104056. [CrossRef]
36. Amend, S.R.; Torga, G.; Lin, K.; Kostecka, L.G.; Marzo, A.; Austin, R.H.; Pienta, K.J. Polyploid Giant Cancer Cells: Unrecognized Actuators of Tumorigenesis, Metastasis, and Resistance. *Prostate* **2019**, *79*, 1489–1497. [CrossRef] [PubMed]
37. Thura, M.; Ye, Z.; Al-Aidaroos, A.Q.; Xiong, Q.; Ong, J.Y.; Gupta, A.; Li, J.; Guo, K.; Ang, K.H.; Zeng, Q. PRL3 Induces Polyploid Giant Cancer Cells Eliminated by PRL3-Zumab to Reduce Tumor Relapse. *Commun. Biol.* **2021**, *4*, 923. [CrossRef]
38. White-Gilbertson, S.; Lu, P.; Esobi, I.; Echesabal-Chen, J.; Mulholland, P.J.; Gooz, M.; Ogretmen, B.; Stamatikos, A.; Voelkel-Johnson, C. Polyploid Giant Cancer Cells Are Dependent on Cholesterol for Progeny Formation through Amitotic Division. *Sci. Rep.* **2022**, *12*, 8971. [CrossRef]
39. White-Gilbertson, S.; Lu, P.; Jones, C.M.; Chiodini, S.; Hurley, D.; Das, A.; Delaney, J.R.; Norris, J.S.; Voelkel-Johnson, C. Tamoxifen Is a Candidate First-in-class Inhibitor of Acid Ceramidase That Reduces Amitotic Division in Polyploid Giant Cancer Cells—Unrecognized Players in Tumorigenesis. *Cancer Med.* **2020**, *9*, 3142–3152. [CrossRef]
40. Paez, A.; Vazquez, E.; Gueron, G. Heme Oxygenase 1 Governs the Cytoskeleton at Filopodia: Pulling the Brakes on the Migratory Capacity of Prostate Tumoral Cells. *Cell Death Discov.* **2017**, *3*, 17020. [CrossRef]
41. Niu, N.; Zhang, J.; Zhang, N.; Mercado-Uribe, I.; Tao, F.; Han, Z.; Pathak, S.; Multani, A.S.; Kuang, J.; Yao, J.; et al. Linking Genomic Reorganization to Tumor Initiation via the Giant Cell Cycle. *Oncogenesis* **2016**, *5*, e281. [CrossRef]
42. Niu, N.; Mercado-Uribe, I.; Liu, J. Dedifferentiation into Blastomere-like Cancer Stem Cells via Formation of Polyploid Giant Cancer Cells. *Oncogene* **2017**, *36*, 4887–4900. [CrossRef]
43. Cortés-Ciriano, I.; Lee, J.J.-K.; Xi, R.; Jain, D.; Jung, Y.L.; Yang, L.; Gordenin, D.; Klimczak, L.J.; Zhang, C.-Z.; Pellman, D.S.; et al. Comprehensive Analysis of Chromothripsis in 2,658 Human Cancers Using Whole-Genome Sequencing. *Nat. Genet.* **2020**, *52*, 331–341. [CrossRef]
44. Kalkavan, H.; Rühl, S.; Shaw, J.J.P.; Green, D.R. Non-Lethal Outcomes of Engaging Regulated Cell Death Pathways in Cancer. *Nat. Cancer* **2023**, *4*, 795–806. [CrossRef] [PubMed]
45. Yang, L.; Fang, J.; Chen, J. Tumor Cell Senescence Response Produces Aggressive Variants. *Cell Death Discov.* **2017**, *3*, 17049. [CrossRef] [PubMed]
46. Dhanasekaran, R. Treacherous Apoptosis—Cancer Cells Sacrifice Themselves at the Altar of Heterogeneity. *Hepatology* **2022**, *76*, 549–550. [CrossRef] [PubMed]
47. Galanos, P.; Vougas, K.; Walter, D.; Polyzos, A.; Maya-Mendoza, A.; Haagensen, E.J.; Kokkalis, A.; Roumelioti, F.-M.; Gagos, S.; Tzetis, M.; et al. Chronic P53-Independent P21 Expression Causes Genomic Instability by Deregulating Replication Licensing. *Nat. Cell Biol.* **2016**, *18*, 777–789. [CrossRef]
48. Zlotorynski, E. The Dark Side of P21. *Nat. Rev. Mol. Cell Biol.* **2016**, *17*, 461. [CrossRef]
49. Zaitceva, V.; Kopeina, G.S.; Zhivotovsky, B. Anastasis: Return Journey from Cell Death. *Cancers* **2021**, *13*, 3671. [CrossRef] [PubMed]
50. Speir, E.; Shibutani, T.; Yu, Z.-X.; Ferrans, V.; Epstein, S.E. Role of Reactive Oxygen Intermediates in Cytomegalovirus Gene Expression and in the Response of Human Smooth Muscle Cells to Viral Infection. *Circ. Res.* **1996**, *79*, 1143–1152. [CrossRef]
51. Zhang, Z.; Tan, Y.; Huang, C.; Wei, X. Redox Signaling in Drug-Tolerant Persister Cells as an Emerging Therapeutic Target. *eBioMedicine* **2023**, *89*, 104483. [CrossRef]
52. Yu, Z.; Wang, Y.; Liu, L.; Zhang, X.; Jiang, S.; Wang, B. Apoptosis Disorder, a Key Pathogenesis of HCMV-Related Diseases. *IJMS* **2021**, *22*, 4106. [CrossRef] [PubMed]
53. Heng, J.; Heng, H.H. Genome Chaos, Information Creation, and Cancer Emergence: Searching for New Frameworks on the 50th Anniversary of the "War on Cancer". *Genes* **2021**, *13*, 101. [CrossRef]
54. Salciccia, S.; Capriotti, A.L.; Laganà, A.; Fais, S.; Logozzi, M.; De Berardinis, E.; Busetto, G.M.; Di Pierro, G.B.; Ricciuti, G.P.; Del Giudice, F.; et al. Biomarkers in Prostate Cancer Diagnosis: From Current Knowledge to the Role of Metabolomics and Exosomes. *IJMS* **2021**, *22*, 4367. [CrossRef] [PubMed]
55. Qiu, X.; Boufaied, N.; Hallal, T.; Feit, A.; De Polo, A.; Luoma, A.M.; Alahmadi, W.; Larocque, J.; Zadra, G.; Xie, Y.; et al. MYC Drives Aggressive Prostate Cancer by Disrupting Transcriptional Pause Release at Androgen Receptor Targets. *Nat. Commun.* **2022**, *13*, 2559. [CrossRef]
56. Xu, K.; Wu, Z.J.; Groner, A.C.; He, H.H.; Cai, C.; Lis, R.T.; Wu, X.; Stack, E.C.; Loda, M.; Liu, T.; et al. EZH2 Oncogenic Activity in Castration-Resistant Prostate Cancer Cells Is Polycomb-Independent. *Science* **2012**, *338*, 1465–1469. [CrossRef] [PubMed]
57. Coulter, J.B.; Easwaran, H. Combining EZH2 and HDAC Inhibitors to Target Castration-Resistant Prostate Cancers. *PLoS Biol.* **2023**, *21*, e3002081. [CrossRef]
58. Rodríguez-Dorantes, M.; Cruz-Hernandez, C.D.; Cortés-Ramírez, S.A.; Cruz-Burgos, J.M.; Reyes-Grajeda, J.P.; Peralta-Zaragoza, O.; Losada-Garcia, A. Prostate Cancer Spheroids: A Three-Dimensional Model for Studying Tumor Heterogeneity. *Cancer Cell Signal.* **2021**, *2174*, 13–17. [CrossRef]

59. Niharika; Roy, A.; Mishra, J.; Chakraborty, S.; Singh, S.P.; Patra, S.K. Epigenetic Regulation of Pluripotency Inducer Genes NANOG and SOX2 in Human Prostate Cancer. *Prog. Mol. Biol. Transl. Sci.* **2023**, *197*, 241–260. [CrossRef]
60. Kleeberger, W.; Bova, G.S.; Nielsen, M.E.; Herawi, M.; Chuang, A.-Y.; Epstein, J.I.; Berman, D.M. Roles for the Stem Cell–Associated Intermediate Filament Nestin in Prostate Cancer Migration and Metastasis. *Cancer Res.* **2007**, *67*, 9199–9206. [CrossRef] [PubMed]
61. Martin, S.K.; Kamelgarn, M.; Kyprianou, N. Cytoskeleton Targeting Value in Prostate Cancer Treatment. *Am. J. Clin. Exp. Urol.* **2014**, *2*, 15–26. [PubMed]
62. Figiel, S.; Vasseur, C.; Bruyere, F.; Rozet, F.; Maheo, K.; Fromont, G. Clinical Significance of Epithelial-Mesenchymal Transition Markers in Prostate Cancer. *Hum. Pathol.* **2017**, *61*, 26–32. [CrossRef] [PubMed]
63. Montanari, M.; Rossetti, S.; Cavaliere, C.; D'Aniello, C.; Malzone, M.G.; Vanacore, D.; Franco, R.D.; Mantia, E.L.; Iovane, G.; Piscitelli, R.; et al. Epithelial-Mesenchymal Transition in Prostate Cancer: An Overview. *Oncotarget* **2017**, *8*, 35376–35389. [CrossRef] [PubMed]
64. Das, D.; Wojno, K.; Imperiale, M.J. BK Virus as a Cofactor in the Etiology of Prostate Cancer in Its Early Stages. *J. Virol.* **2008**, *82*, 2705–2714. [CrossRef] [PubMed]
65. Ahmed, K.; Sheikh, A.; Fatima, S.; Haider, G.; Ghias, K.; Abbas, F.; Mughal, N.; Abidi, S.H. Detection and Characterization of Latency Stage of EBV and Histopathological Analysis of Prostatic Adenocarcinoma Tissues. *Sci. Rep.* **2022**, *12*, 10399. [CrossRef]
66. Lawson, J.S.; Glenn, W.K. Evidence for a Causal Role by Human Papillomaviruses in Prostate Cancer—A Systematic Review. *Infect. Agents Cancer* **2020**, *15*, 41. [CrossRef]
67. Leiros, G.J.; Galliano, S.R.; Sember, M.E.; Kahn, T.; Schwarz, E.; Eiguchi, K. Detection of Human Papillomavirus DNA and P53 Codon 72 Polymorphism in Prostate Carcinomas of Patients from Argentina. *BMC Urol.* **2005**, *5*, 15. [CrossRef]
68. Nahand, J.S.; Khanaliha, K.; Mirzaei, H.; Moghoofei, M.; Baghi, H.B.; Esghaei, M.; Khatami, A.R.; Fatemipour, M.; Bokharaei-Salim, F. Possible Role of HPV/EBV Coinfection in Anoikis Resistance and Development in Prostate Cancer. *BMC Cancer* **2021**, *21*, 926. [CrossRef]
69. Dennis, L.K.; Coughlin, J.A.; McKinnon, B.C.; Wells, T.S.; Gaydos, C.A.; Hamsikova, E.; Gray, G.C. Sexually Transmitted Infections and Prostate Cancer among Men in the U.S. Military. *Cancer Epidemiol. Biomark. Prev.* **2009**, *18*, 2665–2671. [CrossRef]
70. Jary, A.; Veyri, M.; Gothland, A.; Leducq, V.; Calvez, V.; Marcelin, A.-G. Kaposi's Sarcoma-Associated Herpesvirus, the Etiological Agent of All Epidemiological Forms of Kaposi's Sarcoma. *Cancers* **2021**, *13*, 6208. [CrossRef]
71. Münz, C. Latency and Lytic Replication in Epstein–Barr Virus-Associated Oncogenesis. *Nat. Rev. Microbiol.* **2019**, *17*, 691–700. [CrossRef] [PubMed]
72. Chen, Y.; Wei, J. Identification of Pathogen Signatures in Prostate Cancer Using RNA-Seq. *PLoS ONE* **2015**, *10*, e0128955. [CrossRef] [PubMed]
73. Sutcliffe, S.; Till, C.; Gaydos, C.A.; Jenkins, F.J.; Goodman, P.J.; Hoque, A.M.; Hsing, A.W.; Thompson, I.M.; Zenilman, J.M.; Nelson, W.G.; et al. Prospective Study of Cytomegalovirus Serostatus and Prostate Cancer Risk in the Prostate Cancer Prevention Trial. *Cancer Causes Control.* **2012**, *23*, 1511–1518. [CrossRef] [PubMed]
74. Martinez-Fierro, M.L.; Leach, R.J.; Gomez-Guerra, L.S.; Garza-Guajardo, R.; Johnson-Pais, T.; Beuten, J.; Morales-Rodriguez, I.B.; Hernandez-Ordoñez, M.A.; Calderon-Cardenas, G.; Ortiz-Lopez, R.; et al. Identification of Viral Infections in the Prostate and Evaluation of Their Association with Cancer. *BMC Cancer* **2010**, *10*, 326. [CrossRef] [PubMed]
75. Bergh, J.; Marklund, I.; Gustavsson, C.; Wiklund, F.; Grönberg, H.; Allard, A.; Alexeyev, O.; Elgh, F. No Link between Viral Findings in the Prostate and Subsequent Cancer Development. *Br. J. Cancer* **2007**, *96*, 137–139. [CrossRef]
76. Sitas, F.; Carrara, H.; Beral, V.; Newton, R.; Reeves, G.; Bull, D.; Jentsch, U.; Pacella-Norman, R.; Bourboulia, D.; Whitby, D.; et al. Antibodies against Human Herpesvirus 8 in Black South African Patients with Cancer. *N. Engl. J. Med.* **1999**, *340*, 1863–1871. [CrossRef]
77. Sfanos, K.S.; Sauvageot, J.; Fedor, H.L.; Dick, J.D.; De Marzo, A.M.; Isaacs, W.B. A Molecular Analysis of Prokaryotic and Viral DNA Sequences in Prostate Tissue from Patients with Prostate Cancer Indicates the Presence of Multiple and Diverse Microorganisms. *Prostate* **2008**, *68*, 306–320. [CrossRef]
78. De González, A.B.; Urban, M.; Sitas, F.; Blackburn, N.; Hale, M.; Patel, M.; Ruff, P.; Sur, R.; Newton, R.; Beral, V. Antibodies against Six Human Herpesviruses in Relation to Seven Cancers in Black South Africans: A Case Control Study. *Infect. Agents Cancer* **2006**, *1*, 2. [CrossRef]
79. Cinatl, J.; Vogel, J.-U.; Kotchetkov, R.; Wilhelm Doerr, H. Oncomodulatory Signals by Regulatory Proteins Encoded by Human Cytomegalovirus: A Novel Role for Viral Infection in Tumor Progression. *FEMS Microbiol. Rev.* **2004**, *28*, 59–77. [CrossRef]
80. Soroceanu, L.; Cobbs, C.S. Is HCMV a Tumor Promoter? *Virus Res.* **2011**, *157*, 193–203. [CrossRef]
81. Blaheta, R.A.; Weich, E.; Marian, D.; Bereiter-Hahn, J.; Jones, J.; Jonas, D.; Michaelis, M.; Doerr, H.W.; Cinatl, J. Human Cytomegalovirus Infection Alters PC3 Prostate Carcinoma Cell Adhesion to Endothelial Cells, Extracellular Matrix. *Neoplasia* **2006**, *8*, 807–816. [CrossRef] [PubMed]
82. Moon, J.-S.; Lee, M.-Y.; Park, S.W.; Han, W.K.; Hong, S.-W.; Ahn, J.-H.; Kim, K.-S. Androgen-Dependent Activation of Human Cytomegalovirus Major Immediate-Early Promoter in Prostate Cancer Cells. *Prostate* **2008**, *68*, 1450–1460. [CrossRef] [PubMed]

Disclaimer/Publisher's Note: The statements, opinions and data contained in all publications are solely those of the individual author(s) and contributor(s) and not of MDPI and/or the editor(s). MDPI and/or the editor(s) disclaim responsibility for any injury to people or property resulting from any ideas, methods, instructions or products referred to in the content.